USAAMRDL-TR-74-97A

HEAVY LIFT HELICOPTER - CARGO HANDLING ATC PROGRAM

VOLUME I - Detail Design Structural and Weights Analysis, and Static and Dynamic Load Analysis

Boeing Vertol Company
A Division of the Boeing Company
Philadelphia, Pa. 19142

AD A030072

January 1976

Final Report for Period June 1971 - June 1974

Approved for public release;
distribution unlimited.

DDC
SEP 21 1976
A

Prepared for

U. S. ARMY AVIATION SYSTEMS COMMAND
P. O. Box 209
St. Louis, Mo. 63166

COPY AVAILABLE TO DDC DOES NOT PERMIT FULLY LEGIBLE PRODUCTION

EUSTIS DIRECTORATE
U. S. ARMY AIR MOBILITY RESEARCH AND DEVELOPMENT LABORATORY
Fort Eustis, Va. 23604

Copy available to DDC does not permit fully legible reproduction

EUSTIS DIRECTORATE POSITION STATEMENT

This report was prepared by the Boeing Company, Vertol Division, under the terms of Contract DAAJ01-71-C-0840(P6A). The report documents all the detailed design efforts for advanced technology components of the Heavy Lift Helicopter Cargo Handling System. Major system elements included herein are: hoist drives, winch assemblies, load isolators, tension members, signal conductor subsystem, cargo couplings, and system controls.

Approximately 95% of all program objectives was achieved by the designs. The system as designed, with minor modifications, is suitable for installation in a prototype aircraft.

This directorate concurs with the conclusions presented herein.

The technical monitor for this effort was Mr. Jules A. Vichness, HLH Project Office, Systems Support Division.

Pages which are not reproducible can
be obtain from USAAMRDL/SAVDL-EU-TSD
Fort Eustis, Va. 23604

DISCLAIMERS

The findings in this report are not to be construed as an official Department of the Army position unless so designated by other authorized documents.

When Government drawings, specifications, or other data are used for any purpose other than in connection with a definitely related Government procurement operation, the United States Government thereby incurs no responsibility nor any obligation whatsoever; and the fact that the Government may have formulated, furnished, or in any way supplied the said drawings, specifications, or other data is not to be regarded by implication or otherwise as in any manner licensing the holder or any other person or corporation, or conveying any rights or permission, to manufacture, use, or sell any patented invention that may in any way be related thereto.

Trade names cited in this report do not constitute an official endorsement or approval of the use of such commercial hardware or software.

DISPOSITION INSTRUCTIONS

Destroy this report when no longer needed. Do not return it to the originator.

Unclassified

SECURITY CLASSIFICATION OF THIS PAGE (When Data Entered)

REPORT DOCUMENTATION PAGE	READ INSTRUCTIONS BEFORE COMPLETING FORM
1. REPORT NUMBER: USAAMRDL-TR-74-97A	2. GOVT ACCESSION NO.
	3. RECIPIENT'S CATALOG NUMBER
4. TITLE (and Subtitle): HEAVY LIFT HELICOPTER - CARGO HANDLING ATC PROGRAM, VOLUME I, DETAIL DESIGN STRUCTURAL AND WEIGHTS ANALYSIS, AND STATIC AND DYNAMIC LOAD ANALYSIS	5. TYPE OF REPORT & PERIOD COVERED: FINAL REPORT, JUN 71 — JUN 74
	6. PERFORMING ORG. REPORT NUMBER
7. AUTHOR(s): R. Campbell, W. Nutley, J. Shefrin, L. Simpson, B. Solak, D. Stein, G. Wilson	8. CONTRACT OR GRANT NUMBER(s): Contract DAAJ01-71-C-0840(P6A)
9. PERFORMING ORGANIZATION NAME AND ADDRESS: Boeing Vertol Company (A Division of The Boeing Company) Philadelphia, Pa. 19142	10. PROGRAM ELEMENT, PROJECT, TASK AREA & WORK UNIT NUMBERS: Paragraph F.4
11. CONTROLLING OFFICE NAME AND ADDRESS: U.S. Army Aviation Systems Command, P.O. Box 209, St. Louis, Missouri 63166, Attn: AMSAV-PDAC	12. REPORT DATE: Jan 76; 13. NUMBER OF PAGES: 479
14. MONITORING AGENCY NAME & ADDRESS (if different from Controlling Office): Eustis Directorate, U.S. Army Air Mobility R&D Laboratory, Ft. Eustis, Virginia 23604	15. SECURITY CLASS. (of this report): Unclassified; 15a. DECLASSIFICATION/DOWNGRADING SCHEDULE

16. DISTRIBUTION STATEMENT (of this Report)

Approved for public release; distribution unlimited.

17. DISTRIBUTION STATEMENT (of the abstract entered in Block 20, if different from Report)

18. SUPPLEMENTARY NOTES

Volume I of three volumes.

19. KEY WORDS (Continue on reverse side if necessary and identify by block number)

Helicopter	Air Cargo Handling
Heavy Lift Helicopter	Container Handling
Cargo Handling	Hoist Systems
Cargo System Test Rig	Pneumatic Systems
Integrated Test Rig	Suspension Systems

20. ABSTRACT (Continue on reverse side if necessary and identify by block number)

This report presents formal documentation of efforts and results of the cargo handling system segment of the Heavy Lift Helicopter (HLH) Advanced Technology Component (ATC) development program.

DD FORM 1 JAN 73 1473 EDITION OF 1 NOV 65 IS OBSOLETE

Unclassified

SECURITY CLASSIFICATION OF THIS PAGE (When Data Entered)

20. Abstract (Continued)

The purpose of the HLH/ATC program was to minimize technical cost, and schedule risks associated with future HLH system research, development, test and evaluation (RDTE) and production programs. This was achieved by design, fabrication, and testing of specific ATC hardware in three critical air vehicle subsystems:

(a) Rotor/drive system
(b) Flight control system
(c) Cargo handling system

The HLH cargo handling system described herein consists of: tandem pneumatically driven hoists which provide high-speed in-flight stability with pitch attitude optimization and long-reach cargo acquisition and delivery for externally slung cargo; a visual augmentation system to assist the load controlling crewman in acquiring cargo from a hover under conditions of darkness and partial visual obscuration; and a static electricity discharge system to protect ground handlers from shock hazards. The development program consisted of design efforts, hardware fabrication, and testing necessary to confirm the capability of the hardware to meet the design objectives. Results of each major component development are discussed below.

The hoist system met all design objectives in terms of lifting capacity, hoisting speed, structural capacity and variable speed control, including dynamic braking. These characteristics were confirmed by full-scale hardware integrated tests which demonstrated 1,800 hoisting cycles with a 29-ton load at 60 feet per minute and a static pull test of 73 tons. A maximum unloaded payout speed of 84 feet per minute was achieved but fell short of the 120 feet per minute objective. A maximum unloaded reel-in speed of 120 feet per minute was achieved.

The visual augmentation system was adapted from an existing U.S. Army Cobra Night Fire Control System using an 875 line television monitor, an orthographic fish-eye lens and superimposed external cargo handling symbology. The system was demonstrated in the laboratory and was subsequently evaluated in the Boeing Vertol Company Model 347 HLH test bed helicopter.

Both active and passive static electricity discharge systems were developed and tested on a U.S. Army CH-47 helicopter under desert conditions. Insurmountable problems were identified in the area of sensing, which is essential for the active system; therefore, this approach was abandoned. A passive static electricity system, consisting of a resistive grounding line, was designed which meets all program objectives.

TABLE OF CONTENTS

Page

LIST OF ILLUSTRATIONS 4

LIST OF TABLES 13

INTRODUCTION 15

PART 1 - DETAIL DESIGN 16

Overall Cargo Handling System Goals and Objectives 16
Hoist System 17
Hoist Drive System 23
Hoist 121
Load Isolator 168
Hoist Support and Span Positioning (Traverse) Sys. 188
Cable Cutter 215
Suspension System 222
Tension Member 223
Cargo Coupling 286
Signal Transfer System 301
Controls and Displays 345
Visual Augmentation System (VAS) 390
Static Electricity Discharge System 432

PART 2 - STRUCTURAL DESIGN AND WEIGHTS ANALYSIS 453

PART 3 - STATIC AND DYNAMIC LOAD ANALYSIS 466

CONCLUSIONS AND RECOMMENDATIONS 473

LITERATURE CITED 474

LIST OF SYMBOLS 475

LIST OF ILLUSTRATIONS

Figure		Page
1	Multi-Point and Single-Point Suspensions.....	20
2	Integrated Pneumatic Hoist System.....	22
3	Fixed Nozzle.....	34
4	Variable Nozzle.....	35
5	Partial Admission Nozzle.....	36
6	Torque Versus Speed for Fixed and Variable Nozzle Turbines.....	37
7	Nozzle Area Required for a Constant Hoist of 23 Tons at 60 Feet Per Minute Versus Ambient Temperature.....	39
8	Hoist Drive.....	42
9	Hoist Drive Components.....	43
10	Hoist Drive Assembly.....	45
11	ATM and Gearbox Assembly	47
12	Brake Assembly	57
13	Hoisting Turbine Design.....	69
14	Redesigned Hoisting Nozzle.....	71
15	Redesigned Hoisting Wheel.....	72
16	HLH Hoisting Turbine Nozzle Guide Vane Profile (Initial Design).....	73
17	HLH Hoisting Turbine Blade Profile (Initial Design).....	74
18	Redesigned Hoisting Turbine Performance Net Torque (Ft-Lb) versus Speed (RPM).....	75
19	Redesigned Reversing Turbine Performance (Estimated).....	77
20	Reversing Turbine Design.....	79
21	Blade Profiles (Reversing Nozzle).....	80
22	Redesigned Blade Configuration (Reversing Turbine Wheel).....	82

Figure		Page
23	HLH Reversing Turbine Nozzle Guide Vane Profile (Initial Design).....	83
24	HLH Reversing Turbine Blade Diagram (Initial Design).....	84
25	Thrust versus Output Shaft Speed.....	86
26	Hoisting Nozzle Guide Vanes.....	87
27	Hoisting Turbine Wheel Housing.....	88
28	Hoisting Labyrinth Seal Area.....	89
29	Hoisting Turbine Wheel.....	90
30	Reversing Nozzle Guide Vane.....	91
31	Reversing Housing.....	92
32	Hoisting and Reversing Turbine Wheel Assembly	93
33	Pump Element Configuration.....	94
34	Hoist Drive Brake and Separator Plates.....	99
35	Control Valves Installed on the Hoist Drive..	103
36	On-Off Valve.....	105
37	On-Off Valve Schematic.....	106
38	Modulating Valve.....	107
39	Modulating Valve Schematic.....	109
40	Brake Solenoid Valve.....	110
41	Brake Valve Schematic.....	111
42	Hoist Functional Logic Diagram.....	113
43	Hoist Control Unit.....	120
44	Proposal Hoist Design Concept.....	122
45	Baseline Gearing System - Triple Planetary...	123
46	Level Wind Hoist.....	125
47	Single-Point Payout Hoist.....	126

Figure		Page
48	Twin-Drum In-Line Hoist	129
49	Single-Drum Twin-Cable Hoist	130
50	Level-Wind Twin-Drum Hoist	132
51	Single-Point Payout Twin-Drum Hoist	133
52	Structural Interface	134
53	Weight Impact of Increased Tension Member Length	137
54	Drum Support Arrangement	139
55	Dual-Drum Hoist Assembly	140
56	Hoist Assembly	144
57	Hoist Layout Drawings	145
58	Hoist Frame Assembly	155
59	Hoist Components	158
60	Hoist Bevel Drive	162
61	Roller Assemblies	164
62	Cable Cutter Carriage Assemblies	164
63	Cable Angle Sensor Mechanism	166
64	Cable Length Sensor	167
65	Vertical Suspension Natural Frequencies	168
66	Measured Cockpit 1/Rev Vibration	169
67	Load Isolator Schematic	170
68	COZID Load Isolator Concept	172
69	Load Isolation Criteria	174
70	Load Isolator-Load/Deflection Characteristics	175
71	Isolator Equivalent Spring Rate	176
72	Schematic of HLH/ATC Load Isolator	178

Figure		Page
73	Load Isolators	180
74	Load Isolator Assembly	181
75	Cargo and C.G. Variations Accommodated by Tandem Suspension	189
76	Span Positioning System Concepts	191
77	Pneumatic Duct Arrangements	192
78	Schematic of Cable Actuation System	194
79	Track Roller Assembly	195
80	Installation of Hoist in Module	197
81	Hoist Span Positioning Hardware	199
82	Positioning Cable System	207
83	Single Capstan Drum Actuator Layout	210
84	Span Positioning Actuator	212
85	Hoist Installation in Prototype HLH	213
86	Dual Knife Cable Cutter System	216
87	HLH Hoist Cable Cutter Reliability Study	217
88	Single Knife Cable Cutter System	219
89	Cable Cutter Parts and Assembled Units	220
90	HLH Cargo Handling Suspension System	224
91	Cable Load Degradation as a Function of Coefficient of Friction	226
92	Cable Diameter Versus Strength Comparison	228
93	Fatigue Characteristics of Various Cables	232
94	Sections Through Test Cables	239
95	0.78-Inch-Diameter Design Support Test Cables Compared to Diameter and Strength of Commercial, MIL-W-1511, and MIL-C-5425 Cables	242

Figure		Page
96	Cross Sections of 0.78- and 0.70-Inch-Diameter 36 x 7 Warrington Seale Construction Test Cables.	244
97	Typical AISI 4130 Fitting After Being Swaged Onto a 36 x 7 Cable.....	249
98	End Fitting Interface at Coupling Equalizer Bar..	251
99	End Fitting Interface at Single-Point Adapter....	252
100	End Fitting Interface at Hoist Drum.....	253
101	Assembly Sheave Envelope HLH.....	254
102	Cut Through Swaged Shank Specimen, 0.70-Inch-Diameter Cable.....	255
103	Approximate Configuration of ESCO Duplex Sleeve Before and After Swaging.....	257
104	Approximate Configuration of Battelle-Developed Sleeve Before and After Swaging.....	257
105	Cross Section Through Eye-Splice Specimen, 0.70-Inch-Diameter Cable.....	258
106	Design Development Test Fittings	259
107	HLH Tension Member Assembly.....	261
108	HLH Tension Member End Fittings.....	263
109	Tension/Elongation Characteristics of Right-Lay 36 x 7 Cable (Specimen D-1).....	267
110	Tension/Elongation Characteristics of Left-Lay 36 x 7 Cable (Specimen D-2).....	268
111	Tension/Torque Characteristics of Left-Lay 36 x 7 Cable (Specimen D-2, Run 10).....	269
112	Tension/Torque Characteristics of Right-Lay 36 x 7 Cable (Specimen D-3, Run 10).....	270
113	0.78- and 0.70-Inch-Diameter ATC Test Cables Compared to Commercial MIL-W-1511 and MIL-C-5424 Cables.....	277
114	Extension Pendant Design.....	283

Figure		Page
115	HLH Proposal Cargo Coupling Assembly	287
116	Single-Point Operation	288
117	150,000-Pound-Capacity Coupling Design	290
118	210,000-Pound-Capacity Coupling Design	290
119	Coupling Photoelastic Stress Models	293
120	HLH Cargo Coupling Assembly	298
121	HLH Cargo Coupling Assembly	299
122	Major Coupling Hardware	301
123	Single-Point Adapter Sheave and Coupling Assembly	305
124	Single-Point Adapter Pulley	307
125	Single-Point Adapter Assembly	309
126	Proposed External Conductor Sheath	312
127	Signal Conductor Deployment	313
128	Signal Conductor Deployment	314
129	Signal Conductor Reel Assembly	316
130	Reeling Mechanism Response	318
131	Reeling Mechanism Response	319
132	Estimated Runaway Speed HLH Reeling Mechanism	321
133	Operation of Flat Tape Signal Conductor	324
134	Schematic of Signal Conductor Reel Assembly	326
135	Signal Conductor Reeling Mechanism	327
136	External Signal Conductor	329
137	Flat Tape Internal Signal Conductor	333
138	Flat Tape and Mandrel Assembly	331
139	Reeling Mechanism Performance (Sea Level)	337

Figure		Page
140	Reeling Mechanism Performance	338
141	Design Layout of Signal Conductor Reel Assembly	341
142	Contoured Grip Hoist Controller	353
143	Cargo System Control Panel	355
144	Schematic of Cargo Control System	357
145	Cable Tension Indicator	361
146	Cable Length Indicator	363
147	HLH Cable Tension and Cable Length Indicator System	365
148	Interface Electronics Unit	370
149	HLH Cable Tension and Cable Length Prototype Interface Electronics Unit (Internal Construction)	371
150	Cable Length and Tension Block Diagram	373
151	Operating Modes of Cable Tension Indicator	376
152	Internal Construction - Prototype HLH Cable Tension Indicator	379
153	LCC Hoist Controller	384
154	Controls and Displays Components	385
155	Cargo System Control Box	386
156	Signal Conditioning and Control Logic Units	388
157	Visual Augmentation System Concept Block Diagram	394
158	Viewing and Illumination Patterns for SL-7 Class Ship	396
159	Comparison of Lens Responses Considered for VAS.	403
160	Minimum Spectral Transmittance Characteristics for Ideal VAS Prime Lens	406

Figure		Page
161	CNFCS System Simplified Block Diagram.....	407
162	CNFCS Modifications for VAS.....	408
163	Full-Scale Outline of Visual Augmentation System Display.....	409
164	VAS Optical Relay Scheme.....	412
165	VAS Optical Relay System Mockup.....	413
166	EIU Interface Diagram.....	415
167	Symbol Positioning Logic.....	416
168	VAS Symbology Characteristics.....	417
169	CNFCS Components.....	418
170	VAS Control Panel.....	420
171	CNFCS System Modification Block Diagram.....	421
172	CNFCS Camera Mounting.....	422
173	VAS Equipment Location on Model 347 Helicopter.	423
174	VAS Interconnection Diagram.....	425
175	Camera and Turret Outline.....	426
176	MS Servo Amplifier Outline.....	427
177	Signal Processor Outline.....	428
178	Power Distribution Unit Outline.....	429
179	Electronic Interface Unit Outline.....	430
180	Illuminator Outline.....	431
181	Charging Schematics.....	435
182	Accuracy of Voltage Sensing and Residual Shock Energy for HLH Hovering in Dust (Yuma Desert)..	437
183	Physiological Response of Subject Evaluating Anticipated Electric Shock.....	439

Figure		Page
184	Discharge Characteristics of Single Corona Brush	441
185	Resistance as a Function of Voltage for Various Surface Materials.....	444
186	Proposed HLH Resistive Grounding Line.....	449
187	Dual Drum Hoist Assembly.....	459
188	Hoist Drive.....	461
189	Maximum G-Level Experienced with External Loads.	467

LIST OF TABLES

Table		Page
1	Axial and Radial Turbine Features	30
2	Lube Orifice Summary	97
3	Summary of Valve Requirements	104
4	Estimated Weight and Principle Characteristics of the Four Hoist Configurations	134
5	Weight Impact of Structural Reactions	135
6	System Weight Comparison	135
7	End Fitting Criteria	227
8	Strength Improvement Derived Using Fixed Rather Than Free-Ended Cable (18 x 7 Nonrotating Construction)	231
9	Construction Details for Electrogalvanized 36 x 7 Lang-Lay Wire Cable (0.78-Inch Diameter)	241
10	Development Cable - 0.70-Inch Diameter 36 x 7 Construction Characteristics (Right and Left Lay)	245
11	Geometry of 36 x 7 Cable	248
12	Tension Member Detailed Weight Statement per Ship Set	265
13	HLH/ATC Tension Member Development Test Results 0.70-Inch 36 x 7 Cable	272
14	Physical Characteristics of 36 x 7 Cable	273
15	0.72-Inch 36X7 Lang-Lay Construction Characteristics (Right and Left Lay)	275
16	Extension Pendant Concept Study	279
17	Weight Comparison of Steel Cable for Extension Pendant	280
18	Detail Design Summary of Gears	339
19	RCA Analysis of VAS Alternatives - Cost Breakdown per System Element	400

Table		Page
20	Thermal Expansions of Grounding Line Materials	452
21	Cargo System Coupling Device - Summary of Margins of Safety	455
22	Cargo System Hoist Assembly - Summary of Margins of Safety	460
23	Cargo System Air Turbine Motor - Summary of Margins of Safety	462
24	Cargo Handling System Weight Summary	464
25	Load Asymmetry Accommodation	468

INTRODUCTION

The purpose of the Heavy Lift Helicopter (HLH) Advanced Technology Component (ATC) Program was to minimize technical, cost, and schedule risks associated with the future HLH system RDTE and production programs. This was achieved by design, fabrication, and testing of specific Advanced Technology Components (ATCs) in the critical air vehicle subsystems.

The HLH/ATC Program objectives were: to advance the technology of these critical subsystems components so as to improve the future HLH system in areas of weight reduction, performance, mission operational capabilities, and product assurance qualities; to demonstrate these improvements in critical areas by component and dynamic systems integration testing; and to provide a credible component cost data base for a potential HLH system development.

The three design areas listed below were established as critical air vehicle subsystems:

a. Rotor/drive system
b. Flight control system
c. Cargo handling system

Each was organized into a project which defined and conducted a program tailored to meet stated objectives. Final reports were then prepared to document each of these programs. This document contains the results of the Cargo Handling System ATC Program.

The Cargo Handling System final report is divided into three volumes:

Volume I - Cargo Handling System Design

Part 1 - Detail Design
Part 2 - Structural Design and Weights Analysis
Part 3 - Static and Dynamic Load Analysis

Volume II - Fabrication of Test Hardware and Fixtures

Volume III - Results of Tests, Inspections, and Evaluations

PART 1. DETAIL DESIGN

OVERALL CARGO HANDLING SYSTEM GOALS AND OBJECTIVES

The Cargo Handling ATC Development Program consists of three major elements.

a. Tandem dual hoist system with optional single-point hoist capability.

b. Visual augmentation system to assist in acquisition and deposit of external cargo under conditions of reduced visibility.

c. Static electricity dissipation system for potential equalization of the helicopter while hovering in a high triboelectric environment.

Overall goals and objectives of the ATC program are to develop and demonstrate:

Hoist

. Payload	28 Tons
. Life	10,800 Load Cycles
. Useful Tension Member Length	100 Feet
. Pickup Configurations	Dual or Single Point

Visual Augmentation

. Enhancement of load controlling crewman capability.

Static Electricity

. Shock protection for ground handlers.

HOIST SYSTEM

The major elements of the hoist system that are discussed in this section consist of the following:

1. The hoist drive, including the static/emergency brake, air turbine motors for hoisting and reversing, high-speed gear reduction, lubrication system, power connectors, speed sensors and feedback loop, temperature/pressure sensors, and torque sensor.

2. The hoist assembly, including load isolators, cable cutters, low-speed gear reduction, lubrication system, tension member angle sensor, and the hoist span positioning system.

3. Signal/power transfer system conductor reeling mechanism.

4. Control system.

The pneumatic power generation and distribution necessary for the integrated rig testing of the hoisting system is described in Volume II of this report.

Hoist System Criteria

The following specific system requirements were developed:

Hoisting Modes

The system is designed for two hoisting modes:

1. Two-point (Multipoint) suspension mode, utilizing two hoist assemblies, each capable of independent and synchronous, bidirectional variable-speed operation at any load.

2. Single-point suspension mode, utilizing the two hoist assemblies by coupling the suspension system of both hoists with a single-point adapter and hook assembly. Variable bidirectional speed-control capability for variable external load capacities is required.

Operating Ambients

Operating ambient conditions are from -65°F to +125°F at pressure altitudes from 0 to 10,000 feet.

The temperature data are based on the U.S. Army Material Need (MN) document. The altitude limit was selected so as not to inhibit operations at normally experienced density altitudes.

Structural Criteria

Structural criteria for the hoist system are based upon a 28-ton payload. Detail analysis of individual hoist and tension member design criteria may be found in Part 3 of this volume.

P atic Power

The production HLH will have two sources of pneumatic power:

1. Simultaneous bleed from three main propulsion engines.

2. APU generated power.

Redundancy. The primary in-flight pneumatic power source is main engine bleed air. In the event that one engine bleed system fails, yet all three engines are operative, the remaining two bleed systems shall supply adequate bleed air to power all pneumatic systems, including full load hoisting.

In the event one engine fails, the APU shall be used. Full-capacity hoisting power, including the other pneumatic power systems requirements, is to be provided by the APU. Ground operation without main propulsive power shall be provided by the APU-generated pneumatic supply. Electrical and hydraulic power is provided by APU-mounted hydraulic pumps and an air turbine motor-driven generator and hydraulic pumps.

Temperature Limitations. The ATC hoist system design was based on the air supply temperature within the fuselage being limited to 450°F.

Hoist System Control. All facets of the total aircraft pneumatic system control, distribution, priority, and operation must be compatible for the control of the hoist system. The hoist system shall be operated by the pilot, copilot, load-control crewman, and ground-stationed operator. Control priority is reserved for the pilot.

Performance. The system design was based on the two-point suspension mode capable of accommodating the design load at a minimum vertical hoisting velocity of 60 ft/min.

Hoisting velocities with external load capacities less than the specified design load capacity shall be increased proportionately.

Vertical hoisting velocity objective with zero load is 120 fpm. (Proportionate speed reduction due to tension member and coupling weight is acceptable.)

The empty-hook payout speed objective at design-day condition is 120 fpm. This capability is based on zero weight assisting the reversing rotation. Disconnect or clutching between the hoisting driver and the drum is not acceptable.

Component Efficiencies and System Losses The system hardware design was based on component efficiency assumptions and system loss predictions as follows:

1. Low-speed gearing integral with the hoist drum, based on approximately 327:1 gear reduction, is 90 percent at design speed and load.

2. High-speed gearing integral with the air turbine motor driver, based on 10-12:1 gearing reduction, is 95 percent at design speed and load.

3. Cable bending and miscellaneous losses are 5 percent.

4. Pneumatic power transfer pressure losses between the generating sources and the air turbine motor driver are 5 percent of the source pressure absolute.

5. Temperature loss between the source(s) and the drivers is 10 percent of the actual compressor Δ_T based on 80 percent adiabatic compressor efficiency at design-day conditions.

6. Adiabatic turbine efficiency based on design-day conditions at optimum operating point is 79 percent.

7. The constant-speed, shaft-driven, adiabatic compressor efficiency is based on 80 percent at design-day conditions.

Hoist System Design

The initial hoist system concept consisted of two movable hoists installed in tandem tunnels in the bottom of the fuselage. Variable span from 16 feet to 26 feet was provided by mounting the hoists on longitudinal tracks on each bay. Single-point conversion was accomplished by connecting the two tension members with an adapter which converted them to a continuous member. A traveling sheave supporting the coupling maintained symmetrical loads to the two hoists. This configuration is shown in Figure 1.

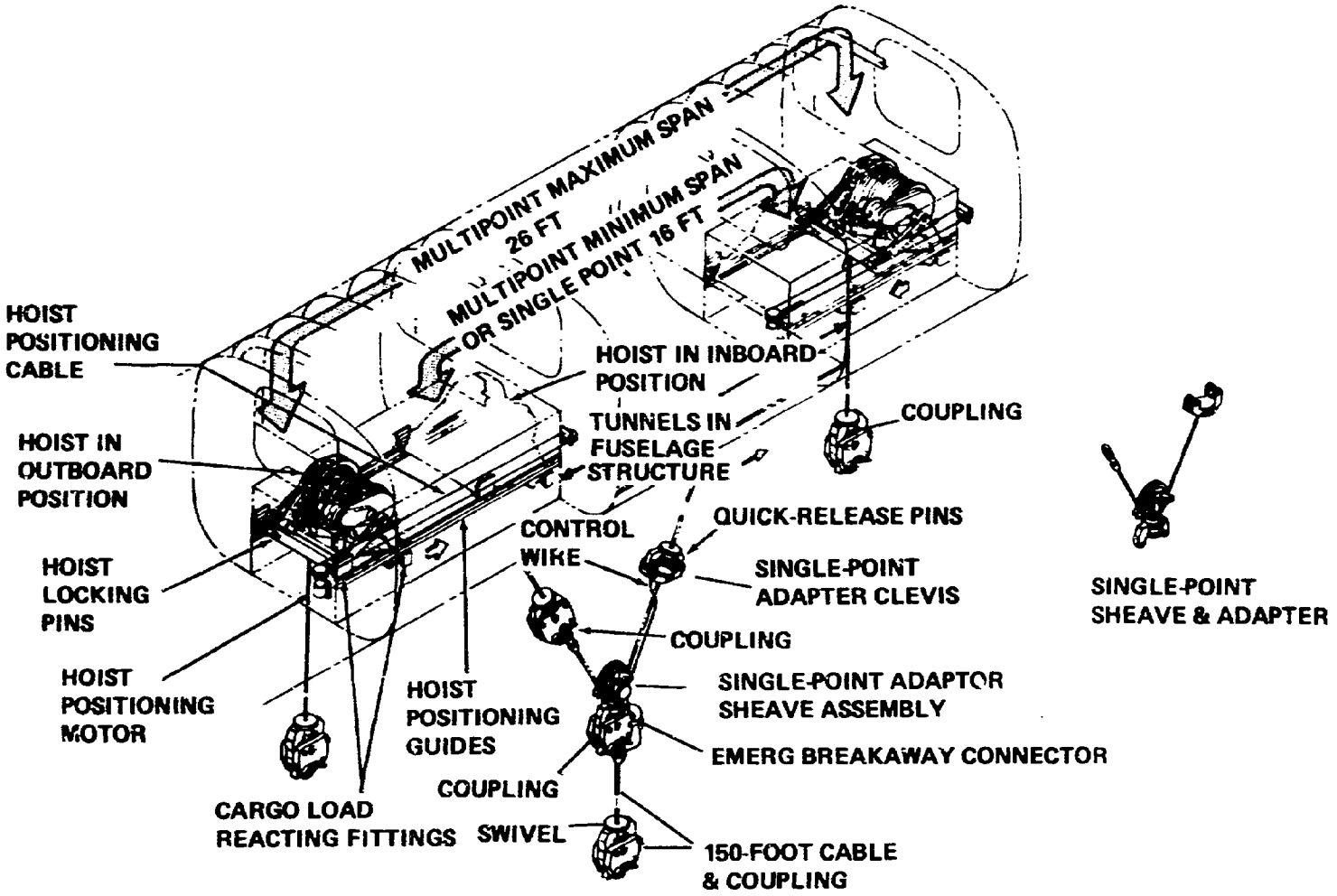


Figure 1. Multipoint and Single-Point Suspension.

The pneumatic system for the hoist drive was integrated with the overall pneumatic system for the other air vehicle subsystems. Telescopic or articulated conductors to the hoists accommodated the variable spans. The power source is either an APU-driven compressor or a main engine bleed, thereby providing power generation redundancy. A schematic of this concept is shown in Figure 2.

The evolution of the various elements of this system and the results of the preliminary design effort to develop the necessary components to implement the general requirements and criteria previously defined are presented in the following sections.

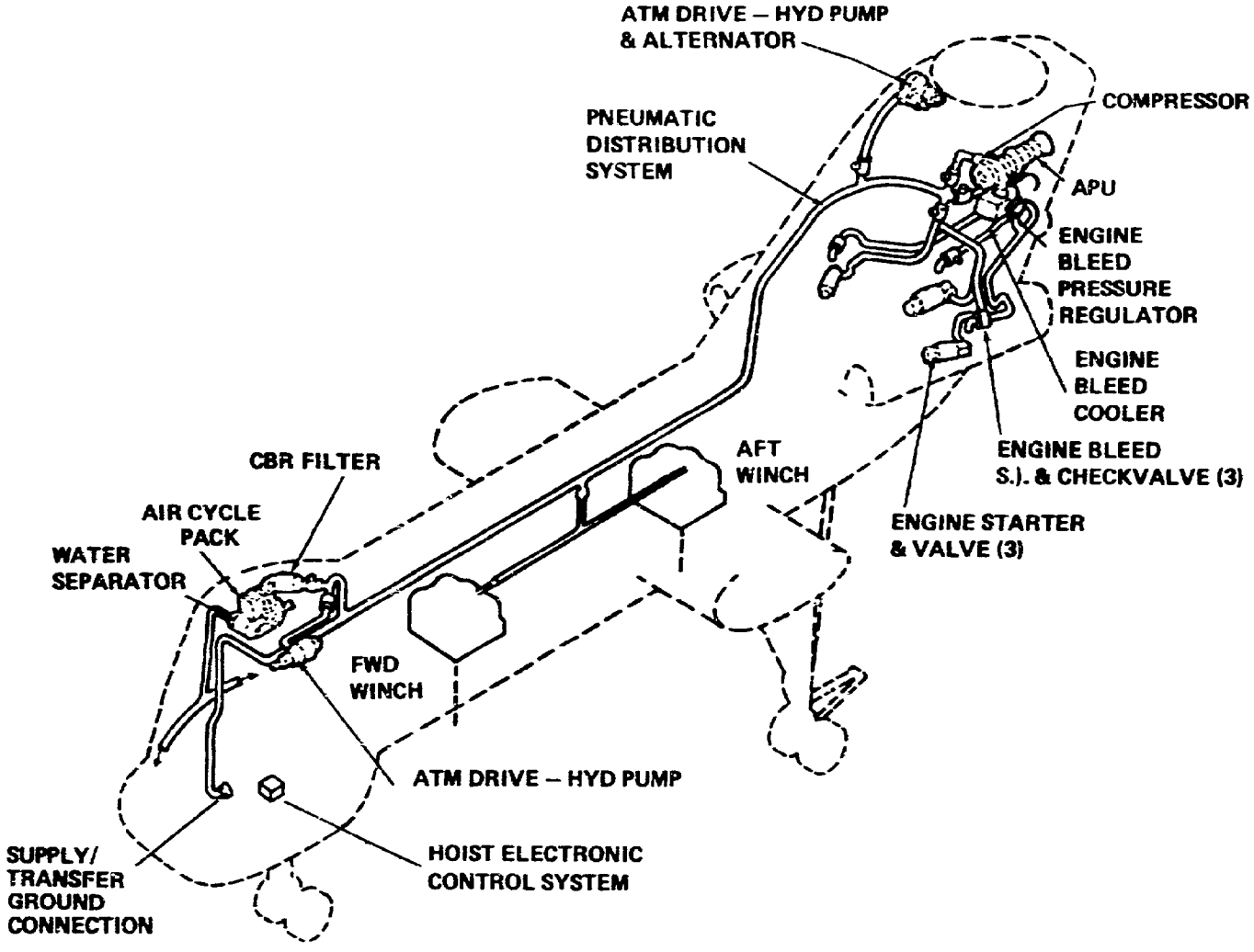


Figure 2. Integrated Pneumatic Hoist System.

Hoist Drive System

Description and Requirements

The hoist drive, alternately referred to as the ATM (Air Turbine Motor), is pneumatically powered. The pneumatic power is supplied through simultaneous bleed of three main propulsion engines or from an APU generated pneumatic power source. The bleed air is "conditioned" to the air quality that meets the hoist system criteria.

Two independent motors of identical capacity and performance characteristics are required for the hoist drive system. The air turbine motor design requirements are based on the criteria defined in the criteria section supplemented by the added specific requirements for the hoist drive which are as follows:

1. Each ATM will be independently controllable or both ATMs may operate in synchronization.

2. Each ATM housing was designed on an integrated basis and shall consist of the following major components.

   a. Hoisting wheel
   b. Nozzle assembly for hoisting
   c. Reversing wheel
   d. Reversing nozzle(s)
   e. Forced lubrication system
   f. Disconnect or clutching

   g. Heat dissipation system
   h. Airflow controller for forward and reverse rotation
   i. Control actuator
   j. Control power generator
   k. High-speed gear reducer
   l. Output shaft
   m. Mounting interface with static/emergency brake
   n. Control interface with static/emergency brake
   o. Signal conductor interface
   p. Static brake

3. The output speed from the high-speed gear reducer at zero load (free-running turbine speed) will be 8,000 rpm. The gear reduction ratio is a function of the hoisting wheel mean diameter selected.

4. Predicated on impulse turbine wheel design, the high-speed gearing output optimum operating point is 4,000 rpm, which corresponds to a hoisting velocity of 60 fpm.

5. The stall torque generating capacity of the wheel is based on its capability to react an 86,387-pound vertical load pull multiplied by the coning angle factor of 1.15 at a lever arm of .782 feet divided by the low-speed gear reduction of 328:1 divided by the high-speed reduction as dictated by the wheel design (equivalent to 236 ft-lb divided by the high-speed gear reduction ratio).

6. Each turbine wheel operating at the optimum point shall be capable of generating 78.6 HP based on 60 fpm hoisting speed. The high-speed gearing output power shall be 74.6 HP, which is based on 95-percent gearing efficiency.

7. For ATM designs utilizing nonclutched reversing wheels, the hoisting wheel design capacity must be increased by an amount equivalent to the reversing wheel drag torque. Higher airflow penalties are acceptable only when definite improvements are demonstrated.

8. The effective nozzle area will be designed for the required horsepower and for the following non-design day conditions:

   a. For design day ambients under 95°F, the system capacity shall equal or exceed design day system capacity.

   b. Reduced system capacity at ambient temperatures above 95°F will be acceptable. However, the percentage change in capacity is not greater than the percentage change in helicopter lift capability consistent with the typical engine lapse rate at normal power settings.

   c. Empty hook hoisting and reversing velocity reduction is acceptable provided the reduction does not exceed the nozzle spouting velocity reduction as a result of colder air supply temperature.

9. Design day pneumatic airflow requirements are based on 4.08 pressure ratio and 414°F temperature available at the turbine.

10. Total design day airflow requirements for both air turbine drivers are based on 60/40 load distribution on either hoist.

11. For non-design day conditions, the airflow requirements will be determined by analysis based on the APU-driven constant speed load compressor, applicable transfer losses and the efficiency deterioration of the air turbine. The minimum analyses shall be conducted for minus 65°F 4000-foot condition, 125°F sea level condition and 95°F 10,000-foot altitude conditions. The valves, nozzle area design, and the control system will be designed for the total operating ambient spectrum.

12. Special provisions to meet 120 ft/min empty hook hoisting under non-design day conditions are not required. The speed reduction will, however, not exceed the theoretical nozzle spouting velocity reduction based on design day condition.

13. Total airflow for powered reversing rotation will not exceed the maximum requirements defined in 10 and 11.

14. Acceptable hoisting nozzle assembly designs were:

    a. fixed geometry
    b. variable geometry
    c. partial admission.

    Substantiation of either concept is required by analysis, which shall define response characteristics, size impact, controllability of the hoist drive system, and turbine efficiencies.

15. For the purpose of 120-ft/min, empty hook payout (reversing rotation) installation of a reversing wheel is acceptable. The reversing wheel shall have adequate capacity to overcome the hoisting wheel aerodynamic drag which is directly coupled (no mechanical disconnect) through the static brake to the

hoist drum. The reversing wheel shall be a module within the ATM housing. Reversing wheel clutching is acceptable. The clutch shall be a module within the ATM housing.

16. The hoisting wheel torque/speed characteristic in the negative region will be compatible with the characteristics of an impulse turbine. These characteristics enable the wheel to perform the dynamic braking function and to identify discrete reverse rotation torque/speed characteristics for a specific airflow for effective rate of descent control with load.

17. To minimize the temperature rise during reversing rotations, installation of additional reversing nozzles to the hoisting wheel is acceptable.

18. A forced lubrication system will be provided.

19. The heat dissipation requirements are based on the efficiency of high-speed gearing, bearing losses and conduction from the air supply temperature. Additional heat is generated during dynamic braking and reverse rotation. Heat dissipation analyses are to be conducted on the basis of three hoisting cycles per hour, each cycle consisting of: full-speed reversing payout, full pacity hoisting, ten minutes of no activity, full-capacity lowering, and empty reel-in. The heat sink is ambient air.

20. The type of airflow controller is predicated on the design of the nozzle assembly. The controller response characteristics to enable variable speed/load accommodations and to provide synchronous speed capability of both hoists are the prime requirements. For fixed geometry nozzle designs, the sliding valve control approach (due to linearity) over the butterfly valve control is preferred. There were, however, no specific valve design requirements.

21. Acceptable types of control power are electrical, hydraulic and/or pneumatic. In the event hydraulic actuating power is used, the motor powering the lubricating pump is to be utilized for this function.

22. The high-speed gear reducer is to be designed for 4,000 rpm shaft output dictated by the hoist interface requirement. The gearing efficiency shall be 95 percent minimum at design operating conditions. Design capacities and speed requirements for the high-speed gearing are consistent with the requirements defined in 3, 4, 5 and 6.

23. The high-speed gearing output shaft is mounted through the static/emergency brake and is directly coupled to the low-speed gearing, which is integral with the hoist drum. Static brake design concepts that are mounted on the high-speed turbine wheel shaft and are integral within the ATM housing may be considered.

24. The static brake design and its operation require the highest order of attention due to its safety function and emergency features.

    The following characteristics were therefore required.

    a. The brake is normally "on".

    b. During hoisting operation, the brake release mechanism does not function until the ATM generated torque is adequate to react the load. Mere substantiation of pneumatic power availability to the ATM is inadequate.

    c. Brake actuating power is generated within the ATM/brake housing.

    d. Application of the brake actuating power shall be gradual and shall not induce accelerations exceeding the levels for which the hoist drive system components (including airframe structure) are designed.

    e. Irrespective of the hoist operator speed selection (airflow), the control system shall be designed in series with the brake release mechanism with an automatic "dwell" (zero speed) period when the brake is being released.

    f. The brake mechanism is engaged whenever zero turbine speed is commanded.

g. The minimum static holding capability of the brake is equivalent of 67,500 ft-lb divided by the appropriate gearing reduction.

h. The brake "normal mode of operation" is designed for on-off condition.

i. One full-capacity dynamic braking operation under maximum loading and velocity conditions is required before brake corrective maintenance, repair or replacement, is required.

j. Brake operation frequent checkout capability shall be provided in the control system and component design. Loss of brake actuating power automatic signal is required.

25. The intelligence and sensor data requiring the ATM control interface consist of the following:

a. Load sensing
b. Tension member angle
c. Hoisting speed, including closed loop speed control
d. Operator to ATM hoisting command signals
e. Position sensing, including proximity switches
f. Temperature/pressure sensors
g. Ambient condition sensors
h. Pneumatic power generator status.

26. For synchronous speed control, the concept of slave and master control shall be employed wherein the master represents the larger load carrying hoist.

Air Turbine Motor Design Analysis

Early analysis of the pneumatically powered hoist drive system power requirements clearly showed that the air turbine is the most suitable motor for this application. The other alternative, the positive displacement motor, was rejected due primarily to its low adiabatic efficiency (less than 50 percent) and unproven performance at 200 percent over design speed required for empty hook reel-in and payout capability.

This would impose intolerable penalties on the engine bleed capacity and dictate APU capacity above that currently available within the HLH/ATC time frame.

The pneumatic approach to the hoist drive system was based on a study[1] conducted by Boeing for the U.S. Army, wherein the weight advantage for a 20-ton hoist system of the pneumatic over the hydraulic approach was 203 pounds against 874 pounds, respectively. This, plus the added advantages of a low-pressure nonflammable power medium, the capability of dynamic braking, the elimination of logistics and the inherent capabiltiy of the turbine to accommodate acceleration loads, resulted in the selection of the pneumatic hoist drive system.

Turbine Design Considerations. The primary consideration in turbine design was the axial versus the radial configuration; applicable to both types is the determination of nozzle design - fixed geometry versus variable geometry. Availability of either combinations with no major manufacturing problems of any system selected has been established. In a recent program funded by the Air Force for an advanced technology small engine, one radial and one axial turbine within the same engine were used as a result of optimization studies conducted. Table 1 shows some of the features of axial and radial turbines.

Early in the program it was decided that in order to pay out (lower) an empty hook, the hoist drive must be powered for the payout mode. The hook weight is not adequate to "pull" the hoist in reverse and overcome the gearing friction. With this in mind, the following turbine wheel and nozzle arrangements were considered:

1. Axial Impulse Turbine With Partial Admission

   This design has a nozzle ring with some nozzles angled in the reverse-rotation direction. Two air supply ports connect the nozzle to the air control valve. This would be designed to progressively throttle the air supply to either set of nozzles, with a central zero position.

   If full reverse speed could be achieved with no more than 30 percent reverse admission, the maximum achievable efficiency in the forward direction should be about 70 percent. The arrangement is simple, but it will not achieve the performance target.

---

1. Stein, D. et al; ADVANCED TECHNOLOGY HIGH-CAPACITY HOIST DRIVE SYSTEM: Boeing Vertol Company; USAAMRDL Tech. Report 72-21, U.S. Army Air Mobility Research and Development Laboratory, Fort Eustis, Virginia; April 1972, AD746629.

TABLE 1. AXIAL AND RADIAL TURBINE FEATURES.

Feature	Radial	Axial
Maximum efficiency, Normal rotation	Good	Good
Maximum efficiency, Reversed rotation	Good	Poor
Reversing nozzle design	Complicated, but reasonably effective	More complicated and not very effective in reverse
Fixed nozzle, Partial admission	Reasonably efficient in both directions	Poor in reverse
Torque speed characteristic	Good	Better
Air consumption characteristic	Increases with speed reduction	Relatively independent of rpm
Most likely design point for torque and airflow	Stall	Maximum HP

2. Axial Turbine With Inner Reversing Blades

This is a full-admission axial - impulse turbine having a pair of axial nozzle rings. The outer nozzle is designed for forward rotation, and the inner one is designed for reverse rotation. Power control is by throttling.

The rotor has normal blades cut on the periphery, and an additional set of blades cut through the rotor to provide reversing blades. These "blades" may be virtually straight-sided slots, since the gas-approach angle will be nearly 90 degrees at maximum speed.

Since the reversing nozzles and blades are at a smaller diameter than the main blades, the maximum reverse speed could in principle be higher than maximum forward speed, with the same nozzle exit velocity.

This arrangement results in the neatest and most compact ATM design with a sufficient degree of design flexibility. However, there could be serious problems in the design and manufacture of the turbine wheel, which would be more highly stressed than a conventional wheel. Given sufficient development time, it is believed that this approach would give the best design for the ATM, but the element of risk is too high for the short development program required.

3. Variable Nozzle Reversible Radial Turbine

This is a simple radial turbine with a nozzle ring having an even number of pivoting nozzle vanes.

With variable angle nozzles, reverse may be approached either through maximum nozzle area or through minimum nozzle area. The former can be done with well shaped nozzles, but it is very bad from a control point of view. Such a nozzle would probably have to be used in conjunction with an inlet control throttle.

Reversing through zero area results in a limitation in nozzle shape, but the nozzle area can be used to control power. At maximum

forward and reverse, the provisional design seems to give a very reasonable nozzle shape; in moving from maximum forward to maximum reverse, half the nozzles rotate through an angle of about 40 degrees, while the interleaving blades move in an opposite direction through an angle of about 14 degrees. From an efficiency point of view, this should be better than throttling, even if compromising nozzle geometry reduces maximum turbine efficiency, since there will be no additional throttling losses. However, the basic characteristics of a radial turbine give a high airflow requirement at stall, and this is sufficient to eliminate this approach.

4. Variable Nozzle Reversible Axial Turbine

Had tests shown that an axial impulse wheel could be driven in reverse at the required speed, the pivoting nozzle design could be used with an axial wheel. However, the nozzle mechanism is more difficult to design for axial directed vanes; also, the performance of axial turbine nozzles is more critically dependent on nozzle shape than is the case with radial turbines. Therefore, the high element of risk eliminates this approach.

5. Single-Axial Wheel With Combined Radial Reversing Stage

This is essentially similar to the concept for a wheel with an inner row of reversing blades, but it avoids weakening the wheel, at the expense of complicating the exhaust ducting.

The shape of the wheel provides a good stress distribution, giving a high bursting speed. The diameter of the radial stage, complete with nozzle ring and a side volute, has to fit inside the nozzle ring of the axial stage. This should be possible since its design speed is twice that of the main stage.

The parasitic drag of the radial stage during normal operation at design speed will not be too high. A 3-inch radial wheel used on a Lucas diesel supercharger takes 5.5 hp at 100,000 rpm when the delivery is shut off. At 50,000 rpm, this would reduce the main stage output power by approximately 2 percent.

The rotor design is such that it can be mounted on a single bearing. The air ducting is complicated by the need to cater to the radial turbine exhaust, but this does not appear to be serious. The only performance shortcoming appears to be the low turbine brake torque available when hoisting an unloaded hook, and this can be catered to in the control system.

6. Twin Wheel Axial Turbine

Although the use of a separate wheel solely for paying out an unloaded hook seems at first to be extravagant, there are definite advantages to this approach.

Since it is required to operate at twice the maximum power, a wheel can be used and can be designed to give its maximum efficiency at a speed where the main wheel efficiency is zero. Also, since windage losses are proportional to the cube of rpm and the fifth power of diameter, the additional losses due to the reversing wheel should be low enough to make declutching unnecessary.

The main wheel design could be a simple conventional profile designed for maximum fatigue life and maximum bursting speed. If this were made from titanium, the bursting speed is at least 50 percent higher than maximum unloaded runaway speed. The design of the reversing wheel can be carefully matched to the drag characteristics of the main wheel, to make excessive reverse speed impossible to achieve. This drag characteristic can only be approximately calculated, and it will need to be established by testing. The only difficulty appears to be in the design of the turbine bearings and their lubrication. The arrangement seems to offer the best possibility for achieving the required hoist performance with the minimum of design risk.

Turbine Nozzle Configuration The selection process of the turbine nozzle configuration for the purpose of hoist-drive control was based on the following configurations:

1. Fixed nozzle design with upstream butterfly valve control - Figure 3.

2. Variable nozzle design - Figure 4.

3. Partial admission nozzle design - Figure 5.

The bidirectional variable speed control with fixed and variable geometry nozzle air-turbine motor designs is accomplished by modulating the airflow into the turbine.

The torque speed characteristics for both nozzle configurations are shown in Figure 6.

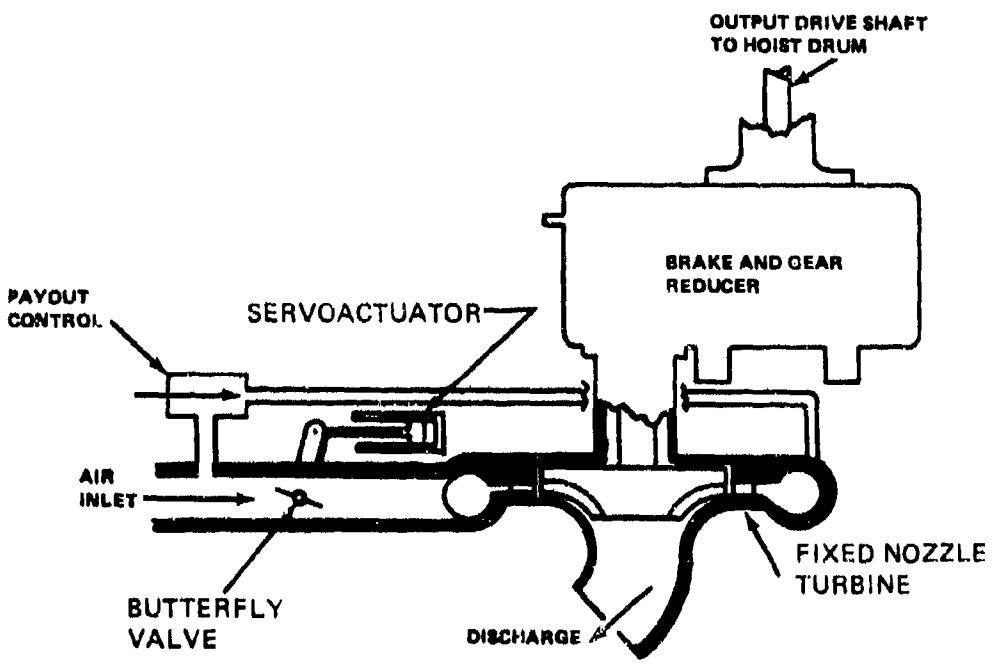


Figure 3. Fixed Nozzle.

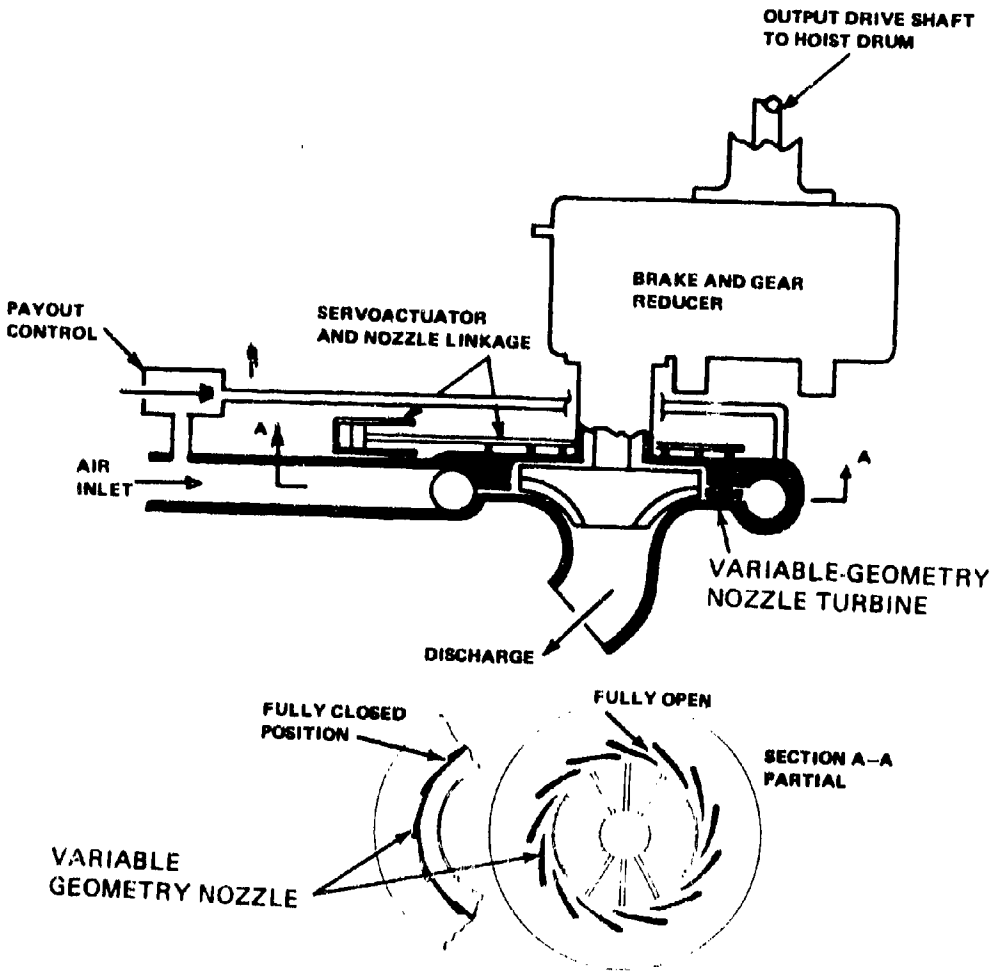


Figure 4. Variable Nozzle.

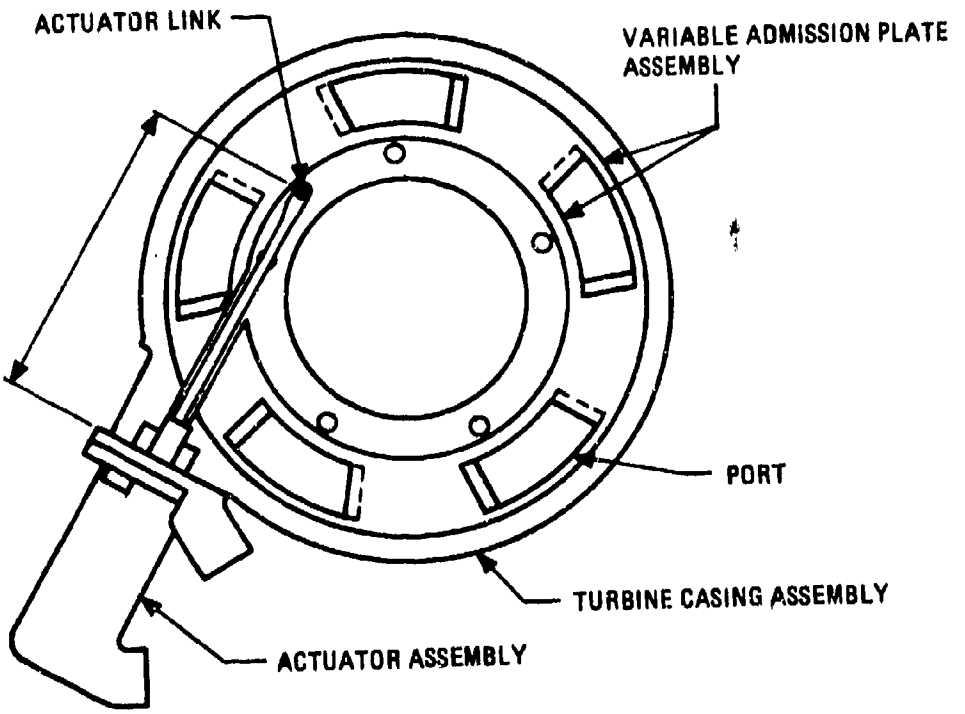
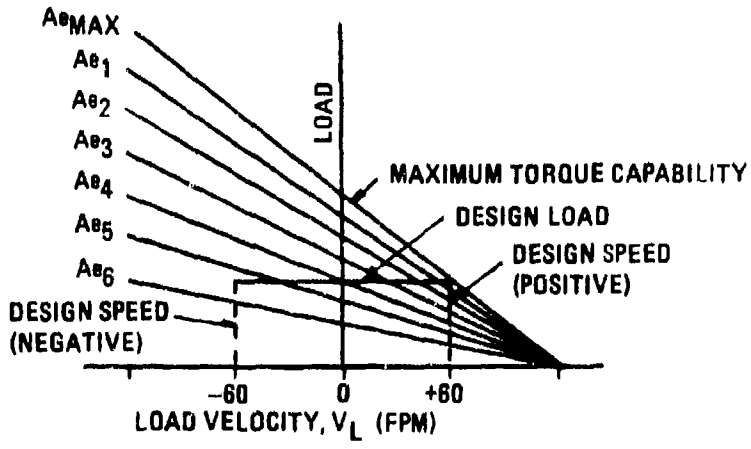


Figure 5. Partial Admission Nozzle.

VARIABLE-NOZZLE TURBINE



FIXED-NOZZLE TURBINE

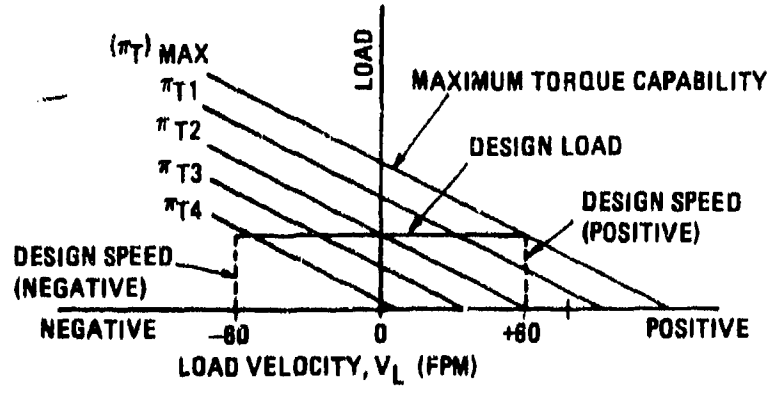


Figure 6. Torque Versus Speed for Fixed and Variable Nozzle Turbines.

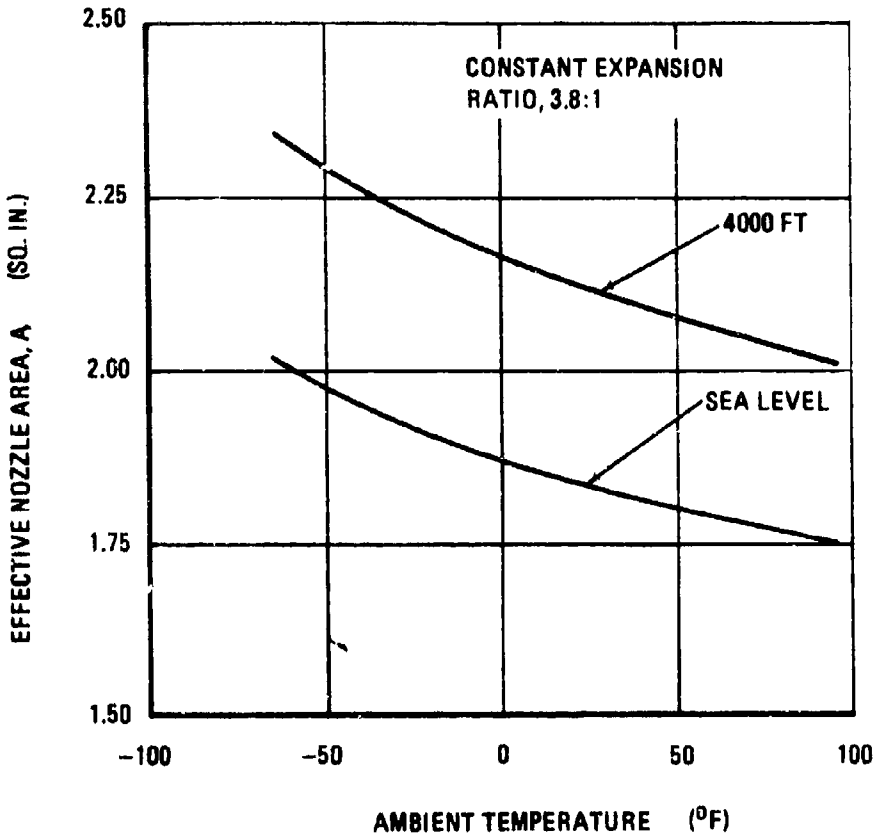
1. Air-Turbine Nozzle Area Analysis

The effective nozzle area design, when based on a hot-day condition, will not permit adequate flow passage to accommodate at least equal hoisting capacity for cold ambients. This is attributable to the fact that the temperature of the air is much colder with the resulting lessening of the supplied air specific energy. The nozzle area design must therefore be based on some colder design-day conditions. (The above is based on a constant pressure ratio operation.) To compensate for the lower specific energy level, more airflow is required, which is available from the increased capability of air delivery from the compressor at the low temperature.

The analyses conducted herein were based on a particular compressor design yielding a 4:1 pressure ratio, which is maintained throughout the entire spectrum of operating ambients from -65°F to +95°F and includes both 4,000 feet and sea level operating conditions. Based on the performance characteristics of the above compressor, the turbine inlet temperature and the respective losses between the compressor and the turbine were calculated. On the basis of degrading turbine performance from the optimum design-day condition of 4,000 feet, 95°F, the nozzle area required for various ambients is as shown in Figure 7.

In order to provide the same hoisting capacity at 4,000 feet, -65°F conditions, the nozzle area required is approximately 11 percent higher than for the equivalent capacity at 4,000 feet, 95°F condition. The corresponding airflow requirement is 36 percent higher at the -65°F ambient condition.

The effective nozzle area must therefore be designed for the -65°F condition in order that no degradation of capacity at this temperature occurs. The adequacy of the increased air delivery from the compressor has been established.



*The intent here is to show the required nozzle area relative variation as a function of temperature based on 85 percent turbine efficiency. In the ATC design the absolute values indicated do not apply since each hoist drive is based on a 16.8-ton capacity (.6 X 28 tons) with turbine efficiencies below 85 percent. The relative nozzle area values are valid.

Figure 7. Nozzle Area Required for a Constant Hoist of 23 Tons* at 60 Feet Per Minute Versus Ambient Temperature.

2. Analytical Data Substantiation

Substantiation of analytical data has been considered the prime order of importance in this study effort. Toward this objective, design support tests were conducted and test data of representative wheel configurations were collected.

The results of these tests are reported in Volume III of this report.

Turbine Selection Summary The performance characteristics of radial and impulse turbines were investigated; the significant parameters affecting system design were compared. These parameters were: overspeed capability, impact on performance under variable ambient operation, turbine wheel diameter, gear reduction requirements, and acquisition and design. A comparison of radial and impulse turbine wheels is particularly significant in the investigation of the dynamic braking.

Based on analytical performance data of the respective wheels, and on the basis of the test data, the following conclusions are drawn:

1. The axial wheels are more suited for variable-speed/load hoist control, due to their linear torque speed characteristics.

2. The radial wheel must be approximately 1.4 times larger in diameter than the axial wheel. The ATM housing is therefore larger.

3. The radial wheel in reverse rotation does not provide the discrete torque intelligence necessary for the rate-of-descent control for hoisting applications.

4. The radial wheel ratio of free-running speed to optimum operating speed does not permit unloaded hook hoisting speeds to be equal to those of the axial wheel.

5. The stall torque of the axial wheel is higher than that of the radial wheel.

6. The variable-geometry nozzle design for the radial wheel is less complex than that for the axial wheel.

7. Neither the axial nor the radial turbine provides high-speed (200 percent) empty-hook payout capability.

8. The efficiency of both wheels is nearly the same.

9. No significant difference in fabrication of either wheel exists, nor is there a substantial cost difference.

Based on the above, the axial wheel and fixed geometry nozzle have been selected as the most appropriate for this application.

Hoist Drive Design

Hoist Drive Assembly

Alternately referred to as the Air Turbine Motor (ATM), the hoist drive assembly is shown in Figures 8 and 10 and consists of:

1. Hoisting and reversing turbine wheel assembly
2. High-speed gearbox
3. Lubrication system
4. Static/emergency brake
5. Housings
6. Pneumatic supply and control valves
7. Hoist control system

The assembly consists of two axial flow turbine wheels mounted back-to-back on a common shaft, one set of fixed nozzle guide vanes for each wheel, associated inlet scrolls, discharge ducting, labyrinth seals, gearbox, and brake assembly (see hoist drive components, Figure 9). The detail design of the hoist drive is illustrated by Sundstrand Drawing EP6003-4510 and EP6003-72, Figures 11 and 12 .

Materials Selection The revised selection of materials for the turbine portion of the design is as follows:

1. Bearings - all M50, except the brake bearings are 52100

2. All aluminum housings - A356-T6 castings

3. Quill shaft, high-speed assembly - 8620 case hardened

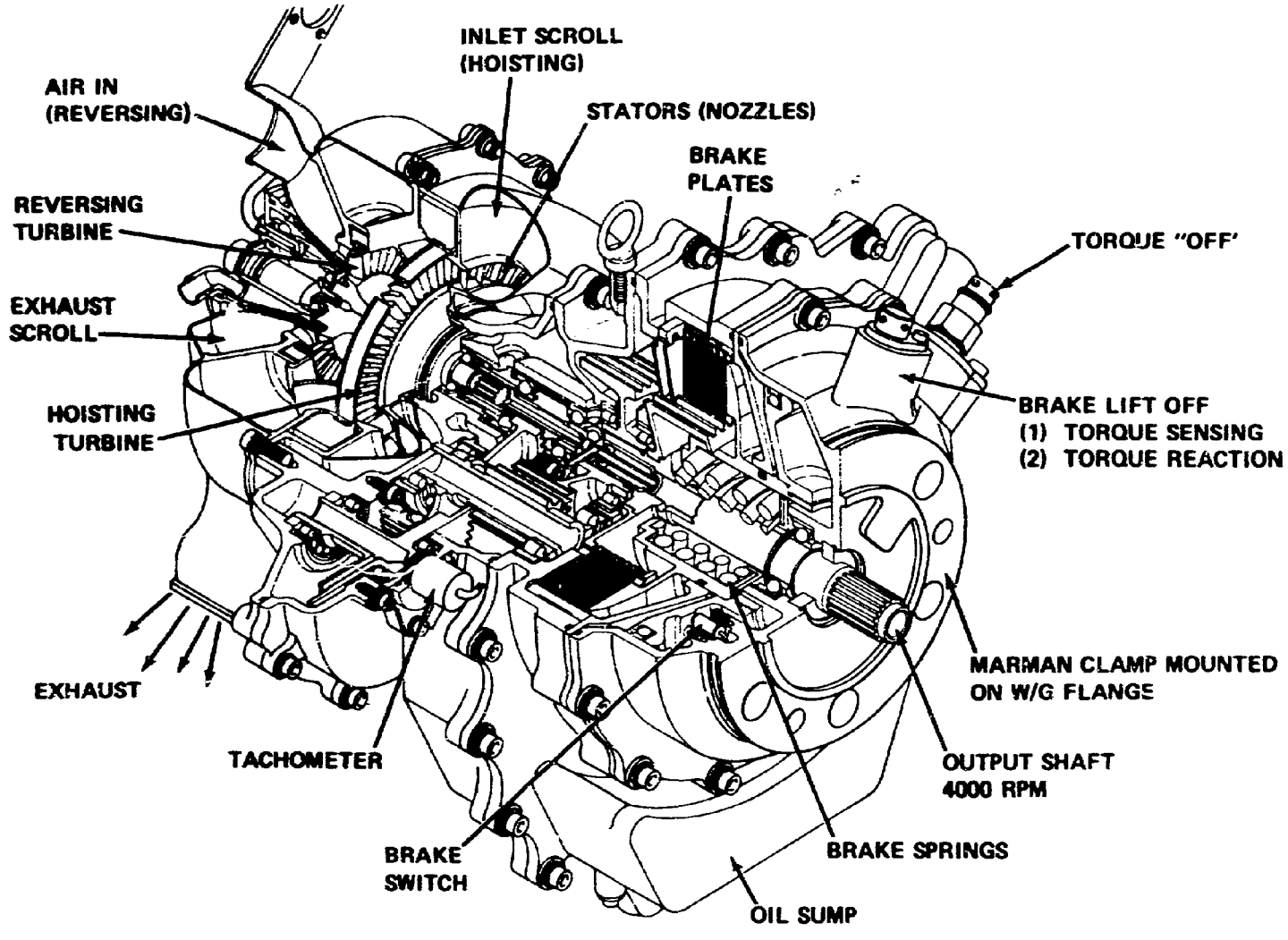


Figure 8. Hoist Drive.

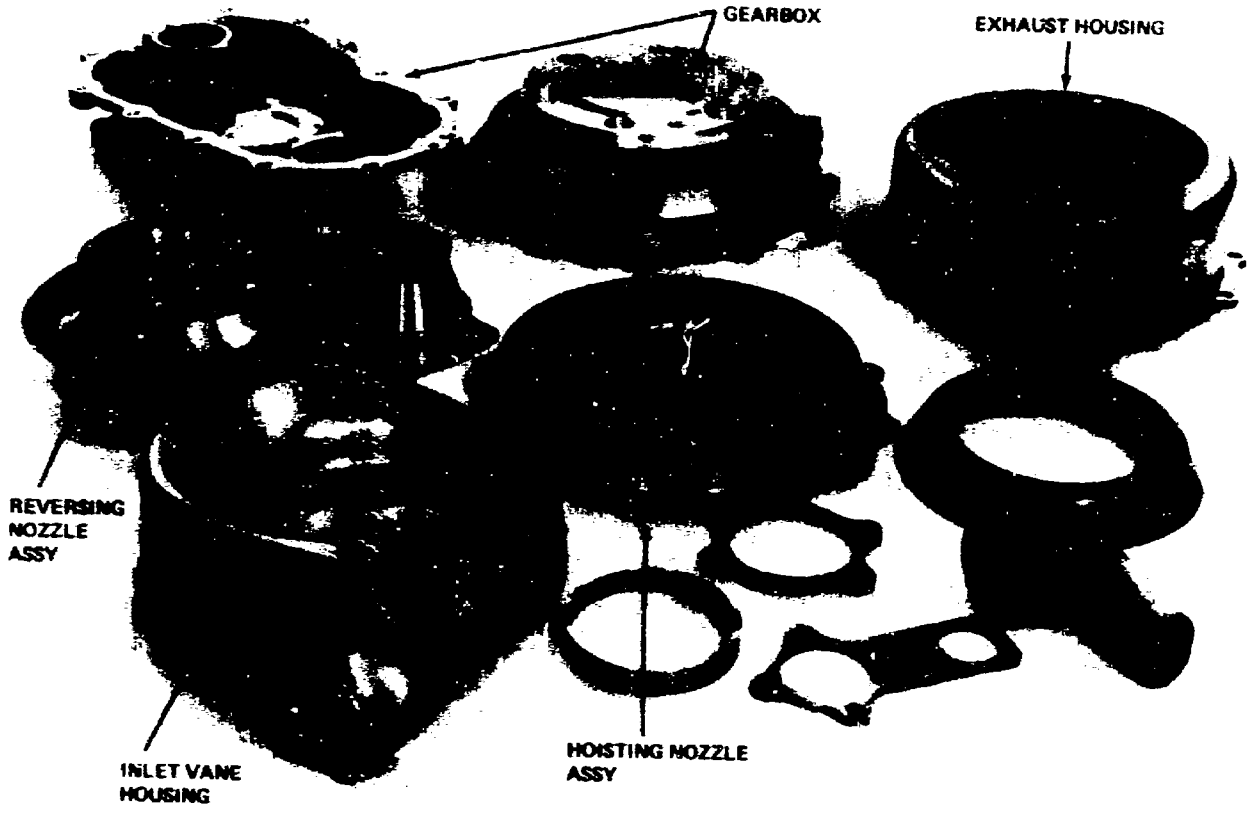


Figure 9. Hoist Drive Components.

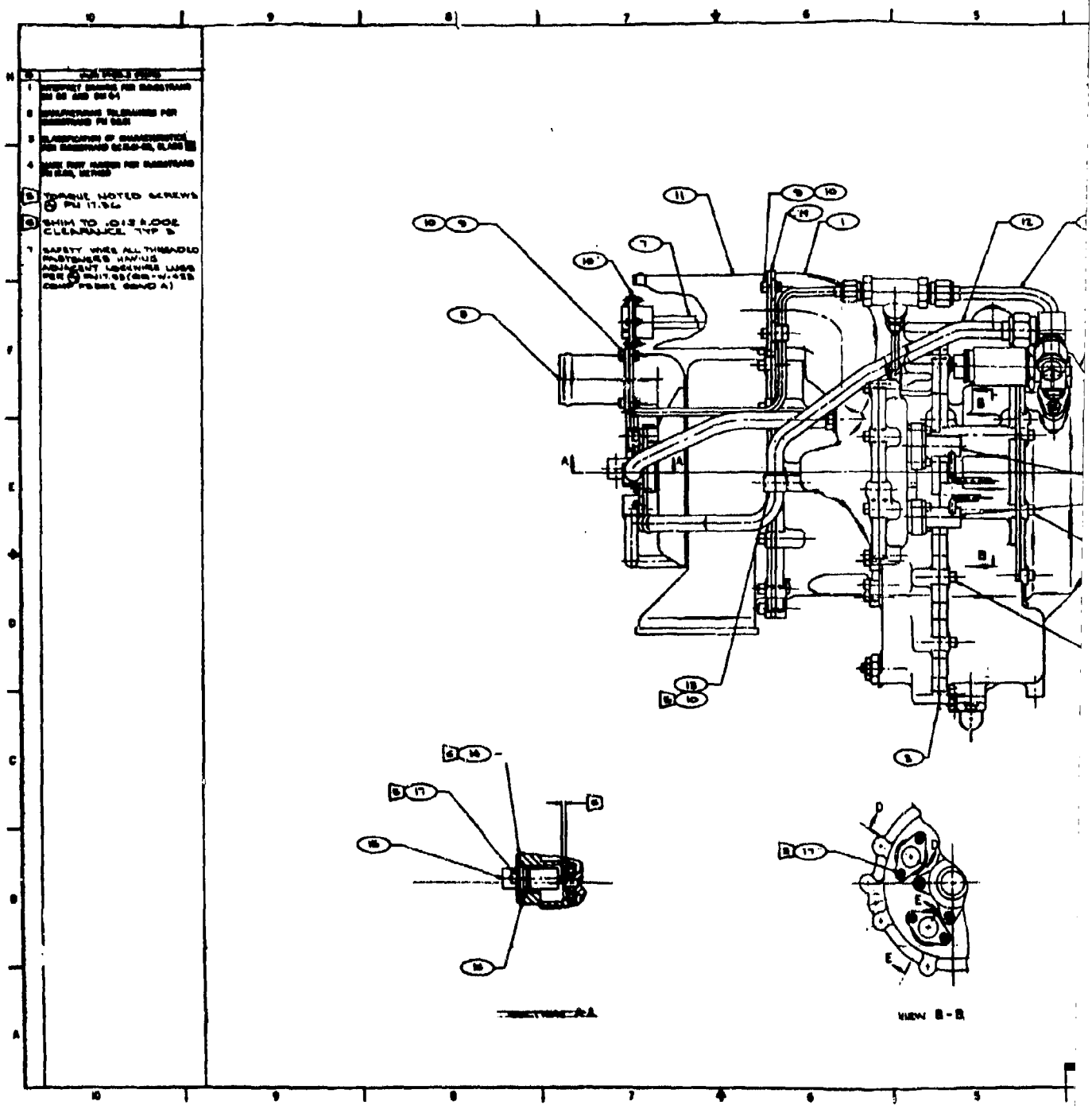
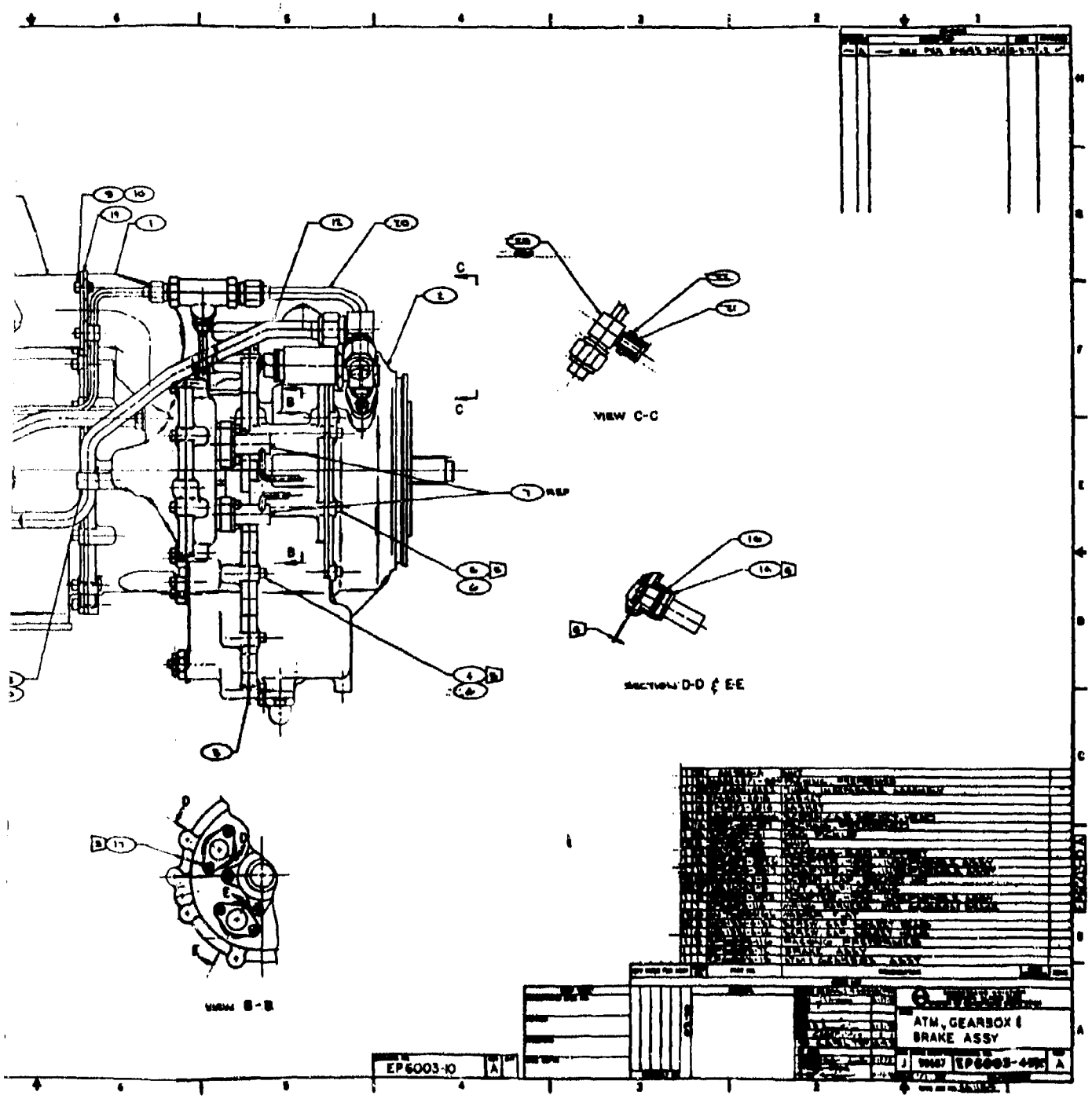


Figure 10. Hoist Drive Assembly.


VIEW C-C
SECTION D-D & E-E
VIEW B-B
ATM, GEARBOX & BRAKE ASSY
EP6003-10

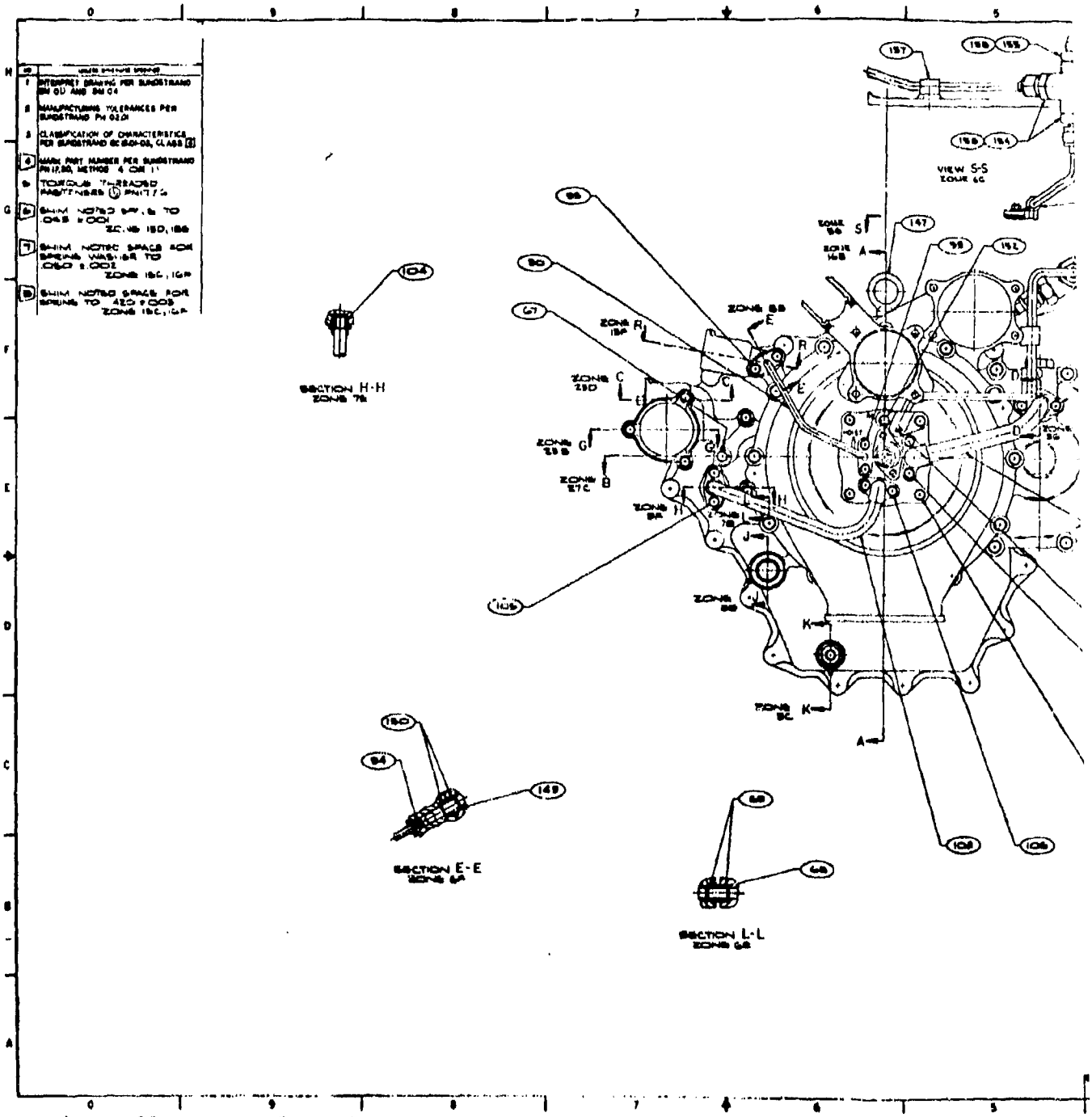
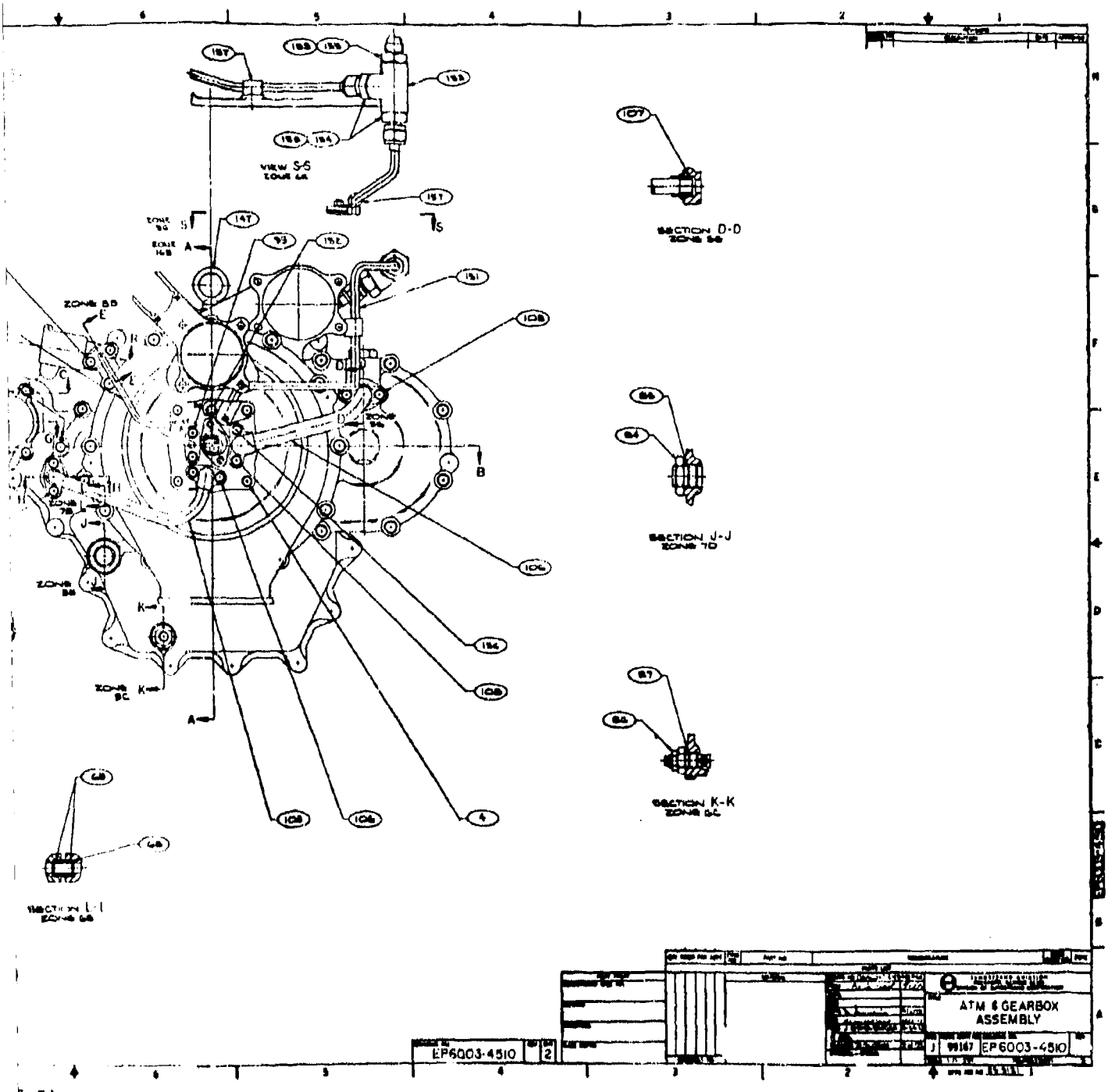


Figure 11. ATM and Gearbox Assembly (Sheet 1 of 5).


VIEW S-S
ZONE 6A
SECTION D-D
ZONE 5B
SECTION J-J
ZONE 7D
SECTION K-K
ZONE 8C
SECTION L-L
ZONE 6B
ZONE 8D
ZONE 7B
ZONE 8A
ZONE 8C
ATM & GEARBOX ASSEMBLY
EP6003-4510
99147
EP6003-4510

E 5).

2

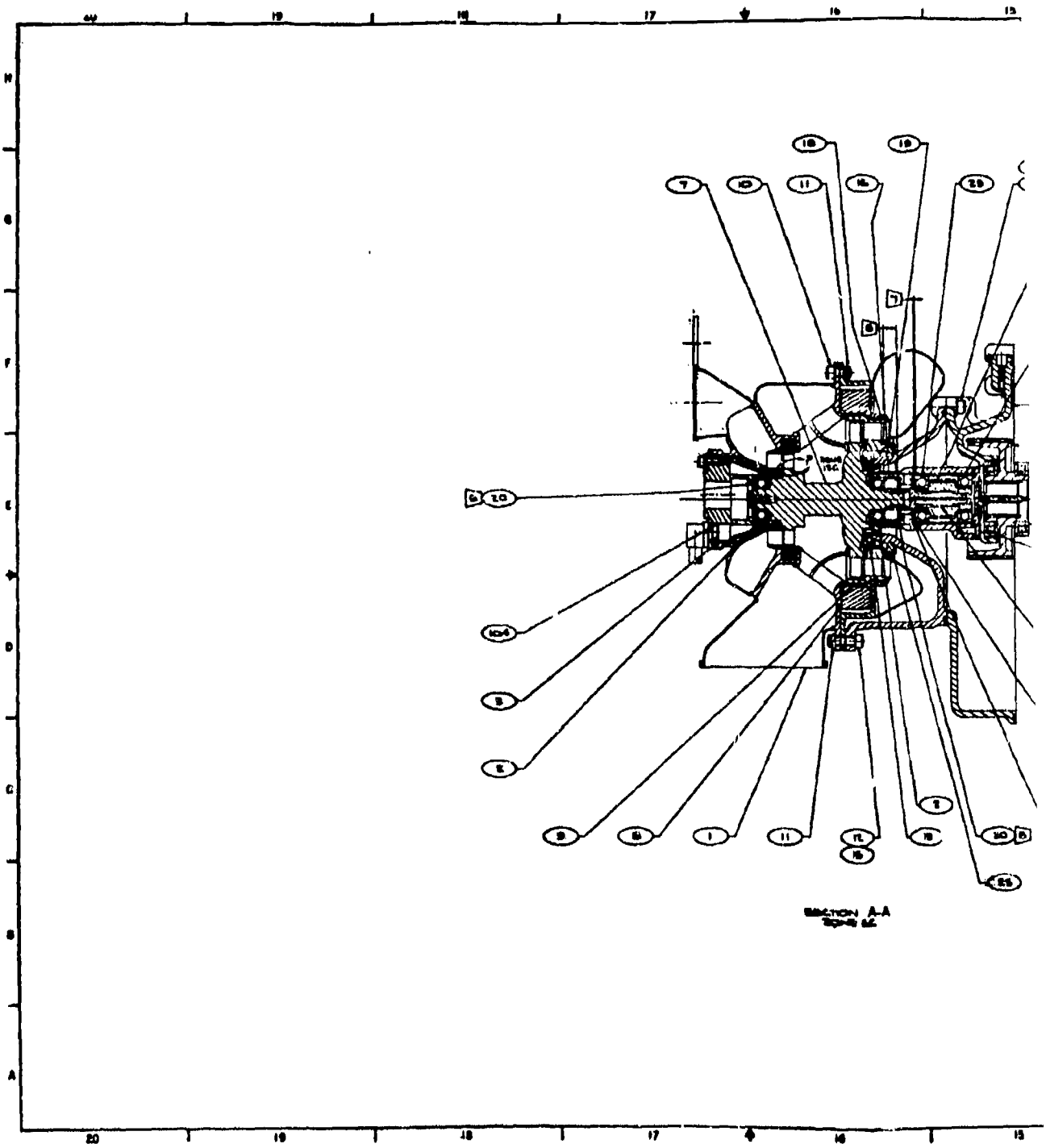
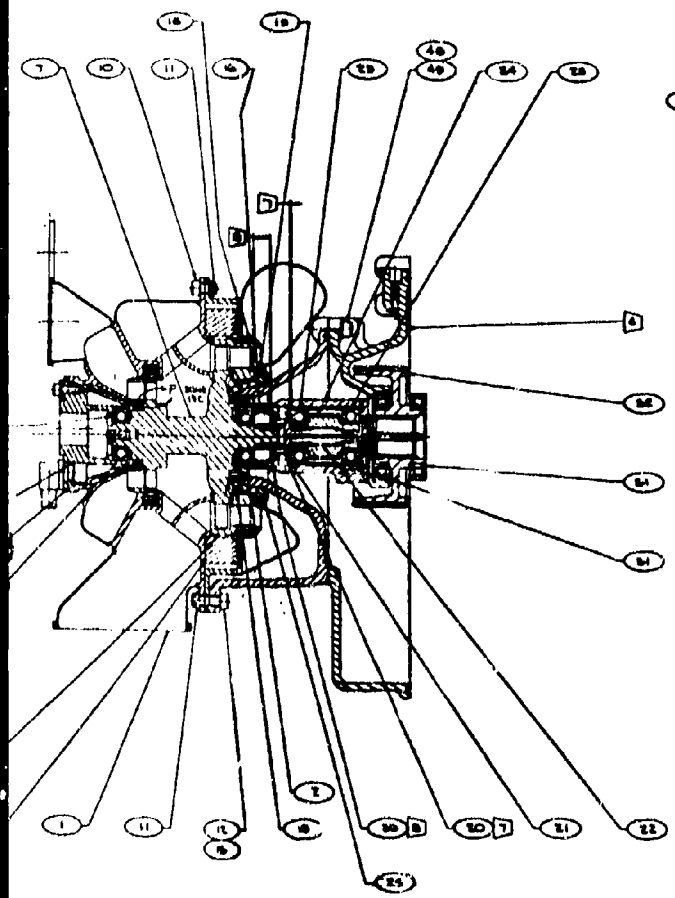
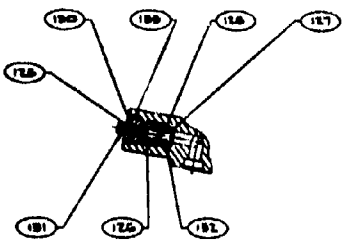


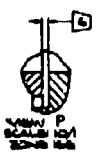
Figure 11. ATM and Gearbox Assembly
(Sheet 2 of 5).



SECTION A-A



SECTION R-R



EP6003-4510 | 3

J 19147 EP6003-4510

2

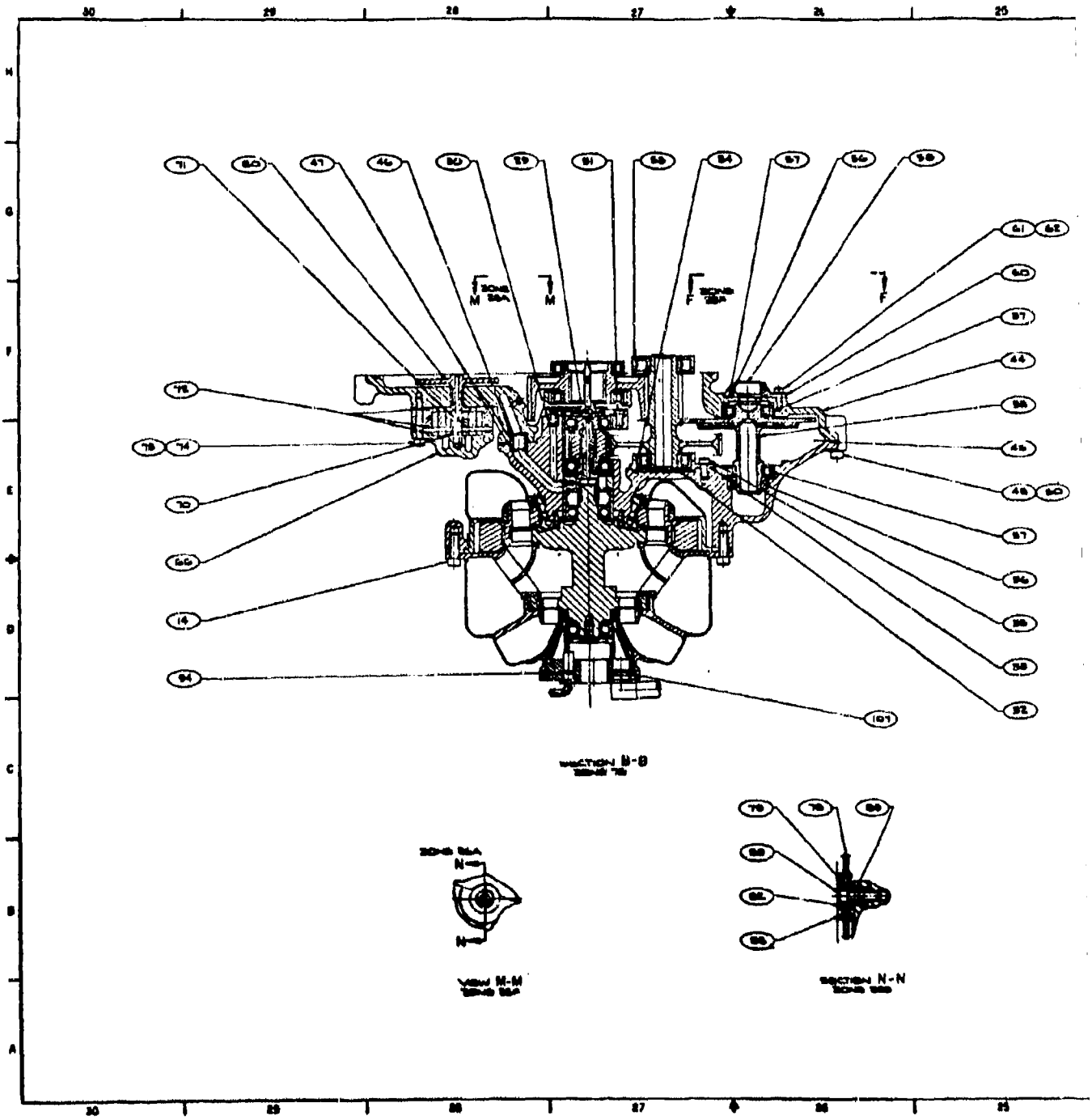
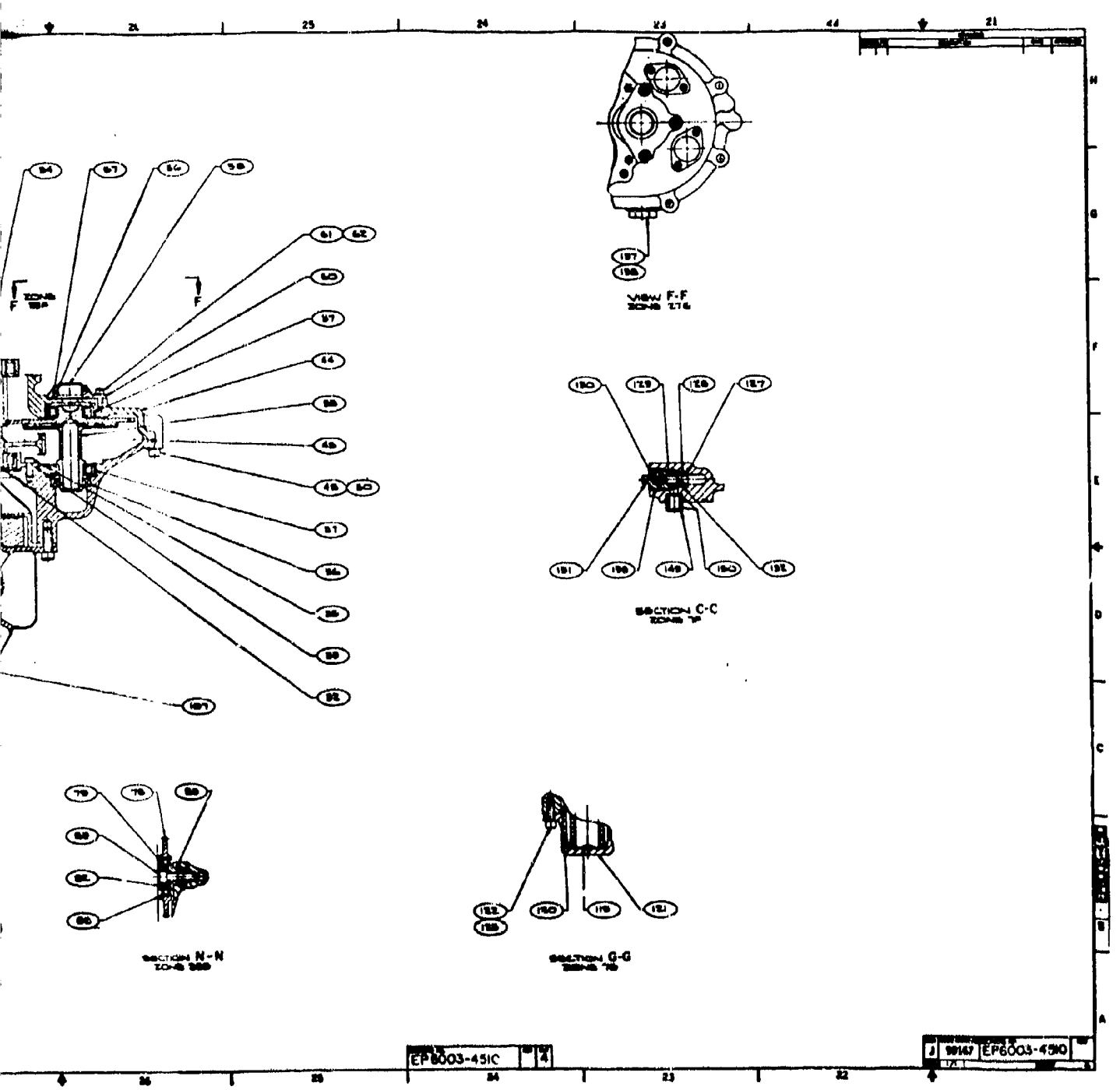


Figure 11. ATM and Gearbox Assembly
(Sheet 3 of 5).


VIEW F-F
SECTION C-C
SECTION N-N
SECTION G-G
EP8003-451C
EP8003-450

2

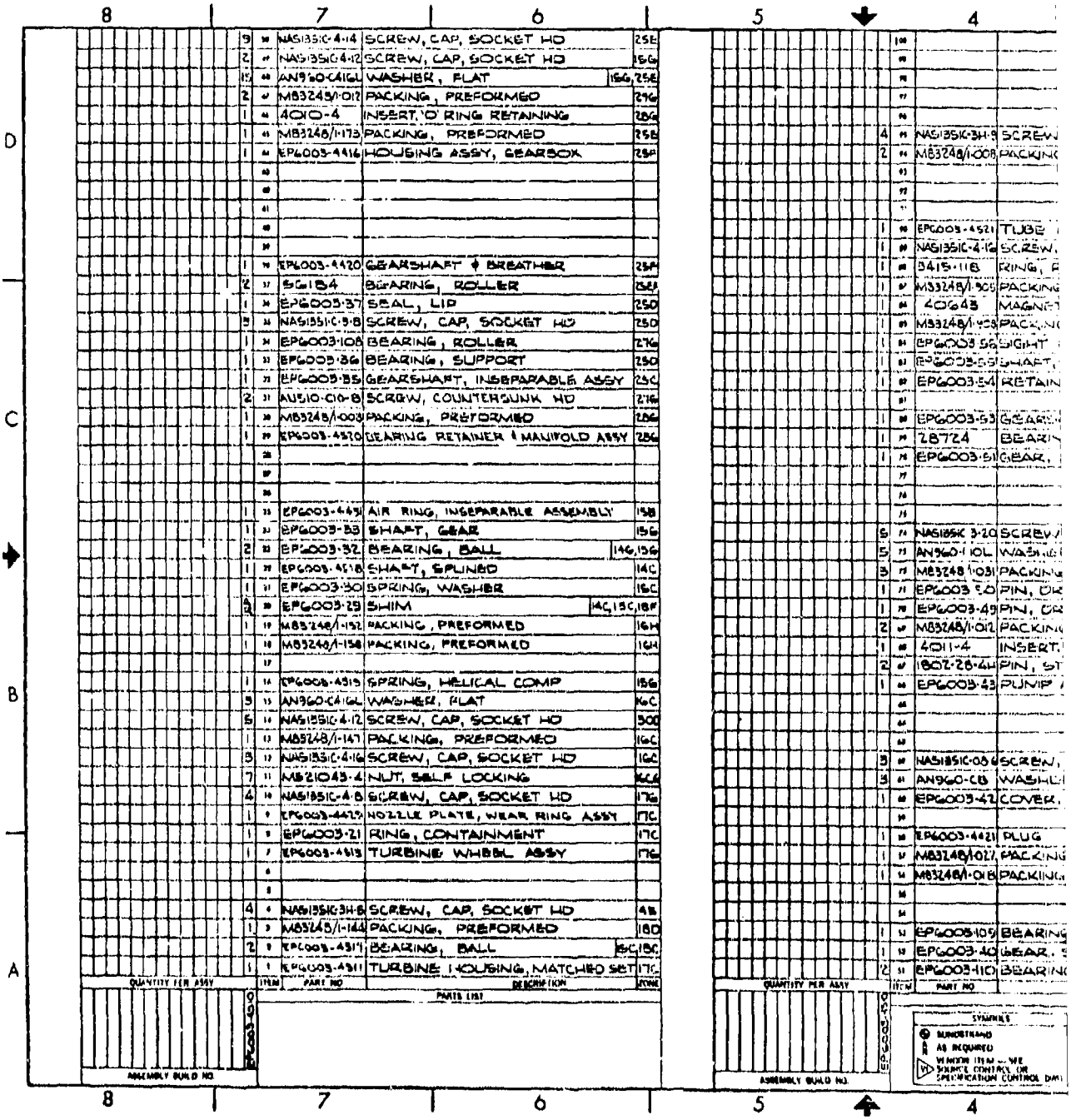


Figure 11. ATM and Gearbox Assembly (Sheet 4 of 5).

ITEM	QUAN	PART NO	DESCRIPTION	ZONE
4	AR	NAS 35K-3H-5	SCREW, CAP, SOCKET HD	5G
2	AR	M83248/1-009	PACKING, PREFORMED	BC
1	AR	EP6003-4521	TUBE ASSY, LUBE	BG
1	AR	NAS 35K-4-16	SCREW, CAP, SOCK HD	2GB
1	AR	5415-118	RING, RETAINING	2GB
1	AR	M83248/1-905	PACKING, PREFORMED	3D
1	AR	4026-43	MAGNETIC CHIP DETECTOR	3C
1	AR	M83248/1-903	PACKING, PREFORMED	3B
1	AR	EP6003-56	SIGHT GLASS	3B
1	AR	EP6003-55	SHAFT, FIXED	2CC
1	AR	EP6003-54	RETAINER, BEARING	2GB
1	AR	EP6003-53	GEARSHAFT, PUMP DRIVE	2BG
1	AR	28724	BEARING, BALL	2CC
1	AR	EP6003-51	GEAR, IDLER	2CC
5	AR	NAS 35K-3-20	SCREW, CAP, SOCKET HD	3DG
5	AR	AN960-C10L	WASHER, FLAT	3DG
3	AR	M83248/1-031	PACKING, PREFORMED	3DB
1	AR	EP6003-50	PIN, DRIVE	3DG
1	AR	EP6003-49	PIN, DRIVE	3DB
2	AR	M83248/1-012	PACKING, PREFORMED	6C
1	AR	4011-4	INSERT, RETAINING 'O' RING	6B
2	AR	1802-28-44	PIN, STRAIGHT, HEADLESS	BF
1	AR	EP6003-43	PUMP ASSY, MATCHED SET	3DC
3	AR	NAS 35K-0806	SCREW, CAP, SOCKET HD	2BG
3	AR	AN960-C8	WASHER, FLAT	2BG
1	AR	EP6003-42	COVER, TACHOMETER	2BG
1	AR	EP6003-4421	PLUG	2BH
1	AR	M83248/1-021	PACKING, PREFORMED	2GG
1	AR	M83248/1-018	PACKING, PREFORMED	2GB
1	AR	EP6308-109	BEARING, ROLLER	2BG
1	AR	EP6003-40	GEAR, SPUR	14B
2	AR	EP6003-110	BEARING, ROLLER	14G

QUANTITY PER ASSY

PARTS LIST

SYMBOLS
- SUNDSTRAND
- AS REQUIRED
- VENDOR ITEM — SEE SOURCE CONTROL OR SPECIFICATION CONTROL DWG

ASSEMBLY BUILD NO

ZONE	LTR	DESCRIPTION	DATE	APPROVED

CONTRACT NO (SEE SHT 1)
PROJ ENGR
QUAL
MFG
MET. ENGR
CHECKER
DRAWN J. ECHELBARGER
APPROVAL & RELEASE

SUNDSTRAND AVIATION
ROCKFORD, ILLINOIS
DIVISION OF SUNDSTRAND CORPORATION

TITLE
ATM & GEARBOX ASSEMBLY

SIZE	CODE IDENT	DWG NO.	REV
E	99167	EP6003-4510	

SCALE — WT ACT CALC LB SHEET 5

2

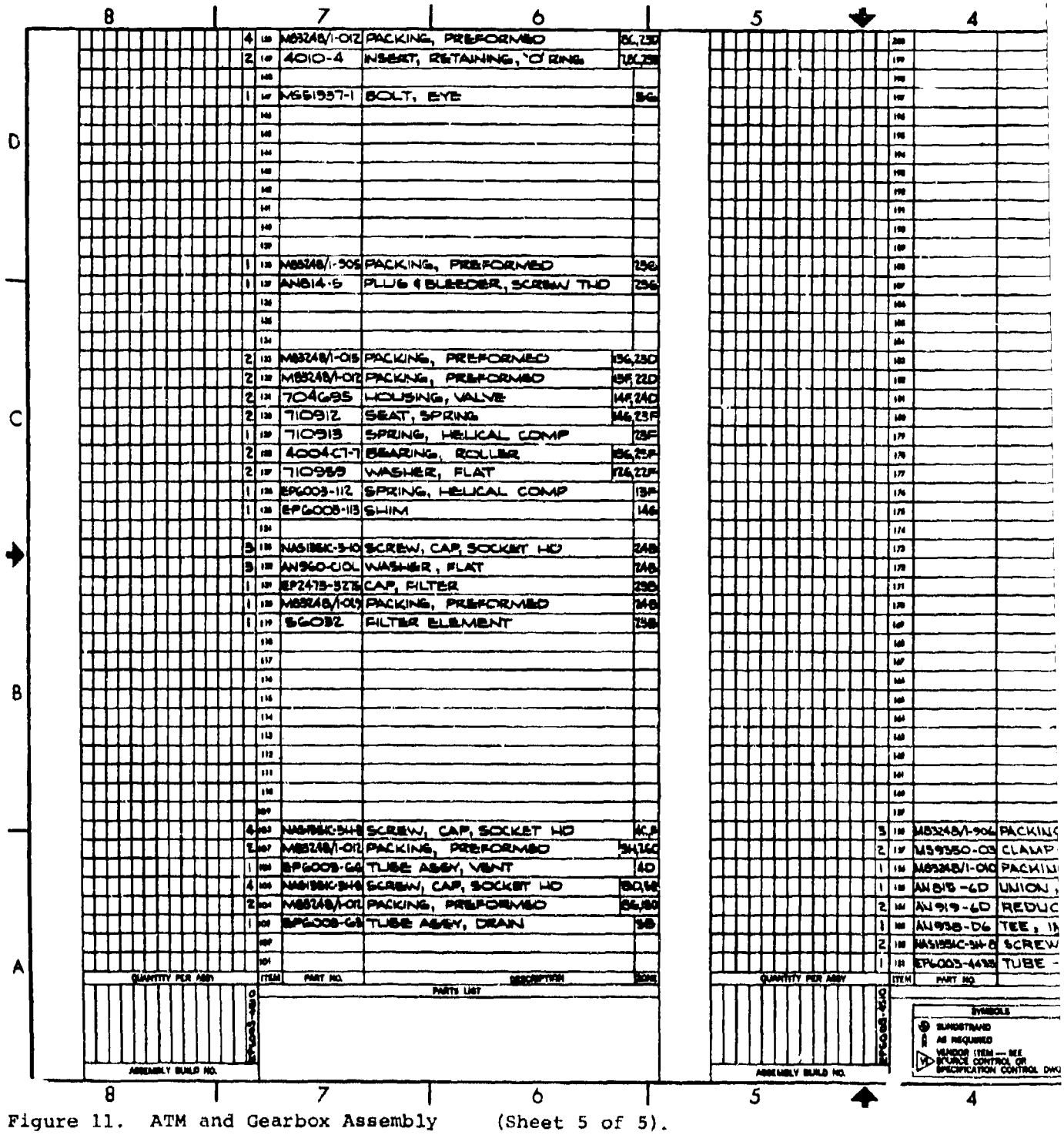


Figure 11. ATM and Gearbox Assembly (Sheet 5 of 5).

ITEM	PART NO.	DESCRIPTION	FDNS
9	MS9348/1-904	PACKING, PREFORMED	5H
2	MS9350-03	CLAMP, TUBE	4A AN
1	MS9348/1-040	PACKING, PREFORMED	4D
1	AN815-6D	UNION, FLARED TUBE	5H
2	AN919-6D	REDUCER - TUBE	5H
1	AN938-D6	TEE, INTERNAL SCREW THD	4H
2	NAS1351C-3H-8	SCREW, CAP, SOC HD	8G
1	EP6003-4498	TUBE - IUSEP ASSY	4P

PARTS LIST

QUANTITY PER ASSY

EP6003-4510

ASSEMBLY BUILD NO.

SYMBOLS

SUNDSTRAND AS REQUIRED

VENDOR ITEM — SEE SOURCE CONTROL OR SPECIFICATION CONTROL DWG

REVISIONS

ZONE	LTR	DESCRIPTION	DATE	APPROVED

CONTRACT NO. (SEE SHT 1)

PROJ ENGR

QUAL

MFR

MET. ENGR

CHECKER

DRAWN J. EKVALL

APPROVAL & RELEASE

APPROVAL—SPECIAL

SUNDSTRAND AVIATION
ROCKFORD, ILLINOIS
DIVISION OF SUNDSTRAND CORPORATION

TITLE

ATM & GEARBOX ASSEMBLY

SIZE	CODE IDENT	DWG NO.	REV
E	99167	EP6003-4510	

SCALE — WT ACT. CALC LB SHEET

2

ITEM	PART NO.	DESCRIPTION	ZONE
5	MS3248/1-904	PACKING, PREFORMED	5H
2	MS9550-09	CLAMP, TUBE	4G 4H
1	MS3248/1-010	PACKING, PREFORMED	4D
1	AN815-6D	UNION, FLARED TUBE	5H
2	AU919-6D	REDUCER - TUBE.	5H
1	AU938-D6	TEE, INTERNAL SCREW THD	4H
2	MS51956C-9H-8	SCREW, CAP, SOC HD	5G
1	EP6003-4498	TUBE - INLET ASSY	4F

QUANTITY PER ASSY

ASSEMBLY BUILD NO.

EP6003-4510

SYMBOLS
- SUNDSTRAND
- AS REQUIRED
- VENDOR ITEM — SEE SOURCE CONTROL OR SPECIFICATION CONTROL DWG

REVISIONS

ZONE	LTR	DESCRIPTION	DATE	APPROVED

SUNDSTRAND AVIATION
ROCKFORD, ILLINOIS
DIVISION OF SUNDSTRAND CORPORATION

TITLE
ATM & GEARBOX ASSEMBLY

SIZE	CODE IDENT	DWG NO.	REV
E	99167	EP6003-4510	

SCALE — WT ACT. CALC LB SHEET

2

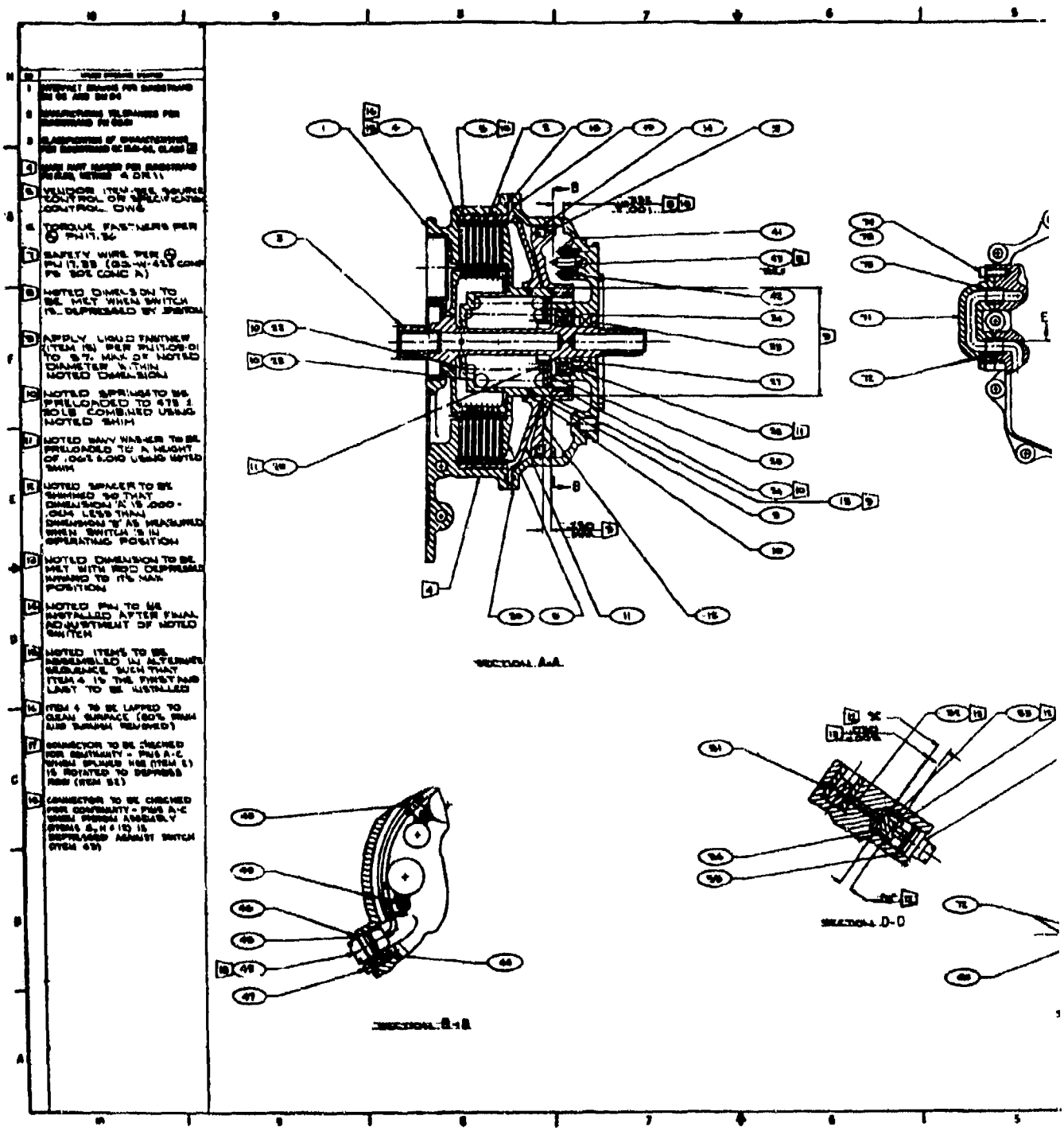
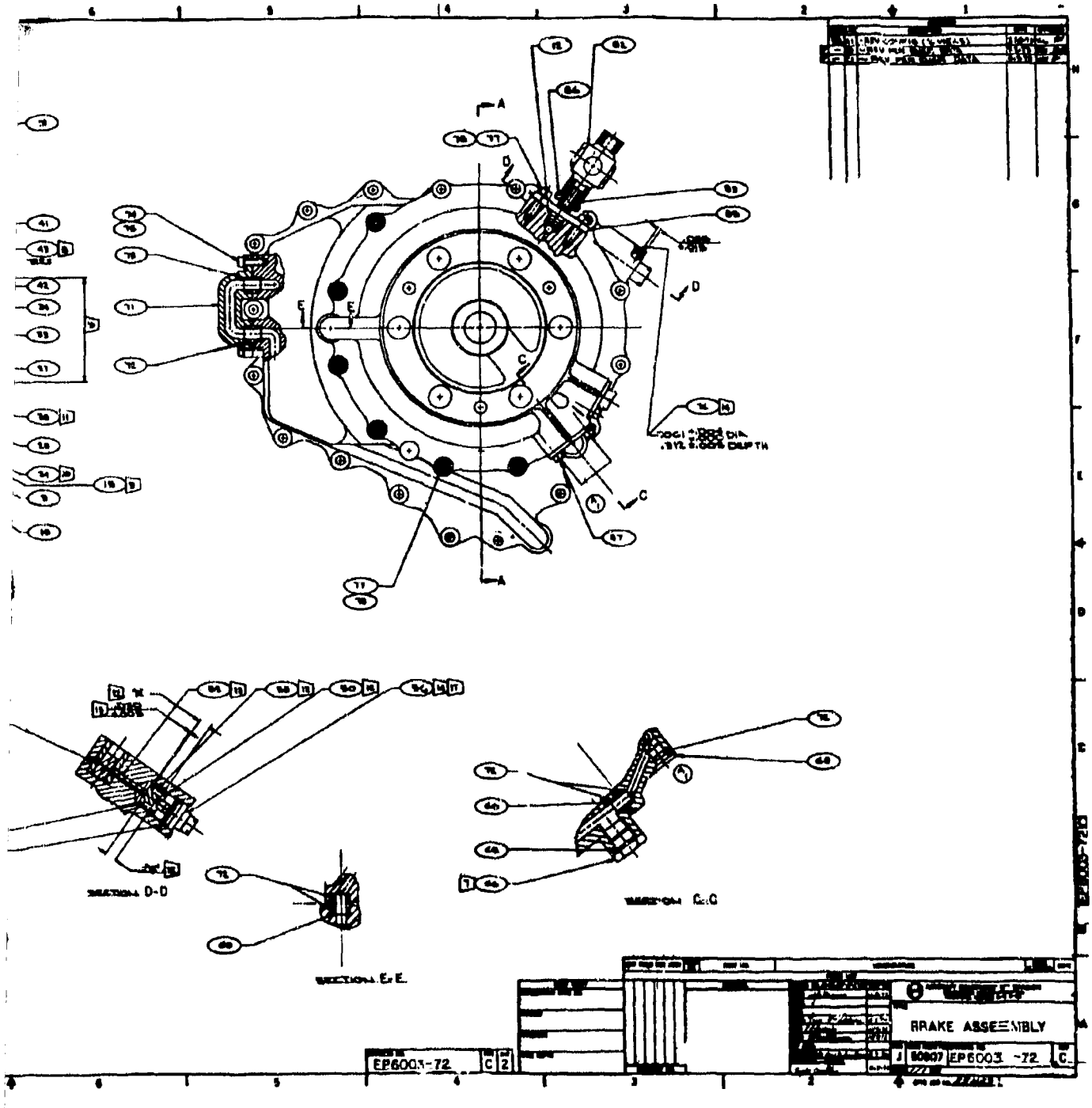


Figure 12. Brake Assembly (Sheet 1 of 2).


SECTION D-D
SECTION E-E
SECTION C-C
BRAKE ASSEMBLY
EP6003-72
EP6003 -72

2

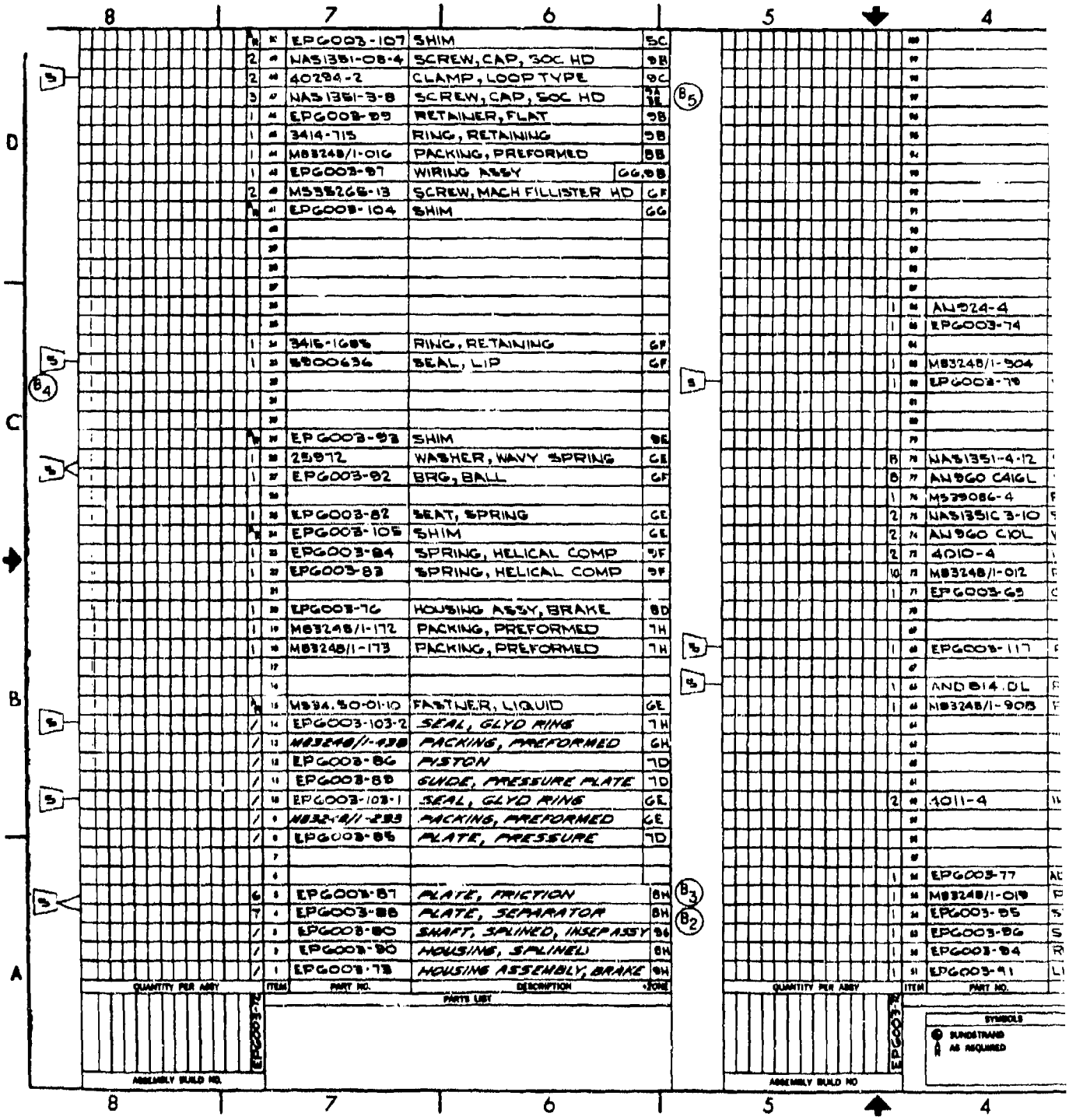
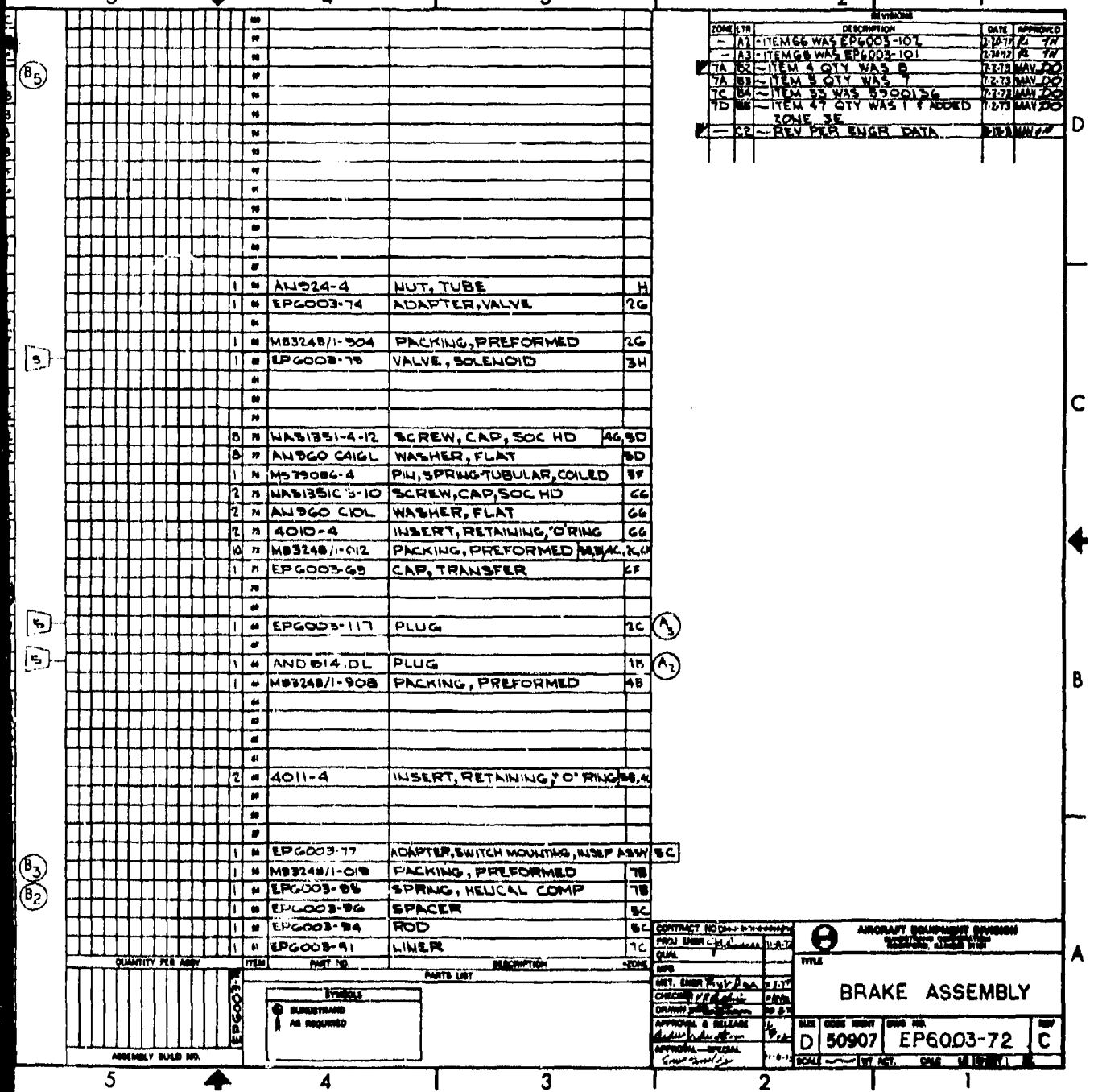


Figure 12. Brake Assembly (Sheet 2 of 2).



ITEM	QTY	PART NO	DESCRIPTION	ZONE
	1	AN924-4	NUT, TUBE	H
	1	EP6003-74	ADAPTER, VALVE	2G
	1	MS3248/1-304	PACKING, PREFORMED	2G
5	1	EP6003-79	VALVE, SOLENOID	3H
	8	NAS1351-4-12	SCREW, CAP, SOC HD	4G,5D
	8	AN960 C416L	WASHER, FLAT	5D
	1	MS79086-4	PIN, SPRING-TUBULAR, COILED	5F
	2	NAS1351C 3-10	SCREW, CAP, SOC HD	6G
	2	AN960 C10L	WASHER, FLAT	6G
	2	4010-4	INSERT, RETAINING, O'RING	6G
	10	MS3248/1-012	PACKING, PREFORMED	5B,4C,4H
	1	EP6003-69	CAP, TRANSFER	6F
5	1	EP6003-117	PLUG	2C (A3)
5	1	AND614.DL	PLUG	1B (A2)
	1	MS3248/1-908	PACKING, PREFORMED	4B
	2	4011-4	INSERT, RETAINING, O' RING	5B,4G
	1	EP6003-77	ADAPTER, SWITCH MOUNTING, W/SEP ASSY	5C
B3	1	MS3248/1-019	PACKING, PREFORMED	7B
B2	1	EP6003-86	SPRING, HELICAL COMP	7B
	1	EP6003-96	SPACER	6C
	1	EP6003-94	ROD	6C
	1	EP6003-91	LINER	7C

PARTS LIST

QUANTITY PER ASSY

ASSEMBLY BUILD NO. EP6003-

SYMBOLS
- SUBSTRAND AS REQUIRED

REVISIONS

ZONE	LTR	DESCRIPTION	DATE	APPROVED
—	A1	- ITEM 66 WAS EP6003-101	7-24-72	[illegible]
—	A3	- ITEM 68 WAS EP6003-101	7-24-72	[illegible]
7A	B2	— ITEM 4 QTY WAS 8	7-2-73	MAV
7A	B3	— ITEM 5 QTY WAS 4	7-2-73	MAV
7C	B4	— ITEM 33 WAS 5900136	7-2-73	MAV
7D	B5	— ITEM 47 QTY WAS 1 # ADDED ZONE 3E	7-2-73	MAV
—	C2	— REV PER ENGR DATA.	8-15-73	MAV

AIRCRAFT EQUIPMENT DIVISION

TITLE: BRAKE ASSEMBLY

SIZE	CODE IDENT	DWG NO	REV
D	50907	EP6003-72	C

SCALE — WT LBS — SHT 1 OF 1

2

4. Brake shaft - 9310

5. Internal brake parts - 6061 T6 aluminum (pistons, brake seal plate, brake ram)

6. Inlet guide vanes - case 17-4

7. Bearing liners - 4340

8. Containment ring - Inconel 718

9. Turbine diffuser vanes - cast 17-4 (entire assembly is cast)

10. Gearing - 9310 carburized

11. Turbine wheels and shaft - Rene´ 95 (discussed below).

In the reversing (or cable lowering) mode of operation, the larger 4.66-inch-diameter hoisting turbine is rotated in the reverse direction at a high rate of speed by the smaller 2.80-inch-diameter reversing turbine. The windage or churning loss that is produced by the hoisting turbine creates a considerable amount of heat which is partially absorbed by the hoisting turbine wheel, resulting in a significant increase in the turbine wheel hub and blade temperature. Extrapolation of initial test results, and further turbine design analysis gave a predicted maximum turbine wheel temperature of approximately 800°F; this was later substantiated in actual prototype testing.

Because of this predicted high temperature environment, a material investigation was conducted to select the optimum material. Among those materials evaluated were:

1. Sundstrand processed Waspalloy (Sundstrand MS14.09-01)

2. Carpenter 455 precipitation hardening stainless steel

3. Inconel 718 (AMS 5662)

4. Rene´ 41

5. Rene´ 95.

The maximum (or runaway) turbine speed in the reverse direction is a critical (800°F) stress situation for the hoisting turbine wheel. The turbine wheel temperature reaches 800°F during dynamic braking condition as

well. Maximum strength at this 800°F anticipated maximum temperature was the primary selection criteria during the material analyses. Hub burst strength was designed with a considerable safety margin at the maximum speed/temperature condition.

René 95 high temperature nickel alloy was chosen for its superior high temperature tensile strength properties. A powdered metal version of the alloy was chosen rather than the cast raw material because Rene' 95 in the wrought or cast condition did not forge well during the early manufacturing process investigations. Forging was deemed a necessary processing requirement to both reduce waste and improve directional strength in the critical turbine wheel hub area. Powdered metal (P/M) Rene' 95 alloy performed well in the manufacturing process in which the P/M blank size, which started at a 4.5-inch-diameter slug, was partially extruded to a 3.0-inch-diameter for the reversing turbine. The 4.5-inch section was then upset to a 5.25-inch diameter for the hoisting turbine.

Turbine Design. The turbine and nozzle blading configurations were designed, with the aid of Sundstrand computer programs, to produce the required stall torque and to optimize efficiency at design point.

Due to the relatively high operating speeds of the ATM, particular attention was devoted to establishing a configuration which would operate subcritical at maximum operating speed. All calculations for the hoisting turbine wheel and nozzle designs were based on 4,000 ft -95°F ambient conditions.

The design point of the turbine was dictated by the stall torque requirement at the output shaft. Additional design conditions consisted of:

1. Hoisting 60% of a 28-ton load at 60 ft/min (80 ft-lb at 4,000 rpm),
2. Hoisting an empty hook at 120 ft/min (8,000 rpm),
3. Paying out an empty hook at 120 ft/min (8,000 rpm).

The stall torque generation requirements for the hoisting wheel were based on accommodating 60% of a 28-ton load at 2.5g, which corresponds to torque of 238 ft-lb at the ATM output shaft.

The reversing turbine design power was based on design

support test data and projected estimates of the windage losses of the hoisting wheel. These estimates were based on a 4-inch-diameter wheel run at 40,000 rpm and corrected for gas density, speed, pitch diameter and the ratio of blade height to pitch diameter.

The bearing on the reversing turbine end of the turbine shaft is sealed off with a labyrinth seal. As originally designed, this seal permitted a significant amount of oil loss during normal operations. This became apparent in the early phases of the design development testing. This leakage problem was solved by machining the labyrinth grooves from the rotating member (turbine) and placing them in a bushing which was pressed into the housing. The diametrical clearance was reduced to between .003 inch and .004 inch and the labyrinth grooves were pressurized with air.

Subsequent test showed that the leakage problem has been resolved. The pressurized labyrinth grooves were incorporated in the design.

Preceding the design development tests, the initial turbine wheel design for the ATM was configured for the following:

1. Hoisting Turbine

No. of stages - 1
Arc of admission - 100%
Rotational speed (60 ft/min hoisting) 43,600 rpm
Power output - 94 hp
Inlet total pressure - 51.8 psia
Inlet total temperature - 874°R
Exhaust static pressure - 12.7 psia
Overall total/static pressure ratio - 4.08
Mass flow - 1.21 lb/sec
Velocity ratio - .415
Specific speed - 66.5
Specific diameter - 1.07
Turbine efficiency - 79%
Stall torque at turbine shaft - 19.1 ft-lb
Turbine pitch diameter - 4.0 in
Blade height at L.E. - .582 in
Blade height at T.E. - .722 in
No. of rotor blades - 66
No. of nozzle guide vanes - 27
Nozzle throat area (total) - 1.357sq-in
Nozzle area ratio - 1.185
Nozzle angle - 14.3°
Rotor inlet blade angle - 28.4°
Rotor exit blade angle - 24.8°

Rotor space/axial chord ratio - .544
Rotor axial chord - .35 in
Rotor maximum thickness/axial chord - 33%
Rotor aspect ratio - 1.86

The hoisting turbine was designed as a single-stage, full admission, predominately impulse type blades with cascade nozzle guide vanes. Five percent reaction was incorporated in order to reduce adverse pressure gradients in the rotor blade passage and the endwall surfaces. The 5 percent reaction was thus intended to improve turbine efficiency.

2. Reversing Turbine

No. of stages - 1
Arc of admission - 00%
Rotational speed - 87,000 rpm
Power output - 31 hp
Inlet total pressure - 51.8 psia
Inlet total temperature - 874°R
Exhaust static pressure - 12.7 psia
Overall total/static pressure ratio - 4.08
Mass flow - .418 lb/sec
Velocity ratio - .456
Specific speed - 69.4
Specific diameter - .98
Turbine efficiency - 75%
Turbine pitch diameter - 2.194 in
Blade height at L.E. - .386 in
Blade height at T.E. - .490 in
No. of blades - 53
No. of nozzle guide vanes - 21
Nozzle throat area - 0.572 sq-in
Nozzle area ratio - 1.185
Nozzle angle - 14.9°
Rotor inlet blade angle - 33.2°
Rotor exit blade angle - 28.8°
Rotor space/axial chord ratio - .522
Rotor axial chord - .25 in
Rotor maximum thickness/axial chord - 33%
Rotor aspect ratio - 1.86

The reversing turbine design was identical to that of the hoisting turbine design philosophy. Based on design support test data, the reversing turbine output power was to overcome the hoisting wheel windage losses estimated to be 31 hp at 120 fpm cable speed, when based on design day conditions of 4,000 ft -95°F.

The above turbine wheel configuration was tested under "sea level" conditions.

This test is reported in Volume III of this report. The test results indicated that the design was inadequate for the following reasons:

1. The hoisting turbine power was below design due to lower than anticipated airflows.

2. The reversing turbine power was below design.

3. The windage losses of the hoisting turbine were higher than expected.

4. The stall torque was inadequate.

5. The turbine efficiency was low.

As a result of these tests, effort was directed toward the redesign of the dynamic components of the ATM.

Several methods of "piecemeal" fixes were evaluated. These included reduction of clearances, development of windage control devices to limit the losses, and attempts to enlarge and clean up the nozzle passages. Minor improvements were achieved; the basic problem, however, was the hoisting turbine wheel, which was designed for limited reaction (rather than pure impulse) and with tapered blades. The prime reason for this design was to meet the efficiency objective. However, this design resulted in windage losses which were far greater than those experienced during the design support test phase with a pure impulse wheel. Therefore, it was decided to redesign both the hoisting and reversing wheels, redesign both nozzle assemblies, and modify the housing to accept a separate nozzle ring rather than one that was part of the casting. This integral design resulted in poor quality and control of the flow passage surfaces.

Turbine consultants were engaged for the purpose of resolving the payout speed and stall torque problem. Detailed turbine configuration trade-offs were conducted by Sundstrand and consultants to determine the optimum redesign configuration. It was decided that impulse blading would be incorporated in both wheels, and nozzles would be redesigned to provide higher airflow and efficiency.

Hoisting Turbine. Performance at sea level conditions indicated a stall torque of 205 ft-lb as compared with the 236 ft-lb design estimate. This was partially caused by the low airflow of 1.28 lb/sec vs. the 1.46 lb/sec design value. The reduced airflow is attributa-

ble to the low nozzle flow coefficient of .86 as compared with .95 used in the design. It is believed that the relatively long narrow nozzle flow passages cause boundary layer buildup and reduced flow coefficients.

A turbine wheel incorporating a small amount of reaction was used in the initial design for efficiency reasons; however, this provides a turbine torque-speed curve somewhat flatter than a pure impulse turbine characteristic, thus tending to reduce stall torque and increase maximum reel-in speed. Generally, an impulse turbine will produce superior stall torque for the same airflow. In order to achieve the stall torque objective, it was decided to provide a redesigned turbine having the following features:

1. A reduced number of relatively short nozzle passages.
2. Increased nozzle throat area for increased airflow.
3. An impulse turbine with symmetrical blading for improved stall torque characteristics.

Hoisting Turbine Windage Losses. A motoring test of the hoisting turbine, driven in the reversing direction, revealed that the windage and friction was 69 hp rather than 37 hp as used in the design. Of the 69 hp, only 8 hp was friction.

A detailed analysis of the windage problem was conducted by Sundstrand, and it was concluded that possibly the reaction blading with the flared axial height passage might be contributing. Also, it was evident that blade height was a key factor. From references it was determined that turbine windage is a function of blade height to the 1.50 to 2.0 power. From the original design support test conducted with two wheels of identical pitch diameter of 4.0 inches, it was determined that the windage horsepower is affected by the blade height (L) and varies as:

$$\text{Windage hp} = L^{1.8}$$

A reduced blade height hoisting turbine, therefore, seemed very desirable from the standpoint of windage reduction.

Hoisting Turbine Design Analysis The objectives of the hoisting turbine redesign were:

1. To increase the stall torque to meet the original design objectives,

2. To reduce the reversing windage to permit the reversing turbine to meet payout speed.

These objectives were to be achieved by designing an efficient enlarged nozzle operating with an impulse turbine having reduced blade height. It was necessary to increase the airflow to fully provide the stall torque and at the same time reduce the turbine blade annulus to reduce the windage hp in the reversing direction.

The initial design of the nozzle and turbine used relatively small nozzle and turbine angles, for example, 14° for the nozzle exit, 28.4° at the turbine inlet, and 24.8° at the turbine exit. This was done for the purpose of maximizing efficiency. The small angles result in greater turbine blade height, however, with corresponding greater windage. In general, greater torque per unit airflow is obtained with smaller angles due to the increased velocity turning in the wheel. Due to the great importance of turbine windage, it was decided to increase the angles, permitting larger airflow with reduced blade height.

A number of designs covering nozzle angle range of 16° to 24° were analyzed. Generally, the higher angles provide less torque, lower efficiency, and reduced reel-in speed. Assuming a velocity coefficient of .95 in the nozzle and .90 across the wheel with 1.50 lb/sec flow, the following stall torque estimates are obtained for three nozzle angles, with turbine angles matched for 0° incidence at rated speed.

*Nozzle Angle	Turbine Angle	Stall Torque
14°	25°	251.
18°	31°	245.
22°	36.9°	234.

*Includes 5 percent allowance for leakage and miscellaneous losses.

At rated speed of 4,000 rpm the comparison of torque and efficiency is as follows:

Nozzle Angle	Torque	Efficiency*
14°	144.	.735
18°	138.	.705
22°	130.	.665

*Includes 5 allowance for leakage and other losses.

The higher nozzle and turbine angles will tend to reduce the maximum reel-in speed. Some margin currently exists, however, at that condition. The above tabulated trade-offs were studied for a number of designs, and the 18° nozzle was tentatively selected.

A specific hoisting turbine design was then determined. It consisted of the following:

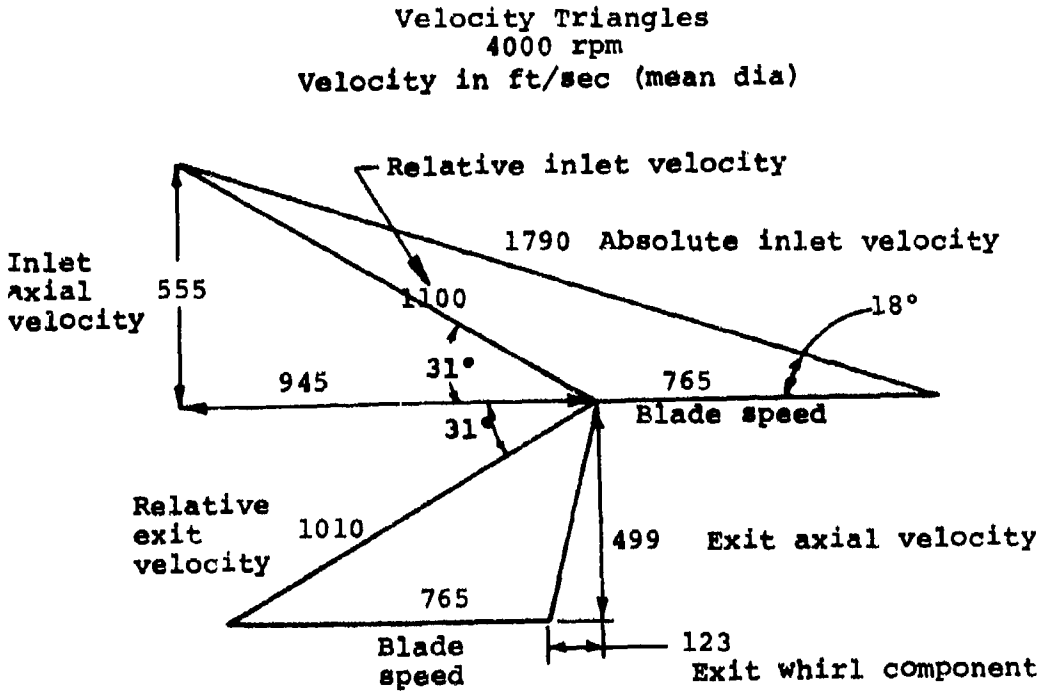
Nozzle angle	18°
Turbine angle	31°
Expansion in nozzle to 20 psia at exit	
Further expansion in wheel to 14.6 psia	
Nozzle height	.52 in
Turbine blade height	.60 in
Nozzle area	1.52 sq in
Estimated efficiency	72%
Estimated stall torque	239 ft-lb
Turbine thrust at maximum reel-in speed	145 lb
Estimated turbine windage	54.8 hp
Turbine blade root stresses 80,000 psi at	8,000 rpm
Nozzle velocity coefficient	.96
Nozzle flow coefficient	.96
Turbine wheel velocity coefficient	.92
Allow 10% for all additional losses (leakage, windage, etc.)	
Airflow*	1.50 lb/sec
Altitude	Sea level

(*Nozzle may be reworked to 1.60 lb/sec flow at sea level.)

The windage losses in the turbine when operating in reverse were analyzed by Sundstrand and by a consulting firm who searched all available information relative to reverse operating turbines. Two methods were used in arriving at the windage hp values. Both methods checked closely at approximately 50 hp at 7,500 rpm. Sundstrand used blade length to the 1.8 power in calculating windage. This was checked by the consultant using other references.

Turbine blade stresses were calculated at 80,000 psi in tension at the blade root. Using 186,000 psi yield for Rene' 95, a 53% speed margin exists at the yeild point. Using 230,000 psi ultimate, a 70% over-speed margin exists to burst.

The velocity diagram for the hoisting turbine is shown in Figure 13.



C_V = .96 Nozzle
C = .96 Nozzle
C_V = .92 Wheel

Allow 10% for all additional losses.

Figure 13. Hoisting Turbine Design.

Hoisting Turbine Wheel and Nozzle. The nozzle is converging/diverging expanding to 20 psia (sea level) at the nozzle exit. Further expansion to 14.7 psia takes place in the gap between the nozzle and turbine. Turbine blade height is greater than nozzle height to permit this expansion to take place. The nozzle diverging section is rather short to minimize boundary layer buildup and maintain a high nozzle efficiency.

The turbine blade height is reduced to reduce windage. As a result, blade angles are increased in order to provide adequate airflow.

The overall design provides an optimized trade-off of stall torque, hoisting torque, payout speed and reel-in speed. Payout speed is emphasized in the design.

Nozzle:

Exit angle - 18°
Throat area - 1.52 sq-in
Exit area - 1.74 sq-in
Airflow - 1.50 lb/sec
No. of vanes - 17
Nozzle height - .52 in
Estimated flow coeff. - .90

Turbine Wheel:

Type of blading - impulse
Blade angle - 31°
Pitch diameter - 4.00 in
Blade height - .600
Passage area - 3.40 sq-in
No. of blades - 66
Blade chord - .350 in
Estimated output stall torque at S.L. - 250 ft/lb

Nozzle coefficients of .96 velocity coefficient and .96 coefficient of contraction were used in formulating the design.

The hoisting nozzle and the hoisting wheel configurations are shown in Figures 14 and 15 respectively. For comparison, the initial design of the hoisting nozzles and the wheel configuration are shown in Figures 16 and 17.

A comparison of the redesigned and the initial hoisting wheel torque versus speed generation capability is shown in Figure 18.

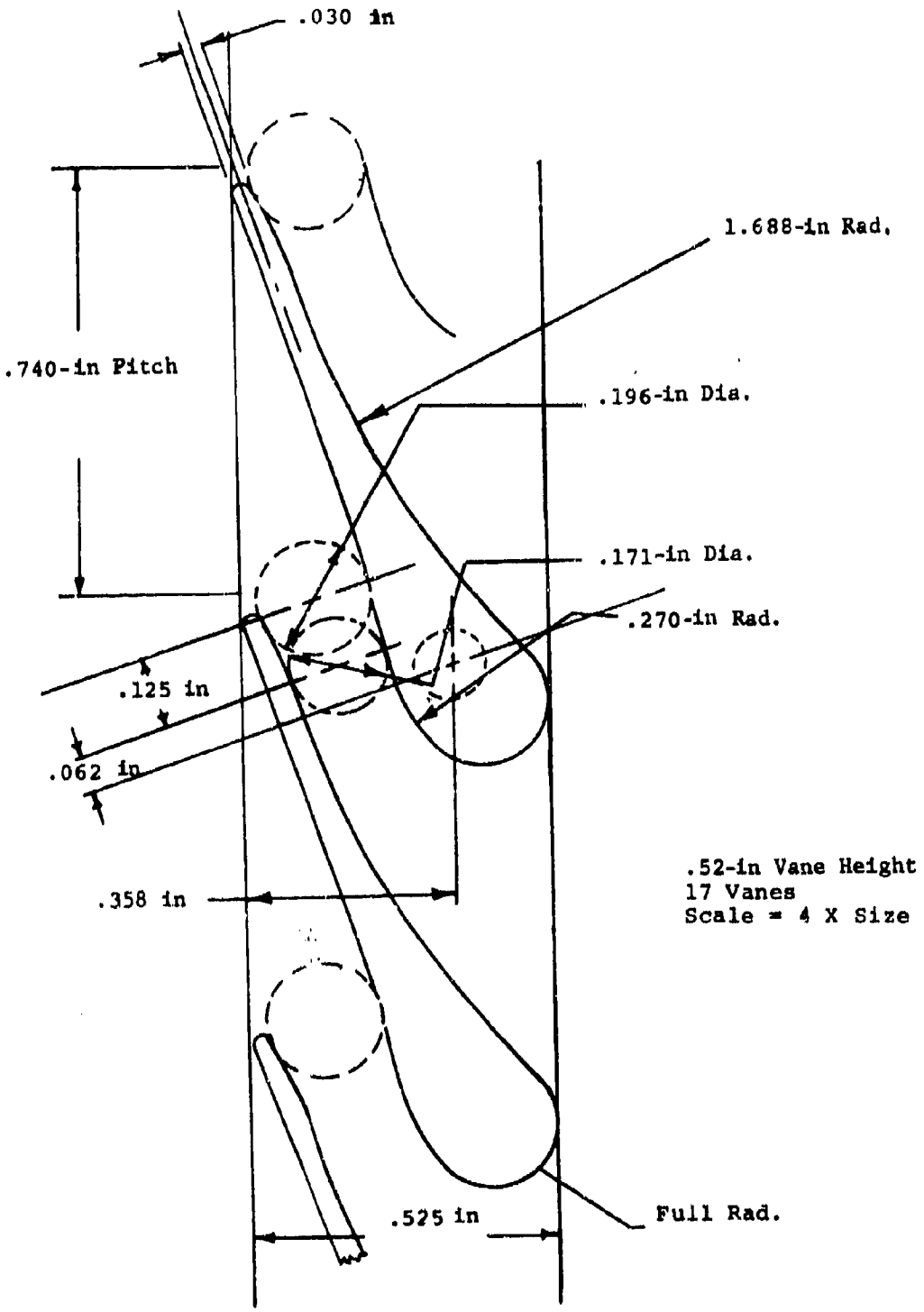
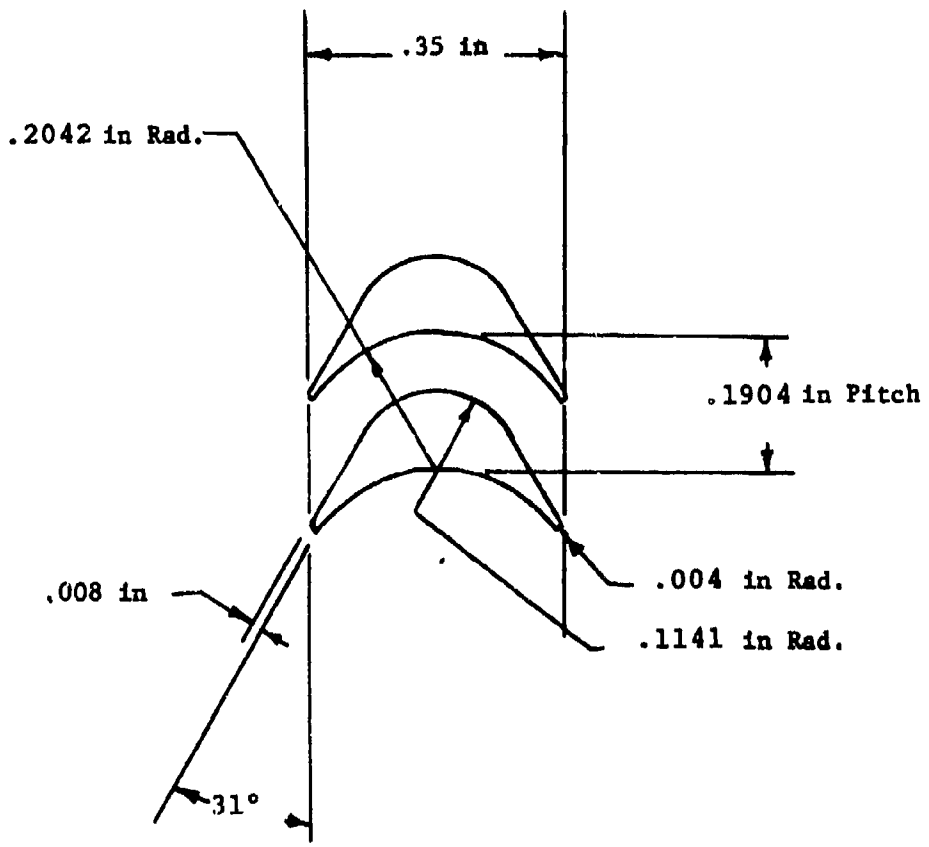


Figure 14. Redesigned Hoisting Nozzle.



Blade Height .600 in
Pitch Dia. 4.000 in
66 Blades
Scale = 4 X Size

Figure 15. Redesigned Hoisting Wheel.

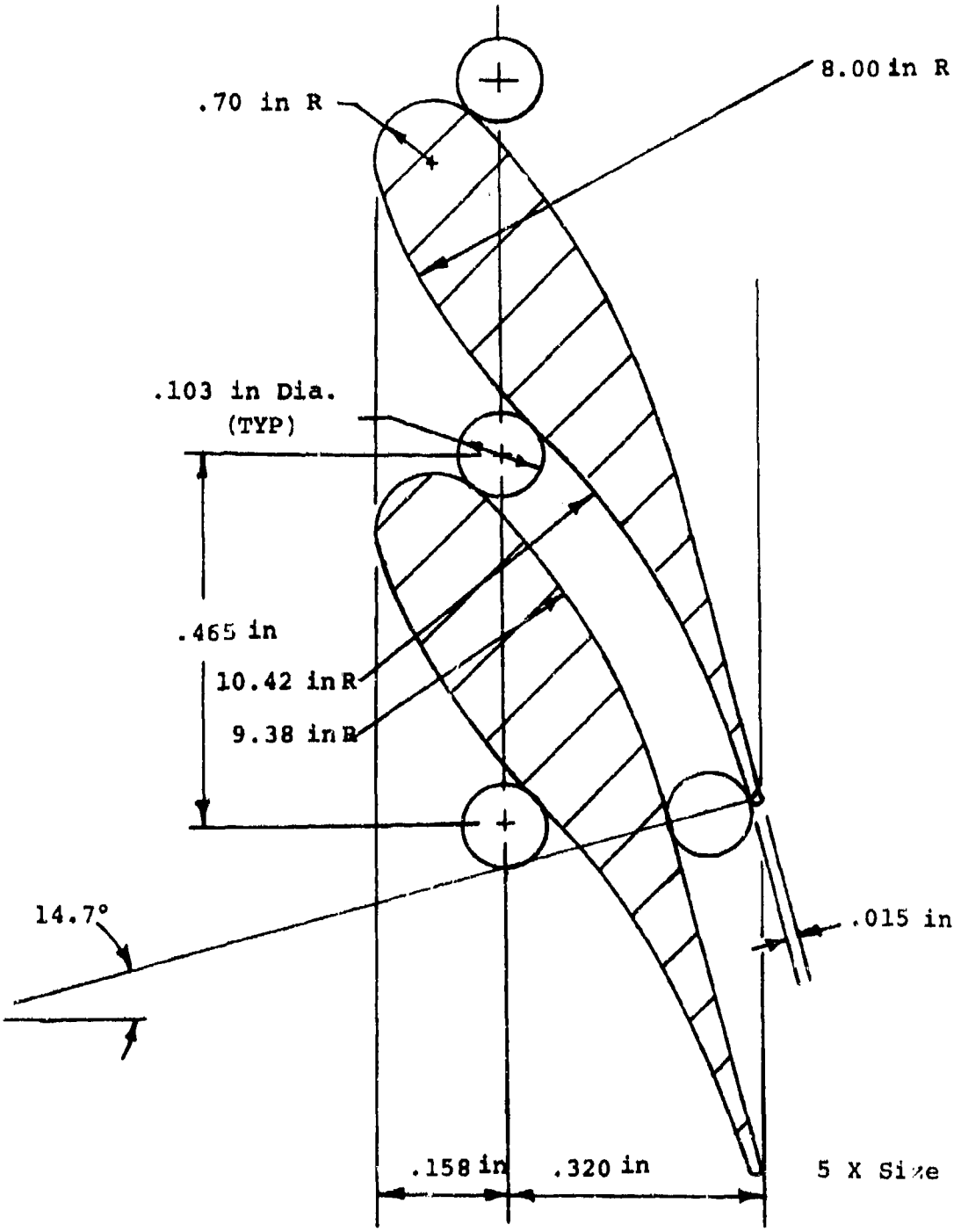


Figure 16. HLH Hoisting Turbine Nozzle Guide Vane Profile (Initial Design).

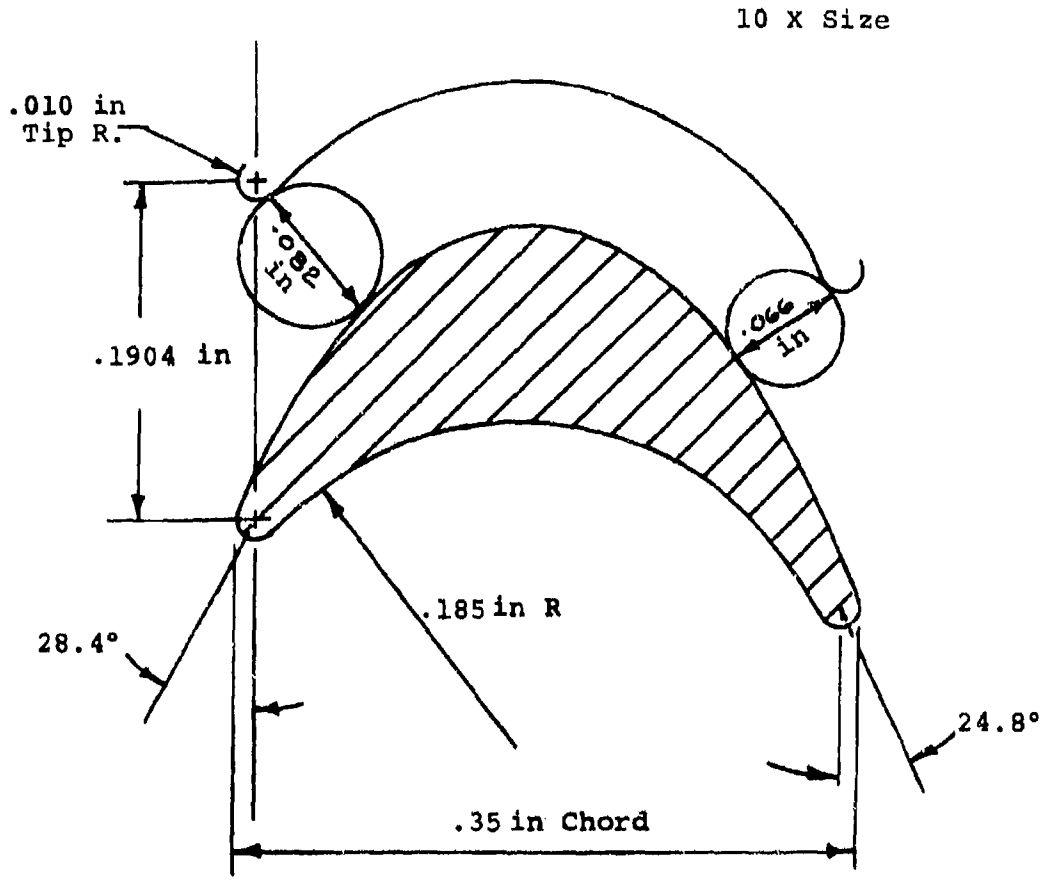


Figure 17. HLH Hoisting Turbine Blade Profile (Initial Design).

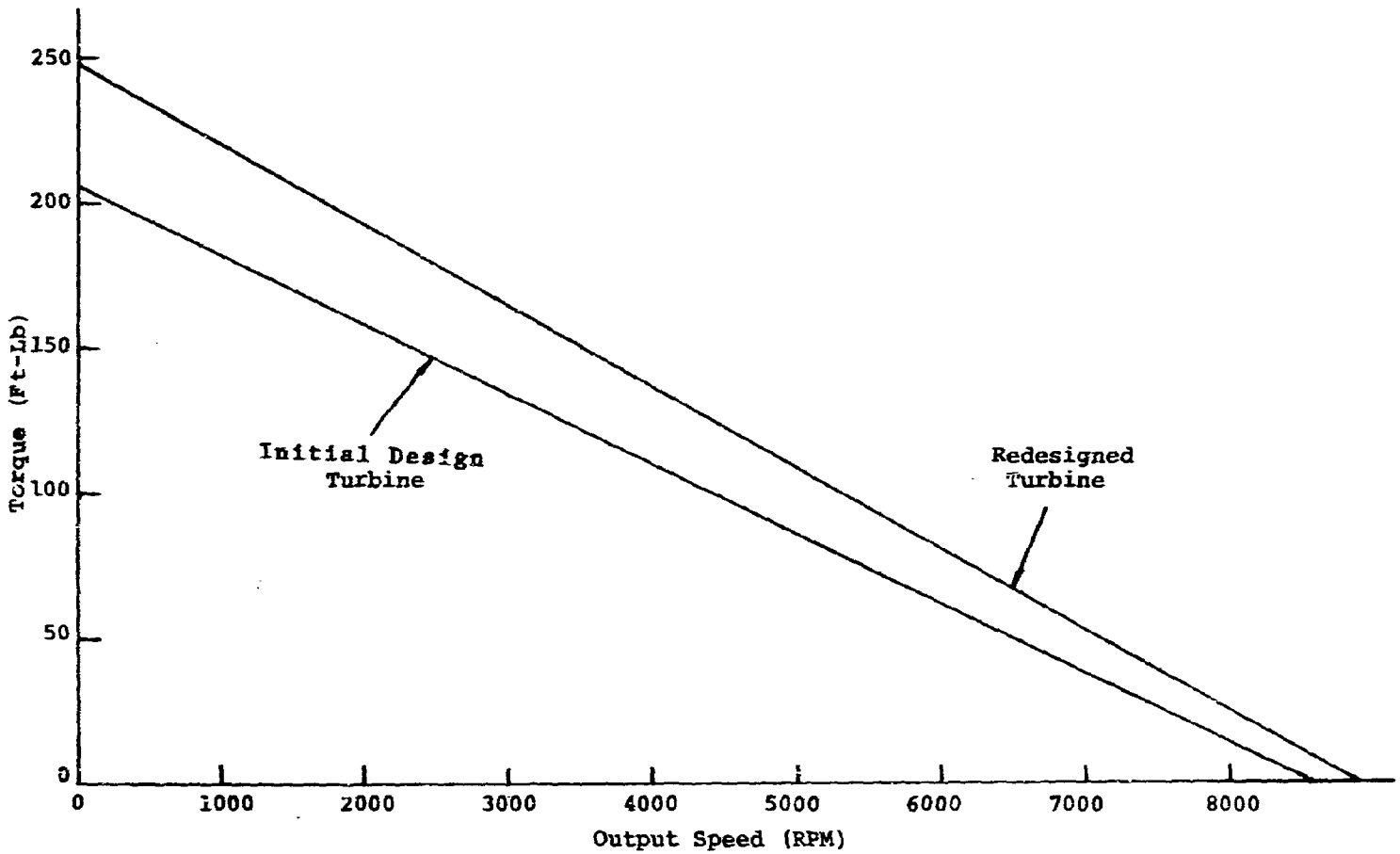


Figure 18. Redesigned Hoisting Turbine Performance
Net Torque Versus Speed.

Both redeisgned nozzles (hoisting and reversing) will be fully machined to provide good surface finish and minimum friction losses. Also, a reduced number of nozzle vanes are being used to reduce the flow surface area, which should result in higher nozzle coefficients.

Reversing Turbine. The reversing turbine must provide sufficient power to drive the hoisting turbine backwards at maximum payout speed. This power requirement is composed of the windage hp of the hoisting turbine running backwards plus the friction hp of the machine.

Based upon design support testing conducted at Sundstrand, this windage and friction value used in the initial design was 37 hp at sea level. The reversing turbine was therefore designed to produce 37 hp at maximum payout speed.

Actual output of 20 hp occurred at approximately 5,000 rpm (see Figure 19). Analysis indicated a low airflow for the nozzle area provided. An airflow of .43 lb/sec was obtained through a .572 sq-in nozzle throat area. This corresponds to a .75 nozzle flow coefficient as compared to .95 used in the design. Overall turbine efficiency at maximum hp was 44%. Poor performance at the turbine nozzle was believed to be a major cause of the low airflow and also the low efficiency. A flow check of the nozzle, without the turbine installed, did not yield increased flow.

An analysis of the turbine wheel indicated that an increased blade solidity would improve turbine efficiency. This could be best accomplished by widening the blade chord.

The reversing turbine was of the reaction type in order to obtain maximum hp at high velocity ratio (U/Co). Maximum hp should have occurred at 8,000 rpm; however, output leveled off at 5,000 rpm, indicating insufficient reaction. It was concluded from analysis that a redesign of the reversing turbine should incorporate the following features:

1. A reduced number of relatively short nozzle passages.
2. Increased nozzle throat area for increased airflow.
3. A turbine wheel with wider chord to provide higher turbine solidity.
4. Much increased turbine reaction to provide maximum hp at maximum payout speed.

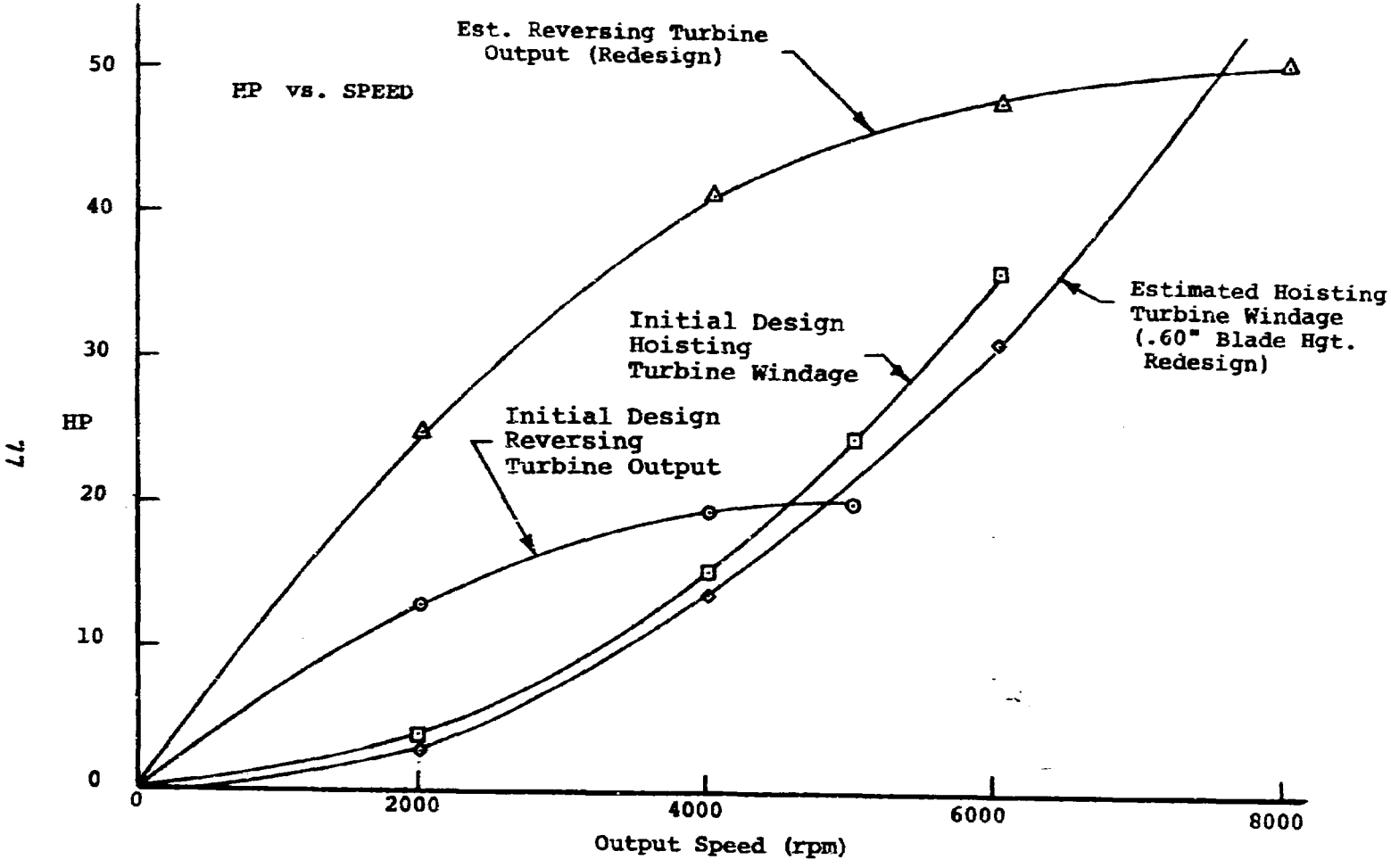


Figure 19 . Redesigned Reversing Turbine Performance (Estimated).

Reversing Turbine Design Analysis. Based upon the hoisting turbine estimated reverse windage, the reversing turbine must produce 50-55 hp to provide maximum payout speed.

Whereas the hoisting turbine operates at rated load at .414 U/Co, the reversing turbine must operate at .460 U/Co. This is past the efficiency peak for such a small turbine and relatively high reaction must be built in.

The design selected has a number of features intended to provide maximum hp at high payout speed. First, the nozzle is designed converging to the throat with no diverging section. Throat pressure is 32.0 psia. In this way the nozzle is enlarged as much as possible in the space available and passes a maximum of flow. Expansion takes place to 20 psia at the turbine inlet, providing reaction of 5 psi across the turbine. Turbine annulus area is increased from the previous design as well to provide maximum flow. Nozzle angle of 18° was selected to retain sufficient air turning at high speed, thus retaining high-speed torque. Nozzle area is now .84 sq-in compared to the previous .57 sq-in; however, the flow rate is doubled from .43 lb/sec to .84 lb/sec. Efficiency is expected to increase from 44% to 60%.

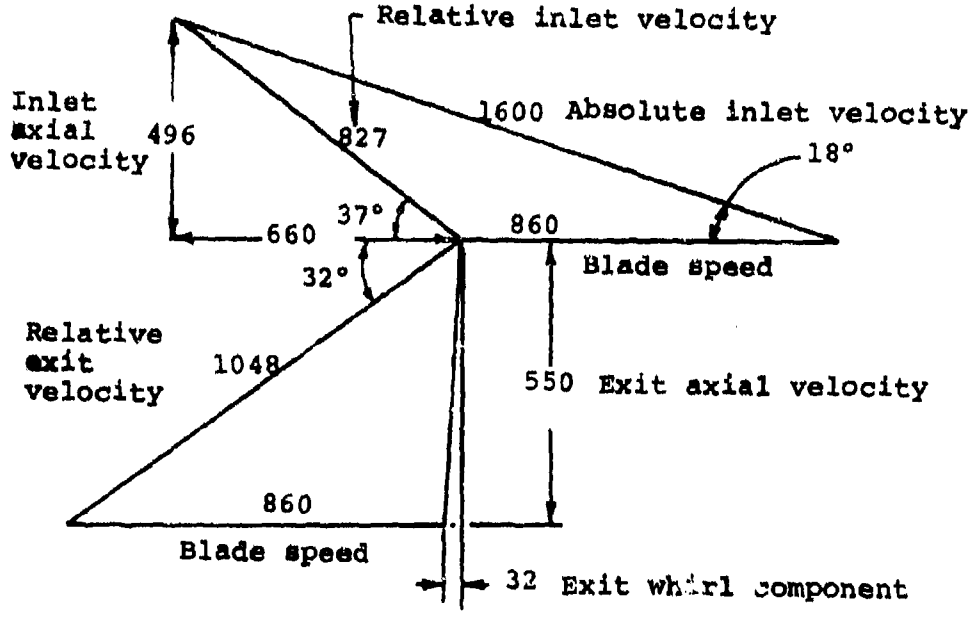
Refer to Figures 19, 20, and 21 for estimated hp, velocity triangles and blade profile curves, respectively. Provisions have been made to rework the throat flow area from .84 sq-in to .93 sq-in if necessary.

In order to improve the solidity, especially toward the rotor O.D., the blade chord was increased from .250 in to .320 in. The number of blades was reduced from 47 to 43 to provide sufficient spacing between the blades at the root for manufacturing and tooling reasons. The two revisions provided optimum turbine solidity.

A specific reversing turbine design was then determined. It consists of the following:

Nozzle angle 18°
Turbine angle 32°
Nozzle height .45 in
Turbine blade height .50 in
Turbine pitch diameter 2.25 in
Turbine blade chord .320
Nozzle expansion ratio 1.86
Turbine expansion ratio 2.19
Expansion in nozzle to 32 psia
Expansion in nozzle/wheel gap to 20 psia
Expansion in wheel to 14.7 psia

Velocity Triangles
8000 rpm
Velocity in ft/sec (mean diameter)



Nozzle C_V = .95
Nozzle C_c = .95
Turbine C_V = .90

Allow 14% for additional losses.

Figure 20. Reversing Turbine Design.

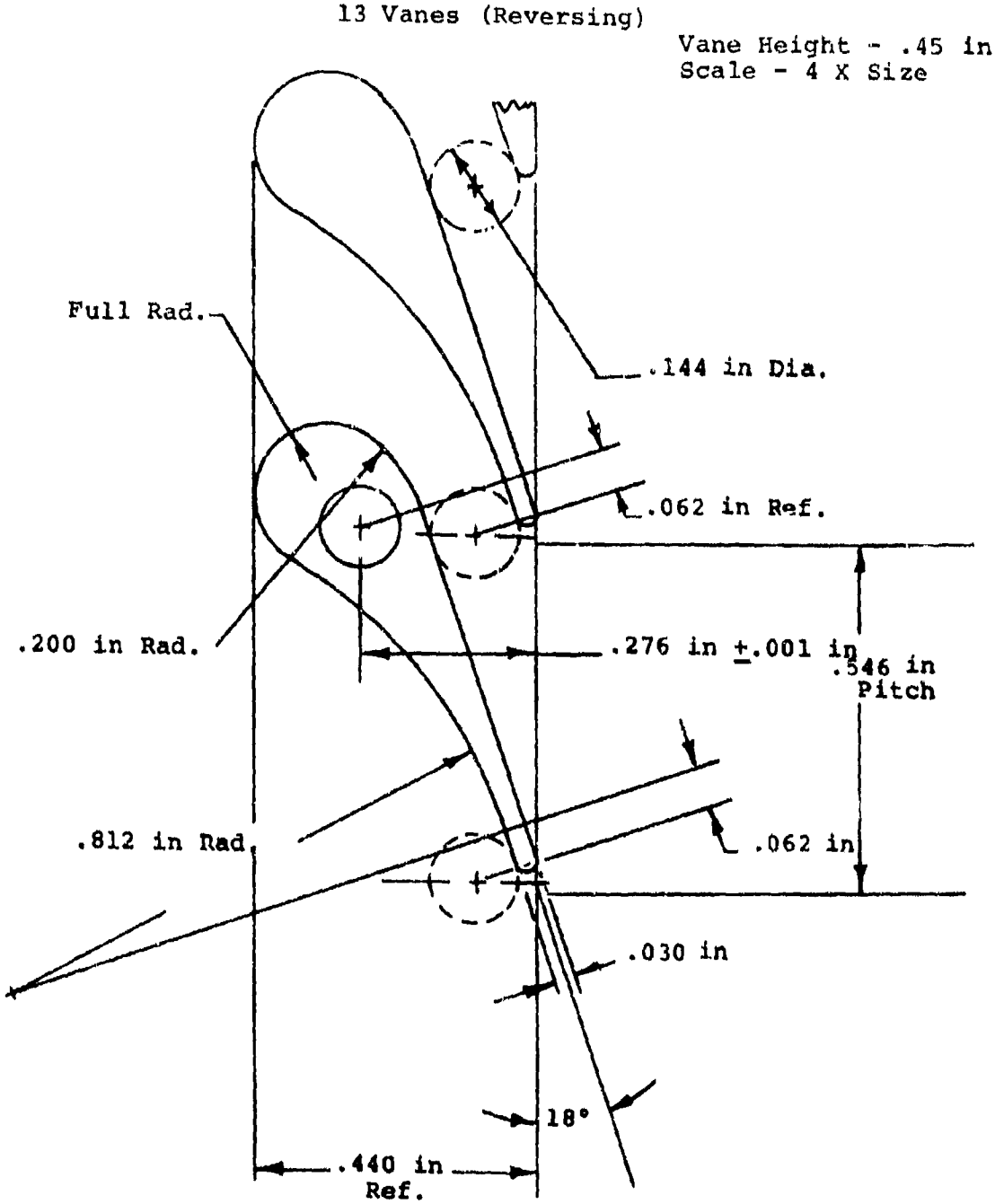


Figure 21. Blade Profiles (Reversing Nozzle).

Nozzle area .84 sq-in
Airflow .82 lb/sec
Estimated efficiency 60%
Nozzle velocity coefficient .95
Nozzle flow coefficient .95
Turbine wheel velocity coefficient .90
Allow 14% for all additional losses (leakage, windage, etc.)
Nozzle may be reworked to .93 lb/sec flow
Altitude - sea level

Nozzle Redesign. A description of the redesigned ATM nozzles is as follows.

Reversing Turbine Nozzle. The nozzle is converging only in order to provide a maximum of flow in the space provided. Downstream expansion takes place in the gap between the nozzle and the turbine wheel and also in the turbine wheel itself. A reaction design is provided to yield peak hp at the design condition of 120 ft/min payout speed.

Nozzle:
- Exit angle - 18°
- Throat area - .84 sq-in
- Airflow - .82 lb/sec
- No. of vanes - 13
- Nozzle height - .45 in
- Estimated flow coeff. - .90

Turbine Wheel:
- Type of blading - impulse
- Blade angle - 32°
- Pitch diameter - 2.25 in
- Blade height - .50 in
- No. of blades - 43
- Blade chord - .320 in
- Estimated output at design speed - 50 hp

The reversing nozzle configuration is shown in Figure 21. The blade configuration for the reversing turbine wheel is shown in Figure 22. For comparison the initial design of the reversing nozzle and the blade configuration are shown in Figures 23 and 24.

Bearing Modification. The axial turbine thrust increases with turbine speed. If the turbine areas are sized to pass the flow at the design speed, usually about half of the maximum speed, then the flow area will be inadequate

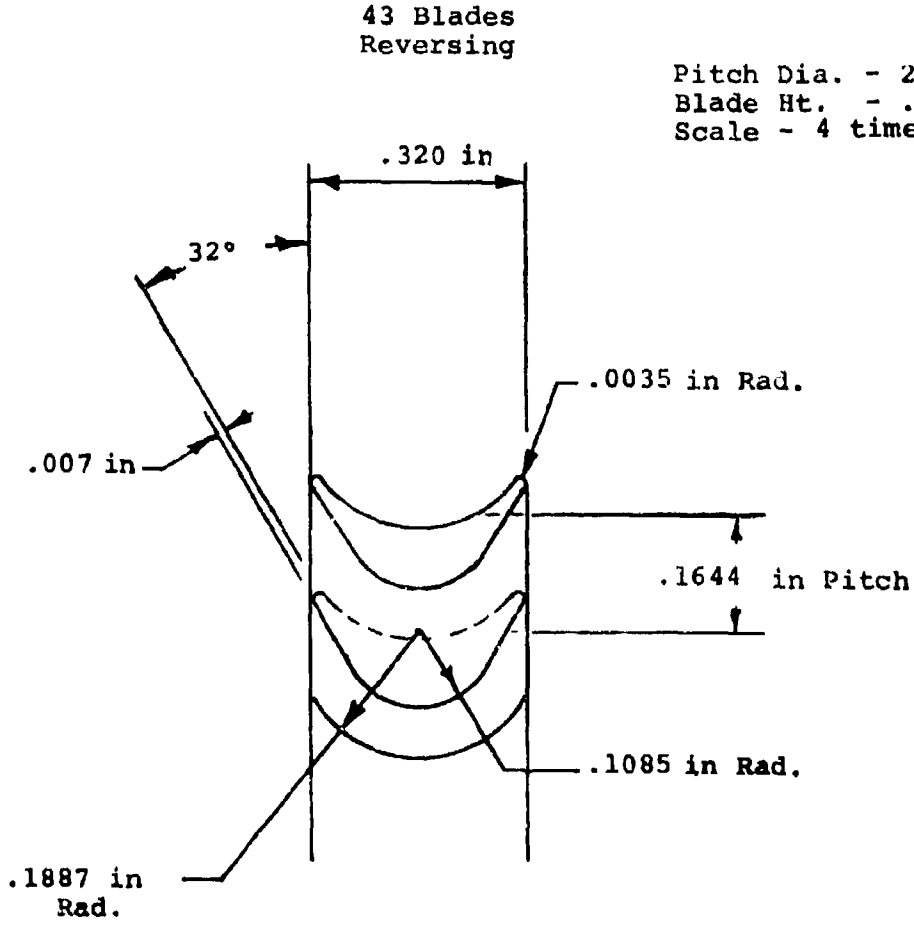


Figure 22. Redesigned Blade Configuration (Reversing Turbine Wheel).

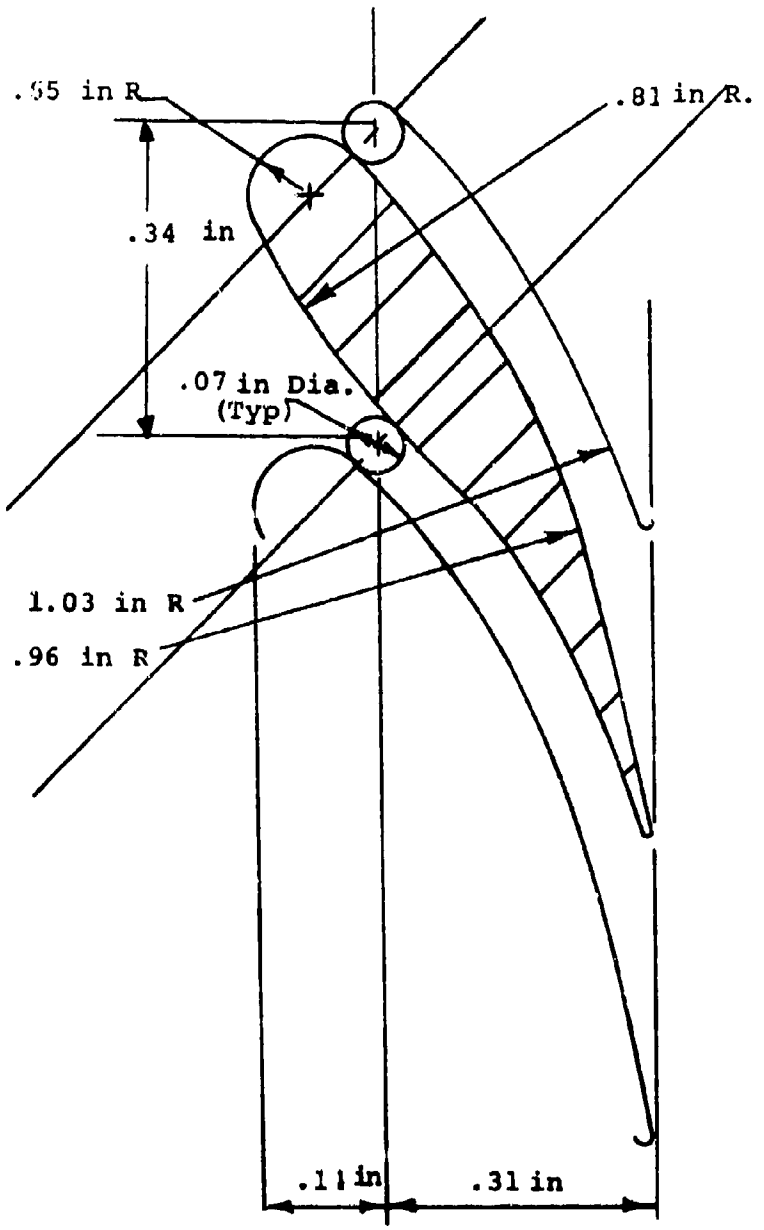


Figure 23. HLH Reversing Turbine Nozzle Guide Vane Profile. (Initial Design)

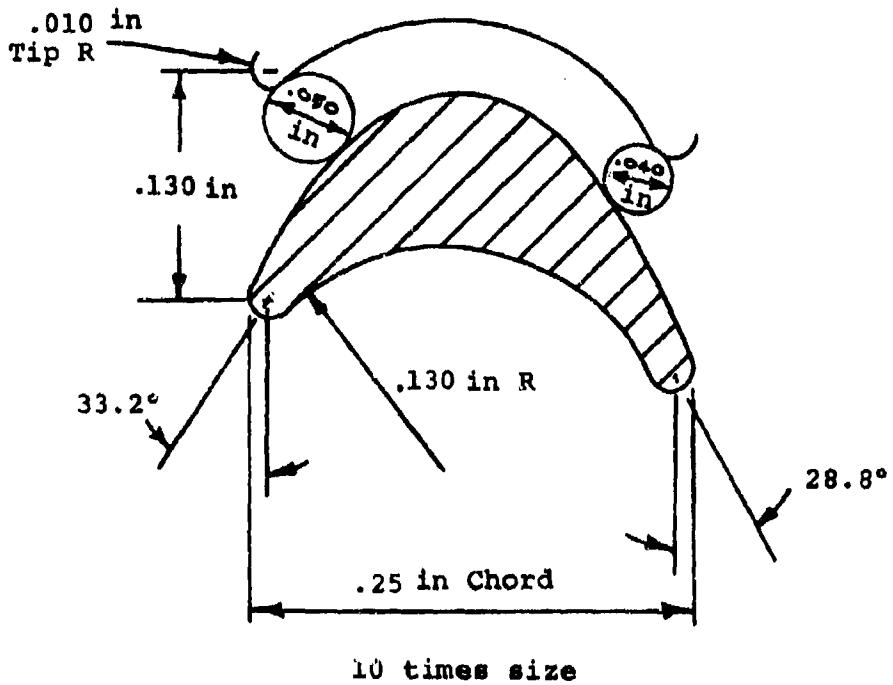


Figure 24. HLH Reversing Turbine Blade Diagram (Initial Design).

at maximum speed. The turbine flow will self-adjust by building up pressure upstream of the wheel, thus creating an axial thrust.

Thrust values determined for the hoisting turbine are negligible up to 4,000 rpm then rise rapidly to 145 lb at 8,000 rpm. The reversing turbine maximum thrust is small, about 20 lb at 8,000 rpm (see Figure 25).

Bearing B-10 life for the original .4724-inch bore JL01 new departure bearings (1.1024 inch OD) at the maximum thrust condition was 109 hours. They were considered marginal for this application. Larger, .5906-inch bore JL02 new departure bearings (1.3780-inch OD) have been selected for the redesigned ATM. The design B-10 life of this bearing is 450 hours, which occurs at maximum reel-in speed.

Lubricant Change. Design support tests conducted with the initial ATM design used MIL-L-23699 lubricant. Testing revealed that viscous drag losses (between brake disc) of this lubricant were higher than with MIL-L-7808 lubricant. The lubricant for the redesigned ATM was, therefore, changed to MIL-L-7808.

Major Redesigned Items. The major items that were redesigned are illustrated in the following figures:

Hoisting nozzle guide vanes	Figure 26
Hoisting turbine wheel housing	Figure 27
Hoisting labyrinth seal area	Figure 28
Hoisting turbine wheel	Figure 29
Reversing housing	Figure 30
Reversing nozzle guide vane	Figure 31
*Hoisting and reversing turbine wheel assembly	Figure 32

*The hoisting wheel was fabricated from René 95 material. The reversing wheel material is Inconel 718.

Lub System. An integral gear type pump, mounted in the gearbox supplies 2.5 GPM at approximately 65 psi. This lube and scavenge pump consists of two standard "gerotor" elements. Each gerotor element consists of a six-tooth rotor, keyed to the drive shaft and meshing with a seven-tooth internal gear. The internal gear rotates in an eccentric ring which is capable of rotating 180°. This half revolution of the eccentric ring permits the flow direction to remain unchanged regardless of the direction of shaft rotation (see Figure 33).

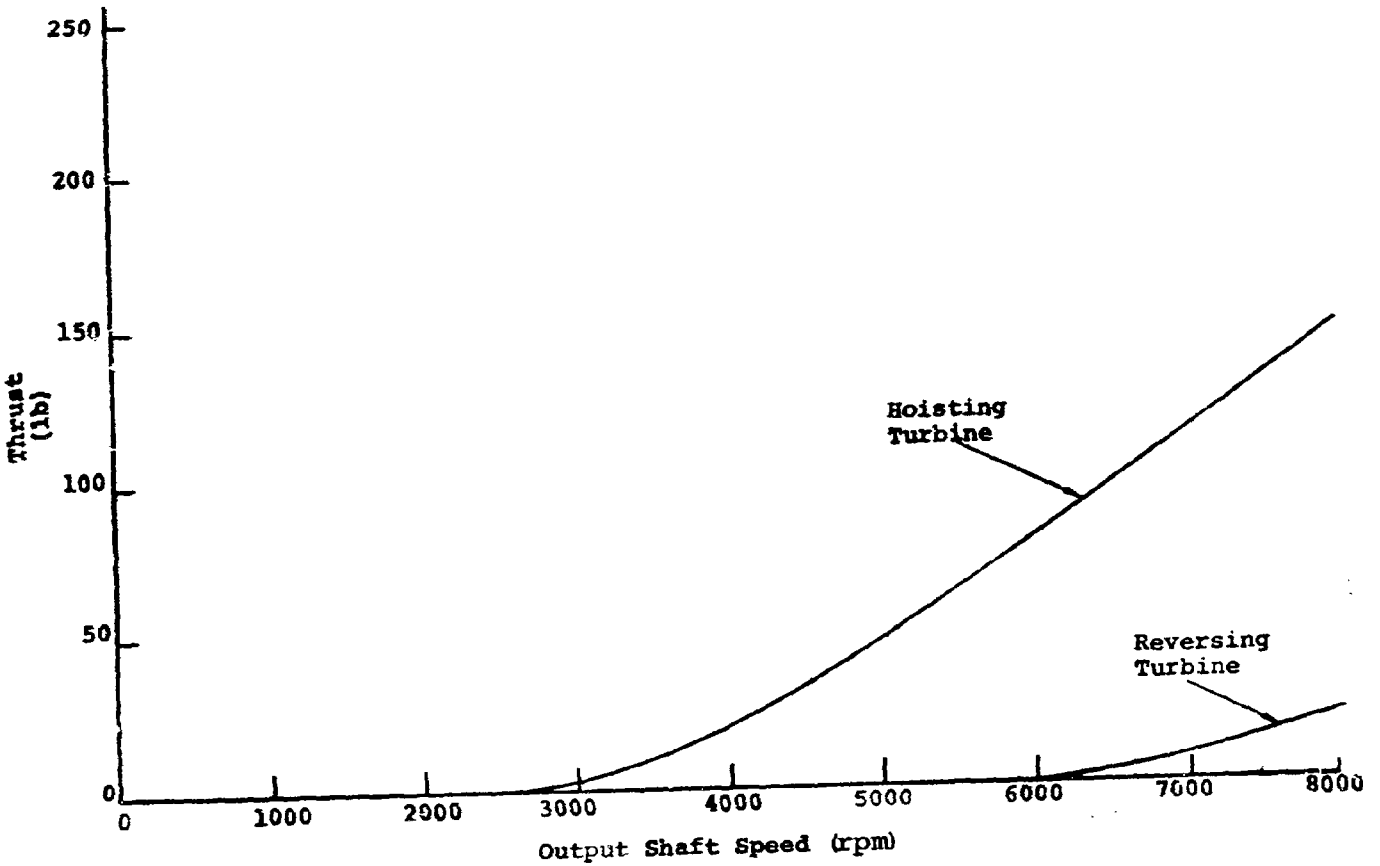


Figure 25. Thrust vs. Output Shaft Speed.



Figure 26. Hoisting Nozzle Guide Vanes.

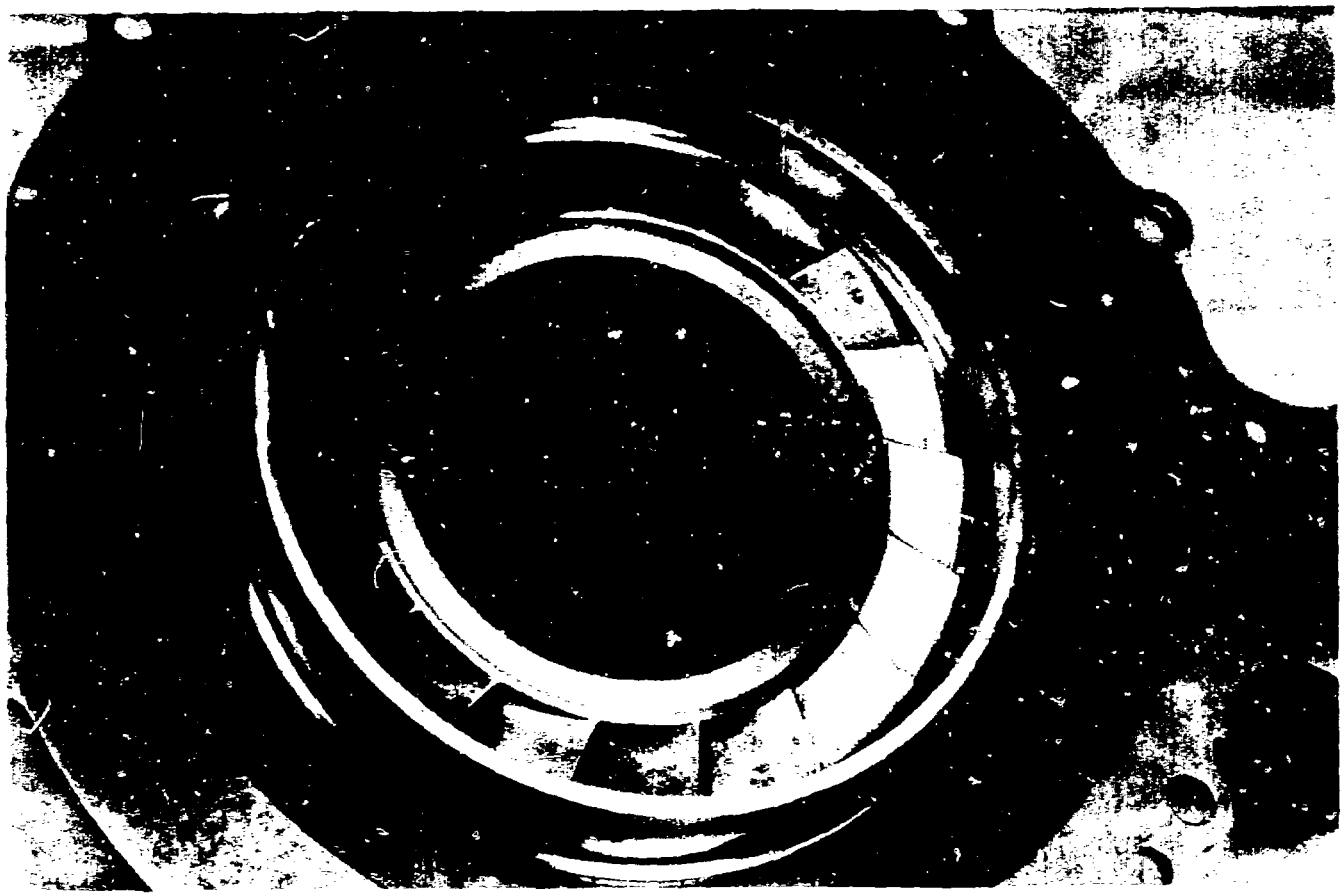


Figure 27. Hoisting Turbine Wheel Housing.



Figure 26 . Hoisting Labyrinth Seal Area.

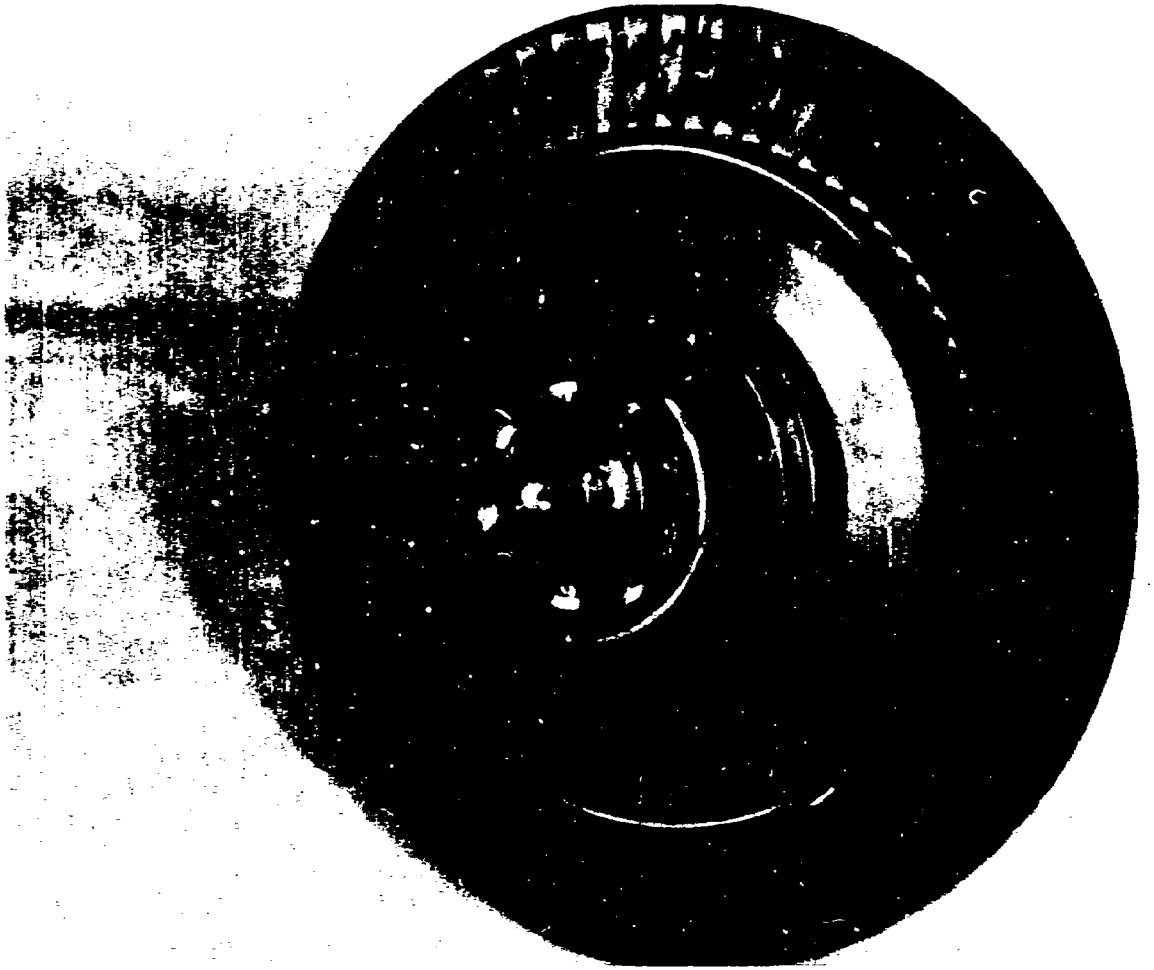


Figure 29. Hoisting Turbine Wheel.

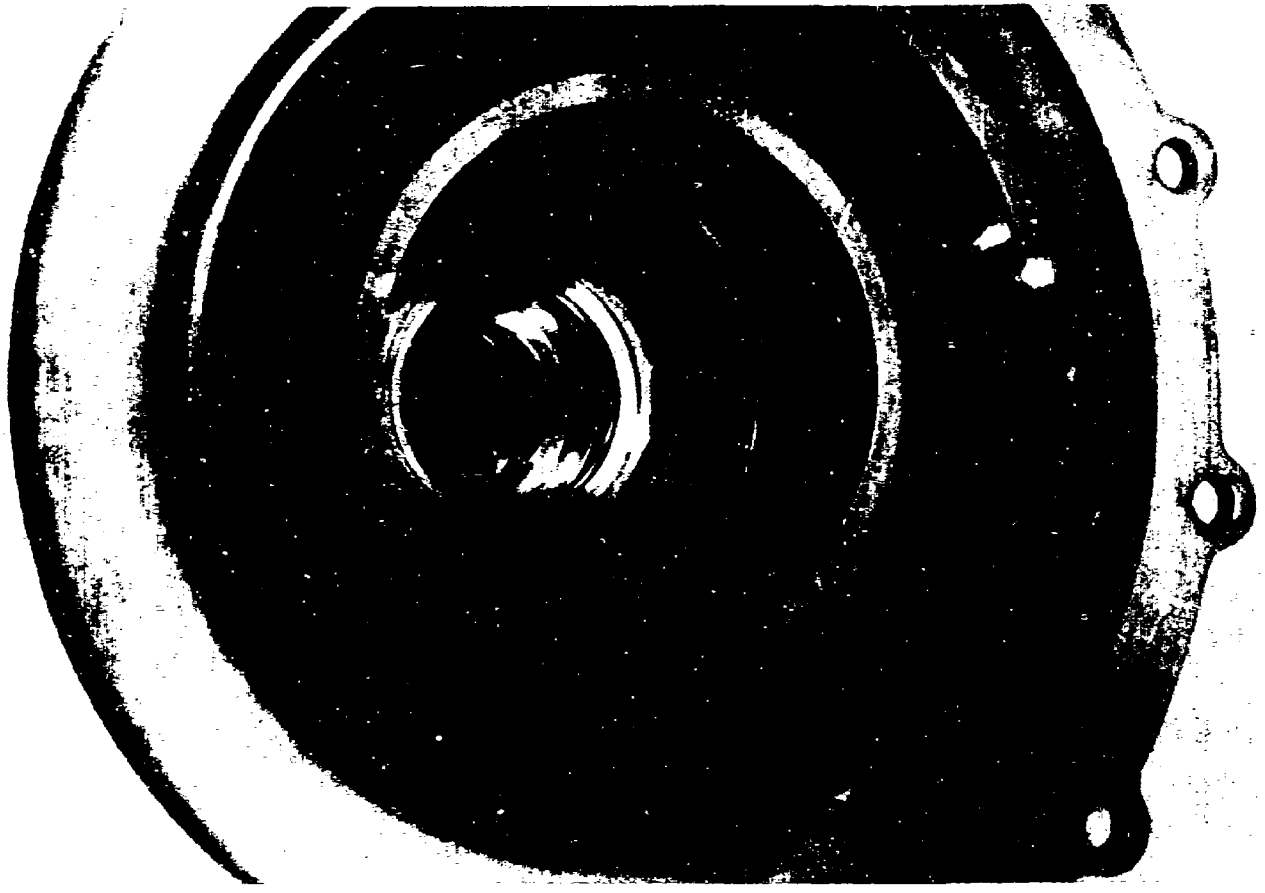


Figure 30. Reversing Nozzle Guide Vane.

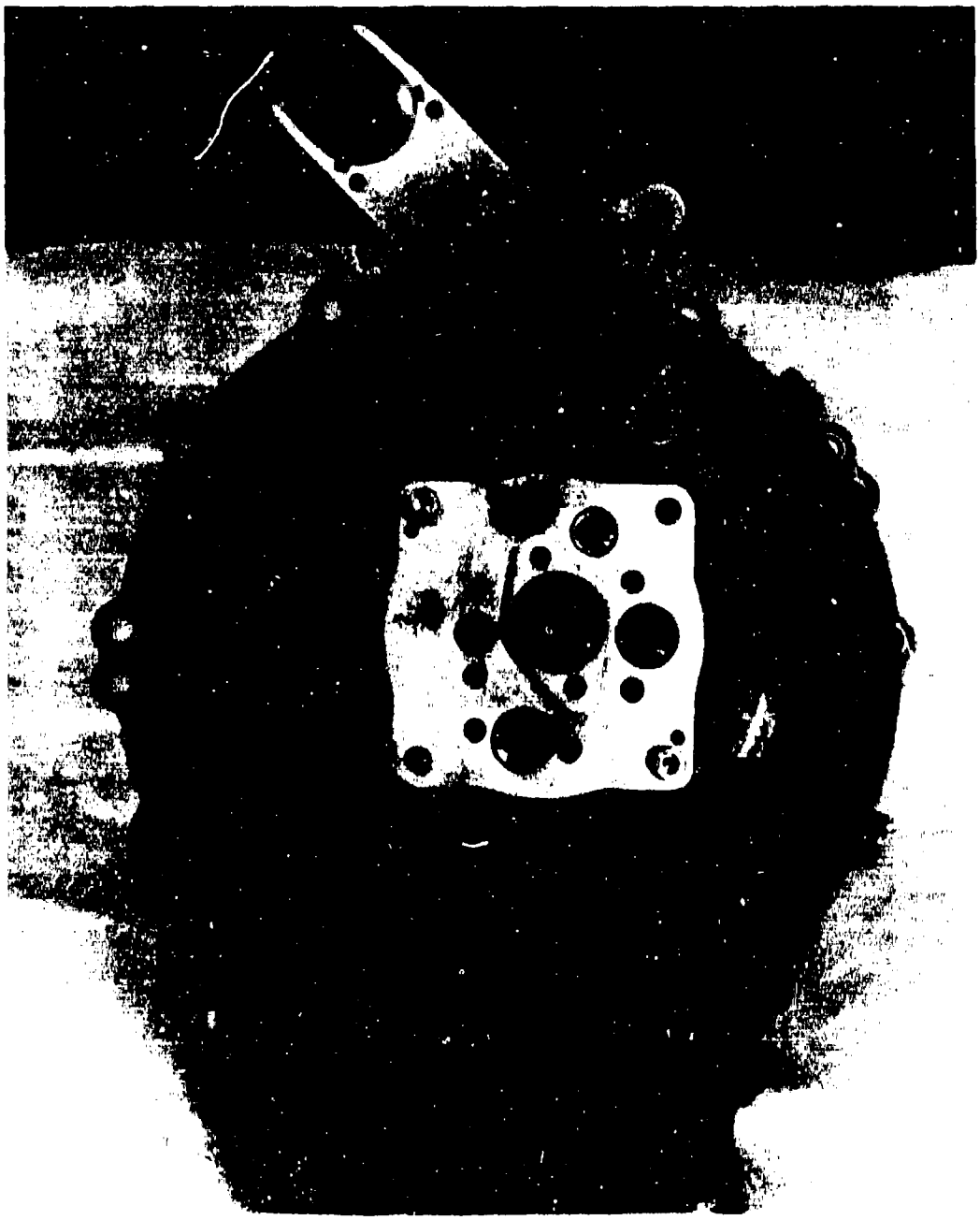


Figure 31. Reversing Housing.

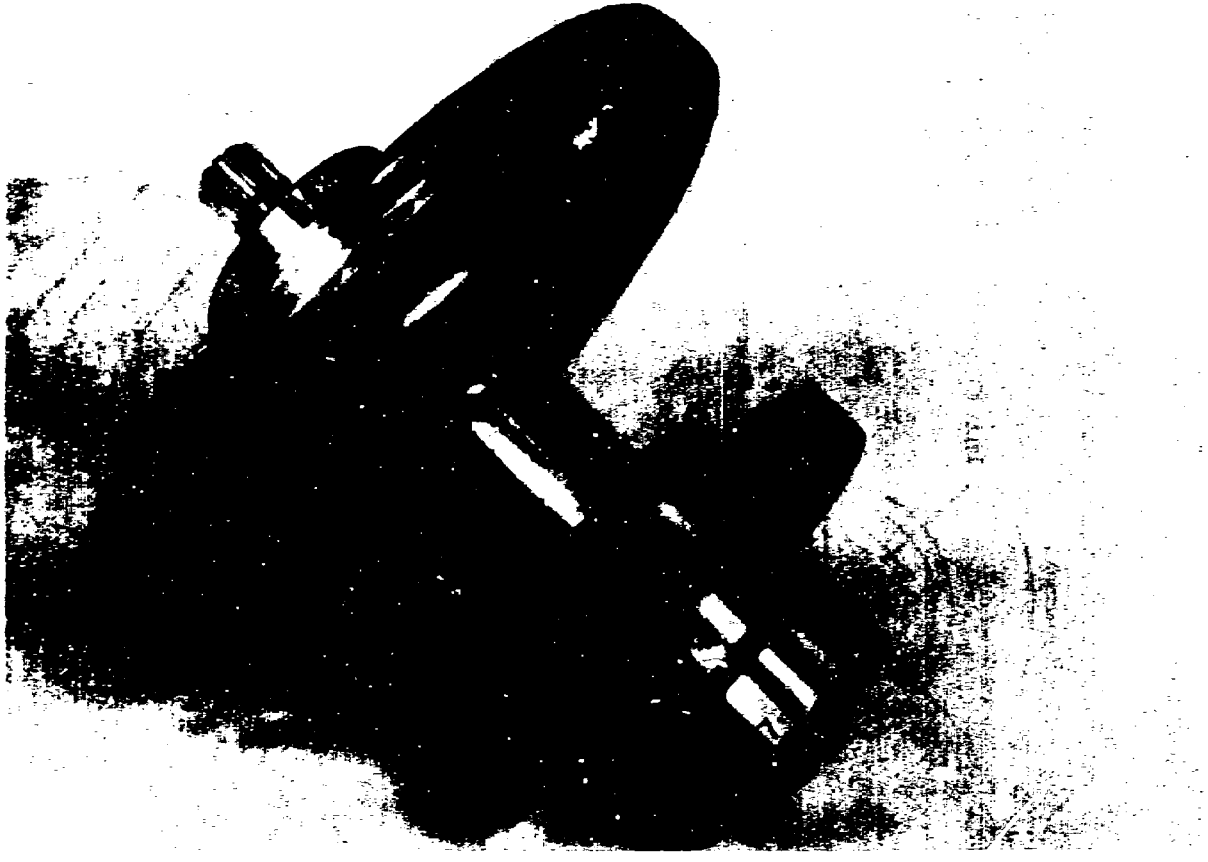


Figure 32. Hoisting and Reversing Turbine Wheel Assembly.

This schematic shows the pump element configuration used in the ATM gearbox. Note that flow direction does not change when rotation is reversed.

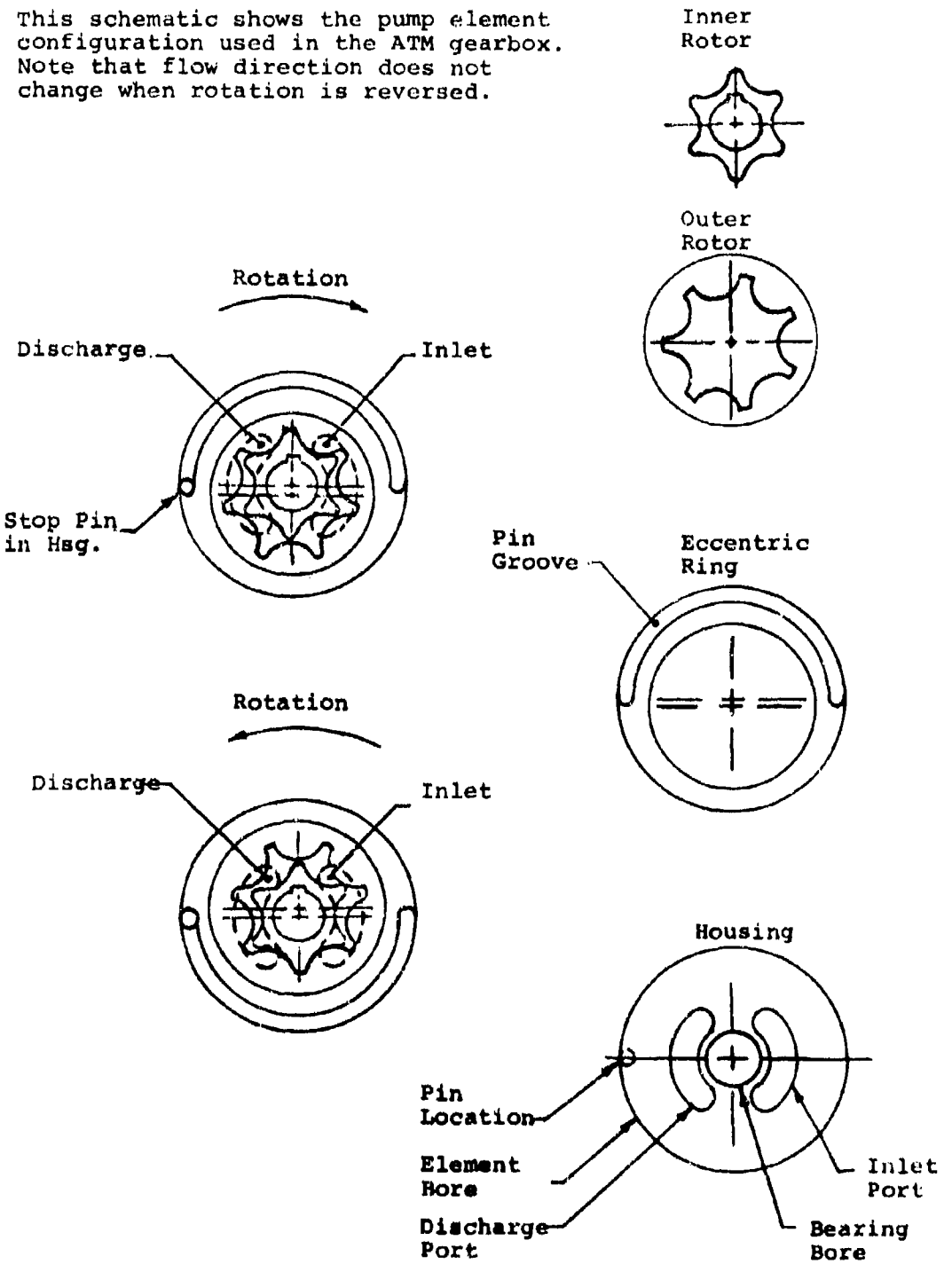


Figure 33. Pump Element Configuration.

Both pumping element inner rotors are pin driven on a common shaft which is supported on bronze bushings at both ends. The pump elements are sized as follows:

Pumping area per revolution of element chosen is 0.2 square inch per revolution.

Design operating speed is $87000 \times \frac{35}{109} \times \frac{20}{70} \times \frac{70}{85} =$ 6,580 rpm.

Required displacement is calculated as follows:

$$\text{Lube} = 2.5 \frac{\text{gal}}{\text{min}} \times 231 \frac{\text{cu-in}}{\text{gal}} \times \frac{1}{6580} \frac{\text{min}}{\text{rev}} = .088 \frac{\text{cu-in}}{\text{rev}}$$

$$\text{Scavenge} = 0.5 \times 231 \times \frac{1}{6580} = .018 \frac{\text{cu-in}}{\text{rev}}$$

Required width of pumping elements is then:

Lube: **.088 cu-in/rev x 1/.2** rev/sq-in = .44 inch

Scavenge: .018 x 1/.2 = .09 inch

Approximate inlet pressure required to fill lube element with no cavitation is $P = \frac{pV^2}{2gc}$

Where: P = oil density
V = mean pumping sector velocity
gc = accel. of gravity

$$V = 6580 \frac{\text{rev}}{\text{min}} \times \frac{.87"}{12} \frac{\text{ft}}{\text{rev}} \times \frac{1}{60} \frac{\text{min}}{\text{sec}} = 25 \frac{\text{ft}}{\text{sec}}$$

$P = 61$ lb/ft^3 (at 60°F)
$gc = 32.2$ ft/sec^2

$$P = \frac{(61)\ (25)^2}{(2)\ (32.2)\ (144)} = 4.1 \text{ psia}$$

This is equivalent to an altitude of 31,000 ft. At altitude design day conditions, ambient pressure is 12.7 psia, a more than adequate inlet pressure.

One GPM is metered through spray nozzles directed at the high-speed bearings and splines. The remainder of the oil flow is used for brake cooling. A second internal gear pump capable of 0.5 GPM scavenges the ATM end bearing cavity and returns the scavenged oil to the sump.

The lube system also contains a replaceable cartridge type filter, and a combination filter bypass valve, pressure differential indicator. The oil sump is an integral part of the gearbox and brake housings. Oil sump size is determined by the heat dissipation requirements of the brake and gearbox and contains five pints of oil. The sump case contains a combination drain plug and magnetic chip collector, and an oil level sight glass plug.

Lubrication and Bearing Modifications. In the design development tests conducted with the initial design, ATM bearing failures were experienced. The analysis of the bearing failures indicated that the failures were due to inadequate lubrication.

The ATM/brake lubrication system was reviewed and several modifications were incorporated. Low system pressures (typically 15 psi vs. 50 psi at rated speed) that had been experienced throughout the program were initially attributed to side clearance losses, pump cavitation, and minor deviations from design porting. A flow measurement of the lube pump output revealed this was not the case. The .5-inch W.H. Nichols gerotor (P/N 6020) produced 2.1 GPM at 4000 RPM brake speed, indicating significant losses elsewhere in the system. A thorough check of all lubrication lines revealed two errors in orifice sizes. In the first case, a 0.62-inch-diameter orifice for the brake bearing was discovered where a .025-inch-diameter orifice should have been. In the second instance, a pipe plug for a .025-inch orifice had been inadvertently omitted from the assembly, leaving an effective orifice of nearly .125-inch diameter.

After these errors had been corrected, several refinements to the system were implemented. The .025-inch-diameter orifices were increased to .030-inch diameter to lessen the chance of plugging. At the same time, the orifice for the brake plates was reduced from .125-inch diameter first to .070-inch diameter and finally to .060-inch diameter, since even under emergency stop conditions, negligible brake plate wear was encountered.

The current oil distribution is summarized in Table 2. The revised system delivers 2.1 GPM with a pressure of 59.12 psi at the design speed.

TABLE 2. LUBE ORIFICE SUMMARY.			
Location	Size (In.Dia.)	Quantity	Flow * (GPM)
Brake Plates	.060	1	.780
Turbine Brgs.	.030	2	.304
Pinion Brgs.	.030	2	.304
Gear Meshes	.030	2	.304
Quill Shaft	.030	1	.152
Brake Brgs.	.030	1	.152
Idler Gear	.030	1	.152

*Calculated @ 4,000 RPM Brake Speed.

High-Speed Gearbox. The gearbox is an integral part of the air turbine motor, brake assembly. It reduces turbine speed by a ratio of 10.9:1 by means of two spur gear meshes. The first mesh is 32 pitch with 35 and 109 teeth; the second mesh is 20 pitch with 20 and 70 teeth.

The high-speed pinion is coupled to the turbine shaft by a piloted, splined quill. A tachometer drive gear, which also functions as a breather, is driven off the jackshaft, as is the lube pump drive gear. The turbine and pinion shafts are supported on spring loaded, angular contact ball bearings. The remaining gear shafts are supported by roller bearings.

The gearbox and brake are lubricated with high temperature turbine oil per MIL-L-7808. The internal gear type pump, mounted in the gearbox, will supply 2.5 GPM of lube oil at approximately 65 psi.

A sectioned view through the high-speed gearbox may be seen on Figure 10.

Static/Emergency Brake. The brake consists basically of a spring loaded disk pack and an air actuated releasing piston. The brake is normally "ON" with the load applied by two concentric helical compression springs. The brake contains porting such that a continuous supply of oil is flowing through the plate-separator clearances during operation. Two electric switches are also part of the braking mechanism.

One switch senses angular displacement between the separator plate spline ring and the housing. This ensures that sufficient turbine torque is applied to the system prior to brake release. A second switch senses axial displacement of the releasing piston, thereby assuring that the brake has been released.

Brake Design Parameters

1. Provide sufficient brake pad area to prevent fusion of the brake disks.

2. Ensure deceleration of the load will not exceed 2g.

3. Ensure reasonable stopping distance if load deceleration is less than 2g.

4. Ensure turbine deceleration torque does not exceed turbine stall torque (236 ft-lb).

Brake Plate Modifications. A mechanical problem developed during the early phase of the design development test is described below.

> In the first test with the ATM and brake, a problem developed with the brake plates. The separator plates used (.060 in thick) were easily distorted by any slippage of the plates under full clamping force. This distortion was caused by the high temperatures generated when the brake shaft was rotated with no inlet pressure to the brake valve. In subsequent testing, the brake and separator plates rubbed, causing the friction material on the brake plates to wear away. A photograph of a set of failed brake and separator plates is shown in Figure 34. Note that the plates near the center of the lower stack were distorted to such an extent that the friction material was completely worn away.

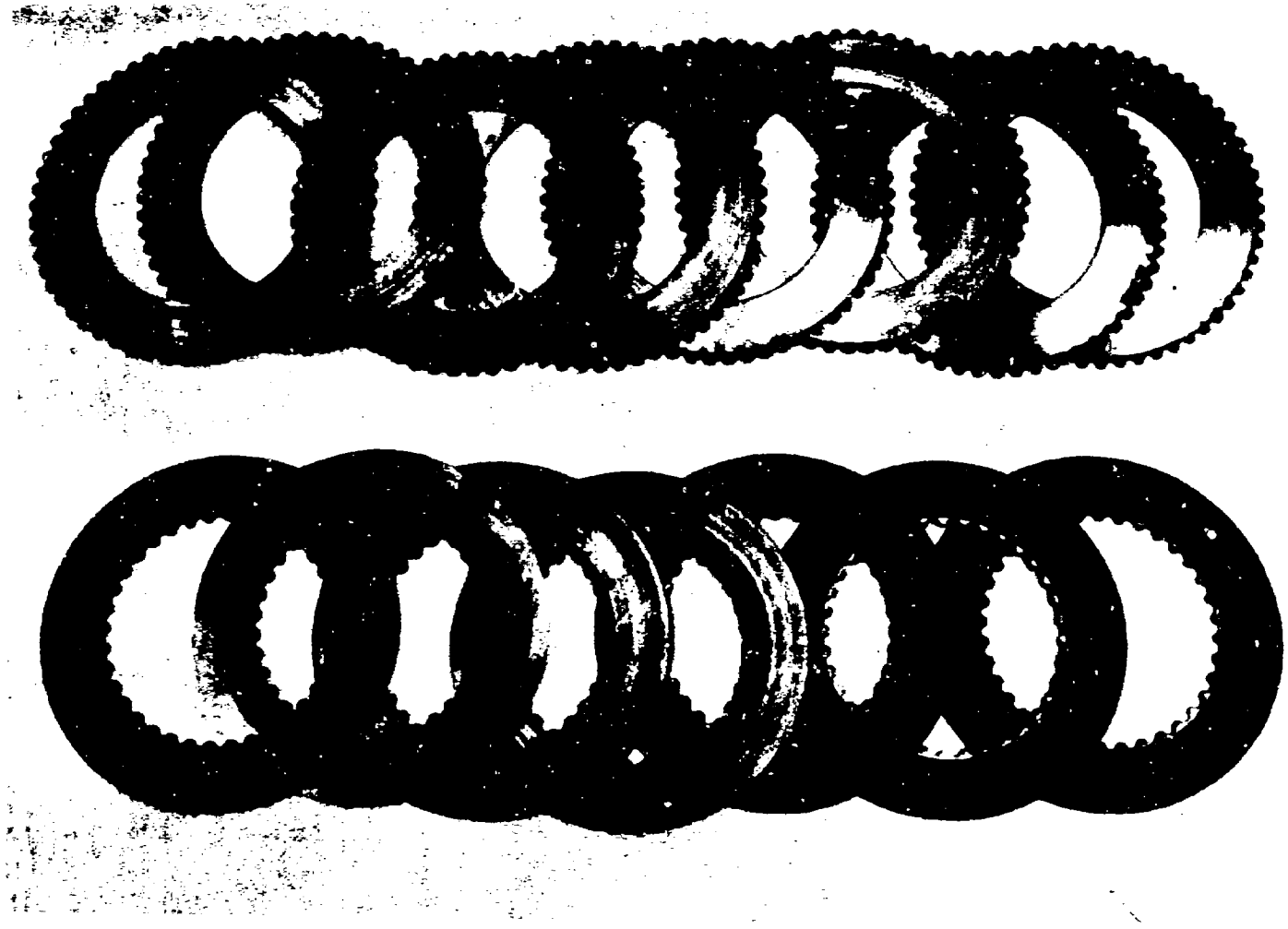


Figure 34. Hoist Drive Brake and Separator Plates.

A fix to this mechanical problem was found and consisted of the following.

The brake problem has been solved by removing one brake plate and one separator plate and increasing the thickness of the separator plates to .084 in. The capability of the brake to perform to design specifications has not been compromised by this reduction in the number of plates.

The addition of these thicker (and more rigid) separator plates has resolved this problem.

Brake Sizing Air pressure available to lift off springs:

Maximum pressure - 43 psi
Minimum pressure - 31 psi
Piston area - 30.2 in^2
Maximum lifting force - 1300 lb
Minimum lifting force - 935 lb
Brake disc size: OD 7.00-inch, ID 4.825-in
Plate thickness - 0.070 in
Liner thickness - 0.022 in
Number brake plates - 6
Brake area (total) - 220 in^2
Number of separator plates - 7
Thickness of S plates - 0.084 in
Total brake stack height - 1.272 in
Total surfaces - 13
Clearance per surface - 0.0156
Total clearance - 0.180 in
Allow piston travel of 0.180 in

Outer Spring Data

Preload - 270 lb
Preload length - 2.08 in
Maximum load - 400 lb
Wire diameter - 0.365 in
Free length - 2.535 in
Spring O D - 2.7 in
Total coils - 5.00
Spring rate - 609.94 lb/in
Working stress - 60,409 psi
Solid stress - 65,475 psi

Inner Spring Data

Preload - 205 lb
Preload length - 2.30 in
Maximum load - 350 lb
Wire diameter - 0.295 in
Free length - 2.841 in
Spring O.D. - 1.900 in
Total coils - 6.75
Spring rate - 506.13 lb/in
Working stress - 71,430 psi
Solid stress - 87,828 psi

Moments of Inertia (at the brake) lb-ft sec^2

Turbine and gearbox - 0.0984
Brake - 0.00096
Gearbox drum and load - 0.00588

Total 0.1053 lb-ft sec^2

Total Energy Dissipated

Turbine energy - 45,600 lb-ft
Load deceleration energy - 2,720 lb-ft
Load holding energy - 47,200 lb-ft
Brake energy - 460 lb-ft

Total energy - 95,980 lb-ft

Heat Generation - Emergency Stop/Temperature Rise

During an emergency stop and assuming that all energy is momentarily absorbed in the separator plates, the heat rise of these plates is calculated as follows:

$\Delta T = \frac{E}{CpW}$ where E = system energy to be dissipated, BTU
Cp = spec ht of plates, BTU/lb-°F
W = weight of plates, lb

$E =$
$E = 95{,}980$ lb-ft x $0.00128 \frac{BTU}{lb\text{-}ft}$
$= 123$ BTU

$Cp = 0.107$

$W = \frac{\pi}{4} (7^2 - 4.825^2) (.084) (7) (0.285) = 3.385$

$\Delta T = \frac{123}{.107 \times 3.385} = 340°F$

This value is low enough to ensure a reasonable margin to take care of nonuniform loading, design assumptions, etc.

Hoist System Valving

The pneumatic supply for each hoist drive is controlled by a valve package consisting of an on-off valve and modulating valves for the hoisting and reverse turbines. In addition, there is an on-off valve controlling the air supply to the brake release piston. Location of the valves when installed on the hoist may be seen in Figure 35, and a summary of valve requirements is shown in Table 3.

The on-off valve is supplied by Whittaker Controls of Los Angeles, California, their part number being 22664. The valve is a 2-1/2-inch aluminum body, solenoid pilot actuated butterfly on-off valve with an 18-to 30-volt DC continuous duty solenoid. The actuator operating pressure is 30 psig to 50 psig. The electrical receptacle mates with a MS 3116E-12-8S plug. Figure 36 shows the valve while attached to the bifurcated duct.

Valve operation is as follows: A 28-volt DC signal to the solenoid positions the pilot valve, which in turn pressurizes the piston actuator cavity. Mechanical linkage moves the butterfly vane open. The piston is spring loaded closed. When the solenoid is de-energized, the pilot valve vents the piston cavity to atmospheric pressure, resulting in the butterfly vane closing the bleed air passage. A schematic of the valve is shown in Figure 37.

From the downstream side of the on-off valve the air duct bifurcates and attaches to the two parallel mounted modulating valves, one valve controlling air to the hoisting turbine wheel and the other valve controlling the supply to the reverse turbine wheel. These two valves are identical. The valves are supplied by Parker Hannifin to their part number 2720110 and are 2-1/2-inch steel body butterfly modulating control valves. The valve operating pressure is 30 PSIG to 65 PSIG, with a proof pressure of 120 PSIG and burst pressure of 240 PSIG. The valve response time from fully closed to fully open to a step change in current from 0 to 250 milliamps is .255 second maximum. The valve inlet flange is per Marman P/N 4560-250S and the outlet flange is per Marman P/N 4550-250S. The electrical receptacle is per MS27479E10C5P.

The torque motor, pilot valve, and actuator portion of the modulating valves were qualified for the L-1011 fixed-wing aircraft air turbine motor. The valve is illustrated in Figure 38.

The modulating valve operation is as follows: The electronic controller supplies current (0 to 250 milliamps) to the torque motor, which positions the pilot valve. The pilot valve, being ported to both sides of the actuator piston, pneumatically

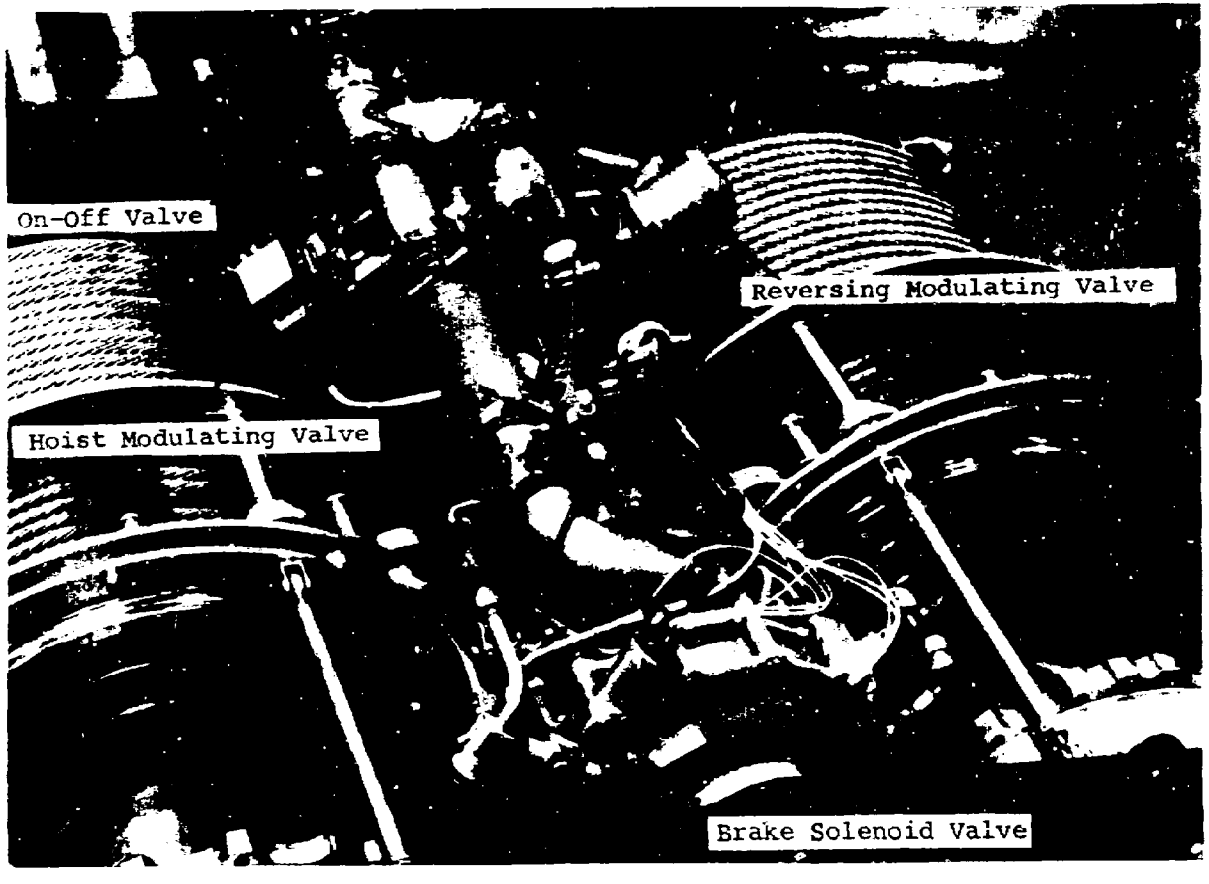


Figure 35. Control Valves Installed on the Hoist Drive.

TABLE 3. SUMMARY OF VALVE REQUIREMENTS

VALVE FUNCTION	DESCRIPTION	VOLTAGE REQUIREMENTS	CURRENT REQUIREMENT	RESPONSE	ALLOW. INT. LEAKAGE CLOSED	ALLOW. Δ P OPEN
ATM SHUT-OFF	NORMALLY CLOSED ON-OFF TYPE	17 VDC MIN. 32 VDC MAX.	500 mA @ 32 VDC - 65°F	2000 MS	.35 LB/MIN	0.5 PSI
HOIST & REV. TURBINE MODULA-TORS	NORMALLY CLOSED CURRENT MODULATED	----------	250 mA @ 16.5 VDC MAX. STEADY STATE + 125°F	250 MS CLOSED TO OPEN 70 MS TO Δ 25 mA CHG	3.0 LB/MIN	-------
BRAKE RELEASE	NORMALLY CLOSED - DISCH. VENTED TO ATMOS. IN CLOSED POS. ONLY ON-OFF TYPE	17 VDC MIN. 32 VDC MAX.	300 mA @ 32 VDC - 55°F	15 MS	0.11 LB/MIN	-------

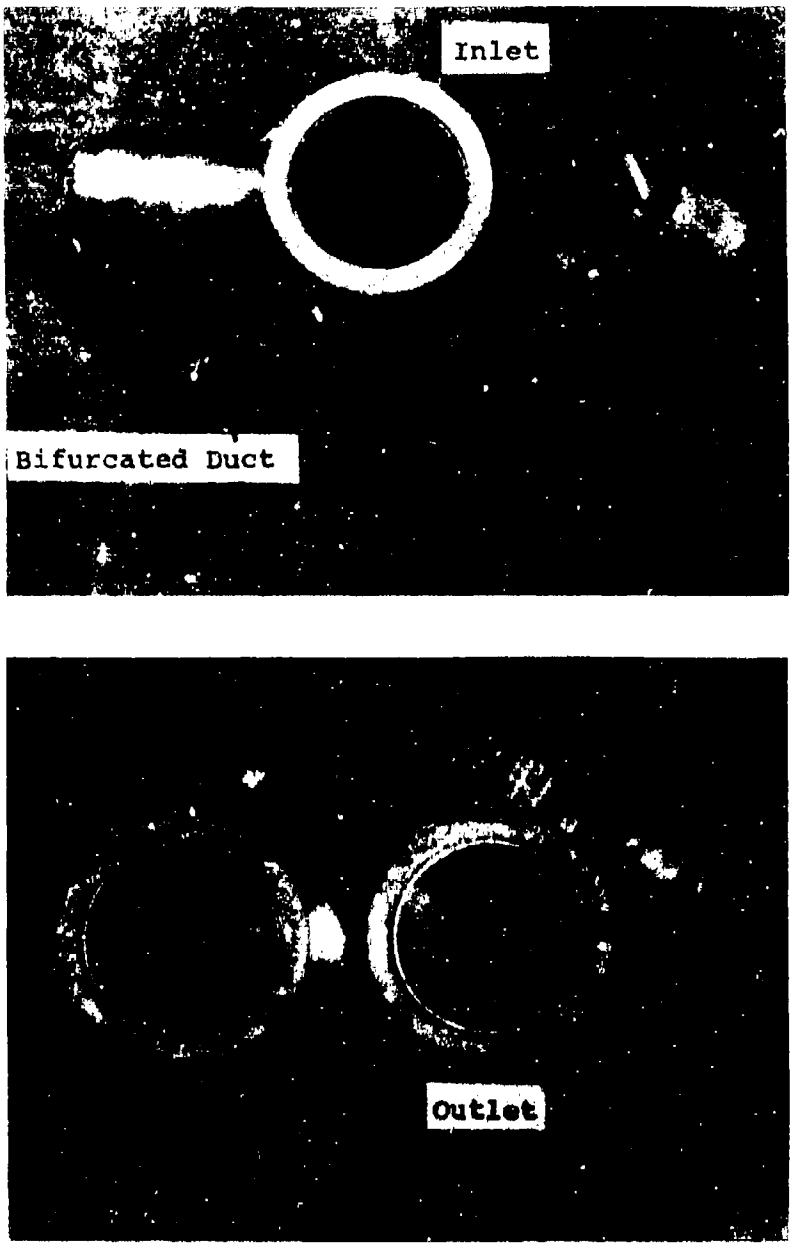


Figure 36. On-Off Valve.

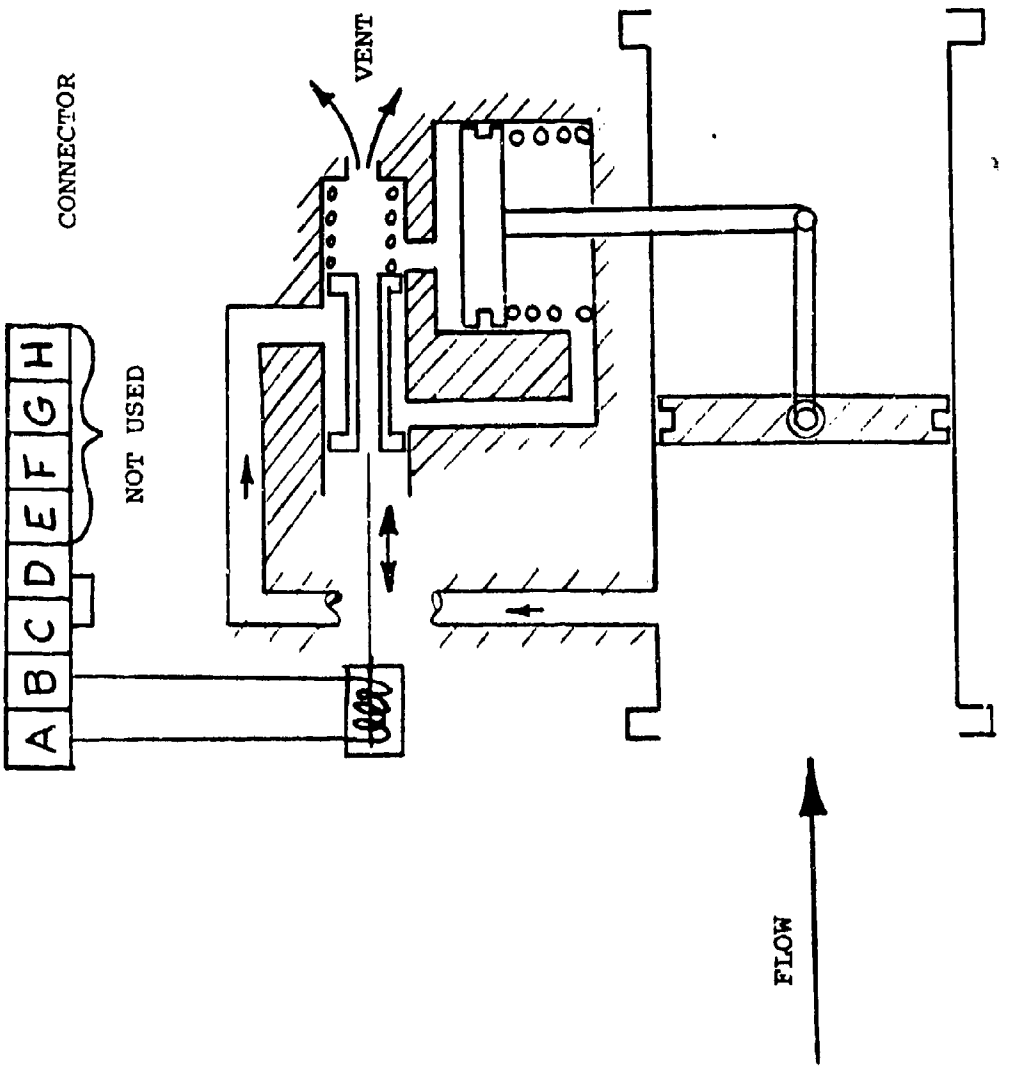


Figure 37 On-Off Valve Schematic.

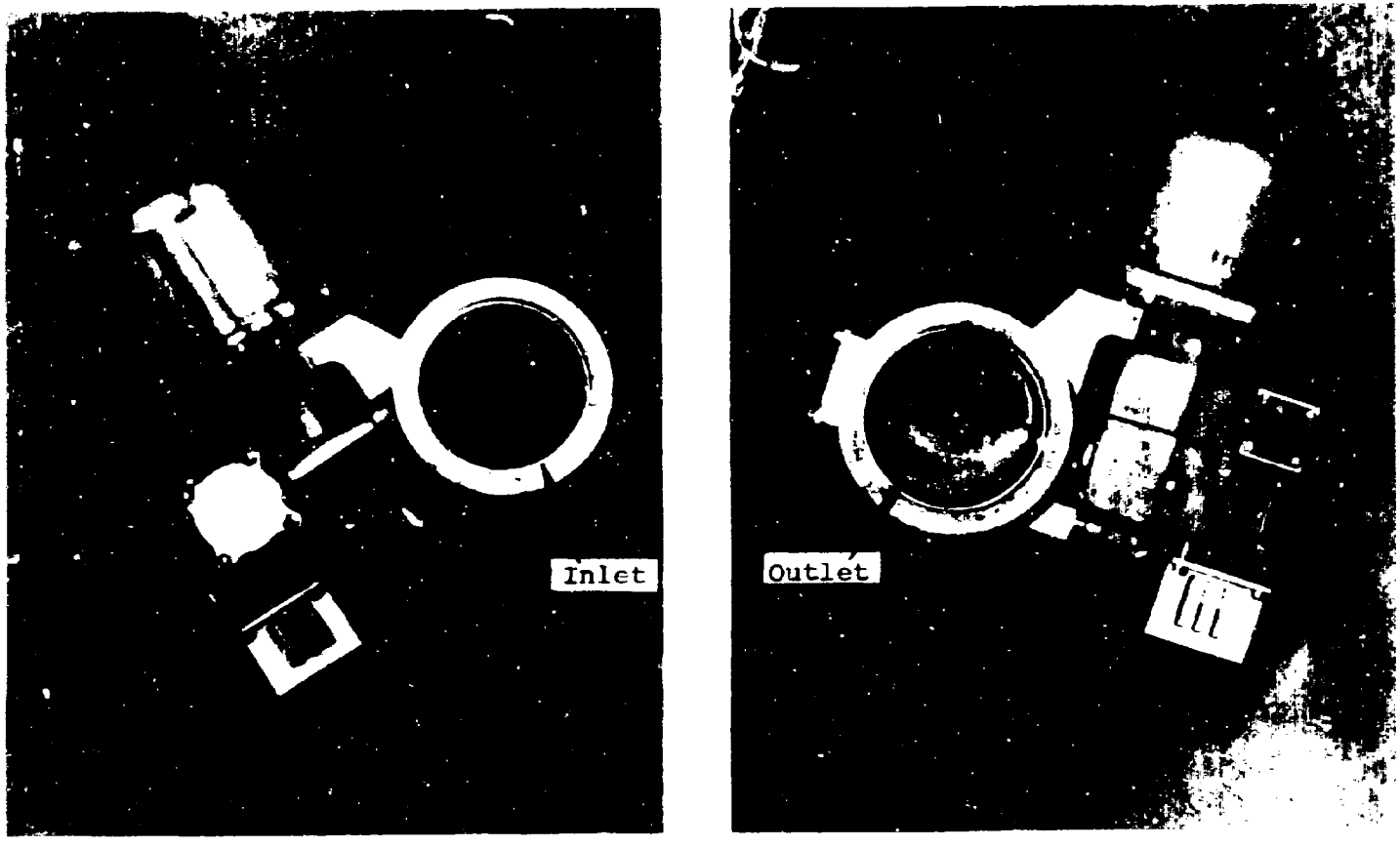


Figure 38. Modulating Valve.

locates the piston. Mechanical linkage from the piston positions the butterfly vane to supply the required bleed air mass flow. A schematic of the modulating valve is shown in Figure 39.

A 2.5-inch-diameter flexible duct from one modulating valve connects to the air inlet of the hoisting turbine. The other modulating valve outlet is reduced to 1.5-inch diameter, and a 1.5-inch flexible duct connects to the inlet of the reversing turbine.

Downstream from the on-off valve and before the inlet to the reverse turbine modulating valve a half-inch-diameter tapping directs air to the brake solenoid valve mounted on the brake assembly. This valve is a three-way two-position, normally closed, solenoid operated valve with an 18-32 volt DC coil. The coil is protected in an explosion-proof and water-tight solenoid enclosure. The rated operating pressure is 10 PSIG to 200 PSIG. Electrical receptacle is per Bendix P/N JT02R2-12-4P. The valve is supplied by the Automatic Switch Company to their part number HVA-162-743E. Figure 40 illustrates the valve.

The solenoid valve is used to pneumatically release the brake assembly, which is normally "ON". Air pressure at 45 PSIG is supplied to the brake valve. When the valve is energized, the air pressure moves the brake piston, which releases the brake. By de-energizing the valve, the brake cavity is vented to atmospheric pressure; therefore, setting the brake. A schematic of this valve is shown in Figure 41.

Hoist Control System. The control system design is shown schematically in the functional logic diagram shown in Figure 42. A description of the HLH control functional logic diagram is as follows.

The speed command from the control station provides a variable reference to the speed comparator. This AC signal has an amplitude proportional to command speed. The phase with respect to the reference phase indicates direction of command speed, up to down. The AC speed command is converted by means of a synchronous phase demodulator to a DC voltage whose amplitude is proportional to command speed and whose polarity is a function of the direction of commanded speed. The range of the DC signal is + 5.0 VDC for $\pm$ 120 ft/min or $\pm$8000 rpm (41.67 mV/fpm or 0.625 mV/rpm).

The DC speed command provides the reference input of a sum and difference amplifier which functions as a speed comparator whose variable speed input is derived from dual magnetic speed and direction sensors on the output shaft of the ATM gearbox. The magnetic speed sensor outputs are converted to DC by a frequency to voltage converter and a six-pole low-pass active filter. The phases of the two magnetic speed sensor outputs are compared to sense direction of rotation of the output

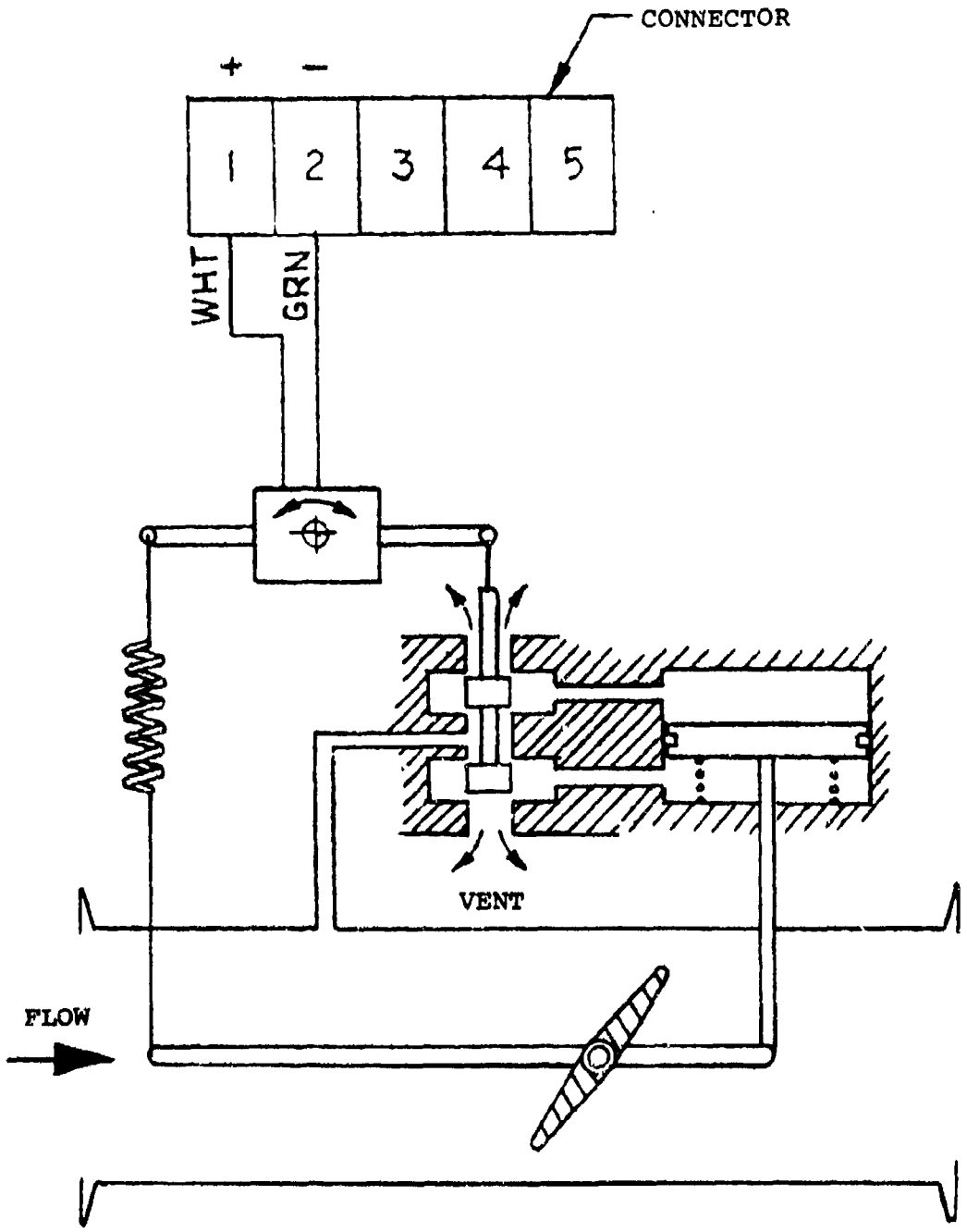


Figure 39. Modulating Valve Schematic.

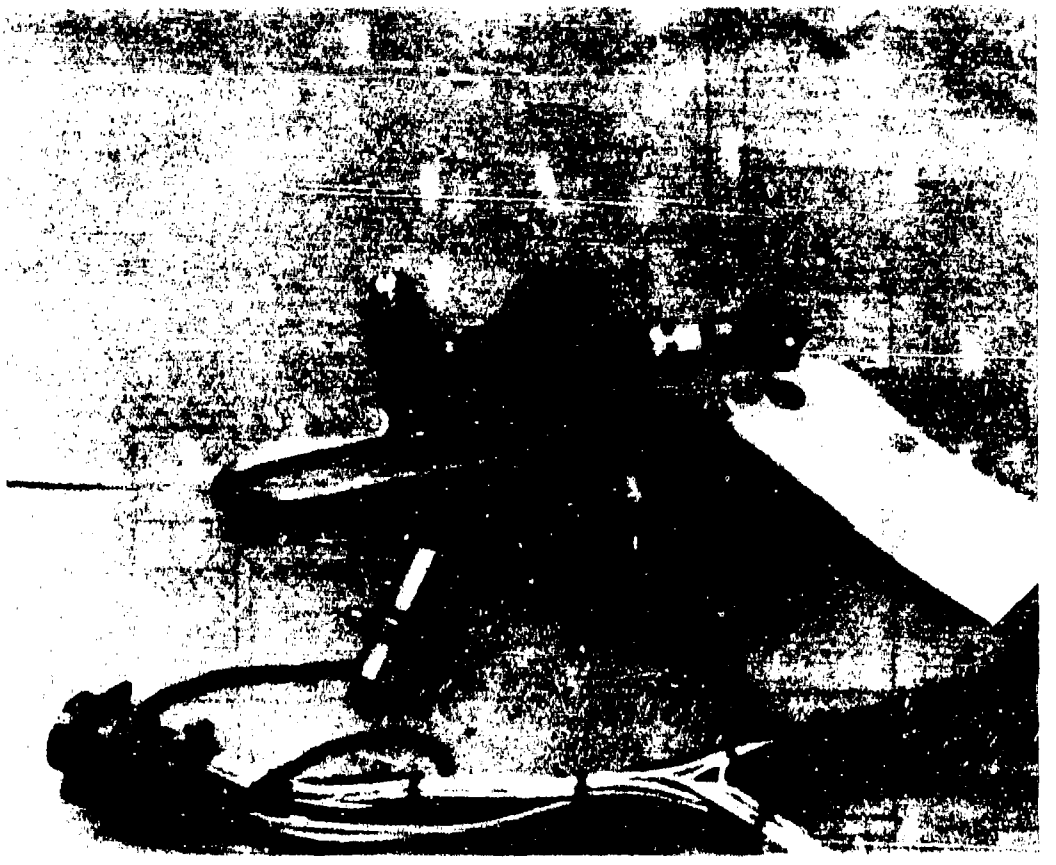


Figure 40. Brake Solenoid Valve.

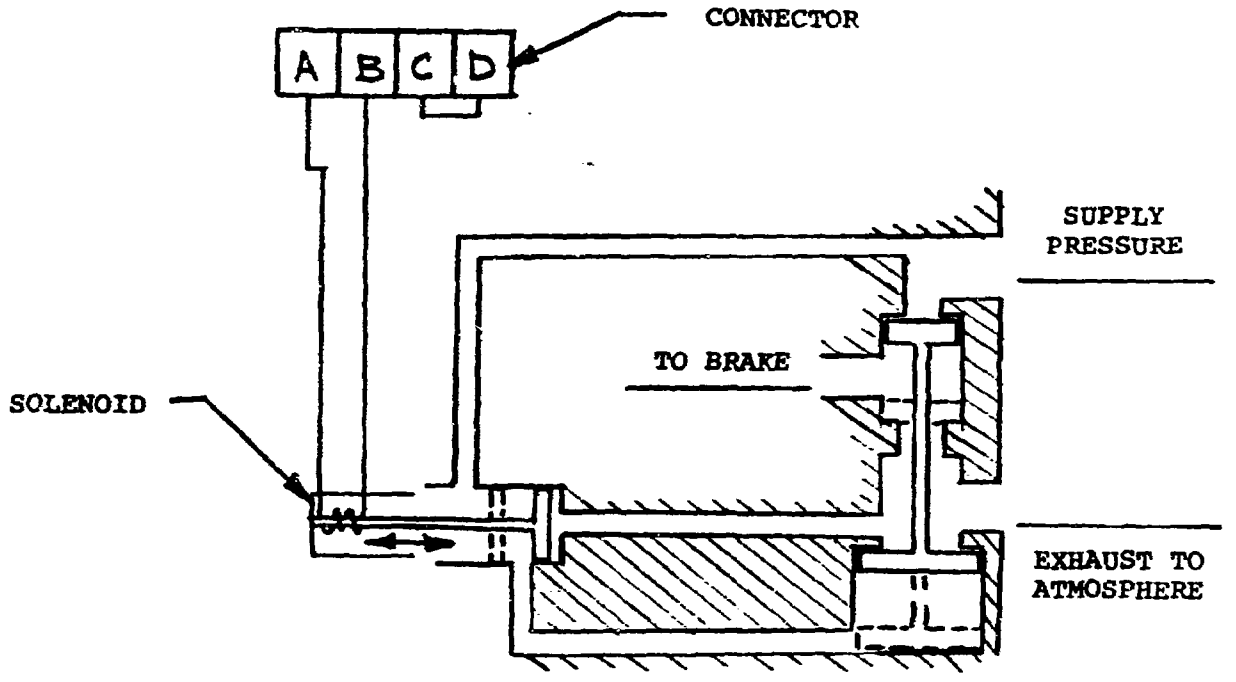


Figure 41. Brake Valve Schematic.

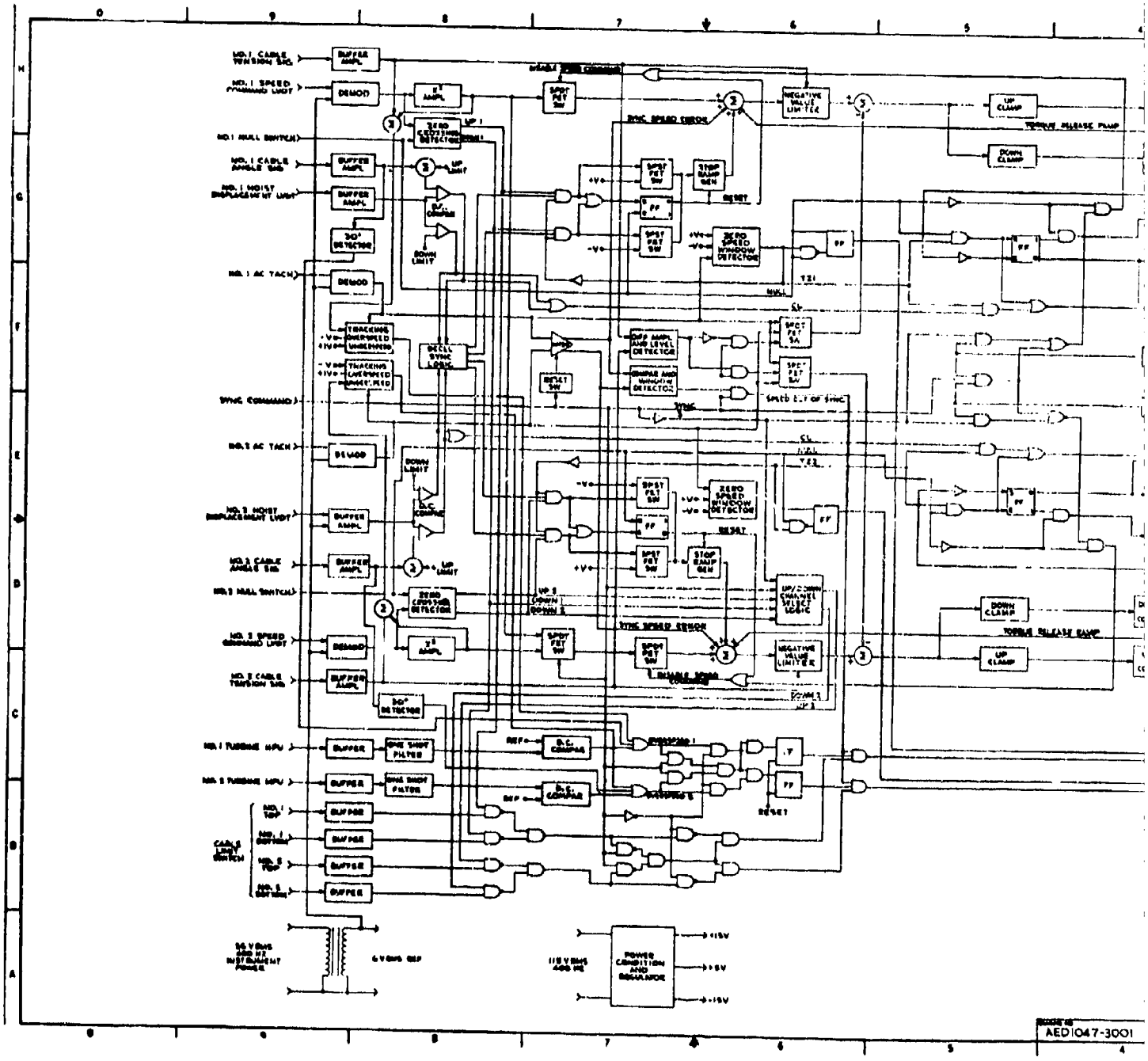
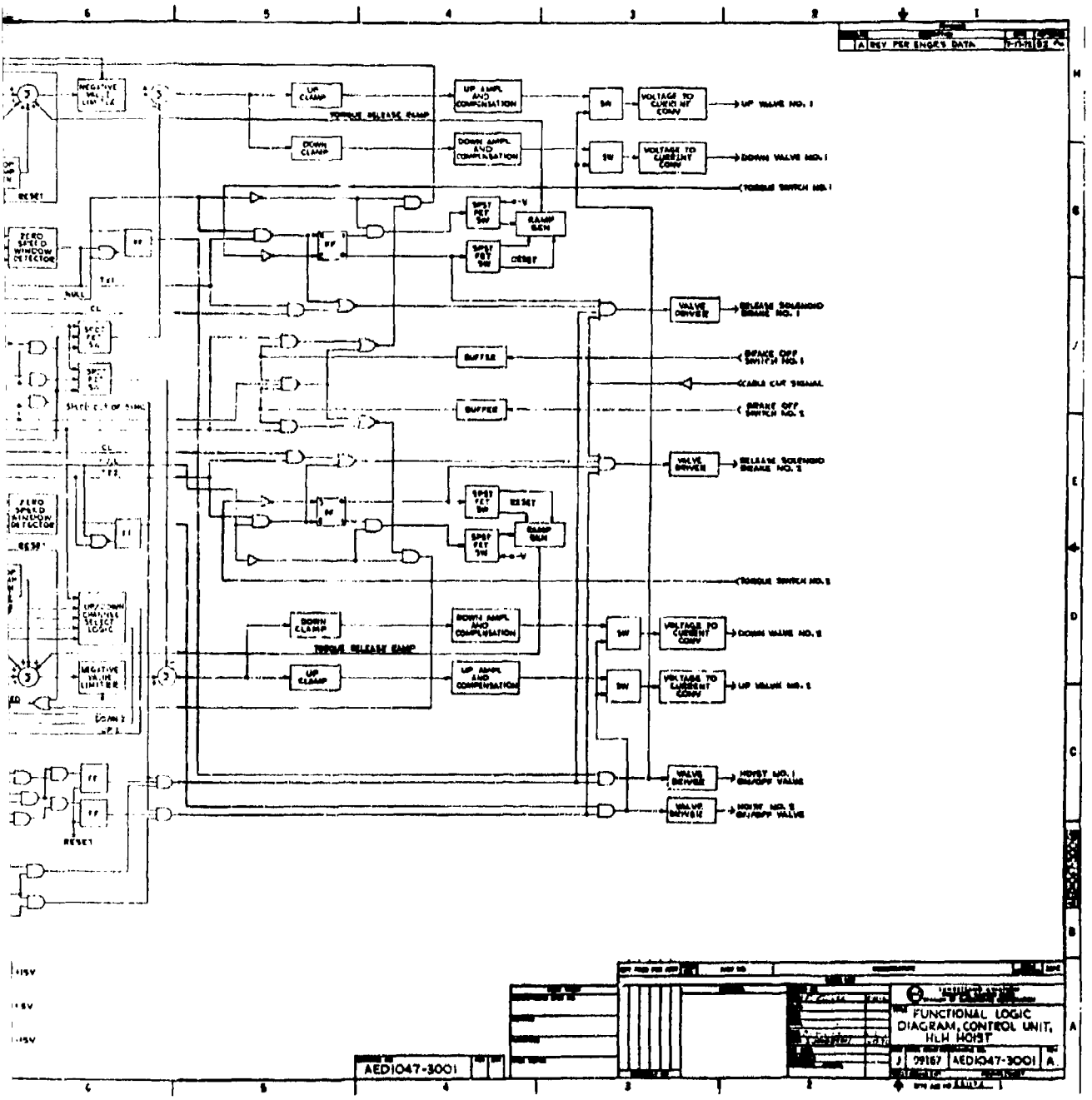


Figure 42. Hoist Functional Logic Diagram.


A REV PER ENGR'S DATA
UP CLAMP
DOWN CLAMP
TORQUE RELEASE CLAMP
UP AMPL AND COMPENSATION
DOWN AMPL AND COMPENSATION
VOLTAGE TO CURRENT CONV
UP VALVE NO. 1
DOWN VALVE NO. 1
TORQUE SWITCH NO. 1
SPEED SET SW
RAMP GEN
ZERO SPEED WINDOW DETECTOR
VALVE DRIVER
RELEASE SOLENOID BRAKE NO. 1
BUFFER
BRAKE OFF SWITCH NO. 1
CABLE CUT SIGNAL
BRAKE OFF SWITCH NO. 2
RELEASE SOLENOID BRAKE NO. 2
TORQUE SWITCH NO. 2
DOWN VALVE NO. 2
UP VALVE NO. 2
HOIST NO. 1 BRAKE OFF VALVE
HOIST NO. 2 BRAKE OFF VALVE
RESET
FUNCTIONAL LOGIC DIAGRAM, CONTROL UNIT, HLH HOIST
AED1047-3001
A

2

shaft. This information is converted to a DC voltage whose amplitude is proportional to speed and polarity as a function of direction. Two other inputs to the reference input of the speed comparator modify the speed command. These will be discussed later.

The conditioned cable tension signal is used to limit the maximum command speed in the down direction to 60 ft/min when a load of 16.8 tons on either hoist is detected. The velocity limitation between 60 and 120 ft/min approximately proportional to load between 0 and 16.8 tons. The up velocity control is not limited by the cable tension.

The output of the speed comparator difference amplifier is inverted and integrated in parallel circuits. These outputs are then summed together to yield a signal in which the speed error is zero and thus a Type 1 control system. The output of the summer is a voltage proportional to the valve angle required to achieve the commanded speed. This output is split to the up and to the down valve voltage to current converter circuits. Clamps are provided in each branch to limit the maximum current to 300 mA and the unused polarity of the signal to zero mA. The up and the down valves are provided with individual amplifiers and compensation circuits since they will in all probability have different requirements. A polarity reversal is required in the down valve amplifier.

Valve disable switches (MVD) are included for each modulating valve to close the modulating valves when the ON/OFF air valve is closed (HVE). The modulating valves will also be commanded to close if a malfunction is detected by the malfunction detection system (MDE).

The two additional inputs to the speed command summing amplifier which modify the speed command reference voltage are the sync speed error and the torque release ramp. These circuits generate voltages which add to or subtract from the demodulated speed command voltage and therefore modify the hoist velocity to meet the immediate demand.

The sync speed error is only present when the two hoists are operated simultaneously and the sync command is present. In this case the difference between the demodulated speed signals from the two ATM's is integrated to produce two error signals of opposite polarities to drive the slower hoist up in velocity and to drive the faster hoist down in velocity.

A deceleration control circuit is used to slow the hoists to a rate of approximately 20-25% of the speed command when the end of permitted cable travel is sensed at 7 and 95 feet. The cable limit switches (top and bottom) are used to stop the hoists at 2 feet or 100 feet. Either limit switch disables the speed command and prevents further response to the speed command. When zero turbine speed is detected, the brake and ON/OFF valves are closed. This condition is maintained until the speed command is returned to null. The system can be removed from the limit switches by commanding a speed in a direction opposite the limit switch which has been tripped. In the synchronized mode the deceleration is initiated by the decel sync logic which monitors both cable length comparator circuits. The first hoist to reach the end of permitted travel decelerates both hoists.

The end of permitted cable travel is sensed by a cable length transducer and a cable angle transducer. Both of these signals are DC voltages with the same range as the speed command voltages. The cable length signal is compared with a fixed down reference voltage and an up reference voltage which is also proportional to the cable angle. At zero degrees cable angle the fixed upper limit predominates,but as the cable angle increases toward 30 degrees the up limit is reduced so that the deceleration control will stop the hoist before 30 degrees is reached.

The second input which modifies the speed command voltage is the torque release ramp. This circuit is used only during the start of the hoist or reverse mode. Its purpose is to verify that the turbine is capable of holding the load prior to releasing the brake. This is accomplished by disconnecting the speed command and generating a short "up" speed ramp until the torque limit switch on ATM output shaft closes. This torque signal is stored and used to reset the ramp to zero and "enable" the brake release solenoid driver. Since turbine speed is still zero and an up or down speed command is detected, the proper logic is set up to release the brake. A brake off switch indicates that the brake has released and this signal is used to reconnect the speed command. During synchronous operation, both brake off signals must be present before the speed command is reconnected. The system will now respond to the speed command until it is removed or until the cable limit comparator detects the end of the permitted cable travel. Either of these conditions will cause the brake logic to set the brake when turbine speed is reduced to less than 150 rpm. A valve driver

consisting of a static switch amplifies the low level logic signal to energize the brake release solenoid.

Zero turbine speed is determined by monitoring the demodulated magnetic speed sensor signal with a voltage window detector, consisting of a pair of level detectors. When the DC voltage proportional to turbine speed is less than the prescribed level representing zero speed (150 rpm), a positive output is generated to the brake release logic and removed from the deceleration control circuit.

During synchronous operation the fore hoist speed command signal is used as the speed reference for both hoists. An analog switch disconnects the aft hoist speed command from the aft speed comparator and connects the fore speed command to both reference inputs of both speed comparators. This assures that any tracking differences between the two speed command signals will not affect synchronous operation.

A null command is generated within the controller by monitoring the speed command demodulator output with a window detector. The detector also generates an up or a down command to "enable"the cable limit circuits and the underspeed detector. The speed command null signal provides one of the "enable" signals to the torque test circuits and the valve control circuits.

A malfunction detection system monitors turbine speed and output shaft speed. The two overspeed detection systems are redundant. The logic is configured so that if each hoist is used independently, detection of an overspeed will shut down the hoist involved, but if the two hoists are operating in sync, any one malfunction will shut down both hoists simultaneously.

The primary overspeed circuit is a tracking overspeed detector which monitors the ATM output shaft via the demodulated magnetic speed sensor signal. This detector reference is the absolute value of the speed command signal plus a voltage equivalent to 15% of the full-scale speed command to determine the overspeed trip level. This voltage is delayed during negative slope changes on speed command (such as reducing the speed command to zero) by a period equivalent to the ATM system response time. Since the variable reference follows the actual speed command, it must be prevented from falling below the turbine speed signal until after the turbine speed has been allowed to decay to zero or at least below the reference. Thus, for low-to-medium speeds this circuit will be able to track the actual speed command and generate an overspeed shutdown well before the turbine

reaches 110% of maximum speed.

An underspeed detector is also used to detect loss of control. Three seconds after the speed command is initiated, the underspeed detector will cause the ATM to shut down immediately if the hoist velocity is less than one-half of the command speed.

The secondary overspeed detector is fixed at 110 percent of maximum speed. Its input is from a third magnetic speed sensor which is located on each turbine shaft. The magnetic speed sensor signal is conditioned and shaped to drive a one shot multivibrator whose on time is equal to one-half the period of MPU frequency at 110% turbine speed. This output is filtered by an active low pass filter to obtain a DC voltage proportional to turbine speed. This proportional voltage is compared with a fixed DC reference voltage in a level detector. If the turbine speed exceeds the 110% limit, the proportional voltage will exceed the fixed reference and the level detector output will switch to and latch up in the overspeed shutdown mode. It will remain latched until the system power is removed.

Control System Speed Sensor Modification. During design development testing of the initial design hoist drives, three tach-generator failures were experienced. After the first failure, the method of mounting was examined and found to be deficient. The tach-generator vendor was contacted for recommendations and, as a result, design changes were made to provide better alignment and support of the outer casing and a damped, but resilient, connection to the shaft. After these changes were incorporated, two additional tachometer failures occurred. Since five were ordered originally, the program was left with two operational tachometers. The vendor was contacted for replacements and a 4-month delivery was quoted. Since the program could not tolerate the 4-month delivery time, it was decided to review the function of the device in the system for alternate approaches to providing the same function.

The advantages of the drag cup tachometer are:

Small size
Speed sensitivity
Directional sensitivity
Constant carrier frequency
Brushless
Linear with speed.

The disadvantages that developed as a result of this application are:

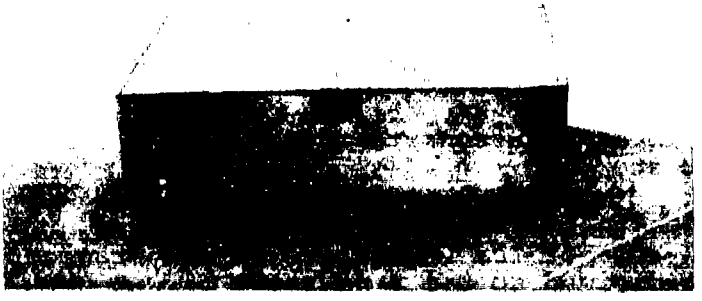
Difficulty in mounting
Poor vendor support
Temperature sensitivity (.1%/°C)
Cost.

In order to overcome these disadvantages and still retain some of the advantages of the drag cup tachometer it was decided to use a magnetic pickup (MPU) assembly, comprised of two MPU's mounted to provide a 90° electrical phase displacement with respect to one another in sensing gear tooth position. In this manner, direction of rotation as well as velocity can be obtained from the signals present. The breather gear would be modified for this by adding 45 slots to the face. With a gear rotation speed of 7000 rpm at a hoist speed of 120 fpm, 45 teeth will give an MPU output frequency of 5250 hz. Since it has been determined that the application of the brake can be tolerated at a maximum hoisting speed of 2.4 fpm, without reducing brake life, the speed sensing circuits must be designed to operate down to 105 hz without introducing cogging or unduly compromising the dynamic compensation of the speed control loop. This can be done by using a high order filter in the MPU signal processing circuitry.

Another advantage of the MPU approach is that a phase locking circuit can be designed into the synchronizing circuit thus providing zero speed error between the two systems during steady-state operation.

The redesign of the circuitry replacing the tach-generators with the magnetic pickups was completed and tested with the initial ATM design. The performance was satisfactory. The redesigned ATMs have the same circuitry utilizing the MPU's instead of the tach-generator.

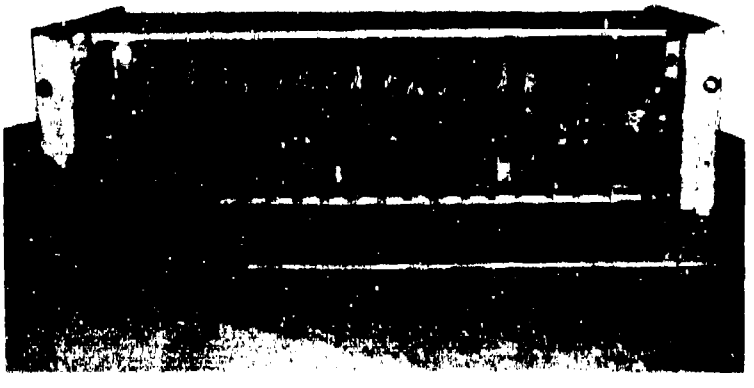
Figure 43 illustrates the hoist control unit.



Front View



Rear View



Inside View

Figure 43. Hoist Control Unit.

HOIST

Design Concept

The hoist design concept as presented in the proposal is reflected in Figure 44. The design represented one assembly of a 22.5-ton capacity dual-hoist system of conventional single-drum level-wind design based upon a 1.0-inch-diameter tension member. Informal in-house studies had rejected the single-point payout (SPP) hoist, as concepts then developed reflected a heavier design than the level wind (LW) hoist. Selection of the low-speed gearing arrangement was the result of a study comparing the following gear systems:

Fixed ring differential system
Four planetary system
Fixed sun differential system
Three-spur, two-planetary system
Two-spur, two-planetary system.

The system selected was a triple-planetary single-spur arrangement as shown in Figure 45.

Preceding the selection of a dual, movable, hoist concept for the proposal system, a number of alternate arrangements had been considered including:

Fixed hoist with movable sheave
Reeved cable system
Hoist installed in line with fuselage.

The fixed hoist with movable sheave would eliminate part of the complexity of moving the complete hoist. However, the additional cable length required a reduction in cable fatigue strength due to the additional bend over the sheave, together with cable fleet-angle problems, caused a considerable increase in projected system weight.

The reeved cable system has the potential of halving the tension member load. The requirement for doubling the cable length with the attendant accommodation problem, cable fatigue due to additional cable bending over sheave, and installation problems eliminated this alternative.

A hoist installation in-line with the fuselage provides a lift consistently on the aircraft center line. However, the resultant sheaves required to accept the longitudinal cable angles made this unattractive from a weight and cable fatigue comparison.

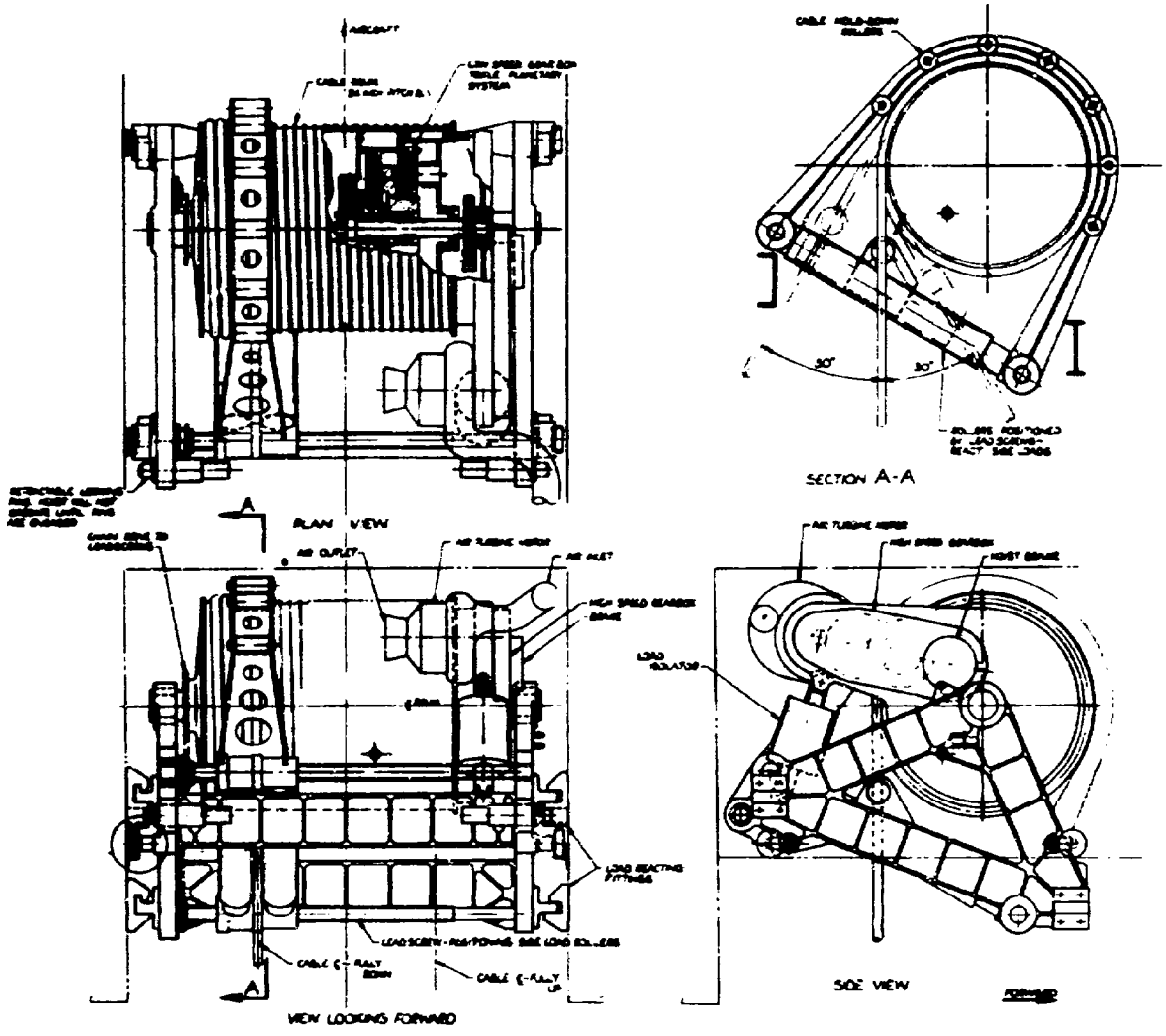


Figure 44. Proposal - Hoist Design Concept.

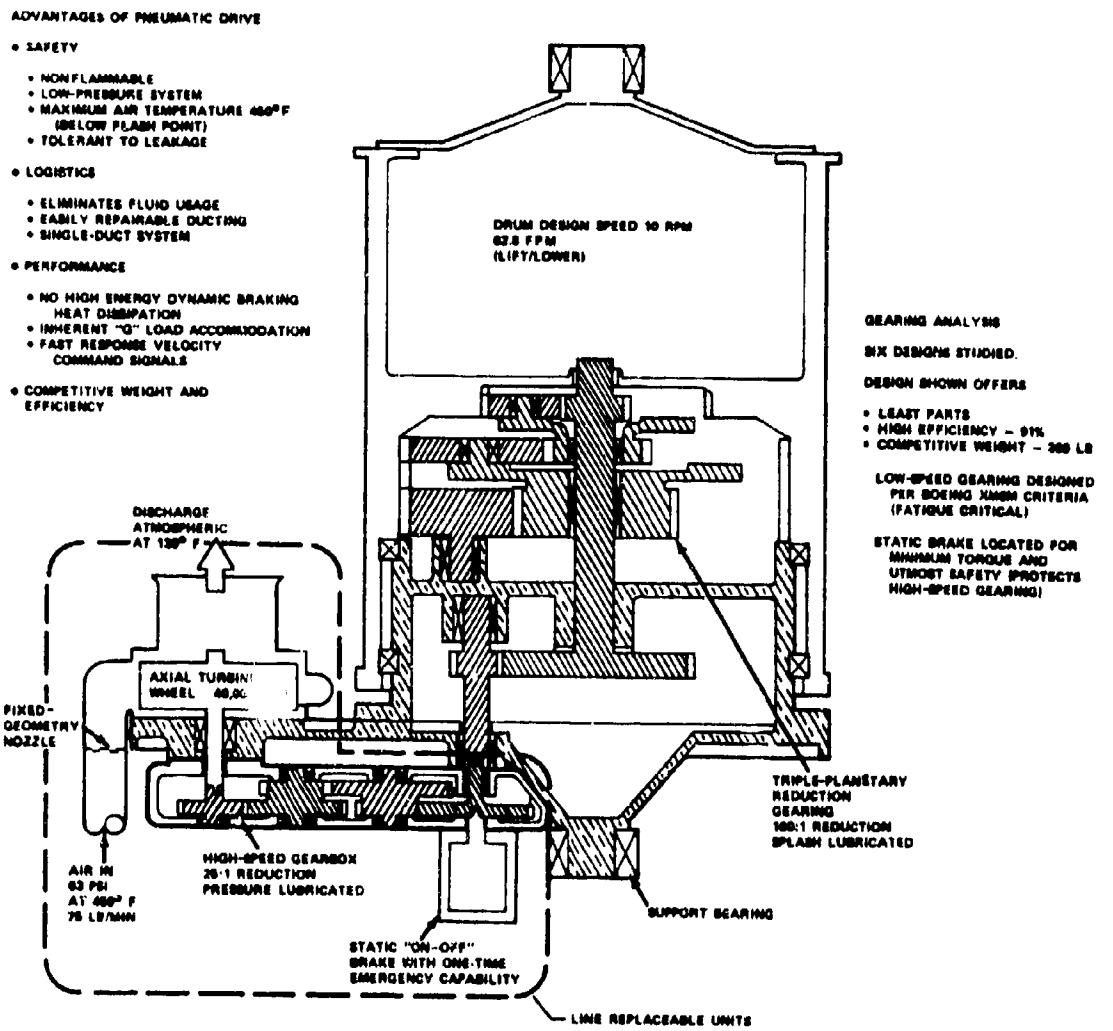


Figure 45. Baseline Gearing System - Triple Planetary.

Preliminary Deployment Concept Trade Study

Subsequent to the proposal submittal and prior to the contract award, a concept for a SPP hoist was developed that was potentially competitive with the LW winch in installed weight with the following advantages:

1. No lateral C.G. shift as the load is lowered or raised.

2. Attachment of an external pod is simplified as location of tension member is always on the aircraft longitudinal centerline.

3. Simple design eliminates a level-wind mechanism and its lead screws, ball-nuts, and drives.

The principal disadvantage was the increased length of the hoist, requiring a wider structural tunnel.

A preliminary design was evolved of the SPP hoist to a depth sufficient for a weight comparison with the conventional LW hoist design submitted in the proposal. The two design concepts are as follows:

Level Wind Hoist

The LW hoist concept is essentially the same as that shown in the proposal and a cross-section of the hoist comparable with the SPP design is shown in Figure 46. The side-load rollers are attached to traversing carriages mounted on a pair of lead screws. The lead screws terminate at the hoist side frames, supported in bearings and driven from the cable drum to synchronize movements. With the cable fully stowed, the hook will exit from the tunnel approximately 9 inches from the aircraft centerline on the LH side. With 100 feet of cable deployed, the cable will be approximately 9 inches from the aircraft centerline on the RH side.

Single-Point Payout Hoist

The SPP hoist concept is shown in Figure 47. The reduction gearing, primary drive, ATM and brake will be essentially the same as those for the LW hoist. Whereas in the LW concept, the final drive is direct from the gearbox to the inside of the drum; in the SPP design the final drive is to a central support tube extending from the gearbox housing to the far support frame. At a location coincident with the aircraft centerline, a flanged disc with integral ribs is mounted on the central support tube.

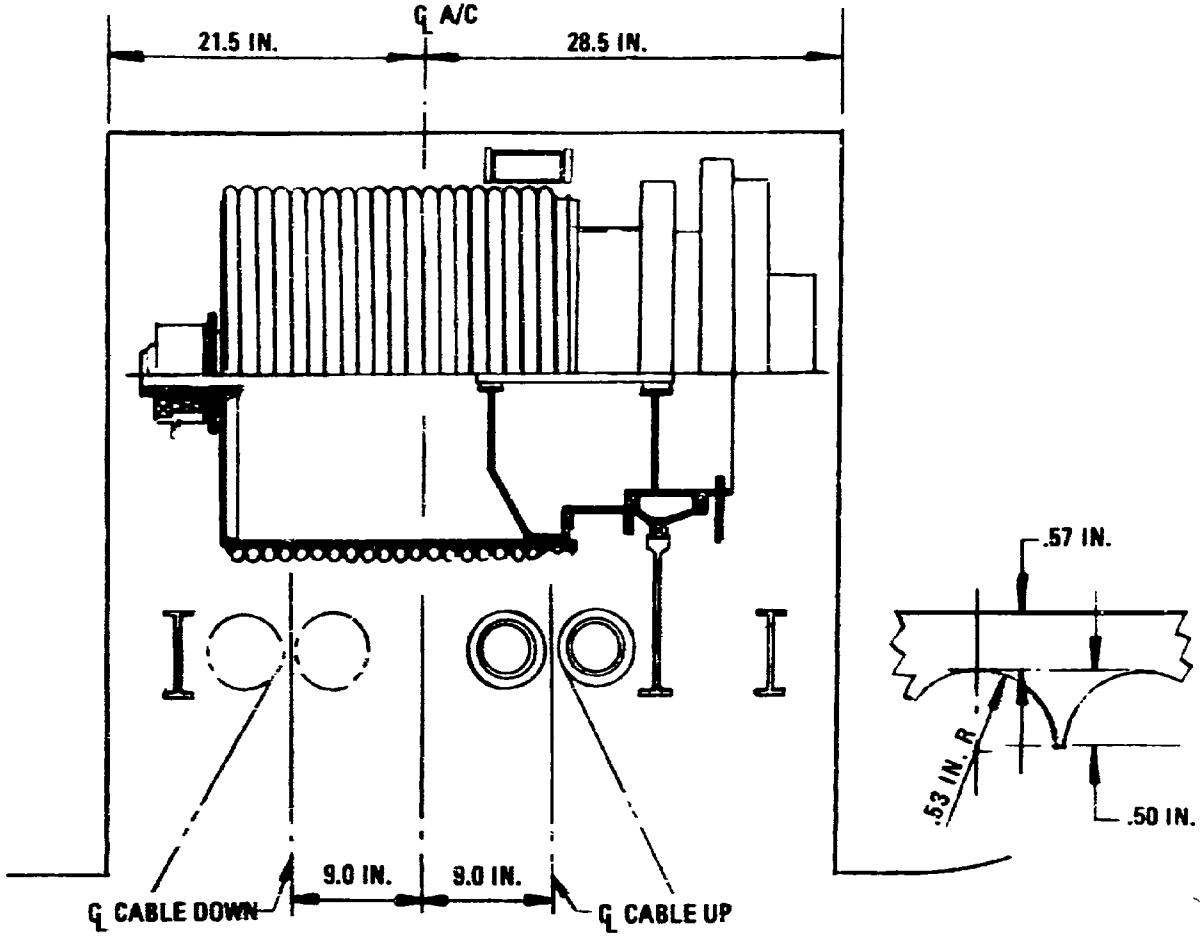


Figure 46. Level-Wind Hoist.

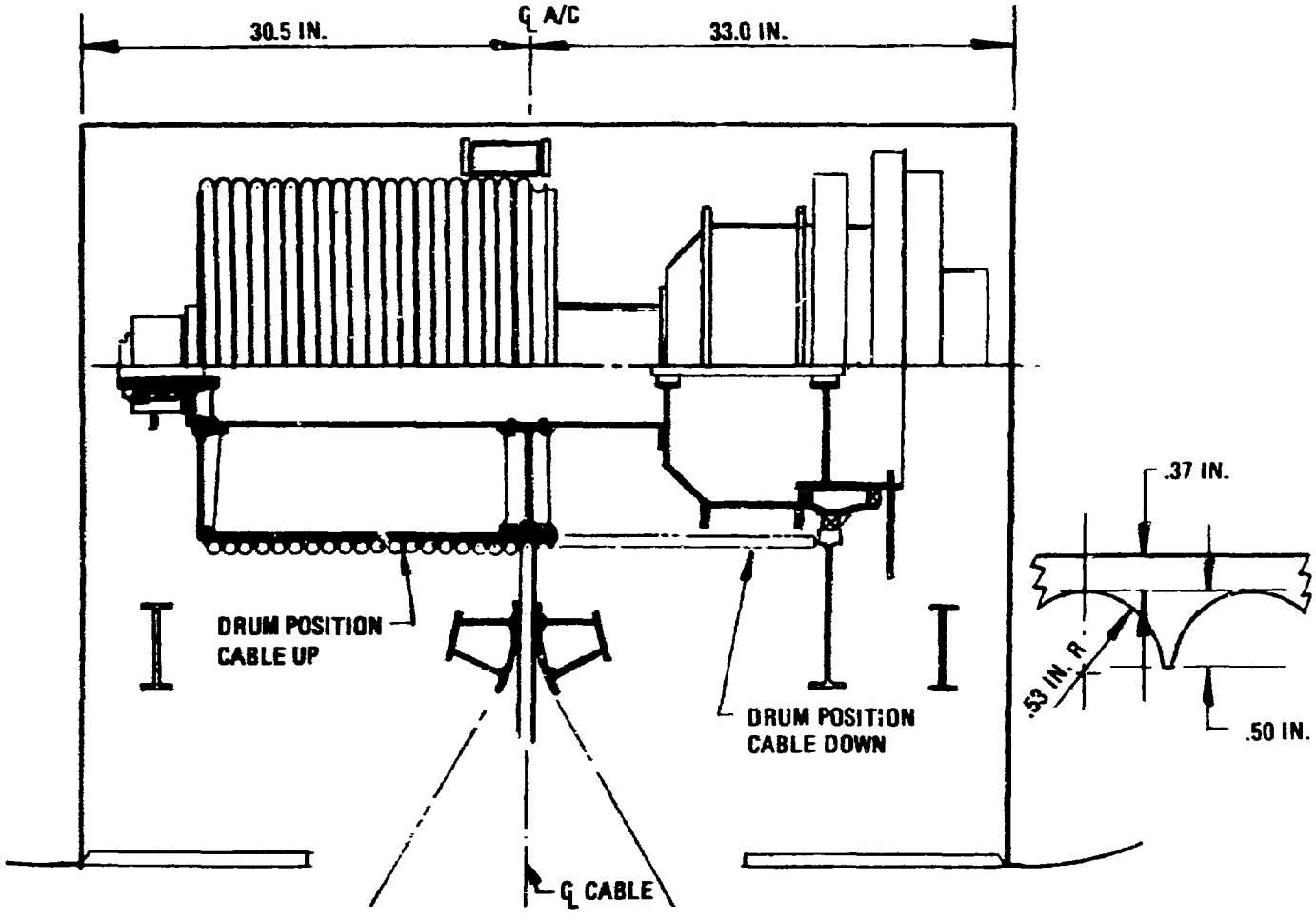


Figure 47. Single-Point Payout Hoist.

The outer rim of this disc mounts a number of linear ball race housings. Grooves on the inside surface of the cable drum match the linear ball races. The balls then support the cable drum and transmit the driving torque. The cable drum has a closure disc at its far end which locates on the central support tube. The outer drum is therefore free to move laterally while under torque. The cable exits between two side-load rollers supported on the hoist lateral frame members. As the cable pays out, the drum will move across the aircraft. A locating roller supported on the hoist frame and running inside the drum cable groove ensures the alignment of cable and drum.

The cable drum is the most significant component in assessment of hoist weight, and due to the SPP design always providing support to the drum at the point of load application, a significant reduction in drum wall thickness can be obtained.

Using the LW hoist configuration as a baseline, the weight difference for the SPP hoist is:

Drum	-70 lb
Level-wind mechanism	-69 lb
Ball spline units	+23 lb
Center support tube	+31 lb
Center support disc	+40 lb
Total	-45 lb

This study concluded that the concept for a SPP hoist was a viable candidate for the HLH hoist design.

Hoist Configuration Study

Release of the HLH ASRD reflected an increase in the cargo handling system capacity requirement from 22.5 tons, as proposed, to 28 tons. This increase in hoist capacity resulted in the projected tension member diameter increasing to 1.18 inches. As manufacturing facilities for cables in excess of 1.0 inch diameter were limited, and to reduce the size of major components such as the cable drum, a number of configurations for dual-cable hoists were evolved.

The advantages of a dual-cable hoist include:

1. Small cables have greater flexibility and higher strength/weight ratios than large cables.

2. Use of handed pairs of cable permits the use of the rotating type of cable construction and eliminates torque on the paired system. Rotating cables generally have higher strengths than nonrotating cables.

3. A dual-cable system provides a possibility of developing a "condition comparator" system to give indication of cable deterioration.

4. Smaller diameter cables are easier to handle, store and install. Cable drums and main support bearings are smaller and easier to fabricate.

Three basic configurations of dual-cable hoist were considered:

Twin Drum In-Line

The configuration shown in Figure 48 consists of two drums mounted on a common axis, driven by a centrally positioned low-speed gearbox. The drums would have opposite handed helices such that with the cables fully up, the cable spacing would be approximately 16 inches; when fully down, the spacing would be approximately 42 inches. The lower end of the cables would terminate at an equalizing beam. The cables pass between side-load rollers as they leave the drums; these rollers are mounted on lead-screws and synchronized to the drum rotation to ensure correct positioning of the cable. Configurations with 24-inch-and 18-inch-diameter drums were considered. The 18-inch-diameter configuration was rejected due to excessive width requirement. With cables fully out, the limit for lateral angle, retaining load sharing on the cables, is approximately 16°. This angle is a function of the length of the equalizing bar and to obtain the 30° angle capability required by the ASRD, this beam would have to be approximately 34 inches long, increasing the tunnel width to 82 inches. A tunnel width in excess of 70 inches would involve a considerable structural weight penalty.

Single Drum, Twin Cable

The configuration shown in Figure 49 is essentially similar to the single-cable level-wind hoist. The principal difference is the drum has a two-start helix, permitting two identical cables to be wound side-by-side. The side-load roller arrangement will require a third roller. The equalizing beam will be short and there will be no side-angle restrictions. The disadvantage of a level-wind hoist, i.e., the cable moving across the aircraft, is inherent in this design.

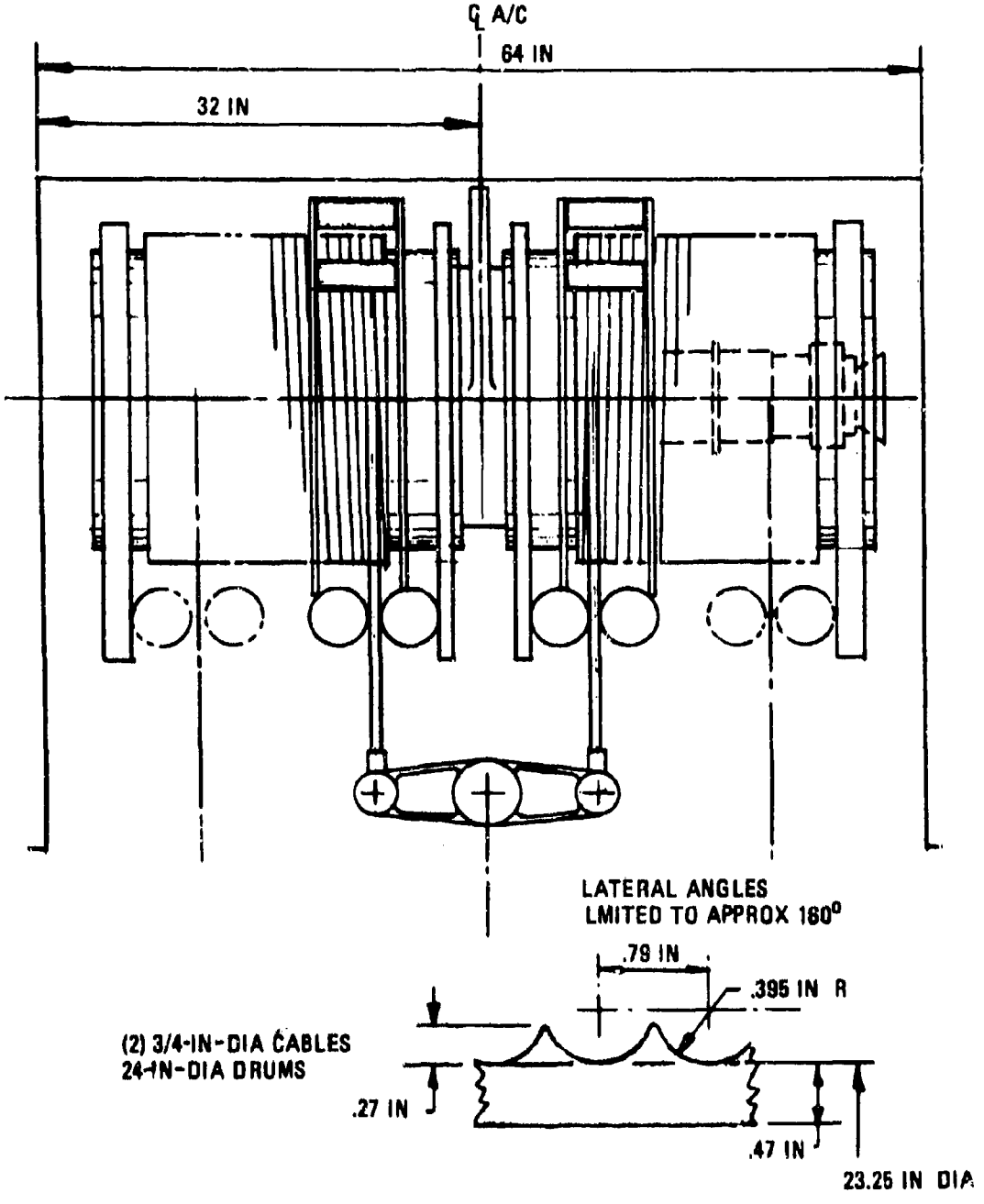


Figure 48. Twin-Drum In-Line Hoist.

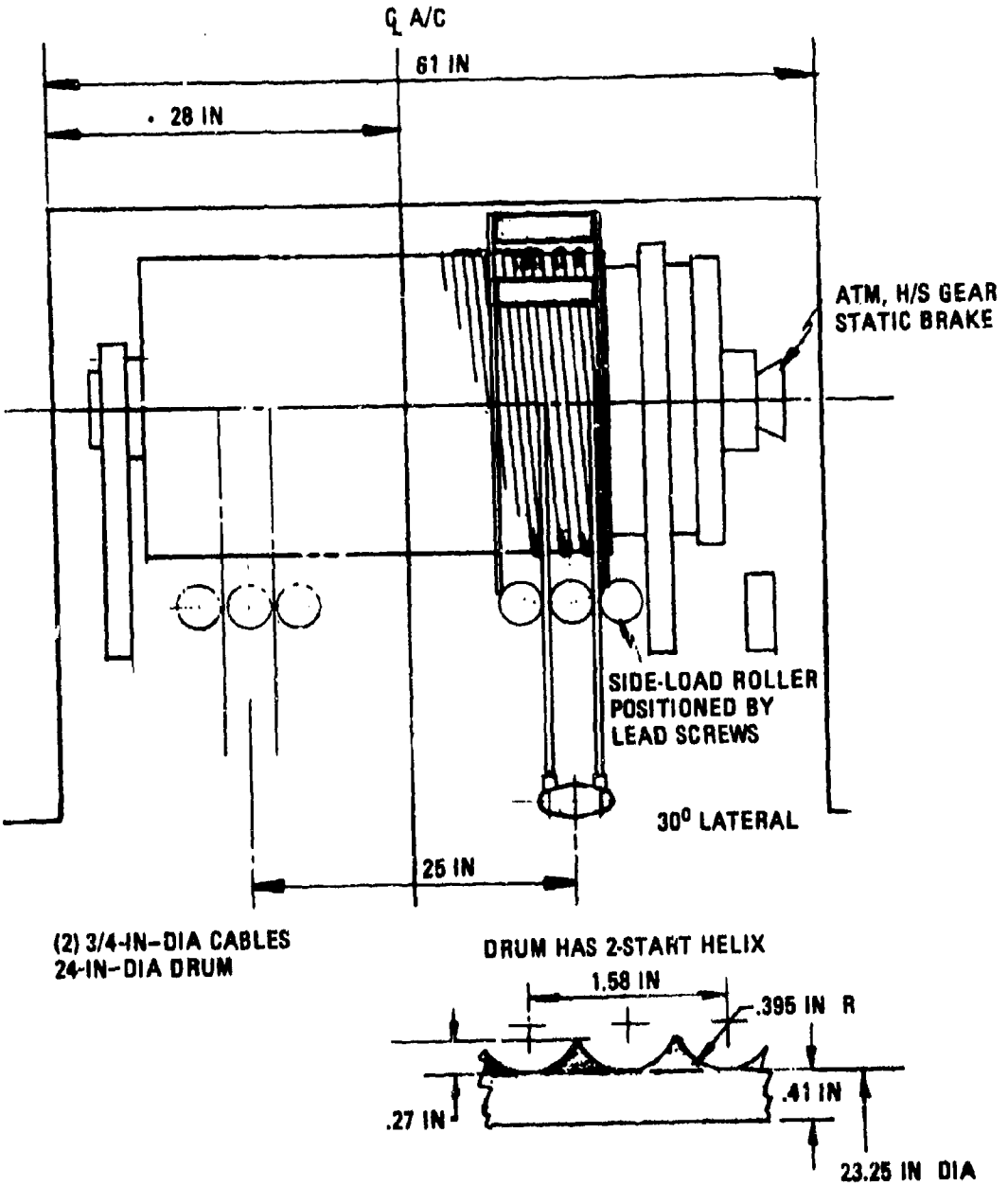


Figure 49. Single-Drum Twin-Cable Hoist.

Twin Drum, Parallel

The arrangement of two drums side-by-side driven from a common ATM and high-speed gearbox would permit either a level-wind or a single-point payout configuration. The configurations are shown in Figures 50 and 51.

This arrangement results in a relatively compact unit with no geometric restrictions to the lateral cable angles. Advantage can be taken of using smaller drums without the unit width being excessive.

A summary of the estimated weight and principal characteristics of the four configurations is shown in Table 4.

Configurations maintaining a single-point payout have some advantages over the level-wind system as presented previously.

An additional advantage of the single-point payout is the reduction in the maximum reaction at the structure interface. For example, the reaction of a corner mount fitting for an ultimate cable tension of 145,000 pounds vertically of the hoist arrangement shown in Figure 51 would be 36,250 pounds. For the configuration shown in Figure 50 , the maximum reaction of a corner fitting could be as high as 87,000 pounds. The configuration shown in Figure 51 utilizes a sliding drum concept requiring the use of multiple linear ball race units as splines. Although a new concept for application to the hoist design, there did not appear to be any significant technical problems.

In addition to the hoist weight comparison, this study also considered the effect of installation weight. The cargo hoist system proposal weight breakdown included 175 pounds for track and fittings, of which 140 pounds was for the load-reacting fittings on the tunnel side wall. Additionally, the structure weight breakdown had 300 pounds allocated to direct backup for the hoist installations. Considering this as one total, 440 pounds, and adjusting for the increased load due to the system capacity increase, results in 440 x 1.25 = 550 pounds of installation structure.

Assuming that this 550 pounds is a direct function of the sum of the maximum reactions of the level-wind hoist illustrated in Figure 50 and is comparable to the proposal installation, the structure weight will vary, as shown in Table 5, based on the installation geometry shown in Figure 52.

The total system and structural backup weights for the four configurations are shown in Figure 6.

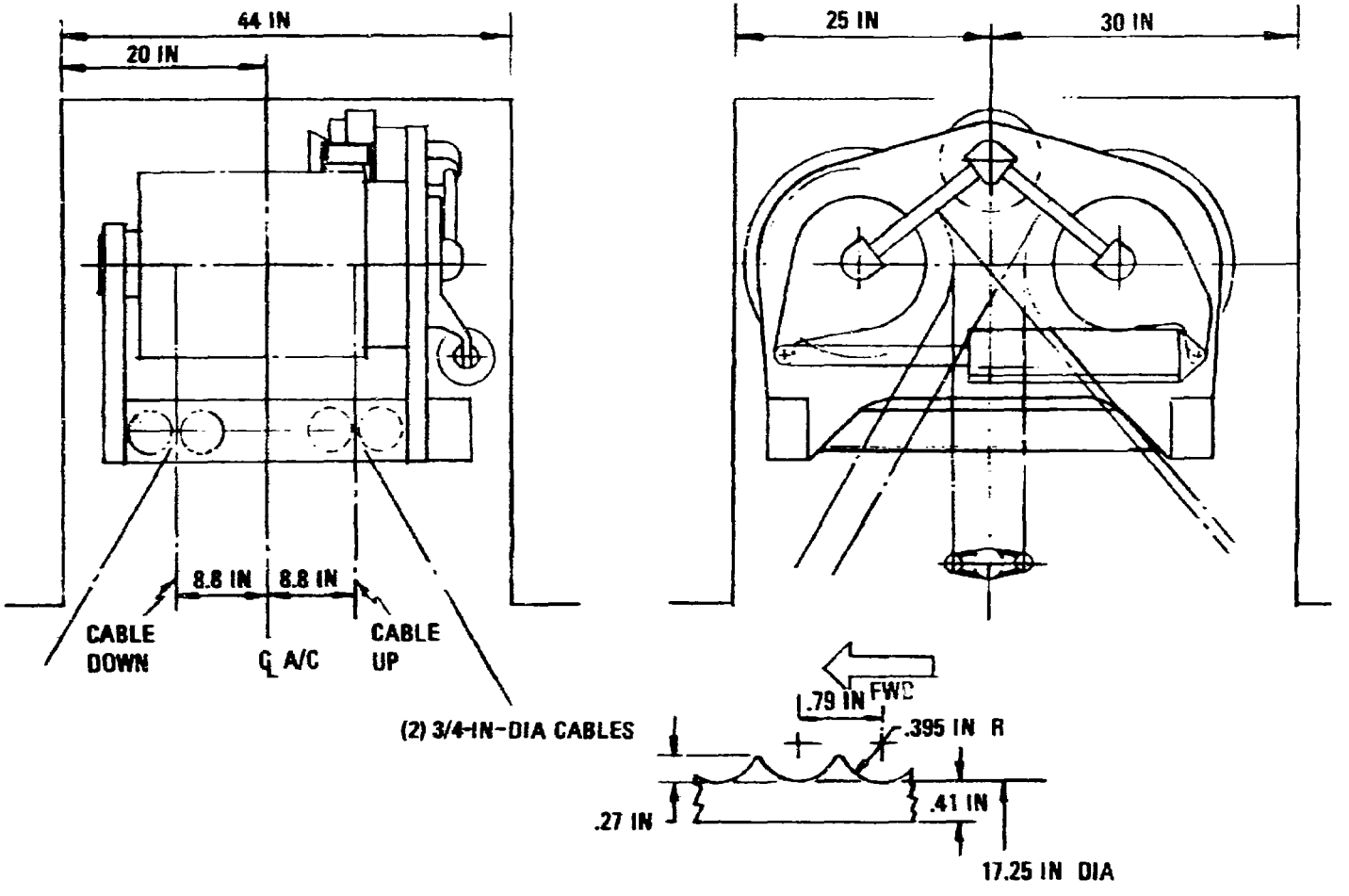


Figure 50. Level-Wind Twin-Drum Hoist.

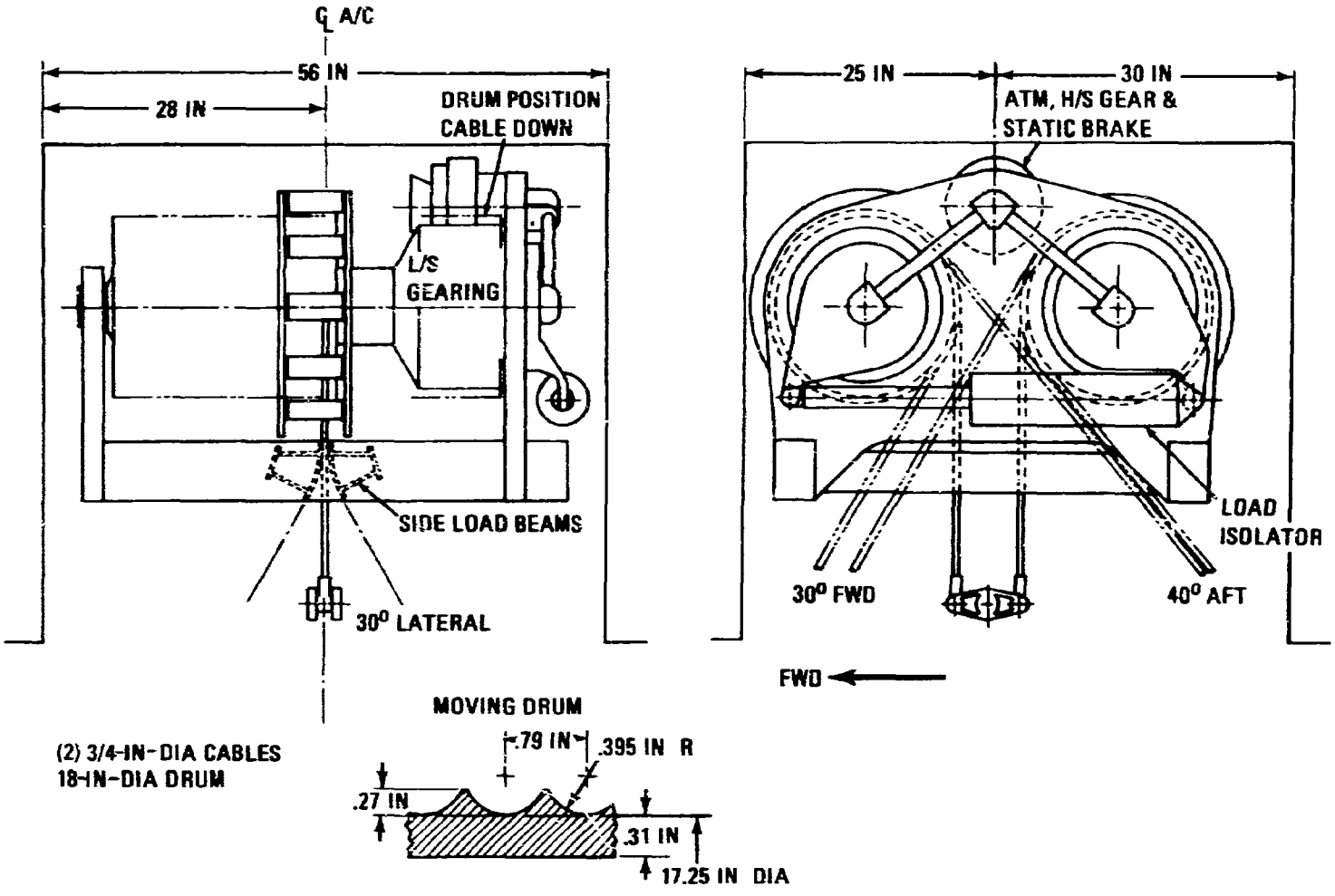


Figure 51. Single-Point Payout Twin-Drum H .

TABLE 4. ESTIMATED WEIGHT AND PRINCIPAL CHARACTERISTICS OF THE FOUR CONFIGURATIONS.

Config.	Weight (Lb)	Tunnel Width (In)	Lateral Cable Angle	Single Point (SP) or Cable Travel (IN)	M ◊	R ◊
Fig. 48	1369	64.0	± 16°	SP	4	4
Fig. 49	1244	61.0	± 30°	± 12.5	3	1
Fig. 51	1142	56.0	± 30°	SP	2	2
Fig. 50	1202	44.0	± 30°	± 8.8	1	3

*Preliminary weight analysis. Includes: Cable Drum; Drum Support Frame; Low-Speed Gearing; Level Wind or Equivalent Mechanism; Provisions for Cable Cutter.

Drum thickness determined by stress unit based on SMR 364 and use of Carpenter Custom 455 steel of 280,000 psi ult. strength.

◊ Order of preference as defined by Product Assurance Group in terms of Maintainability M and Reliability R.

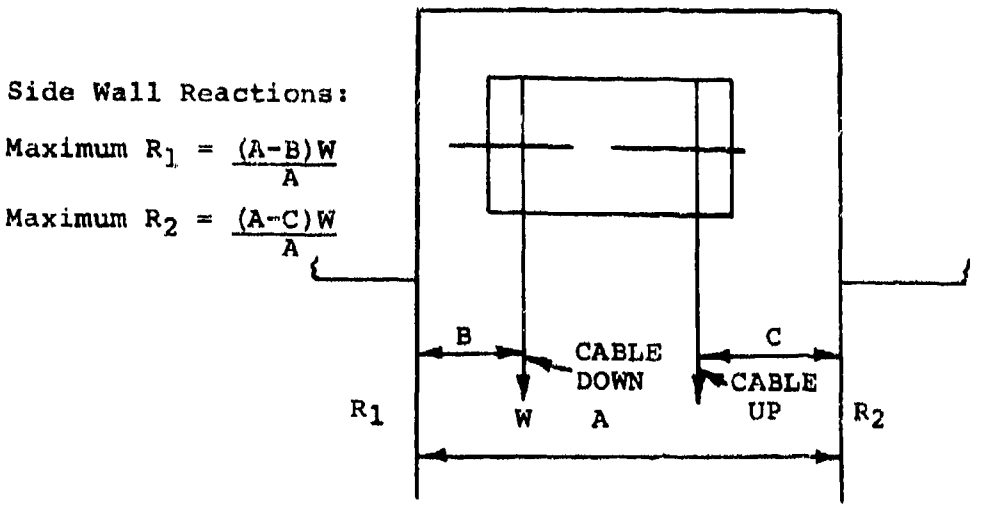


Figure 52. Structural Interface.

TABLE 5. WEIGHT IMPACT OF STRUCTURAL REACTIONS.

Config.	A	B	C	MAX R_1	MAX R_2	$R_1 + R_2$	Structural Wt (Lb)
Fig. 48	64.0	32.0	32.0	.5 W	.5 W	W	405
Fig. 49	61.0	15.5	20.5	.75W	.66W	1.41W	570
Fig. 51	56.0	28.0	28,0	.5 W	.5 W	W	405
Fig. 50	44.0	11.0	15.4	.75W	.65W	1.40W	567

Structural Weight - 68% Allocated to Structure
32% to Hoist System

Structural Weight Proportional to $R_1 + R_2$

The structural weight was integrated with the hoist, cable and remaining system weights to provide the overall system weight comparison shown in Table 6.

TABLE 6. SYSTEM WEIGHT COMPARISON.

Config.	Two Hoist Drum & Support Assys.	Two Cable Assys.	Instl. Struct.	Remaining Weight	Total	Struct.* Wt. Inc. in Total	System Total
Fig. 48	2738	542	405	975	4660	275	4395
Fig. 49	2488	542	570	975	4575	387	4188
Fig. 51	2284	524	405	975	4188	275	3913
Fig. 50	2404	524	567	975	4470	385	4085

Remaining Weight: Includes ATM, Isolators, Cable Cutters, Span Positioning System, etc.

*Structural Weight: 68% of installation weight carried as structure weight in aircraft weight breakdown.

The parallel twin-drum as a SPP configuration was selected as the basis for development due to the favorable installed weight forecast, the possibility of measuring individual cable tensions and the redundancy of the low-speed gearing.

Extended Reach Impact

The weight impact of an increase in useable cable length beyond 100 feet is shown in Figure 53.

The delta of 13.35 pounds per additional foot of tension member length was derived from detail considerations of drum size, frame size, tension member and signal conductor lengths, and the necessary structural changes resulting from the increased tunnel width required. A further problem with cables in excess of 100 feet was the inability to obtain a suspension system natural frequency above 1.5 Hz considered as the desirable lower limit for the desired suspension frequency range.

Selected Concept

The selected concept was established as a twin, parallel drum, hoist with cable payout on the aircraft centerline.

The design load capability requirement of 33,600 lb and ultimate capability of 150,000 lb was determined as shown in Part 3 of this volume. Operating speeds of 60 ft/min at design load and 120 ft/min at no load with drive input speeds of 4000 rpm and 8000 rpm, respectively, were established from the contract requirement and the interface with the hoist drive.

The design life of 10,800 cycles and cable angle capability of 30° forward and lateral, 40° aft, result from the basic criteria established in the criteria section of this volume.

Concept Development

The selected hoist supplier, Western Gear Corporation of Lynwood, California, developed the basic configuration into a detail design. A key design feature of the twin-drum, single-point payout configuration is the practical application of a recirculating ball spline support and drive system for the cable drum. Beaver Precision Products of Troy, Michigan, designers and manufacturers of precision ball-spline and ball-screw actuators, were contracted by Western Gear to design and produce the drum support spline system.

Western Gear developed a mathematical model of the supporting framework to provide a design tool for a minimum weight design. The mathematical model presents the structure as a

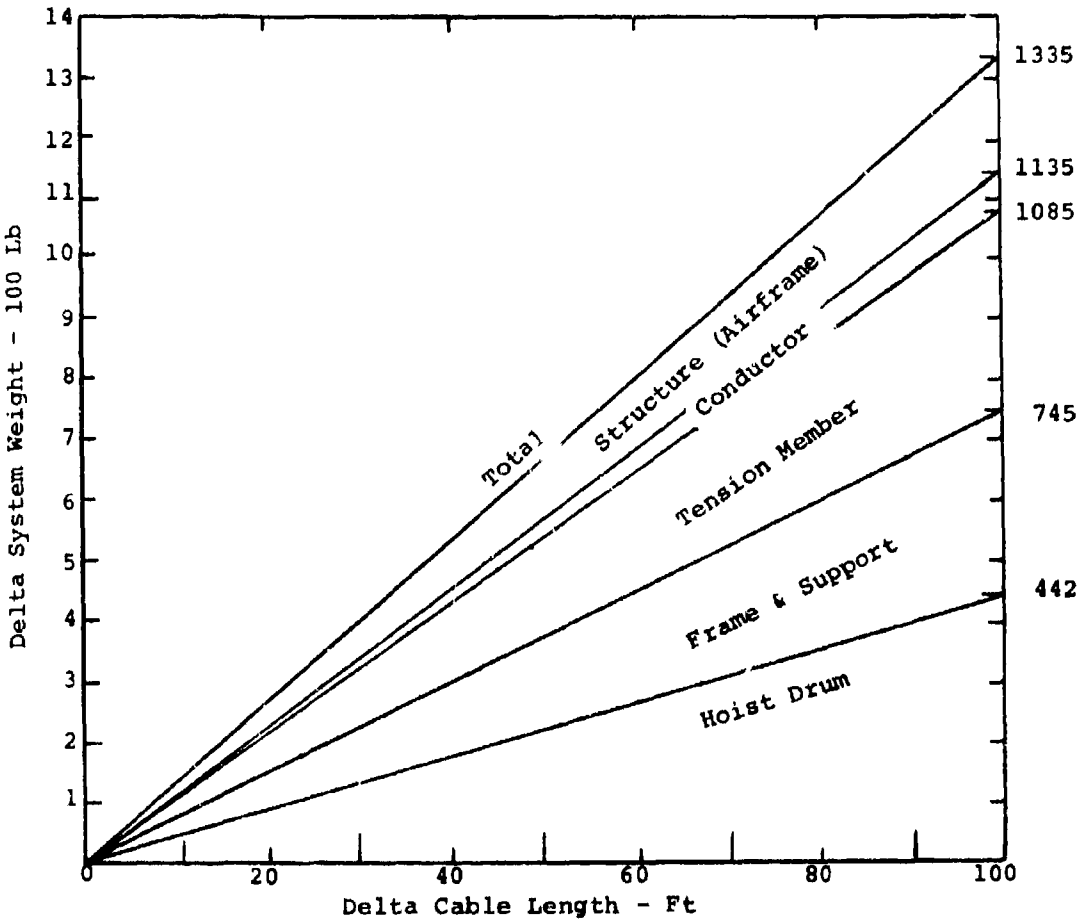


Figure 53 . Weight Impact of Increased Tension Member Length.

series of elements between node points with the mathematical analysis to derive stress levels and deflections for each element or node. This data is presented in a form compatible with available computer facilities such that the properties of each element can be revised and a new analysis obtained rapidly. Use of this program permitted the design to be reviewed and adjusted for optimum stress levels at ultimate loads while retaining acceptable deflections at design and limit loads. Use of this program permitted weight reductions in the main bearing and gear support frames subsequent to freezing the design concept.

A major area of the hoist design not amenable to accurate analysis was the drum wall thickness requirement. In the selected configuration using the sliding drum supported by linear ball races, the drum design becomes stiffness critical rather than strength critical. To prevent jamming of a loaded drum over the ball supports when the drum traverses (see Figure 54), the spline manufacturer dictated that the drum radial deflection should not exceed .014 inch. To provide information on radial deflections, a design support test was conducted by Western Gear where a section of drum was subjected to loads induced by a wrapped cable, and the deflections were measured. The test was repeated for a total of three drum thicknesses. This test is described in Volume III of this report.

As a result of this test, a drum wall thickness of .34 inch was determined to be adequate . Two further tests were conducted prior to completion of the detail design. One test established that the selected drum material and finish would show satisfactory wear characteristics when abraded by the tension member, and the second test applied an ultimate load to the ball spline and support structure to ensure adequate strength. These tests are described in Volume III of this report.

Preliminary Hoist Design

The configuration of the hoist is shown in Figure 55. The air turbine motor, high-speed gearbox and brake assembly is mounted above the twin drums and drives the two low-speed gearing assemblies through two shafts with bevel gears at either end. The input to the low-speed gearing is through the axis of drum rotation.

The low-speed gearing is a simple three-stage planetary system with each stage driving a common outer ring. The third-stage planets are mounted on an end plate that can rotate about the drum axis.

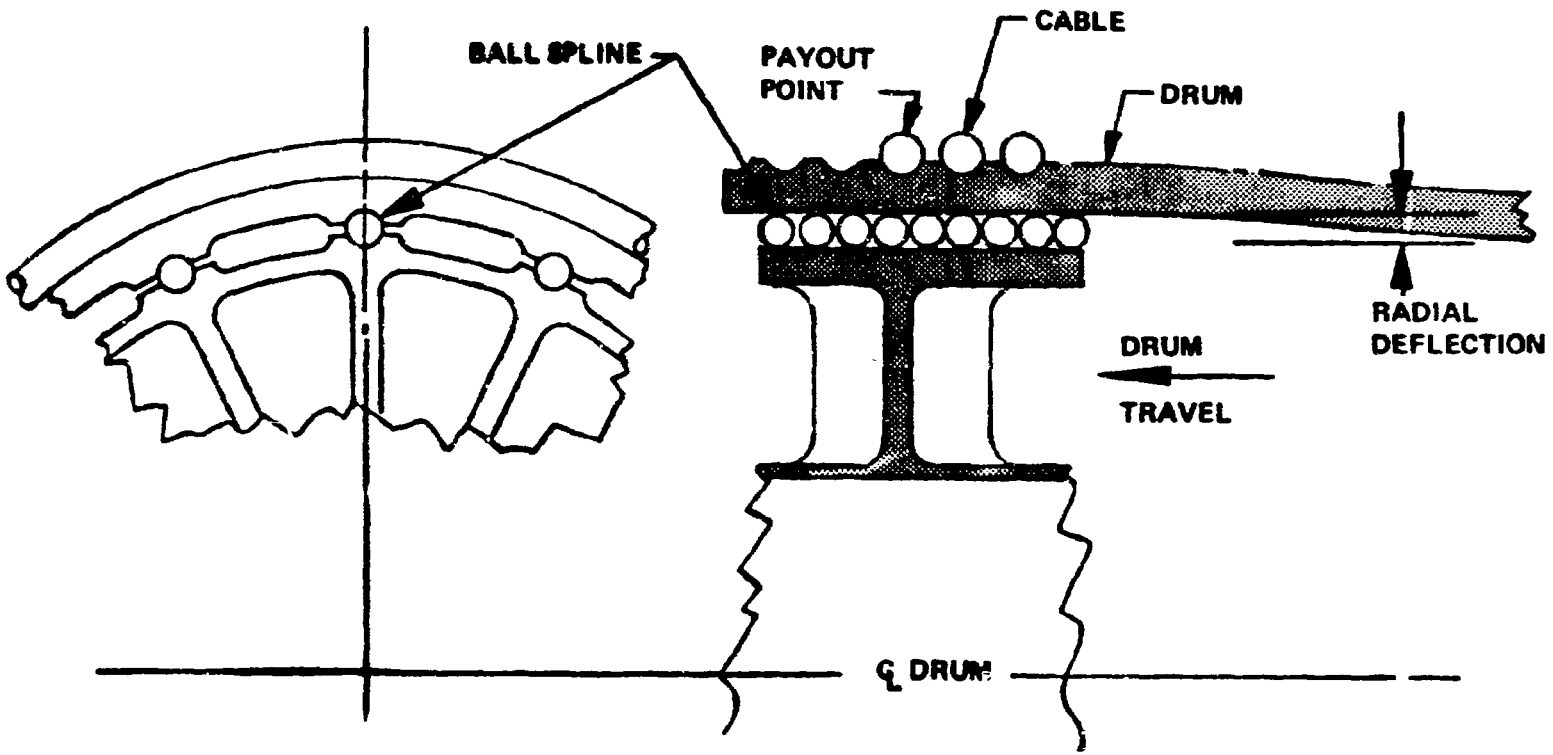


Figure 54. Drum Support Arrangement.

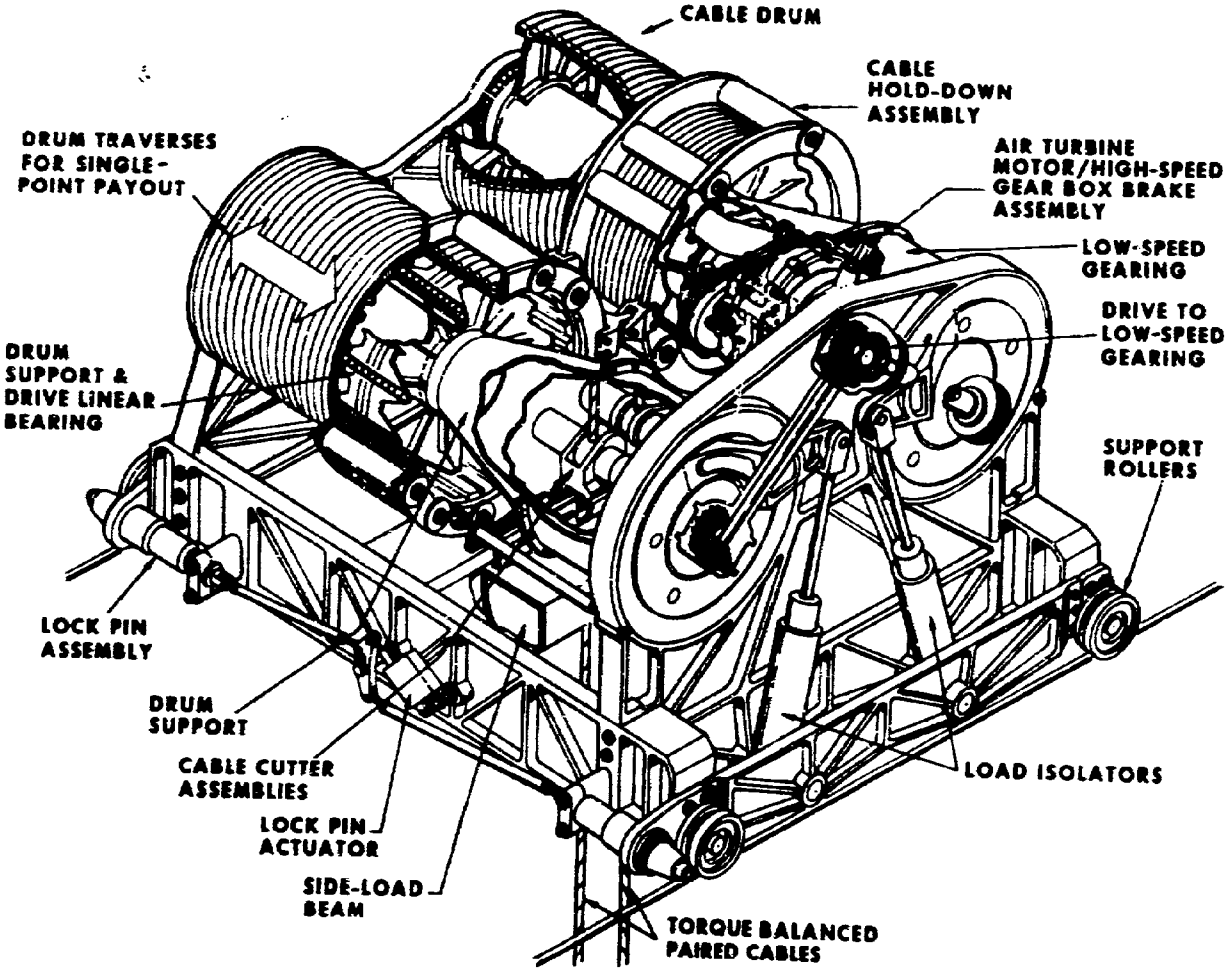


Figure 55 . Dual-Drum Hoist Assembly.

Rotation is prevented by the load isolator attaching to an arm integral with the end plate. The opposite end of the load isolator is attached to the hoist frame, thus the load isolator reacts all the torque applied by the cable over the drum.

The outer ring gear forms the housing for the gear assembly and has the drum support member extending to the bearing in the winch bearing support frame member. A driving flange is mounted on the drum support member at the point of cable payout. The outer surface of the driving flange mounts 12 equally spaced linear ball spline units. These units have return tubes to permit the balls to recirculate and eliminate ball skidding.

The inner surface of the cable drum has 12 longitudinal grooves to match the ball spline units on the driving flange. The drums are therefore free to move axially while being restrained radially by the ball spline. The drum has a closing flange at the far end with a sliding bearing on the outer surface of the drum support member.

The outer ring gear is supported by a large diameter bearing at the load isolator end of the hoist and in turn supports the gear end plate with its integral load isolator arm.

The cable leaves the drum and exits from the hoist between two structural members designed to react side loads due to lateral cable angles. Between the side-load members and the drums the cables pass through the two cable cutters. The cutters are mounted on individual carriages and are free to move along the length of the side-load beam as the cable longitudinal angle changes.

The cable hold-down assembly is a fully floating ring and roller arrangement located by tie rods to the gear support frame. The assembly is therefore independent of drum and support deflections. A pair of profiled rollers engage in the drum groove to provide the drum translation force.

A major problem throughout the concept development phase was the projected hoist weight.

Three major areas with potential for weight reduction were examined at the Preliminary Design Review. These areas were:

1. Drum Support Spline
2. Drum Support Structure
3. Frame Design.

At that time, the unit weight was projected at 1,400 pounds. A subsequent design review on September 28, 1972, revealed that some progress had been made in reducing the weight in these areas, and identified weight savings in two further areas.

1. Cable angle sensing arrangement. A revised concept resulted in a weight reduction in the order of 5 pounds per hoist.

2. Side load beam wear plates. Reduction of thickness of the steel wear plates from .064 to .032 inch reduced the weight by 4 pounds per hoist.

The critical design review reflected an estimated weight based on detail design drawings of 1,270 pounds.

Detail changes made during the hoist fabrication resulted in the actual weights of the assemblies ranging between 1,225 and 1,230 lb.

Further areas with potential for weight reduction include:

1. Side load beams. The two side load beams are currently fabricated as titanium welded assemblies. A design utilizing 7075 aluminum extrusions may result in weight savings. A change in the design criteria to reduce the inertia factor when the cables are at high lateral angles would result in a proportional change in side load beam weight.

2. Side frame members. The existing design of forward and aft side frame members reflects machined parts from 7075 aluminum billets. A fabricated box section beam with integrated mounting fitting would be more efficient.

3. Bearing and gear support frames. The bearing and gear support frames are machined from 7075 aluminum plate stock. Consideration should be given to the use of closed die forgings for these parts with an evaluation made of a material change to 6Al-4V titanium. The use of closed die forgings would possibly permit the economic use of titanium with the frame sections revised to reflect the higher allowables.

4. Drum support member. The drum support structure is machined from a 4340 steel hammered forging. Alternative designs using drawn tubes may result in a lighter weight structure.

5. Reduced number of "dead" wraps. The drum and support design dictates a minimum length of drum from the payout point necessary to accommodate the ball spline. This length results in approximately 4-1/2 dead wraps with 100 feet of cable deployed. Tests have shown that three dead wraps are required to dissipate the load to an acceptable value at the cable button. A design should be developed with the objective of reducing the 4-1/2 dead wraps to 3 while retaining a satisfactory support geometry. Additionally, the possibility of increasing the design capacity of the drum button to further reduce the number of dead wraps should be investigated.

6. Drum end plate. A material change for the drum end plate from steel to titanium would result in a weight saving in the order of 3 lb per drum.

7. Miscellaneous details. A review of the roller hold-down assemblies and the miscellaneous details and fasteners could result in further weight reductions.

Design studies are required in all these areas to establish the actual weight delta possible. A preliminary estimate suggests that some 75 lb could be removed, resulting in a hoist weight in the order of 1150 lb.

Detail Design

The assembled hoist is shown in Figure 56. The detail design is illustrated by Western Gear drawing 42198R100 reproduced as Figure 57.

The principal assemblies of the hoist are:

Frame Assembly
LH & RH Support Structure
LH & RH Drum Assemblies
LH & RH Planetary Drive Assemblies
Bevel Gear Assemblies
Roller Assemblies

Frame Assembly

The hoist frame assembly consists of seven major elements. The bearing support frame, gear support frame, isolator beam, together with the forward and aft side frames are machined from 7075-T651 aluminum. The left-and right-hand side load beams are welded titanium subassemblies. Figure 58 shows the initial frame assembly set up for line boring of the bearing housings.

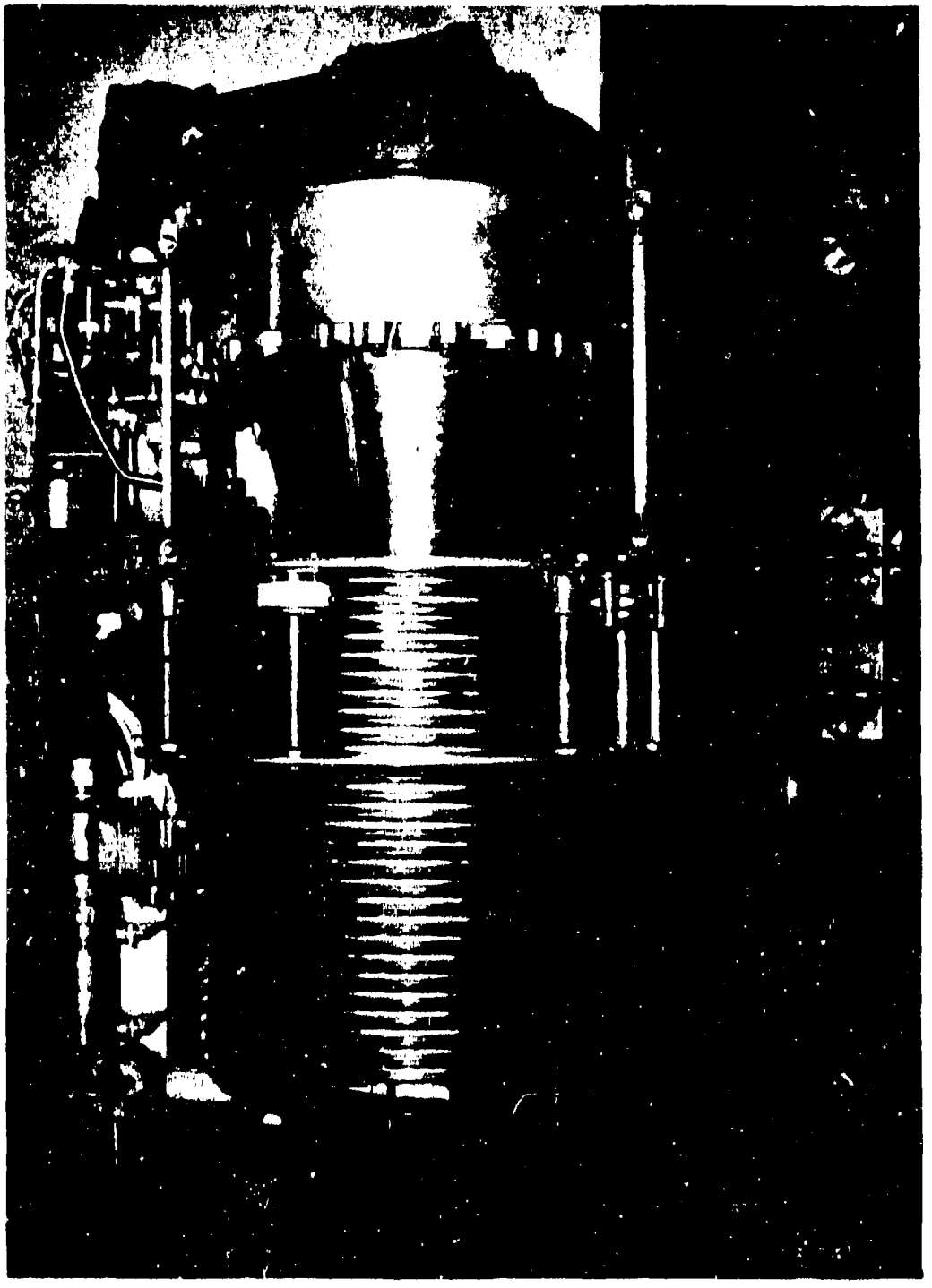
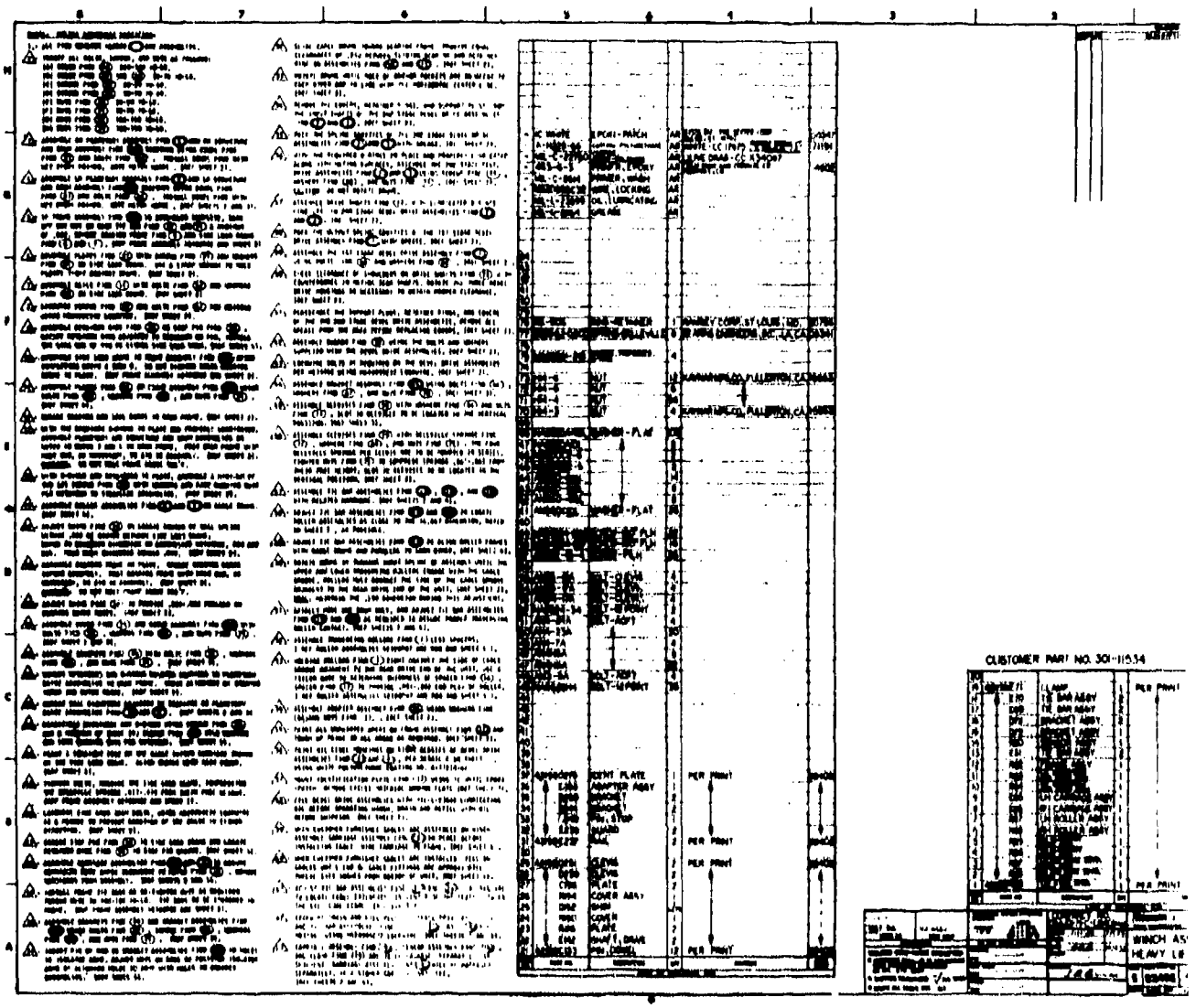
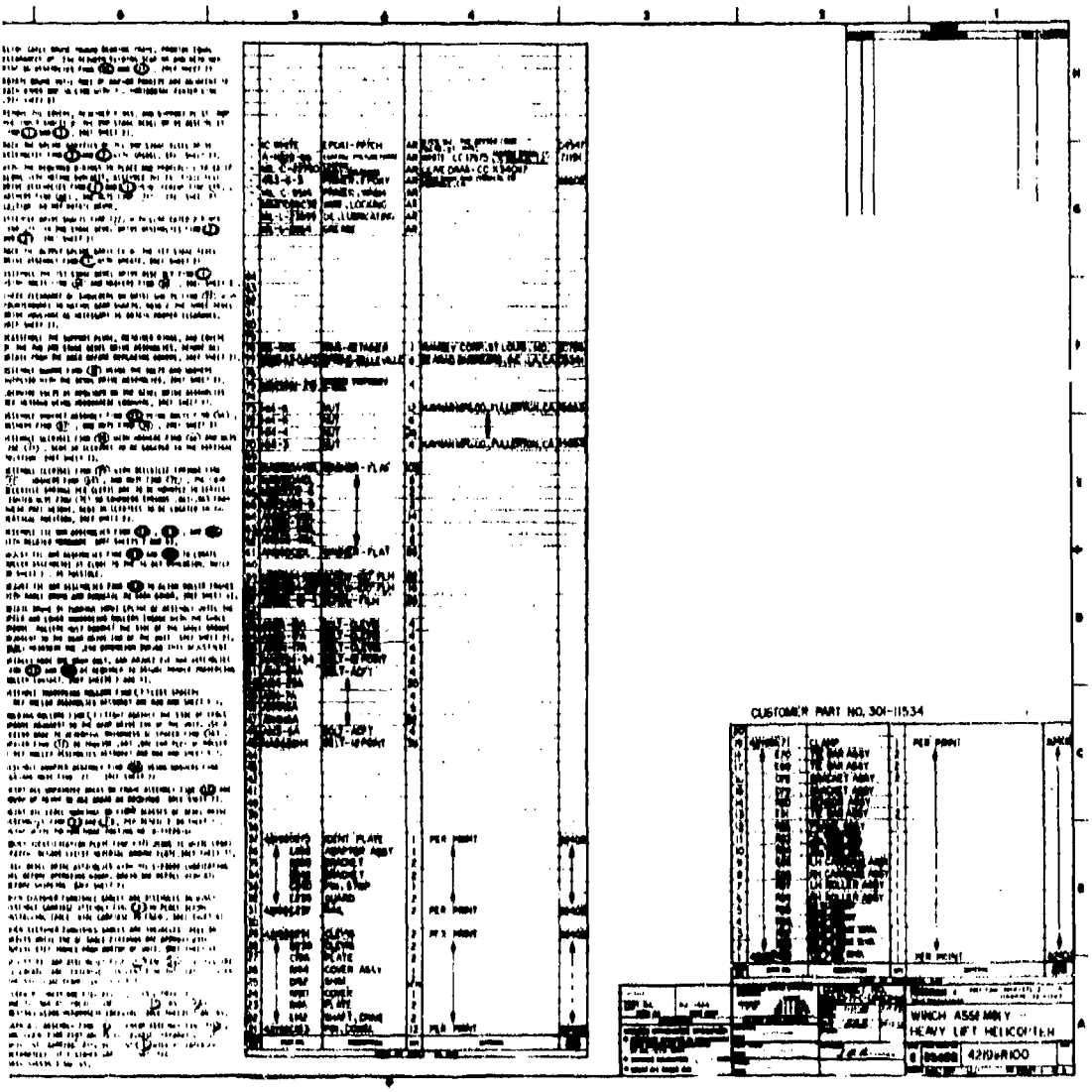


Figure 56. Hoist Assembly.



COPY AVAILABLE TO DDC DOES NOT
PERMIT FULLY LEGIBLE PRODUCTION

Figure 57. Hoist Layout Drawings (Sheet 1 of 5).



OPY AVAILABLE TO DDC DOES NOT
ERMIT FULLY LEGIBLE PRODUCTION

Hoist Layout Drawings (Sheet 1 of 5).

2

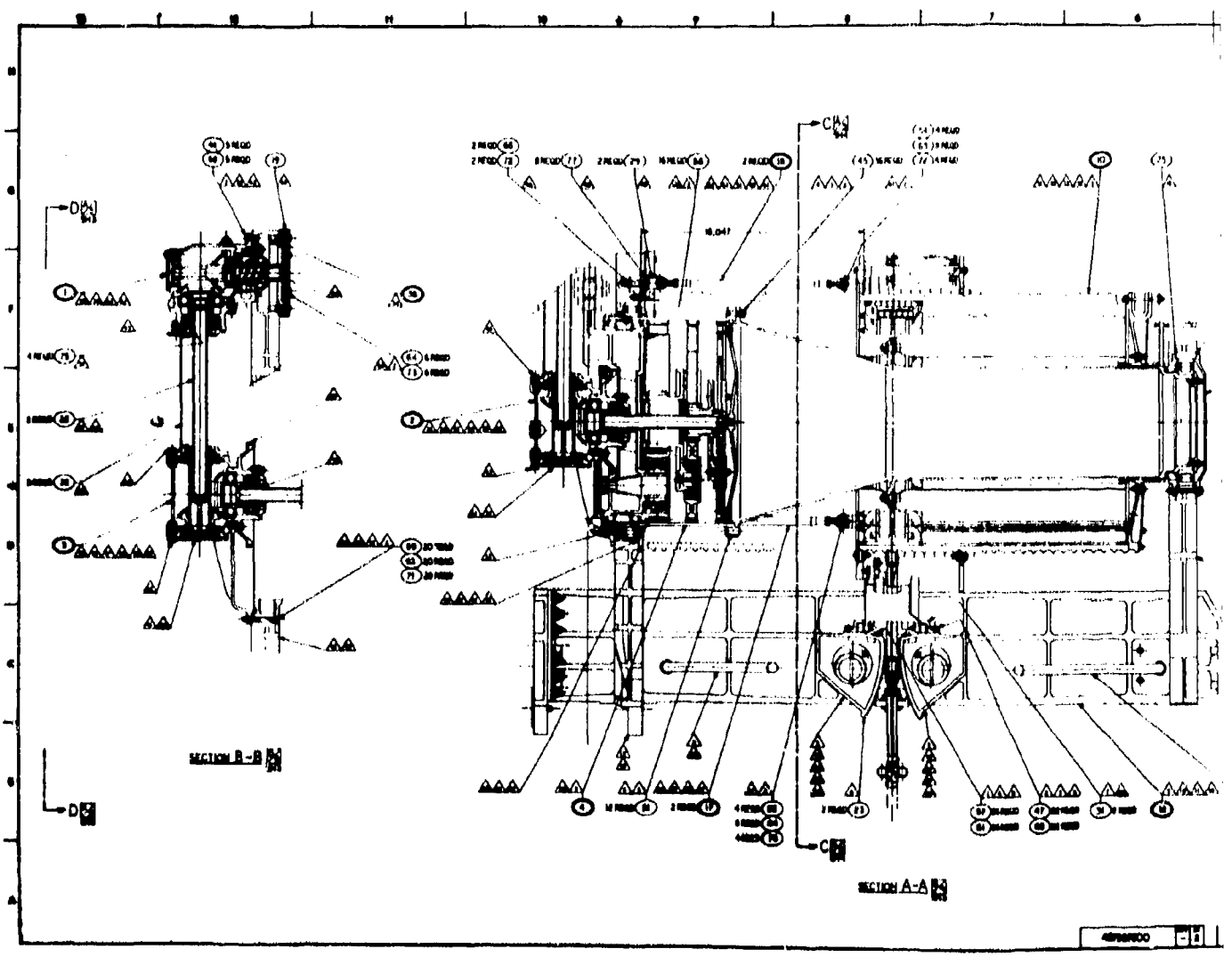
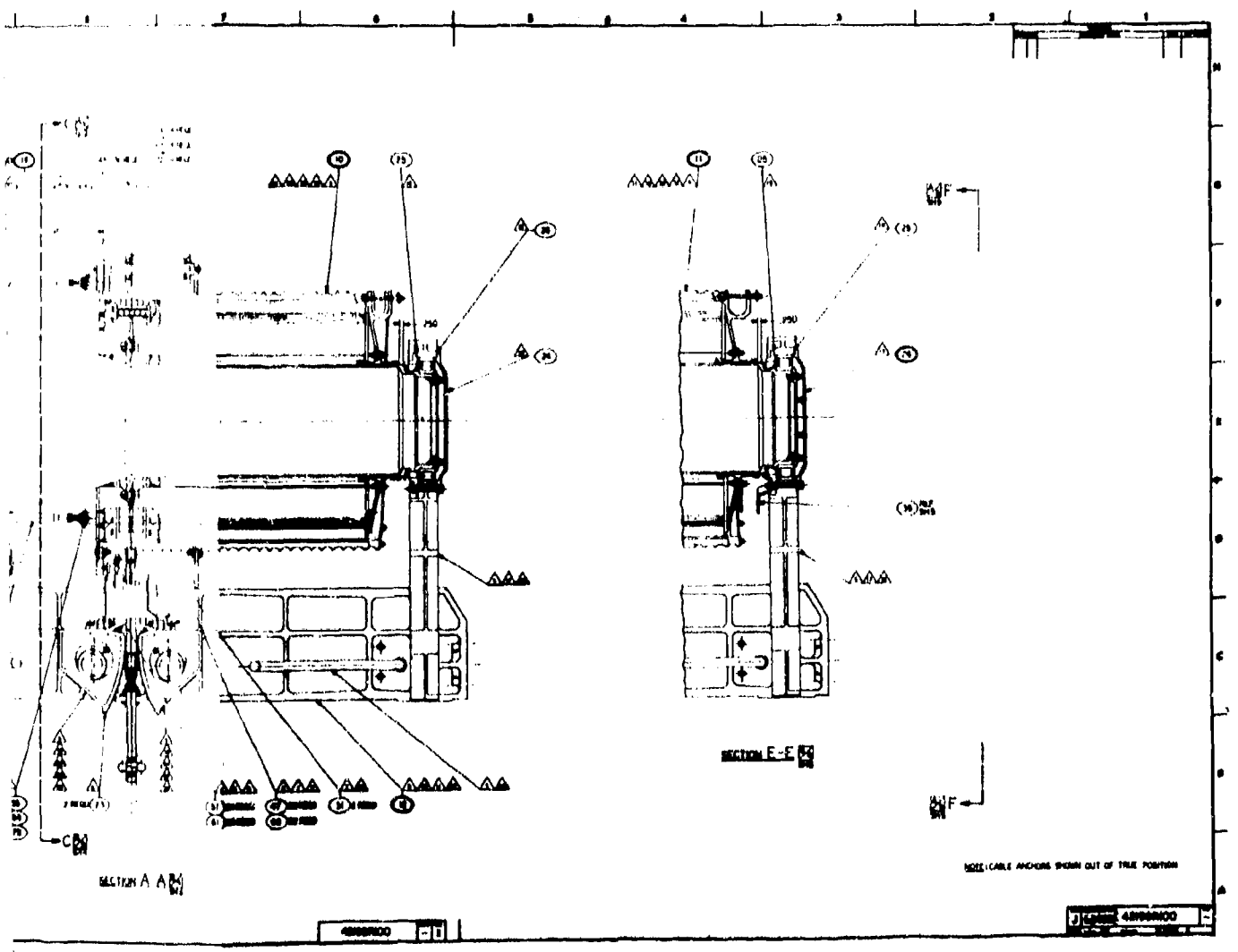


Figure 57. Continued (Sheet 2 of 5).


SECTION A-A
SECTION E-E
NOTE: CABLE ANCHORS SHOWN OUT OF TRUE POSITION

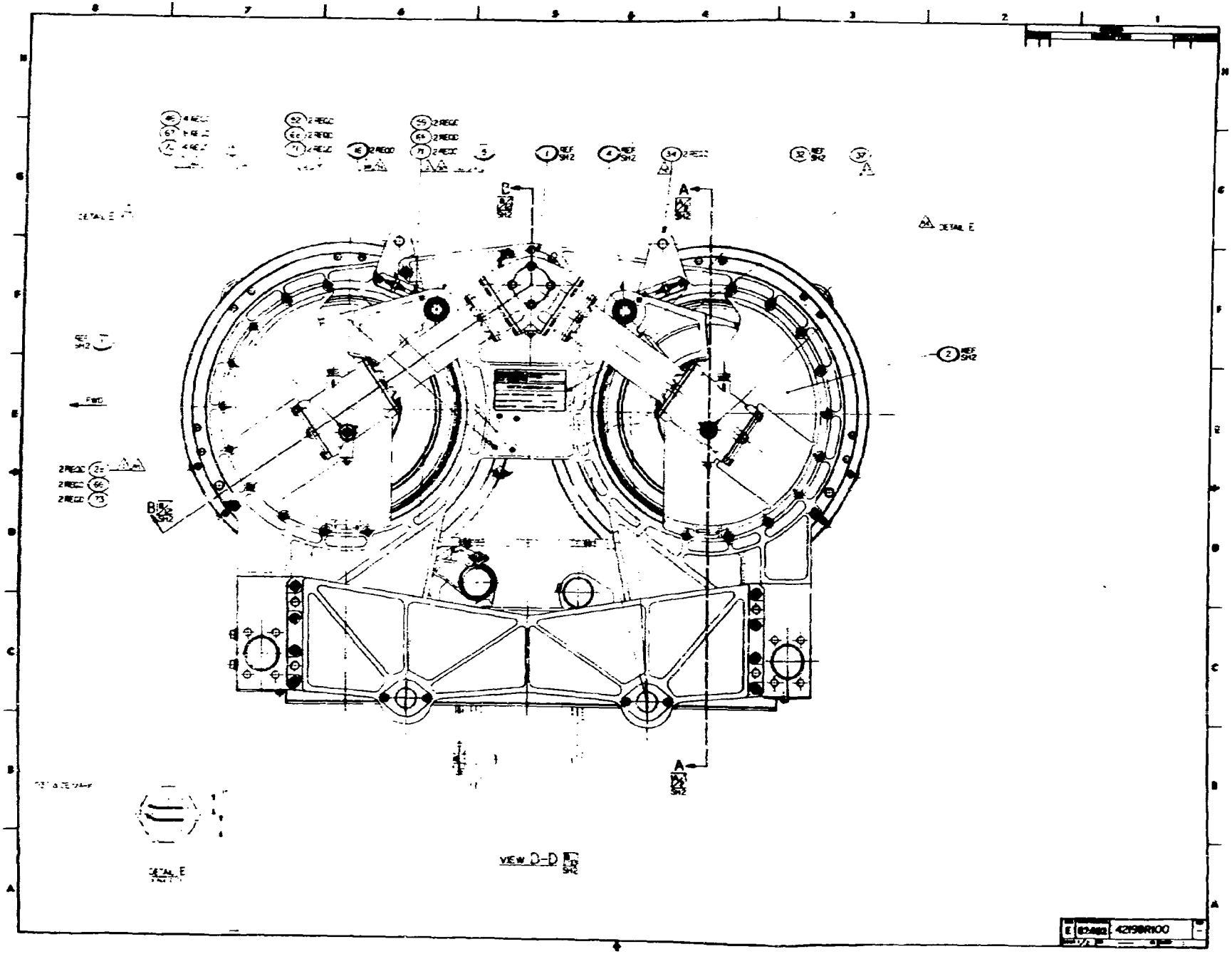


Figure 57. Continued (Sheet 3 of 5).

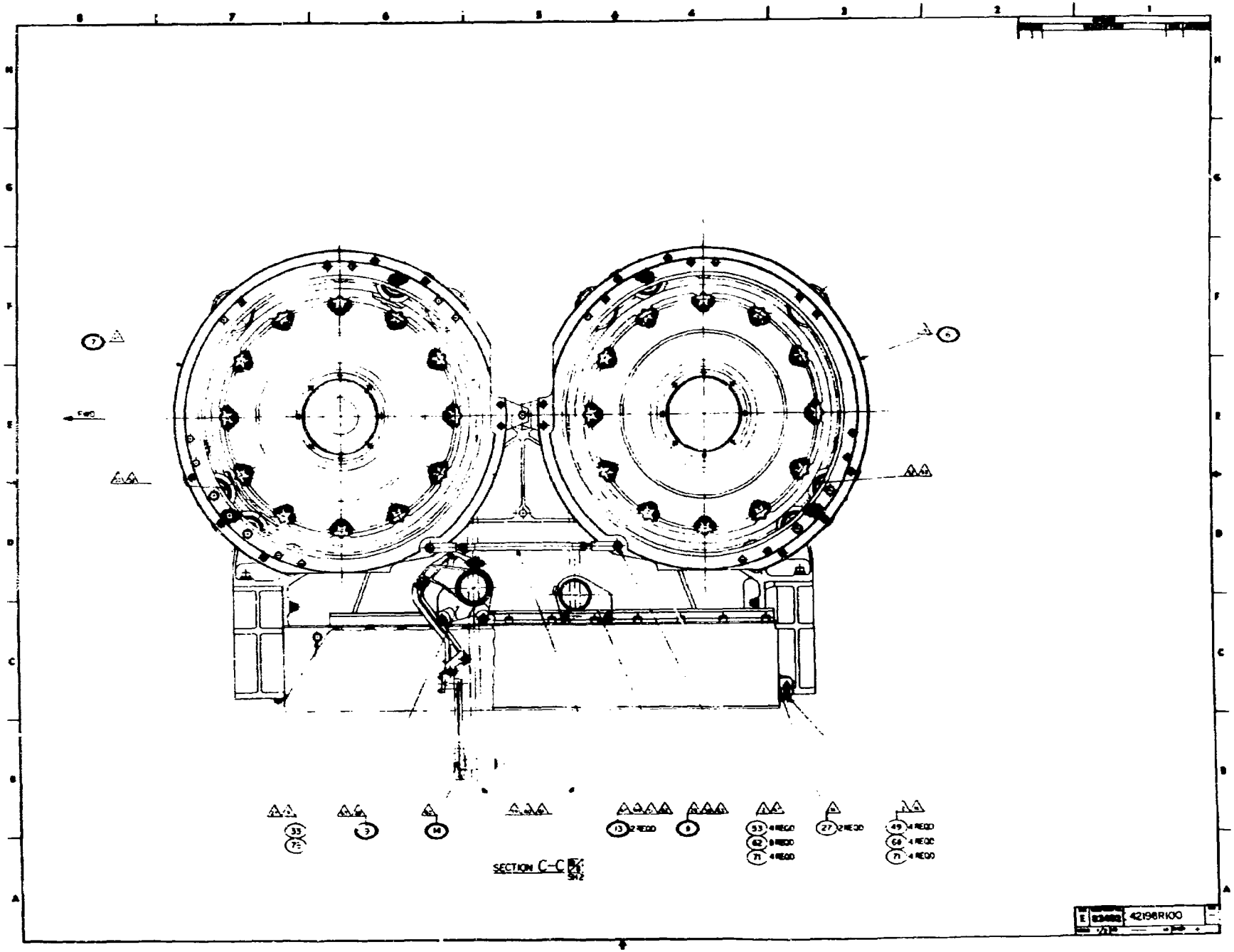


Figure 57. Continued (Sheet 4 of 5).

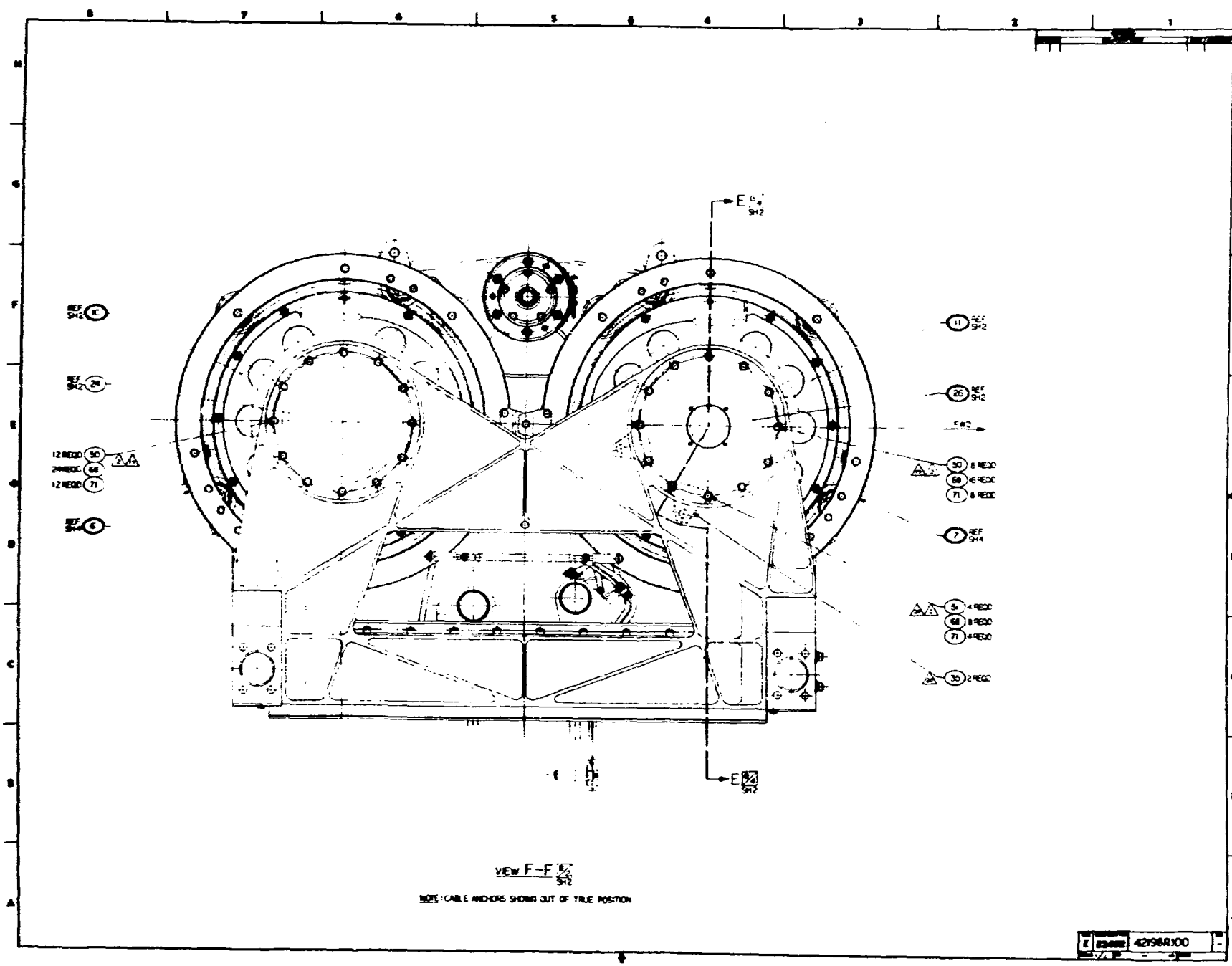


Figure 57. Concluded (Sheet 5 of 5).

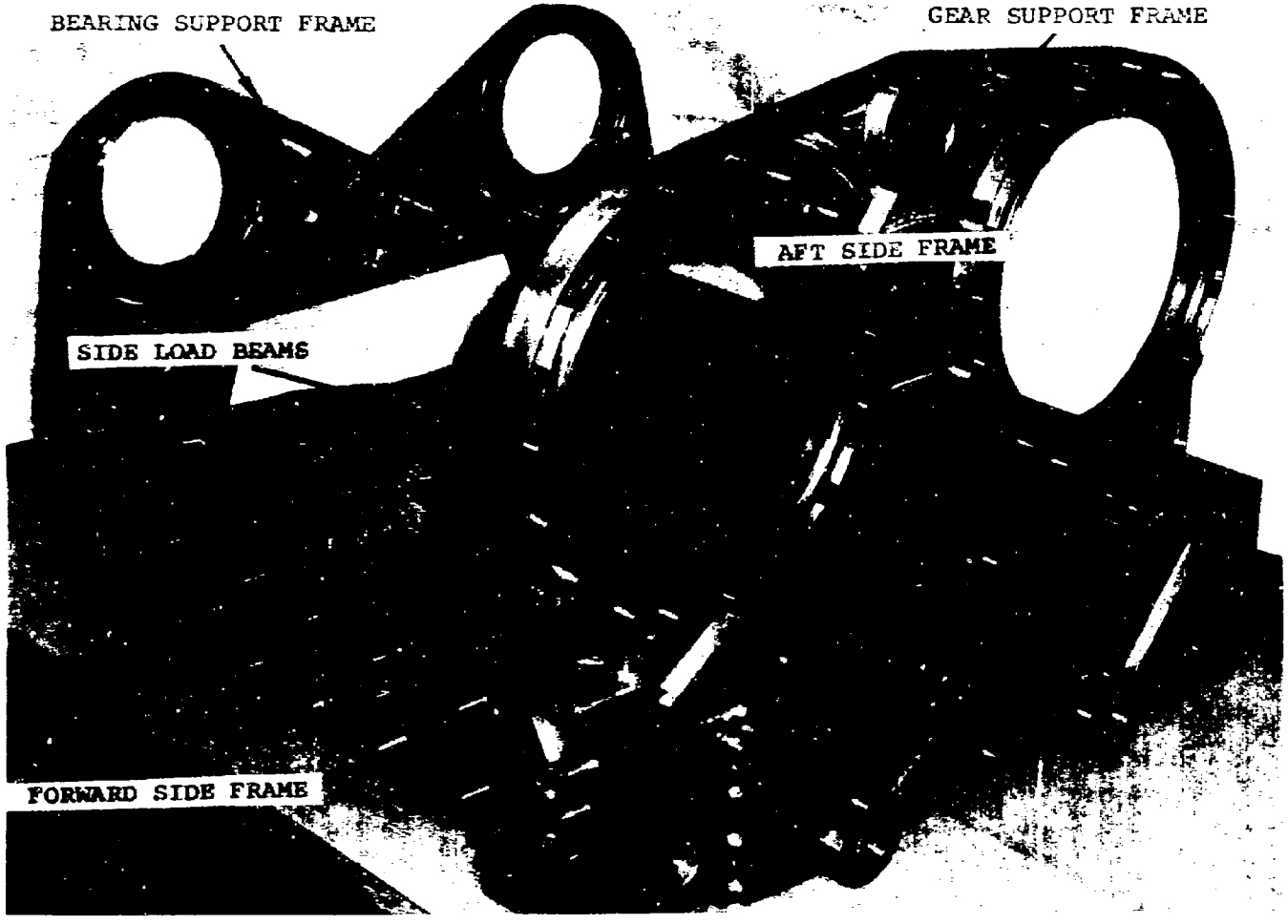


Figure 58. Hoist Frame Assembly.

7075-T651 aluminum was selected as the principal frame material due to its high strength/weight ratio with satisfactory stiffness characteristics, ready availability and good machinability. Titanium was selected for the side load beams due to the need for a high strength weldable material.

The gear support and bearing support frames provide housings for the bearings that locate and hold the drum support structure and are in turn attached to the forward and aft side frames. Additionally, the gear support frame has the drive unit attachment provisions between and above the bearing housing bores. The attachment consists of three shear pins and a quick-release clamp, permitting rapid assembly or removal of the drive unit.

Lifting points are also provided on the gear support frame, consisting of two profiled plates each attaching to two bolts in the upper frame area. At the same locations, brackets are mounted to provide a means of holding and adjusting the load isolator attachment arm prior to installing the load isolator. The side frames have provisions at either end for support fitting attachments.

The isolator beam is also attached to the side frames parallel to the gear support frame; the load isolator being located between the two members.

The titanium side load beams are positioned between the side frames and disposed such that the cables pass out through the slot formed between the two beams.

Attachment to the side frames uses a titanium shear plug and tension bolts. The side-load beams have a curved surface of 10.0-inch radius presented toward the cable such that the beams will support the cable when the cable exits at a lateral angle and hence react the side loads resulting from the angle. The curved surface of the beam has a replaceable hard-chrome plated steel wear plate to resist abrasion from the cables.

The beam is of a built-up box section with internal ribs. The curved surface and end attachment provisions are machined after welding. The upper surface of the beam supports a track and retention member for the cable cutter carriages.

Diagonal tie rods are installed between the side frames to increase the horizontal plane stiffness of the assembly.

Support Structure and Drum Assembly

The LH and RH structure and drum assembly are essentially of opposite hand except that the LH assembly has provisions for the length sensor installation and cable up limit switches.

Included in this assembly are the following major components: cable drum, ball spline flange, closure flange, and center support structure. Figure 59 shows these components.

The cable drum is fabricated from vacuum melt 9310 steel, helically grooved on the outside to suit the cable and longitudinally grooved on the inside to suit the support spline. The twelve equally spaced grooves for the support spline are case-hardened to a R_C56-60 value while the basic drum is hardened to R_C32-42. The cable groove has a .74 inch lead and a groove configuration to suit a .70 diameter cable, the RH drum having a RH helix and the LH drum a LH helix. Protective finish is electroless nickel plate.

Supporting the drum at the point of cable payout are twelve linear ball bearing units mounted on a flanged disc assembled to the center support structure. Each linear ball bearing unit has an integral return tube for the balls, felt seals to exclude dirt, and a grease fitting for lubrication. Material used for the flange is 9310 steel case hardened in the ball groove area, with an electroless nickel finish.

The closure flange incorporates the cable drum terminal and has a low friction sliding bearing mounted to its inner diameter. Attached to the cable drum by a series of bolts, the closure flange provides support for the drum end as it slides along the center support structure. The pocket for the cable terminal has provisions for a quick-release pin to retain the cable terminal when installed. The closure flange is also 9310 steel with an electroless nickel finish. The sliding bearing is a Teflon impregnated cloth lining bonded to a steel housing.

The center support structure extends from the low-speed gear housing to the bearing support frame. Fabricated from a 4340 steel forging, the support structure is heat treated to a hardness of R_C32-38. Attached to the gear housing at its outside diameter the support tapers down to the location for the ball spline flange and continues as a parallel tubular section to the supporting bearing. The finish of this component is electroless nickel plate.

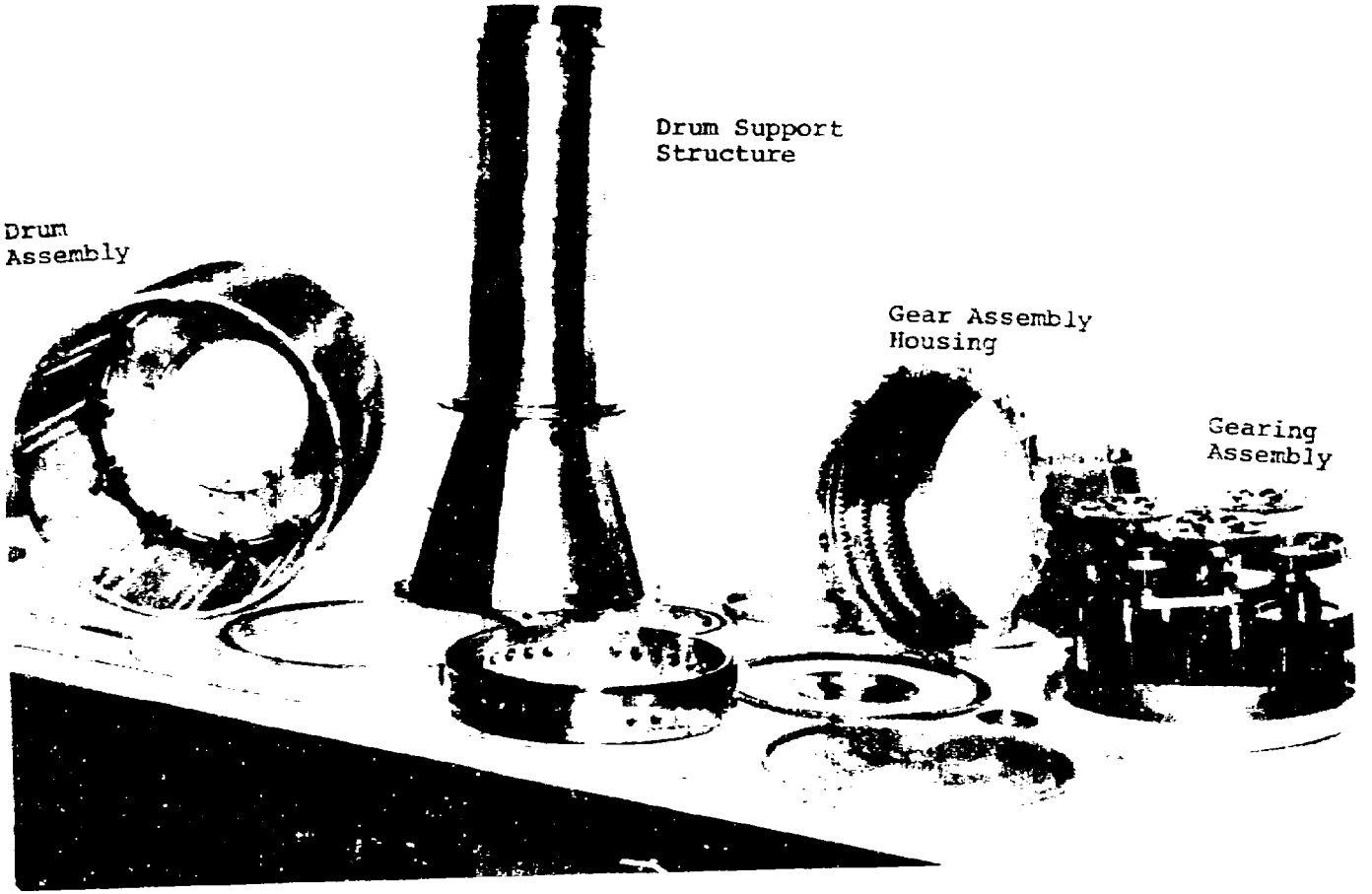


Figure 59. Hoist Components.

Planetary Drive Assemblies

The LH and RH planetary drive assemblies are essentially identical except that the third-stage carriers are of opposite hand.

The three-stage planetary system has the input to the first-stage sun gear and the output from the common ring gear that also forms the cylindrical housing of the assembly, with an overall reduction of approximately 274:1. Sun gears of all three stages are free to float between their planet gears to ensure uniform loading on all planets. The third-stage planets are mounted on a carrier supported by a set of taper roller bearings in the cylindrical housing. An arm extends from this carrier outside of the housing to attach to the upper end of the load isolator. This carrier can then rotate relative to the housing and to the main supporting frame within the limits of the load isolator movement. All the torque due to the loaded cable operating over the drum is reacted through the gearing by the load isolator. All gears are machined from 9310 vacuum melt steel forgings. Gear teeth are carburized and hardened to R_C60-64; core and uncarburized areas are R_C35-42. Lubrication of the planetary system is by grease to MIL-G-21164. During the demonstration program MIL-G-83363 grease was evaluated in one hoist assembly.

The principal subassemblies and components of the planetary drive are: housing, first-stage planetary assembly, second-stage planetary assembly, third-stage planetary assembly, sealing plate, and main support bearing.

The housing has the internal ring gears for the second and third stage together with the support teeth for the first-stage ring gear machined on the inside surface. An external flange provides attachment locations for the center support structure on one end of the cylinder; the opposite end has a mounting surface for the main support bearing.

The first-stage planetary assembly includes the input shaft/sun gear; carrier with integral sun gear for the second stage; three planet gears and a ring gear. The input shaft extends from the second-stage bevel drive, past the third-and second-stage planetaries and terminates as the sun gear. The planets are mounted to the carrier by ball bearings. The ring gear locates, and is retained, inside the housing.

The second-stage planetary assembly consists of three planet gears mounted by two-row spherical roller bearings to the carrier. The first-stage sun gear is an integral part of the carrier hub.

The third-stage planetary assembly has five planet gears mounted to the carrier by two-row spherical roller bearings. The carrier includes the load isolator attachment arm and has two taper roller bearings mounted to the outside diameter. These bearings locate and support the assembly inside the housing. The carrier is machined from a 4340 steel pancake forging.

The sealing plate is located inside the housing at the flanged end. This plate, machined from 7075-T651 aluminum alloy, seals the planetary gearing from the center support structure and provides the end restraint for the three sun gears.

Outside the housing, adjacent to the third-stage carrier, the main support bearing is located. This single-row spherical roller bearing is located in the gear support frame, and together with the bearing located on the center support structure, provides the support for the principal rotating components.

Bevel Gear Assemblies

The input drive from the air turbine motor and high-speed gearbox enters the hoist above and between the two drum centerlines. The first-stage bevel gearbox takes the drive through 90° and has two outputs. Each output drives into a second-stage bevel gearbox by a torque shaft, where the drive is again taken through 90° into the planetary drive systems. The two second-stage boxes are similar except that the output of the RH box is opposite to that of the LH box, providing the opposite rotations necessary to the two cable drums. The gears are machined from 9310 steel, with the teeth carburized and heat-treated to R_c60-64. Housings are machined from A356 aluminum alloy castings. All three assemblies are lubricated with MIL-L-23699 oil.

The first-stage assembly has a female spline to accept the ATM drive; the spline being part of a coupling incorporating a spring loaded brake. Insertion of the ATM drive spline forces the coupling to move axially, separating the tapered face on the coupling away from a mating face that is part of the housing. When the ATM drive is withdrawn, the two faces contact and provide a brake to prevent the drums rotating. The coupling drives the pinion, which in turn drives the two output

bevels. Input and output gears are supported by pairs of single-row ball bearings. A magnetic chip detector is incorporated in the drain plug; a dip-stick and vent plug are mounted on the upper surface of the housing. This assembly has a speed reduction ratio of approximately 1.19:1.

The second-stage bevel assembly has input and output bevels supported by pairs of single-row ball bearings mounted in the housing, which is attached to the gear support frame. The output bevel provides support for the input shaft to the planetary assembly. A tubular drive shaft connects the first-and second-stage assemblies. This shaft may be disassembled to permit one drum to be rotated independent of the other when necessary for initial set-up or adjustment. This bevel assembly has a 1:1 speed ratio. The housing has a magnetic chip detector, oil level sight gage and combined filler/breather plug. The elements of the bevel gear assemblies are shown in Figure 60.

Roller Assemblies

The LH and RH roller assemblies are generally similar but of opposite hand. The assemblies have two principal functions:

1. To traverse the drums during cable payout or reel-in.

2. To hold down the cable to the drum under conditions that tend to place the cable in compression.

Each assembly consists of two aluminum alloy plate rings with eight rollers of various configurations mounted between the rings. The rings are installed around the drum assemblies and are located from the gear support by two link assemblies. Radial movement is prevented by a link between the LH and RH assemblies together with a pin and slot joint at the drum horizontals centerline. This arrangement allows the ring assemblies to follow the deflections of the cable drums.

Each assembly has three steel contoured rollers that locate in the cable drum groove. As the drum rotates, the helix of the drum groove, restrained by the contoured rollers, forces the drum to translate along its axis. To permit the drum to rotate without moving axially, necessary when assembling or removing a cable, the contoured roller may be withdrawn from the groove by rotating the eccentrically mounted roller shaft. A lock pin ensures positive positioning in the engaged or

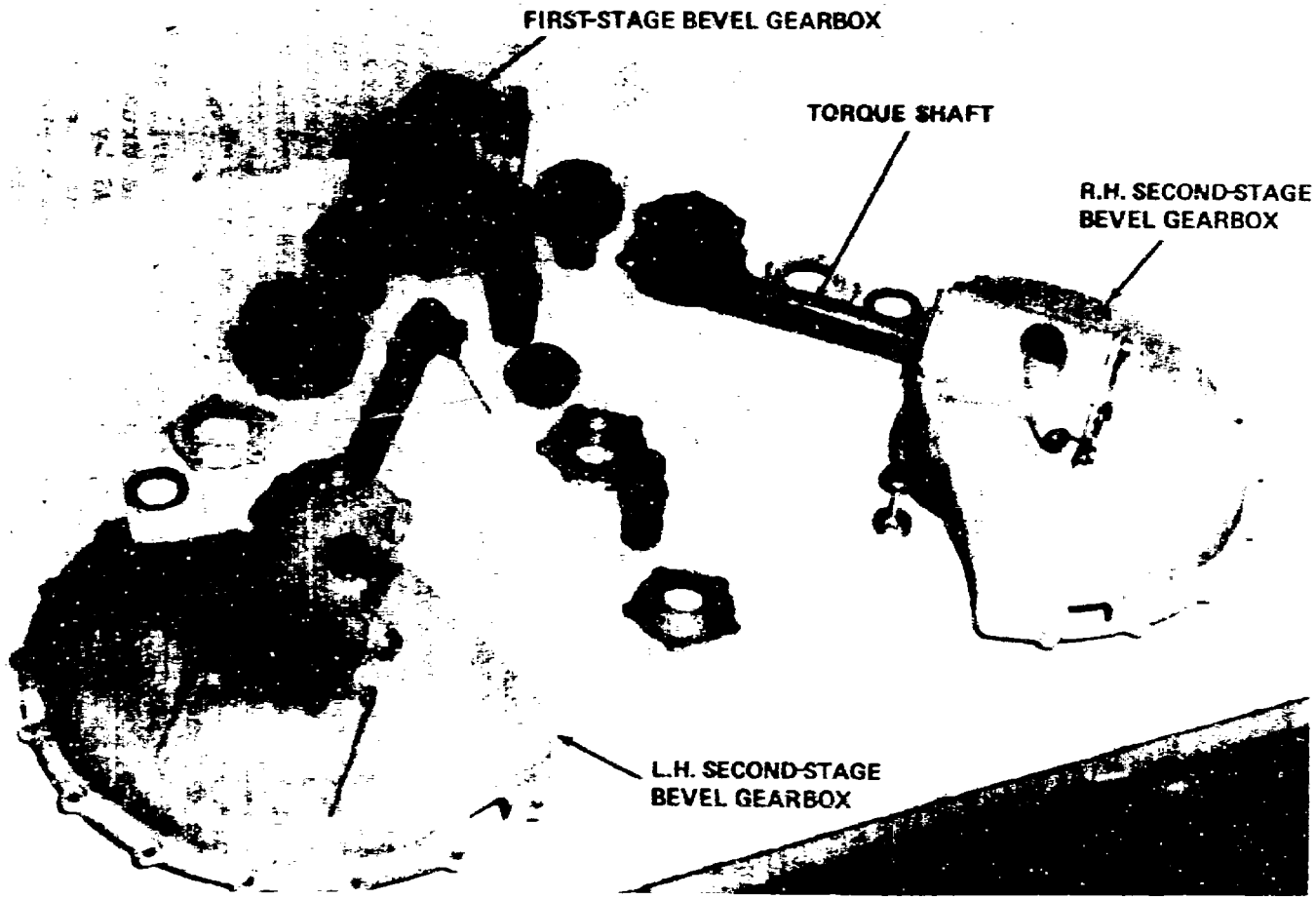


Figure 60. Hoist Bevel Drive.

disengaged positions. Five additional rollers are arranged with a nominal clearance above the installed cable to prevent the cables leaving the drum. These rollers are machined from aluminum alloy with a polyurathane cover. Two of these rollers have a larger diameter portion at the gear support frame end to provide location on the drum when the cable is removed. All rollers are mounted on a pair of single-row ball bearings. These assemblies are shown in Figure 61.

Miscellaneous Features

Additional features of the hoist not included in the preceding descriptions of major assemblies consist of; cable cutter carriages, cable angle sensing mechanism, cable length sensor, and limit switch arrangement.

To provide emergency means of jettisoning the load in-flight, a cable cutter is assembled about each cable. The cutter is mounted in a 17-4PH investment cast steel carriage with four rollers attached. The rollers are located in the rails mounted to the top surface of the side-load beams, permitting the carriage to move along the beam as the cable departure angle changes. The LH and RH carriages are similar except that the LH carriage has the cutter mounted slightly higher than in the RH carriage to minimize interference between the carriages at extreme cable angles. The carriages are shown in Figure 62. Teflon lined bearings are installed in each carriage to mount the cable cutter. The LH cutter has an extended bearing to provide an installation surface for the cable angle sensing mechanism. The RH cutter must be positioned before the two cables are installed; the LH cutter can be installed subsequent to the cables.

The cable angle sensing mechanism provides an electrical signal as a function of the longitudinal or lateral angle the cable makes relative to the vertical centerline of the hoist. This signal is used together with cable tension, to compute the load weight and provide a displacement signal to the flight control system. The signal is provided by linear transformers, one for longitudinal angles and one for lateral angles. The longitudinal angle sensor is mounted on a bracket rotating on the extended bearing for the cable cutter on the LH carriage assembly. The sensor shaft has a lever arm lirked to a point on the cutter carriage such that rotation of the bracket causes equal angular movement of the sensor shaft. The outer end of the bracket mounts a curved arm; each end of this arm has nylon rollers that contact the cable. Changes of cable angle result in rotation of the bracket due to the nylon rollers

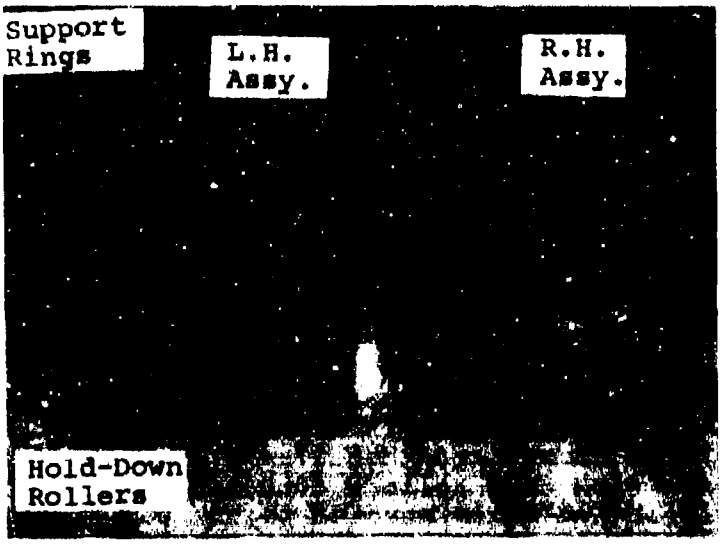


Figure 61. Roller Assemblies.

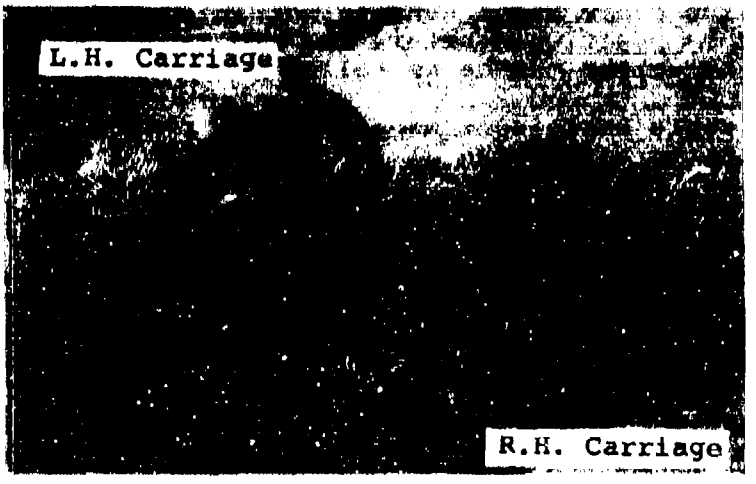


Figure 62. Cable Cutter Carriage Assemblies.

following the cable. An extension to the lower portion of the curved arm has mounting provisions for the lateral angle sensor with the centerline of the sensor in a longitudinal plane, i.e., parallel with the side load beams. Pivoted on this centerline and clamped to the sensor shaft is a lever arm extending down below the side load beams. The lower end of this lever mounts two side-by-side nylon rollers that straddle the cable. Side movement of the cable will deflect the two rollers, rotating the lever arm and hence the angle sensor. The cable angle sensor mechanism assembly can be seen in Figure 63. The bracket, curved arm, and extended lever are investment castings in stainless steel.

The cable length sensing mechanism is shown in Figure 64. A signal that is a function of the length of cable deployed is provided by measuring the number of turns of the cable drum from the cable up position. The linear transformer is mounted to the stationary bearing retainer of the LH drum support structure by means of an inner housing. The sensor input shaft is attached to the outer housing located and keyed to the rotating bearing retainer by means of a 48:1 speed reducing gearhead. Thus, the 20.5 turns of the cable drum, approximately 100 ft of cable result in approximately 154° of sensor shaft rotation, the output signal being a function of shaft rotation.

While the control circuit for the hoist drive operation provides speed reduction at each end of the cable travel through the length signal, overriding limit switches are provided for up and down limits. There are two up limit switches, one for normal cable up that ensures the swaged cable end fitting does not pass through the cable angle sensing mechanism and another for a "stowed" up position, where the cable is up such that the swaged end is between the side load beams. These switches are proximity sensors, mounted on individual brackets at the bearing support frame. The brackets attach by two of the bearing retainer bolts, permitting adjustment in intervals about the center support.

The target is mounted on a bracket attached to two bolts on the drum end plate, also adjustable for radial location. As the target passes in front of the switch within approximately .20 inch, the switch will operate. Cable fully out is limited by a micro switch operated by the drum as it approaches the gear support frame. The switch is actuated by a lever deflected by the drum, the switch being mounted on a bracket attached to the gear support frame.

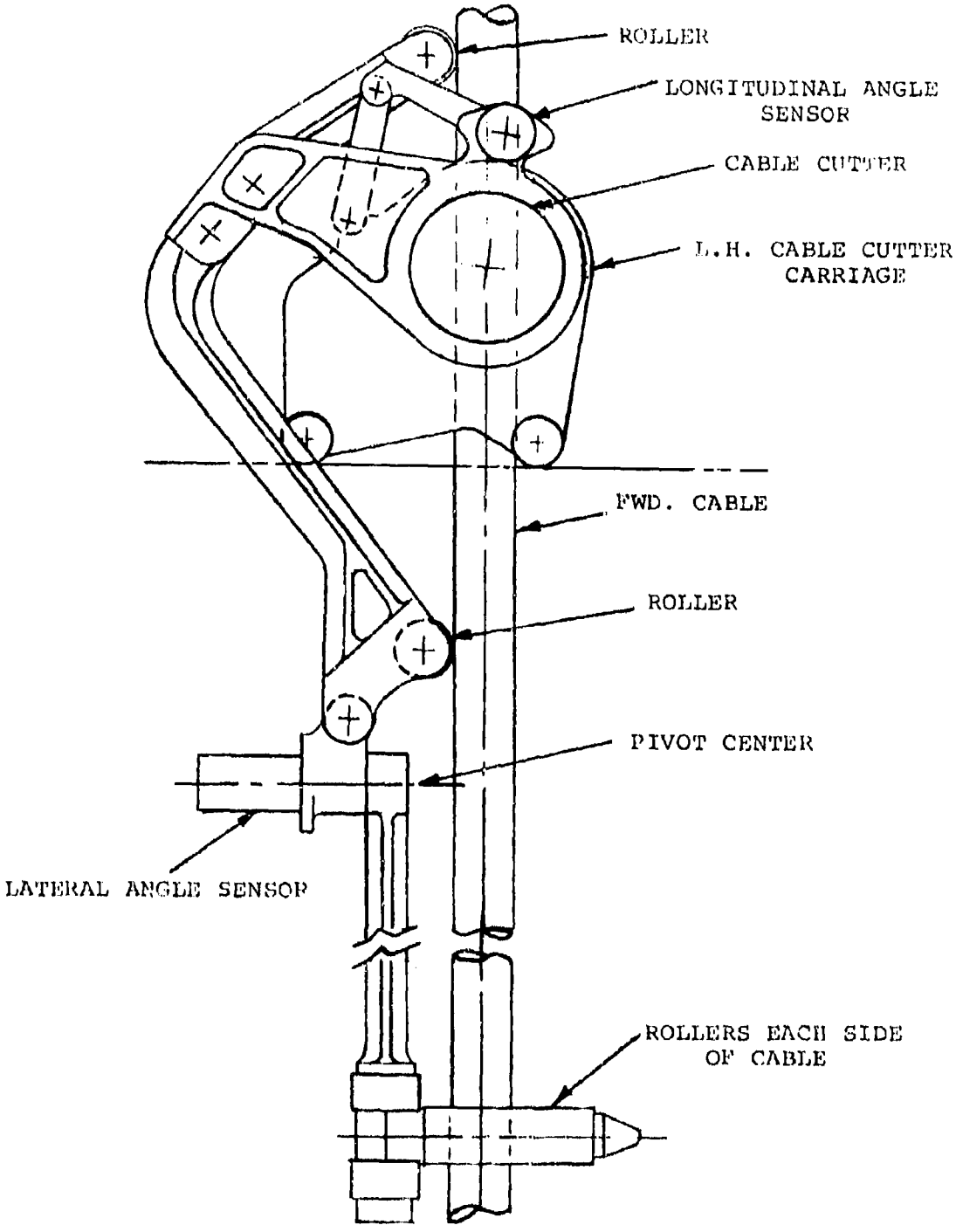


Figure 63. Cable Angle Sensor Mechanism.

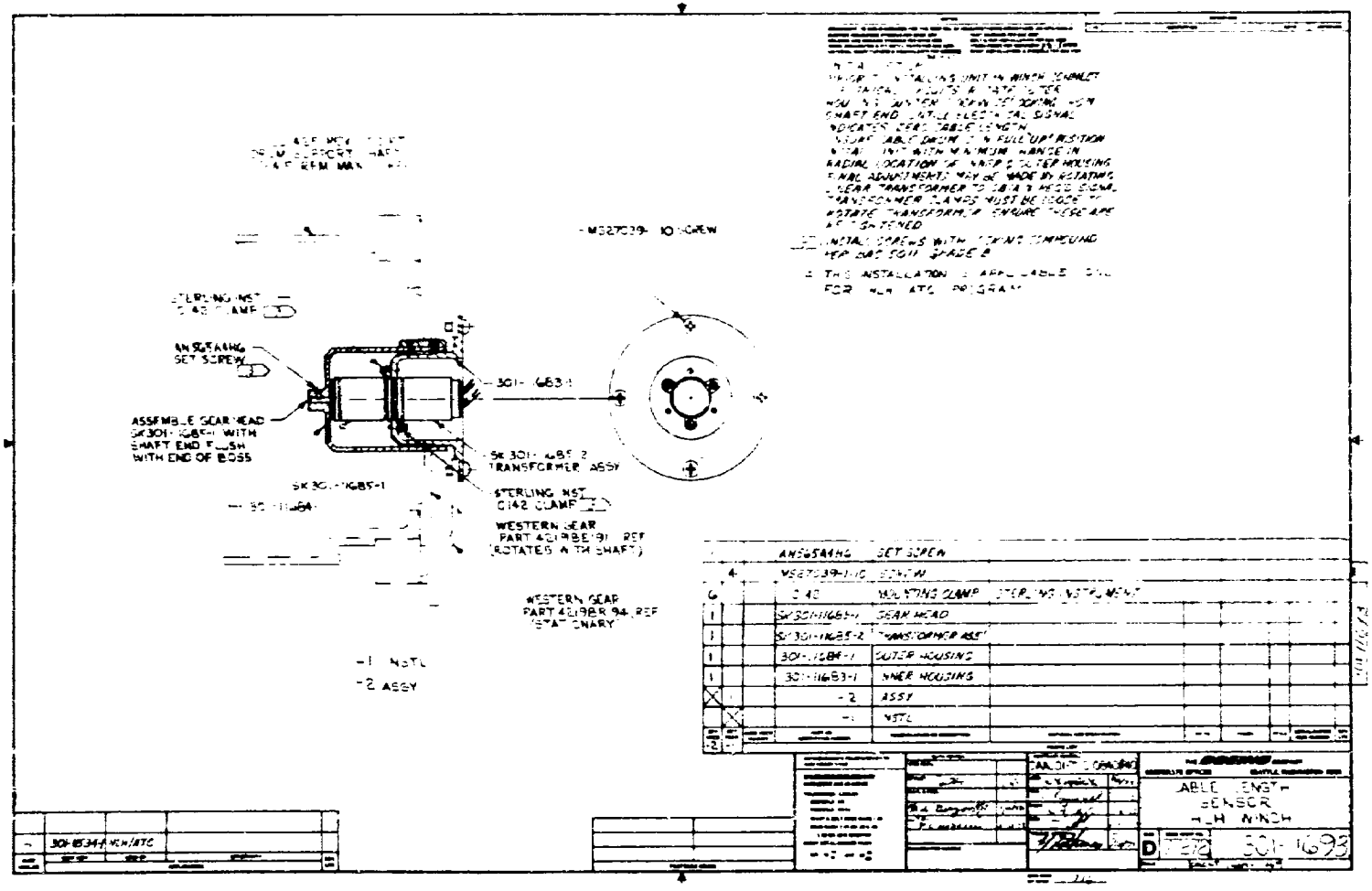


Figure 64. Cable Length Sensor.

LOAD ISOLATION

Proposal Configuration

The requirement to maintain the natural frequency of the external cargo suspension system between 1.5 and 2.0 Hz was recognized through the extensive experience and experimental programs with externally suspended loads conducted with the CH-47 helicopter.

An objective of a 2.0 Hz upper limit resulted from this experience, which showed that suspension frequencies must be kept below 75% of the 1/rev frequency of the rotor to avoid resonance of the load.

The 1.5 Hz lower limit was set to avoid coupling with normal pilot control inputs.

Figure 65 illustrates the projected suspension system natural frequency without load isolation.

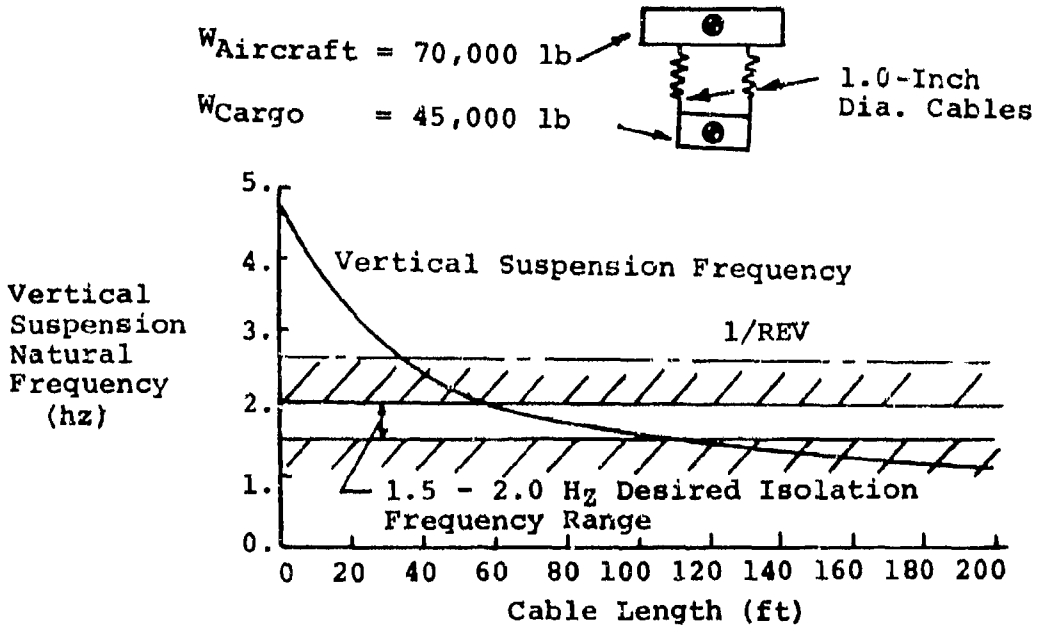


Figure 65. Vertical Suspension Natural Frequencies.

Recorded data on the effect of a resonant load on the cockpit vibration level for a CH-47A carrying a 12,000-lb external load is shown in Figure 66. An HLH vibration level objective line is also shown to indicate the necessity for the load isolators.

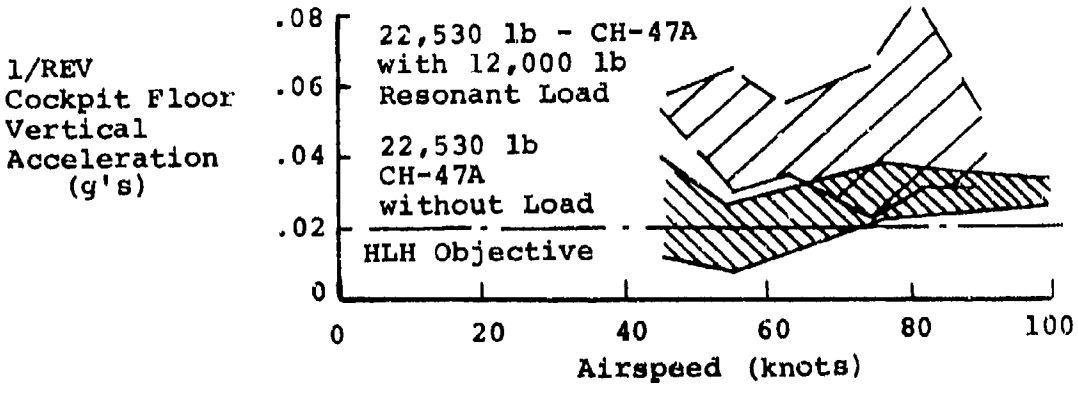


Figure 66. Measured Cockpit 1/Rev Vibration.

Several methods of introducing the isolator into the suspension system were considered. The simplest, most direct method would be to install the isolator between the coupling and the end of the tension member. However, this installation would increase the height of the coupling substantially and also eliminate any active or semiactive system.

Also considered was the suspension of the complete hoist assembly by the isolators. Design layouts established that this would be a complex and heavy method, increasing the problems of hoist repositioning. The selected method was to install the isolator such that it would react the torque of the cable over the drum. Isolator movement results in drum rotation. The basic hoist is static, simplifying mounting and position changing. Additionally, the isolator is essentially between the load and the hoist low-speed gearing, providing some shock load protection for this assembly.

Due to the variable length of cable that is available with the HLH hoist system, the isolator schematic as presented in the proposal was for an active oil/air system where the spring rate changed with changing load by means of regulating the air pressure within the isolator. The schematic is shown in Figure 67.

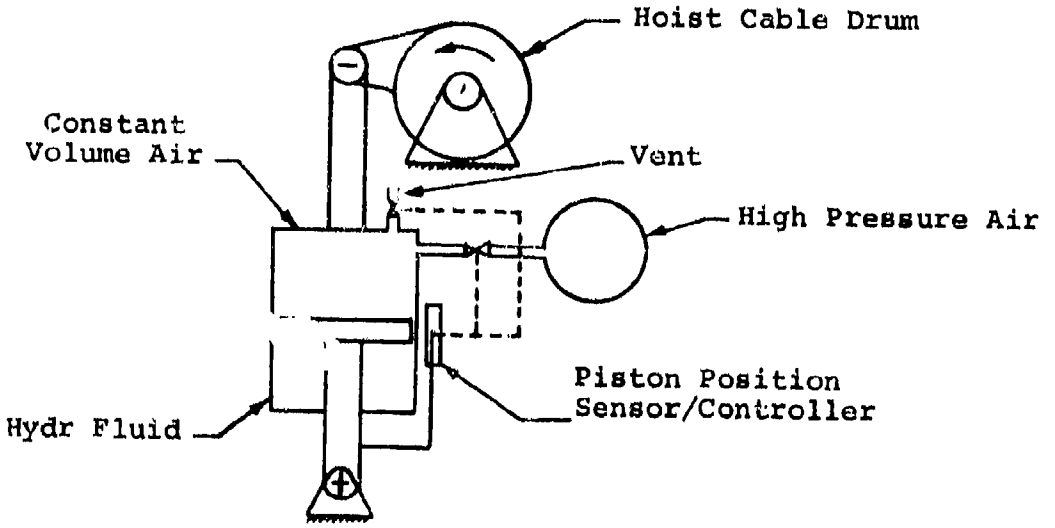


Figure 67. Load Isolator Schematic.

Preliminary Criteria and Configuration Development

Subsequent to the contract award, further dynamic analysis together with a review of the mechanization of an isolator installation indicated that a liquid spring could possibly fulfill the isolation function. In order to establish a physical envelope, the following criteria were developed:

1. Isolation would be limited to hoist loads between 10,000 lb and maximum load.

2. Isolation would be active to 1.5 g on maximum load.

The selection of the load range was based upon experience with external loads carried by the CH-47. This experience established that when the external load to aircraft weight ratio is below 0.3, there is no requirement for isolation. Experience with external loads has also shown that at high load weight to aircraft weight ratios inertia factors were unlikely to exceed 1.5 g.

As an alternate system, discussions were held with Kaman Aerospace Corporation to explore the application of their Cable Operated Zero Impedance Device (COZID) to the HLH/ATC load isolator requirement. The COZID is an anti-resonance device, as opposed to an isolator, and has the desirable characteristic of a tuned frequency independent of external load weight. Analytically, it is the only concept which meets all established load isolator requirements, including the grouping of suspension frequencies between 1.5 and 2.0 Hz to avoid control coupling and vertical bounce. The COZID is fully passive, mechanical, and possesses a minimal sensitivity to temperature changes.

The COZID concept was reviewed and a layout of a possible configuration to suit the hoist envelope was completed and is shown schematically in Figure 68. In this configuration, the hoist torque is reacted by a spring member; the torque-plate movement is amplified and rotates a tuning weight on a radius arm. Maximum arm movement is limited to 40 degrees. A four-phase development program was proposed to produce ATC hardware.

Following a review of the development effort, the COZID configuration was eliminated as resolution of the problems of mechanization appeared to be beyond the resources of the ATC program, and detailed studies of liquid spring characteristics modified by installation geometry offered a more economic solution.

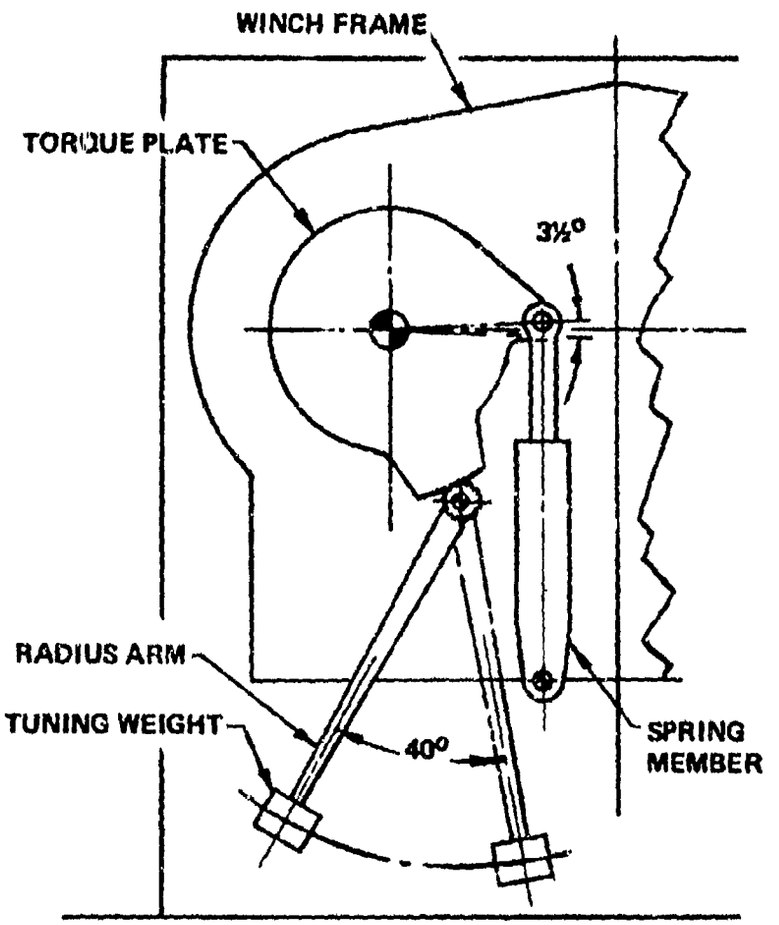


Figure 68. COZID Load Isolator Concept.

Requirements and Criteria

The general requirements and criteria for the load isolator were:

1. Prevent amplification of steady state 1/rev induced vibration of the aircraft.

2. Reduce the possibility of pilot induced oscillation at 1/rev.

3. Make fuselage natural frequencies independent of cargo mass.

4. Damp out transient vertical responses of the aircraft/load system caused by gusts or other disturbances.

The load isolator criterion is illustrated in Figure 69.

Data from the tension member development program was used to predict the tension member spring rate and plot isolator requirements for varying tension member lengths.

The load isolator desired characteristics to obtain the maximum range of cable lengths within the suspension natural frequency range of 1.5-2.0 Hz are shown in Figure 70. The resulting effect of this spring rate when integrated with the installation geometry is shown in Figure 71.

Load Isolator Preliminary Design

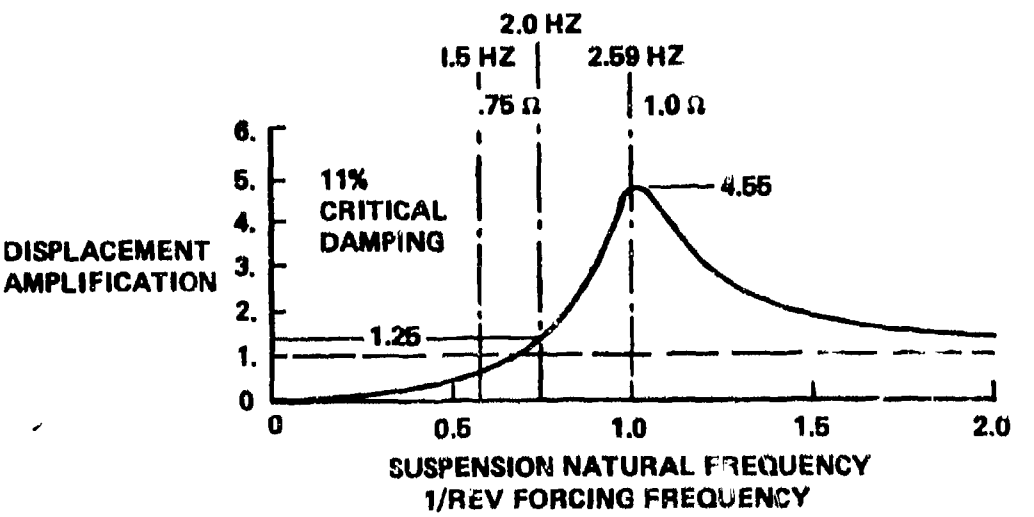
The principal problem in the use of a liquid spring for the load isolator is that of temperature compensation. The specification temperature range of -65°F to +160°F would mean that the initial load on an uncompensated spring could range from 0 to 16,000 lb. Three systems for temperature compensation were considered:

1. Electrically heated unit
2. Hydraulic pressure compensation
3. Air charged recuperator

The electrically heated unit would normally be operated at, or close to, the upper specification limit. Problems associated with this approach include:

1. High installed system weight
2. Need for electrical supply to the isolator
3. Lower reliability due to the addition of electrical components
4. Long warm-up time required before system is active.

- MINIMIZE RESPONSE TO 1/REV ROTOR FORCES BY TUNING SUSPENSION MODE FREQUENCIES TO .75/REV OR LOWER.



- RESULTING DESIRED ISOLATION MODE FREQUENCY RANGE IS 1.5 TO 2.0 HZ FOR A 1/REV FREQUENCY OF 2.59 HZ (156 rpm).
- KEEP SUSPENSION NATURAL FREQUENCIES ABOVE 1.5 HZ TO AVOID AIRCRAFT CONTROL PROBLEMS.

Figure 69. Load Isolation Criteria.

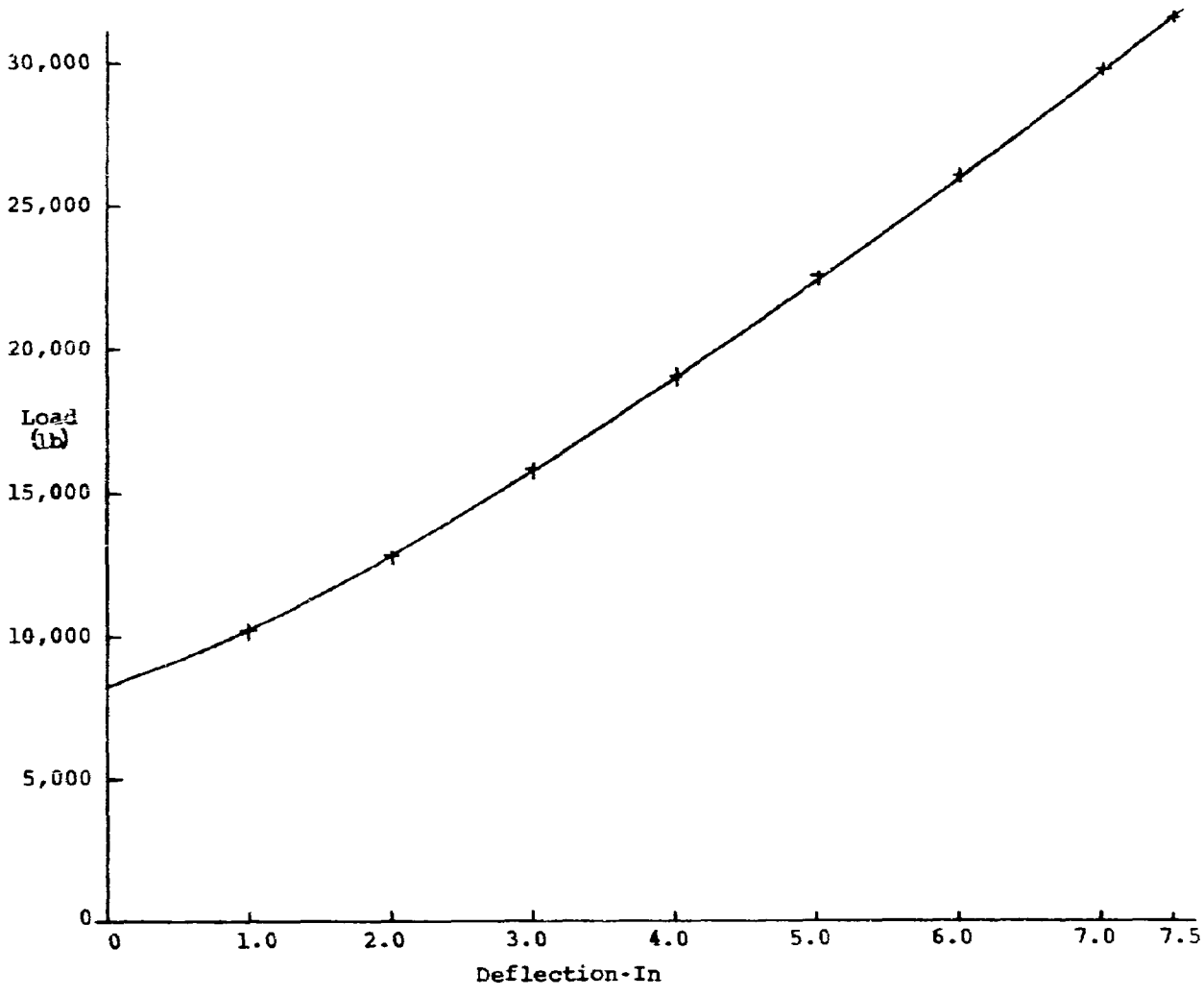
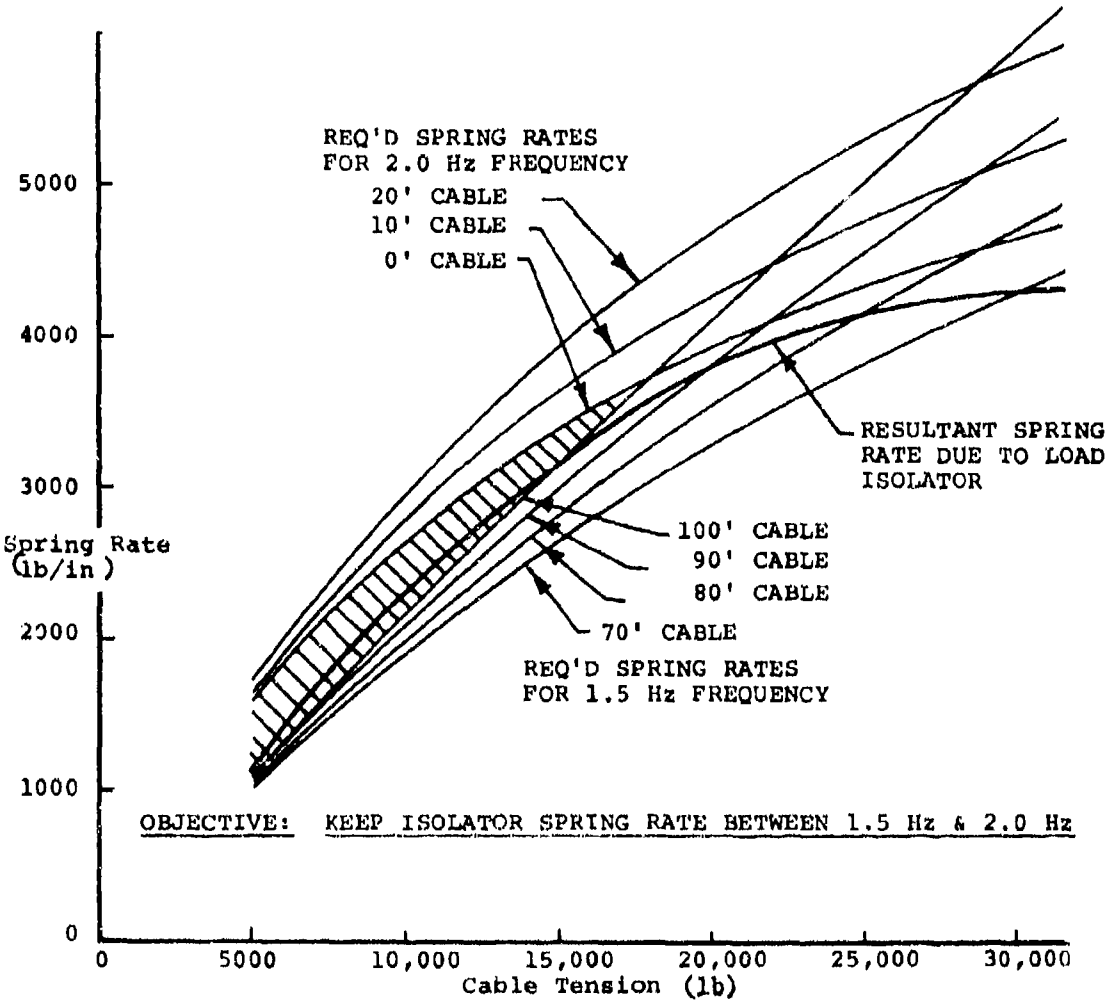


Figure 70. Load Isolator - Load/Deflection Characteristics.



Load Isolator Stroke - 7.5 inches
Cable Diameter - 0.72 Inch

Figure 71. Isolator Equivalent Spring Rate.

The hydraulic pressure compensated unit required the isolator fluid pressure to be exposed to the aircraft hydraulic system press via a stepped piston unit. The aircraft hydraulic system thus provided a reference pressure for the unit each time the aircraft was prepared for flight. Problems associated with this approach included:

1. Need for a hydraulic supply to the isolator
2. Complexity of additional hydraulic components reduces reliability
3. High installed weight.

The air-charged recuperator design has a separate recuperator chamber attached to the liquid spring. Fluid on one side of the recuperator piston is charged to the minimum spring fluid pressure by an air or nitrogen charge in the recuperator chamber. The recuperator piston has differential areas such that the fluid charge is in the order of twice the air or nitrogen pressure. While the liquid spring is fully extended, the recuperator fluid has direct passage to the spring fluid. Initial movement of the spring rod closed a valve, isolating the spring fluid from the recuperator. This concept is shown in Figure 72.

The addition of the recuperator reduces the effect of temperature change on the spring characteristics; however, the volume of fluid required to provide satisfactory compensation over the -65° to +165°F range resulted in a unit weight heavier than the target. Alleviating this requirement to a range of -25°F to +125°F results in a reduction in weight to the target. This does not inhibit high temperature operation and only constrains low temperature operation below -25°F in that to maintain full isolation capabilities, a minimum cable payout will have to be established until the unit warms up. Since this is accomplished in a relatively few cycles, it should impose no operational constraint.

The air charged recuperator system was selected. The decision was based principally on the fact that the isolator is a self-contained unit independent of the aircraft systems, with a resultant improvement in reliability and weight.

The unit that was selected is a nitrogen-charged recuperator compensated liquid spring, which has been developed into the design described below. Eight load isolators were produced to this design with an additional unit for test purposes. Development testing was conducted in parallel with production, and initial results showed the need for modification to the units to reduce the unit stiffness at the low temperature extreme of the environmental range. The reduction in stiffness was obtained by increasing the displaced fluid volume

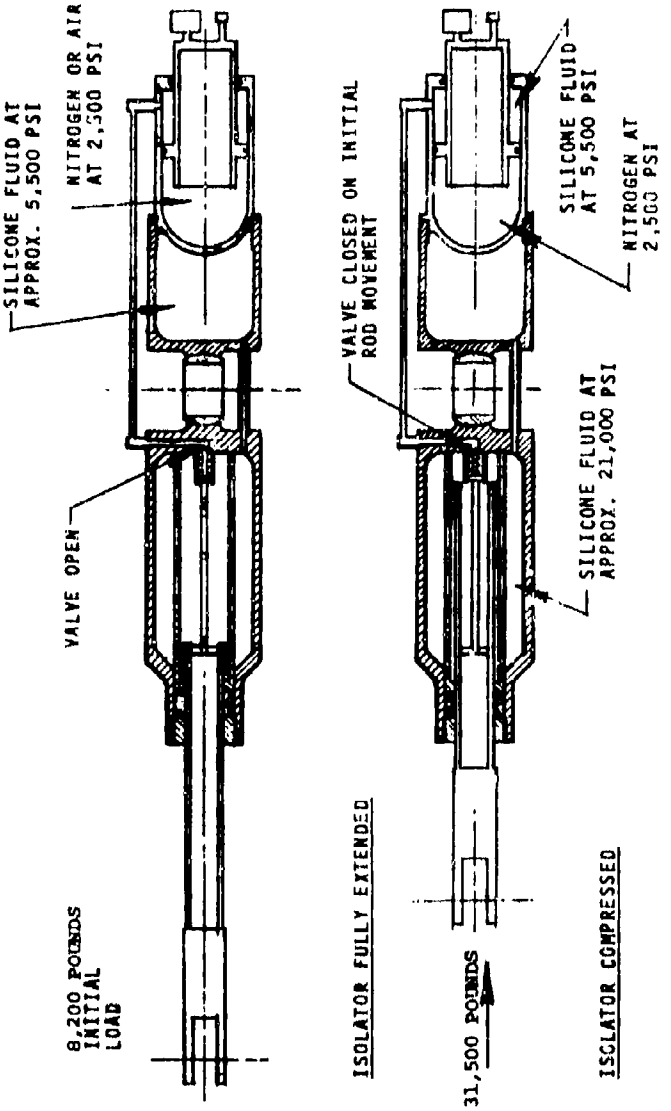


Figure 72. Schematic of HLH/ATC Load Isolator.

approximately 10%. Changing the piston rod diameter from 1.3125 inches to 1.25 inches provided the required 10% volume increase and retained positive margins for the unit strength. Existing piston rods were reworked to the new diameter. New gland packs and gland nuts were required. The isolator is installed on the hoist assembly reacting the torque through the third-stage planet carrier. A combination of installation geometry and liquid spring characteristics results in the spring rate/cable tension curve necessary to limit the suspension system natural frequency below 2.0 Hz and above 1.5 Hz for the maximum practical range of cable lengths.

General Description

The load isolator consists of a liquid spring using high compressibility silicone fluid with a nitrogen-charged recuperator chamber built into the assembly. The piston rod terminates in a clevis end which mounts over the hoist planetary reaction arm and includes a load cell for axial load sensing. The cylindrical spring fluid housing has a self-aligning bearing installed to suit the hoist mounting provisions, splitting the fluid volume into two interconnected areas. Below the spring fluid housing is the recuperator chamber. The recuperator piston has differential areas such that the working fluid pressure is approximately twice that of the nitrogen charge. When the liquid spring is fully extended, the recuperator fluid has direct passage to the spring fluid, providing the datum pressure, to partially compensate for pressure changes due to temperature variation. Initial movement of the piston rod closes a valve isolating the spring fluid from the recuperator. Maximum fluid pressure at full stroke is approximately 23,000 psi.

The recuperator piston provides a visual indication of the correct fluid volume; a pressure gage indicates the nitrogen pressure. Figure 73 shows two load isolators.

Detail Design

The detail design of the isolator is shown on the Dowty Rotol Assembly Drawing 200646102 (Figure 74).

The pressure cylinder is machined from maraging steel heat treated to 260,000 psi. The spherical support bearing for the isolator is installed at approximately mid-length, causing the internal volume to be split into two areas. Machined passages connect the two volumes. Each end of the cylinder is threaded on the inside diameter; the larger cavity has the end cap containing the gland assembly installed, the other has the recuperator cylinder. Adjacent to the support bearing, a passage connects a valve seat installed in the base of the larger cavity to an external fitting and tube

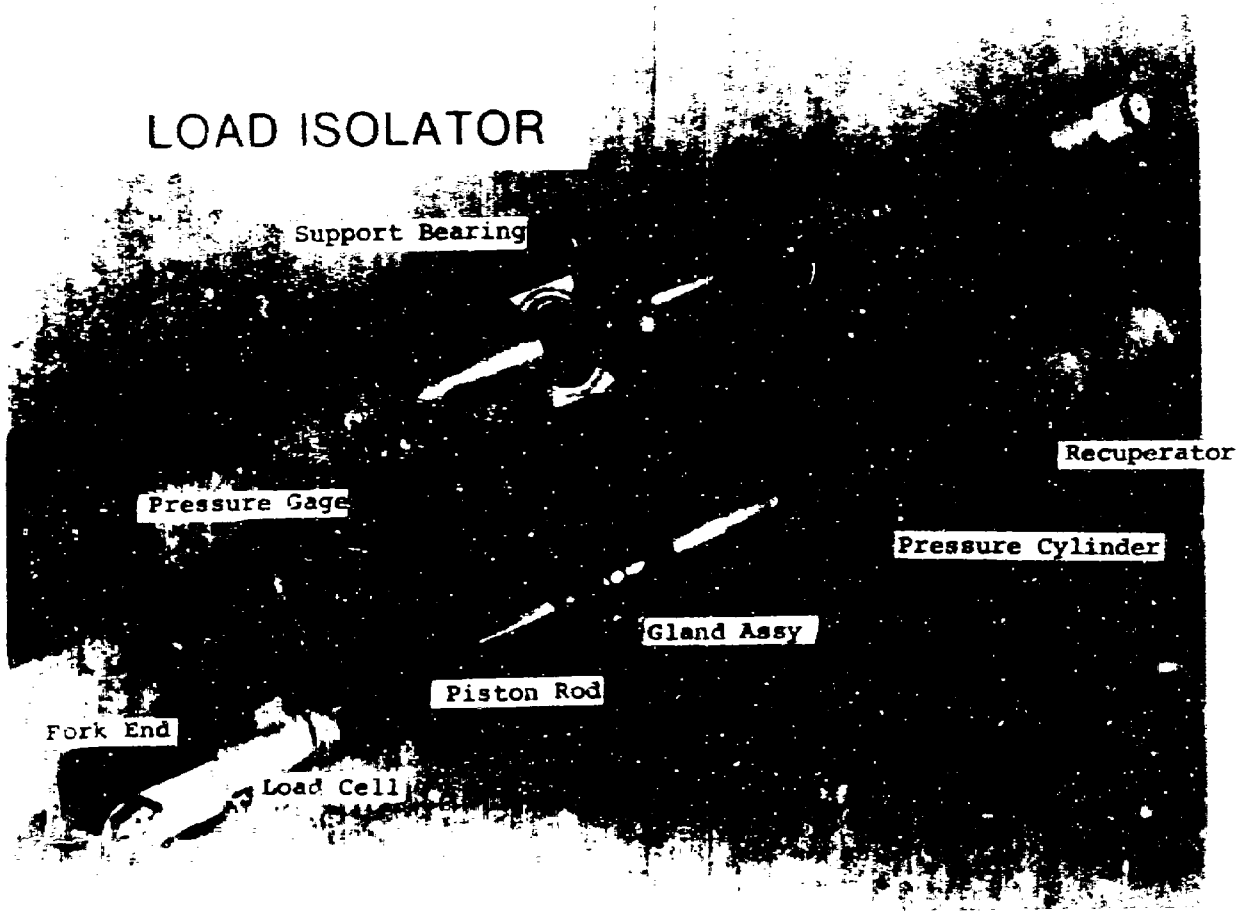


Figure 73. Load Isolators.

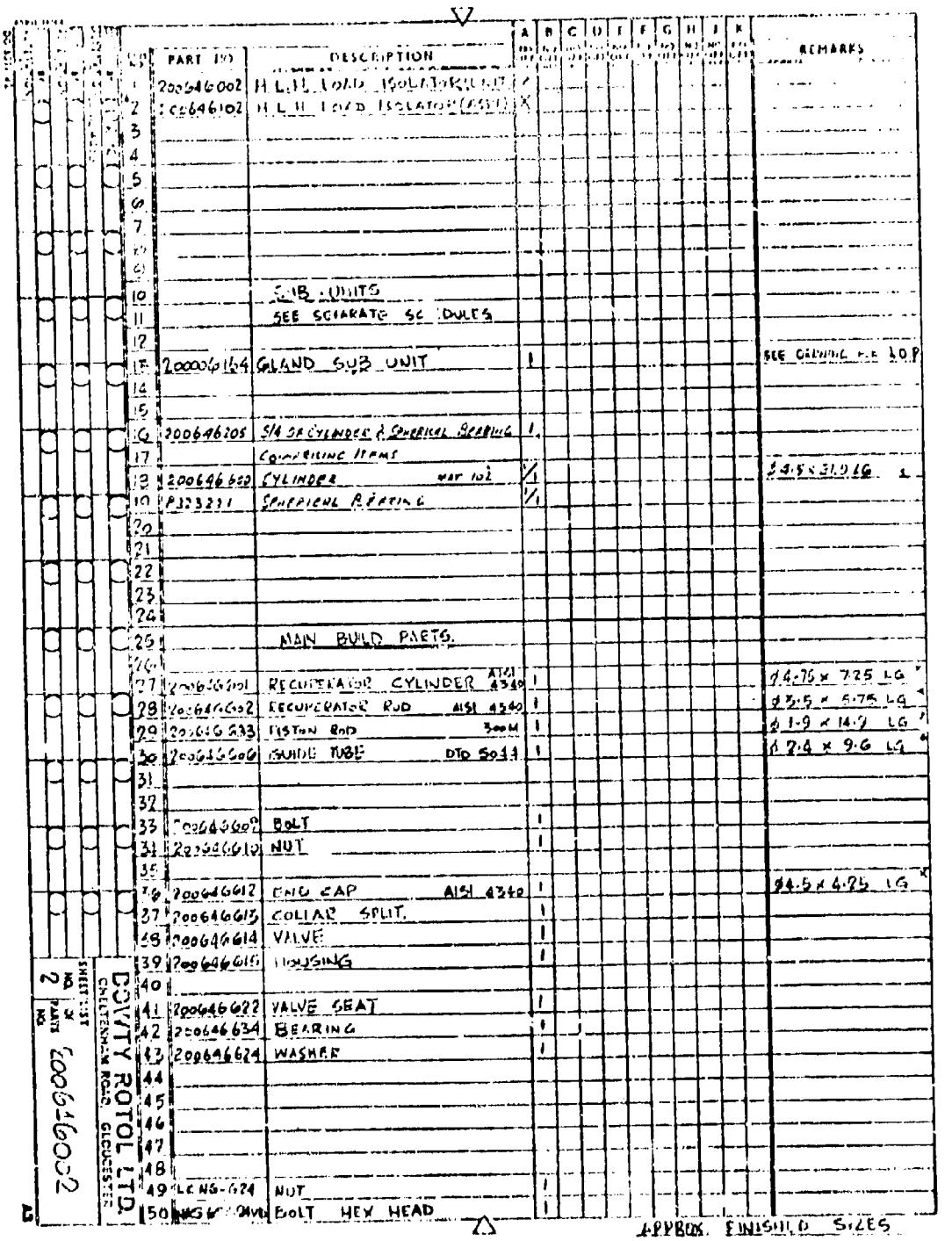
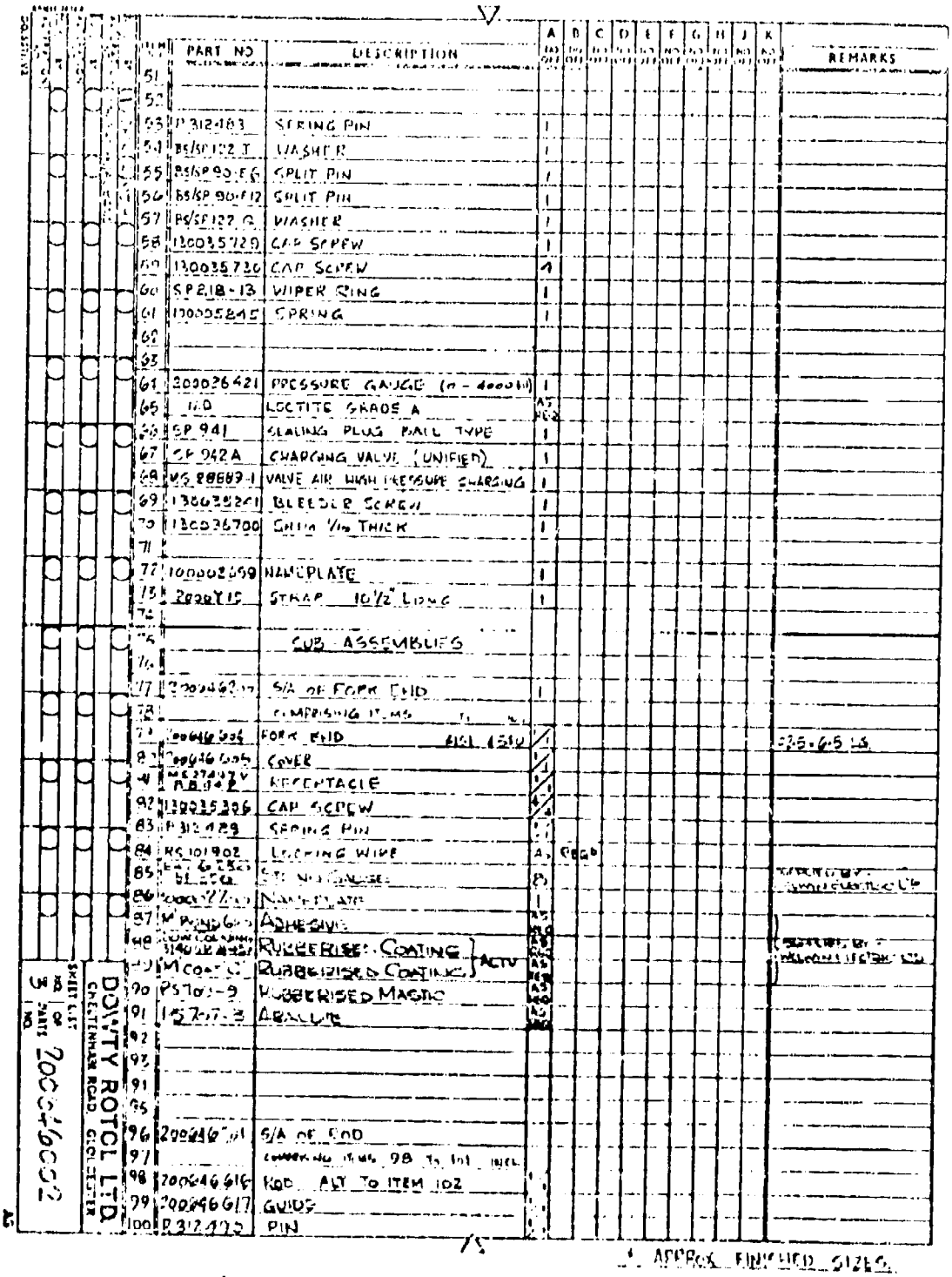


Figure 74. Load Isolator Assembly.
(Sheet 1 of 4)



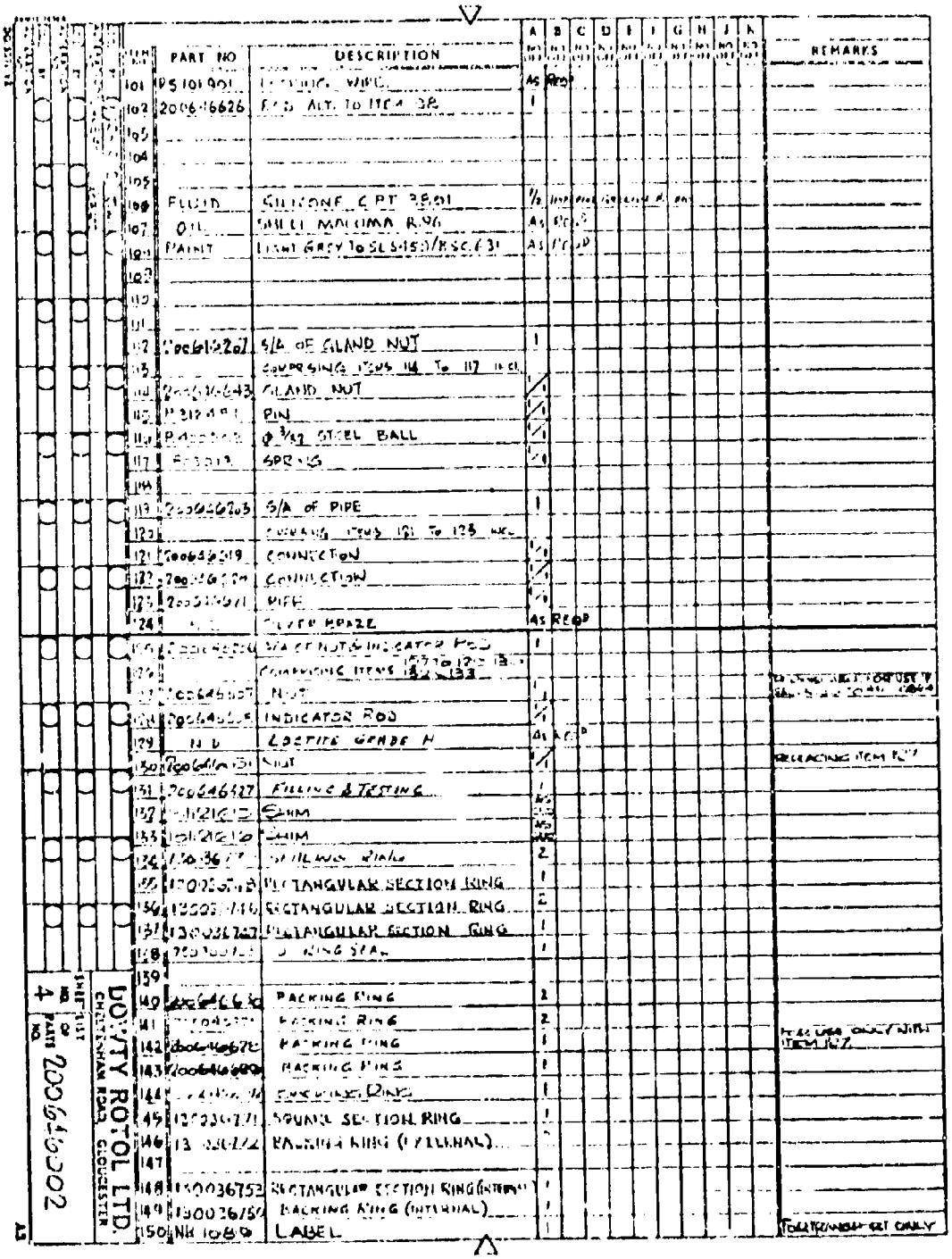
ITEM	PART NO	DESCRIPTION	A	B	C	D	E	F	G	H	J	K	REMARKS
53	P312483	SPRING PIN	1										
54	BS/SP122 T	WASHER	1										
55	BS/NP90-E6	SPLIT PIN	1										
56	BS/SP90-F12	SPLIT PIN	1										
57	BS/SP122 G	WASHER	1										
58	1300355720	CAP SCREW	1										
59	1300355730	CAP SCREW	1										
60	SP218-13	WIPER RING	1										
61	1300058455	SPRING	1										
62													
63													
64	200026421	PRESSURE GAUGE (0 - 4000 PSI)	1										
65	N.D	LOCTITE GRADE A	AS REQ										
66	SP 941	SEALING PLUG BALL TYPE	1										
67	SP 942A	CHARGING VALVE (UNIFIED)	1										
68	MS 28889-1	VALVE AIR HIGH PRESSURE CHARGING	1										
69	1300355241	BLEEDER SCREW	1										
70	1300356700	SHIM 1/16 THICK	1										
71													
72	100002659	NAMEPLATE	1										
73	2828Y15	STRAP 10½" LONG	1										
74													
75		SUB ASSEMBLIES											
76													
77	200046[illegible]	S/A OF FORK END	1										
78		COMPRISING ITEMS [illegible]											
79	200046 605	FORK END	1										2.5-6.5 LS
80	200046 606	COVER	1										
81	MS 27407 V P.B.S.4 Z	RECEPTACLE	1 4										
82	1300355396	CAP SCREW	4										
83	P312489	SPRING PIN	1										
84	RS 101902	LOCKING WIRE	AR	REQD									
85	[illegible]	[illegible]	[illegible]										[illegible]
86	[illegible]	NAMEPLATE	1										
87	M [illegible]	ADHESIVE	AS REQ										
88	[illegible]	RUBBERISED COATING } ACTV	AS REQ										
89	M Coat C	RUBBERISED COATING } ACTV	AS REQ										
90	PS 101-9	RUBBERISED MAGIC	AS REQ										
91	157-7-3	ARALDITE	AS REQ										
92													
93													
94													
95													
96	200046[illegible]	S/A OF ROD											
97		COMPRISING ITEMS 98 TO [illegible] INCL											
98	200046 616	ROD ALT TO ITEM 102	1										
99	200046 617	GUIDE	1										
100	P312 [illegible]	PIN	1										

DOWTY ROTOL LTD. CHELTENHAM ROAD, GLOUCESTER

SHEET LIST NO 3 SHEETS 2 OF 3 NO 200046[illegible]

1. APPROX FINISHED SIZES.

Figure 74. Continued
(Sheet 2 of 4)



ITEM NO	PART NO	DESCRIPTION	A	B	C	D	E	I	G	H	J	K	REMARKS
101	PS 101 901	[illegible] WIRE	AS	REQ'D									
102	2006-6626	R.H.D. ALT. TO ITEM 38	1										
103													
104													
105													
106	FLUID	SILICONE C.P.T. 35.01	1/2	Imperial Gallons									
107	OIL	SHELL MACOMA R.96	AS	REQ'D									
108	PAINT	LIGHT GREY To SLS-150/BSC.631	AS	REQ'D									
109													
110													
111													
112	2006-6207	S/A OF GLAND NUT	1										
113		COMPRISING ITEMS 114 To 117 INCL.											
114	2006-6643	GLAND NUT	1										
115	[illegible]	PIN	1										
116	[illegible]	Ø 3/32 STEEL BALL	1										
117	[illegible]	SPRING	1										
118													
119	2006-6603	S/A of PIPE	1										
120		COMPRISING ITEMS 121 To 125 INCL.											
121	2006-6619	CONNECTION	1										
122	2006-6618	CONNECTION	1										
123	2006-6617	PIPE	1										
124	[illegible]	SILVER BRAZE	AS	REQ'D									
125	[illegible]	S/A OF NUT & INDICATOR ROD	1										
126		COMPRISING ITEMS 127 To 133 INCL.											
127	2006-6607	NUT	1										
128	2006-6606	INDICATOR ROD	1										
129	N.D.	LOCTITE GRADE H	AS	REQ'D									
130	2006-6630	SEAT	1										
131	2006-6627	FILLING & TESTING	1										
132	[illegible]	SHIM	AS	REQ'D									
133	[illegible]	SHIM	AS	REQ'D									
134	[illegible]	SPRING WASHER	2										
135	[illegible]	RECTANGULAR SECTION RING	1										
136	[illegible]	RECTANGULAR SECTION RING	2										
137	[illegible]	RECTANGULAR SECTION RING	1										
138	[illegible]	O RING SEAL	1										
139													
140	[illegible]	PACKING RING	2										
141	[illegible]	PACKING RING	2										
142	[illegible]	PACKING RING	1										
143	[illegible]	PACKING RING	1										
144	[illegible]	PACKING RING	1										
145	[illegible]	SQUARE SECTION RING	1										
146	[illegible]	PACKING RING (EXTERNAL)	1										
147													
148	1300 36752	RECTANGULAR SECTION RING (INTERNAL)	1										
149	1300 36754	BACKING RING (INTERNAL)	1										
150	NK 1088	LABEL	1										

DOWTY ROTOL LTD. CHELTENHAM ROAD, GLOUCESTER

SHEET LIST 4 PARTS NO. 2006-6302

Figure 74. Continued
(Sheet 3 of 4)

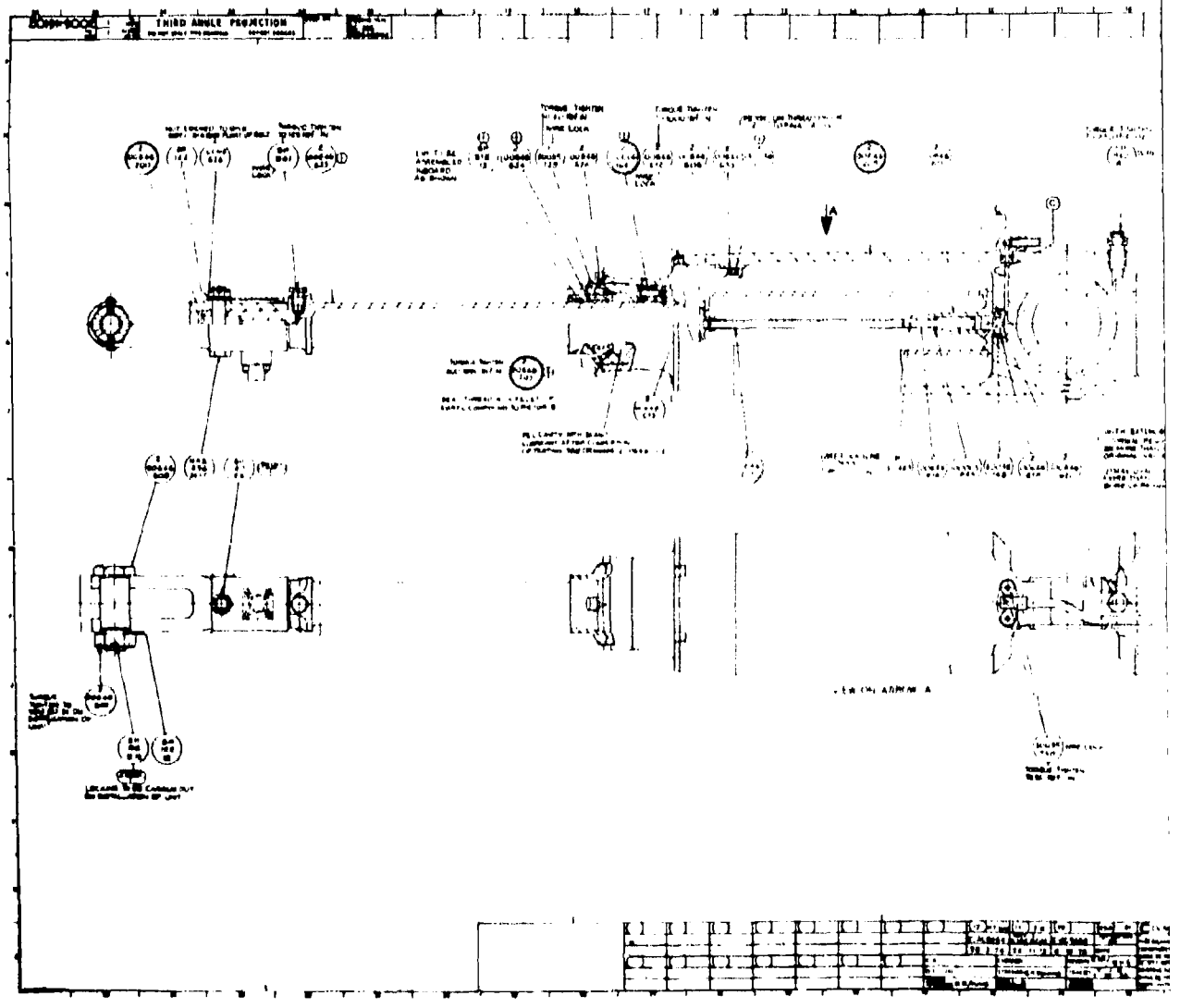
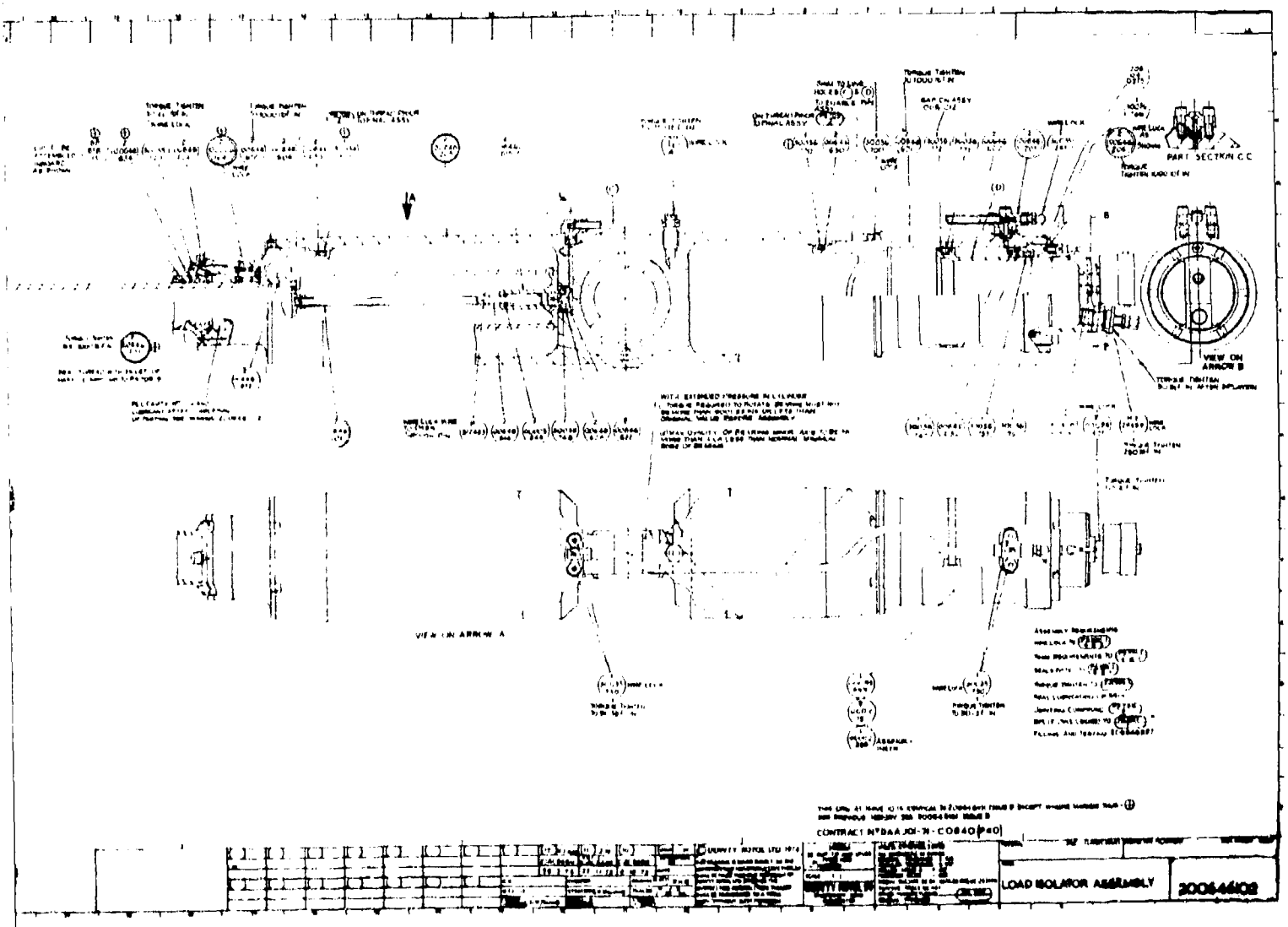


Figure 74. Load Isolator Assembly
(Sheet 4 of 4).



oad Isolator Assembly
(Sheet 4 of 4).

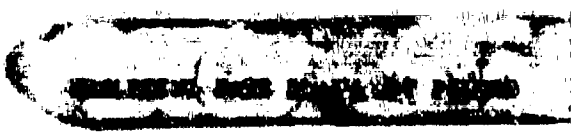
connecting to the recuperator cylinder.

The recuperator cylinder machined from 4340 steel heat treated to 200,000 psi is completely sealed from the pressure cylinder except for the external tube connection. An integral piston and rod can move inside the recuperator, with the piston rod extending through a sealing nut closing the recuperator. The base of the piston rod, external to the cylinder, contains an MS28889-1 charging valve and a pressure gage. The sealing nut has an indicator rod assembled and marked to provide a visual indication of the piston rod position and hence in conjunction with the pressure gage reading an indication of the correct fluid quantity. Nitrogen fills the volume inside the piston rod and above the piston; fluid fills the area below the piston,which is vented to the pressure cylinder by the external tube.

The gland assembly, installed in the pressure cylinder at the opposite end to the recuperator, includes the gland housing, sealing gland, and gland nut. The sealing gland is clamped between the gland nut and the piston guide tube. The piston guide tube extends to the base of the cavity and traps the valve assembly to the pressure cylinder. The piston rod passes through the sealing gland, being supported by the guide tube when the rod moves into the cylinder. When fully extended, a lip on the piston reacts the valve from its seat by means of a tubular link. On initial movement of the piston rod the valve is closed by a spring contained in the valve housing, ensuring the recuperator fluid has passage to the spring fluid only when the piston rod is fully extended.

The hollow piston rod is machined from maraging steel heat treated to 275,000 psi tensile strength. A detachable fork end is assembled to the external end of the piston rod such that the end load is reacted by a shoulder on the rod; the attaching bolt being installed in oversize holes. The fork end has a strain-gage type load sensing element bonded to its outside diameter with an aluminum protecting shroud. An MS27497 type connector is provided for the 28-volt supply and output wiring.

The assembly is filled with silicone fluid type CPT3801 through a charging valve in the pressure cylinder adjacent to the support bearing. Bleed screws are provided at the outer end of the piston rod and through the fluid area of the recuperator to ensure complete filling. The gland nut contains a reservoir for lubricating oil.



HOIST SUPPORT AND SPAN POSITIONING (TRAVERSE) SYSTEM

Proposal Configuration

Studies directed toward the definition of an optimum span for the dual-point lift system indicated that no single span would satisfy all the projected loads for the HLH. A prime requirement for the HLH will be the placement and extraction of 20-foot-long containers from the hold of containerships. To ensure cable clearance inside the hold, it is essential that the lifting span be less than 20 feet. Also, the requirement to use the dual-point lift as a single-point lift by the addition of an adapter would be more readily fulfilled by a short lifting span. To accommodate a 40-foot-long load, however, requires a lifting span in excess of 20 feet to obtain the maximum advantage from the dual-point lift system. Flight tests conducted in 1969 with a two-point system on a CH-47 helicopter had shown that good load stability could be maintained with lifting span to load length ratios in the order of 0.6. Based on this ratio, the minimum lifting span for a 40-foot container would be 24 feet. A lifting span variable between 16 feet and 26 feet was selected as a design objective, these limits ensuring compliance with the above requirements.

Integration of the hoist installation within the proposed structural configuration of the HLH fuselage, and maintaining the allowable CG envelope, dictated a maximum movement of the aft hoist of 50 inches. The boundaries of this movement being limited by major structural members. The forward hoist installation was therefore configured for a 70-inch travel.

It was originally conceived that the hoist lifting span would be infinitely variable between the maximum and minimum limits. Studies of the structural requirements to fulfill this objective showed weight penalties in excess of 1,000 lb over the use of discrete lifting locations at each end of the hoist travel. Additionally, no operational requirement was foreseen that would require lifting spans other than those established by the installation geometry, i.e., 16 feet, 26 feet and some intermediate span. Typical cargo characteristics and appropriate lifting spans are shown in Figure 75.

The proposal therefore presented the basic arrangement for the forward hoist to have a 70-inch travel and the aft hoist a 50-inch travel. With these dimensions, four separate lifting spans would be available: 16 ft-0 in, 20 ft-2 in, 21 ft-10 in and 26 ft-0 in.

Trade Studies

Subsequent to the contract award, a study was completed on alternate methods of moving the hoist assembly between

HOIST SPAN PLOT CODE	CARGO CHARACTERISTICS (FSF U.S. ARMY CHARACTERISTIC SHEETS) MODEL/DESCRIPTION	WEIGHT TONS	LENGTH FEET	CG OFF-SET FEET
a	CONTAINERS	22.4 28– 1/8	20 30 40	1.0 1.5 2.0
	WEAPONS & VEHICLES			
b	M35 – 2½ T. 6 x6 TRUCK	6.4	16.0	1.60
c	M113 – ARM. PERS CAR.	10.1	11.5	1.50
d	M577 – ARM. CMD PAST	11.4	12.0	.91
e	M106 – ARM. S.P. 107	12.2	11.6	.90
f	890258 – 5T TRUCK	13.3	20.0	5.8
g	5FD – TRUCK – 15T	14.3	19.0	3.0
h	XM511 – SHERIDAN TANK	16.0	16.6	1.32
i	LR – TRUCK	16.2	22.5	0.00
j	SB–3001 – TRUCK	17.6	18.6	3.1
k	D8 – TRACTOR	18.1	9.4	.19
l	TD–18–182 – TRACTOR	19.4	9.5	.71
m	M109 – 155M HOWITZER	25.2	18.6	1.30
n	TD–24–241 – TRACTOR	27.0	8.9	.30
o	304 – CRANE SHOVEL	27.6	12.4	1.8
p	PLATFORMS & GONDOLAS	10 28– 1/8	20 40	1.5 2.6

CARGO CHARACTERISTICS

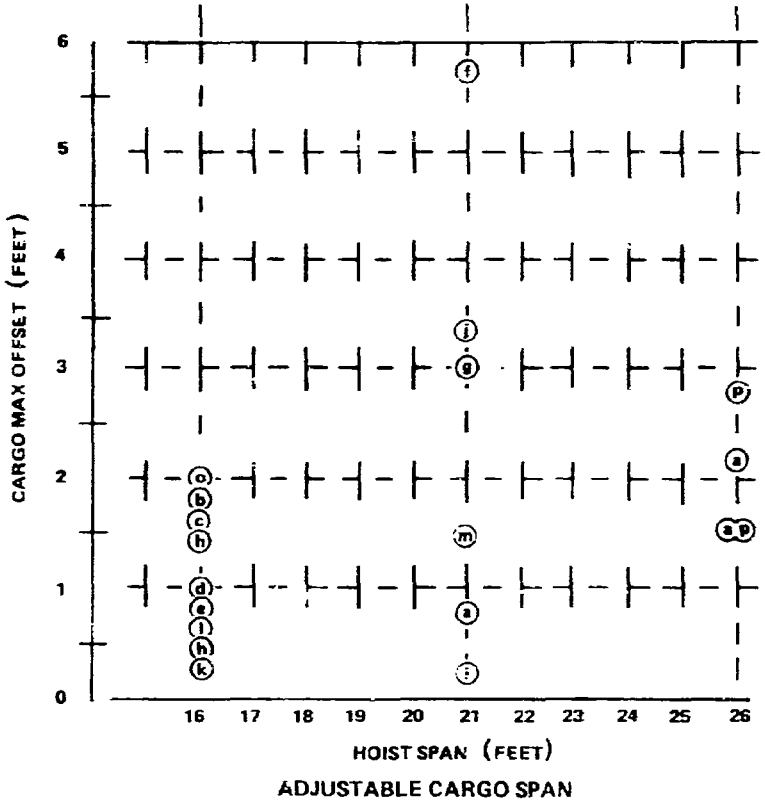


Figure 75. Cargo and CG Variations Accommodated by Tandem Suspension.

operating locations. Two basic systems for positioning the hoist were considered and developed to a depth sufficient to establish weight comparisons. The two systems compared were roller and track and swinging arm arrangements. These concepts are illustrated in Figure 76. A weight analysis based on electrical actuator/capstan-drum and cable powered systems did not show any significant weight advantage for either concept.

A reliability review did show that the reduced number of critical functioning parts on the track and roller system would result in an arrangement with higher reliability. Based on this review and an assessment that the roller-and-track system would involve a lower-risk design, the decision was made to proceed with this concept.

The pneumatic duct interface was considered as part of this study and several duct arrangements were compared, as shown in Figure 77. A distribution duct consisting of two articulated lengths was selected as the preferred arrangement to avoid the potential problems associated with telescopic tubes.

As a result of interface studies with the Airframe Design Group, revised fuselage structural concepts were devised which permitted two equal length hoist tunnels, each allowing a 60-inch hoist position change. This change provided three lifting spans: 16 ft-0 in, 21 ft-0 in, and 26 ft-0 in; and had the advantage of simplifying the structural design and reducing the tooling and the number of different parts. The span positioning system would also be simplified, and all parts of the actuating arrangement would be common to both bays.

It was also established that a single-level track would be used rather than a bi-level track to reduce the weight.

A study was conducted to establish the possibility of showing an overall weight saving by increasing the length of the hoist frame to permit using three airframe fittings per side in each bay instead of four. The study established that the existing geometry of hoist frame and four airframe fittings per side was lighter.

Requirements, Criteria and Objectives

The principal requirements and criteria include:

1. Hoist position may be changed in flight or on the ground.

2. Hoist will not change position when carrying a load.

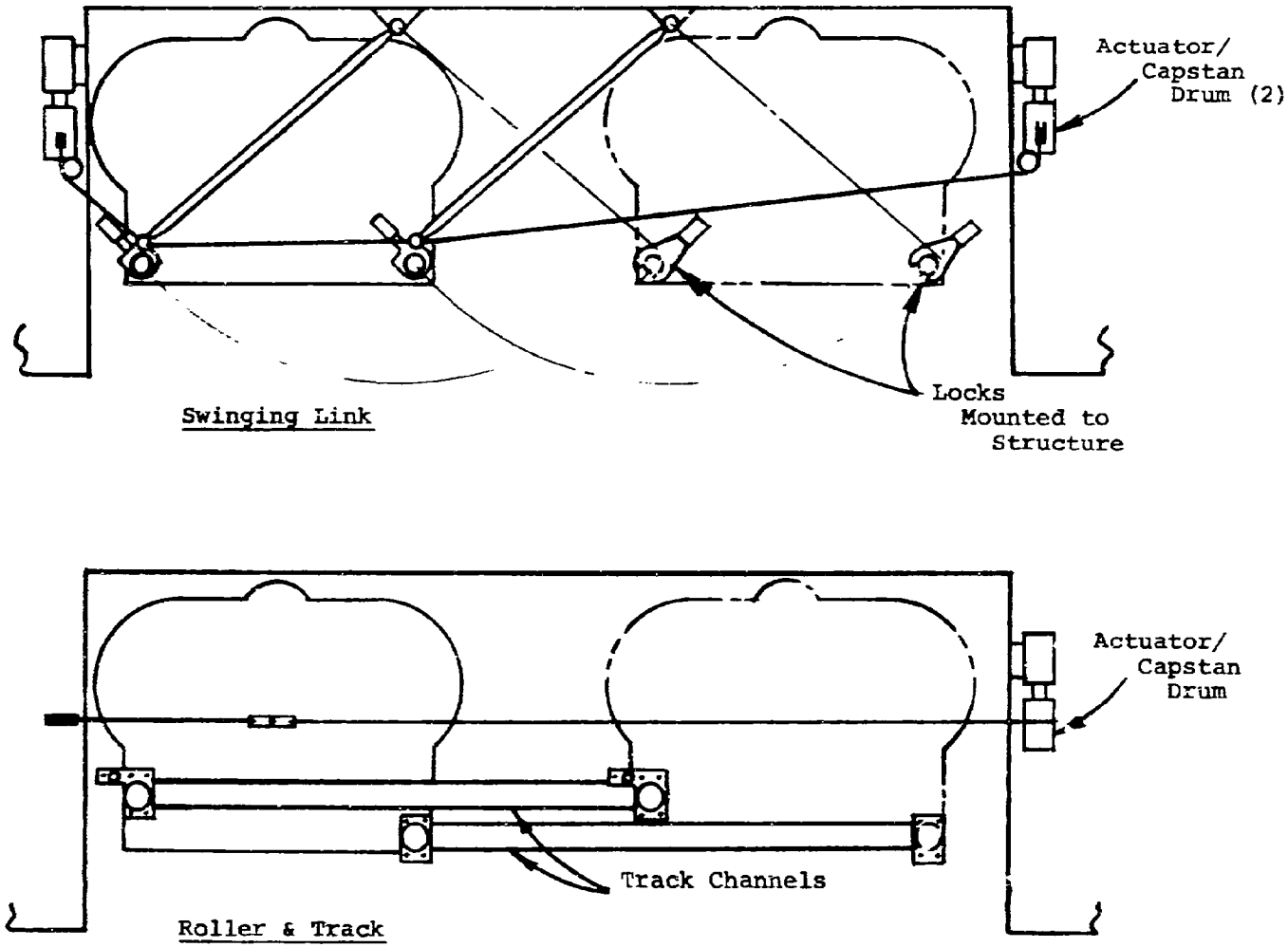
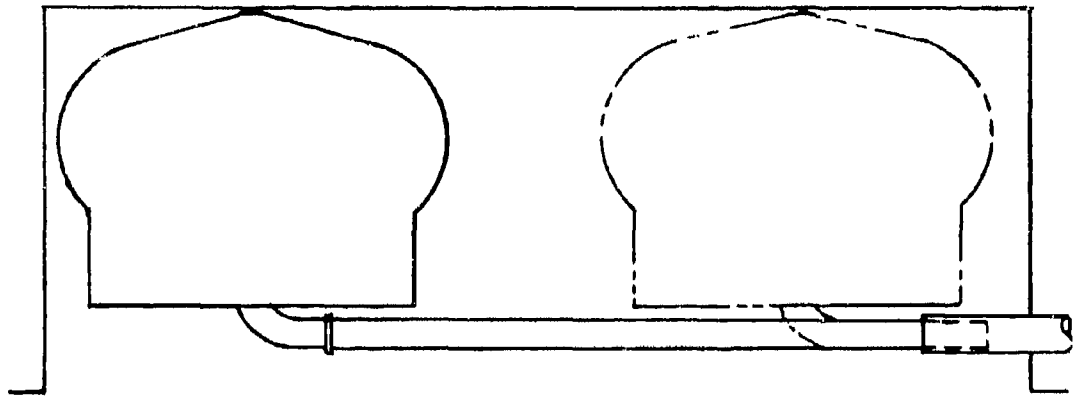
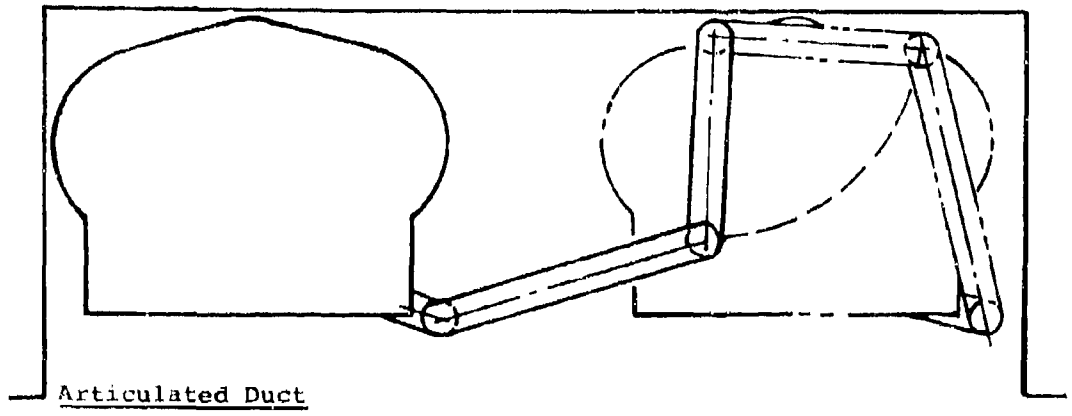


Figure 76. Span Positioning System Concepts.



Telescopic Duct



Articulated Duct

Figure 77. Pneumatic Duct Arrangements.

3. Hoist position changes will be accomplished within 1 minute.

4. Hoist positioning system will be designed for a minimum life of 5,400 position changes. This number is based upon an aircraft design life of 3,600 flying hours; three hoist cycles per flight hour and one position change every second hoist cycle.

Preliminary Design

The design developed for the ATC Program is based on supporting the hoist by four roller fittings and locking into the airframe by two retractable lockpins. The four rollers are mounted at a single level requiring one rail on each sidewall. At the load position the rollers engage in shallow depressions in the load-reacting fittings. The rollers are configured such that when repositioning, the aft roller will not engage in the forward roller fitting, and the forward roller will not engage in the aft roller fitting, providing a smooth transition.

The two lockpins are mounted on the forward member of the hoist frame and are actuated by a single actuator and linkage system, also mounted on the same frame member.

The hoist is repositioned by a dual cable arrangement powered by an electrical motor/gearbox/capstan assembly, electrically interlocked such that operation is only possible with no load on the hoist. Figure 78 shows the cable arrangement schematically.

Design Support Testing

An ultimate test was conducted on a roller assembly (Figure 79) to establish the lateral load capability of the support bearing retention, resulting in a failure load approximately 50% above the design ultimate requirement. Other areas of the design were amenable to analysis.

The system actuator was functioned at design load and demonstrated at design limit stalled load.

With these areas of design confirmed, the following design was committed for fabrication and installation in the Integrated Test Rig.

General Description

The span positioning system involves two areas of effort:

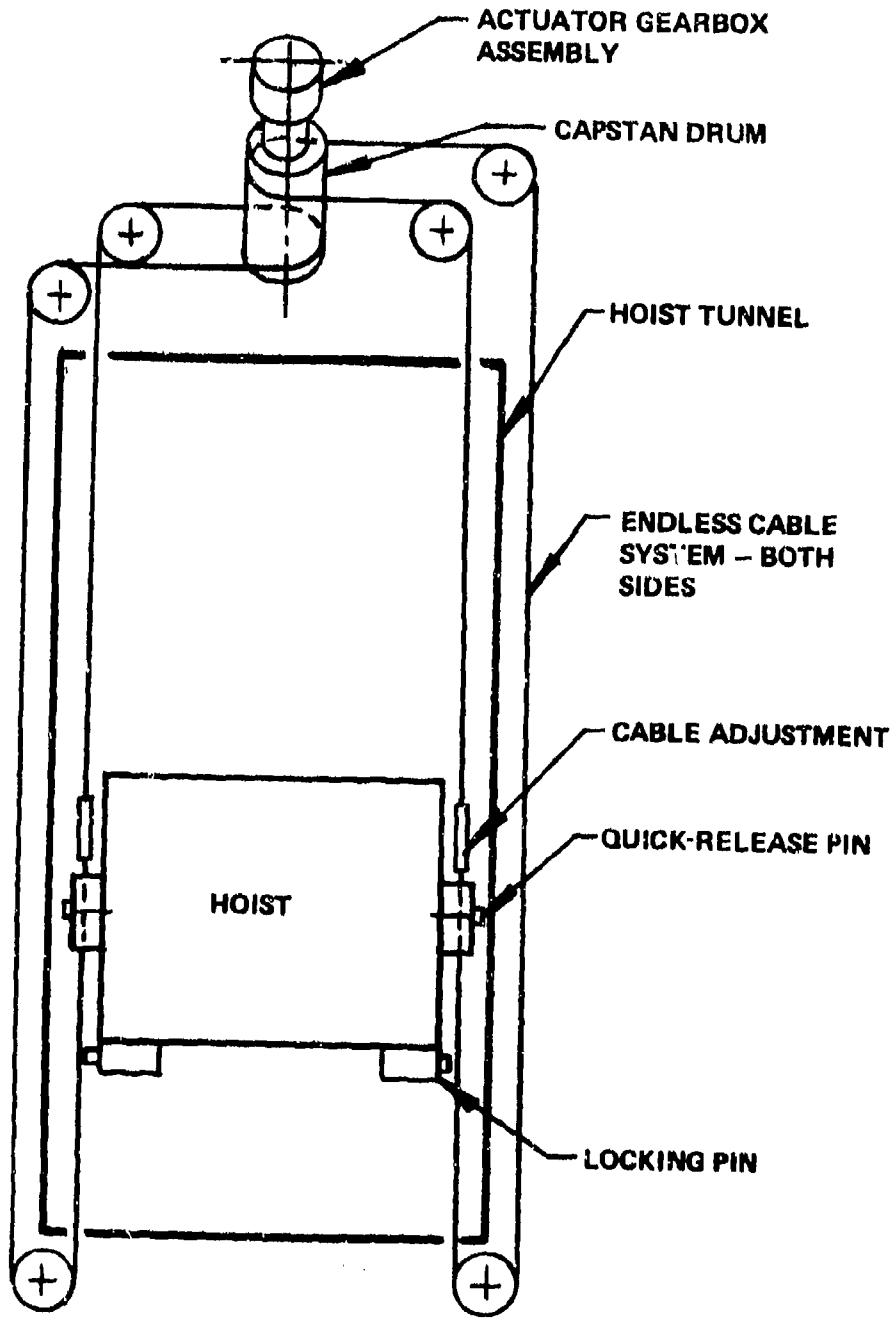


Figure 78 . Schematic of Cable Actuation System.

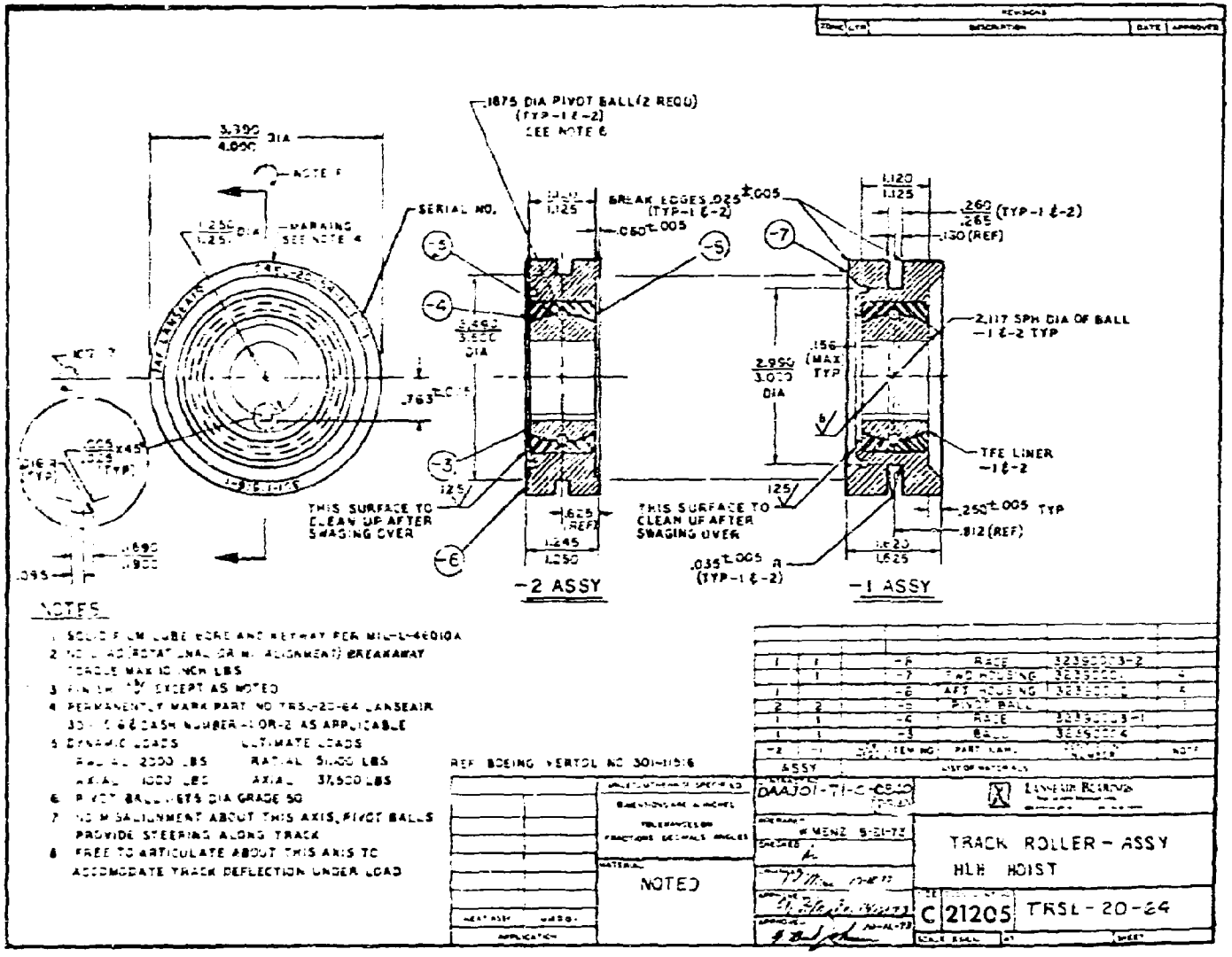


Figure 79. Tank Roller Assembly.

1. Components and systems directly mounted to the hoist assembly, and

2. Hardware and systems mounted on the Integrated Test Rig module.

Generally, the hoist-mounted hardware reflects flightworthy, lightweight design, while the module-mounted hardware, with the exception of the system actuator, represents rig design with no effort made to produce lightweight hardware.

The rig module consists of two longitudinal channel members of welded steel construction, spaced to accept the width of the hoist assembly and with sufficient length to accommodate the hoist at either end of the 5-foot travel.

Lateral members join the module ends and provide mounting surfaces in the test rig. The basis for the module concept is the provision of a completely built-up hoist assembly together with all the span positioning hardware and to function and adjust all the positioning features prior to installing in the 70-foot-high tower.

The hoist is supported by four roller fittings that operate in two sets of rails positioned on the module longitudinal channels. Two lockpins, retractable by a single actuator, are mounted on the forward hoist frame member. These lockpins engage in slots in the module when the hoist is in an operating position. Electrical interlocks ensure the hoist will not operate until the pins are completely engaged.

Two cable circuits extend along the length of the module, attach to the hoist and, by an arrangement of pulleys, assemble around a single electrically powered capstan drum. Figure 80 shows the hoist mounted in the module.

Detail Design

The hoist mounted components consist of roller mounting fittings, rollers, lockpin assemblies, linkage and linear actuator. The module mounted hardware consists of upper and lower rails, rail attachment plates, pulley attachment brackets, pulleys, capstan actuator and actuator mounting provision cable circuits and limit switch for hoist position and lockpins.

Hoist Mounted Components

Boeing Vertol Drawing 301-11534 (Figure 81) shows the span positioning hardware installed on the hoist. The four rollers are machined from stainless steel, with a spherical bearing assembled at their center. This

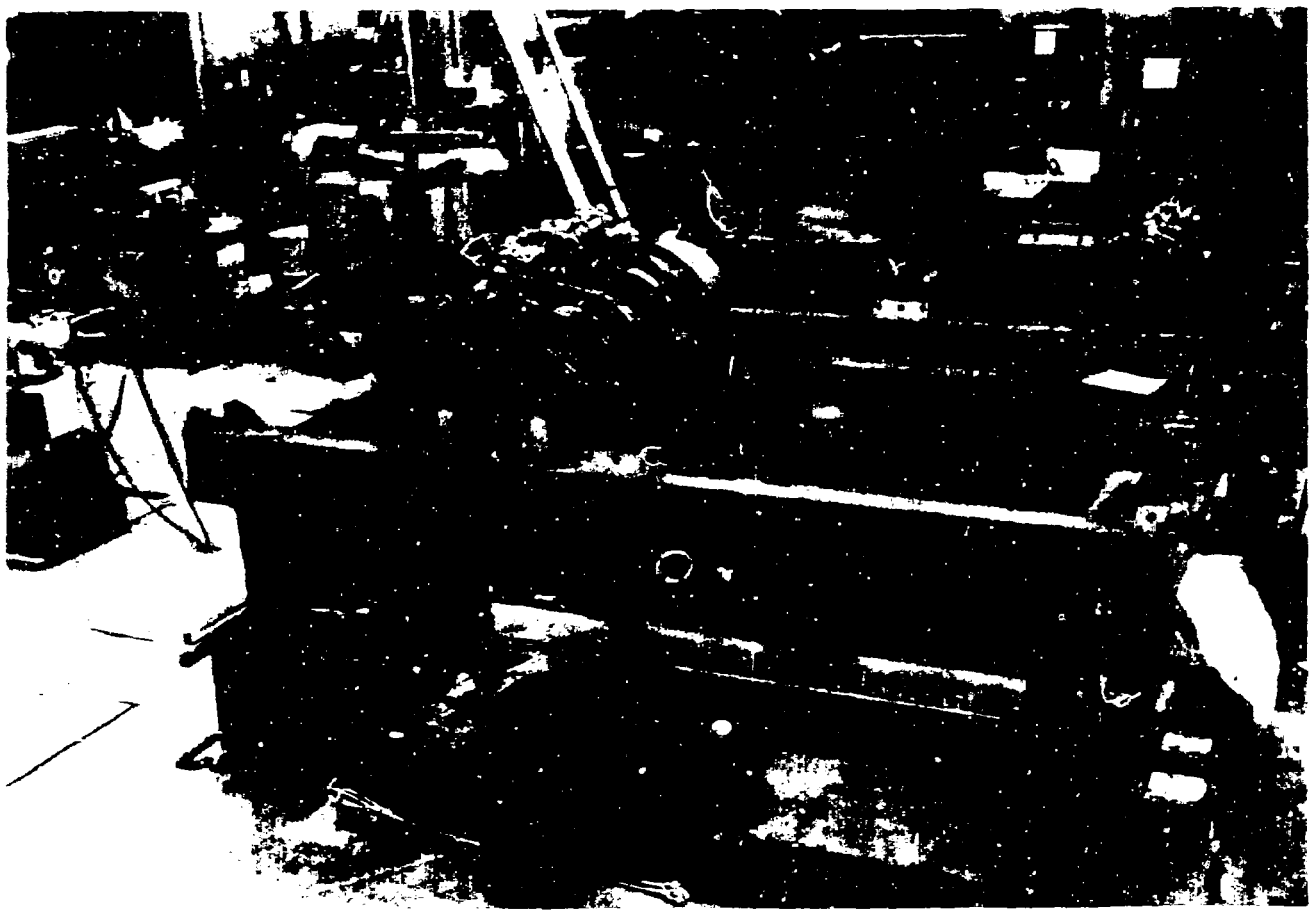


Figure 80. Installation of Hoist in Module.

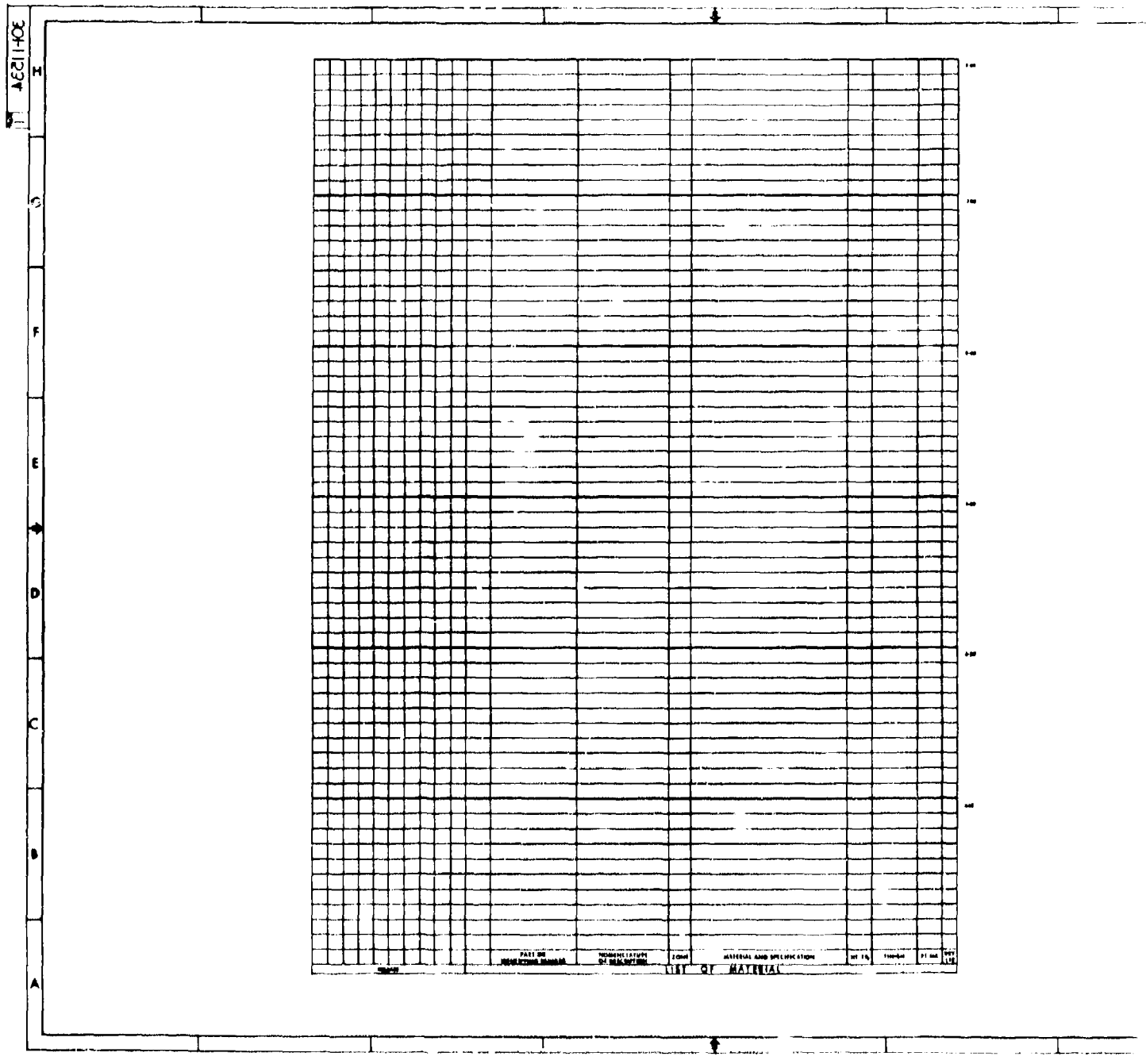


Figure 81. Hoist Span Positioning Hardware (Sheet 1 of 3).

PRECEDING PAGE BLANK-NOT

2	2		MS 627-120	BOLT	A
2	2		MS 627-85	BOLT	A
2	2		MS 338-808-12	KEY	
2	2		MS 338-808-17	KEY	
AR	AR		MS 20995NC40	SAFETY WIRE	
	2		MS 24665-287	COTTER PIN	
	7		MS 24665-154	COTTER PIN	
4	4		AN 960-716	WASHER	A
8	1		AN 960-516L	WASHER	B
	6		AN 960-416L	WASHER	
16	18		AN 960-816L	WASHER	
8			AN 960-1016L	WASHER	B
	1		AN 310-5	NUT	
	2		AN 310-8	NUT	
	5		AN 310-4	NUT	
16	16		BAC N10B 12BL	NUT	
2	2		BAC N10B-12BL	NUT	
2	2		BAC N10B-10L	NUT	
2	2		BAC N10DR-G2B	NUT	
4	4		BAC N10B 6L	NUT	A
	3		AN4-11	BOLT	
	2		AN4-7	BOLT	
16	16		AN3-15A	BOLT	
2	2		MS 33536A25	CSK BOLT	
2	2		MS 340CA26	CSK BOLT	
-2	-1		PART NO IDENTIFYING NUMBER	NOMENCLATURE OR DESCRIPTION	ZONE / MATERIAL AND SPECIFICATION / WT LB / FINISH / REV LTR

LIST OF MATERIAL

CAGE IDENT NO. 11533
DWG NO. 301 11534 1

2

NOTES:

1. THIS ASSEMBLY REPRESENTS THE STANDARD REQ'D FOR INSTALLATION ON THE INTEGRATED TEST RIG.
2. THIS ASSEMBLY REPRESENTS THE STANDARD AS RECEIVED FROM WESTERN GEAR CORP & WILL BE THE BASIS FOR BUILD-UP INTO A -1 ASSEMBLY.
3. INSTALL WITH WET ZINC CHROMATE PRIMER
4. INSTALL WITH A LIGHT COAT OF GREASE PER MIL-G-23827
5. TORQUE NUTS TO 480-630 IN-LB
6. INSTALL LOCKWIRE PER BAC 5018
7. THESE PARTS MAY BE DISASSEMBLED WHEN -2 ASSY IS RECEIVED.
8. TORQUE NUTS TO 230-360 IN-LB
9. FOR BOEING WIRING SEE SK301-11674
10. CABLE CUTTER IS A G.F.E. PART SUPPLIED BY FRANKFORD ARSENAL PHILA PA
11. LIMIT SWITCH SUPPLIED BY EDC THROUGH BOEING VERTOL ENGINEERING FOR FUNCTIONAL SUITABILITY ASSESSMENT

	B 050-02	LIMIT SWITCH	1 DC LYNWOOD WASH [11]			B
	7ENT-G	LIMIT SWITCH	MICRO SWITCH FREEPORT ILL			A
						B
	5800011	HOIST DRIVE	BUNDSTRAND AVIATION ROCKFORD ILLINOIS			A
	SK301-10253-2	CABLE RH				B
	SK301-10253-1	CABLE LH				B
13908	13400-C495	CABLE CUTTER	FRANKFORD ARSENAL PHILA PA [10]			P1
06824	SYLC 50287	ACTUATOR	BARBER-COLMAN, ROCKFORD ILL			
	200646001	LOAD ISOLATOR [12]	DOWTY BOTOL LTD, GLOUCESTER ENG			P1
81205	42138 R001	WINCH ASSY	WESTERN GEAR CORP, LYNWOOD CALIF			P1

PART OR IDENTIFYING NUMBER	NOMENCLATURE OR REVISION STATUS	ZONE	MATERIAL AND SPECIFICATION	NO. REQ'D	FINISH	PART OR IDENT NO.	REV LTR
1	QT MATERIAL						

BASIC RIVET CODE

CODE IDENT NO
DWG NO 301-11534

301-11534	NEXT ASSY	USED ON	APPLICATION	PART NO.	PREVIOUS REV	REV LTR

3

NOTES -

(1) THIS ASSEMBLY REPRESENTS THE STANDARD BUILD FOR INSTALLATION ON THE INTEGRATED TEST RIG

(2) THIS ASSEMBLY REPRESENTS THE STANDARD AS RECEIVED FROM WESTERN GEAR CORP & WILL BE THE BASIS FOR BUILD UP INTO A -1 ASSEMBLY

(3) INSTALL WITH WET ZINC CHROMATE PRIMER

(4) INSTALL WITH A LIGHT COAT OF GREASE PER MIL-G 23827

(5) TORQUE NUTS TO 480-650 IN LB

(6) INSTALL LOCKWIRE PER BAC 5048

(7) THESE PARTS MAY BE DISASSEMBLED WHEN -2 ASSY IS RECEIVED

(8) TORQUE NUTS TO 250-360 IN-LB FOR BOEING WIRING SEE BAC301-11674

(10) CABLE CUTTER IS A G.F.E. PART SUPPLIED BY FRANKFORD ARSENAL PHILA PA

(11) LIMIT SWITCH SUPPLIED BY EDC THROUGH BOEING VERTOL ENGINEERING FOR FUNCTIONAL SUITABILITY ASSESSMENT

REVISIONS			
		SEE DCN INC ADCN 1	
	B	SEE DCN	

	2		301-11710	ADAPTER
		1	301-11693-1	CABLE LOCKING
	2		301-11883-2	SPACER
	2		301-11883-1	MOUNTING PIN
		2	301-11529-1	LINK ASSY
		1	301-11652-4	PIN ACTUATOR
		1	301-11952-3	PIN LEVER
		1	301-11882-1	LEVER ASSY
	2		301-11881-3	DIMPLED WASHER
	2		301-11880-1	RETAINING WASHER
	3		301-11881-1	BRACKET
	8		301-11515-6	SUPPORT BLOCK
	2		301-11515-1	LOCKPIN ASSY
	2		301-11516-1	FWD ROLLER
	2		301-11516-2	AFT ROLLER
	1		301-11514-4	RH AFT FITTING
	1		301-11514-3	LH AFT FITTING
	1		301-11514-2	RH FWD FITTING
	1		301-11514-1	LH FWD FITTING
X	1		-2	HOIST ASSY
X			-1	HOIST ASSY
-2	-1			

QTY | PART OR IDENTIFYING NUMBER | NOMENCLATURE OR DESCRIPTION | ZONE | MATERIAL AND SPECIFICATION | MT TO | FINISH | MT NO | NEXT ASSY

THE BOEING COMPANY
VERTOL DIVISION MORTON PENNSYLVANIA

HOIST ASSY
CARGO SYSTEM
HLH

SIZE B | CODE IDENT NO 77597 | 301-11534

301-11534 | 1 | B

4

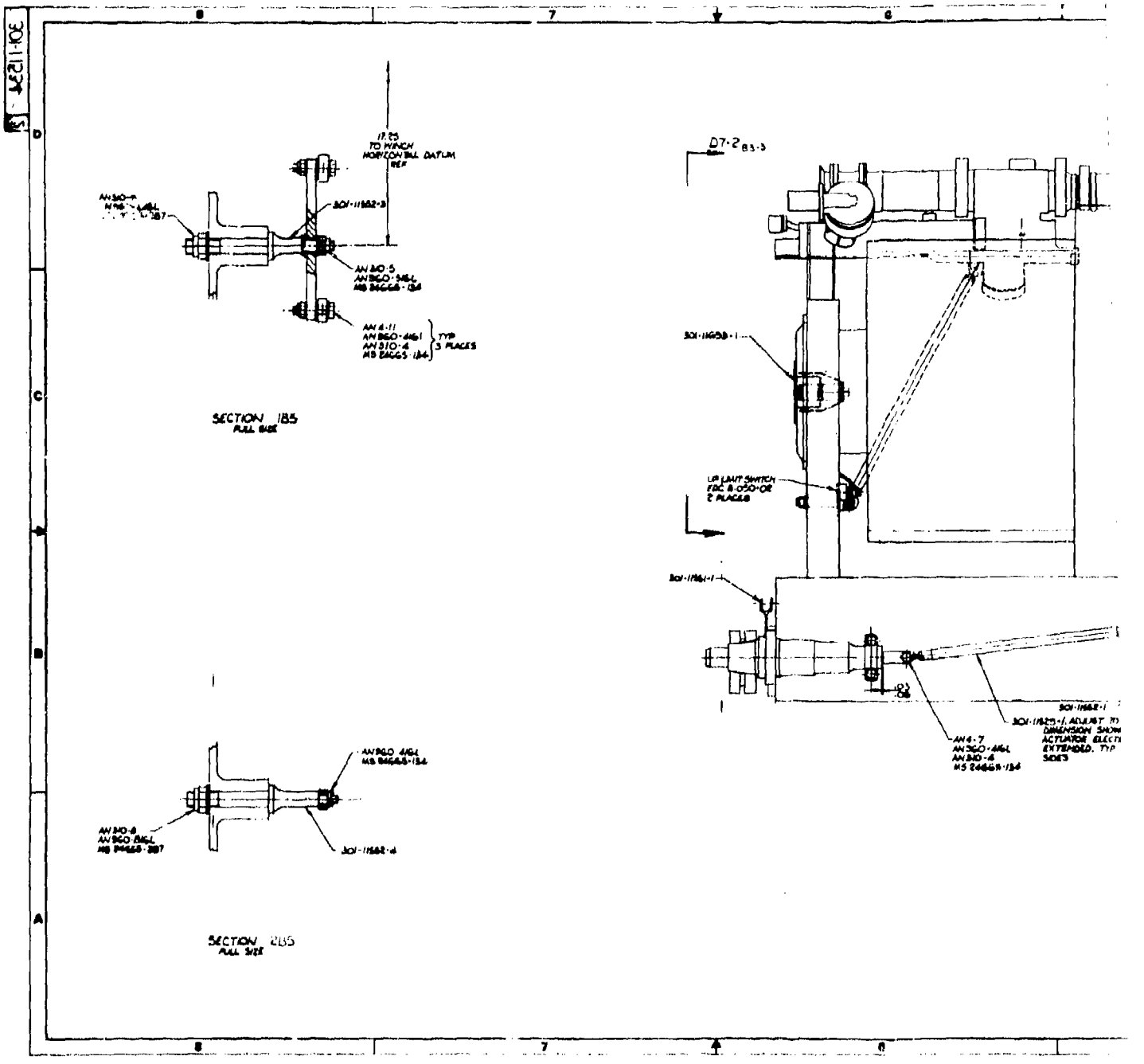
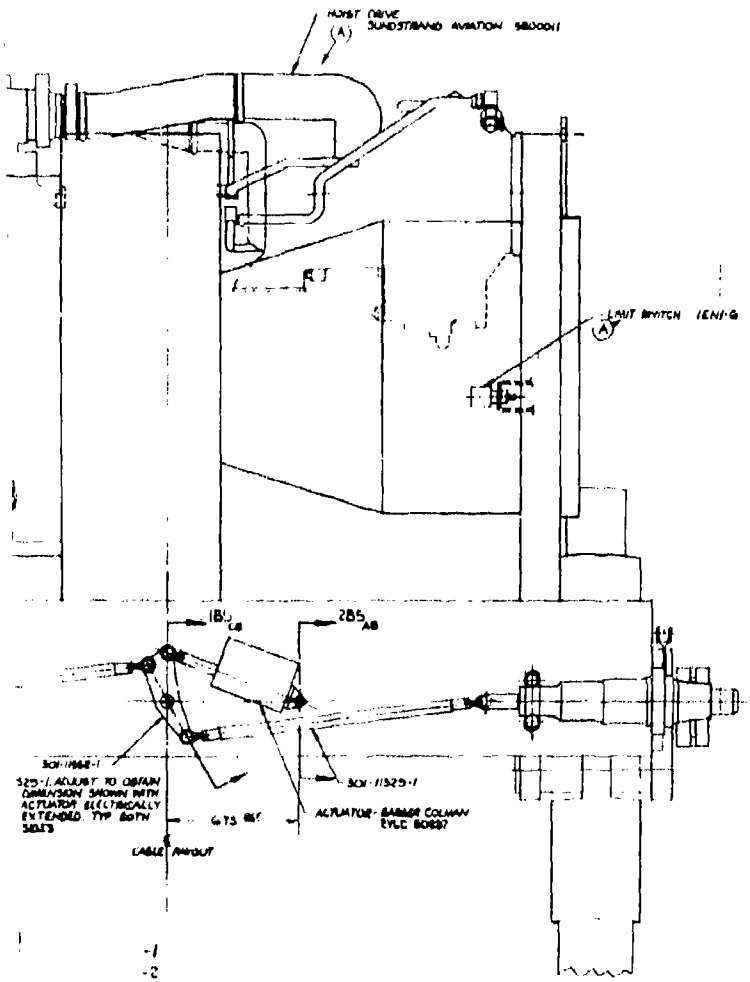
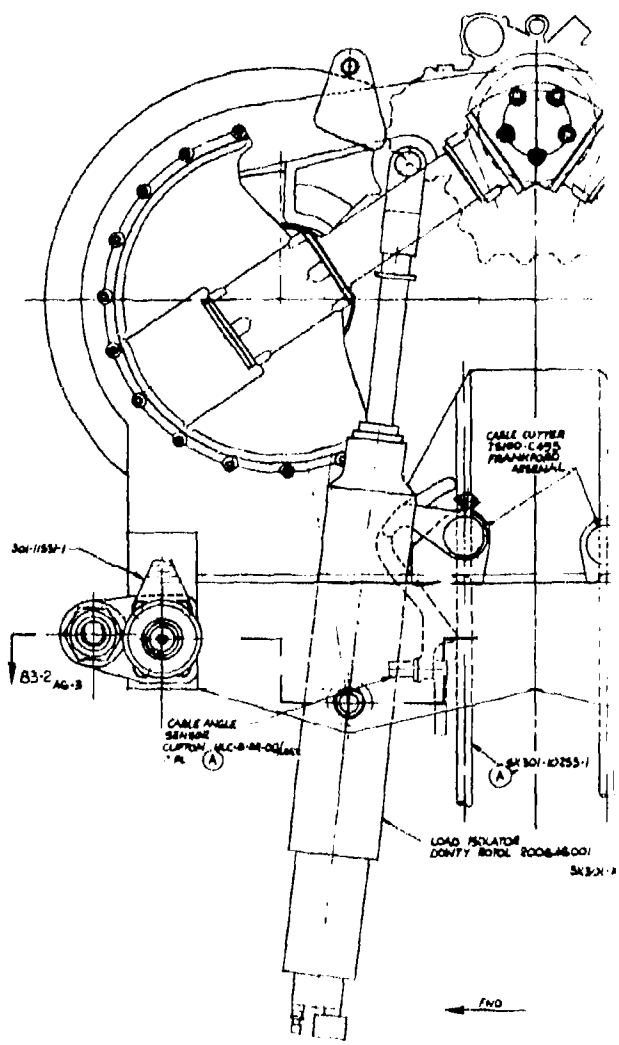


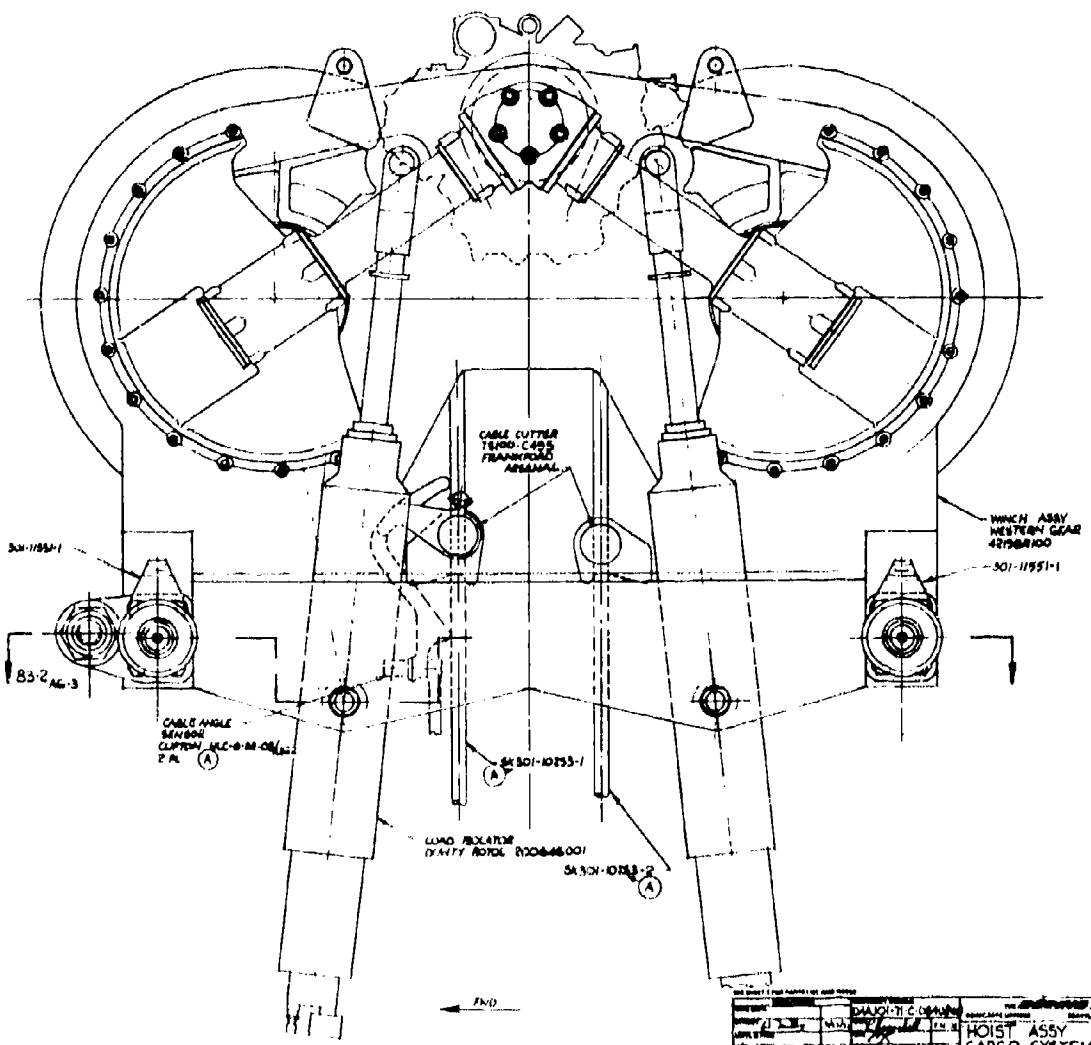
Figure 81. Continued (Sheet 2 of 3).





301-11534 -1 -2

1 2



HOIST ASSY
CARGO SYSTEM
H-H
J 77272 301-11534

301-11534 A2

301-11234 S

3

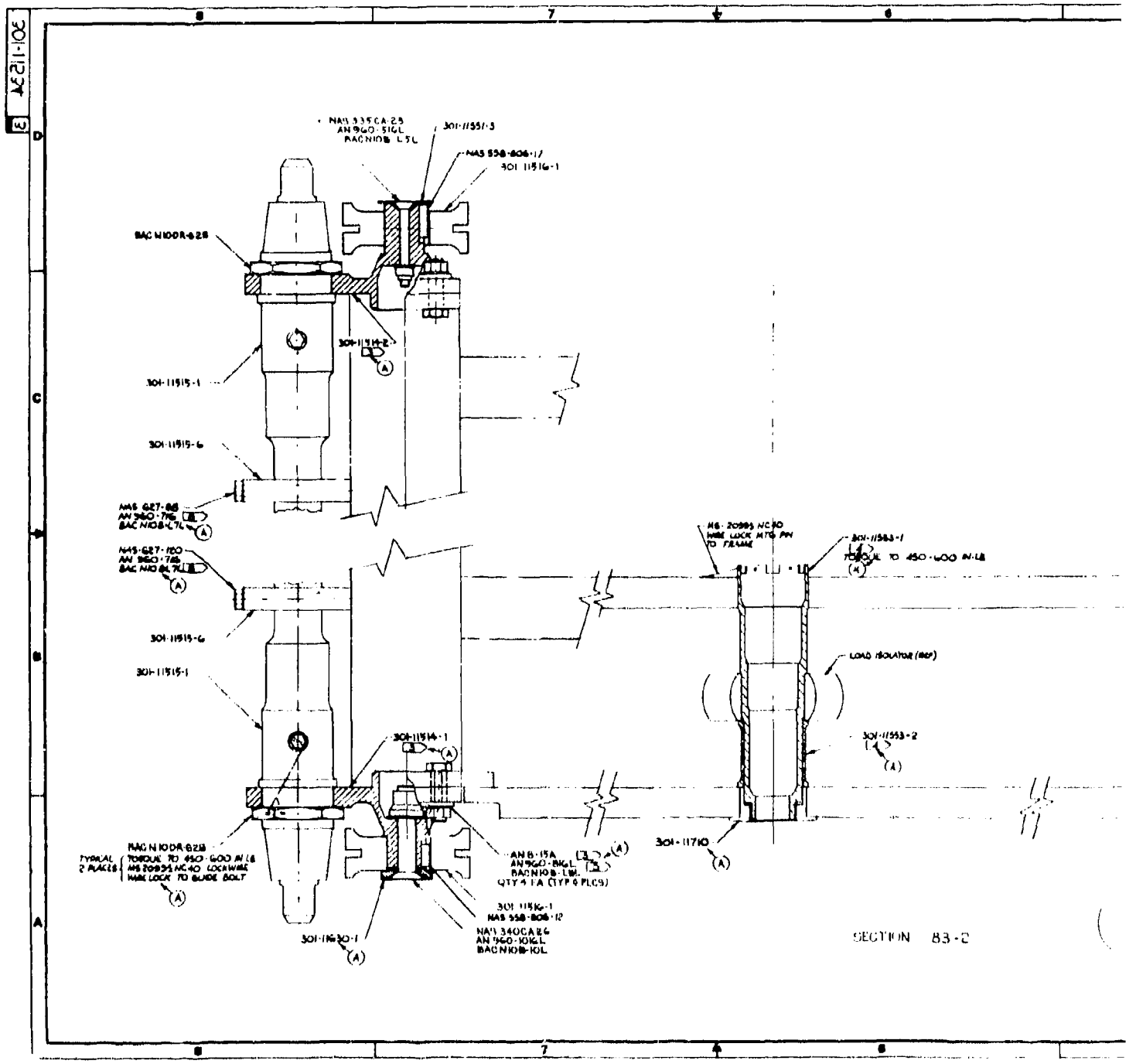
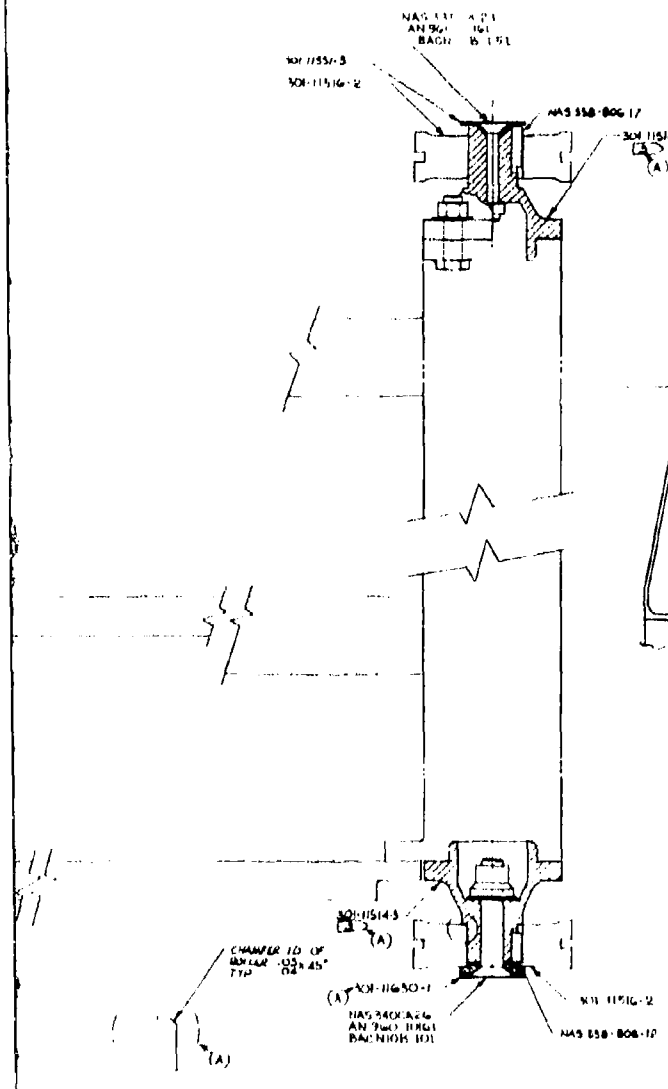
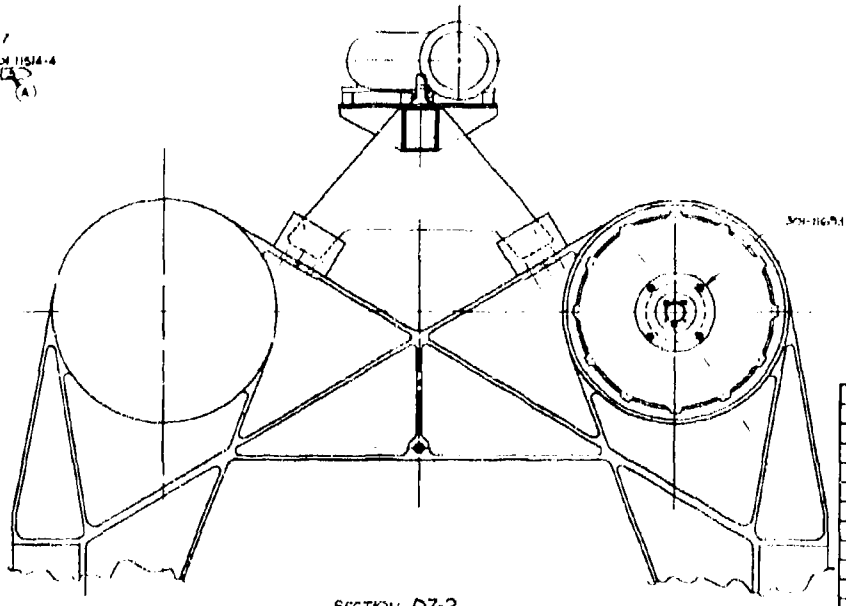


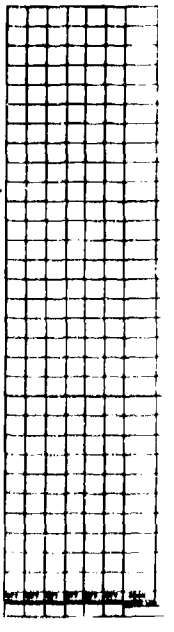
Figure 81. Concluded (Sheet 3 of 3).

PRECEDING PAGE BLANK-NOT FILMED

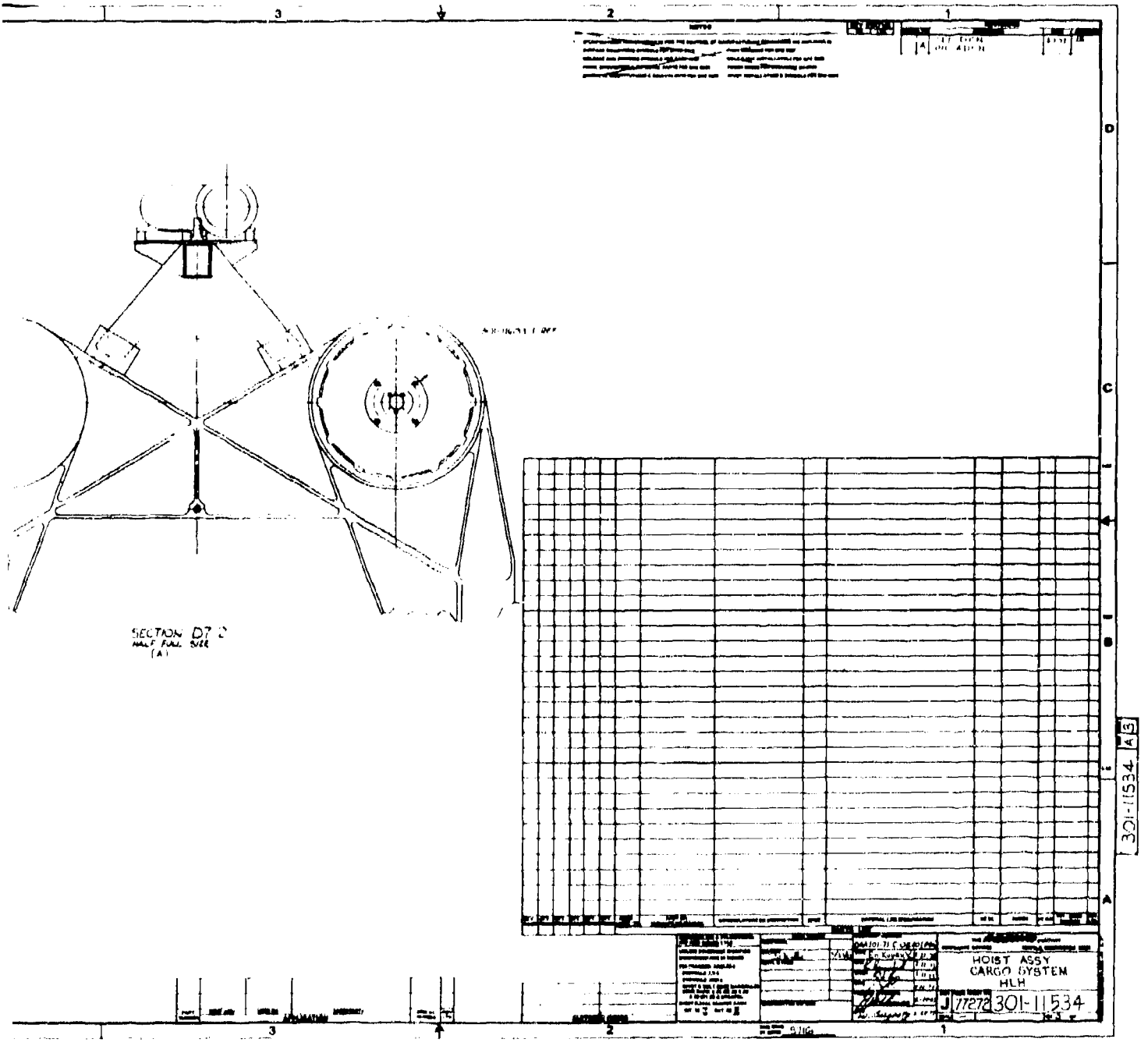




SECTION D7-2
HALF FULL SIZE
(A)



301 11534 A 5


SECTION D7 C
HALF FULL SIZE
(A)
HOIST ASSY
CARGO SYSTEM
HLH
J 77272 301-11534
301-11534 AB

bearing is restricted to align in a roll plane only, the objective being to ensure roller and track alignment under high loads. A keyway in the bearing bore mates with a key on the mount fitting to retain the radial location of the alignment feature. The spherical surface rotates on a Teflon impregnated fabric liner. Each roller has a circumferential groove machined central to the tread to match a flange along each track, providing alignment and reacting side-loads from the hoist. The two rollers on the drive side (LH side) of the hoist are restrained axially while the RH side rollers are free, within limits, to move axially to line-up with the track width. The forward and aft rollers have differing configurations of tread width and groove depth such that, in conjunction with the track configuration, the forward rollers will not locate in the track recess for an aft roller, or the aft roller in the forward recess. This feature provides for a smooth position change.

The roller mounting fittings are machined from 4340 steel heat-treated to 180-200 kips. Each fitting is attached to the hoist with four bolts; a cylindrical extension on the fitting engaging in a recess in the hoist frame for vertical load transfer. The two forward fittings extend forward of the hoist frame and provide support for the two lockpin assemblies.

Each lockpin assembly consists of a sliding pin, spring-loaded to the engaged position, and assembled in a housing attached to the forward hoist frame. The principal parts of the system are machined from 4340 steel. At the center of the hoist frame a bellcrank lever is linked to each locking pin by an adjustable tubular link and powered by a Barber-Colman actuator SYLC 50237. The actuator is attached to the hoist frame by a shouldered pin.

Module Mounted Hardware

The upper and lower rails are machined from mild steel stock with inserts of 4340 steel at the load reacting locations. The track has an integral flange to match the hoists support rollers and shallow recesses at the load carrying positions. Attachments to the module side wall are through four mild-steel doubler plates shimed as necessary to maintain track alignment and spacing. The doubler plates contain slots for the hoist lockpins at each operating location.

The positioning cable system is shown on Boeing Vertol drawing 301-11634 (Figure 82). Pulleys are standard

PRECEDING PAGE BLANK-NOT FILMED

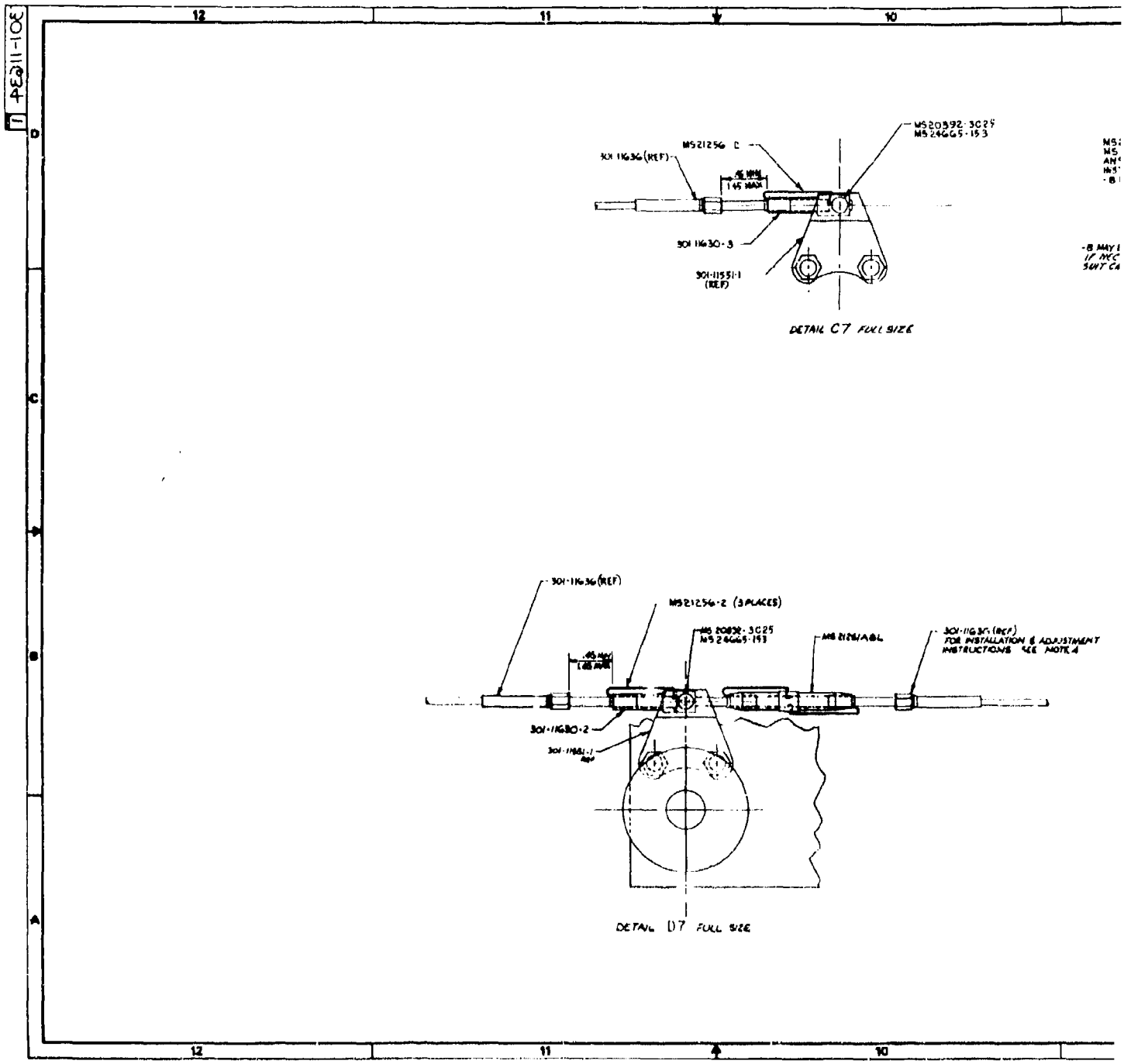
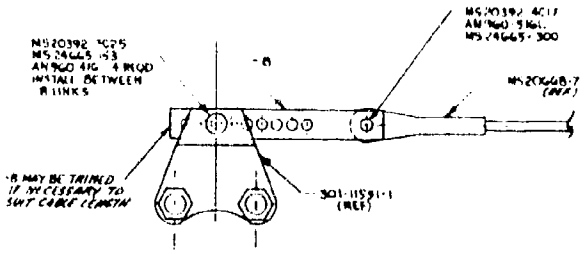
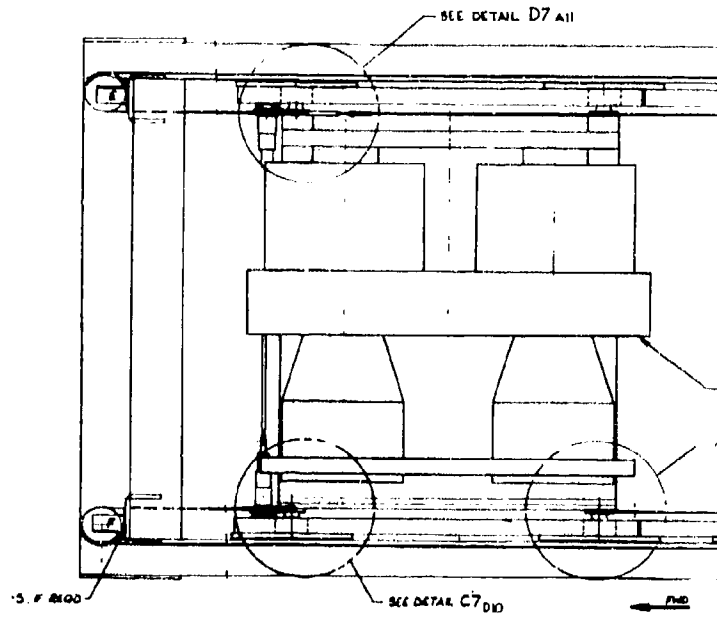


Figure 82. Positioning Cable System.

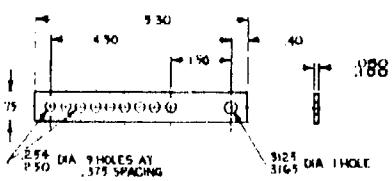


DETAIL C6 FULL SIZE

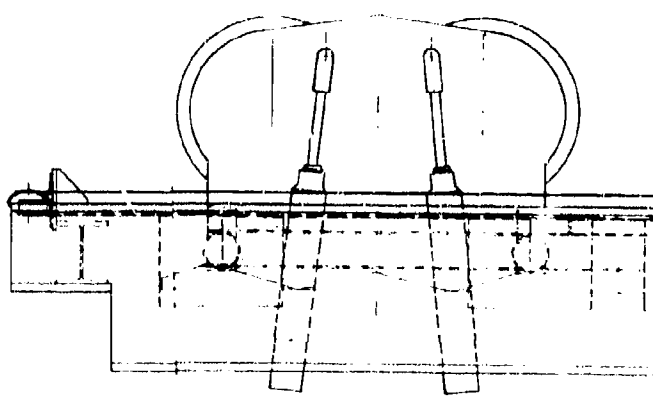


PLAN VIEW

-1 INSTALLATION

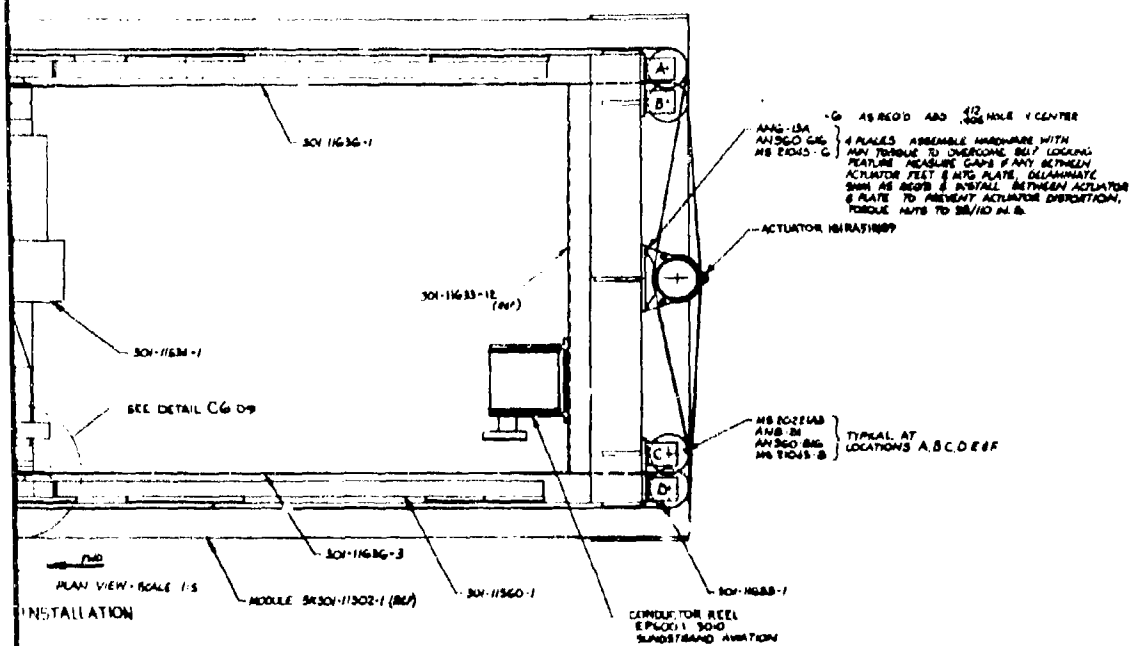


DETAIL -8 FULL SIZE

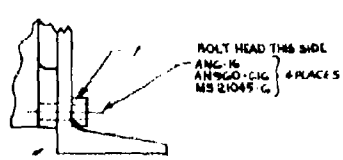


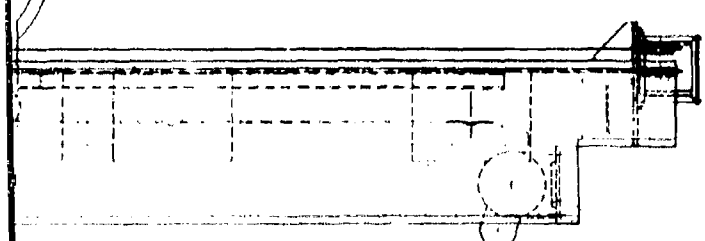
301-11634 A1

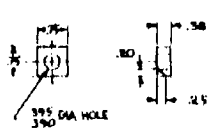
2

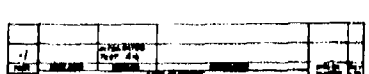


NOTES (CONT)









301-11634 A 1

3

1		MS 24665-300	SPLIT COTTER		
1		AN960-416	WASHER		
1		MS 24665-417	PIN		
4		AN960-416	WASHER		
1		301-11690-3	CABLE FITTING		
4		AN6-16	BOLT		
4		MS 21045-6	NUT		
8		AN960-616	WASHER		
4		AN6-18A	BOLT		
1	DOWTY EQUIPMENT		ACTUATOR	D4	
3		MS 24665-153	SPLIT COTTER		
2		AN960-416	WASHER		
6		AN960-516	WASHER		
6		AN5-24A	BOLT		
10		MS21045-5	NUT		
1		NSE12518BL	TURNBUCKLE BODY		
6		MS20821A5	PULLEY		
4		MS 21256-2	LOCKING CLIP		
3		MS 20392-3C25	PIN		
1		301-11636-3	CABLE ASSY	C3	
1		301-11630-2	CABLE FITTING	B11	
1		301-11636-1	CABLE ASSY	B9	
1		301-11633-1	SYSTEM SCHEMATIC	C4	
1		301-11960-1	LAYOUT WINCH TRACK	C5	
1		301-11934-1	HOIST ASSY	C6	
1	99193	EP6003-3010	CONDUCTOR REEL	B5	SUPERSEDING AMMTON DRAWING
2		-8	LINK	A9	.10 × .75 × 5.50
4		-7	WASHER	A4	.38 × .75 × .75
4		-6	SHIM	D4	M/F BAC 5408 DUO
AS REQD		-5	SHIM	C7	.05 × 4.0 × 7.0
		-1	INSTALLATION		

BOLT HEAD THIS SIDE
ANG 16
AN960-616
MS 21045 6
} 4 PLACES

INSTALLATION OF HOIST IN INTEGRATED TEST RIG

J7722 301-11634

301-11634 A1

4

5-inch-diameter aircraft items mounted on mild steel brackets welded to the module. The single capstan drum actuator is shown on Western Gear Corporation drawing 181RA51R189 (presented as Figure 83), and illustrated on Figure 84. The capstan drum is supported by two bearings installed in a mounting bracket at each end of the drum. Attached to the lower mounting bracket, inside of the drum, is the removable reduction gear and drive motor assembly, the final reduction being through a single-stage planetary with the internal gear mounted directly to the drum. The electrical drive motor is a 28V 400 cycle unit of approximately 0.25 hp. The reduction gear provides a final drum speed of 4 rpm, resulting in a time of 48 seconds for a hoist position change. Provisions are included on the actuator for manual operation by depressing and rotating a squared shaft at the upper end of the drum.

Electrical limit switches are actuated by the hoist at each end of its travel, stopping the positioning actuator and initiating lockpin insertion. When fully home, the lockpins operate limit switches which signal that the hoist is positioned and ready to operate.

Hoist Installation in the HLH Prototype

As part of the efforts to reduce weight and cost of the HLH prototype, the longitudinal span positioning capability of the cargo handling winches has been eliminated and provision made for an 18-foot fixed winch span. This change was possible, as recent flight tests have indicated that it was not necessary to preserve the .6 span ratio, that is the ratio between the load length and the distance between the winches, in order to stabilize lightweight containers.

To determine the effect of the fixed 18-foot span on an empty 40-foot container, a wind tunnel program was run at the University of Maryland. Various arrangements of suspended 20-foot and 40-foot containers at scaled empty weights were flown. Suspension lengths were also varied from 10 feet to 30 feet and asymmetrical configurations utilized to investigate longitudinal attitudes.

Results of these tests indicate that the empty 40-foot container is much less sensitive to suspension configurations and longitudinal attitudes than the empty 20-foot container. They also indicate that an 18-foot winch span is suitable for both 20-foot and 40-foot containers.

The installation of the hoist in the airframe will therefore have the four roller mounting fitting assemblies replaced

REPRODUCIBILITY OF THE ORIGINAL PAGE IS POOR

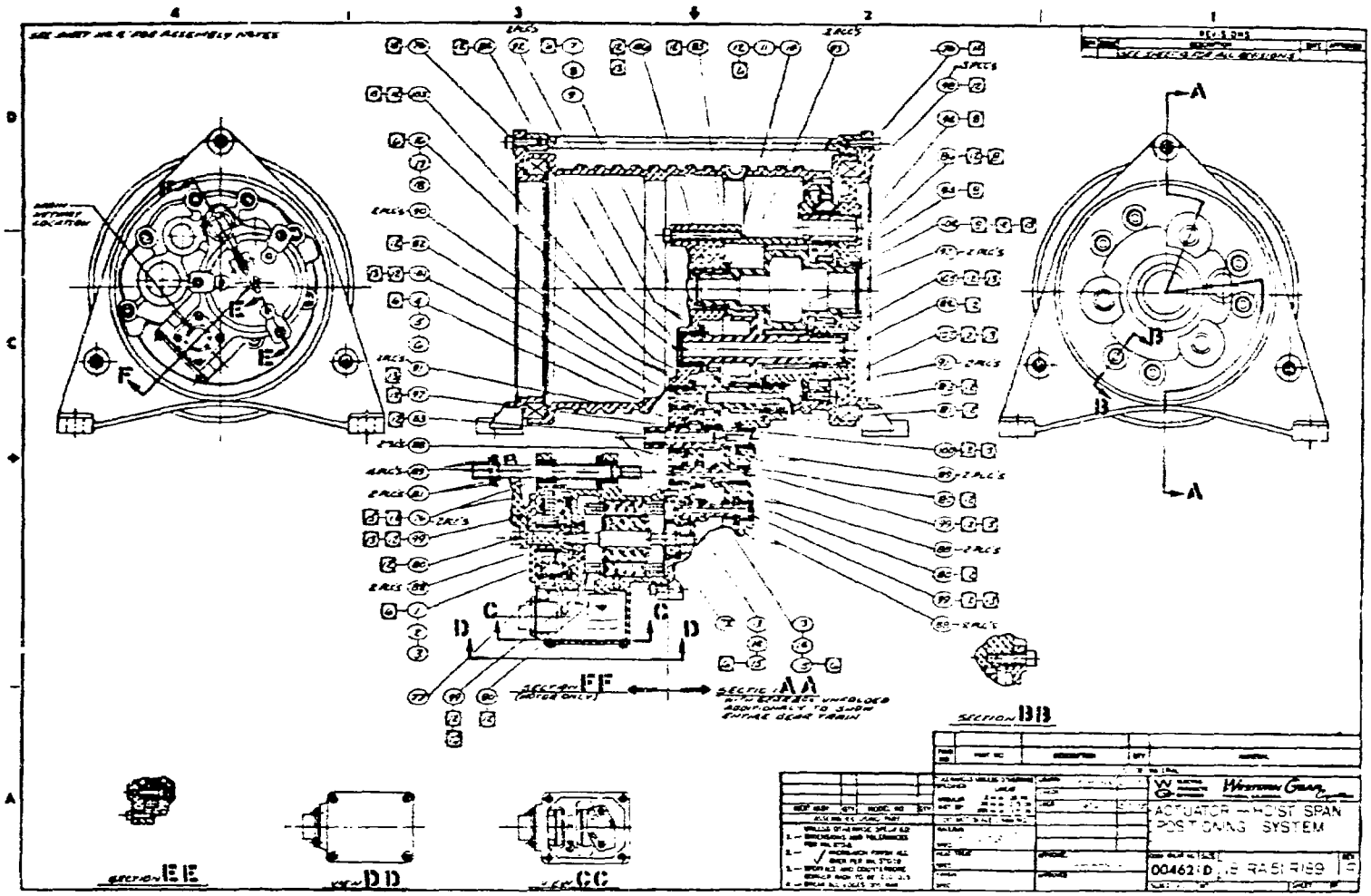


Figure 83. Single Capstan Drum Actuator Layout.

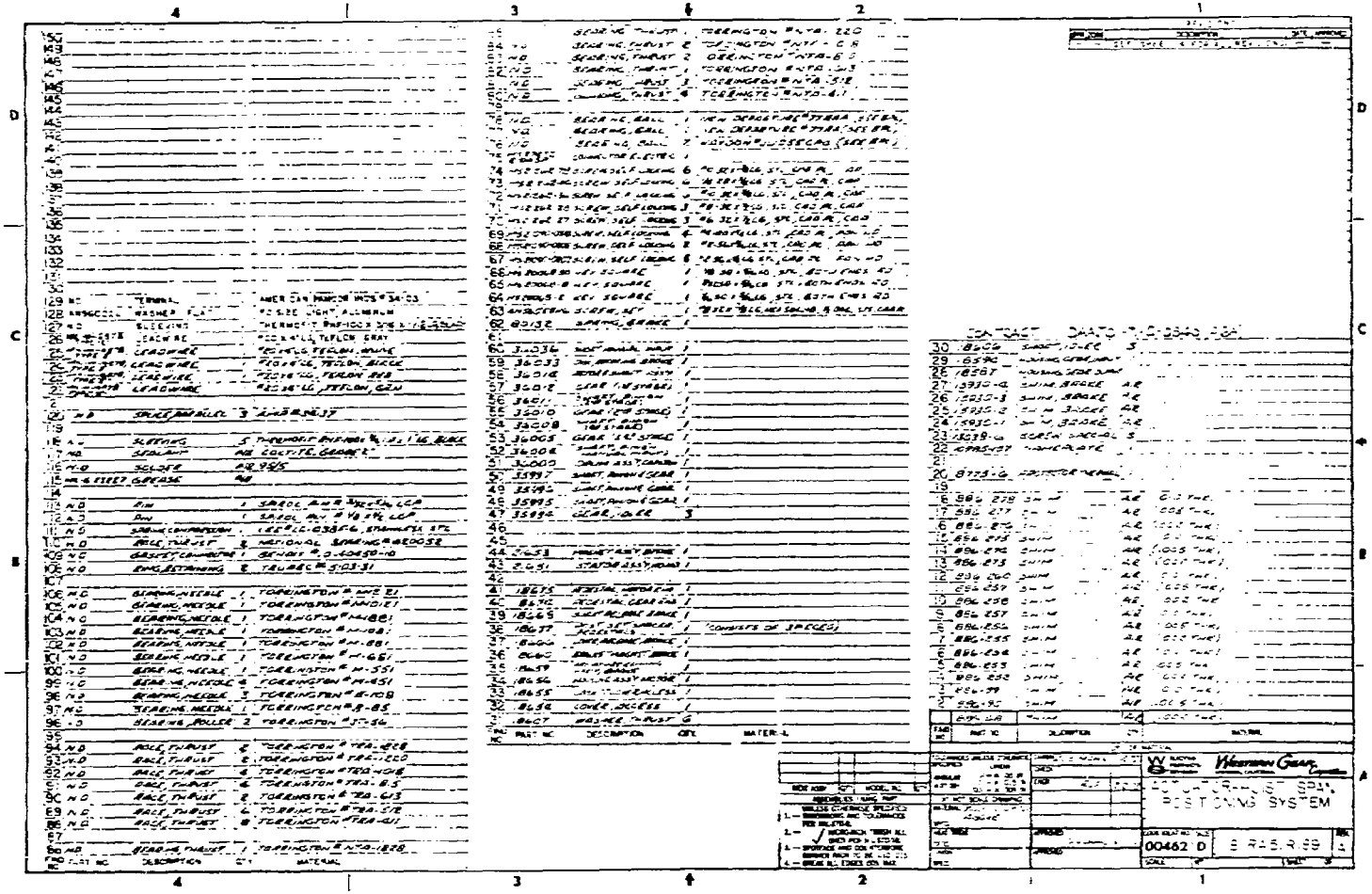


Figure 83. Continued.

with fittings permitting direct attachment to the airframe. The locking pin assemblies and actuator will be removed from the hoist frame. Figure 85 illustrates the hoist installation in the HLH Prototype.



Figure 84. Span Positioning Actuator.

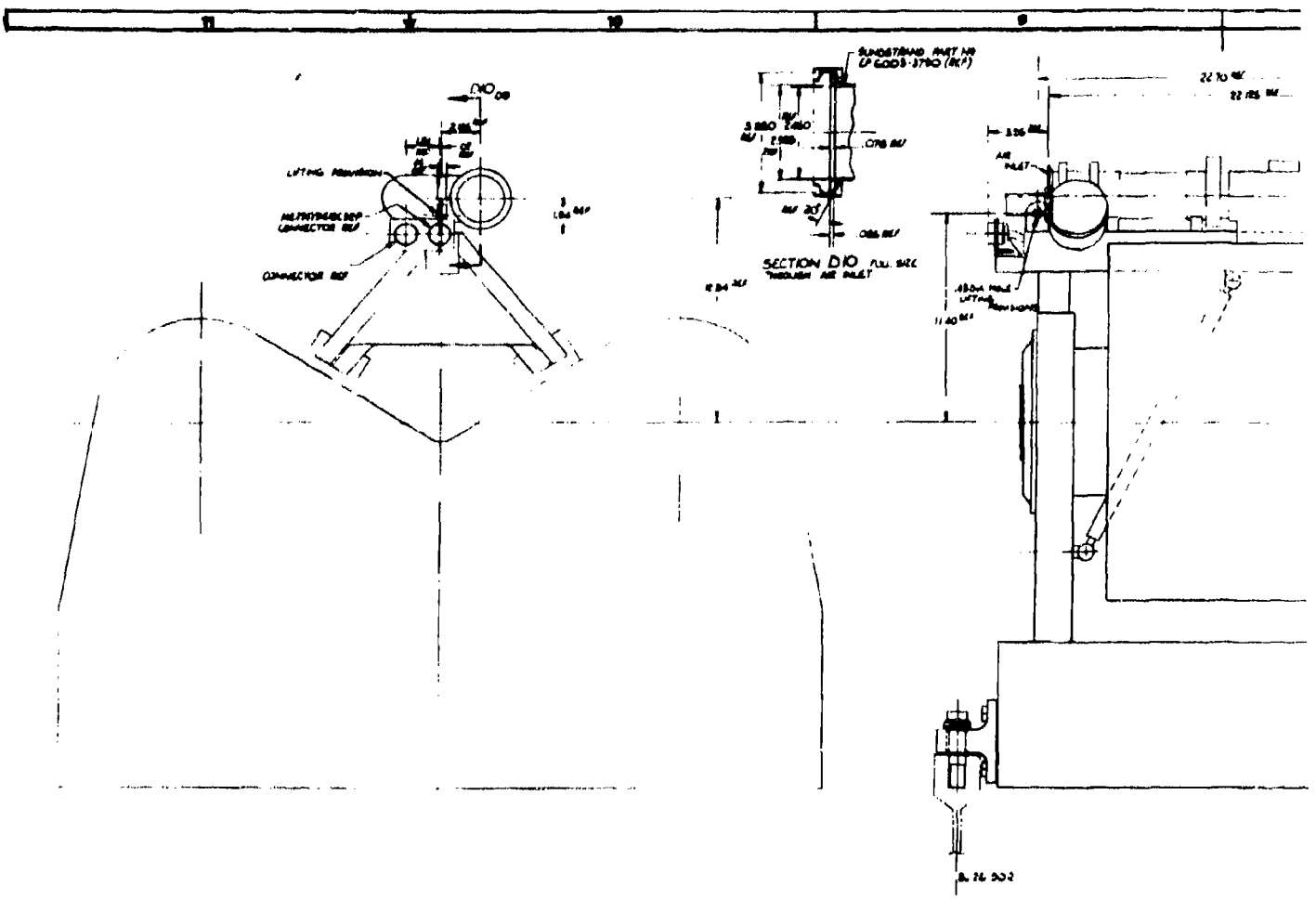
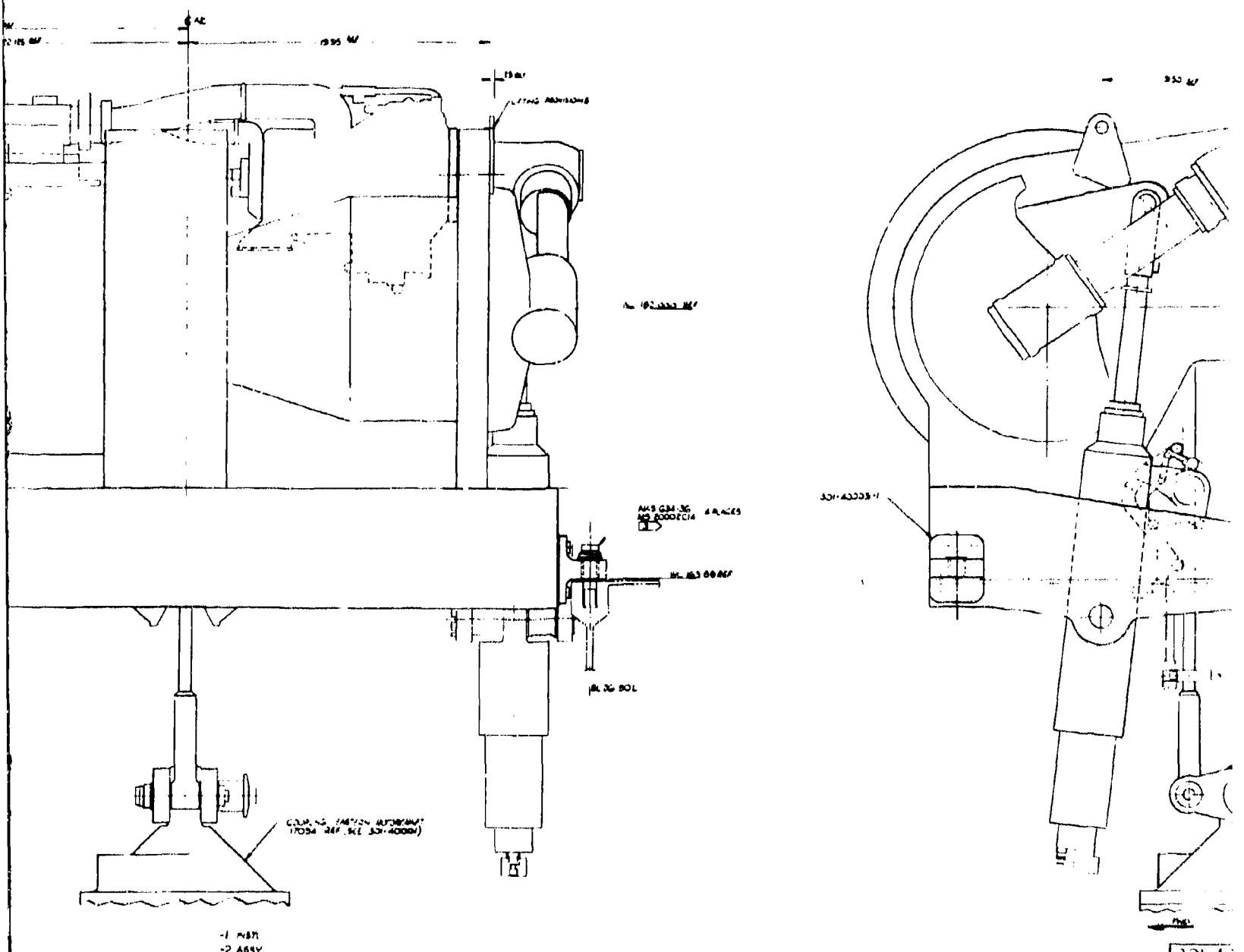
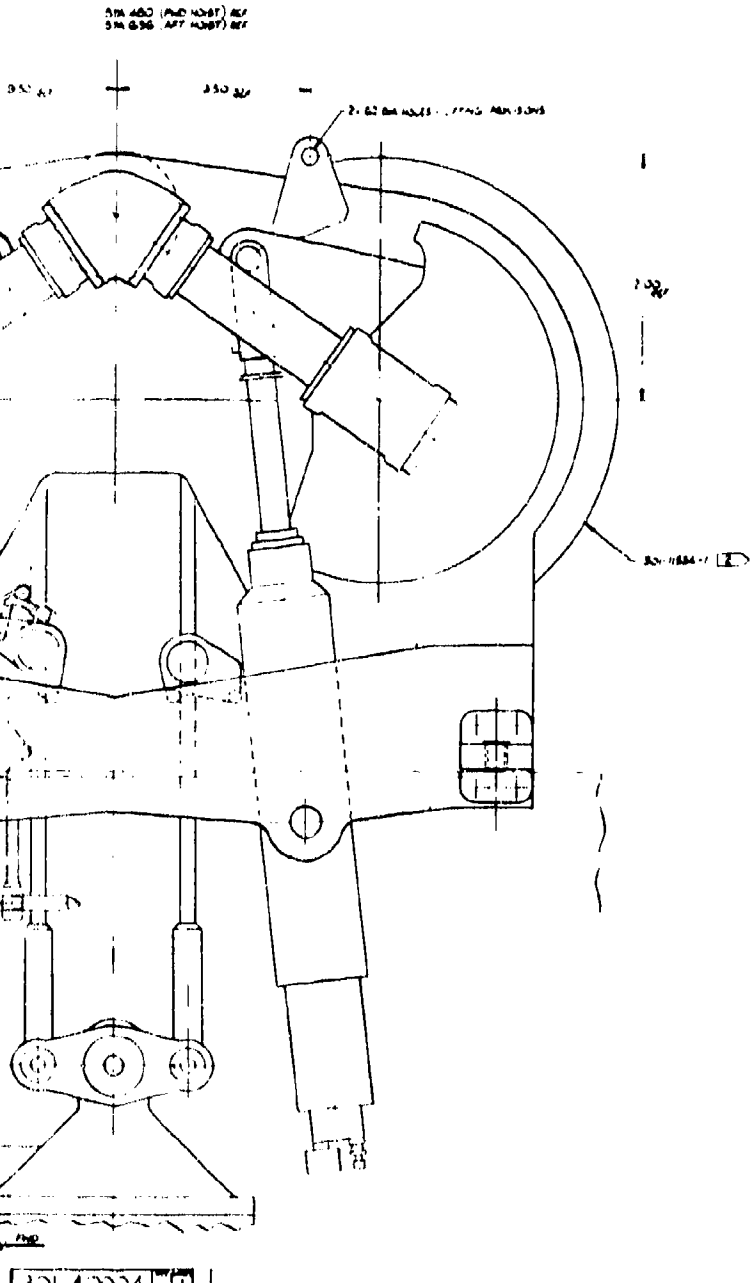


Figure 85. Hoist Installation in Prototype HLH.

301-40004 | 1



1 2



(2) THE FOLLOWING PARTS ARE TO BE REMOVED FROM 331-11534-1 ASSY TOGETHER WITH ATTACHING HARDWARE :

PART NO	DESCRIPTION	QTY
331-11534-1	LH FWD FTG	1
-2	RH FWD FTG	1
-3	LH AFT FTG	1
-4	RH AFT FTG	1
331-11516-2	AFT ROLLER	2
-1	FWD ROLLER	2
331-11518-1	LOCKPIN ASSY	2
-5	SUPPORT BLOCK	2
331-11551-1	BRACKET	2
331-11530-1	RETAINING WASHER	8
331-11531-3	UMBILO WASHER	2
331-11552-1	LEVER ASSY	1
-3	PIN LEVER	1
-4	PIN ACTUATOR	1
331-11529-1	LINK ASSY	2
91-LC 30287	ACTUATOR (AMBIENT COUPLING)	1

SEE DRAWING 331-11534 FOR LOCATION OF PARTS REMOVED PARTS TOGETHER WITH ATTACHING HARDWARE TO BE BAGGED, TAGGED & RETURNED TO RCA. TAG WILL RECORD PART NOS & SERIAL NO OF WINCH

(3) TORQUE BOLTS TO 1500-1800 INCH POUNDS

	4	MS 35002 C14	WASHER
	4	NAS 624 3G	BOLT
	1	331-43003-1	FITTING INSTL
	1	331-11534-	HOIST ASSY AFT
		-2	HOIST ASSY
		-1	HOIST INSTL

331-40004 T

3

NOTES

1. [illegible]

(1) THE FOLLOWING PARTS ARE TO BE REMOVED FROM 301-11534-1 ASSY TOGETHER WITH ATTACHING HARDWARE :

PART NO	DESCRIPTION	QTY
301-11536-1	LH FWD FTG	1
-2	RH FWD FTG	1
-3	LH AFT FTG	1
-4	RH AFT FTG	1
301-11546-2	AFT ROLLER	2
-1	FWD ROLLER	2
301-11515-1	LOCKPIN ASSY	2
-6	SUPPORT BLOCK	2
301-11551-1	BRACKET	2
301-11550-1	RETAINING WASHER	8
301-11551-3	GUARD WASHER	2
301-11552-1	LEVER ASSY	1
-3	PIN LEVER	1
-4	PIN ACTUATOR	1
301-11529-1	LINK ASSY	2
STD NO 2287	ACTUATOR (BARREL COUPLER)	1

SEE DRWG NO 301-11534 FOR LOCATION OF PARTS REMOVED PARTS TOGETHER WITH ATTACHING HARDWARE TO BE BAGGED, TAGGED & RETURNED TO PCA TAG WILL RECORD PART NOS & SERIAL NO OF WINCH

(2) TORQUE 83.75 TO 1530-1800 INCH POUNDS

	4	MS 20002C14	WASHER	
	4	AMS 23- 36	BOLT	
	1	301-43005-1	FITTING INSTL	
	1	301-11534-	HOIST ASSY, ATC1	(2)
1		-2	HOIST ASSY	
		1	HOIST INSTL	

MATERIAL 0840(943)

WINCH INSTL
HLH PROTOTYPE

J 77872 301-40004

1 4

CABLE CUTTER

Requirements

Cable cutter requirements were initially defined as listed below and shown on Figure 86.

1. One cutter assembly for each cable.
2. Dual knives in each cutter.
3. Dual powder charge for each knife.
4. Dual initiator with a dual bridge wire for each knife.

Proposals were received from four experienced manufacturers. These proposals included one from Frankford Arsenal using only one cutter. Their past experience indicated that one cutter would always cut the cable.

An evaluation was conducted which included a reliability study of possible combinations of single or dual knife applications. The basic premise being that the cables would be completely cut when required and that they would not fire when not required to assure safety of the aircraft and personnel.

Figure 87 shows the reliability figures with the combinations of single and dual cutters, initiators, powder charge, and bridge wire. These were evaluated for reliability, redundancy and hardware complexity.

The cutter assemblies (1 through 8) shown in Figure 87 are described below. All assemblies have dual powder charge.

1. One knife, one initiator, and single bridge wire for each initiator.

2. One knife, one initiator, and dual bridge wire for each initiator.

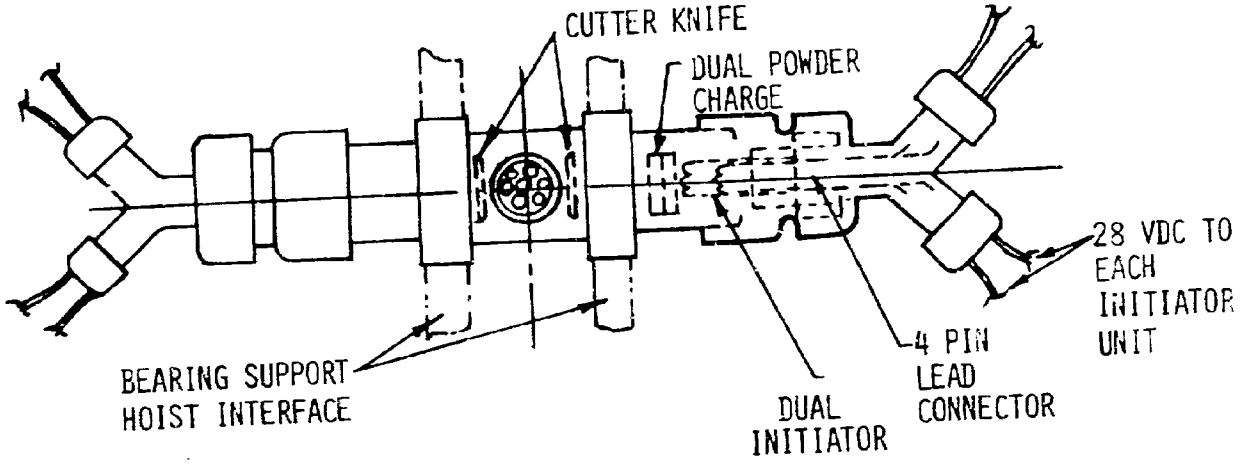
3. One knife, dual initiator, and single bridge wire for each initiator.

4. One knife, dual initiator, and dual bridge wire for each initiator.

5. Dual knife, one initiator, and single bridge wire for each initiator.

6. Dual knife, one initiator and dual bridge wire for each initiator.

PRECEDING PAGE BLANK-NOT FILMED



RELIABILITY AND REDUNDANCY

- DUAL INITIATOR SYSTEM FOR EACH CUTTER
- DUAL CUTTER KNIVES
- MULTIPLE POWER LEADS
- TEST CIRCUIT FOR EACH INITIATOR
- DUAL POWDER CHARGE

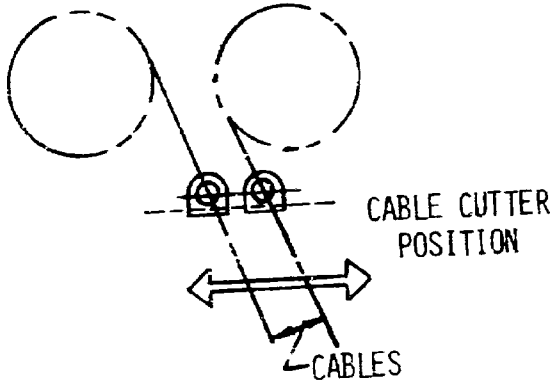
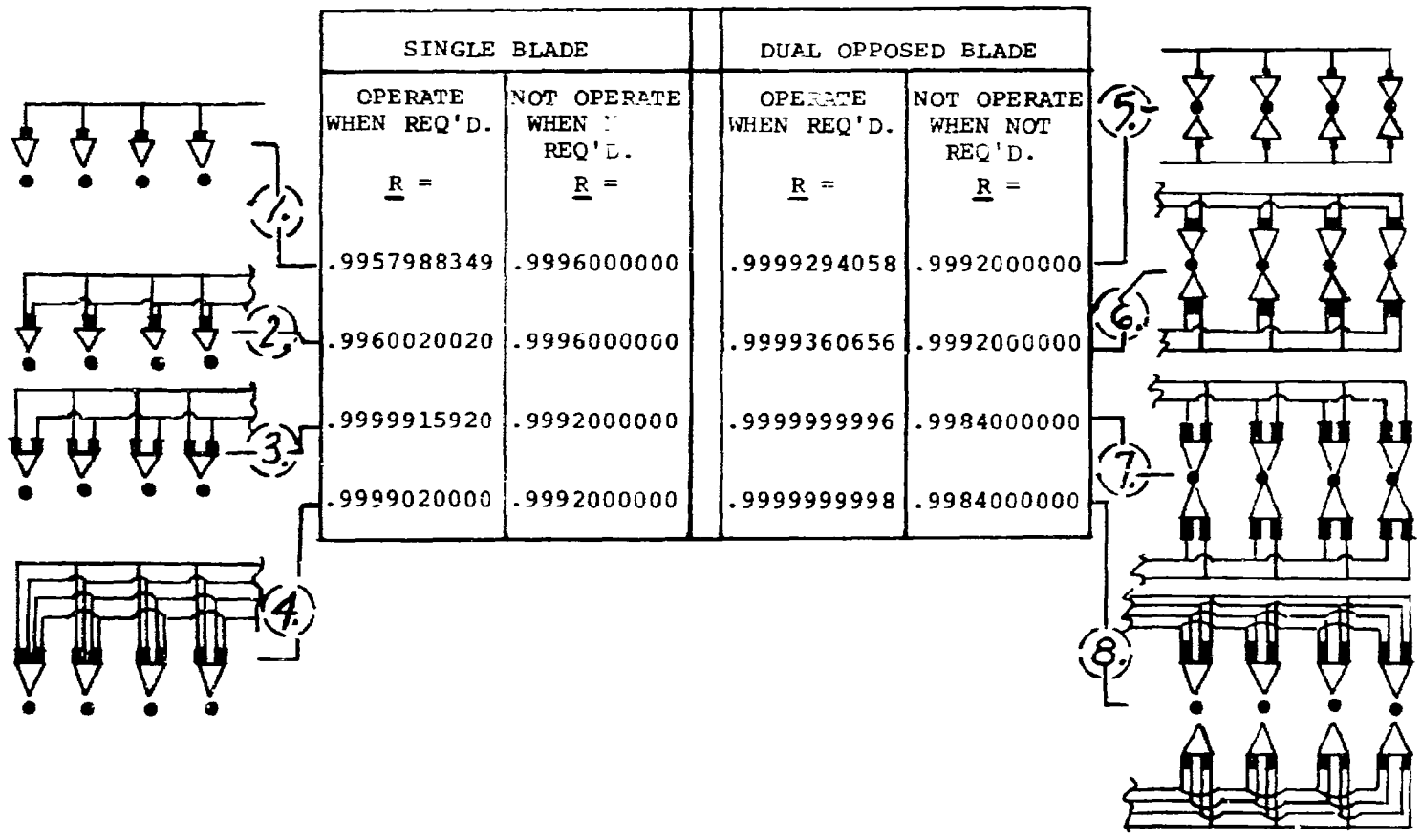


Figure 86. Dual Knife Cable Cutter System.



	SINGLE BLADE		DUAL OPPOSED BLADE	
	OPERATE WHEN REQ'D. R =	NOT OPERATE WHEN NOT REQ'D. R =	OPERATE WHEN REQ'D. R =	NOT OPERATE WHEN NOT REQ'D. R =
1.	.9957988349	.9996000000	.9999294058	.9992000000
2.	.9960020020	.9996000000	.9999360656	.9992000000
3.	.9999915920	.9992000000	.9999999996	.9984000000
4.	.9999020000	.9992000000	.9999999998	.9984000000

Figure 87. HLH Hoist Cable Cutter Reliability Study.

7. Dual knife, dual initiator, and single bridge wire for each initiator.

8. Dual knife, dual initiator, and dual bridge wire for each initiator.

The reliability figures in the study indicate that configuration 3 has the greatest reliability "for operating when required" except the analogous configurations with dual knives, and the highest reliability "for not operating when not required" except for the two single initiator configurations. Therefore, this configuration,consisting of dual initiators, single knife, and single bridge and dual charges, was selected as the best compromise for safety and reliability.

The final design, shown schematically in Figure 88 , consists of:

1. One cutter assembly for each cable.
2. Single knife for each cutter assembly.
3. Dual powder charge for each knife.
4. Two initiators with a single bridge wire for each.

The initiator is a standard MIL-I-23659C unit as proposed by Frankford Arsenal. The proposal per Frankford Arsenal was accepted by AVSCOM, St. Louis, for the initial contract of the ATC Program. Subsequently, design and initial testing were completed.

Testing at Frankford Arsenal confirmed the satisfactory operation of the cutter over the required temperature range. Interface requirements with the hoist resulted in two changes:

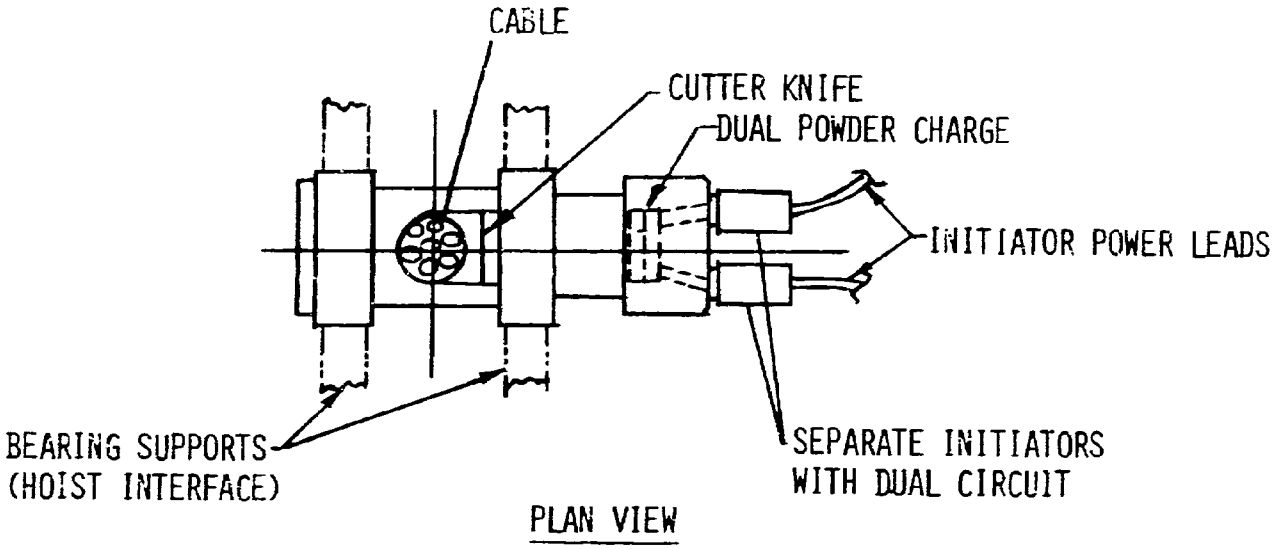
1. To provide a longer bearing surface by reducing the diameter of the end cap, and

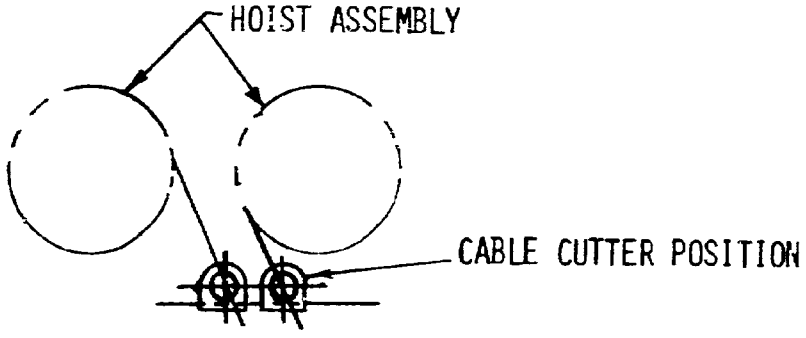
2. Replacing the holes provided in the anvil retainer to facilitate assembly with four equally spaced slots.

A description of the cable cutters supplied for the ATC Program is presented below.

Detail Design

The assembled cutter consists of the following principal parts: body, blade and piston assembly, initiators, cartridge head, anvil, anvil retainer, and cable liner. These parts, together with an assembled unit, are shown in Figure 89.





RELIABILITY AND REDUNDANCY

- TWO SEPARATE INITIATORS
- SINGLE ELEMENT CIRCUIT FOR EACH INITIATOR
- MULTIPLE POWER LEADS
- DUAL POWDER CHARGE
- SINGLE CUTTER KNIFE

Figure 88. Single Knife Cable Cutter System.

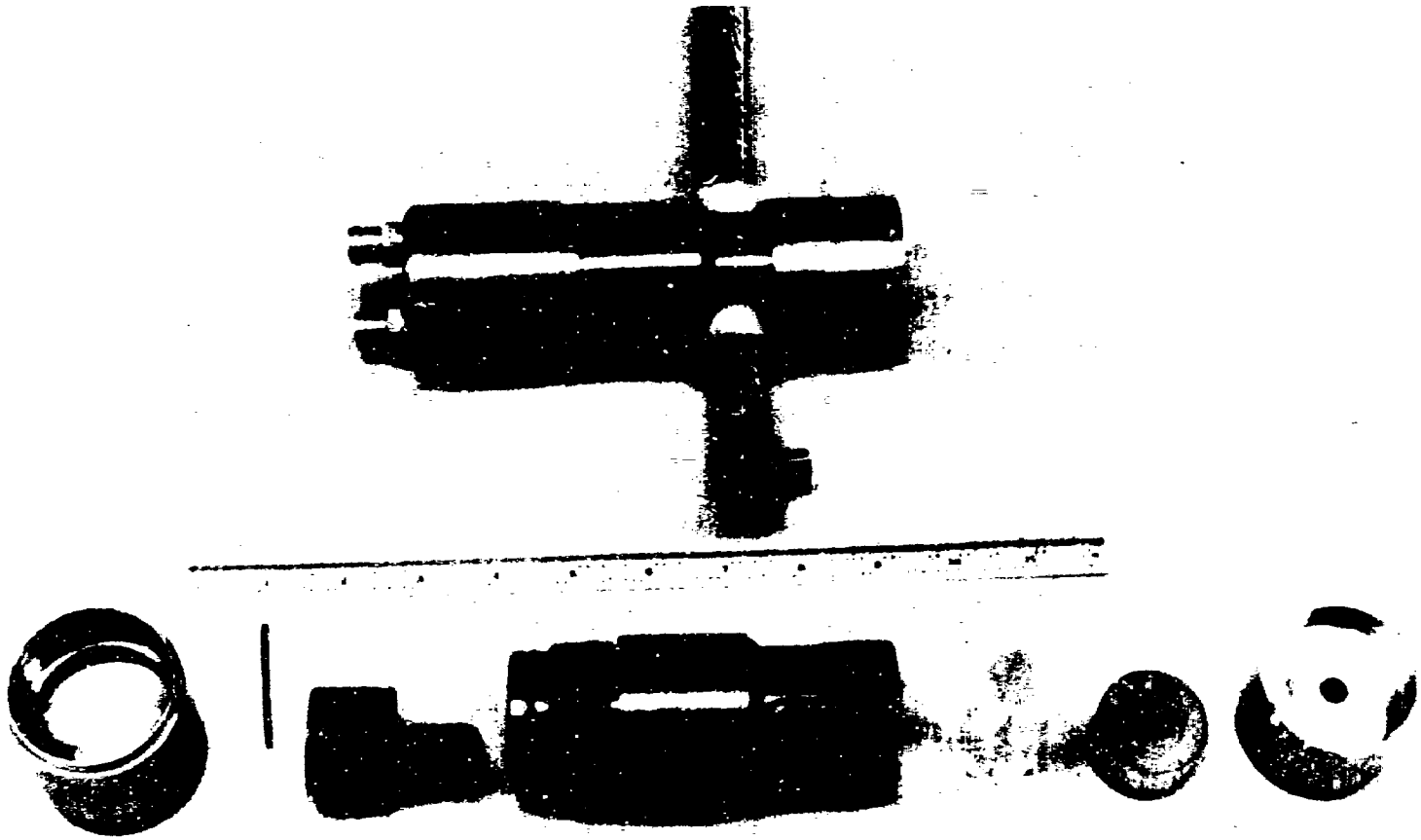


Figure 89. Cable Cutter Parts and Assembled Unit.

The cylindrical body has external threads at either end with a through bore to suit the blade piston. The blade piston is retained to one end of the body by a copper shear pin that also aligns the blade to be normal to the cable. The cartridge head containing the dual initiators and propellant is assembled to the threaded portion of the body at the piston end. Opposite to the piston end of the body the anvil retainer, with the anvil assembled, is threaded such that when fully engaged the anvil is touching the cable liner. The body has a longitudinal slot to permit assembly about an installed cable. The nylon cable liner is split longitudinally, also to facilitate installation. The body, anvil retainer, cartridge head and blade are machined from steel; the piston and anvil are from aluminum alloy. With the cable and cable cutter carriage installed on a hoist, installation of the cutter requires the body, with the piston, blade, cartridge head and ignitors preassembled, to be inserted through one side of the carriage with the slot about the cable. The anvil retainer, with the anvil preassembled, is then threaded to the body through the opposite side of the carriage. The two halves of the cable liner must be assembled about the cable before the anvil retainer is fully installed.

The outside surface of the anvil retainer and the body between the cartridge head and the cable liner provide the bearing surface for the cutter in the carriage.

SUSPENSION SYSTEM

The principal elements of the suspension system consist of the tension member, the coupling, the signal transfer system, the single-point adapter and the extension pendant.

Design Requirements and Proposal Configuration

The suspension system presented in the HLH/ATC proposal was based on a system requirement for a 22.5-ton payload. The dual tandem hoist configuration necessitated a 1.2 factor to accommodate asymmetrical loads, which together with an acceleration factor of 2.5 and ultimate factor of 1.5 required each of the tension members to have an ultimate capacity of 101,000 lb.

The proposed configuration utilized single steel cables of nonrotating construction with integral wire rope cores for the tension members. Electrical conductors for signals and power transfer between the aircraft and the coupling were enclosed within a sheath surrounding the tension member. The proposed diameter of the tension member was based upon developments in materials and construction permitting a 20% increase in cable strength above existing capacity.

The ATC ASRD reflected a requirement for an increased capacity system of 28 ton payload. This requirement, together with a reassessment of aerodynamic and system geometry factors, results in the suspension system requiring an ultimate strength capacity of 300,000 lb as derived in Part III of this volume.

A review of the tension member needed to match this ultimate strength requirement showed that each hoist would need a cable in the order of 1.25 inch diameter. Cable diameters in excess of 1.0 inch present severe development problems due to the limited number of facilities capable of fabricating such cables. This consideration, together with the weight penalties associated with the large-diameter hoist drums required, resulted in the selection of a dual cable tension member concept.

Each tension member will consist of two steel cables, one of left-hand construction, and one of right-hand construction, terminating at a connecting member or "equalizing bar" to ensure equal load sharing. The

coupling will be suspended from the mid-point of the equalizing bar. The "paired" cables ensure a torque-balanced suspension member.

Tension Member

Requirements and Criteria

Multipoint Tension Members - The multipoint (MP) suspension system consists of two identical (interchangeable) tension member assemblies which share the load on a 60/40 load distribution between hoists. Each hoist tension member pair will be capable of supporting 60% of the maximum payload since the CG asymmetry may occur either forward or aft of the longitudinal geometric center of the cargo.

The multipoint tension member capacity, or minimum breaking strength (MBS), is 150,000 pounds.

Single-Point Tension Members - The single-point adapter (SP) lift system consists of a cable/sheave adapter assembly suspended from the multipoint system.

The single-point load carrying element supports the freely moving sheave, coupling, swivel, extension pendant (if used) and cargo and shares the load equally in each of its legs under all flight conditions, as shown in Figure 90.

The single-point tension member capacity based on the load equalization (CG always centered below the sheave) is 120,800 pounds, i.e., 60,400 pounds per cable.

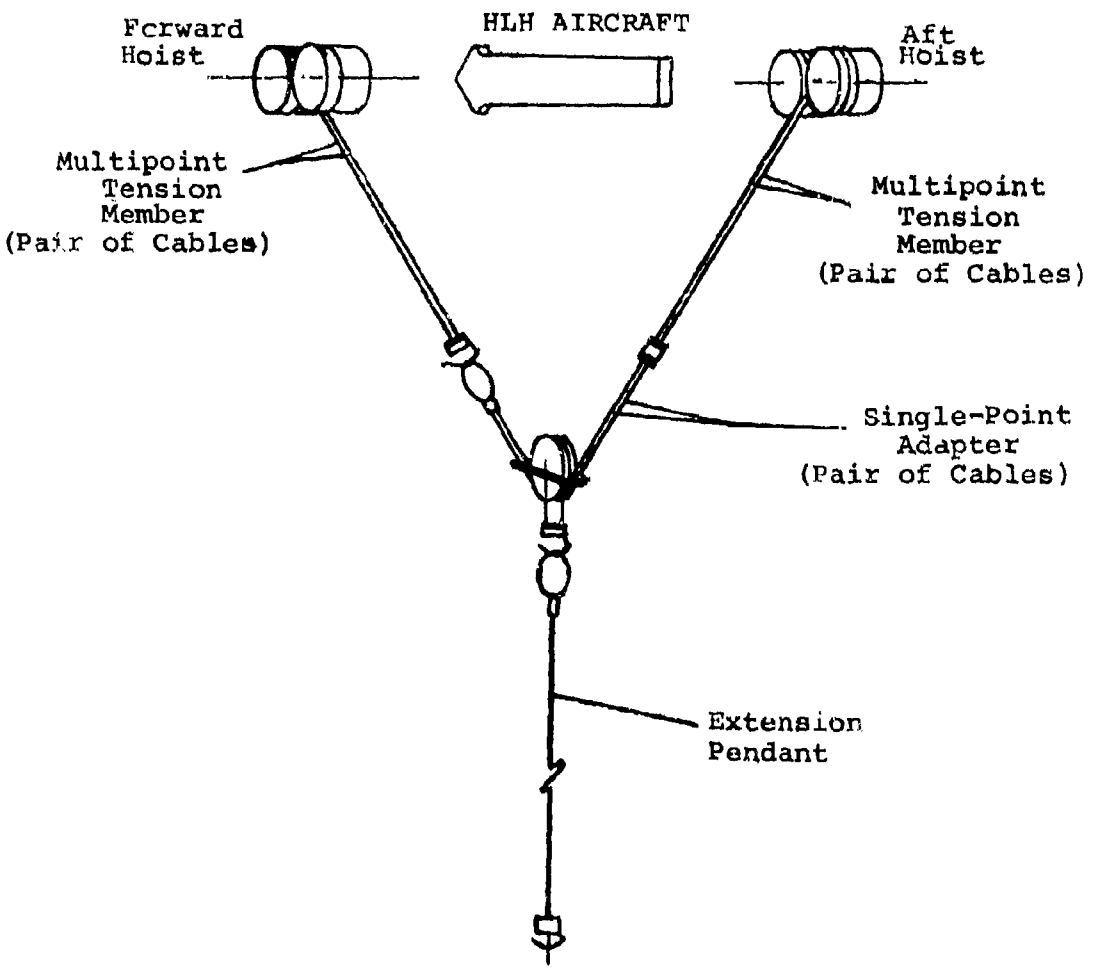


Figure 90. HLH Cargo Handling Suspension System.

Extension Pendant. The 150-ft extension pendant (EP) consists of a tension member used between the single-point adapter and the load. It will be used to supplement the single-point reach of the suspension system.

The pendant tension member capacity (P_{EP}) is based on lifting the maximum design payload

$$P_{EP} = 56{,}000 \times 2.5 \times 1.5$$

$$= 210{,}000 \text{ pounds}$$

End Fittings - Strength Criteria. End fittings will be provided at both ends of each tension member cable to serve as the load transfer (interface) to mating parts.

The hoist drum attachment strength requirement is 20,000 based on 3 dead-wraps and a coefficient of friction of 0.05, as shown in Figure 91.

Each end fitting will meet or exceed the criteria shown in Table 7.

Studies and Analysis Methods

Tension member design does not follow explicit technological patterns. Cable design and manufacturing are largely based on empirical methods, individual manufacturing experience and proprietary techniques. Large safety factors and a broad derating policy are normally used throughout the industry. Production is geared to high-volume, low-cost products which meet minimum specification (catalog) strength levels in order to achieve high utility under a variety of service conditions.

Since the cable diameter largely determined the hoist drum dimensions, and, therefore, the hoist weight and torque requirements, the primary design objective was to minimize cable diameter. This was done by maximizing the cable strength-to-weight ratio and by using a finite life requirement (of the HLH/ATC program) instead of an infinite life requirement.

The following studies were conducted to meet the above objectives:

1. Tension member materials
2. Tension member constructions
3. Strength-to-weight ratio
4. Stored energy
5. Anticorrosion coatings
6. Nonmetallic tension member feasibility

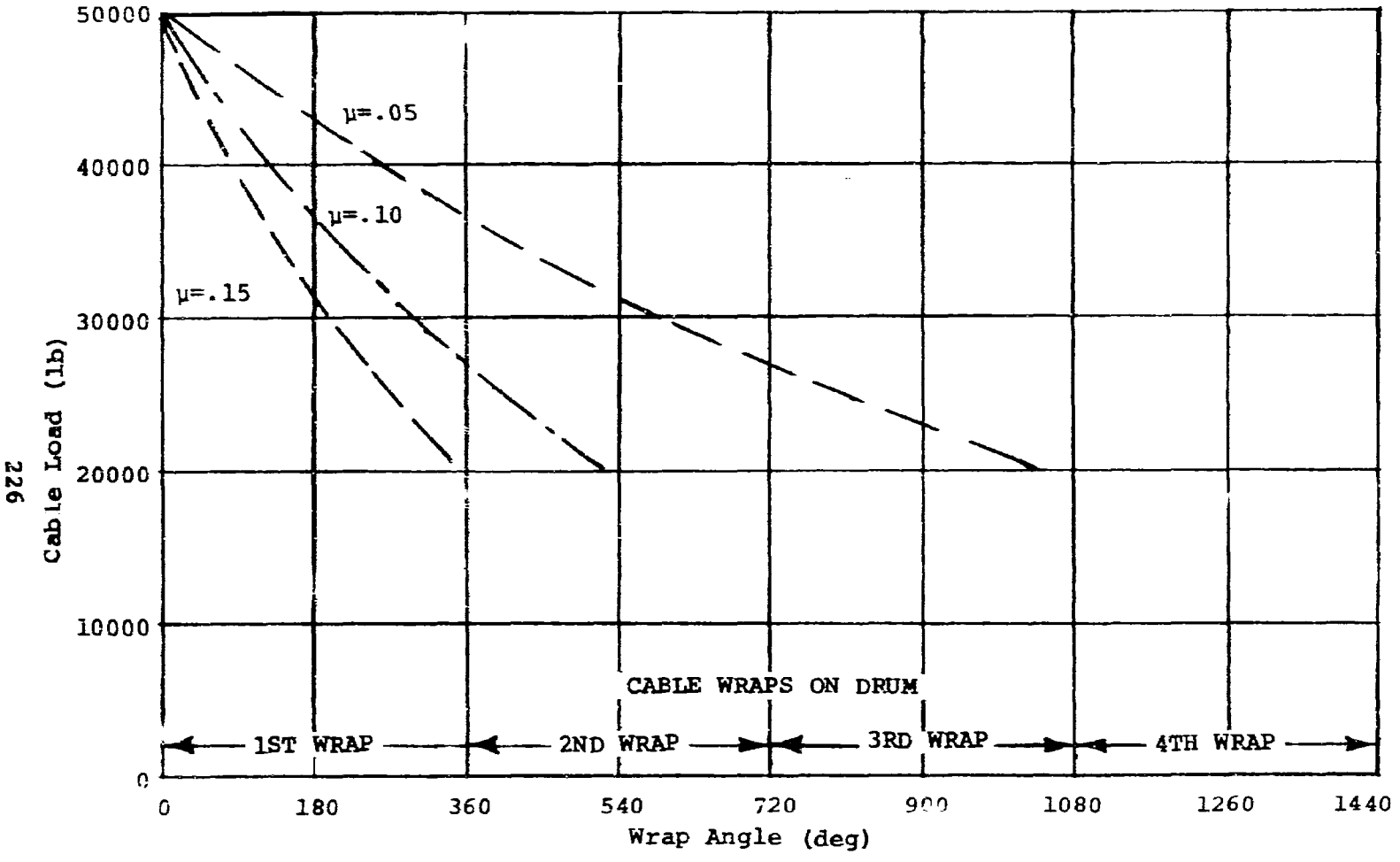


Figure 91. Cable Load Degradation as a Function of Coefficient of Friction.

TABLE 7. END FITTING CRITERIA.		
End Fitting (Interface)	Design Loads* (Pounds)	
	Limit	Ultimate
Equalizer Bar	50,000	75,000
Adapter (Single-Point)	40,300	60,400
Coupling Load Beam	40,300	60,400
Winch Drum	20,000	30,000
Extension Pendant	142,000	213,000

*Limit Load - No Yield
Ultimate Load - No Rupture

To provide a preliminary tension member size permitting the hoist and drive design to be initiated, current technology cable strengths were compared with cables of improved strengths known to be under development. This comparison, shown in Figure 92, uses the data for MIL-W-1511 and MIL-C-5424 cables as the basis for production technology. Known developments, A and B, permit a broadband projection to be made of possible diameter/strength ratios of improved cables.

Tension Member Materials

Metallic cables (wire rope) in the HLH/ATC capacity range are normally made using wire strength specifications in the minimum range of 230,000 to 250,000 psi, depending upon wire size. Earlier airborne cargo hoist studies by the U.S. Army have indicated excessive weights of the hoist designs, influenced by the use of these materials.

Tension member design for the ATC program was based on use of the highest strength wire or fibers that could be produced by existing fabrication processes in the ATC

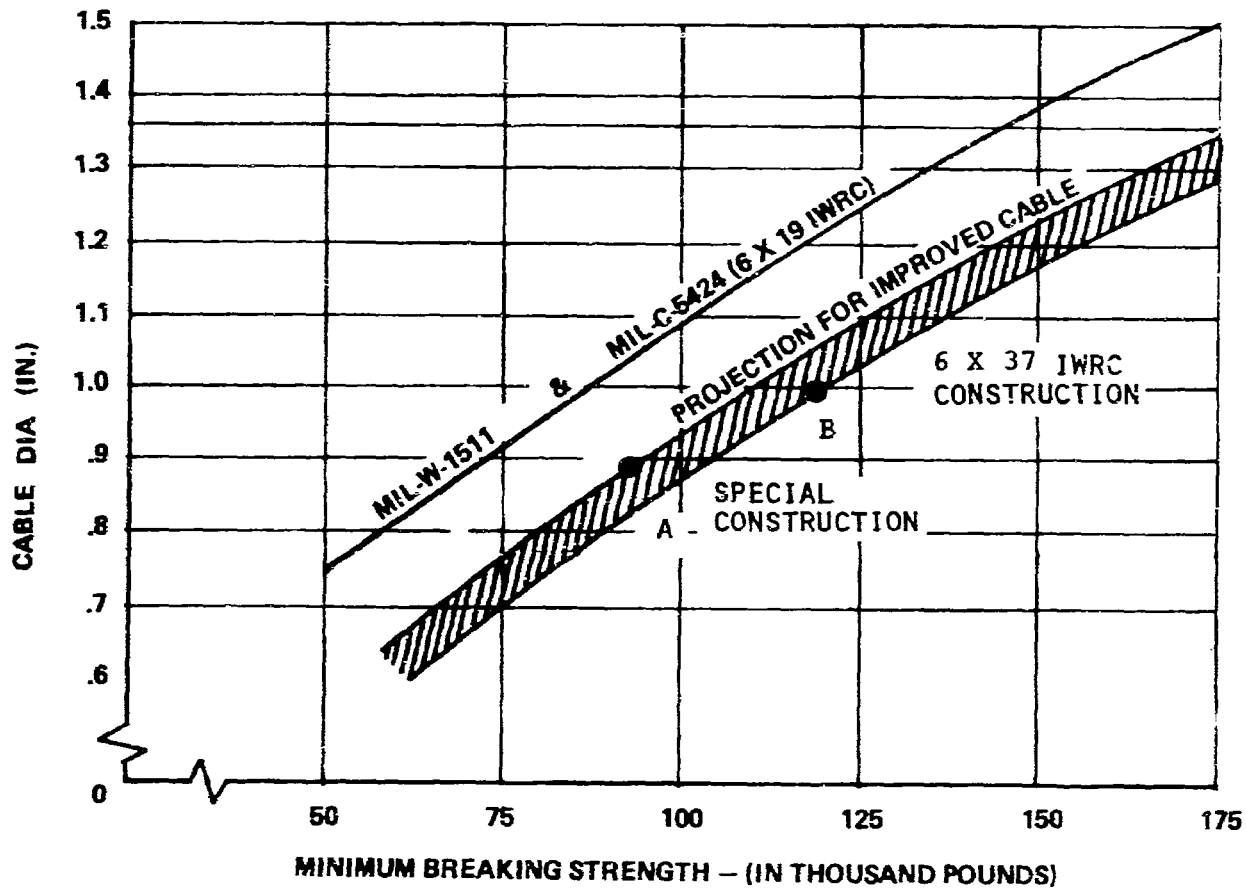


Figure 92. Cable Diameter Versus Strength Comparison.

time frame (of the order of 350,000 psi) providing a strength improvement of at least 40%.

Thus, steels which develop tensile strengths in the 300,000 to 400,000 psi range with a high usable ductility were reviewed. These metals were also to be nonfretting, formable, and have an acceptable work hardening characteristic curing useful life. Coatings to improve the corrosion resistance of steels were also reviewed.

Usable competitive organic fibers reviewed had exceedingly low density, but had tensile strengths in the range of 300,000 - 380,000 psi, and were resistant to common solvents, chemicals, flame ultraviolet light, pollution, abrasion and high temperature.

Materials considered for design support evaluation were: in the metallic category, bright carbon steel as a baseline, drawn-galvanized carbon steel, and stainless steels, 18-2 Mn and 17-7 PH; and in the fiber category, PRD-49-Type III and its companion, Fiber "B".

The materials selected for investigation were based on the following reasoning:

1. Bright carbon steel as baseline material to afford a comparison with existing test data available for different cable constructions. This material has the best known strength and ductility but has no corrosion resistance.

2. Galvanized, drawn carbon steel has the best overall strength, ductility and corrosion resistance, but not the best strength-to-weight ratio.

3. 18-2 Mn and 17-7 PH have good strength, ductility and corrosion resistance, but have not been applied to cables.

4. A new coating with corrosion and abrasion resistance is (electroless) Nickel-Boron. Its use on wire subject to drawing and construction into cable had not been explored.

5. In organic fibers, Kevlar 49 (PRD-49 Type III) and Kevlar 29 (Fiber B) merited investigation due to their high fiber strength, high modulus, and exceedingly low density and elongation.

Materials reviewed and eliminated in the studies include the following:

Material	Rejected For
302	Relative lower strength and ductility although good corrosion resistance.
NS-355	Relative lower fatigue strength than carbon steel (also material being removed from market).
MP-35N	Cost prohibitive (by an order of magnitude) although characteristics are applicable.
Titanium	Low fatigue strength and high galling susceptibility (for available alloys).
Fibers	
Boron	Stiffness
Graphite	Stiffness and notch sensitivity
Glass	Poor abrasion resistance
Nylon	Low tensile strength and high elongation
Dacron	Low tensile strength and high elongation

Tension Member Construction

The tension member design concept is for an all-steel torque balanced, paired cable assembly. Nonmetallic fibers to be tested have no previous utilization in rope construction, necessitating the primary design being based on a metallic cable.

Previous studies had indicated areas where there was a potential for significant increases in strength and fatigue life. A review of existing data showed that the strength/weight ratio of a steel cable increased as the diameter decreased. A comparison of cables of rotating and nonrotating construction showed a considerable increase in strength for rotating-type cables. These factors influenced the selection of the torque balanced, paired cable concept.

Since both cables are attached to a fixed connector rather than a swivel, both cables are automatically torque balanced through the connecting member.

Torque-balance will be achieved by using a pair of cables, each of opposite hand (one left and one right hand) of the same construction. Each cable will be designed as a mirror-image of the other to develop identical strength, torque (of opposite sign), and elongation under all load conditions. When loaded in

parallel, as an assembly, they will develop the design capacity without rotation about their common axis.

A further distinct advantage of the dual-drum approach is that lang or regular lay rotating cables can be used. Both of these constructions are stronger than non-rotating cables.

Use of cables with "fixed" rather than "free-swiveling" end conditions also provides a significant increase in available tensile strength from the same cable diameter and construction. This is shown from comparative tensile tests of four 18 x 7 nonrotating constructions in Table 8.

TABLE 8. STRENGTH IMPROVEMENT DERIVED USING FIXED RATHER THAN FREE-ENDED CABLE[2] (18x7 Nonrotating Construction.)

Cable	One End Free	Fixed	Improvement In Strength
A	100,500	132,000	32%
B	80,000	121,500	52%
C	97,000	132,600	38%
D	91,000	128,400	42%

Use of rotating (lang) lay cable instead of nonrotating constructions (same diameter) provides a 2:1 improvement in fatigue strength[3] with D/d = 0/1 (see Figure 93).

The feasible life cycle projections also shown in Figure 93 are based on Navy test data and are shown for constant load cases for D/d ratio of 20/1 and 24/1 and both non-rotating and rotating type constructions. The minimum life at a 20/1 D/d and 100% design load, as estimated for the rotating lang-lay type construction, provides approximately a 3-to-1 margin over the ATC requirements.

Roebling and other manufacturers have recommended lang-lay wire rope as having greater flexibility, abrasion resistance and fatigue life for the same strength, grade and construction. By comparison with regular rotating and nonrotating construction, the lang-lay has shallower wire crossing angles. The Navy fatigue data

2. Gibson, P. T., et al; TORSIONAL PROPERTIES OF WIRE ROPE; ASME Report 69-DE-34; 1969.

LOAD		BEARING PRESSURE RATIO	D/d	HOISTING CYCLES AT FAILURE	
				CONSTRUCTION	
% DESIGN	POUNDS			ROTATING LANG LAY (6 x 25)	NON ROTATING (18-7)
100	40,500	.0073	20/1	36,000	18,400
125	50,000	.0088	20/1	31,000	16,400
100	40,500	.0061	24/1	41,000-40,000	21,000
125	50,000	.0077	24/1	34,000-40,000	17,600

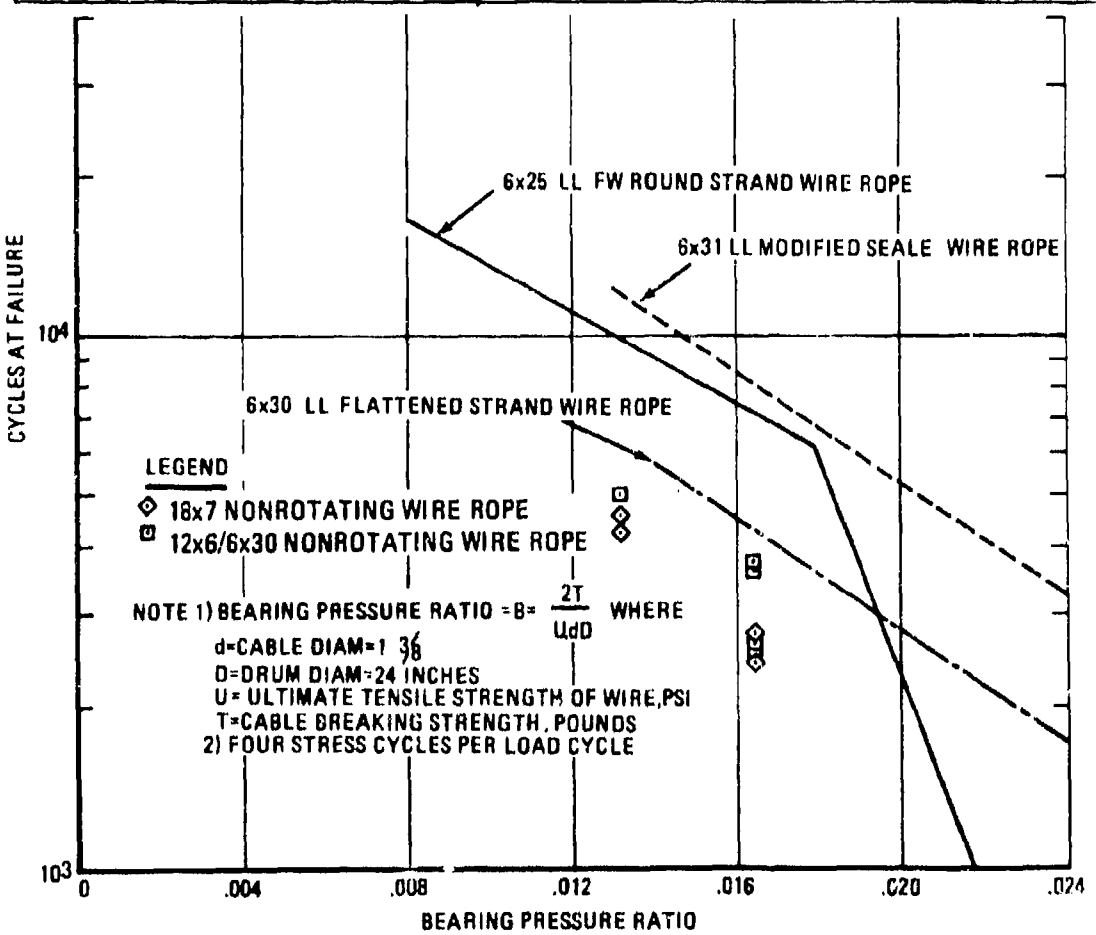


Figure 93. Fatigue Characteristics of Various Cables.

shows acceptable life expectancy in large-size cables. Since direct and comparable fatigue data is not available, design support tests were designed to include several lang-lay constructions which could be compared with data available on 3/4-inch cable of regular-lay constructions.

This study concluded that both regular and lang-lay rotating cable constructions would be assessed in the design support tests.

The maximum cable diameter was limited to 1-1/8 inches. Cables exceeding this diameter are extremely stiff and do not lend themselves to practical airborne application because they require very large drum diameters and produce excessive weight penalties.

The flexibility criteria selected for the HLH/ATC design and development program was 24/1 with an objective of 20/1 established for design support tests. The final design D/d will be selected based on the cable life margin determined from test.

The critical bending stress induced in the tension member at its point of tangency with the drum or sheave should be included in the strength criteria. The bending stress cannot be readily calculated, however, as it is influenced by many simultaneous factors among which are relative movement of individual wires and strands, under load. Industry practice has been to increase the safety factor or to add a percentage of the payload to compensate for bending. Normally, demonstration is by a straight tensile pull test.

To assure the proper incorporation of the bending effect losses in the ATC program, the design was based on actual test demonstration of the strength criteria with one end of the tension member wrapped around a drum.

In the field, the cable life is affected by many degrading factors including the combined effects of wear, abrasion, handling damage, random loading, and maintaining lubrication. These were evaluated in design support tests. A simulated drum interface (drum material, surface, contour and helix angle) to include the effect of degradation due to wear and wrap pressure (compression) loading was used in the design study tests.

Close conformity between the drum groove and the cable during operation under load was used to provide proper support for maintaining the cable shape and to afford proper load distribution between adjacent wires and strands. U.S. Navy tests[3] have demonstrated a 15% fatigue life improvement with close fitting cable/sheave grooves.

Accordingly, design support test components were designed with a +.010 - .000 fit based on cable diameter at no load compared to the cable industry practice of allowing 1/32 inch groove clearance.

Structural wire cores were selected for the design for two reasons: (1) an increase of 7-1/2% in strength for the same cable diameter and (2) elimination of troublesome core conductors for coupling signal transfer.

Other benefits derived in using a pair of small-diameter cables as a tension member are: load sharing between member elements, a means of condition sensing, higher flexibility and strength-to-weight ratio, and simplified producibility.

Strength-To-Weight Ratio

A stringent weight target of 1.7 pounds/foot was selected for the 150,000-pound design in steel. This is based on existing high strength cable samples with a margin (weight reduction) for development based on the low life cycle requirement. The use of Kevlar 49 in a competitive strength indicated an achievable weight objective of 1.2 pounds/foot.

Strength-to-weight ratio goals in this weight basis for the tension member were as follows:

Material	Unit Strength/Weight (lb/lb wt/
Carbon Steel	$\frac{150,000}{1.7} = 88,200$
Stainless Steel	$\frac{150,000}{2.0} = 75,000$
Kevlar	$\frac{150,000}{1.2} = 125,000$

The lower target for stainless was due to its reported increased brittleness in wire strengths in the desired working range of 300,000 to 350,000 psi.

---

3. Black, R.; MARK 7 ARRESTING GEAR PURCHASE CABLE AND DECK PENDANT DEVELOPMENT PROGRAM: NAEC Report ENG-7625, Naval Air Engineering Center, Philadelphia, Pennsylvania; May 1970.

Stored Energy

The amount of energy which can be recovered from the tension member during unloading becomes important when cable failures are considered. This recoverable stored energy can be transformed into spring back of the cable which could then strike the fuselage or rebound into the rotors.

An analysis was performed to determine the height of cable motion after a cable failure. The method[4] used was to determine the velocity of the end of the remaining cable shortly after a cable failure. The resulting height of motion of the end of the remaining cable was determined from this velocity.

The approach is to express the initial static displacements due to the load carried by the cable in terms of cable longitudinal natural modes and to determine initial conditions for model generalized coordinates. The total velocity of the end of the remaining cable is then found at a time equal to one-quarter of a period of the first longitudinal mode of the remaining cable. At this time, the total longitudinal displacement of the cable will first pass through zero and all the initial strain energy will be converted to kinetic energy. Assuming that the tension member cannot carry compression, the velocity at this time will determine how high the end of the remaining tension member can go. The height of cable motion was found to be a function of the ratio:

$$\frac{f_{tu}^{2}}{E\,\gamma}$$

where: f_{tu} = tensile ultimate stress in cable
E = modulus of elasticity (Young's Modulus)
γ = effective material density = cable weight per unit length divided by net cable tension material area.

The larger this ratio, the higher the height of cable motion. This height can be reduced by the following changes, either singly or in combination:

1. Arbitrarily increasing nonstructural cable weight.
2. Increasing the cable material modulus of elasticity.
3. Lowering the cable stress levels.

---

4. Jacobsen, Ayre; ENGINEERING VIBRATIONS; McGraw-Hill Book Company, New York, New York; 1958; Page 474

Of these three possibilities, nonsturctural cable weight increases and lower cable stress levels are diametrically opposite tension member design objectives of low weight and high strength-to-weight ratio. This leaves increases in modulus of elasticity as the only area where stored energy considerations can be reflected. The tension member material/construction selected for the preliminary design had a modulus of elasticity of 19.7 x 10^6 psi. This compares with a nominal wire rope modulus range of 12 to 15 x 10^6 psi. The 36 x 7 electro-galvanized swaged strand lang-lay carbon steel cable had the highest modulus of elasticity within the group of constructions tested.

The analysis indicates, however, that cable springback sufficient to strike the fuselage can occur at a 1.0G stress level with cable lengths shorter than about 50 feet. Springback sufficient to reach the rotor plane is possible at cable lengths less than about 17 feet.

This analysis justifies the requirements for a cable cutter system at the upper end of the tension members and the stipulation that inflight load jettison at the cargo coupling be mechanically precluded.

Tension Member Anti-Corrosion Feasibility Study

The tension member development for the HLH/ATC included the investigation of stainless steels, as well as carbon steel, in order to select the best candidate material on a strength-to-weight ratio. The degree of corrosion resistance of stainless steel depends on the specific material involved. For carbon steel cable, zinc coatings have afforded the best corrosion resistance. The proper lubricant for both materials should also assist in inhibiting corrosion. Stainless steel cable development was discarded on the basis of the low strength levels obtained in the early phase of design support tests. Therefore, an investigation of corrosion protection of non-stainless materials was essential.

The specific degree of corrosion resistance for field use is unknown; however, the problem is mitigated by the HLH design requirement for a limited life cable rather than one of unlimited life.

The objective of this design support study was to determine the feasibility of using an untried electroless nickel-boron coating to resist corrosion on high-strength carbon steel wire, and to determine the compatibility of the coating with the processes involved in cold wire drawing and wire rope construction. Another

important attribute of the Ni-Bo coating was its abrasion resistance. While this characteristic could also be used to advantage in possibly improving cable life, it was of secondary importance.

Tests were conducted using nickel-boron coatings and zinc coatings over nickel-boron on a typical high-strength carbon steel. Both coatings were compared to drawn zinc coated wires. These tests are reported in Volume III of this report.

Test results proved that:

1. Zinc applied to nickel-boron coating after drawing, .1 mil thick, did not provide adequate corrosion protection.

2. Zinc applied to nickel-boron coated wire by the hot dip process before drawing did not survive the drawing process adequately to provide adequate corrosion protection.

Nonmetallic Tension Member Feasibility Study

The objective of the HLH/ATC tension member development program was to develop a tension member for the cargo carrying subsystem using the latest technical advances in materials and construction techniques within constraints of time and manufacturing feasibility.

One avenue of pursuit was to determine the feasibility of using nonmetallic fibers for their high strength-to-weight ratio characteristics; in particular, Kevlar 49 and 29 fibers for a tension member applicable to the development of an optimum size/weight hoist.

This feasibility study consisted of two phases of design support tests. The first phase included static and environmental tests; the second, an evaluation of fatigue characteristics and a determination of tensile properties using simple end termination techniques. The test specimens consisted of fiber bundles or "building blocks" of 1/8-inch diameter. Variations in yarn twist, fiber finish, and bundle construction were evaluated to determine their influence on achieving maximum fiber strength utilization. Tests included tensile elongation, over-a-drum tensile strength, and bundle fatigue characteristics when bent over a (hoist) drum. Fiber stresses

representative of actual conditions were used. Temperature, abrasion, and ultraviolet degradation factors were investigated. These tests are reported in Volume III of this report.

As a result of these tests, the following conclusions were made. Based strictly on strength characteristics, a cable suitable for the ATC tension member application (75,000 pounds cable ultimate with D/d-24/1) could be developed in the range of 1-3/16 to 1½ inches depending upon construction efficiency. These tension member designs would result in an estimated weight saving over the use of steel wire in the tension member in the range of 63 to 40%, respectively. However, in order to fully capitalize on this weight benefit for the present hoist concept, the PRD cable must be capable of operating at a lower D/d than now contemplated for steel cable. The fatigue life of each of the 1/8-inch fiber bundle configurations tested at a D/d of 24/1 was lower than required (10,800 cycles) at the representative fiber bundle design load (25% of ultimate strength). However, the data shows a trend of increased life with larger cable size (36,480 to 48,600 denier) and with the added protection of an outer abrasive-resistant sleeve. Full-scale tests must be done to further define the influence of these factors on Kevlar 49 and 29 cable applications.

Ultraviolet degradation and abrasion effects are time dependent losses which may be alleviated by jacketing with appropriate synthetic material. Increased diametral and weight effects of jacketing were not included in the projections. While jacketing will not decrease the Kevlar weight advantage significantly, it will increase cable diameter; a disadvantage if outside size is a critical competitive factor. Also, the final cable diameter using a fiber construction will be larger in diameter than now anticipated for a steel cable design, thereby requiring a longer drum or a new hoist configuration.

No significant conclusions were drawn relative to the terminal designs used because of the sensitivity to nonuniform fiber loading within the bundle. However, bundle "center breaks were achieved with some tabbed samples and the ½-inch rope tensile tests with epoxy terminals, indicating the need for special techniques in terminal fabrication.

Based on the above, it is concluded that development of a Kevlar configuration with maximum fiber strength utilization, minimum diameter, and an adequate fatigue life was not compatible with the HLH/ATC time frame.

Metallic Tension Member Development

In order to establish the optimum configuration for a metallic tension member, a program of design support test was established. These tests also verified the "paired cable" torque balanced concept.

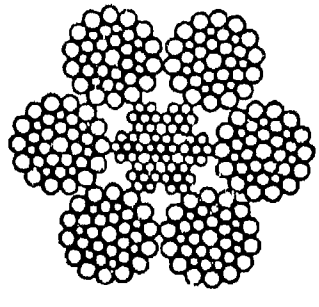
Design Support Tests consisted of:

1. Paired cable torsion and rotation demonstration
2. Cable tension/elongation measurements
3. Cable bending fatigue tests
4. Cable tension-over-drum tests
5. Tension/elongation tests of candidate wire materials
6. Torsion tests of candidate wire materials

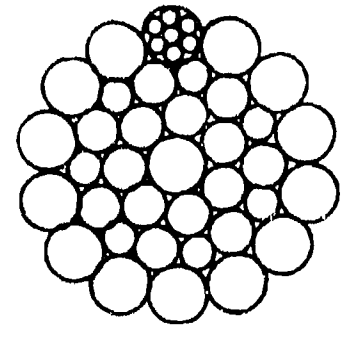
Materials and constructions evaluated were:

Materials	Construction
Bright Carbon Steel	6 x 36 Regular Lay
Bright Carbon Steel	6 x 36 Lang Lay
Electro-galvanized Carbon Steel	6 x 36 Lang Lay
Electro-galvanized Carbon Steel	36 x 7 Lang Lay
17-7 PH Stainless	6 x 36 Lang Lay
18-2 M_n Stainless	6 x 36 Lang Lay

The two construction configurations are shown in Figure 94. Details of these tests are included in Volume III of this report.



6x36 Warrington-Seale, IWRC Construction.



36x7 Swaged-Strand Construction. (Each of the 36 elements actually is a seven-wire swaged strand)

Figure 94. Sections Through Test Cables.

Conclusions Drawn from Design Support Tests

Tension member design support testing demonstrated that the 0.78-inch-diameter electrogalvanized, .36x7, swaged strand, lang-lay, Warrington-Seale construction exceeded the design performance requirements of the ATC program. The advantages of the 0.78-inch-dia. 36x7 material/construction combination over the other steel cables compared are summarized below:

1. Highest tensile strength.

2. Highest strength-to-weight ratio.

3. Highest efficiency.

4. Meets fatigue spectrum loading criteria with acceptable remaining tensile strength. Bending fatigue 150% overload for 10,800 cycles had no perceptible effect on the strength of the cable.

5. Insensitive to drum groove wear due to bending fatigue (including operation at 150% overload).

6. Material has acceptable corrosion resistance. There was no significant cable degradation due to bending fatigue and salt-fog exposure.

7. Material is insensitive to stress corrosion.

8. Its construction characteristics are desirable:

   a. It has the highest elastic modulus.

   b. It develops the lowest torque.

   c. It exhibits the least permanent elongation or constructional stretch and a proportional limit well above required limit load.

The characteristics of tested 36 x 7 cable are shown in Table 9. The cable diameter/strength relationship compared to available cable and original design projections are shown in Figure 95.

While the 36 x 7 EGCS did not meet the ATC weight objective selected, it was used as a basis for a lighter weight cable design.

TABLE 9. CONSTRUCTION DETAILS FOR ELECTROGALVANIZED 36x7 LANG-LAY WIRE CABLE (0.78-INCH DIAMETER).

Wire Location	Wire Diameter (Inch)	Ultimate Tensile Strength (10^3 psi)	Total Number of Wires	Wire Breaking Load (Lb.)	Aggregate Wire Strength (Lb.)
Outer 14 strands	0.046	309	84	514	43,176
Outer 14 strands	0.049	314	14	592	8,288
Int. 7 strands	0.038	330	42	374	15,708
Int. 7 strands	0.041	322	7	425	2,975
Int. 7 strands	0.029	348	42	230	9,660
Int. 7 strands	0.031	350	7	264	1,848
Inner 7 strands	0.038	330	42	374	15,708
Inner 7 strands	0.041	322	7	425	2,975
Core strand	0.056	307	6	756	4,536
Core strand	0.059	306	1	837	837
			Total Aggregate Strength		105,711

Metallic Area = .330 Sq. Inch
Measured Weight = 1.219 lb/ft

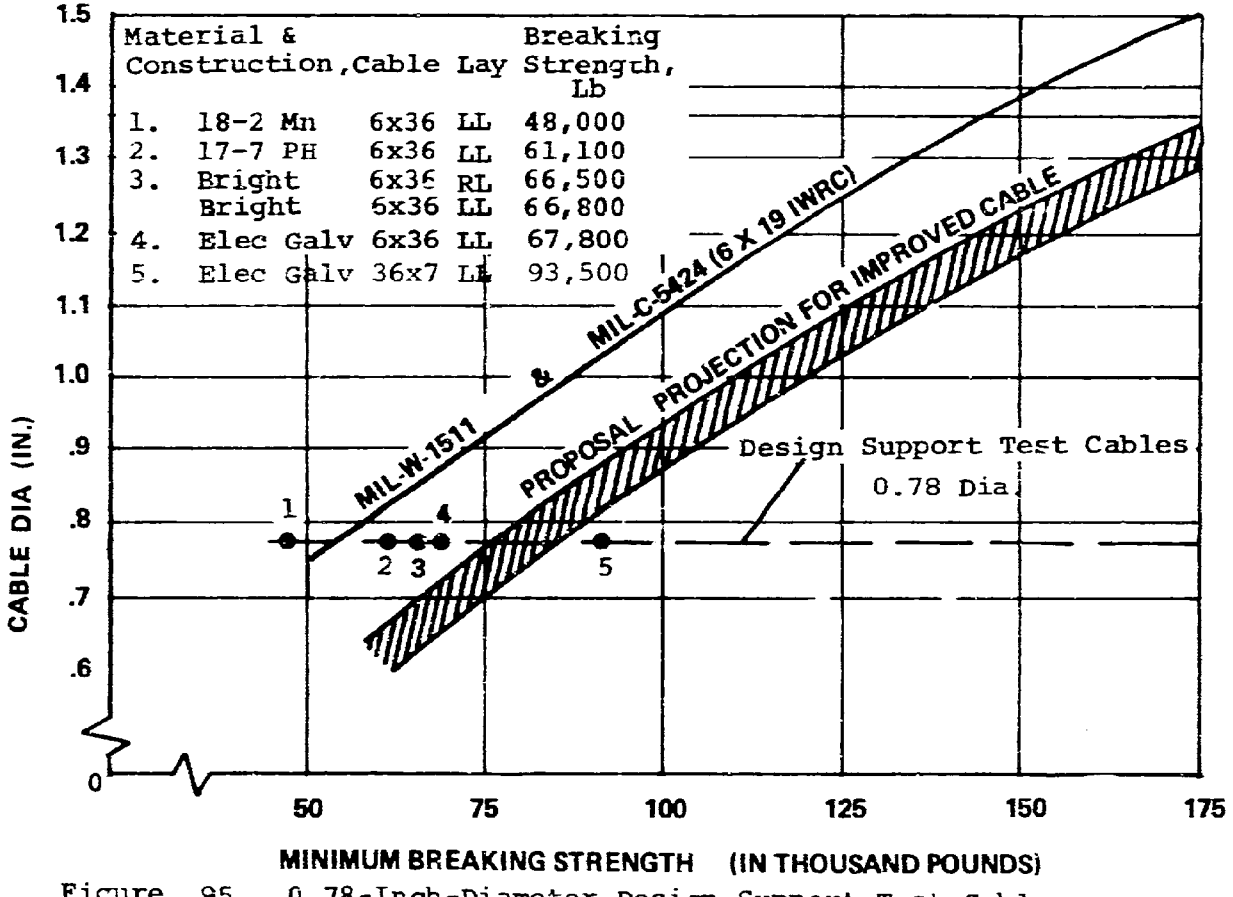


Figure 95. 0.78-Inch-Diameter Design Support Test Cables Compared To Diameter And Strength of Commercial, MIL-W-1511, And MIL-C-5424 Cables.

Cable Preliminary Design

As a result of the higher than required breaking strength achieved with the 0.78-inch, 36x7 design support cable, a cable of 0.70-inch diameter of the same construction was selected for development.

The 0.78-inch-diameter cable used mill run wire, which developed an average wire tensile strength of 320,000 psi. The diameter reduction was based on wire drawn to an average of 350,000 psi strength and geometry projections of achieved breaking strength versus cable area. The strength-to-weight ratio of this new cable was estimated to be 76,400 compared to 50,000 for .75-inch-diameter mil spec cable. Also, it was an improvement over the 0.78-inch-diameter test cable, which had a strength-to-weight ratio of 71,400.

Calculated weight for the 0.70-inch-diameter cable was .982 lb/ft compared to the weight goal of .85 lb/ft. The cable weight saving with the 0.70-inch diameter resulted in approximately 140 lb per aircraft. This was considered to be a worthy ATC objective. The 0.70-inch-diameter cable configuration is described in more detail in the paragraph entitled "Cable Detail Development Design".

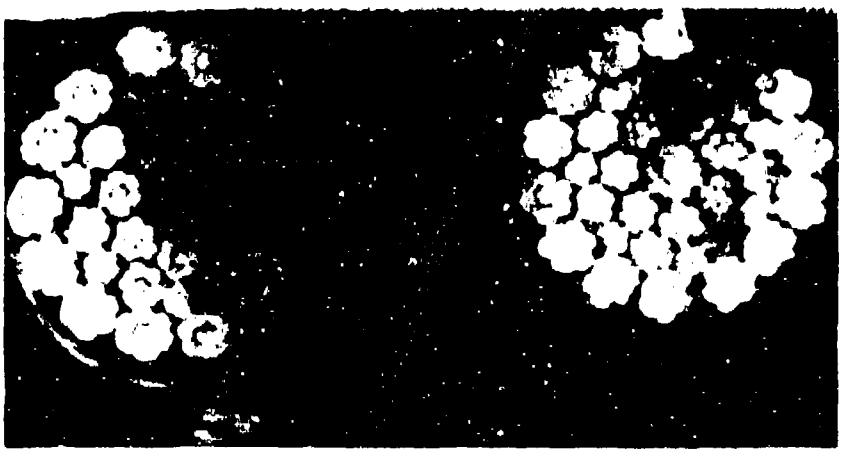
Since multipoint and single-point cable strength requirements are relatively close (i.e., 75,000 and 61,300 lb, respectively) the same cable design was used for both applications.

The preliminary design cable diameter of 0.70-inch makes it possible to reduce the hoist drum length and diameter. The D/d for the development cable design based on the hoist drum selected is 26.7/1, although tests have shown that a D/d of 20/1 was satisfactory for cable life and wear considerations.

Cable Detail Development Design

The 36x7 wire and strand construction used for development tests is as shown in the photograph in Figure 96. Details of the alternate strand sized in the second layer (Warrington-Seale arrangement) and a comparison of the compacted strands in the 0.78-inch and 0.70-inch diameters are shown.

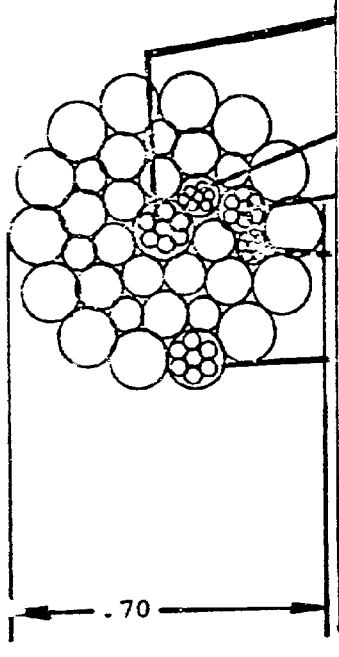
Wire and strand characteristics in the right- and left-hand development test cables are listed in Table 10. Computed



0.78-in Dia. 0.70-in Dia.

Figure 96. Cross Sections of 0.78-Inch and 0.70-Inch Dia., 36x7 Warrington-Seale Construction Test Cables.

TABLE 10. DEVELOPMENT CABLE - 0.70-INCH DIAMETER 36x7 CONSTRUCTION CHARACTERISTICS RIGHT AND LEFT LAY.



Strands				Cable Lay			
				Right		Left	
				Wire			
No.	Layer Location	Diameter (In.)	Total No. Used	Measured Strength (psi)	Aggregate Strength (lb)	Measured Strength (psi)	Aggregate Strength (lb)
1	Core	.053	1	331,342	731	331,342	731
		.061	6	339,726	4,163	339,726	4,163
7	1st	.036	7	345,817	2,463	345,817	2,463
	Inner	.034	42	367,874	14,028	367,874	14,028
7	2nd	.036	7	345,817	2,463	345,817	2,463
	Inner	.034	42	367,874	14,028	367,874	14,028
7	2nd	.028	7	365,408	1,575	365,408	1,575
	Inner	.026	42	382,348	8,525	382,348	8,525
14	Outer	.044	14	341,986	7,280	346,590	7,378
		.041	84	365,092	40,488	325,696	36,120
Total Metallic Area,sq.in.= .264							
Average Wire Stress,psi=				362,942		346,770	
Calculated Aggregate Breaking Strength (lbs) =					95,744		91,478

"Aggregate Breaking Strengths" (ABS) were 95,744 lb and 91,478 lb for right- and left-hand cables, respectively. These strengths were based on average measured wire strengths of 362,942 psi for the right-lay and 346,770 psi for the left-lay cables using wires from two sources. To achieve these wire strengths, a hot dipped galvanized coating instead of electrogalvanizing was used.

The 4,266-lb difference between the cable strengths was due to the use of lower strength wires in the 14 outer strands of the left-lay cable. The complete right-lay cable, as well as the core and inner layer of the left-hand cable, were fabricated from wires supplied from one source with a minimum strength of 30,000 psi over the catalog strength values for each wire size used. The wires drawn by the second source had a strength requirement of 20,000 psi over commercial catalog minimums. Otherwise, except for mirror-image twist, the cables were to be identical.

The cable size and weight design estimates are based on $\pm$.001 tolerance on each wire used. Final characteristics were also subject to the influence of strand compacting (swaging). The cables as tested were as follows:

	Actual		Calculated
	Right	Left	
Diameter, in.	.695	.695	.695 to .710
Weight, lb/ft	.948	.960	.982

By comparison the design support test 0.78-inch-diameter cable weight was 1.219 lb/ft.

Cable Fabrication

A manufacturing problem occurring in swaging of the outer strands (365,092 psi wire strength) (see Table 11) necessitated the use of the second source wires in the left-lay cable. Using these wires, the estimated minimum breaking strength (MBS) for the right and left cables, based on projections of construction losses, were 79,000 and 77,000 lb, respectively.

The pattern of wire lay lengths (pitch of twist within strands) and L/d ratios in the 0.70-inch cable were slightly larger than used in the 0.78-inch-diameter cable. This change was based on cable fabricating experience which indicated that a lower efficiency would result from use of the high strength wire. Compensation was, therefore, built into the new cable by increasing strand lay lengths. A complete dimensional analysis of the construction of both the 0.78-and 0.70-inch cables is given in Tables 9 and 10.

End Fitting Description

The tension member design required the development of 100% end fittings for all cable terminations except where restrained to the drum (button fitting). (A 100% fitting is one whose mechanical gripping strength is greater than the minimum breaking strength of the cable.) With the selection of cable construction and wire material completed, a design basis was needed for cable end terminations (end fittings) which were compatible with the 36x7 design.

The approach selected was to use the 0.78-inch-diameter 36x7 design support test candidate cable for initial tests. The swaged type end fitting was selected over the fiege and spelter socket types from the experience gained during design support tests. A typical swaged shank/cable specimen used to develop the end fittings is shown in Figure 97.

Once the basic guidelines for achieving an adequate mechanical grip were established, tests with the 0.78 inch cable were discontinued and the final shank configuration was defined with the 0.70-inch-diameter cable.

End Fitting Design

Tension member end fitting designs were made to conform to the interface space limitations and requirement as shown in Figures 98 through 101.

TABLE 11. GEOMETRY OF 36 x 7 CABLE.

Cable Physical Property	Cable Measurements		
	Design Support Cable	Development Cable	Development Cable
Cable Lay Direction	Left	Right	Left
Cable Lay, l, inch	6.56	5.59	5.34
Cable Diameter, d, inch	0.789	0.695	0.695
l/d	8.31	8.04	7.68
° Outer Layer Strands			
Strand lay, l_1 inch	1.02	1.04	1.10
Diameter, d_1 inch	0.136	0.120	0.119
l_1/d_1	7.50	8.67	9.24
° First Inner Layer Strands-Large(a)			
Strand lay, l_2, inch	0.84	0.86	0.90
Diameter, d_2, inch	0.111	0.098	0.097
l_2/d_2	7.57	8.78	9.28
° First Inner Layer Strands-Small			
Strand lay, l, inch	0.62	0.66	0.69
Diameter, d_3, inch	0.084	0.075	0.074
l_3/d_3	7.38	8.80	9.32
° Second Inner Layer Strands(a)			
Strand lay, l_4, inch	0.84	0.87	0.89
Diameter, d_4, inch	0.111	0.099	0.098
l_4/d_4	7.57	8.79	9.08
° Core Strand			
Strand lay, l_5, inch	0.98	1.05	1.03
Diameter, d_5, inch	0.164	0.145	0.144
l_5/d_5	5.98	7.24	7.15

(a) Two layers of strands were made from the same wires and, therefore, were nearly identical in geometry. Measurements were made after swaging.

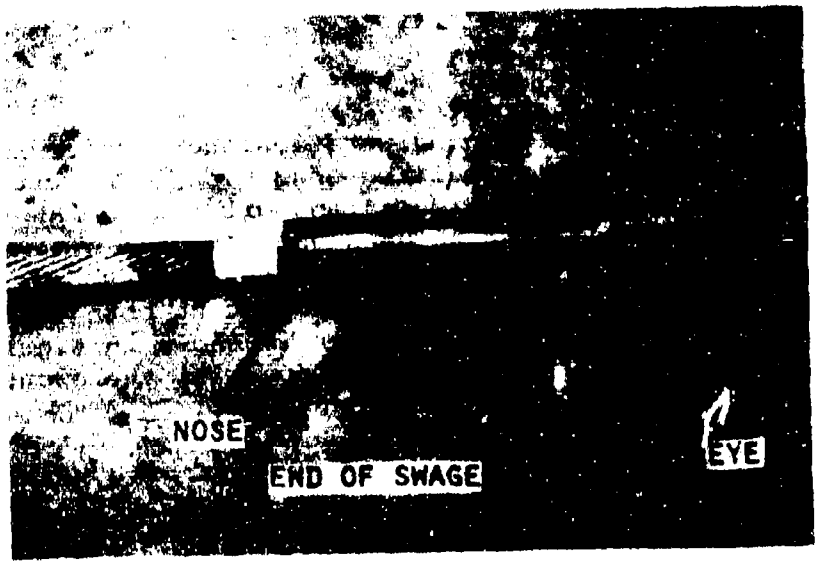


Figure 97. Typical AISI 4130 Fitting After Swaging Onto a 36x7 Cable.

Figure	B/V Drawing	Title
98	301-11149	Interface-Coupling Equalizer Bar
99	301-11170	Interface-Single-Point Adapter
100	301-10322	Interface-Hoist Drum
101	301-10271	Assembly, Sheave Envelope (Coupling Load Beam)

These interfaces required development of configurations of three end fitting types as follows:

1. Eye with swaged shank
2. Swaged button
3. Eye splice

Standard MS bushing components were used.

End fittings requiring swaging were designed empirically using AISI 4130 in the normalized condition. End fitting tests provided swaging configurations within the interface length limitations, each of which developed full ultimate cable strength of the 0.70-inch-diameter 36x7 cable. A sectioned swaged shank specimen representing both the equalizer bar and the single-point adapter is shown in Figure 102. The "eye" designs required to become part of the swaged shank fittings were validated in separate tests.

Each of the "eye" portions of the specimens were heat treated using MIL-H-6875F procedures - achieving a measured hardness of Rc 39 equivalent to a tensile ultimate strength of 176,000 psi to minimize the weight of the fitting.

After each eye was defined, the swaged shank and eye design portion of the fittings were combined into a single component. Following the test, the eye sections of these terminals were reconfigured (material added) to assure that the assembly of the single-point adapter included one left- and one right-lay cable. Assembly of two like cables was made impossible even if bushings were omitted from the mounting bolt. These components were then fabricated as individual test samples, differentially heat treated, and evaluated in the static and fatigue portions of the development test program. The same procedure was also applied to the development and validation of the eye-splice configuration.

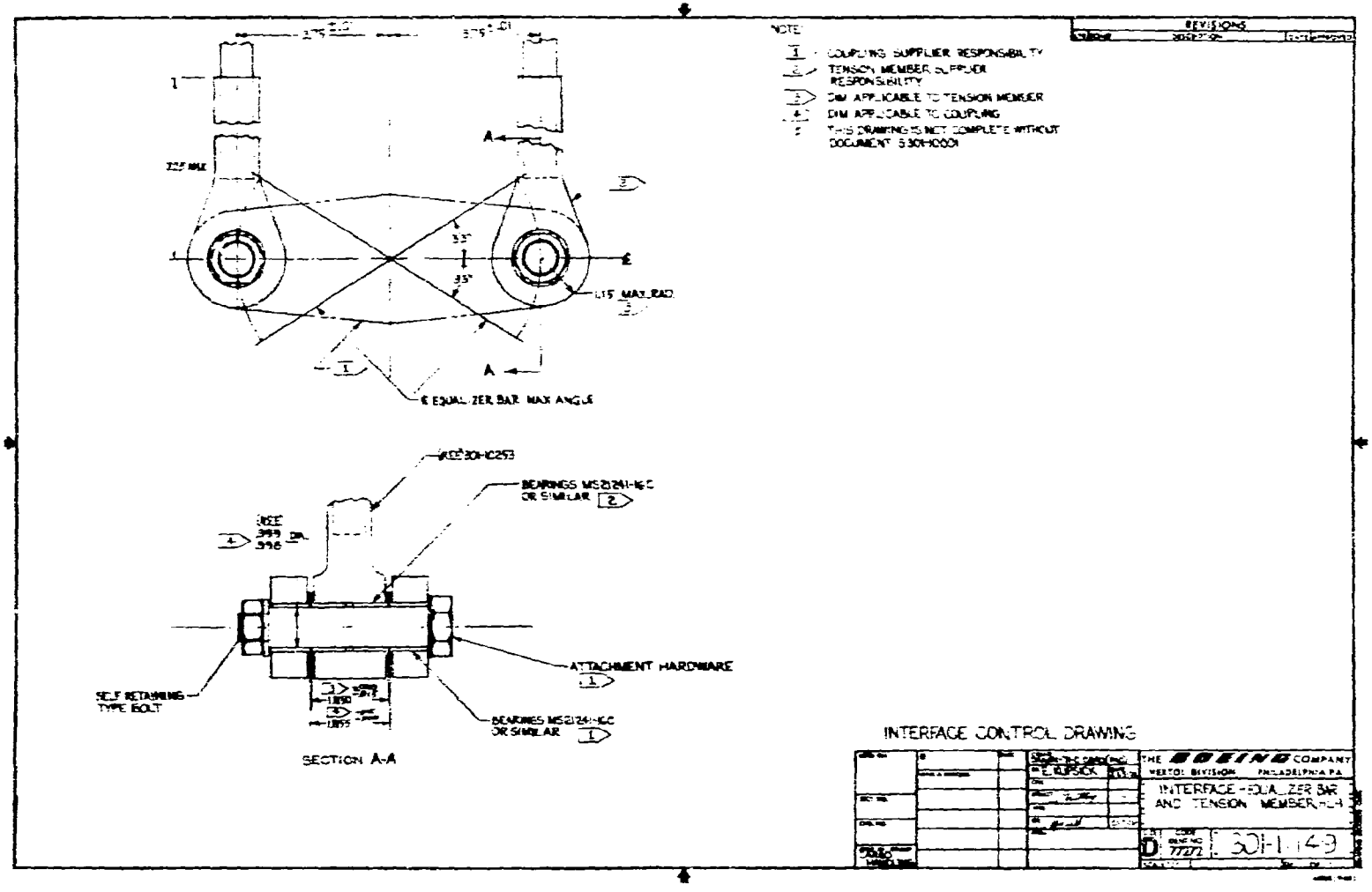


Figure 98. End Fitting Interface at Coupling Equalizer Bar.

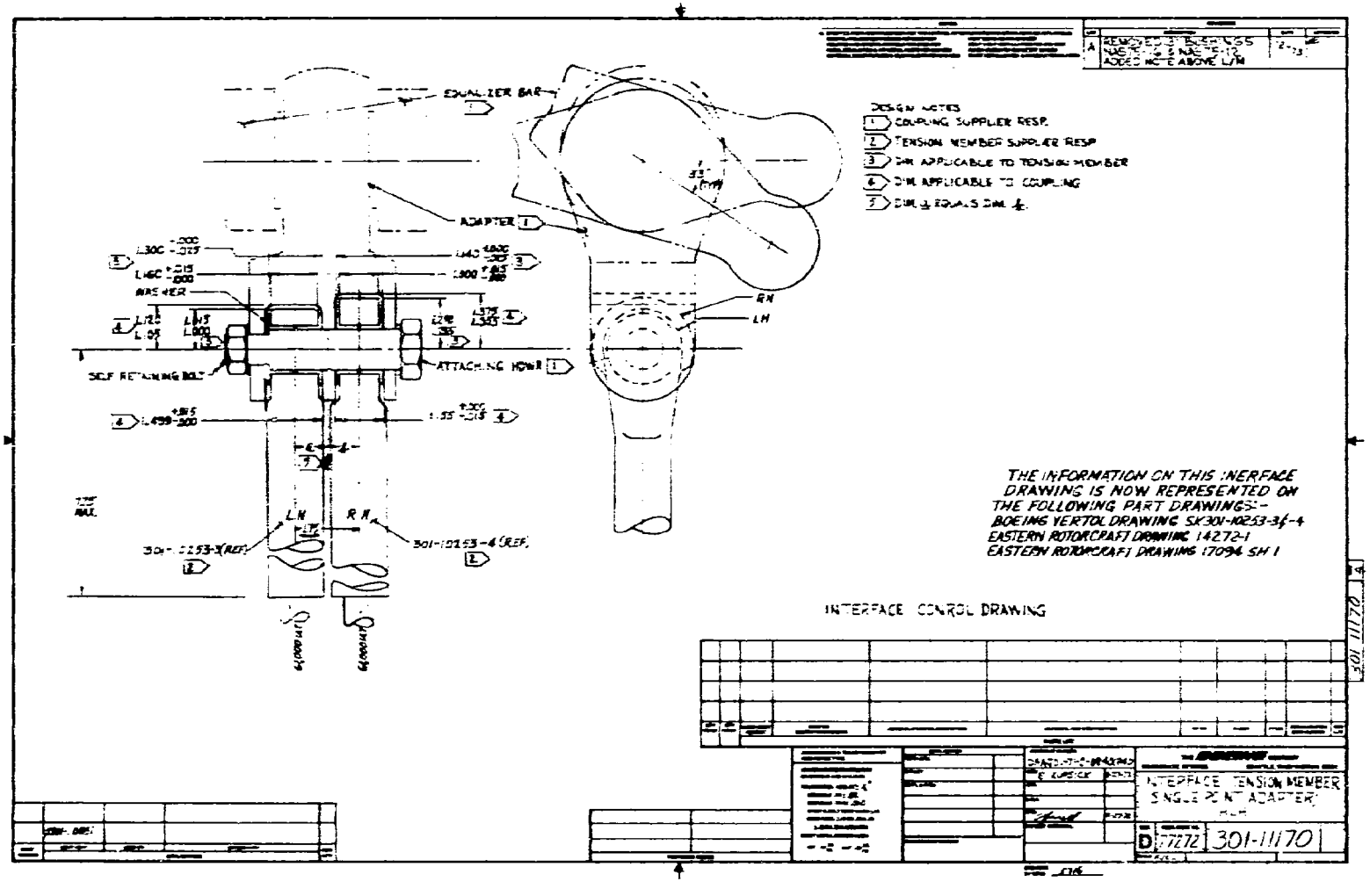


Figure 99. End Fitting Interface at Single-Point Adapter.

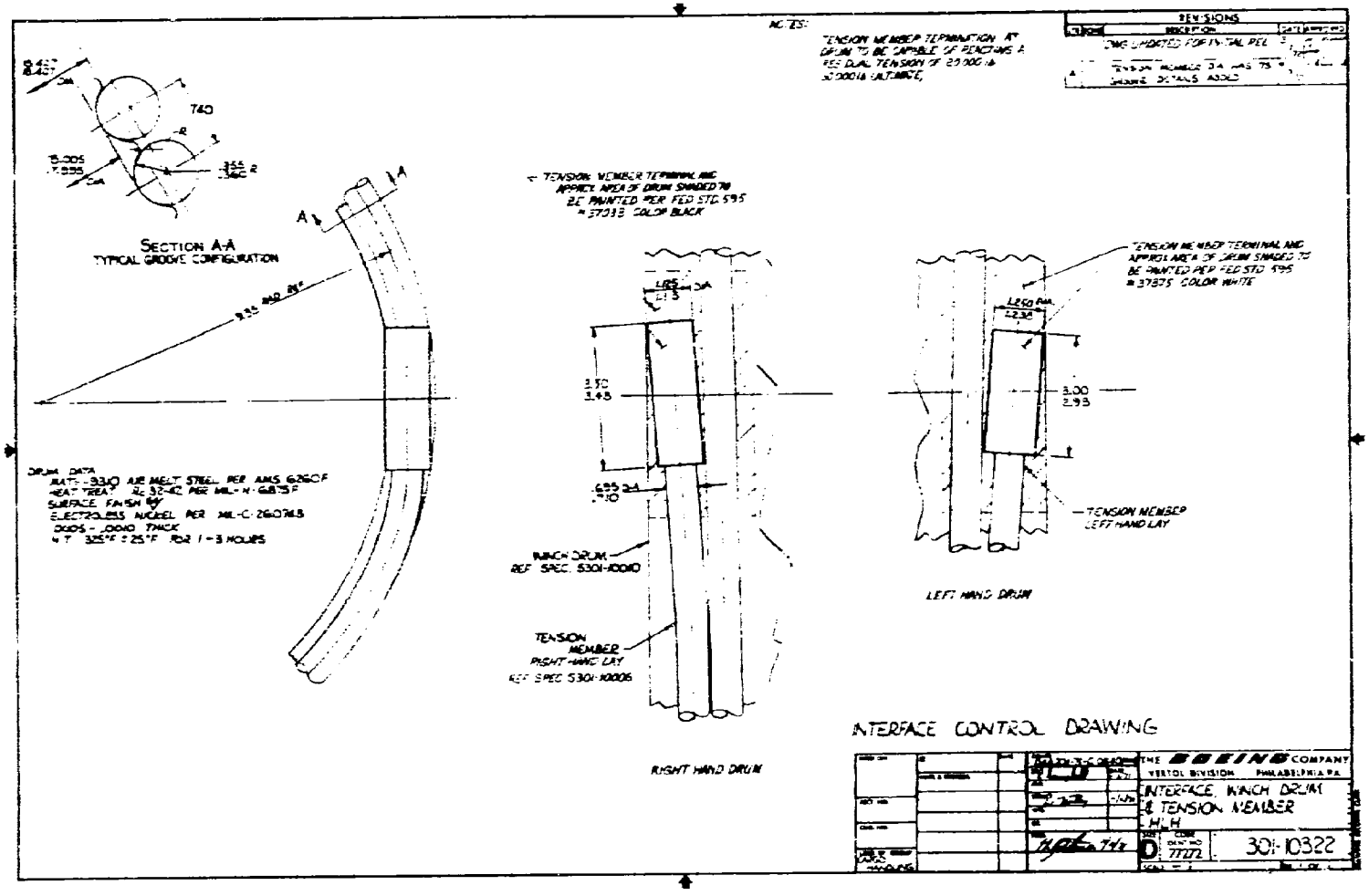


Figure 100. End Fitting Interface at Hoist Drum.

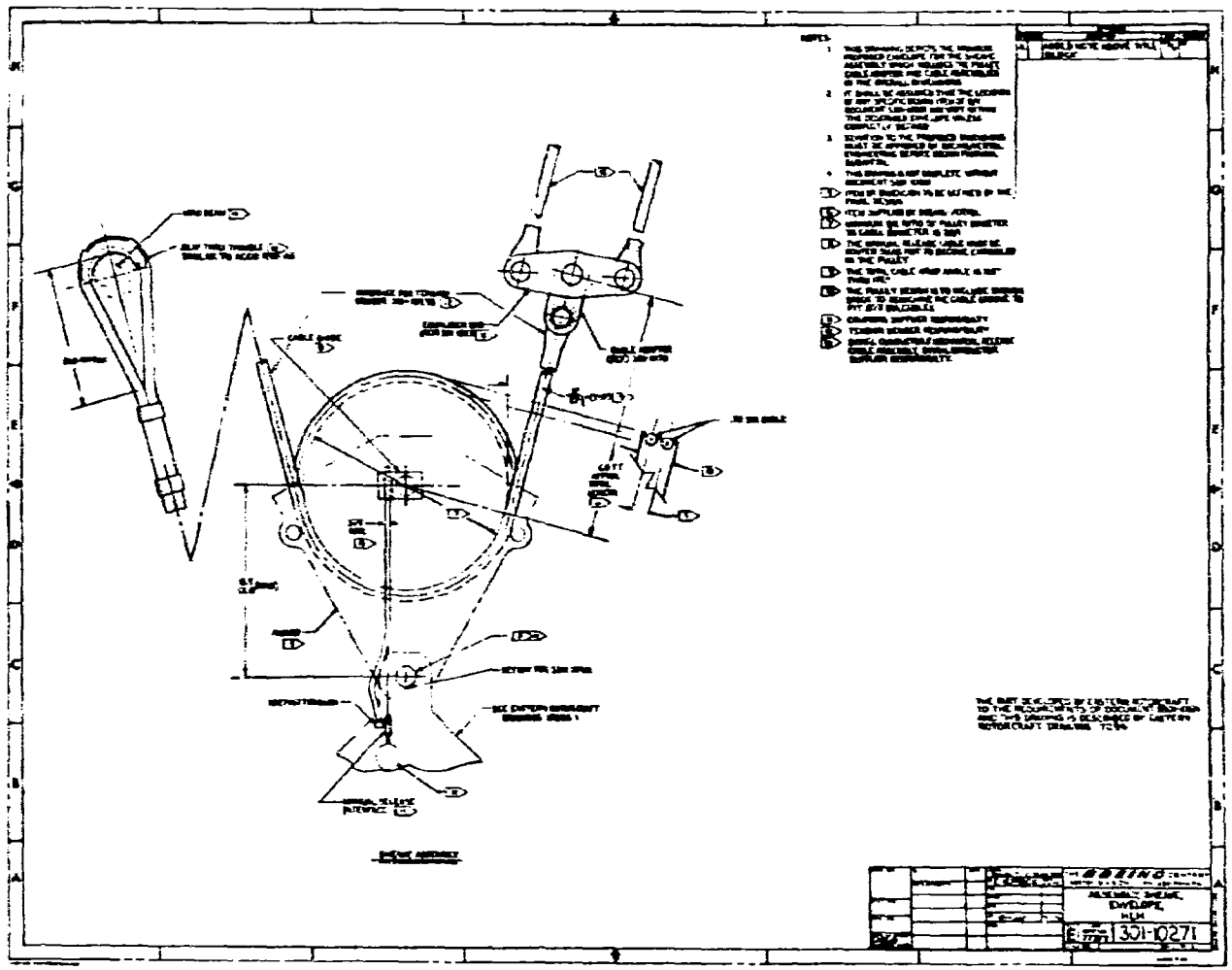


Figure 101. End Fitting Interface - Single-Point Adapter to Coupling.

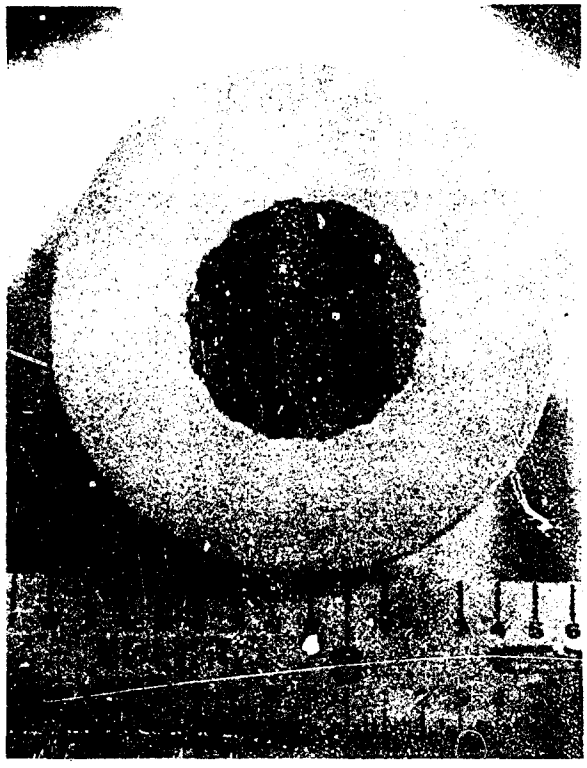


Figure 102. Cut Through Swaged Shank Specimen, 0.70-Inch-Diameter Cable.

Commercial hardware was initially evaluated for the eye-splice for the load beam attachment of the single-point adapter. Swaging of these commercial duplex sleeves resulted in severe distortion of the 36x7 cables and failure at the edge of the sleeve. Failing load levels were unacceptable. Design of a dual-hole sleeve made development of full cable strength possible for the eye-splice. A comparison of the two swaged configurations are shown in Figures 103 & 104, with a section through the final swaged joint shown in Figure 105.

The drum button tests were limited to static testing only, since these terminations are only subjected to pure tensile loading.

The development test fittings are shown in Figure 106.

Tension Member Assemblies

The tension member configurations consisting of the cable and the various end fittings that were developed are defined by the following drawings:

SK301-10253 "Tension Member Assembly for HLH ATC Cargo Figure 107 Handling System"

SK301-11561 "End Fitting, Tension Member, HLH" Figure 108.

Tension member weights are presented in Table 12.

Design Development Tests

Static, fatigue and corrosion tests were conducted on a 0.70-inch-diameter cable and three end fitting types, based on HLH/ATC requirements. The following is a summary of the results of these tests.

Cable Static Tests (Straight pull and tension-over-drum)

Results of cable static tests were satisfactory. Cable elongation and torque characteristics were stable showing only slight nonlinearity at partial load conditions. The torque balance between left and right cables was near perfect with design load and 100 ft payout. The calculated cable twist was approximately 5°. Right-lay cable strength loss due to bending over a hoist drum (D/d ratio, 26.7/1) was 2.4% of the ultimate load (left-lay cable bending loss not determined). The right-lay cable efficiency was 81.5% of the aggregate wire strength. The left-lay cable efficiency was 82.1%. Internal wire breakage (pinging) started 10,000 lb below ultimate



Figure 103. Approximate Configuration of ESCO Duplex Sleeve Before and After Swaging.

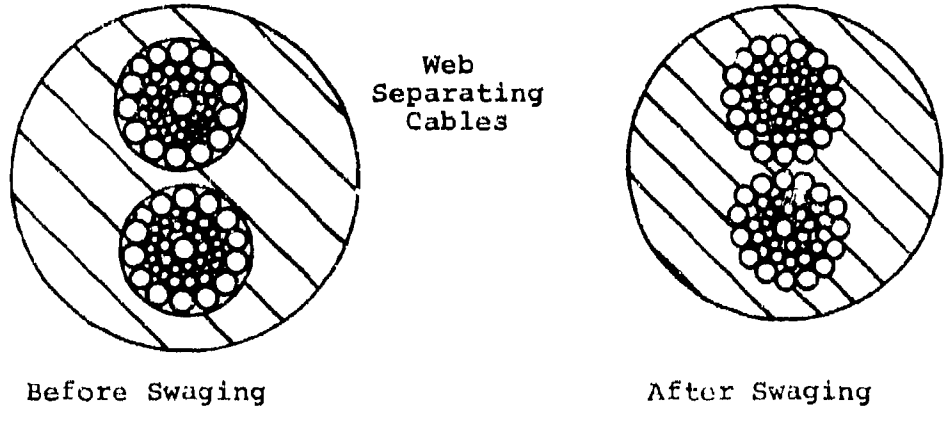


Figure 104. Approximate Configuration of Battelle-Developed Sleeve Before and After Swaging.

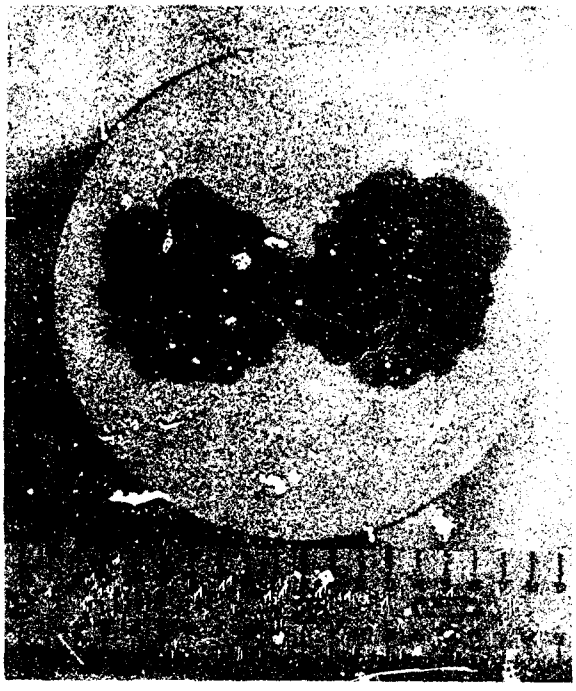


Figure 105. Cross Section Through Eye-Splice Specimen, 0.70-Inch-Diameter Cable.

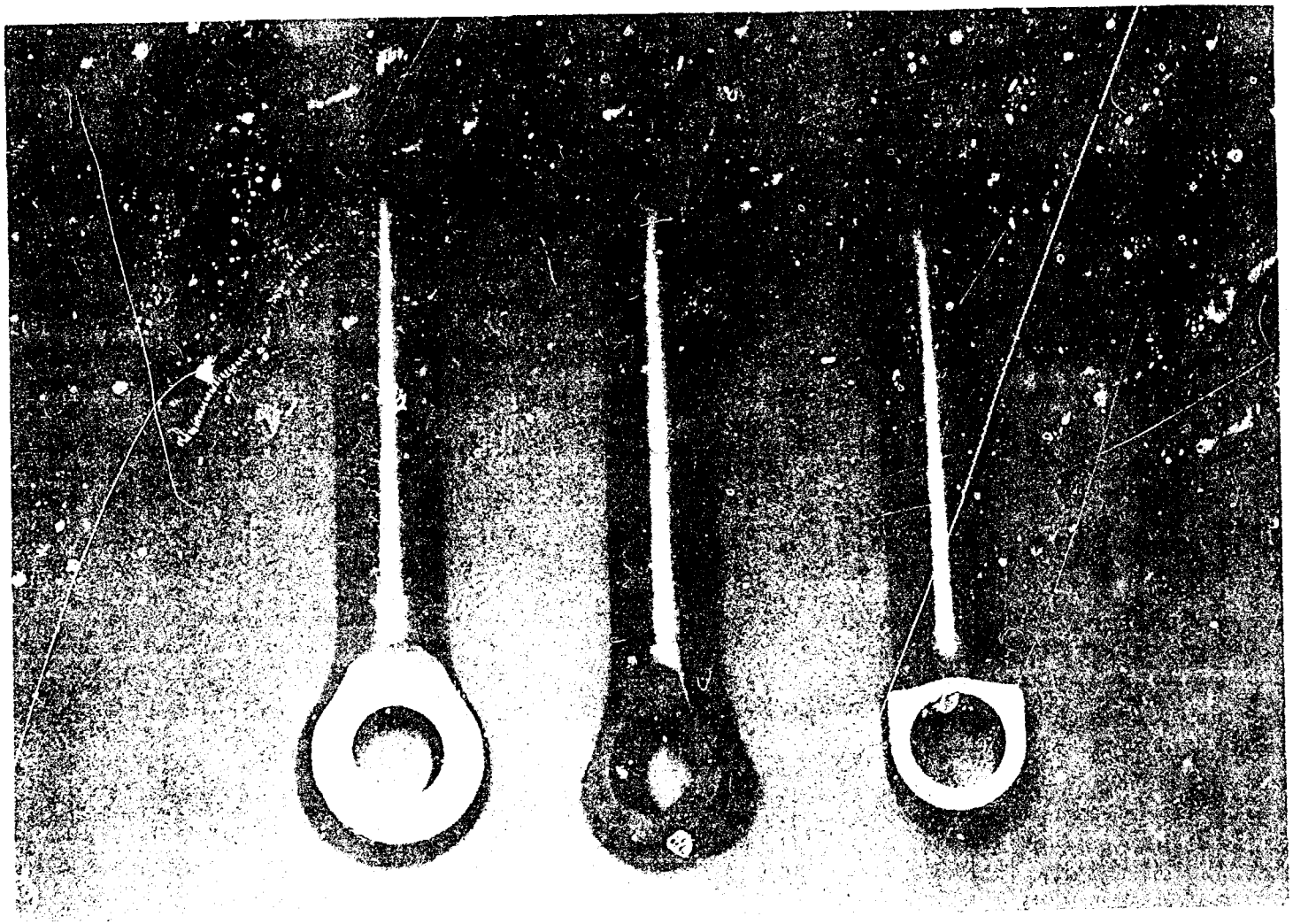


Figure 106. Design Development Test Fittings.

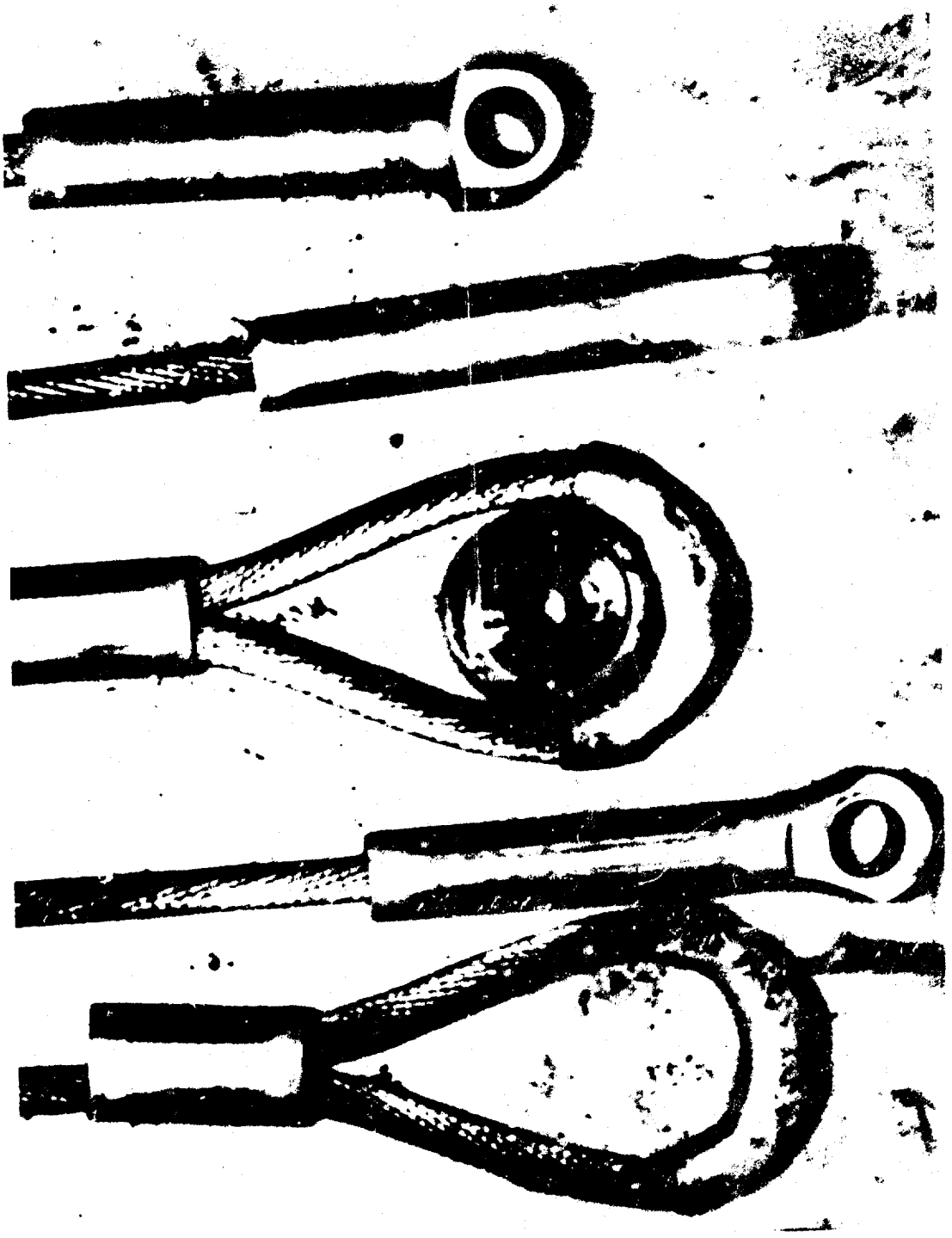


Figure 106. Continued.

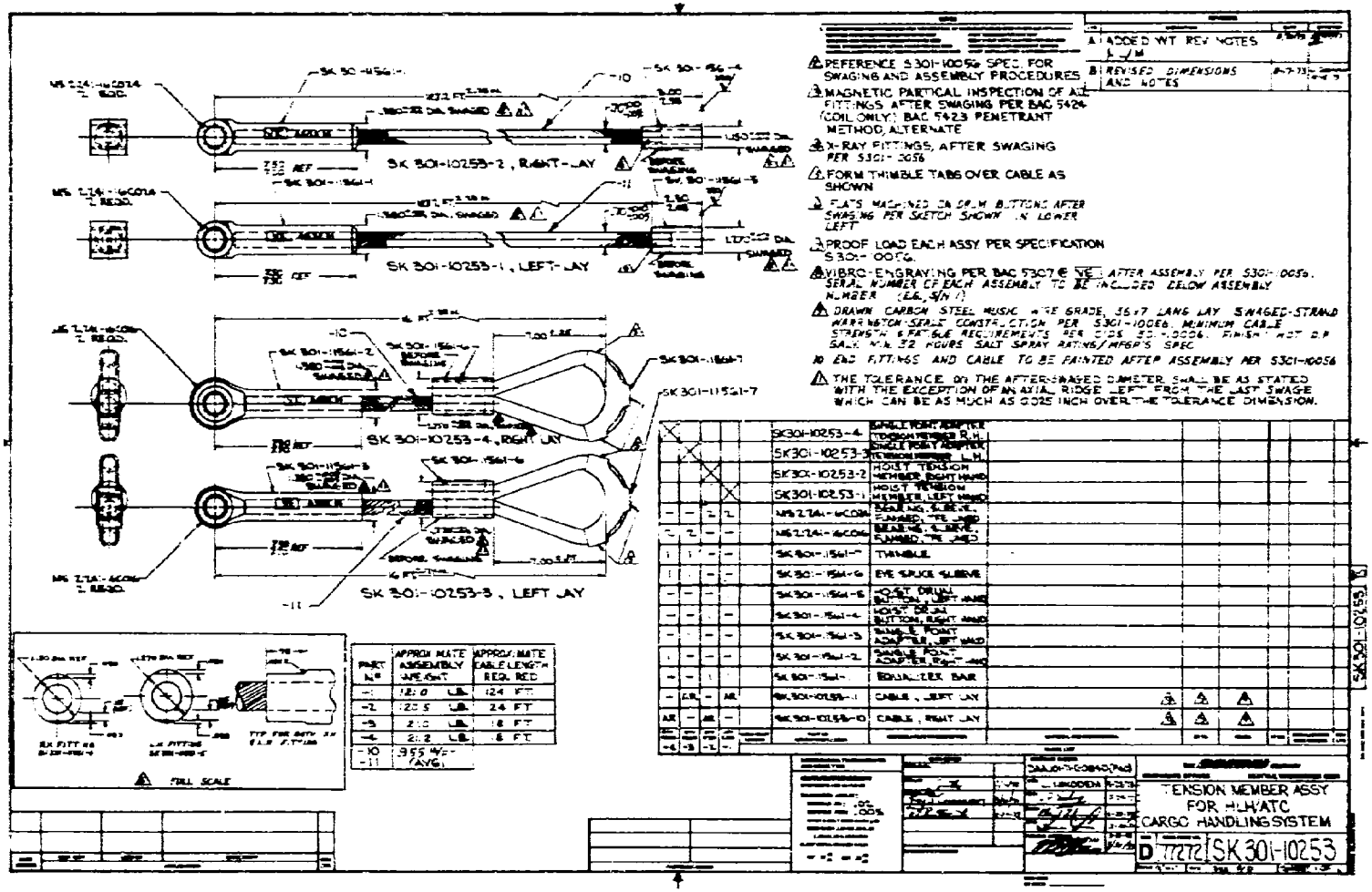


Figure 107. HLH Tension Member Assembly.

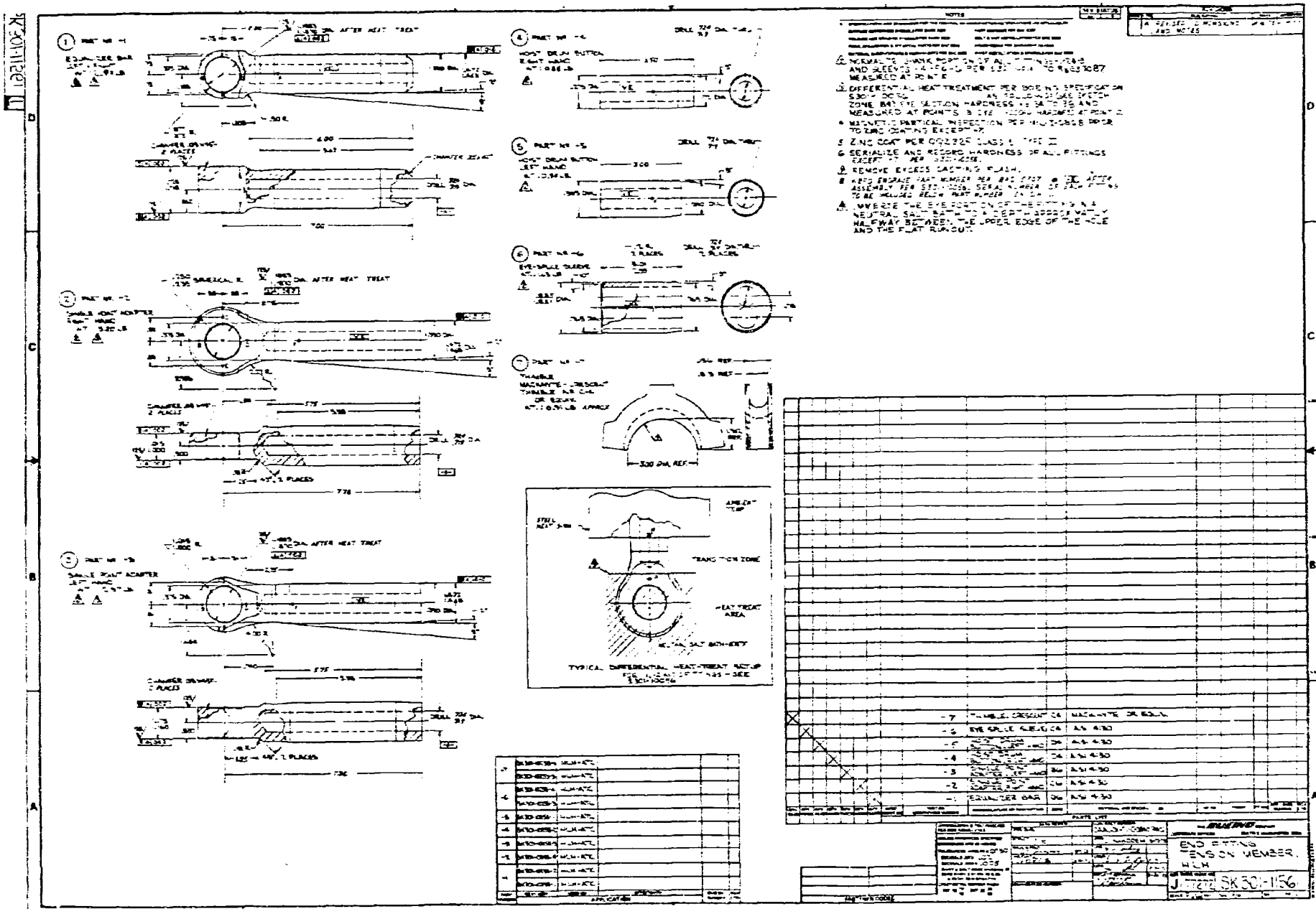


Figure 108. HLH Tension Member End Fittings.

TABLE 12. TENSION MEMBER DETAILED WEIGHT STATEMENT PER SHIP SET. (REF. SK301-11561A AND 301-10253B)

Subsystem			Pounds
Multipoint			
Cable	123.2' x .955 lb/ft x 4 Ship Sets	=	483
Fittings	2 Per Cable x 4 Cables		
Equalizer Bar*	2 Units	=	24
	SUBTOTAL, MULTIPOINT	=	507
Single-Point			
Cable	16' x 2 Ship Sets x .955	=	42.2
Fittings (Load Beam)	2		
Fittings (Adapter)	2		
Adapter*	1	=	8.0
	SUBTOTAL, SINGLE-POINT	=	50.2

*With Hardware

(but significantly above limit load of 50,000 lb) indicating that optimum load distribution between strands was not achieved.

Curves showing cable elongation and torque characteristics for both right-and left-lay are plotted in Figures 109, 110, 111, and 112.

End Fitting Static Tests

In the end fitting static tests, two failures were encountered:

1. A swaged shank slipped due to imperfect swaging, and

2. An eye-splice sleeve split because of material imperfections.

Both designs were modified to avoid these problems and retesting was accomplished satisfactorily.

Fatigue Tests - Cable/Fitting Assemblies

Fatigue, fatigue combined with corrosion and fatigue life cycle tests were conducted using a drum-to-cable diameter ratio of 26.7/1. Fatigue loading in each case included repeated bending and tension following a spectrum loading schedule. The first two tests, programmed 10,800 load cycles (one life cycle), were completed with tension member components in satisfactory condition. The extent of cable strength deterioration due to these tests was determined by tension-over-drum (TOD) static test. The maximum ultimate strength losses (referred to pure tensile strength) were higher than anticipated, and are as follows:

Post-Fatigue Static Ultimate Strength Loss

1. After 10,800 bending/tension cycles = 9.8%
2. After 10,800 bending/tension cycles and 240 hours of salt-fog exposure = 20.3%.

A 3.8% loss was the acceptable limit to meet design criteria. Excessive strength loss due to corrosion require assessment due to the very severe test condition which is estimated to be much more severe than the field usage requirements. Fatigue life tests were terminated by outer strand failures after 3.0 and also 3.6 life cycles. A third sample was subjected to 4.63 life cycles (50,000 load cycles) without failure. All three samples survived a limit load static test after 2.0 life

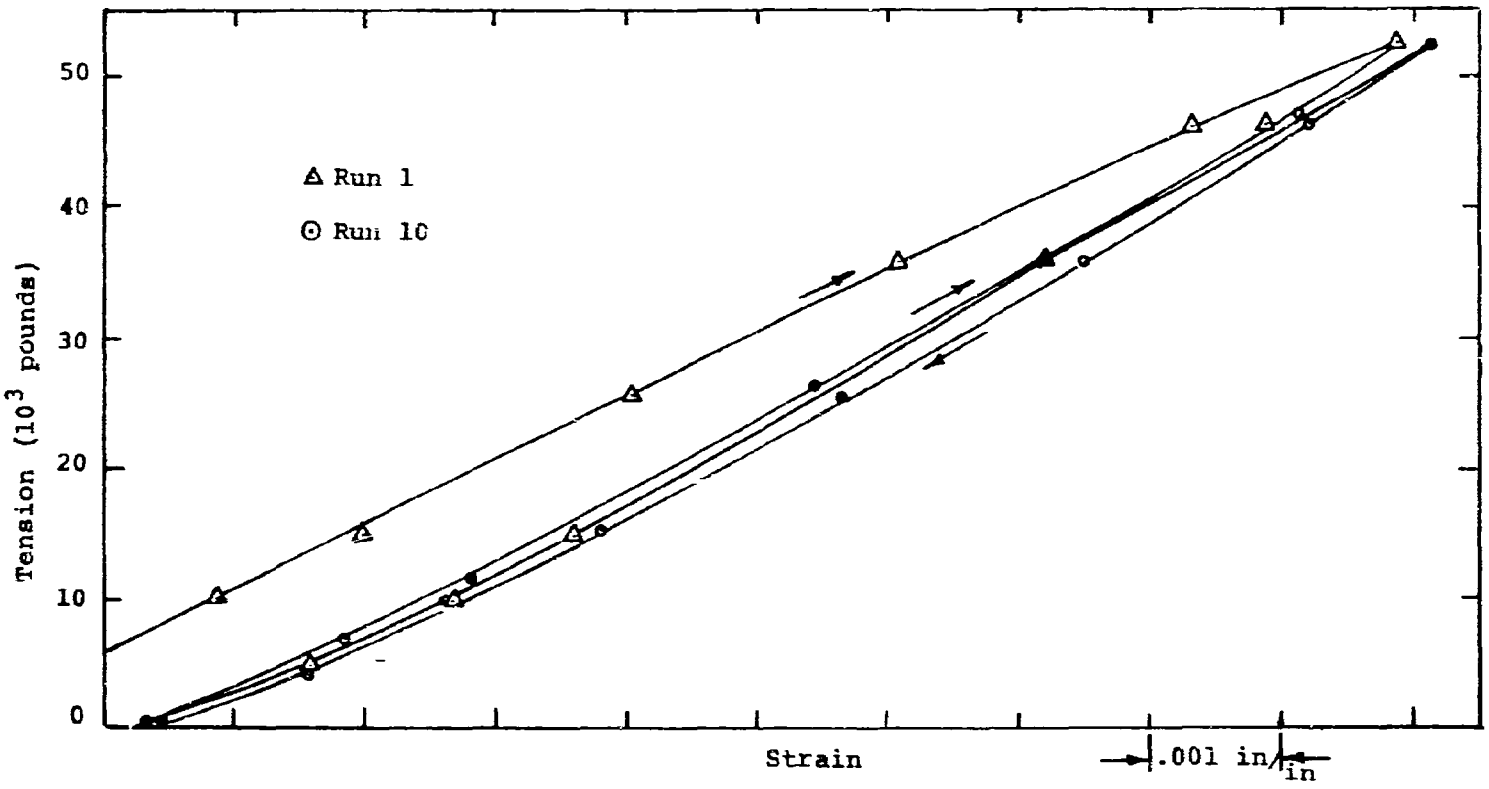


Figure 109. Tension/Elongation Characteristics of Right-Lay 36x7 Cable (Specimen D-1).

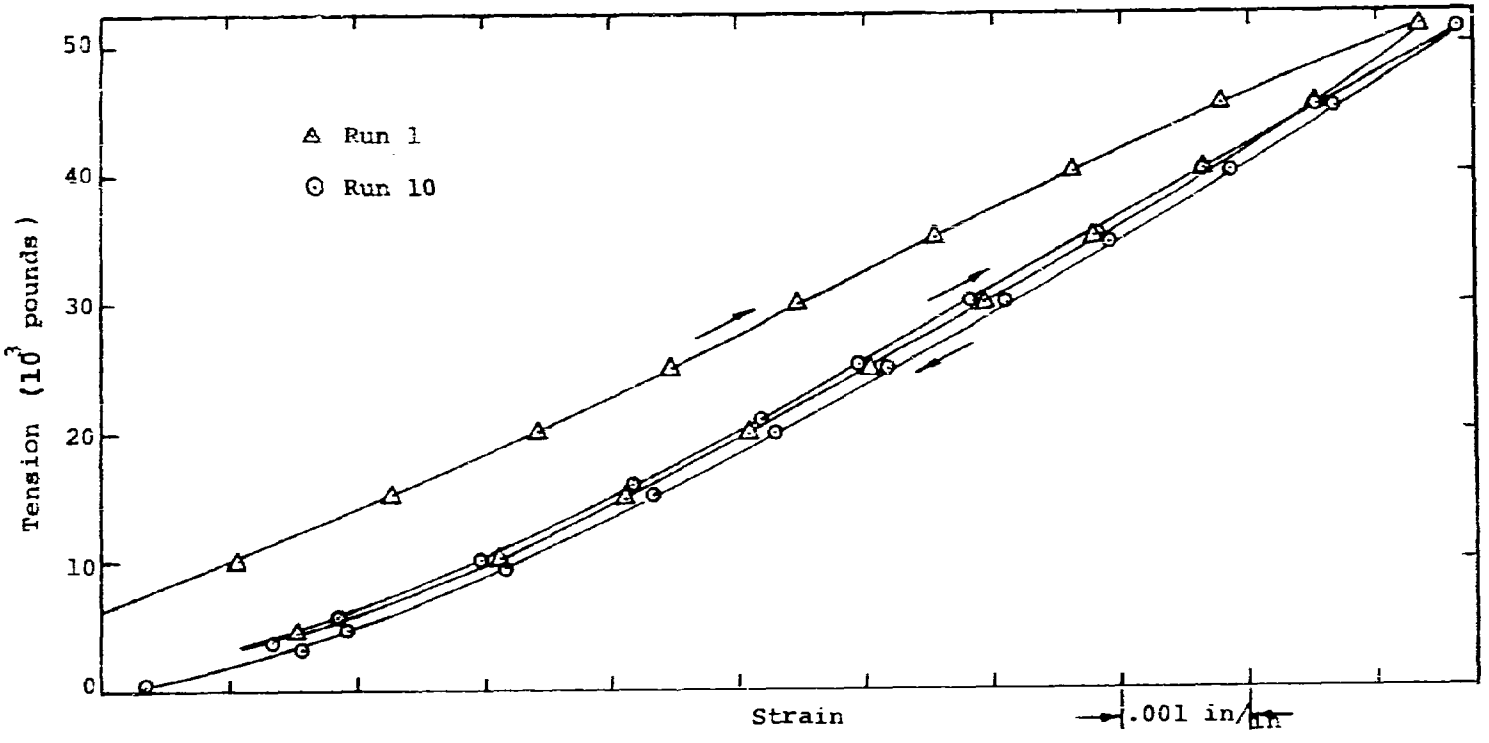


Figure 110. Tension/Elongation Characteristics of Left-Lay 36x7 Cable (Specimen D-2).

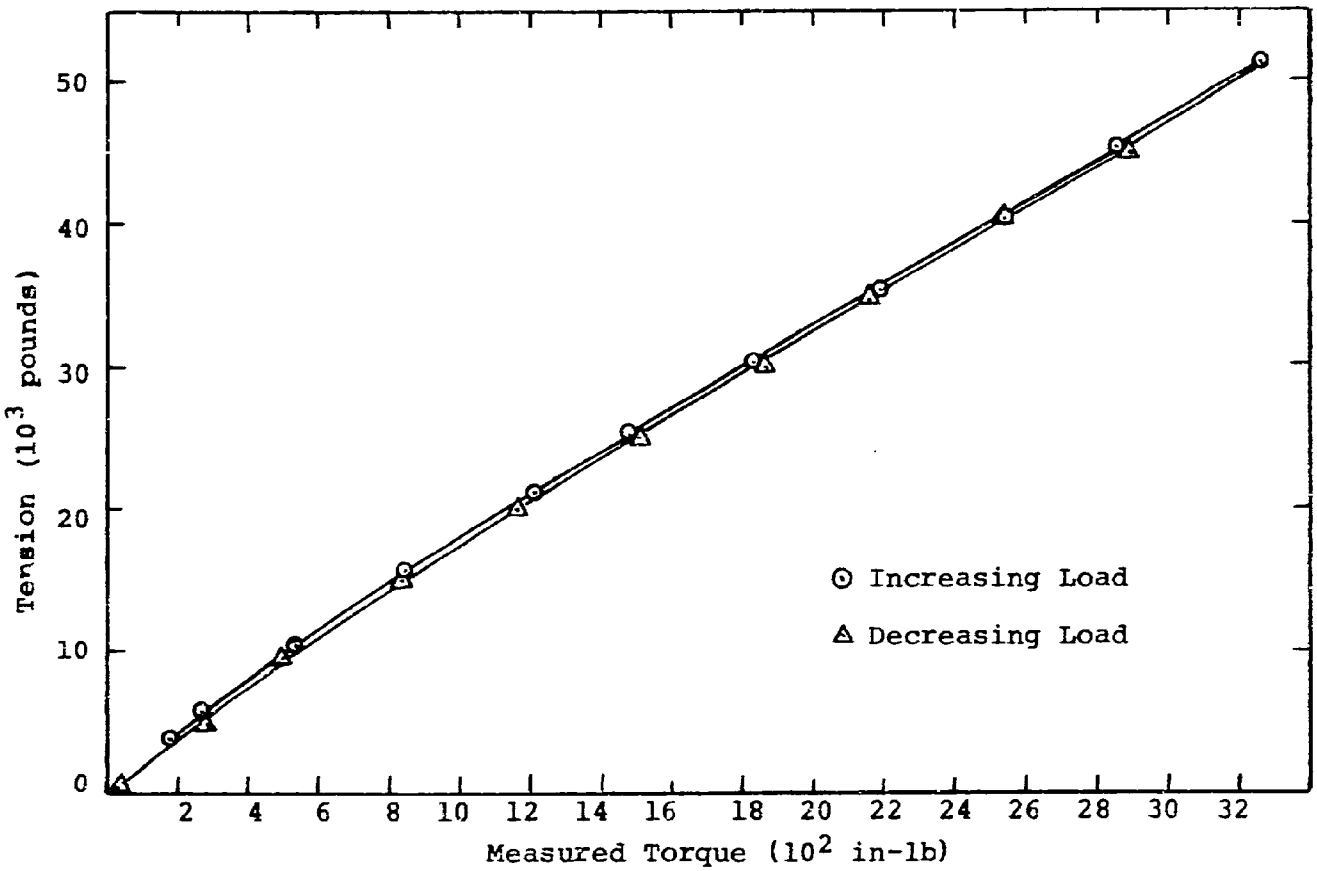


Figure 111. Tension/Torque Characteristics of Left-Lay 36x7 Cable (Specimen D-2, Run 10).

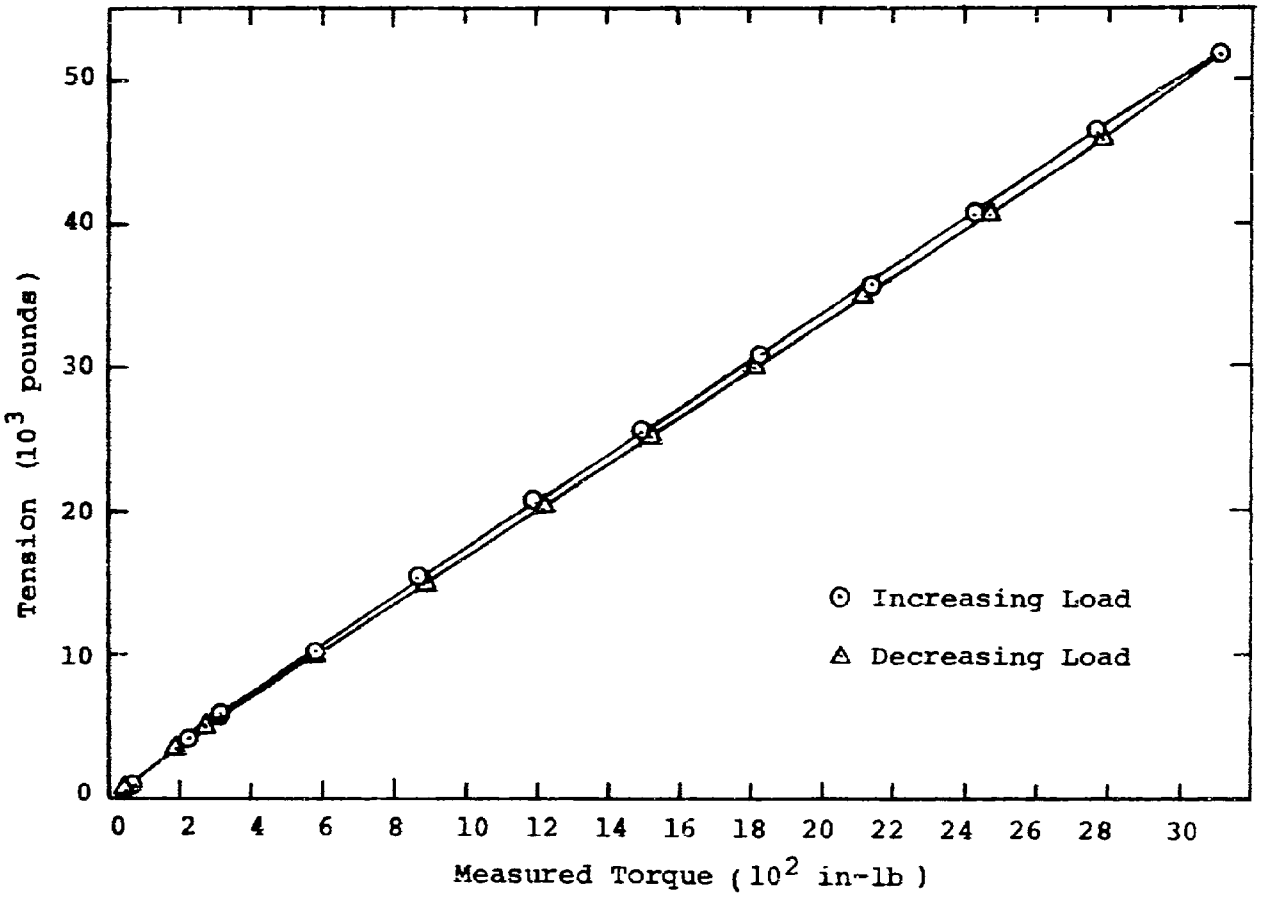


Figure 112. Tension/Torque Characteristics of Right-Lay 36x7 Cable (Specimen D-3, Run 10).

cycles. A fourth sample failed the limit load test after 2.0 life cycles. The results of tension-over-drum validation test after fatigue testing are tabulated in Table 13.

Supplemental 0.78-Inch-Diameter 36x7 Tests

The test results shown in Table 13 indicate that some of the criteria were not met. To understand the discrepancy of performance between the 0.70-inch-diameter cable and the 0.78-inch-diameter cable, and to provide a better base for defining design refinements, additional tests with the 0.78-inch cable were conducted. In these tests, the efficiency of the 0.78-inch-diameter cable was established at 88.5% and the TOD bending loss at 1.25% when bent over a 24.1 D/d. (A more severe bending condition than used in the 0.70-inch-diameter - 26.7/1 D/d test).

A summary of the 0.70-and 0.78-inch-diameter cable characteristics established by test are listed in Table14.

Conclusions and Recommendations from Design Development Tests

The tension member tests of the 0.70-inch-diameter 36x7 cable using high-strength (363,000 psi average) galvanized carbon steel wire and end fittings demonstrated the following:

1. The cable and end fittings (as modified after failure) met all static criteria.

2. The cable did not meet 75,000-lb bend-over-drum ultimate strength following completion of 10,800 bending and tensile fatigue cycles under spectrum loading. The UTS deviation was 5,100 lb.

3. The end fittings satisfactorily met fatigue criteria.

4. Corrosion criteria is not considered relative to field use and should be revised for future design evaluation tests.

5. Supplemental tests of the 0.78-inch-diameter cable demonstrated its superiority over the 0.70-inch-diameter in efficiency, lower bending loss and better interstrand load distribution at ultimate load.

TABLE 13. HLH ATC TENSION MEMBER DEVELOPMENT TEST RESULTS 0.70-INCH 36 x 7 CABLE.

Specimen Test Plan Code	Test Description	Test Criteria (lb)	Minimum Test Value (lb)	Evaluation
A(RL)	Tension Ultimate	75,000	78,000	Satisfactory
A(LL)			75,100	Satisfactory
D	Limit Load	50,000	>50,000	Satisfactory
A(RL)	Tension-Over-Drum	75,000	76,100	Satisfactory
E(RL)	Fatigue:Bend-Over-	Limit:50,000	50,000	Satisfactory
E(LL)	Drum/Tension, Spectrum Loading	Ult.: 75,000	69,900	Unsatisfactory
G(RL)	Corrosion/Fatigue: Bend-Over-Drum/ Tension, Spectrum Loading	Limit:50,000 Ult.: 75,000	46,500 62,100	Unsatisfactory Unsatisfactory

NOTES: 1) All specimens were proof-loaded to 50,000 lb. before test.
2) Drum D/d = 26.7/1.
3) BOD/T: Tension varied, 0 to spectrum load each bend cycle.
4) **BOD/T/C:** 240 Hours of salt-fog exposure applied after 3600 BOD/T fatigue cycles. Test resumed to complete 10,800 BOD/T cycles after corrosion.
5) RL: Right-Lay Cable
LL: Left-Lay Cable

TABLE 14. PHYSICAL CHARACTERISTICS OF 36 x 7 CABLE.

Cable Physical Characteristics	Values		
	Design Support Cable	Development Cable	Development Cable
Cable Diameter, Inches	0.789	0.695	0.695
Lay Direction	Left	Right	Left
Weight, lb/ft	1.219	0.948	0.960
Breaking Strength, lb. (Straight Tension)	93,490	78,000	75,100
Breaking Strength, lb. (TOD) (a)	92,300	76,100	--
Strength-to-weight ratio, lb./lb/ft	76,800	82,276	81,218
Wire Aggregate Strength, lb. (Calc.)	105,700	95,700	91,500
Cable efficiency, percent	88.5	81.5	82.1
Cross sectional area, $in.^2$ (Calc.)	0.330	0.264	0.264
Elastic modulus, $lb/in.^2$	19.7×10^6	20.9×10^6	20.9×10^6
Average wire strength, $lb/in.^2$	320,100	363,000	346,800
Torque at 20,000 lb. tension, lb/in	1.584	1.160	1.120
(a) D/d Ratio	24.1/1	26.7/1	

Based on the results and analysis of the development tests, it has been determined that a 0.72-inch-diameter cable using millrun electrogalvanized music wire will meet HLH/ATC static and fatigue criteria when run on the ATC hoist (D/d ratio of 26/1).

Revised Cable Design

Based on the 0.78-inch-diameter 36x7 construction, and based on minimum commercial strength (millrun) electrogalvanized music wire grade with an average wire tensile strength of 315,000 psi, a 0.72-inch-diameter cable will have an aggregate breaking strength (ABS) of 95,827 lb. This calculated ultimate strength assumes the same efficiency as demonstrated by the 0.78-inch cable. Fatigue resistance (with D/d ratio of 26/1) should be improved over that demonstrated by the 0.70-inch-diameter cable, by improved wire ductility permitting selection of strand L/d ratios based on the 0.78-inch-diameter cable design.

A description of the 0.72-inch-diameter wire sizes, the L/d's and calculated strand and cable strengths are listed in Table 15. Estimated weight for this cable is 1.04 lb/ft. The strength-to-weight ratio is estimated to be 79,000 lb compared to 76,800 for the 0.78-inch-diameter cable.

Revised End Fitting Design for 0.72-Inch Cable

Neither weight nor size increases were required in the redesign of the swaged shank end fittings for the 0.72-inch cable.

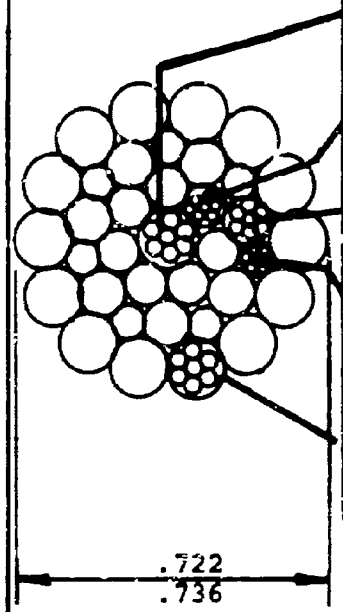
Fittings developed for the 0.72-inch-diameter were identical in geometry to the specimens used in the 0.78-inch-diameter cable tests except for the reduced wall thickness required to accommodate the larger cable (.797-.804-inch bore). The 19 swaged fittings configured for the larger cable were tested over the range of slip-to-cable rupture without failure. Sufficient test background, therefore, exists to reconfigure the SK301-11561 end fitting designs for the 0.72-inch-diameter cable without redevelopment with only the following changes:

1. Change cable hole sizes in the -1 through -6 fittings from 0.70-to 0.72-inch diameter.

2. Use the next largest commercial swaging die size on -6 (two-hole) end fitting to maintain the proper wall thickness.

3. Increase hardness of the normalized section of the shank for swaging from R_B 83-87 to R_B 85-89 to maintain +.09 margin of safety in neck down sections of -1, -2, and -3 end fittings.

Table 15. 0.72-Inch 36X7 Lang-Lay Construction Characteristics (Right and Left Lay).



Strands		Wire				Strands		
No.	Layer Location	Diameter (In.)	No. Used	Minimum Catalog Strength psi (10^{-3})	Aggregate Strength Pounds	Calculated Strength Pounds	Lay Len. In.	L/d
1	Core	.056	1	300,000	738.9		1.0	6.5
	(.154)	.054	6	303,000	4163.6	4,902.5		
7	1st Inner	.038	7	318,000	2524.5		.72	7.0
	(.103)	.036	42	321,000	13723.0	16,247.5		
7	2nd Inner	.038	7	318,000	2524.5		.72	7.0
	(.103)	.036	42	321,000	13723.0	16,247.5		
7	2nd Inner	.029	7	333,000	1539.7		.54	7.02
	(.077)	.027	42	337,000	8103.9	9,643.6		
14	Outer	.047	14	309,000	7505.4		.88	6.94
	(.127)	.045	84	309,000	41281.2	48,786.6		

Calculated Aggregate Breaking Strength, Pounds = 95,827
Total Metallic Area, sq. in. = .304

ATC Tension Member/MIL-SPEC Comparison

The achievements made in the HLH/ATC tension member development program are shown graphically in Figure 113.

The cable diameter/strength relationships of the 0.78-inch-diameter design support, 0.70-inch design development and the proposed 0.72-inch-diameter cables are compared with available commercial aircraft cable and the original design projections.

The ATC program size/strength expectations have been exceeded with proportional weight savings made directly in the cable and reflected in the hoist design. The percentage of strength improvement provided by the ATC cables over the MIL-SPEC minimums using a 3/4-inch diameter as a reference were:

0.78-inch-diameter with millrun wire = 174%
0.70-inch-diameter with high strength wire = 180%

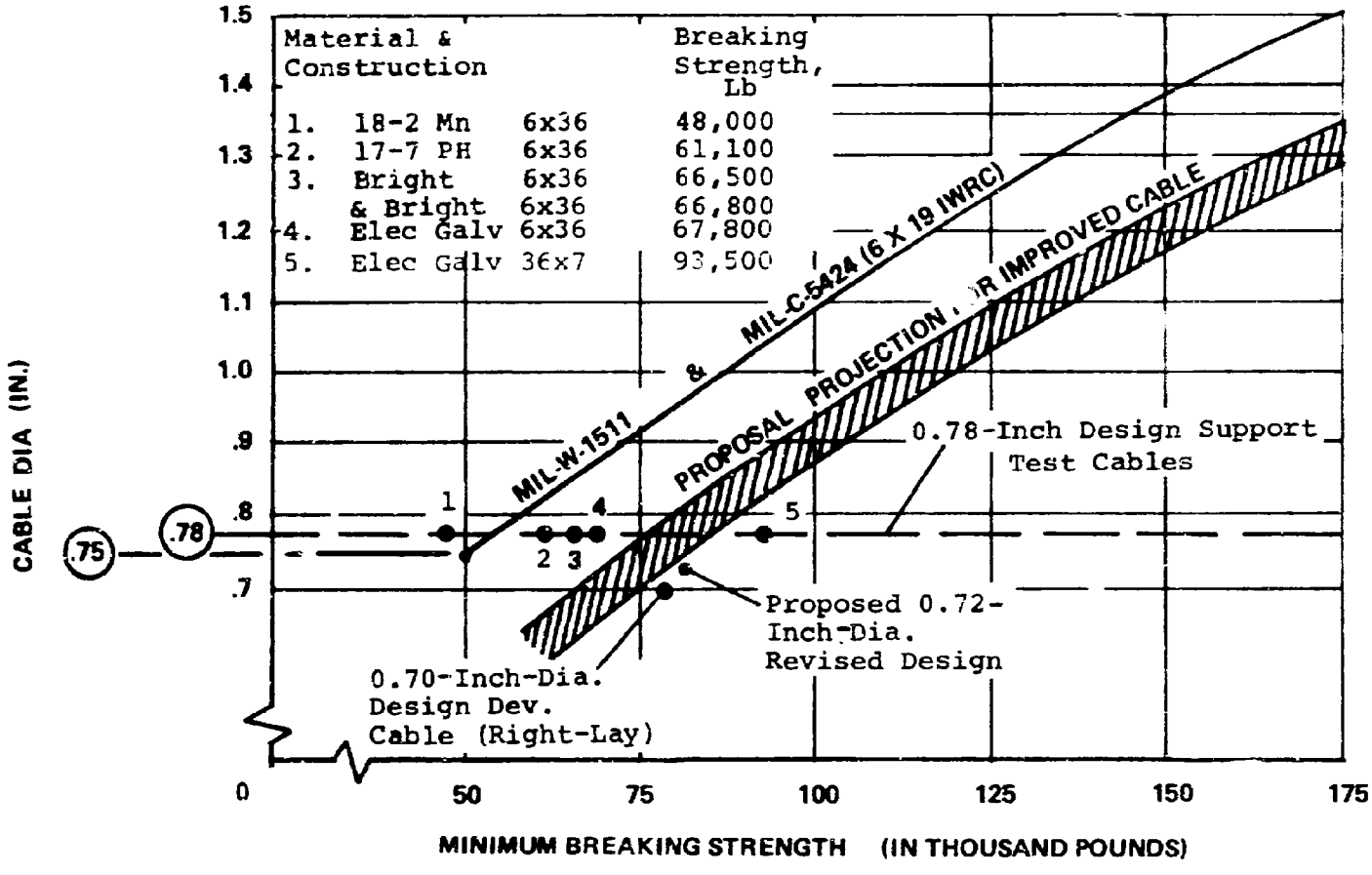


Figure 113. 0.78-and 0.70-Inch-Diameter ATC Test Cables Compared to Commercial MIL-W-1511 and MIL-C-5424 Cables.

Extension Pendant Preliminary Design

The proposal concept for the extension pendant consisted of a single large-diameter nonrotating cable of 150-foot length. It was to be suspended from the single-point adapter/coupling-swivel/sheave assembly and supported by a controllable coupling at its lower end. The control cable was an external circular conductor supported by the pendant with connectors at each end.

The lift capacity of the assembly was 22.5 tons at 2.5 g and 35 tons at 2.0 g.

The HLH ATC contract established the system capacity as 28 tons at 2.5 g, requiring the pendant to have an ultimate load capability of 210,000 lb. The extension pendant will be an item of Ground Support Equipment whose operational requirements include:

1. Minimum weight for ease of handling.
2. Maximum flexibility for ease of handling.
3. Ruggedness to take abusive use.
4. Small package size to facilitate transport.
5. Zero or low torque to minimize load twisting and cable unlaying.

The pendant load requirement is pure tensile since it will not be used on a drum or sheave and, therefore, not be subject to bending fatigue or associated compressive stresses. However, bending will occur when coiling for transport, and damage may occur when impacting the ground on release.

Several concepts for pendant assemblies were studied using 1, 2, 3, or 4 cables with sheave or equalizer bar terminations at the lower coupling. Table 16 summarizes the pendant concepts considered with the selection factors considered. Table 17 provides a weight comparison for the cable portion of the various pendants.

While all multi-cable configurations eliminate "free end" cable losses, the lowest cable weight would be obtained from the triple-cable arrangement identified as the tri-line/adapter concept . The cables are identical to the .70-inch-diameter ATC tension member components. Torque balance is maintained by using one LH and one RH lay cables with the third cable assembled from two half-length cables, one LH and one RH. Therefore, the resultant assembly uses four cables, two

TABLE 16. EXTENSION PENDANT CONCEPT STUDY.

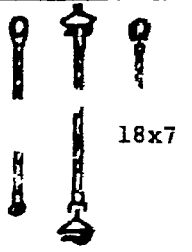
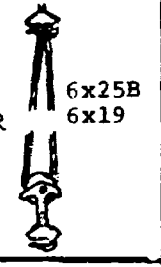
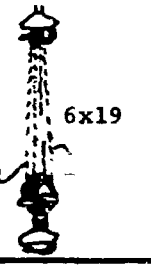
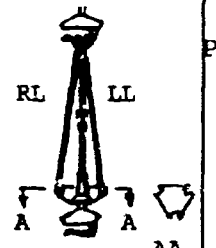
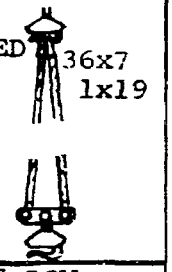
CONCEPT	SINGLE LINE	DUAL/SHEAVE	DUAL-PAIRED/ SHEAVE	TRI-LINE/ ADAPTER	EQUALIZER BAR
					
CABLE WEIGHT	HIGH	HIGH	HIGH	LOW	36x7 LOW 1x19 HIGH
CABLE STIFFNESS	HIGH	MODERATE	LOW	LOW	36x7 LOW 1x19 HIGH
HANDLING	POOR	FAIR	GOOD	GOOD	36x7 GOOD 1x19 POOR
CABLE REPLACEMENT	COMPLETE ASSY.	COMPLETE ASSY.	COMPONENT	COMPONENT	COMPONENT
STORAGE VOLUME	HIGH	MODERATE	LOW	LOW	36x7 LOW 1x 19 HIGH
PENDANT TORQUE	BALANCED	LOW	ZERO	ZERO	ZERO
LOAD PATH	SINGLE	DUAL	DUAL	TRIPLE	DUAL
CABLE	COMMERCIAL	COMMERCIAL	COMMERCIAL	HLH/ATC	36x7 LIKE ATC 1x19 COMM.
FITTINGS	COMMERCIAL	COMMERCIAL	COMMERCIAL	LIKE ATC	PAIRED-LIKE ATC
SHEAVE, ADAPTER OR EQUAL. BAR	NONE	COMMERCIAL	COMMERCIAL	SPECIAL	SPECIAL
CABLE WIRE	COMMERCIAL	COMMERCIAL	COMMERCIAL	SPECIAL	COMMERCIAL

TABLE 17. WEIGHT COMPARISON OF STEEL CABLES FOR EXTENSION PENDANT

Cable Construction	Dia. In.	UTS		Bal. Torque	Material	Cable System		Configuration
		Tons (a)	Lb. (b)			Lb/Ft	Lb/Tot	
18 x 7 - NR	1-3/4	114	228,000	Yes	Monitor	5.30	795	Single Line
(2) 6 x 25 B	1-1/8	57.9	232,000	No (d)	IPS	2.28	683	Dual - Sheave
(2) 6 x 19	1-1/4	64.6	258,000	No (d)	VHS	2.34	702	Dual - Sheave
(4) 6 x 19	7/8	32.2	268,000	Yes (c)	Monitor	1.23	728	Dual - Paired Sheave
(3) 36 x 7	0.70 (e)	37.5	225,000	Yes	HDGCS	.982	442	Tri-Line/Adapter
(2) 36 x 7	7/8	113	226,000	Yes	EGCS	1.54	460	Paired/Equalizer Bar
(2) 1 x 19	1	61	244,000	No (d)	EGHS (f)	2.10	620	Paired/Equalizer Bar

NOTES: NR - Nonrotating Cable (All others are rotating constructions).
(a) - Cable Capacity
(b) - System Capacity (213,000 lb. required)
(c) - Paired Cables: One Left, One Right Lay to Balance Torque
(d) - Torque of Two Cables Additive but Cable Does Not Unlay
(e) - Special noncommercial wire strengths
(f) - Bridge Strand - Prestressed with Min. $E = 24 \times 10^6$ but less flexible than standard cables
EGCS - Electrogalvanized Carbon Steel
HDGCS - Hot-Dipped-Galvanized Carbon Steel
EGHS - Extra Galvanized High Strength
VHS - Acco High Carbon Steel (Very High Strength)
IPS - Improved Plough Steel
Monitor - United States Steel Improved Plough Steel

at 150 feet and two at 75 feet. This design does require a complex equalizing fitting at the lower end. Each cable terminal, together with the coupling attachment, would require gimballing to ensure load sharing.

The relatively large number of parts required for this design, together with the complex equalizing fitting, resulted in this concept being rejected.

The next-lightest cable arrangement was the paired cable/equalizer bar concept. A pair of 36x7 cables of similar construction to the hoist tension members would require minimum diameters of .85 inch. To simplify and reduce construction cost, a standard cable diameter of 7/8 inch was selected. This concept requires simple equalizing bars at the lower terminal similar in concept to the design used for the hoist tension member.

As the tension member weight was close to the tri-line concept and significantly lower than any other concept, the paired cable/equalizer bar was developed into the pendant design.

Proposed Extension Pendant Design

The design developed from the preceding concept is detailed on drawing SK301-1562 Rev. A, reproduced as Figure 114. The two cables terminate in eye splice fittings at the upper end and swaged eye fittings at the lower end. The cable is of 36x7 construction using millrun wire. The design is based on the original .78-inch-diameter cables used for the tension member design support tests. Swaged cable fittings are designed by extrapolation of data available from the end fitting design development tests. The equalizing bar is designed as a steel machining to reduce the size necessary as an aluminum fitting and ensuring physical interface with a coupling.

The coupling is identical to the two HLH couplings to reduce development cost. The electrical release system would not be employed; the coupling being opened by ground personnel using the manual knob only.

The above design is developed on the basis of capability of releasing the complete pendant from the basic single-point configuration, thus requiring the single-point coupling to be retained. An alternate lower weight system would require the single-point coupling to be removed and the upper ends of the

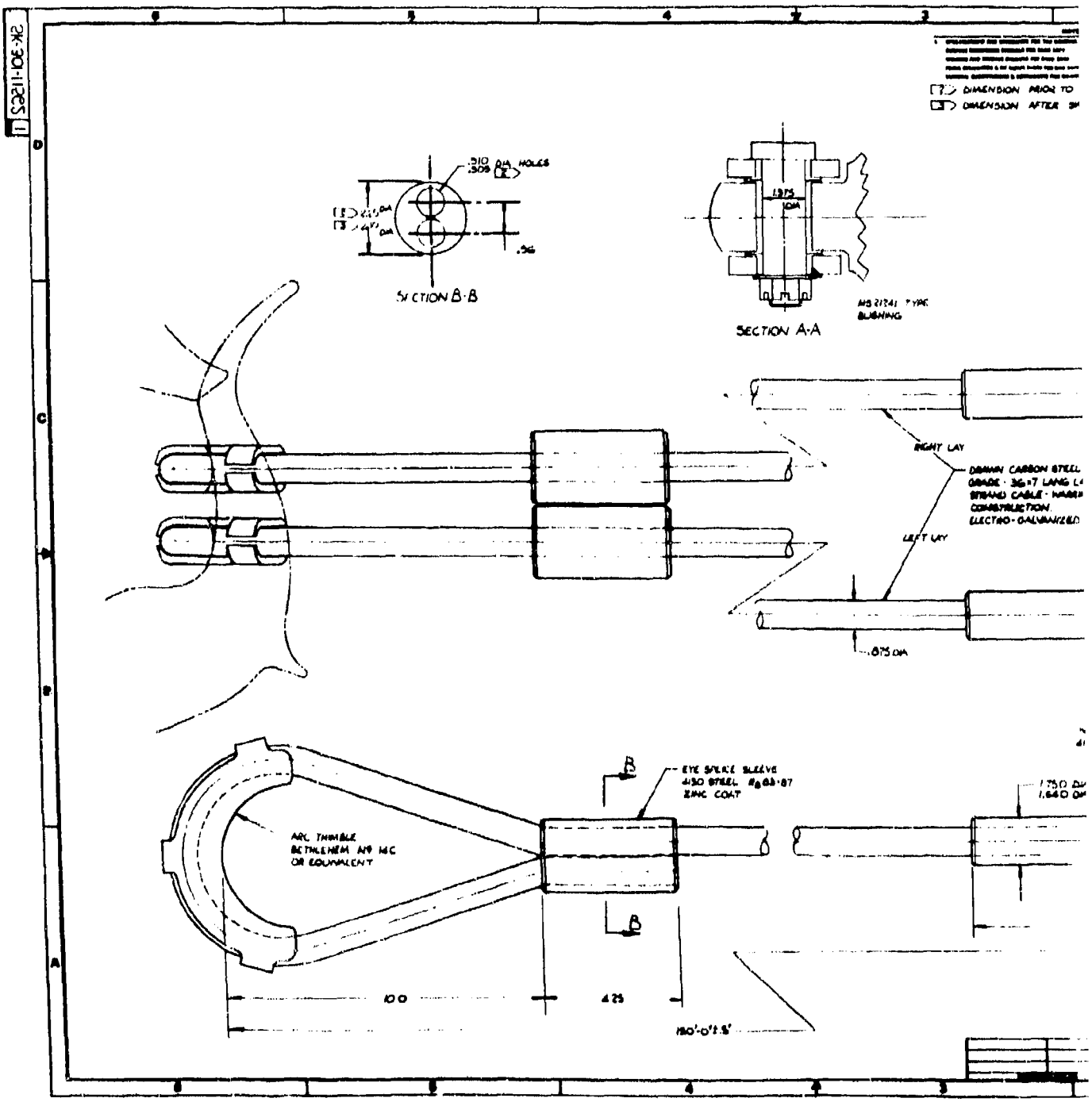
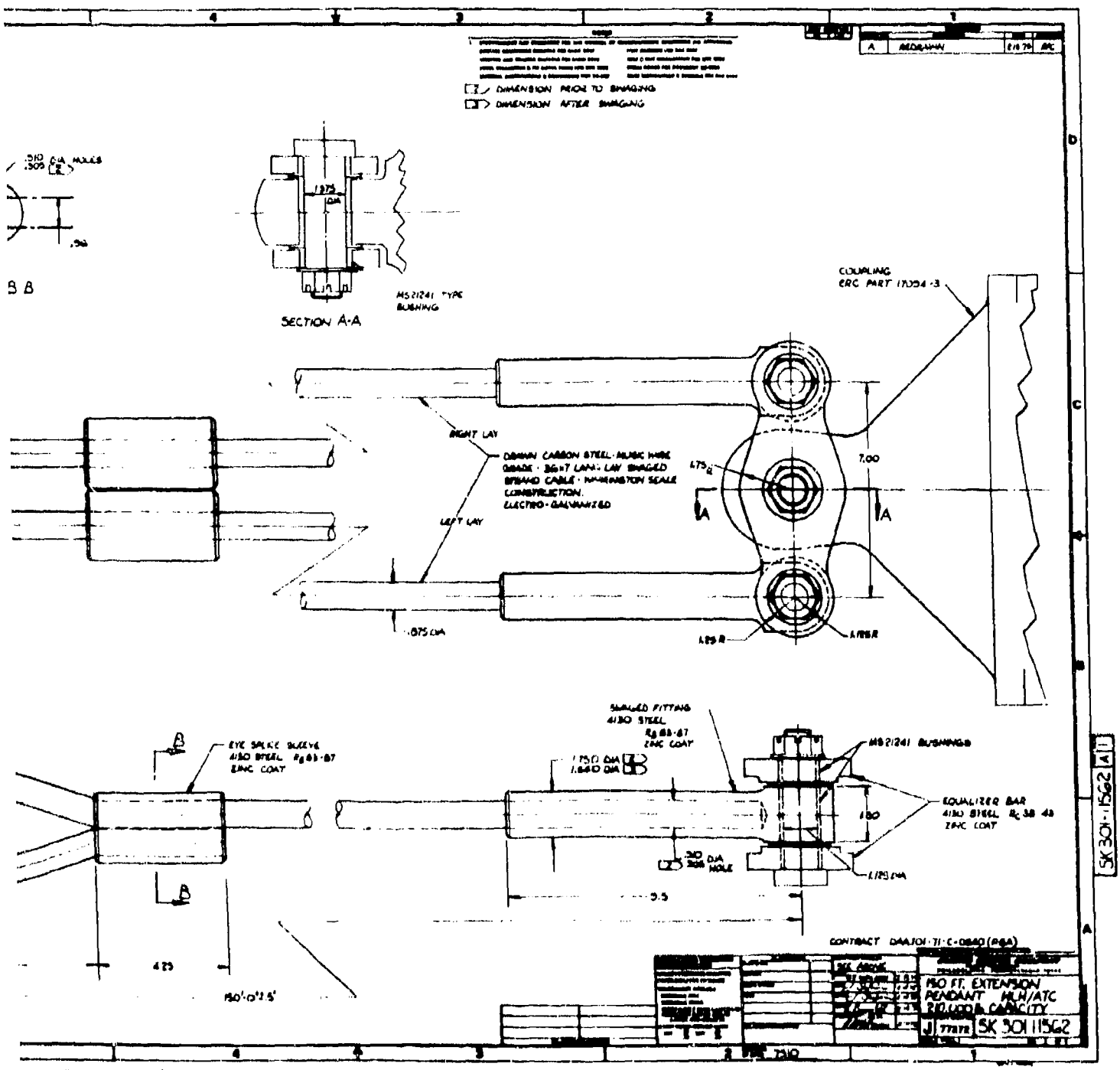


Figure 114. Extension Pendant Design.

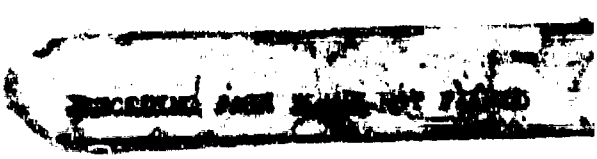


Pendant Design.

cables to terminate in a swaged clevis fitting suitable for attaching to the single-point sheave side plates. The removed coupling would then be attached to the pendant equalizing bar. This concept does delete the ability to remotely drop the pendant and increases conversion time by the need to remove the coupling and install the cable fittings.

The advantages would be to reduce the pendant weight by approximately 100 lb (coupling weight less weight of adapter fitting) and provide the opportunity to make the lower coupling releasable from the aircraft by means of an extension to the conductor cable.

The increased conversion time, and the possibility of separating the coupling from the aircraft, prevented this concept being selected as the pendant design.



CARGO COUPLING

Proposal Configuration Description

The following is the coupling assembly description that was presented in the ULH proposal document.

For the 22.5-ton system capacity requirement, each coupling was designed for 33.75 tons limit load based on the following:

1. Each coupling carries 60% of 22.5 tons, which results in 13.5 tons.

2. Multiplying this value by 2.5 g load factor we obtain 33.75 tons.

The coupling proposed incorporated a positive force latch that protects against inadvertent release and prevents release when hook load exceeds 1,000 pounds. Weight reduction of 20% was projected by the use of titanium structural parts. The feasibility of this application of titanium was based on more than 650,000 hours of Boeing operating experience on the CH-47 titanium cargo hook. Parts count in the coupling swivel were also reduced by two-thirds, and size was reduced by the use of high capacity bearings and dry lubricants. See Figure 115 for the coupling proposal drawing.

The envelope shaded area depicts an existing cargo hook of 20,000-28,000 lb capacity. The unshaded portion shows the then expected areas of improvement and envelope reduction to produce a coupling to fit the 22.5-ton requirement of the aircraft.

Design requirements included a new high strength swivel of smaller envelope and a new type of slip ring design to eliminate corrosion. Higher strength materials such as titanium were to decrease the weight as well as the envelope.

To accomplish a single-point cargo transport, a single-point adapter assembly was designed. Figure 116 shows the installation of the single-point adapter to the dual tension member system. It is composed of a sheave and cable assembly connected at one end to one coupling load beam and connected to the other tension member through an adapter after the removal of one coupling. This allows the load C.G. to shift under the aircraft and maintains equal load sharing between the hoist tension members at all times.

Subsequently, the cargo system design capacity was increased from the 22.5 tons to 28 tons. The 2.5 g load factor was retained. The design effort that follows was based on the 28-ton capacity.

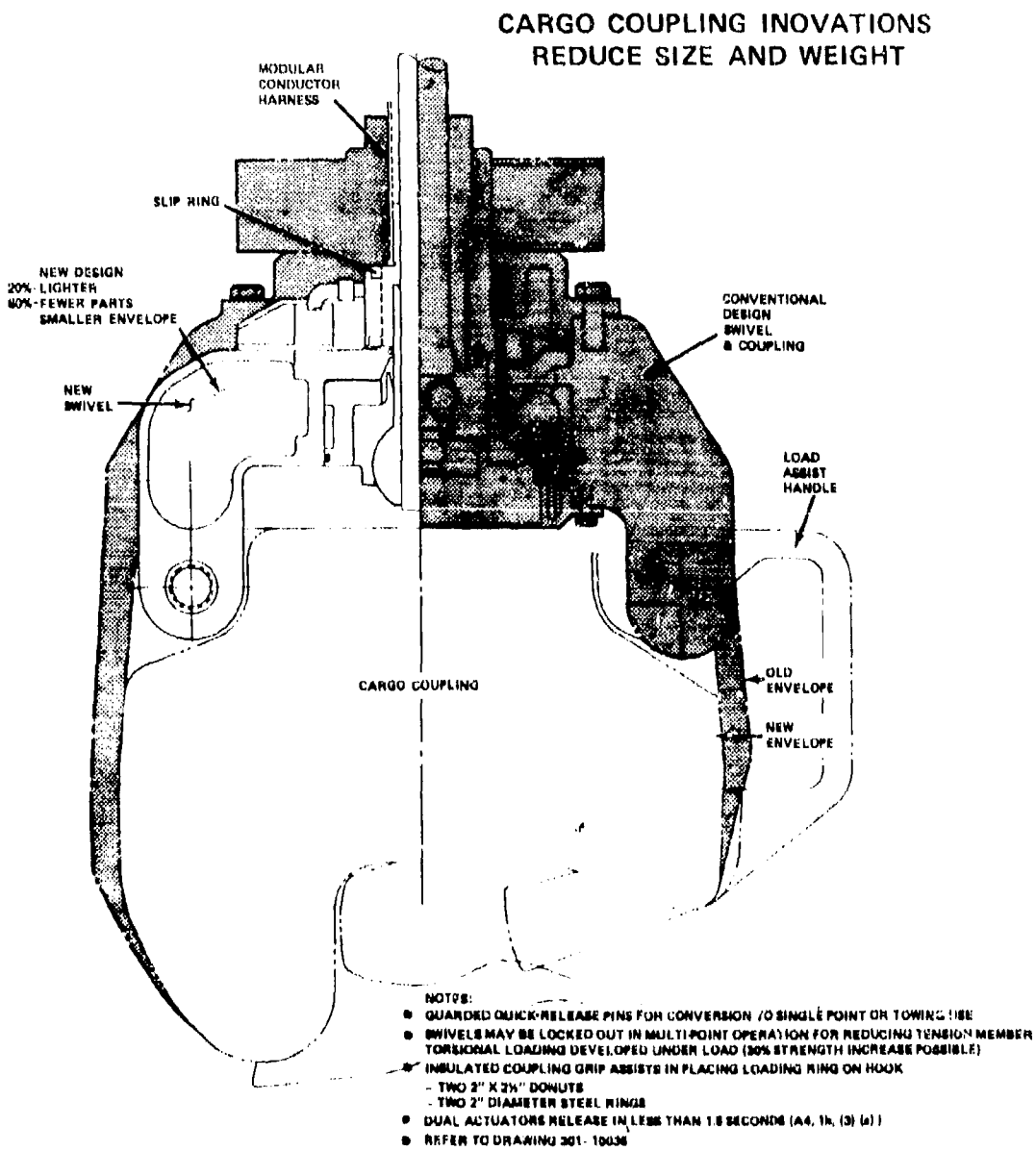


Figure 115. HLH Proposal - Cargo Coupling Assembly.

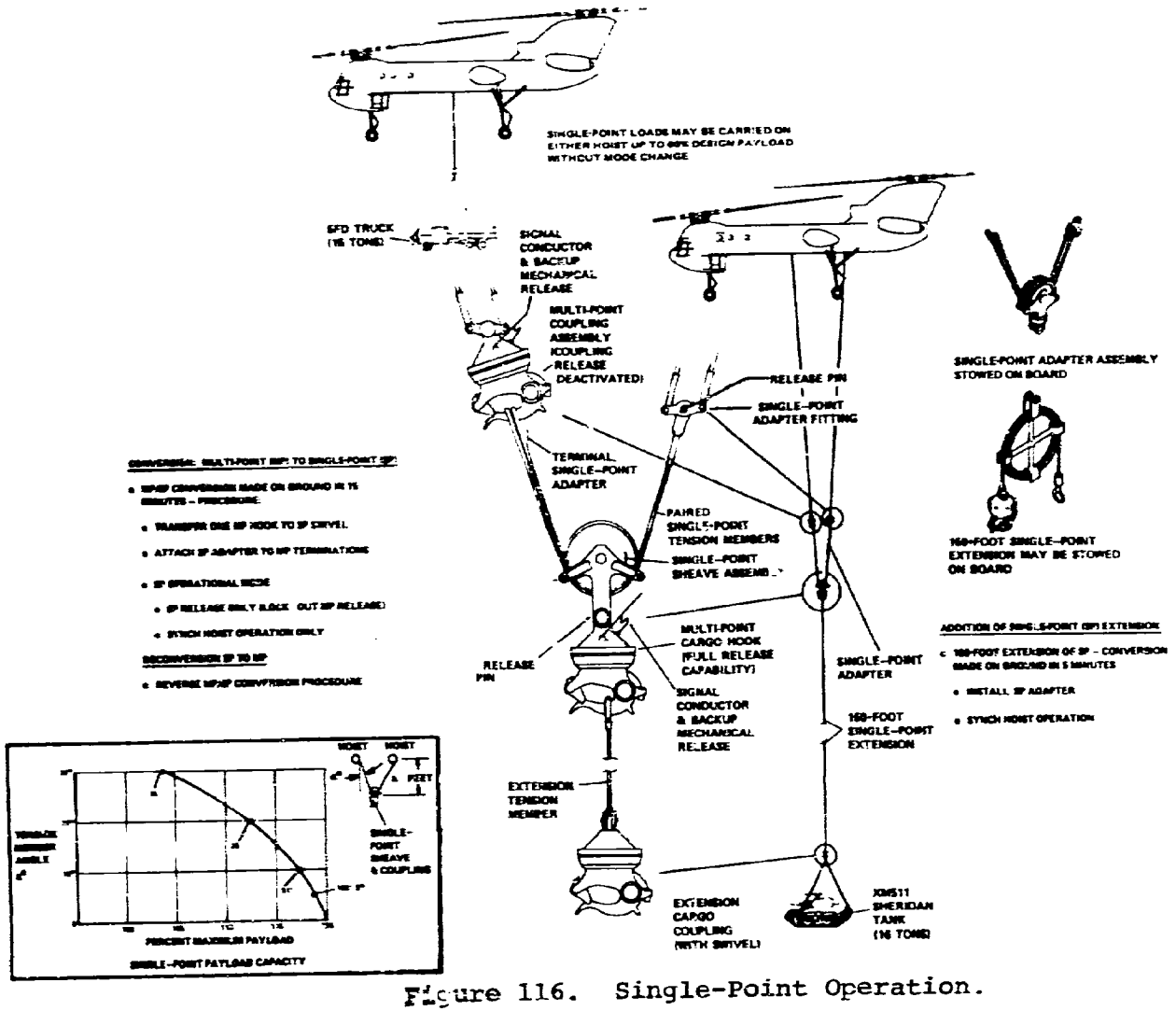


Figure 116. Single-Point Operation.

A single coupling design for both the single- and the two-point suspension modes had been decided upon in the early phase of the design. The coupling assembly was designed for an ultimate load of 210,000 lb, which accommodates the single-point suspension mode and is overdesigned for the two-point suspension mode. The rationale for this decision follows.

1. The capacity of each tension member system when operated in the two-point suspension mode is based on a 60-40 percent load split. Coupled with the additional requirements of accommodating a 30-degree coning angle plus the added load due to the downwash, each tension member system is designed to an ultimate load capacity of 150,000 pounds.

   When operating in the single-point suspension mode the system is capable of an ultimate load capacity of 210,000 pounds (56,000 x 2.5 x 1.5).

2. The expected design weight of each coupling assembly is 120 pounds for the 210K design.

3. Assuming a direct ratio of coupling weight to ultimate load the 150,000-pound unit will weigh 86 pounds.

$$\left(\frac{150K}{210K} = \frac{X}{120}\right)$$

   a. Referring to Figure 117 we require two multi-point couplings (86 pounds each) plus a single-point coupling of 120 pounds, resulting in a total weight of 292 pounds.

   b. Assuming two 210K couplings are designed per Figure 118, the total weight equals 240 pounds (2 x 120) + 10 pounds for an adapter. The net weight saving is 42 pounds (292 - 252).

   c. Engineering nonrecurring costs are less by using one type of capacity coupling.

   d. Manufacturing costs are less for one coupling design because of less machining setups and changes in operations.

   e. Logistics costs are less for one coupling for all configurations.

Two 86-pound couplings at 172 pounds total for the multi-point load plus an extra 120-pound coupling for the single-point load.

TOTAL:	172 pounds
	120 pounds
	292 pounds

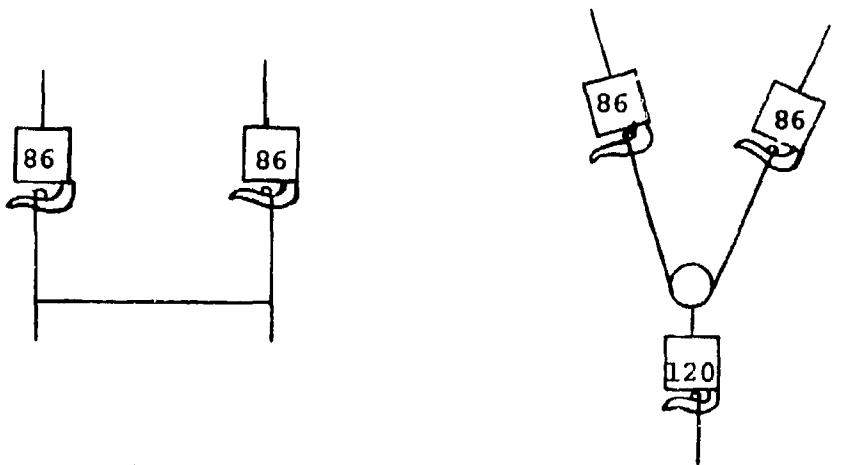


Figure 117. 150,000-Pound-Capacity Coupling Design.

Two 120-pound couplings at 240 pounds total for both multi- and single-point modes plus an adapter to replace the one coupling reinstalled in the single-point mode.

TOTAL:	240 pounds
	10 pounds
	250 pounds

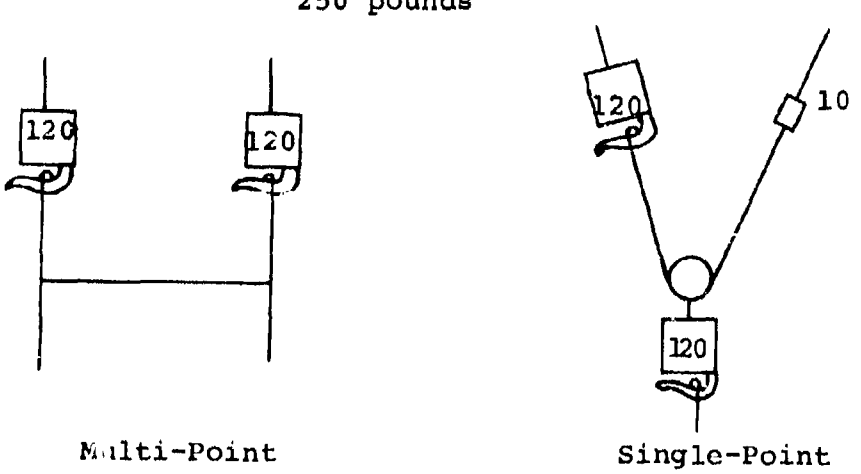


Figure 118. 210,000-Pound-Capacity Coupling Design.

Design Criteria and Objectives

The initial design of the coupling was based on the following principal criteria and objectives:

1.	Design capacity	56,000 lb
2.	Limit load capacity	140,000 lb
3.	Ultimate load capacity	210,000 lb
4.	Design life with following load spectrum:	10,800 cycles

% cycles	% design capacity
10	125
75	100
10	50
5	25

5.	Normal release system	dual electrical
6.	Backup release system	remote mechanical
7.	Ground release system	manual
8.	Release prevention	above 1,000 lb
9.	Swivel capability	full
10.	Signal systems	redundant
11.	Throat area	for two 2x2-1/2-inch section slings or two 2-1/4-inch-dia. rings

Design Studies and Analyses

A number of design studies and analyses were conducted to formulate the final coupling design. These studies included the following:

1. Open throat load beam versus other configurations
2. Load beam configurations
3. Load beam material
4. Electrical release power requirements

Open Throat Load Beam Versus Other Configurations

The preliminary open throat shape, of either an "L" or a "C" configuration, was based on the experience gained during actual in-field conditions over a period of many years and many cargo hook configurations. The open throat is based on ease of loading the hook with a sling with one motion only, that of slamming the sling ring into the open throat area. No other design allows this freedom and quickness of load acquisition in one continuous motion.

Cargo hooks used in past installations include those which require the load beam to be opened first, before acquisition of the sling. It then must be closed by hand. All designs of this type double or triple the acquisition time.

A study of the open throat design was conducted using the throat area requirement to determine the geometry of the load beam open throat. It must be large enough to accommodate two large steel shackles 2-1/4 inches in diameter or two nylon donuts with cross sections of 2 x 2.5 inches. A geometry study of the load beam opening excursion versus the position of the pivot point established the general shape of each configuration.

Load Beam Configuration Study

The primary objective was to establish a design weight differential between an "L" shape and a "C" shape load beam. A design study was conducted using both the "L" and "C" shape load beams in order to finalize an acceptable design which allowed the lightest weight and smallest envelope. This included a study of the operating kinematics to release the load beam.

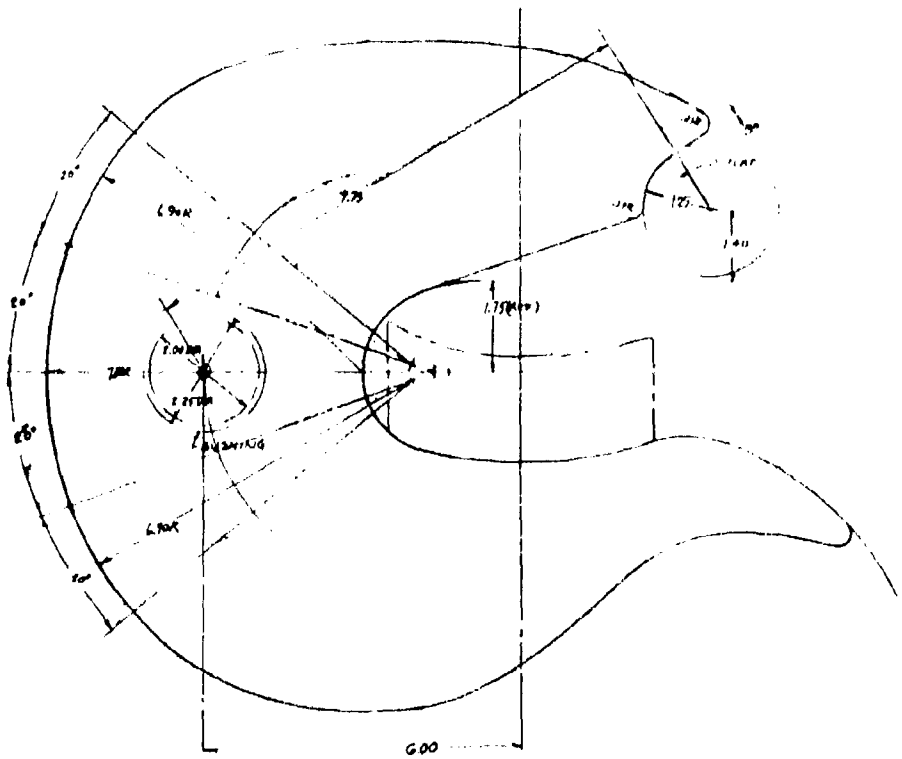
The operating mechanism of the load beam was established by a trade-off of weight versus power to actuate the release mechanism to open the load beam. While the "C" shape is heavier, it requires less operating power to release.

In order to confirm the configuration of the coupling load beam, a photoelastic stress model analysis[5] of an "L" and a "C" shape configuration was conducted in accordance with the ATC contract.

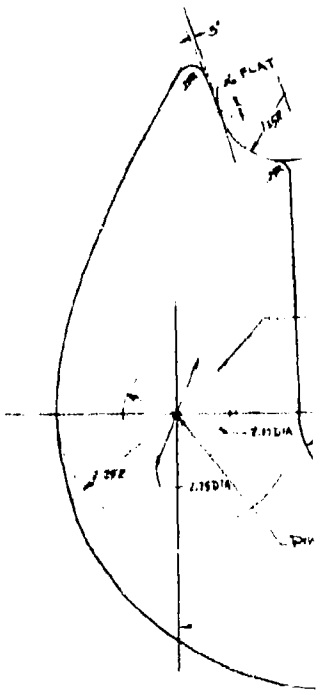
The selected approach employed a two-dimensional photoelastic plastic modeling technique which used a constant thickness model to provide geometric profile information, as shown in Figure 119.

A three-dimensional model analysis would permit a more complete determination of the overall stress distribution in the load beam; however, a two-dimensional model was felt to be adequate for this investigation since the most highly stressed plane would be on the centerline of symmetry, which could be satisfactorily represented by a flat plastic model. The overall stress distribution throughout the model would also be readily apparent.

5. Nutley, W.; TECHNOLOGY DEVELOPMENT REPORT - MODEL 301 HLH/ATC CARGO HANDLING SYSTEM COUPLING; Boeing Vertol Company; USAAMRDL Technical Report 73-88, U.S. Army Air Mobility Research and Development Laboratory, Fort Eustis, Virginia June 1973.



-2 OUTLINE OF LOAD BEAM
FOR CARGO HOIST COUPLING
"C" SHAPE
(SAME AS -1 EXCEPT AS SHOWN)
[4]

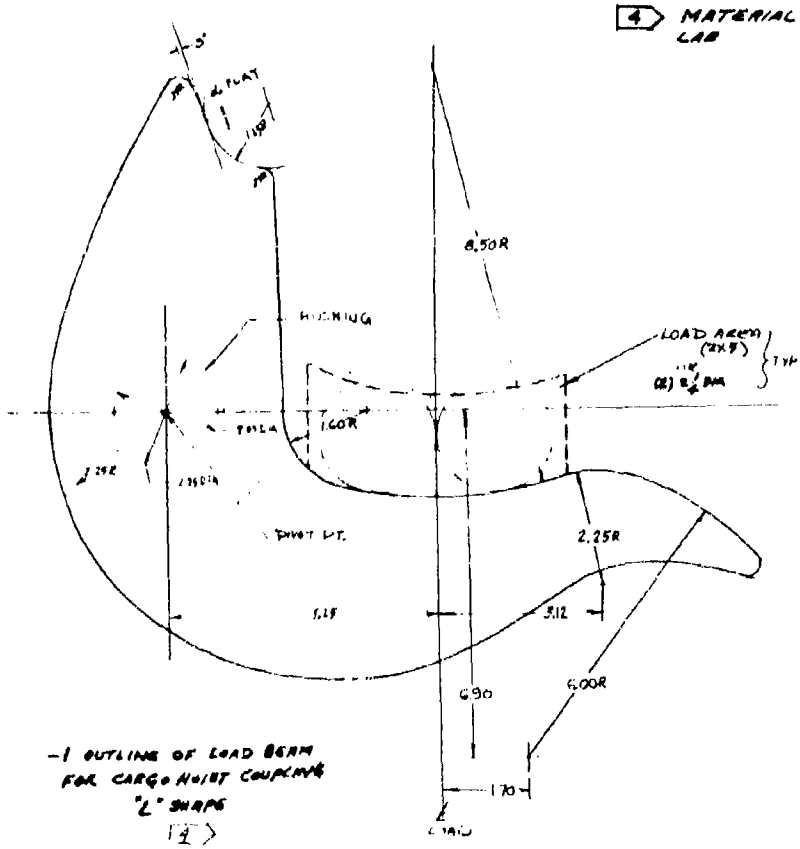


-1 OUTLINE OF LOAD BEAM
FOR CARGO HOIST COUPLING
"L" SHAPE
[2]

Figure 119. Coupling Photoelastic Stress Models.

NOTES:

1. -1 & -2 PATTERNS TO BE USED TO MAKE A TWO DIMENSIONAL PHOTOELASTIC MODEL FOR SIMULATED LOAD TESTS.
2. LOAD TO BE SIMULATED IS 66,000 LB WKG LOAD
3. THE LOAD MARK IS NOTED AS A NYLON SLING 2×6 INCHES OR TWO (2) NYLON SLINGS 2×2 1/2 INCHES OR TWO 2 1/2 DIA STEEL SHACKLES.
4. MATERIAL & THICKNESS TO BE DETERMINED BY TEST LAB



-1 OUTLINE OF LOAD BEAM FOR CARGO HOIST COUPLING "L" SHAPE

4

Since the representation required was at the centerline of symmetry of both types of beams, full-scale models at these planes were manufactured from 1/4-inch-thick plastic. The results of the two-dimensional photoelastic test models confirmed the general size of an I shape, which in turn established the type of materials to be used.

Further photoelastic testing would not be effective since the load beam is a thick, high-strength steel member that is critical under ultimate load. The photoelastic model only projects the elastic limit of the material and gives little indication of the load distribution beyond that point. It was therefore decided to subject the coupling load beam to a load test to destruction. With the use of strain gages, the load and associated deflections can be plotted, from which the strength margins can be determined and weight saving modifications accurately defined.

Load Beam Material Study

A load beam material study was conducted to determine the type of material to be used. In addition to Titanium, the following high-strength steels were considered:

4340M VASCO Max 250 VASCO Max 300 Republic 9N14Co-.30C Hy Tuff, Crucible Steel	Low Alloy Steel
Armco PH 13-8 Mo Carpenter Custom 455 per Spec AMS 5617 Carpenter Custom 455 ELC per Boeing Spec. BMS 7-213	Maraging Stainless Steel

Titanium was eliminated as a candidate material. The larger sections required compared to high-strength steel resulted in higher moments about the pivot which offset the superior strength-to-weight ratio of the titanium.

Low alloy steels were eliminated due to the problems in providing adequate corrosion protection.

The maraging stainless steels have high strength without the corrosion protection problems. Carpenter Custom 455 was selected as it combined the physical properties required with availability and relative economy.

PRECEDING PAGE BLANK-NOT FILMED

The material was available to Specification AMS 5617 or Boeing Specification BMS 7-213. The Boeing Specification was selected since it resulted in better control of the material properties.

Electrical Release Power Requirements

AC and DC powered solenoids were considered for the load beam actuators. AC solenoids are generally larger, less efficient, heavier and less reliable than DC solenoids. DC solenoids were therefore selected.

Previous studies had determined that approximately 140 feet of electrical conductor would be required to accommodate the full 100 feet of tension member payout. The voltage drop in the 140 feet of conductor is prohibited when a 28-volt DC supply is used. The study concluded that 115-volt AC power would be the most satisfactory supply down to the coupling housing. The supply is then rectified to 67-volt DC for the solenoids.

Design Support Tests

A series of subsystem design support tests have been conducted to evaluate and substantiate the overall design and new concepts of the coupling system. These included the following:

1. Push Rod Test
2. Load Beam
   a. Ultimate Test
   b. Coating Test
   c. Sealing Test, including Sand and Dust
   d. Latch Test
3. Pivot Bearing Test
4. Pulley Coating Test.

These tests, together with the design development tests, are described in Volume III. From the preceding studies, together with the design support and development tests, the following design was evolved.

General Description of the Coupling

The coupling is designed to ensure that the load beam cannot be opened, under any mode of operation, when the load is in excess of approximately 1,000 lb. Normal release for the beam is electrical; dual solenoids operate the release linkage; and each solenoid is capable of independent hook release. A remote mechanical release is available through the external conductor reeling mechanism in the event of both solenoids

being inoperative. Additionally, a ground release knob allows the beam to be opened at the coupling. The load beam will relatch automatically after the load is dropped from the hook.

The load beam is pivoted between two halves of a lower housing and shaped such that rotation is normally prevented by a compression member also pivoted within the lower housing. The compression member is linked through an over-center mechanism, to the release solenoids. The lower housing mounts a high capacity thrust bearing, retained to the housing by a special nut. The outer race of the bearing is retained by the upper domed housing, permitting the lower housing and load beam to rotate relative to the upper housing.

A diaphragm between the upper and lower housings provides the mounting surface for the release solenoids and electrical components. All linkages between the upper and lower housing are located concentric to the bearing centerline such that lower housing rotation is not restrained. All the electrical equipment is mounted within the upper dome, and therefore has no rotation, eliminating the requirement for sliprings.

The upper housing is conically shaped, terminating in a single lug, normally attached to the center of the suspension member equalizing beam. The equalizing beam is pin-jointed to the ends of each cable of the dual suspension system, ensuring equal load distribution between the two cables.

Removal of the upper housing provides access to all mechanical and electrical equipment mounted on the diaphragm.

The load beam is spring powered to the closed position; loading being accomplished through a pivoted keeper that prevents the loaded attachment from being removed until the load beam is actuated open.

To allow the coupling to be used for either single- or dual-point operations, the design load capacity is 56,000 pounds with a design limit load of 140,000 pounds.

Figures 120 and 121 illustrate the complete coupling.

Detail Design

While there are no major subassemblies to the coupling, the design structure may be conveniently considered as three major areas: upper housing, lower housing, and load beam. The housings each contain actuation and/or signalling mechanisms with the swivel thrust bearing being the interface between the two housings. Figure 122 illustrates the major

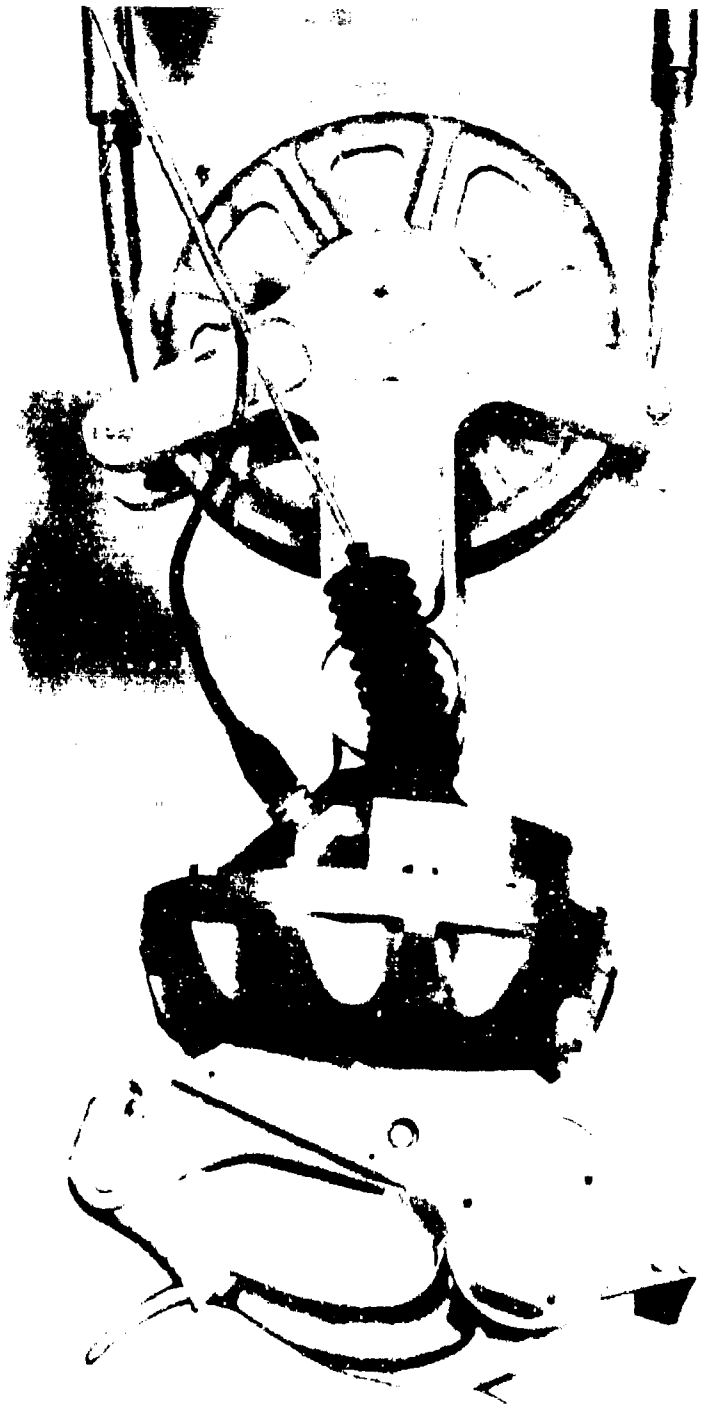


Figure 120. HLH Cargo Coupling Assembly.

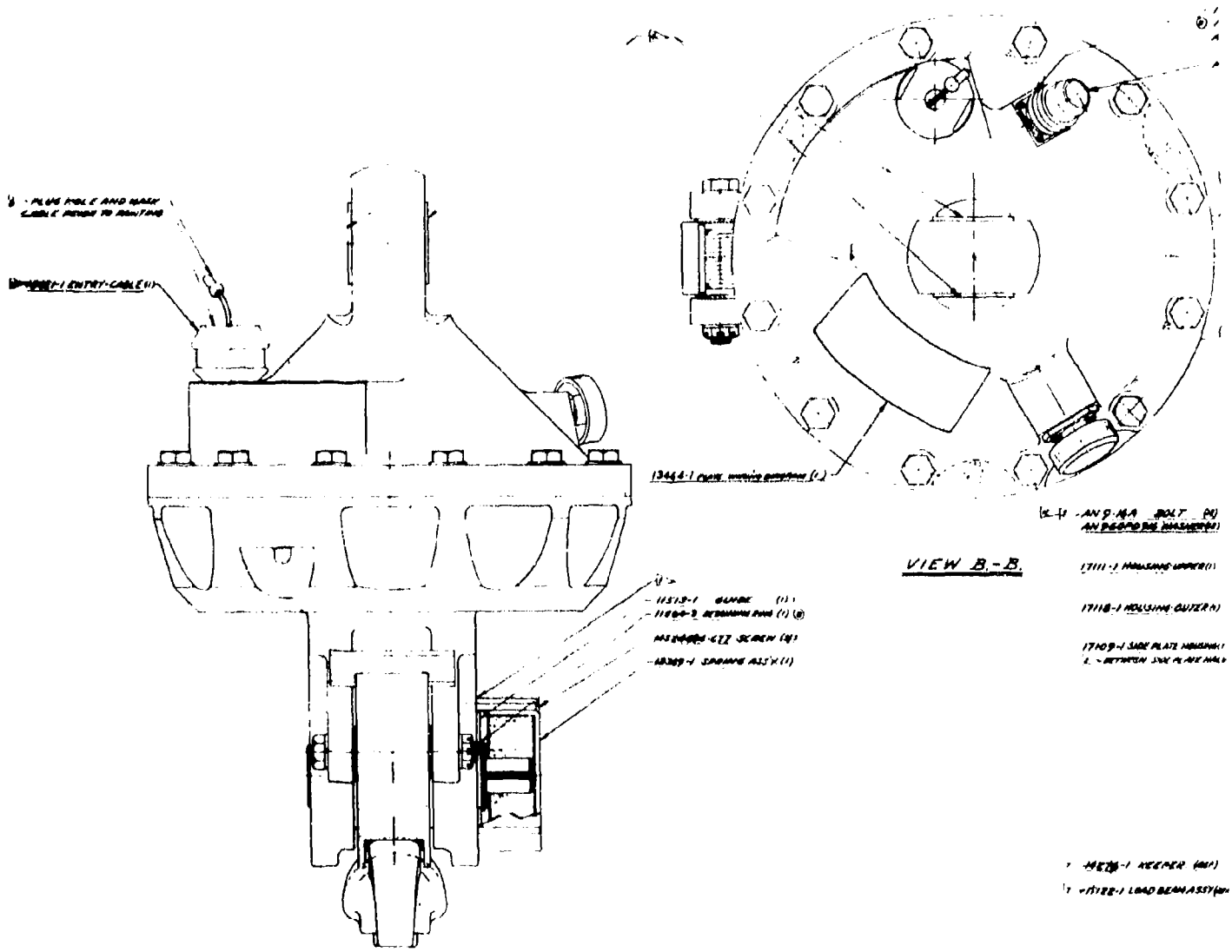
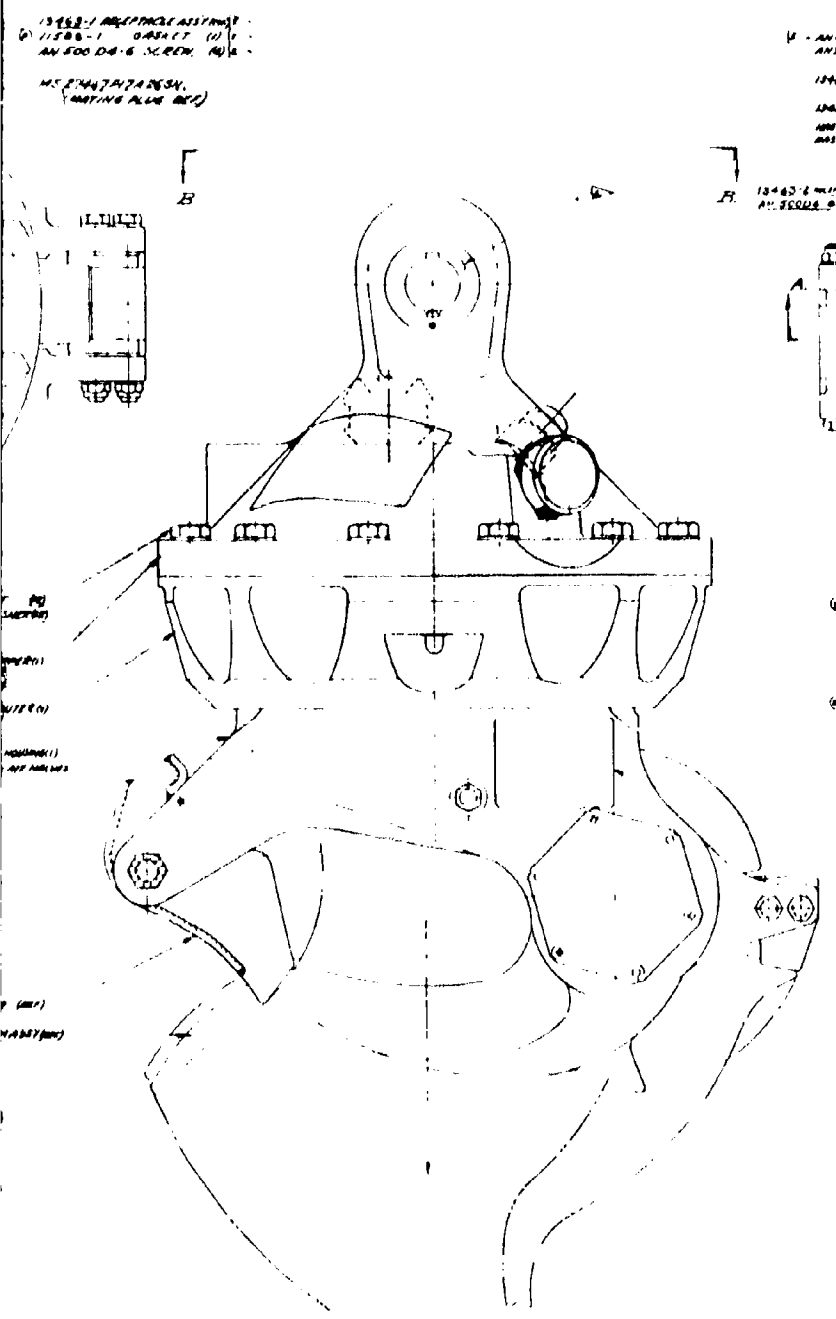


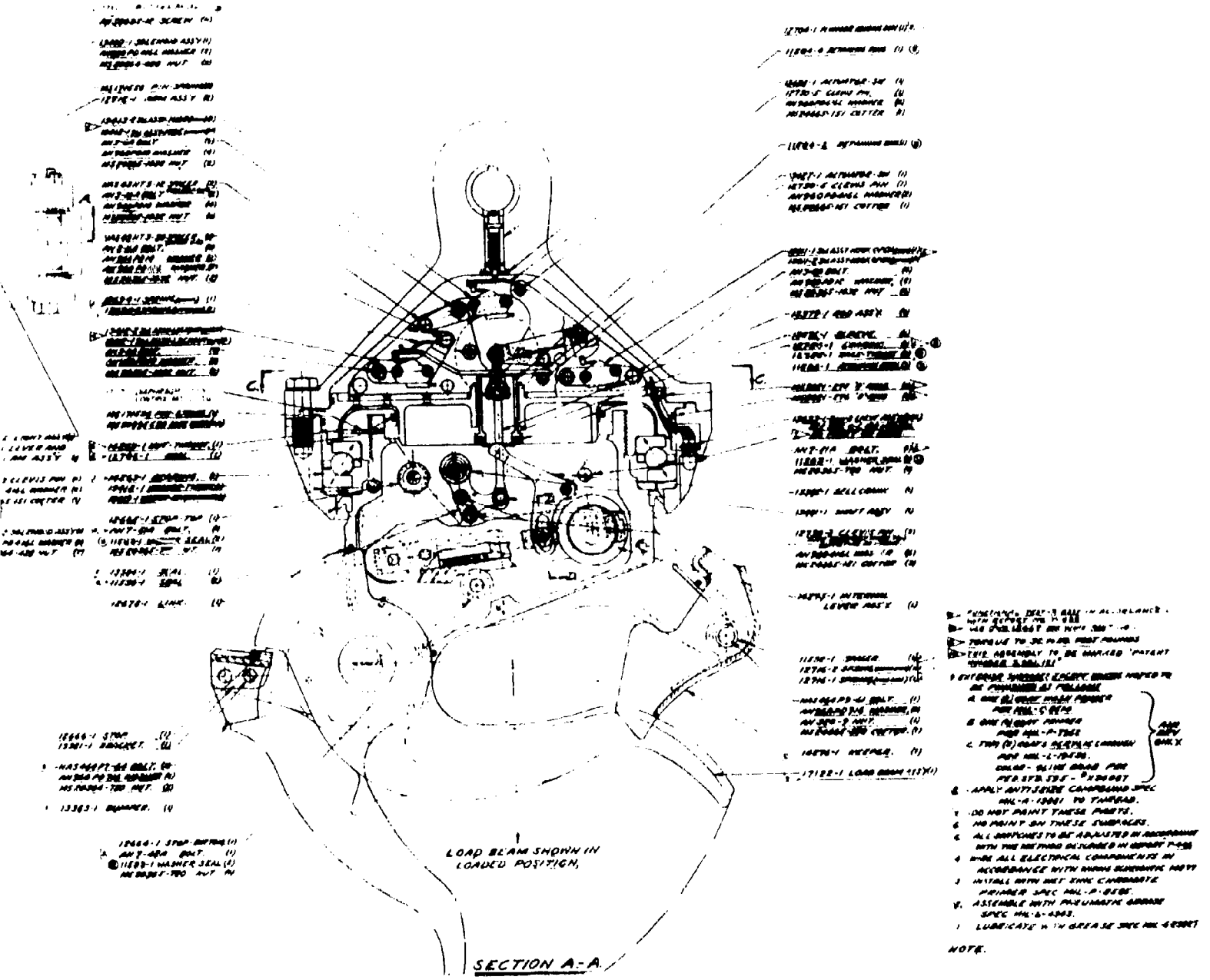
Figure 121. HLH Cargo Coupling Assembly.



SECTION C.-C

SECTION D.-D

2



3

structural components of the coupling.



Left to Right - load beam, internal lever, lower housing, bearing support ring, diaphragm, upper cone with manual release boot, equalizer bar (1 of 2).

Figure 122. Major Coupling Hardware.

Upper Housing

The upper housing is fabricated in two parts, the bearing support ring and the domed attachment cover. The two parts are attached by a series of tension bolts, the diaphragm being trapped between the two parts. The domed cover, while basically conical in shape, has projecting housings to mount the manual release, remote mechanical release and electrical harness connectors. The apex of the cone has an integral lug to install between the equalizing bar side

RECEIVED [illegible] NOT FILMED

plates, the connection being made by a quick-release pin. A bushing within the lug has longitudinal keyways to align the quick-release pin and to ensure the plunger installed within the lug will be depressed by a projection on the quick-release pin to operate an electrical switch inside the dome when used in the single-point mode. Below the domed cover the bearing support ring provides the housing for the lower race of the swivel thrust bearing and is attached to the cover by 12 tension bolts. The domed cover and the bearing support ring are machined from 7075-T7351 aluminum alloy. The bearing support ring has three light assemblies arranged about the outside periphery for operations in darkness.

Between the two upper housing sections is the diaphragm member. Fabricated from 7075-T651 aluminum alloy, the diaphragm has two angle members attached in parallel along chords of the diameter such that they straddle the diaphragm center. Attached to each angle is a solenoid with its axis in line with a diameter of the diaphragm. Each solenoid has an operating arm with a roller attached. When the solenoids are energized, the operating arms lift a lever pivoted between the two angles, which in turn lifts a push-pull rod located on the vertical centerline of the coupling. The push-pull rod has a ball-bearing assembly at the upper end, allowing the lower portion to rotate without restricting or affecting vertical movement. The angle members also support three pairs of micro switch assemblies and the pivot centers for two switch actuating arms.

At the center of the diaphragm, a signal transfer sleeve is free to slide in a bushing installed in the diaphragm. The inside diameter of this sleeve permits the push-pull rod actuated by the solenoids to pass without restriction.

Extending from the end of each solenoid is the continuation of the shaft that supports the operating arm. One solenoid shaft has a coupling permitting the shaft to be operated by the manual release knob mounted to the outside of the domed housing. The other solenoid shaft is coupled to the remote mechanical release linkage.

The remote mechanical release linkage is operated by the outer sheathing of the coupling signal conductor cable. The signal conductor reel provides a relatively constant tension to the outer sheathing to minimize the effects of air drag when the helicopter has forward speed. For emergency release this tension can be increased for a short duration. The release mechanism must therefore be capable of reacting the constant tension without rotating the solenoid shaft, and only operate with the higher tension. Integral with the operating lever of the release mechanism is a cam face with a

detent shaped to match a spring-loaded roller. Adjustment of the Belleville washer spring stack allows the force required to move the operating lever to be made higher than the constant tension of the conductor cable and lower than the tension available for emergency release.

The electrical connections from the signal conductor cable enter the domed housing through an MS27467 type connector plug.

Lower Housing

In order to assemble the internal lever, operating linkage and load beam, the lower housing is split along its vertical centerline and machined in matched halves. The upper portion of the housing locates inside the upper half of the thrust bearing and is threaded to assemble the bearing retaining nut. This nut, machined from 4130 steel, is configured to trap the inside diameter of the housing and prevent the two housing halves from deflecting inward. Machined from 7075-T7351 aluminum alloy, the housing halves have Teflon lined bearings installed for the pivot point of the load beam and the internal lever.

The internal lever is normally in a position to prevent the load beam being pivoted open. Actuation of the solenoids or the mechanical release systems causes the central push-pull rod to release an over-center linkage and lift the internal lever clear of the load beam, permitting the load beam to open. The internal lever has a roller in contact with the load beam, spring loaded by a stack of Belleville washers such that with a load on the beam in excess of approximately 1,000 lb the roller will be pushed in line with the end face of the lever. The lever end face and load beam contact face have a geometry which ensures that increase in load will always tend to retain the internal lever in the locked position. While the nominal lock-out force is 1,000 lb, the system hysteresis causes the lock-out to be effective at a load in the order of 1,700 lb when the load is applied, and to be released at approximately 900 lb when the load is removed.

Compression of the roller spring stack in the internal lever also causes a bellcrank assembly to rotate, lowering the sleeve through the center of the diaphragm and operating a pair of microswitches. These switches remove all power from the release solenoids and signal that the load beam is locked. The lever mounted in the upper housing that actuates the push-pull rod, and hence positions the internal lever, also operates a pair of microswitches. These switches indicate a "hook open" or "hook closed" condition. The two halves of the

lower housing are joined by three bolts. Two of these bolts are located to be upper and lower stops for the internal lever.

The pivot bearings for the load beam are installed in extensions to the lower housing, effectively forming two side plates. A stop for the load beam in the fully open and closed position is mounted between these extensions, and mounting provisions for the load beam return spring located concentric with the pivot bush are provided on one side only. Also mounted on extensions of the housing is the welded steel keeper. Spring loaded to the closed position, the keeper closes the throat of the coupling, preventing sling donuts on the beam from sliding off until the coupling is opened. The coupling is loaded by pushing the sling donuts past the spring loaded keeper which then returns to the closed position.

Load Beam

The load beam is fabricated in two parts, the beam itself and the pivot that has an interference fit in the beam. Both parts are machined from a maraging stainless steel Carpenter Custom 455; heat treated to Rc43-47. The beam is configured with a radius of 1.5 inches on the load-carrying portion of its upper surface. A clock-type torsion spring rotates the load beam to the closed position after the beam has been opened. This spring is contained in a housing mounted to the side of the lower housing concentric with the load beam pivot.

Single-Point Adapter

The concept of a single-point adapter for converting from a dual suspension system to a single-point mode has remained valid from the original proposal to the current design described here. Flight testing with the 347 helicopter, proved the concept was practical; development testing with the coupling has demonstrated the strength of the ATC design.

General Description

Conversion from dual hook to a single-point configuration is achieved by removing one of the couplings from its equalizing bar, assembling a fitting attached to a paired cable and sheave arrangement in its place, and attaching the other end of the paired cable to the load beam of the remaining coupling. The moved coupling is now assembled to the sheave, becoming the single-point attachment. The paired cables are of identical construction to the main tension member. Figure 123 illustrates the sheave arrangement.

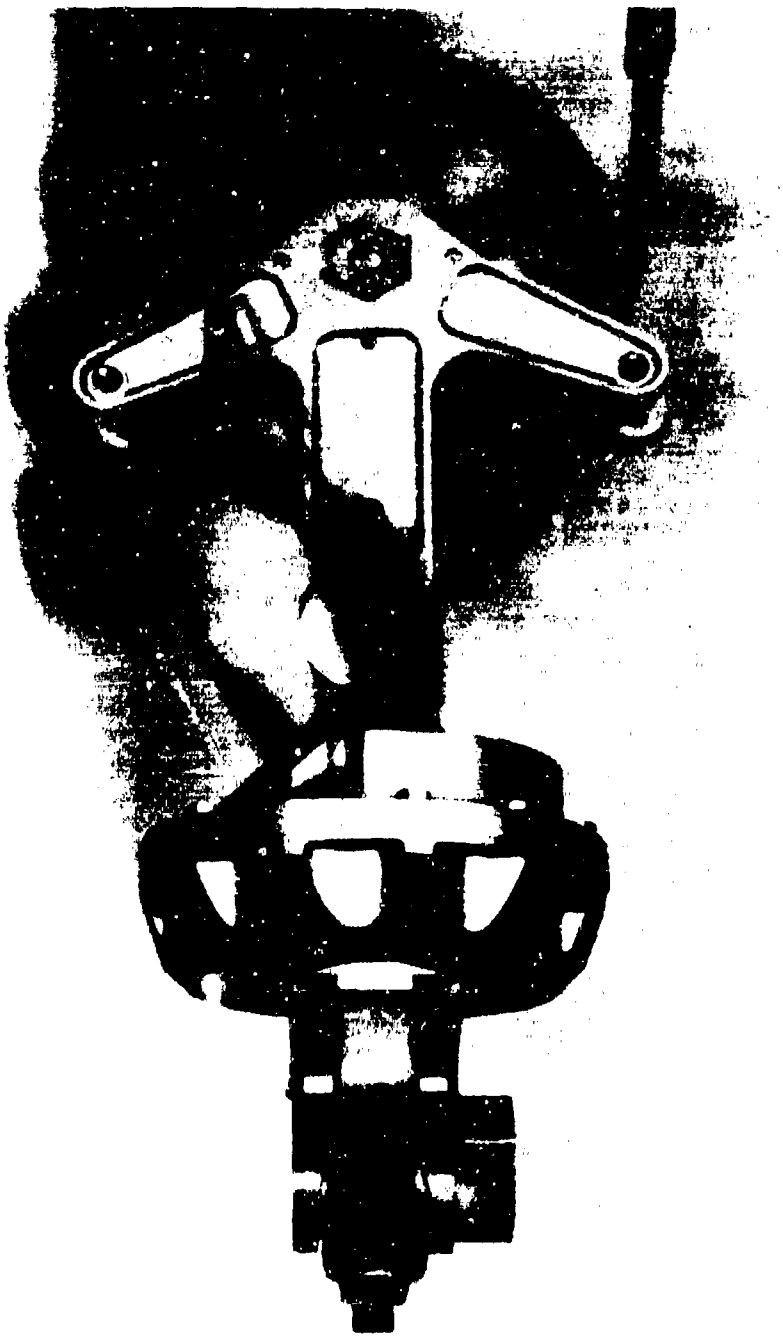


Figure 123. Single-Point Adapter and Coupling Assembly.

Detail Design

The single-point adapter consists of the following elements: paired cables, adapter fitting, pulley and side plate assembly.

The paired cables terminate in individual eyes at one end and swaged terminals at the other end. The eyes are formed over a thimble with two swaged buttons to retain the returned cable end. The swaged terminals assemble into the adapter, arranged such that the left-hand and right-hand terminals cannot be interchanged in the adapter fitting, ensuring that the two cables will always be of opposite lays. The adapter fitting is machined from Carpenter Custom 455 stainless steel, with a double clevis to accept the cable terminals. The two terminals are retained by a single bolt. The fitting then adapts from the double clevis to a single lug identical to the lug on the coupling upper housing, and assembles to the equalizing bar assembly by the same quick-release pin that retained the coupling.

Assembled on the two cables is the pulley and side plate assembly. The pulley is a double grooved wheel of 15.4 inches mean diameter, machined from 7075-T651 aluminum alloy with a hard anodize finish on the grooves. The two identical side plates are also machined from 7075-T651 aluminum alloy and extend from the center of the pulley to the attachment point for the coupling. Extensions of the side plate provide locations for cable guard pins to prevent the cables leaving the pulley grooves. Teflon lined bearings are installed in the side plate for the coupling attachment pin and in the pulley for the pivot pin. The pulley is shown in Figure 124.

The coupling attachment pin has a projecting key that when installed will actuate a mode switch inside the coupling to electrically isolate the coupling still assembled to the tension member. This arrangement ensures that release will take place only at the single-point coupling.

Mounted on one side plate adjacent to the pulley center, is a fairlead to guide the conductor cable and prevent interference with the pulley arrangement. Figure 125 describes the single-point adapter.



Figure 124. Single-Point Adapter Pulley.

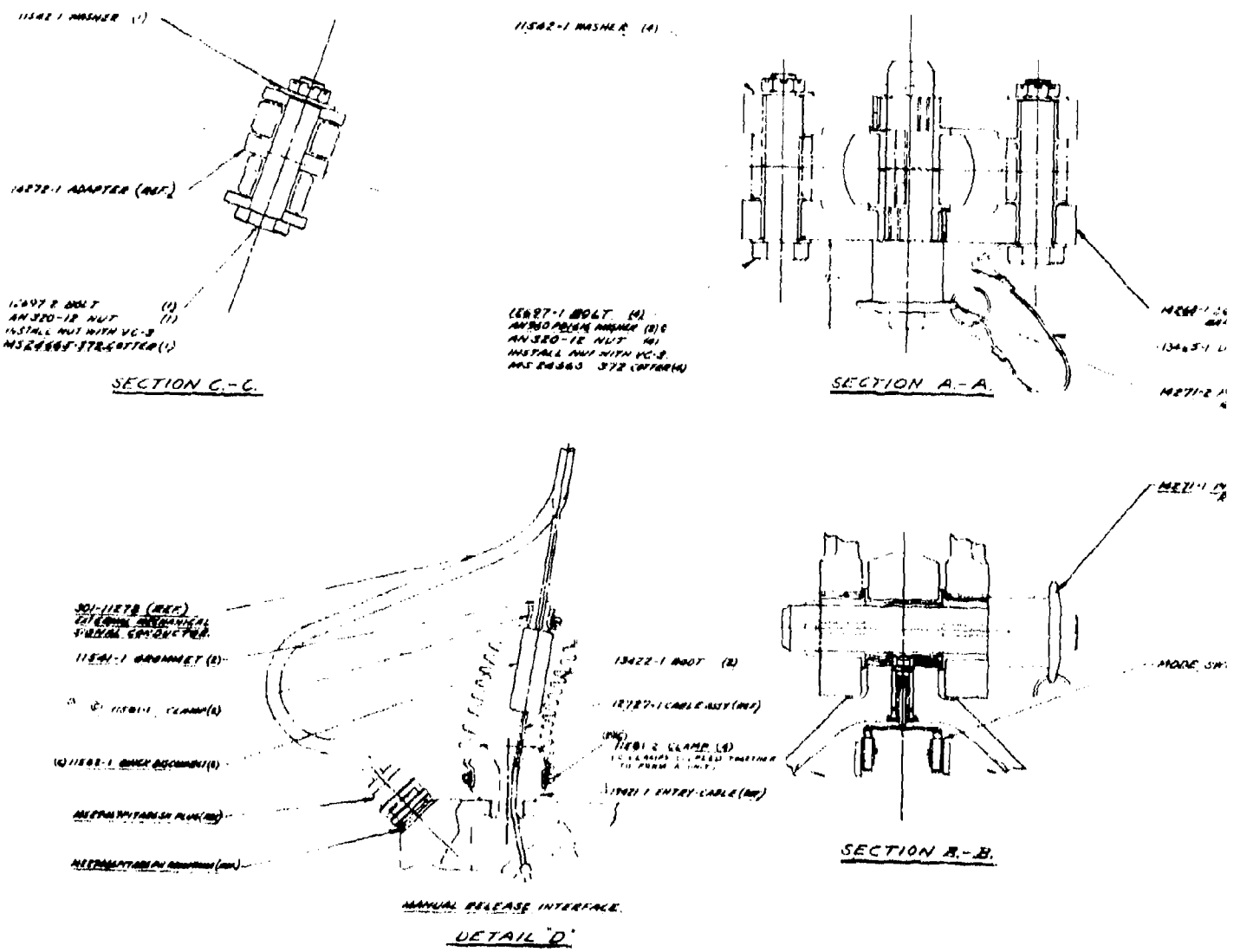
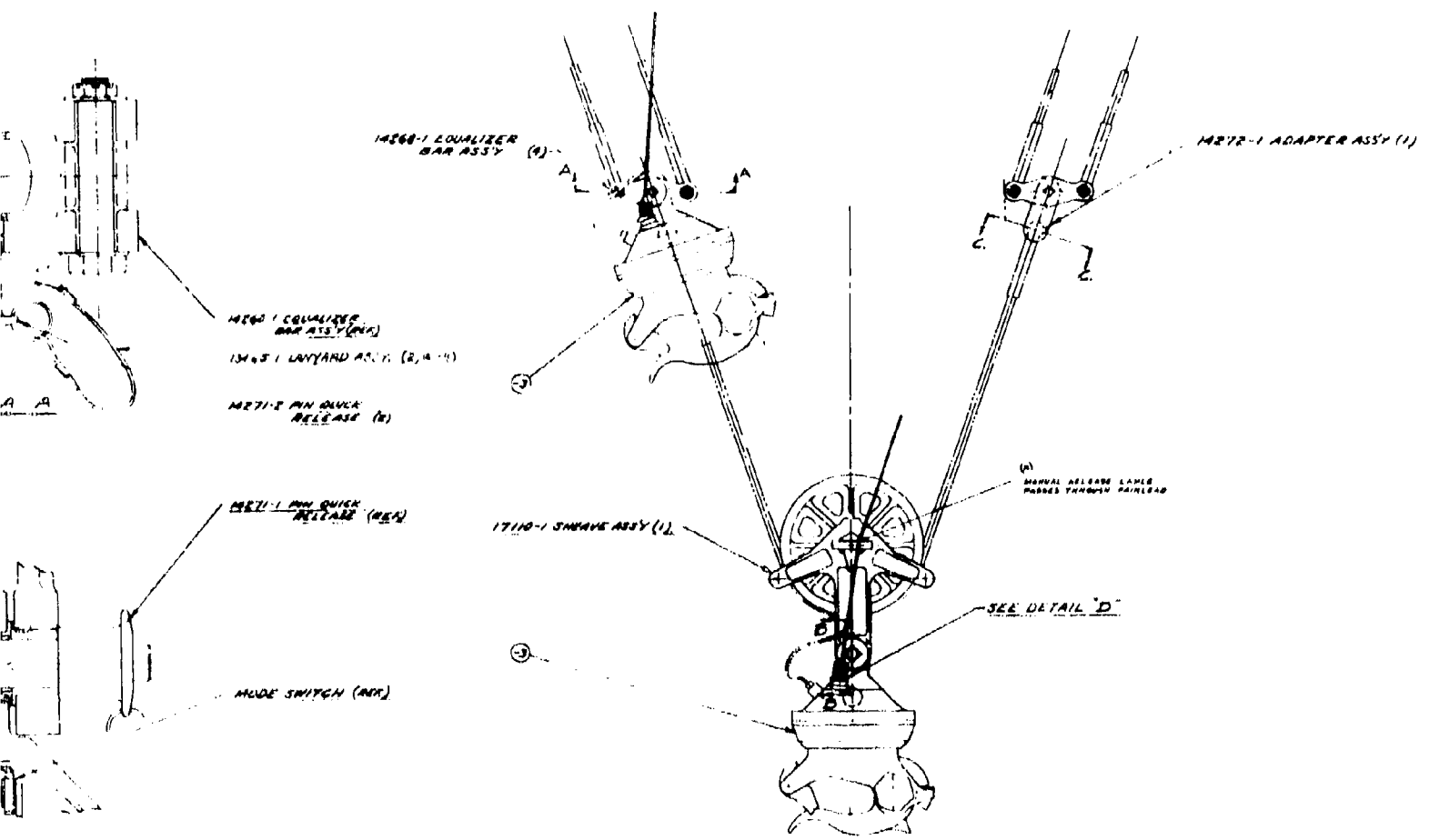


Figure 125. Single-Point Adapter Assembly.



(6) PAINT THIS PORTION OF PIN & ENTIRE LANYARD ASSY PER NOTE "B" OF THIS DWG. ON SHT 2 OF 2.
(7) THIS ASSEMBLY TO BE MARKED "PATENT NUMBER 3,884,161" PER NOTE "A"

2

SIGNAL TRANSFER SYSTEM

Proposal Configuration

The HLH proposal presented a configuration of an external sheath of embedded conductors that is automatically wrapped around a single hoist cable. This is shown in Figure 126.

The sheath terminated at the coupling end in a slip ring assembly.

The hoist end of the system passed through a closing die in which the flat tape was enclosed around the tension cable by the die and interlocked in place. The closing die extends below the hoist.

Upon exiting from the cable through the closing die, the flat tape was stored on a reel drum powered through the hoist system. Reference Figure 127.

Subsequent to the proposal submission, other methods of deploying the signal conductor cable were considered. One concept is shown in Figure 128. The conductor stowage drum is mounted below the hoist payout area in a horizontal plane with the tension member passing through the center. The stowage drum would be stationary with a deployment guide rotating about the outside of the drum. A constant torque power device would tend to power the guide to position the conductor on the drum. Payout of the tension member would pull out the conductor, cause the guide to rotate and wind the conductor cable about the tension member. Reeling in the tension member would permit the guide to rewind the conductor on the stowage drum.

Trade Study

The ATC contract ASRD dictated a cargo system capacity of 28 tons, increased from the 22-1/2-ton system presented in the proposal. This increase resulted in a reevaluation of the tension member and the adoption of the paired-cable concept in place of the original single cable.

The paired cable tension member resulted in the rejection of the sheath concept for the conductor system and precluded further consideration of the horizontal stowage drum concept as both arrangements were directed toward a single cable tension member. Additionally, a new design objective for a remote mechanical backup coupling release was introduced and the preceding concepts could not accommodate this feature.

A trade study was conducted to evaluate three systems: (1) internal wiring within the center of the tension member,

PRECEDING PAGE BLANK-NOT FI

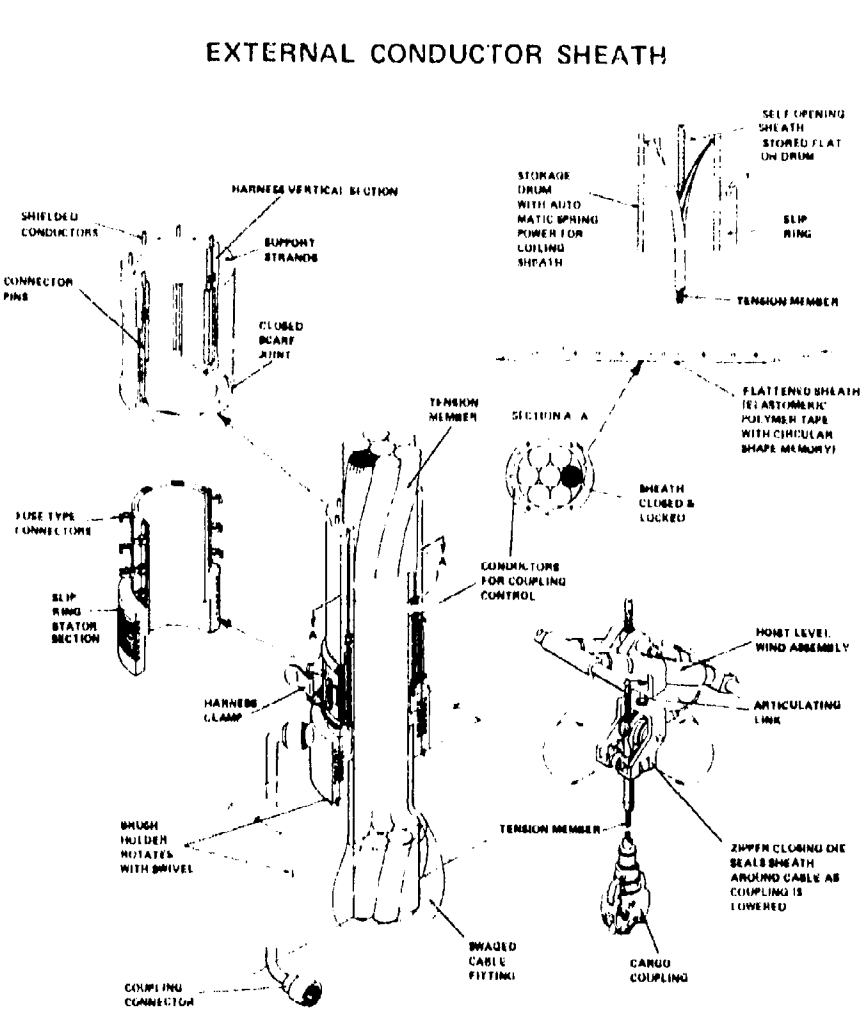


Figure 126. Proposed External Conductor Sheath.

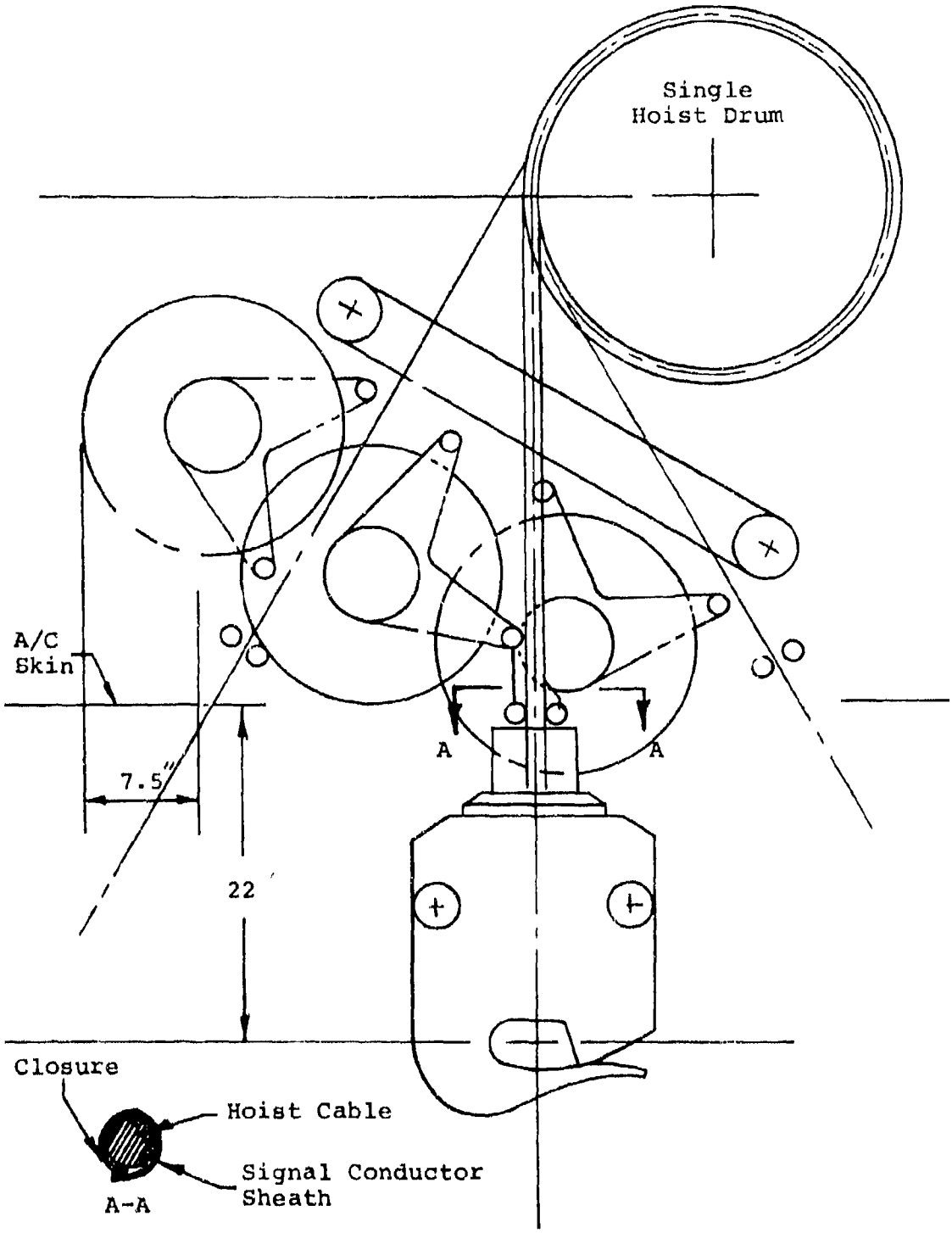


Figure 127. Signal Conductor Deployment.

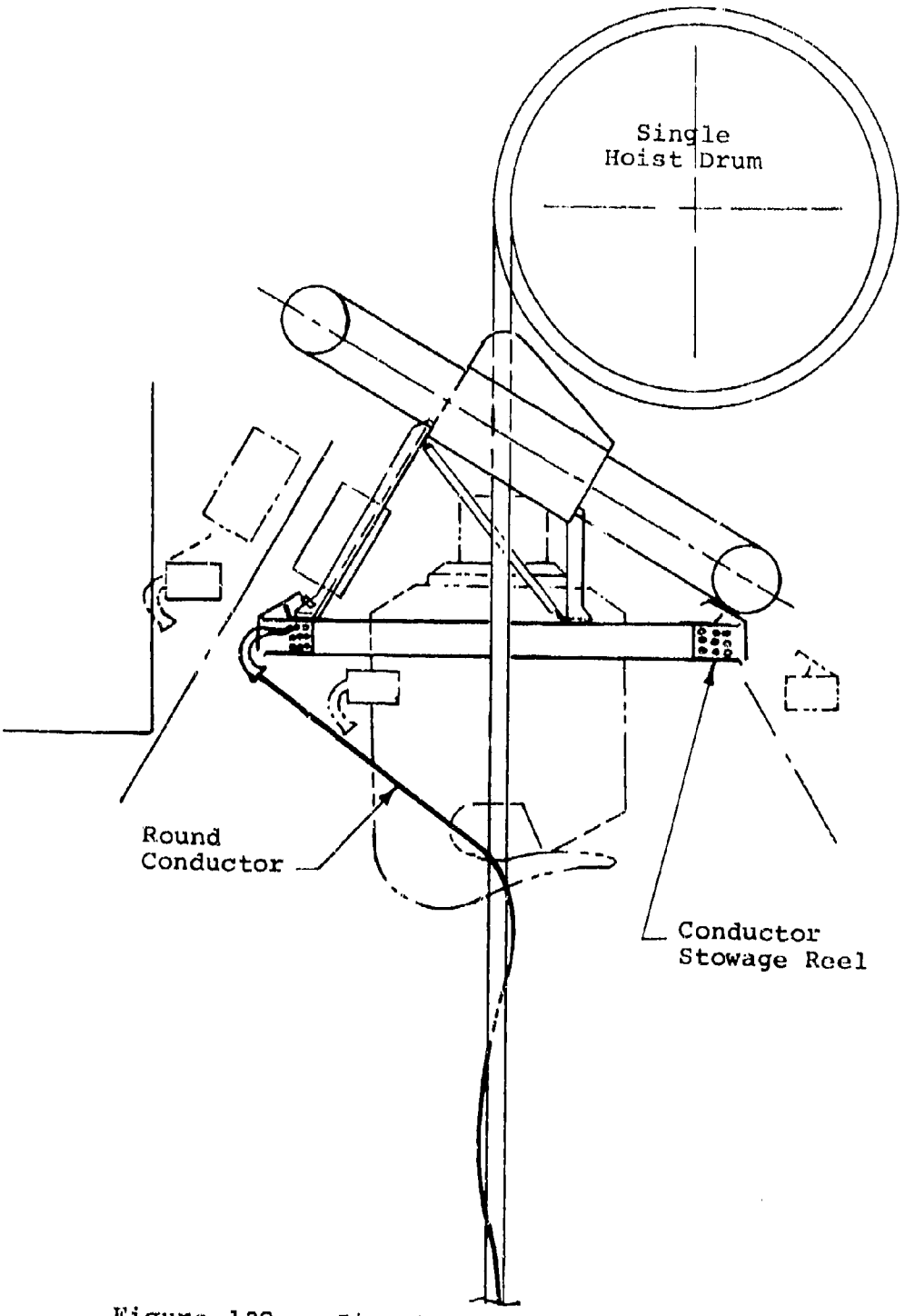


Figure 128. Signal Conductor Deployment.

(2) a remote electronic signal system with a transmitter mounted on the coupling, and (3) an external conductor cable independent of the tension members.

The independent external conductor cable and reel was selected as this arrangement was compatible with providing a remote mechanical release and could utilize a signal transfer concept in the reel to eliminate the need for slip rings. The same study evaluated several reeling concepts to meet the following list of design objectives:

1. Compatible with the paired cable hoist system.

2. Provide the ability to be used as a mechanical load release of the coupling.

3. Withstand continuous air loads throughout the load cycles of 3600 flight hours.

4. Follow the excursion of the coupling in whatever mode is being used without undue or abnormal wear.

5. Provide storage of the signal conductor when the coupling is retracted or extended in an orderly fashion and prevent snarling with any portion of the suspension system, in any operating mode.

6. Provide a power limited constant torque against the signal conductor to maintain a constant tension on the conductor.

7. Provide a power limited means of tripping the mechanical release of the coupling without over stressing the signal conductor system.

Reel Configuration

The signal conductor reel study evaluated several different types of reel configurations from the simplest reel with no deployment control to a sophisticated reel with a level wind mechanism. From this study, it was ascertained that the reel should be pneumatically powered, driven by an air turbine motor as shown in Figure 129.

Air Turbine Motor

An objective was to design the turbine stage to produce the cable tension/cable speed characteristics specified as follows:

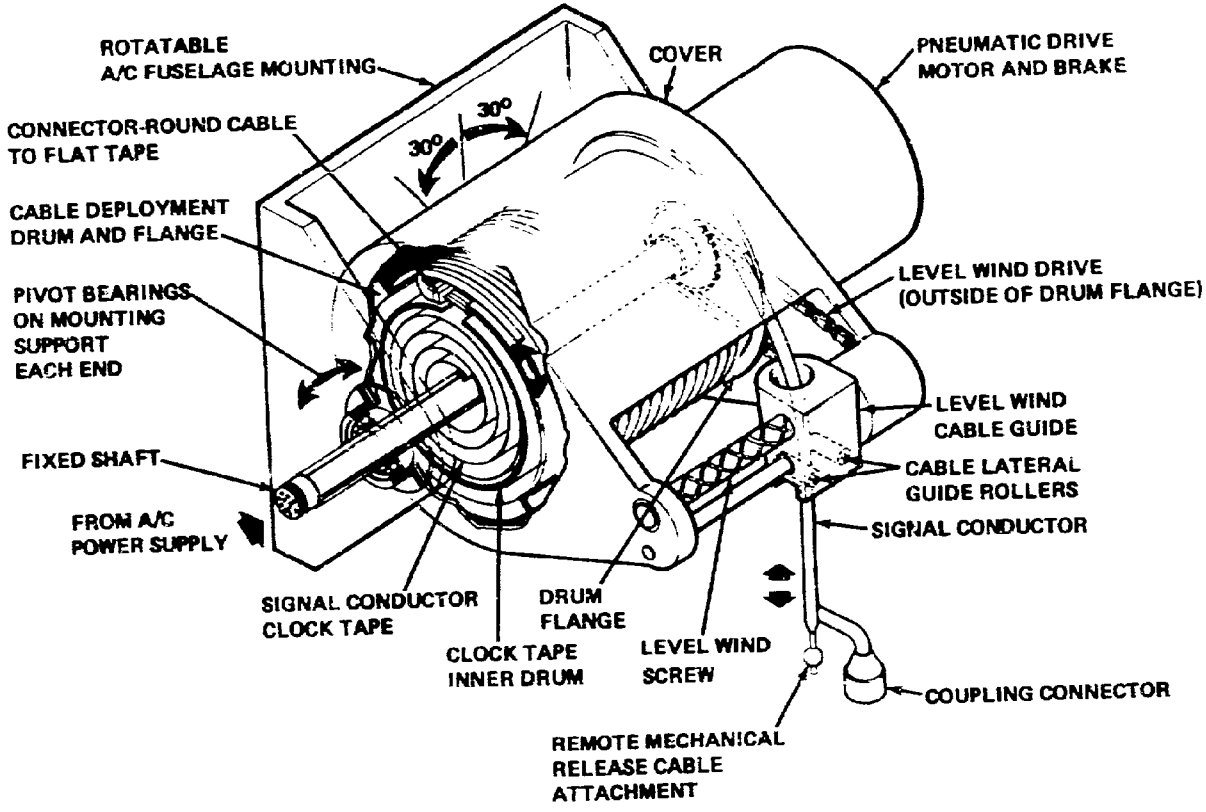


Figure 129. Signal Conductor Reel Assembly.

1. A steady tension on the cable assembly of between 80 and 100 lb at cable speeds of between zero and 130 ft/min.

2. An additional tension jerk on the cable assembly providing a total tension of 350 lb at zero cable speed for hook release.

The above characteristics are obtained with an air supply at the turbine of 51.8 psia and 414°F on a design day of 4,000 ft altitude and 95°F ambient temperature.

The turbine wheel size was chosen to ensure small mass flow requirements from a low polar moment of inertia system. This was achieved by using an existing Sundstrand wheel design with nozzles tailored for this application. The wheel is a single-stage axial impulse design having symmetrical buckets generated on the disc by electrochemical milling. Manufacture of the wheel could thus be accomplished with existing tooling. Three convergent/divergent circular nozzles are utilized. One supplies air for the steady tension requirements. Hook release torque is generated by activating the additional nozzles. The hook release valve is normally closed.

Reduction Gear

Initial consideration of the reel design proposed using a harmonic reduction drive between the air turbine motor and the reeling drum.

Figure 130 presents the estimated performance of the reeling mechanism with a 140:1 harmonic drive. The efficiency of the harmonic drive was assumed to be 75% in both directions. Due to the low efficiency of the harmonic drive, the cable would undergo a wide variation in tension over the anticipated modes of operation. It should be noted from Figure 130 that the force needed to payout the cable is greater than the weight of the empty hook. It was decided that it would be difficult, if not impossible, to obtain the desired results (low variation in tension, tension well below hook weight) with the 140:1 harmonic drive. Figure 131 presents the mechanical response of the reeling mechanism which would employ a harmonic drive with a lower ratio (80:1).

The use of the harmonic drive was ruled out after consultation with representatives of the USM Corporation, manufacturer of the harmonic drive components. During normal operation, the harmonic drive would be subjected to a maximum load of 450 in-lb on the low-speed shaft. When the hook release tension is applied, the load increases to 1580 in-lb, also on the low speed shaft. In order to shear the shear section,

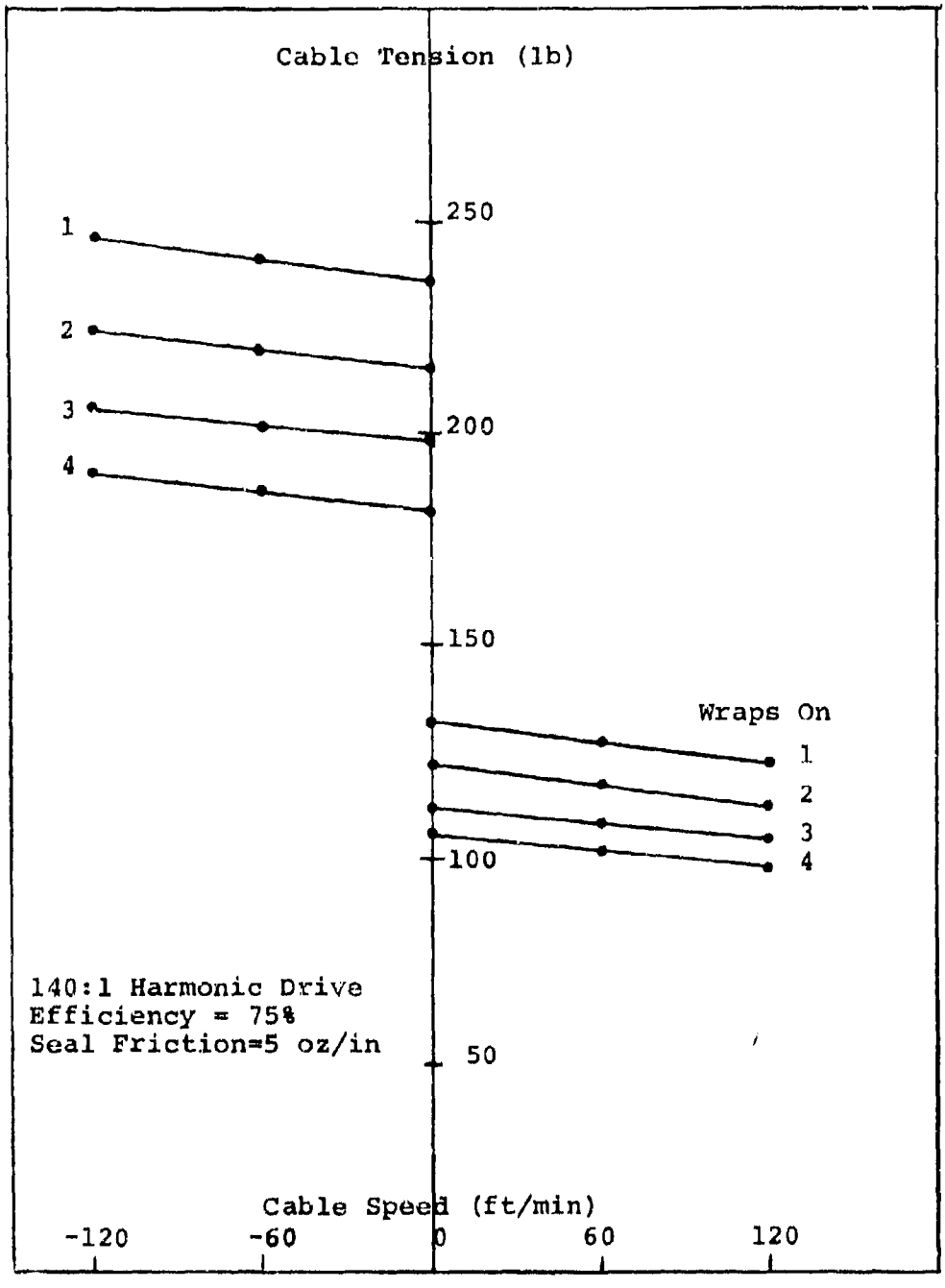


Figure 130. Reeling Mechanism Response.

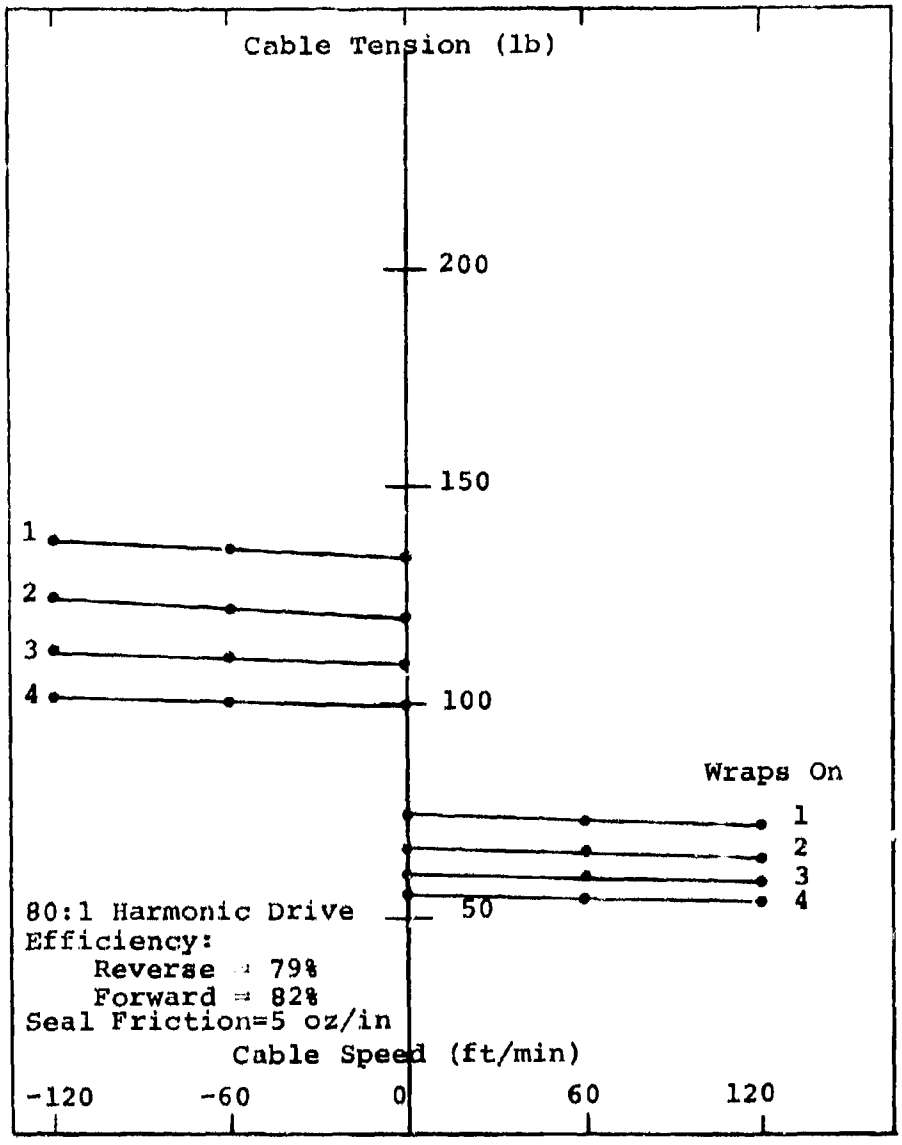


Figure 131. Reeling Mechanism Response.

the harmonic drive would have to withstand loads of up to 3160 in-lb. An oversized harmonic drive with special modifications would be required. The bearing which makes up the wave generator would be specially made for a low tolerance fit. Even with these special modifications, the performance of the shear section would be questionable. By going to an oversized harmonic drive to withstand the shear torques, the efficiency was dropped to 62 to 65% in the forward direction and 72% in the reverse direction. This is due to the fact that at normal loads, the harmonic drive would be operating at a smaller fraction of rated load, resulting in a lower efficiency.

The mechanism remains active and supplies cable tension whenever the helicopter was operating. This means that the turbine would run away after the cable cutters were used and the load in free-fall sheared the shear section. From calculations of the turbine output power and turbine windage, estimated from design support testing, the maximum speed of the turbine was estimated to be 36,300 rpm (as shown in Figure 132). This speed is high enough to cause the wave generator of the harmonic drive to burst. The gears in a spur gear reduction would be unaffected, however, by this runaway condition.

In summary, it was decided to replace the harmonic drive with a spur gear reduction for the following reasons:

1. Low overall efficiency of the harmonic drive.
2. Necessity of an oversized harmonic drive, with further reduced efficiency.
3. Added cost and time required for special modification of wave generator bearing in the harmonic drive.
4. Questionable performance of the harmonic drive during shearing of the shear section.
5. Destruction of the harmonic drive after runaway.

External Round Conductor Configuration

The following requirements were established for the external conductor:

1. It must follow the coupling excursion without becoming entangled in other associated systems.
2. It must be resistant to all different environments.

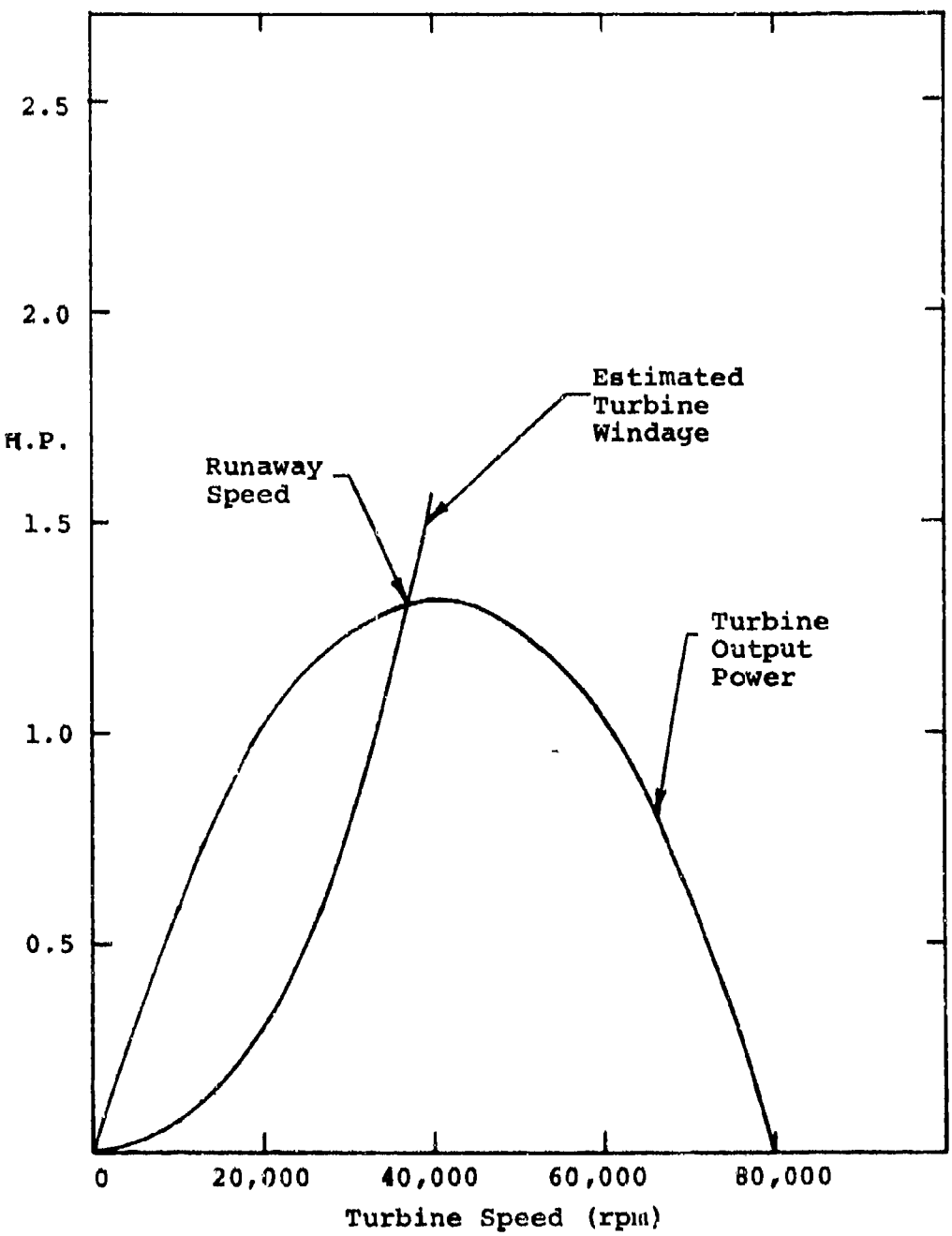


Figure 132. Estimated Runaway Speed - HLH Reeling Mechanism.

3. It must be a small diameter to keep air loads to a minimum.

4. It must be strong enough to sustain repeated mechanical releases.

5. It must have the ability to be wrapped in three layers on the storage reel without impairment.

The signal conductor serves the following purposes:

1. It must carry the signals for the condition of the coupling as to whether it is open, closed or locked.

2. It must carry the power requirements to actuate the rotary solenoids to open the load beam mechanism.

3. It must provide a means of a remote mechanical backup release system.

4. It must be of a dual construction in that the inner conductors do not carry the air loads or release loads imposed upon it.

The breaking strength of the sheath was demonstrated by design support testing at between 800-900 lb. The effective mechanical release tension of the coupling was established at 350-500 lb. The breaking strength is within the objective 1.5 factor of safety at 500 lb x 1.5 = 750 lb minimum breaking strength.

Signal Transfer

A primary objective of the entire signal conductor system is to obtain high reliability. Normally, a signal conductor that is wound on a reel will require slip rings or some other sliding electrical interface between the rotating and non-rotating parts. Slip rings are subject to many mechanical problems and require maintenance. To increase reliability, the slip rings have been eliminated in favor of a single flat multiple conductor tape that coils and uncoils like a clock spring. This method allows continuity of the electrical circuitry between the rotating drum and the fixed point of electrical supply. A solid mechanical connection is maintained throughout.

A flat, flexible tape with buried copper electrical ribbons, is used as the transition medium from the rotating to non rotating portions of the aircraft mounted reel support. This

tape is wound like a clock spring which may also be reverse wound over itself. The flat tape is enclosed within a secondary drum inside of the conductor reel. The operation of the flat tape may be seen in Figure 133.

Detail Design

Following the preceding design studies, the detail design of the signal transfer system was evolved. Figure 134 shows a schematic of the complete assembly, and Figure 135 shows the assembly installed in the test rig.

The complete signal transfer system is composed of the following elements:

1. The external signal conductor round cable assembly connecting the coupling to the conductor storage reel assembly.

2. The flat tape within the storage reel which eliminates the reel slip rings and permits a solid mechanical electrical connection from the round conductor to the aircraft power source.

3. Signal conductor reeling mechanism.

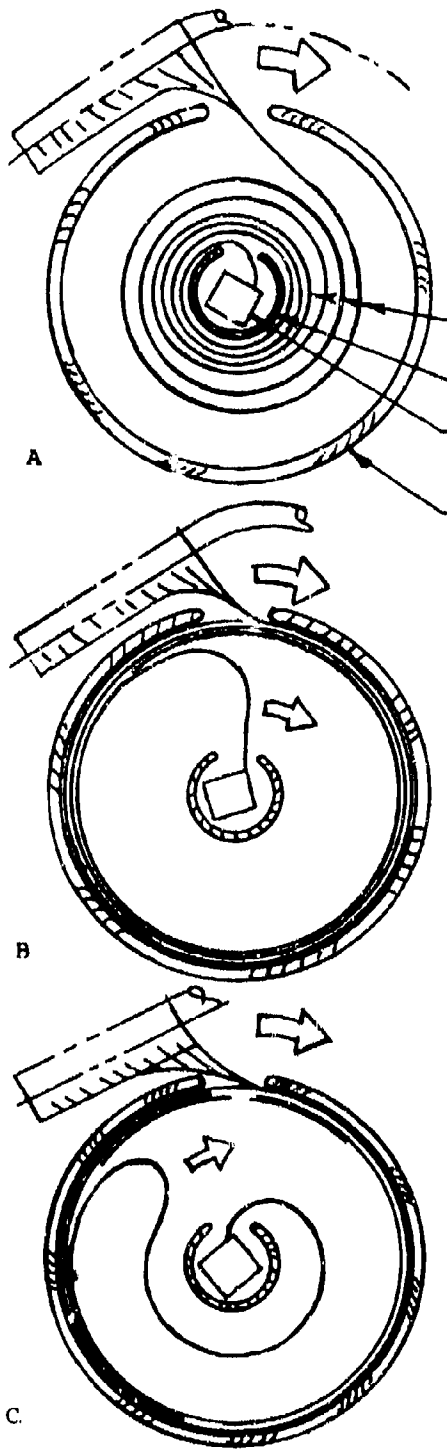
External Signal Conductor

The external conductor cable is composed of 19 copper stranded wire assemblies surrounded by a corrosion resistant steel braided sheath which also serves as the means of transmitting power to the coupling mechanical release system. The cable construction is illustrated in Figure 136.

The braided sheath of the cable is separated from the conductors at each end of the cable assembly. The electrical conductors are then looped in order to keep them unloaded when tension is applied to the supporting braid. Only the braided end of the coupling feels the mechanical 350-500 lb release load and the normal 80-100 lb constant takeup tension. The loads at the drum end are dissipated through a minimim of three dead wraps on the drum. A strip-off feature allows the braided end at the drum to break at 50% of the 800-900 lb ultimate of the coupling ends. This is to protect the reel and mechanism in the event of load jettison and cable tension snap-back.

Flat Tape Conductor

The flat tape internal signal conductor used as the transition medium from the rotating to the stationary portions of reeling mechanism consists of 24 bare copper



1. Flat tape inner drum rotates with the main cable drum.
2. Tape wound up on inner fixed shaft. Main cable is not deployed.

Tape

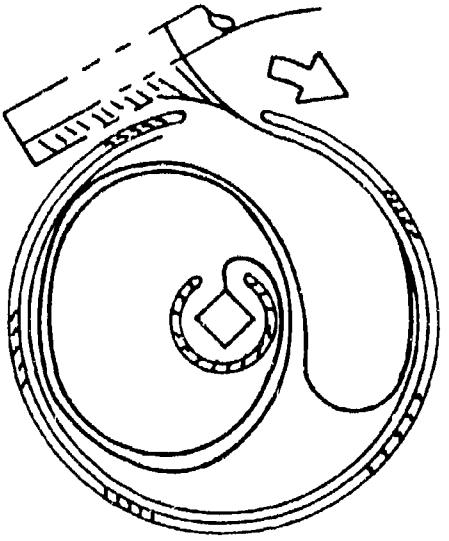
Fixed shaft (Nonrotating)

Fixed lead to A/C supply (Nonrotating)

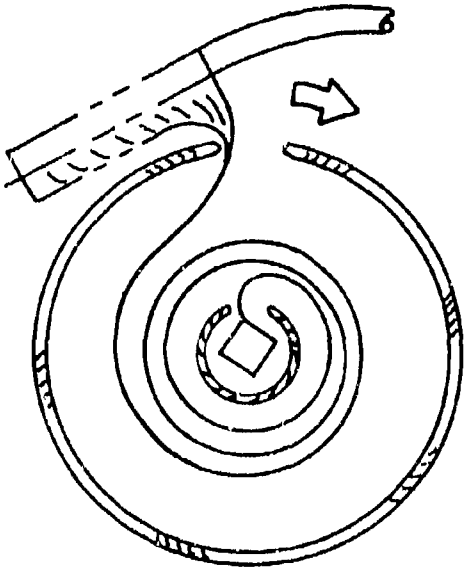
Tape drum rotates with main drum

3. Flat tape wound completely out inside of inner drum
4. Main conductor is 50% deployed.
5. As the main conductor continues to be deployed, the flat tape begins to reverse itself by wrapping upon the fixed inner shaft in the opposite direction.
6. The main conductor deployment now exceeds the 50% mark.

Figure 133. Operation of Flat Tape Signal Conductor.



7. The flat tape continues to reverse on itself as the main conductor is deployed.



8. The tape is shown almost completely in reverse of "A" with the main conductor almost fully deployed.

9. As the main conductor is wound "in", the tape will again reverse itself around the fixed shaft until it again is completely wound upon the main drum in its original starting position at "A".

Figure 133. Continued.

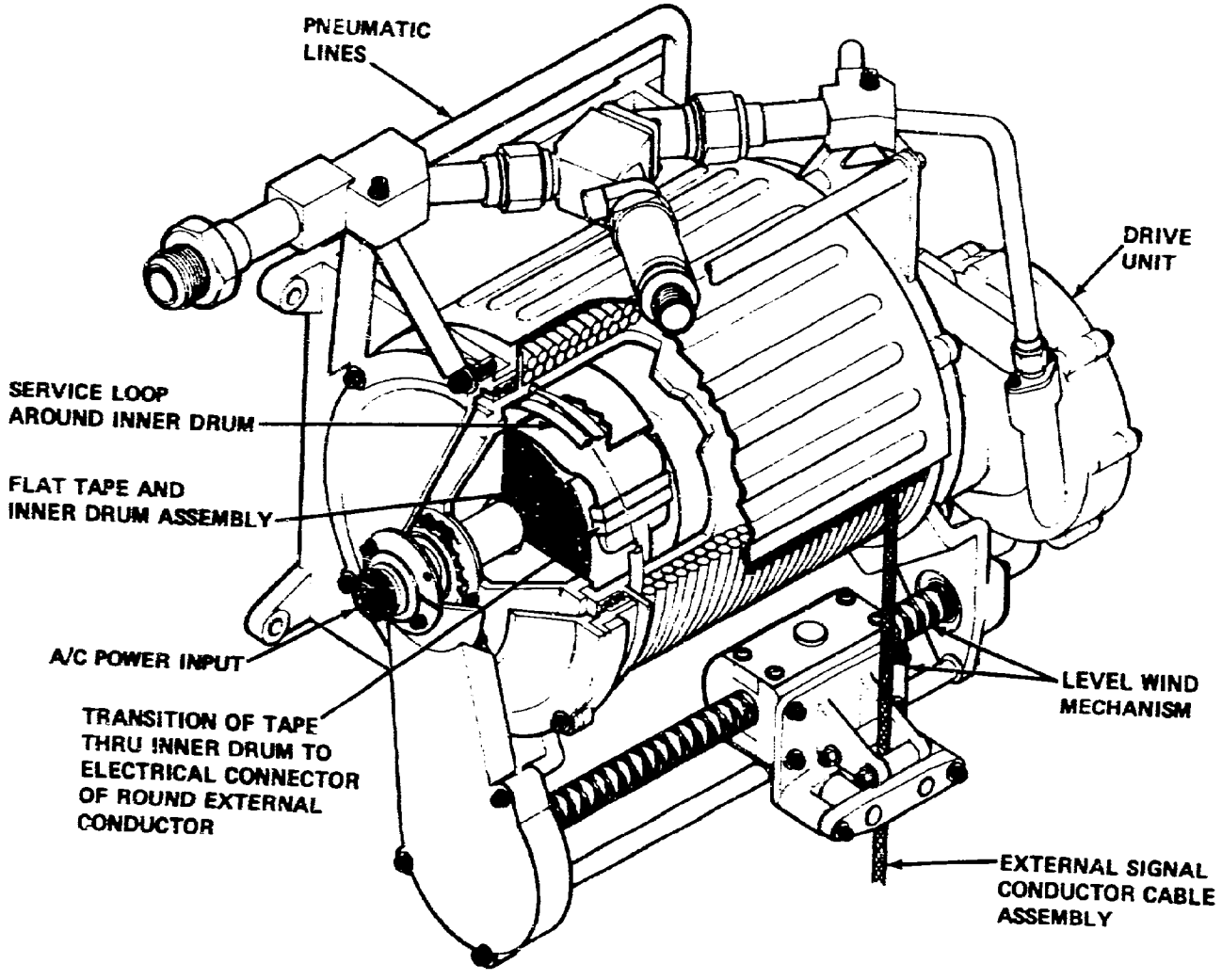


Figure 134. Schematic of Signal Conductor Reel Ass -y.

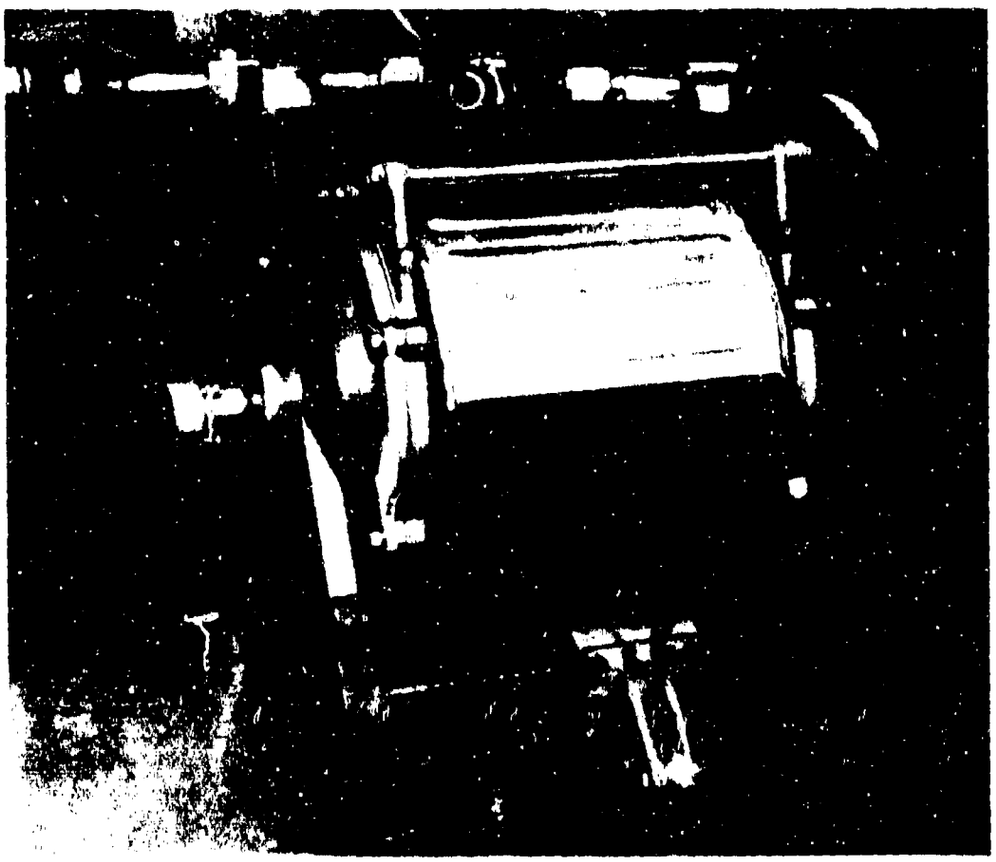
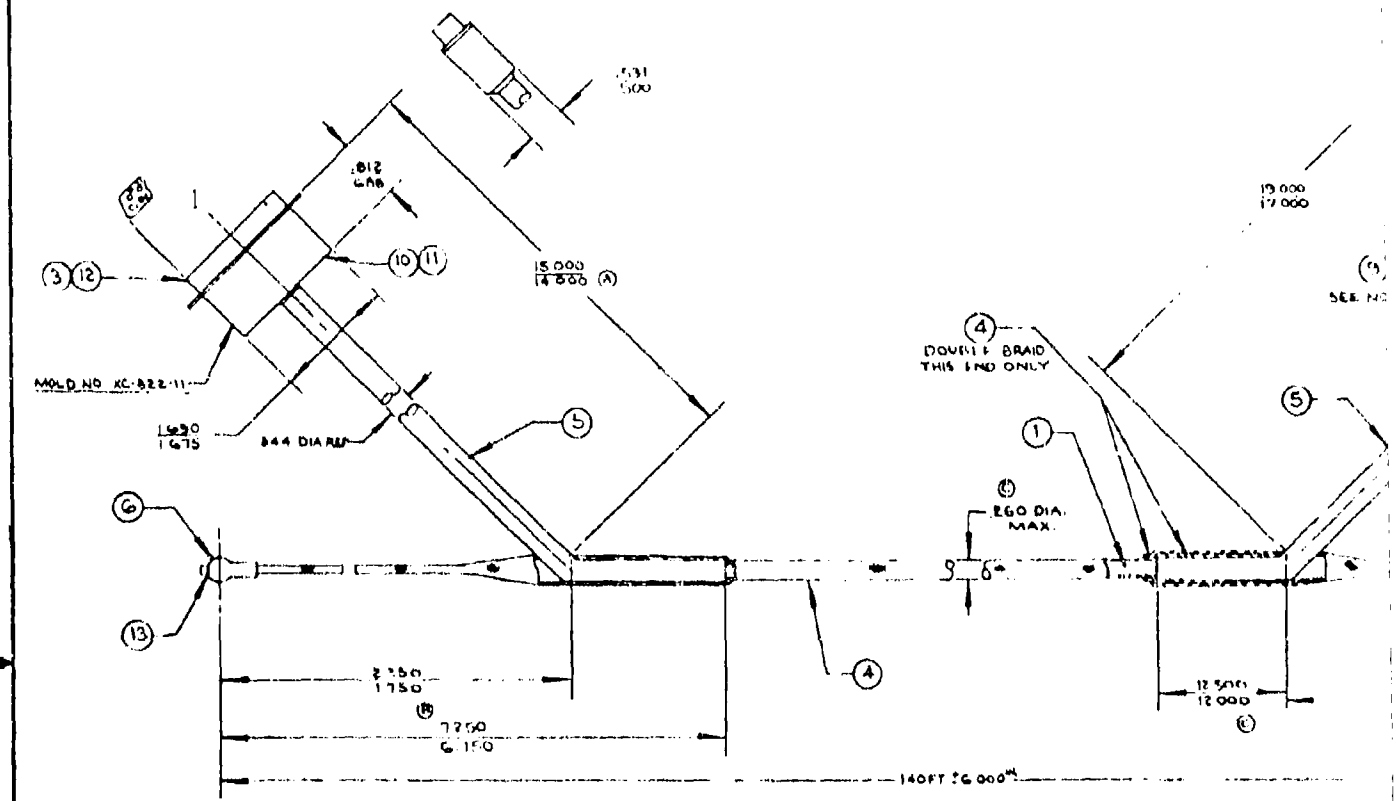
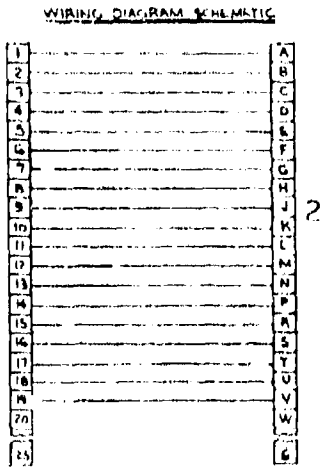


Figure 135. Signal Conductor Reeling Mechanism.





NOTES:

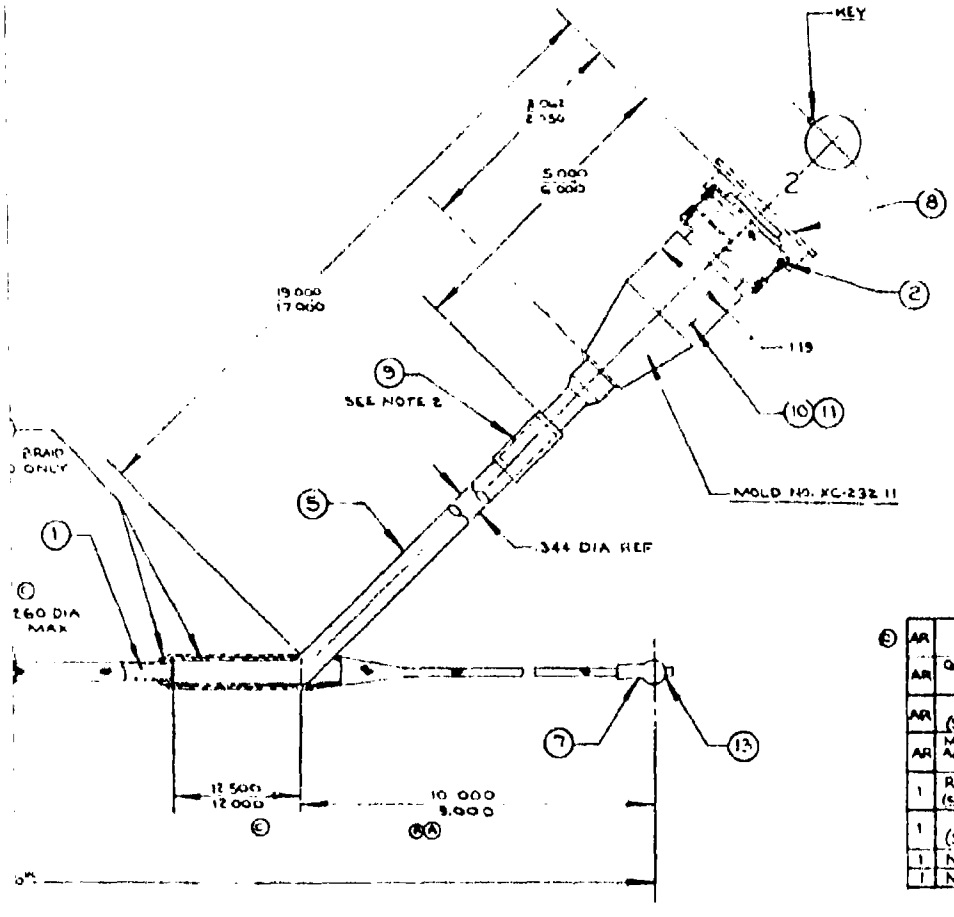
1. SEE DRAWING T-35880 FOR REQUIRED PRIMERS.
2. KINGSLEY STAMP IDENTIFICATION INFORMATION ON ITEM NO. 9 USING 1/8 HIGH WHITE GOTHIC STYLE CHARACTERS. IDENTIFICATION INFORMATION TO BE AS FOLLOWS:

   7879/501-11278-1
   9162S/TEM-N18AE

3. INSULATION RESISTANCE SHALL BE 100 MEGOHMS MINIMUM BETWEEN EACH CONDUCTOR AND ALL OTHER CONDUCTORS AND BETWEEN EACH CONDUCTOR AND THE OUTER BRAID WITH 50VDC APPLIED.

Figure 136. External Signal Conductor.

DATE	REVISION	BY	APPROVALS
1-7-13	A		
1-9-13	B	ITEMS 5 AND 8 [illegible]	
2-8-13	C	12.500-12.000 WAS 7.00 ± .50 WEIGHT 12.5 MAX WAS 12.0 260 DIA MAX WAS .250 DIA MAX REVISED NOTE 3 ITEM 3 WAS MS24394/1-3 ADDED ITEM 13	



Ⓔ	AR	AMS 4770 (S-4771-4)	13	SOLDER-SILVER	KESTER SOLDER Co. CHICAGO, ILL.
	AR	QQ-S-511 SN60 (S-2019)	12	SOLDER-SOFT	FORM W CORE P2 TYPE RA
	AR	4054 (S-20973)	11	POTTING COMPOUND	ACME WIRE Co. HAMDEN, CONN
	AR	MIL-STD-417 SIZE 25 A, B, C, E, J, F2 (S-25021)	10	MOLDING COMPOUND	AIREX INC. PORTLAND, CONN
	1	RNF 100 SIZE 1/2 (S-26145-BA-250)	9	TUBING-BLK THERMOFIT 250V,	RAYCHEM TUBES INC REDWOOD CITY CAL
	1	EC-22 (S-7876-8)	8	CAP-PROTECTIVE	PROTECTIVE CLOS BUFFALO, N.Y.
	1	MS20664C6	7	END BALL	
	1	MS20664C4	6		

TLM-41202

C

Ⓐ(2)	1	219 I.D x .062 WALL (S-25762-219 GRADE 4)	5	TUBING-NEOPRENE	MIL-C-13777 4½ FT
	AR	T-35700-3-4	4	BRAID-WIRE CRES	
Ⓒ	1	M24308/3-3 (S-28936) N/D	3	CONNECTOR-RECTANGULAR	CANNON ITT SANTA ANA, CAL.
	1	MS27467T17A26SN (S-28329) N/D	2	CONNECTOR-PLUG	BENDIX CORP.
	1	WR-1002 BG	1	CABLE 19 COND 22 GA.	

PART NO.	ITEM	NOMENCLATURE
12-11-12	3	

TLM-41202

capicon / REVERE ELECTRONIC DIVISION

600 NORTH COLONY ROAD WALLINGFORD CONN 06492

UNLESS OTHERWISE SPECIFIED

MATERIAL SHARP EDGES AND CORNERS	FINISH	MATERIAL AND FINISH SURFACE TREATMENT	
ALLOWABLE TOLERANCES			
FRACTIONS	DECIMALS	ANGLES	
	.XX ± .01		

NEXT ASSY | USED ON

APPLICATION

LEAD ASSEMBLY ELECTRICAL MOLDED

		CODE IDENT NO 50625	SIZE D
			DRAWING NUMBER TLM-41202
	WEIGHT 12.5 LBS MAX	SCALE NONE	SHEET OF

DO NOT SCALE DWG

SOURCE DWG NO. 501-11278

PRIMERS.

FORMATION ON ITEM NO. 9 CHARACTERS, IDENTI- LOWS:

DO MEGOHMS NO AT OTHER UCTOR AND THE

strip conductors 0.006 x 0.065 inch section, embedded in a Polyimide insulating material, the finished section being 2.5 inches wide and .014 inch thick. The 20-foot-long tape shown in Figure 137 has one end potted to the central, stationary, shaft of the conductor reel, such that the electrical connections are made within the shaft to an MS type connector on the outside of the reel. The other end of the tape terminates in a rectangular connector that mates with the external conductor at the inner surface of the drum. Figure 138 shows the tape assembled to the shaft.

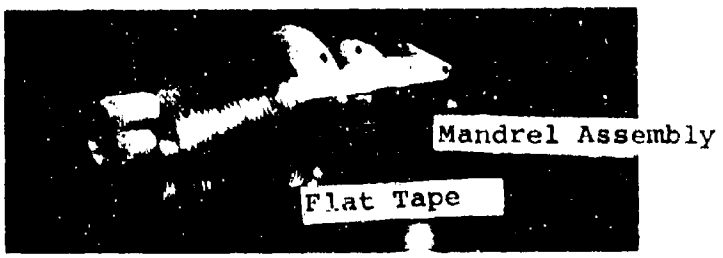


Figure 138. Flat Tape and Mandrel Assembly.

Signal Conductor Reeling Mechanism

The reeling mechanism contains the following basic components:

1. An air turbine with three inlet nozzles. One nozzle imparts normal operating torque and the other two, plus the nozzle imparting normal operating torque, are used to impart alternate hook release torque.

2. A gear reduction between the turbine and cable reel.

3. A drum capable of receiving 140 feet of .25-inch diameter signal conductor cable.

4. A level wind mechanism which distributes the signal conductor in even layers onto the reeling drum.

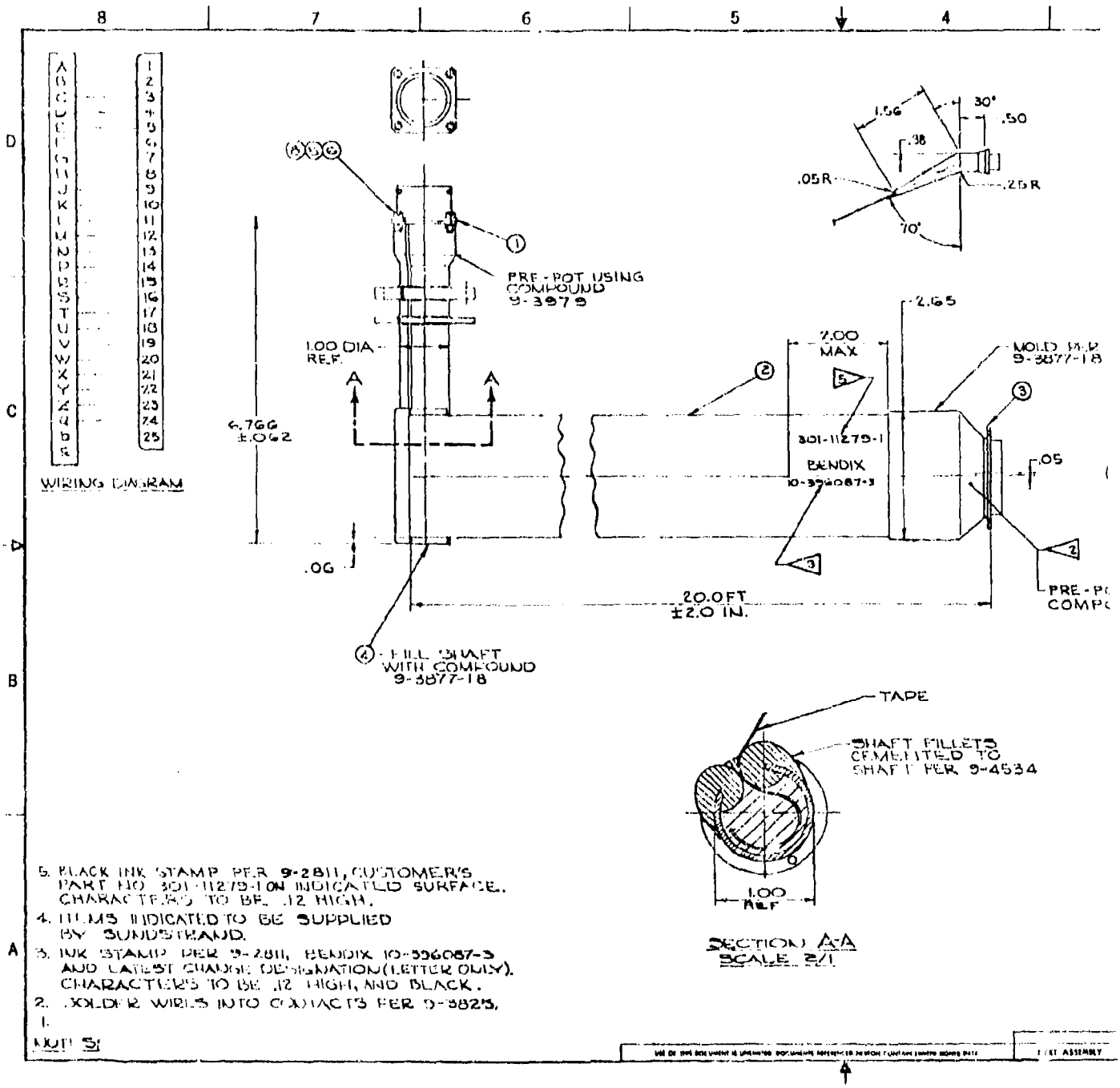
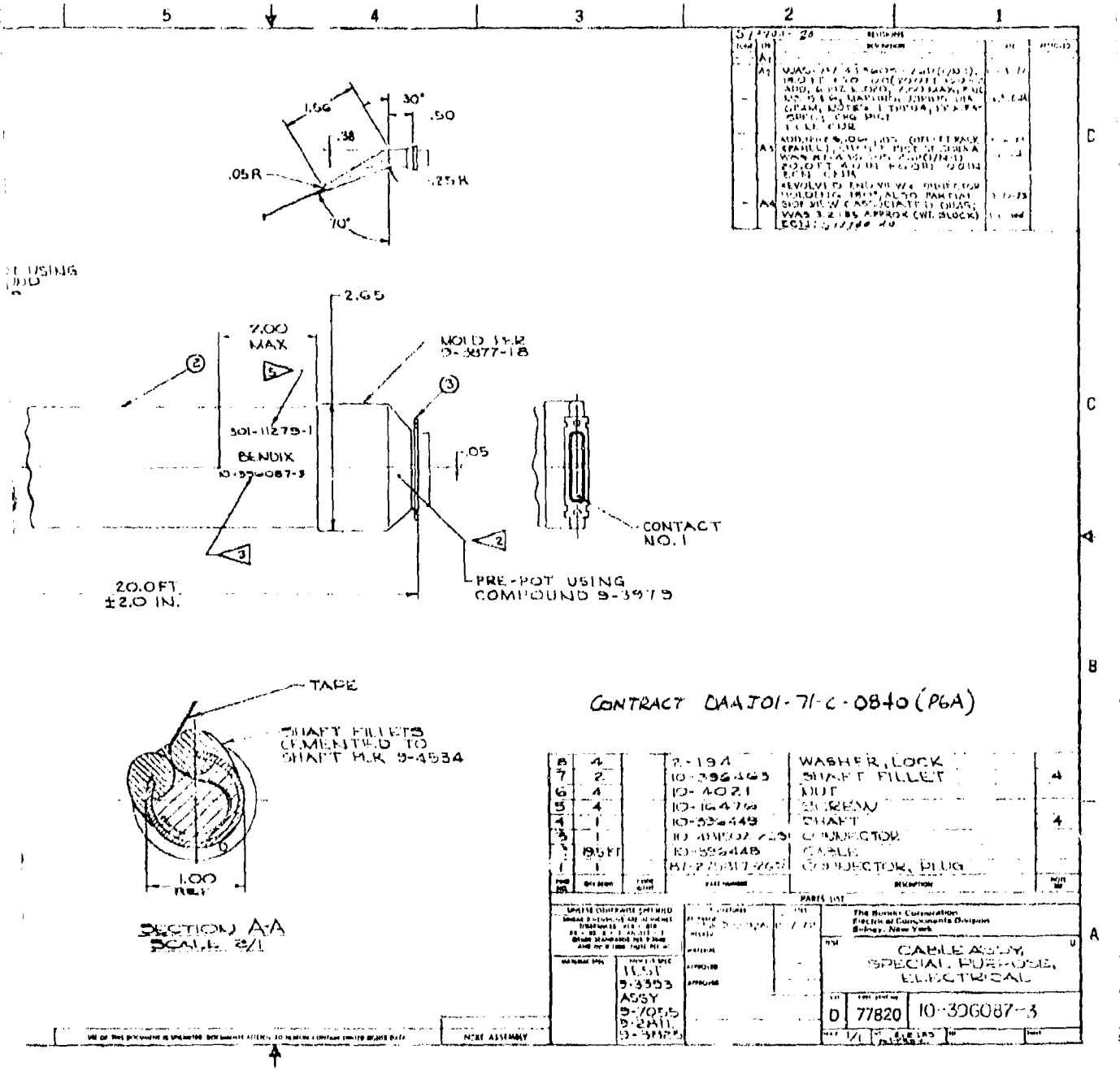


Figure 137. Flat Tape Internal Signal Conductor.


5
4
3
2
1
1.56
30°
.50
.38
.05R
.25R
70°
2.65
2.00
MAX
MOLD PER
9-3877-18
501-11279-1
BENDIX
10-306087-3
.05
CONTACT
NO. 1
20.0 FT.
±2.0 IN.
PRE-POT USING
COMPOUND 9-3979
TAPE
SHAFT FILLETS
CEMENTED TO
SHAFT PER 9-4534
1.00
REF
SECTION A-A
SCALE 2/1
CONTRACT DAAJ01-71-C-0840 (P6A)
WASHER, LOCK
SHAFT FILLET
NUT
SCREW
SHAFT
CONDUCTOR
CABLE
CONDUCTOR, PLUG
PARTS LIST
The Bendix Corporation
Electrical Components Division
Sidney, New York
CABLE ASSY,
SPECIAL PURPOSE,
ELECTRICAL
D
77820
10-306087-3
NEXT ASSEMBLY

1 Conductor.

5. A signal transfer mechanism. This mechanism consists of an electrical conductor tape roll which is connected to a stationary arbor at its inside end and to the revolving cable reel at its outside end.

The air turbine was designed to produce a steady tension on the conductor cable of between 80 and 100 lb at all cable speeds and be capable of providing a tension of approximately 350 lb at zero cable speed for the coupling release.

The turbine wheel size was chosen to ensure small mass flow requirements from a low polar moment of inertia system. This was achieved by using an existing Sundstrand wheel design with nozzles tailored for this application. The wheel is a single-stage axial impulse design having symmetrical buckets generated on the disc by electrochemical milling. Manufacture of the wheel could thus be accomplished with existing tooling. Three convergent/divergent circular nozzles are utilized. One supplies air for the steady tension requirements. Hook release torque is generated by activating the additional nozzles. The hook release valve is normally closed.

Turbine Wheel Design Data

Pitch diameter - inch	4.152
Blade height - inch	0.325
Blade chord - inch	0.25
Blade angle - deg	27
No. of blades	82
Speed at maximum cable speed - rpm	4,300

Normal Tension Nozzle

No. of nozzles	1
Nozzle angle - deg	20
Nozzle throat diameter - inch	0.208
Airflow rate (design day condition) - lb/sec	0.032
Normal tension range - pounds	60 to 120
Normal speed range	120 ft/min reel-in to 120 ft/min payout

Hook Release Nozzle Design

No. of nozzles	2
Nozzle angle - deg	20
Nozzle throat diameter - inch	0.3004
Airflow rate (per nozzle) - lb/sec	0.0667
Hook release tension - pounds	300

The turbine wheel has an integral shaft supported by two ball bearings within a cast aluminum housing. The nozzles are mounted in this housing. A closure plate that also forms the turbine containment ring contains the exhaust-ports. The exhaust from the constant tension nozzle is ducted to the center of the level wind shaft to prevent freezing of the level wind mechanism.

The air supply for the three nozzles is provided by a single connection to the aircraft pneumatic system. Downstream of this connection the tube bifurcates; one line going directly to the constant tension nozzle, the other line connecting to a normally closed solenoid valve. From the outlet side of the valve, the tube divides to provide individual connections to the coupling release nozzles. The valve is electrically operated "open" when a remote mechanical release of the coupling is required.

The estimated reeling mechanism performance at sea level, 95° day condition and 4000 ft, 95° day condition is shown in Figure 139 and Figure 140, respectively.

A 14-tooth gear pinion is attached to the turbine shaft, providing the input to the reduction gear assembly. Total reduction is approximately 64:1. Two jackshafts provide pinion and gear sets to achieve this reduction with the final drive being on the centerline of the drum. Jackshafts and the final drive gear are supported on roller bearings within a cast aluminum housing. The gears are splash lubricated by MIL-L-7808 oil. Table 18 provides the design data of the reduction gears.

The final drive gear is connected to the conductor cable storage reel by a short splined shaft, configured to provide a shear section as a mechanical fuse. This section is designed to shear when the torque exceeds the coupling release torque by a factor of 1.5. Thus, in the event that an external cargo was jettisoned, the inertia of the turbine wheel would cause this section to shear before the reel speed could damage the gears or the turbine.

The storage reel is machined from an aluminum casting with a 6.5-inch outside diameter. The reel accommodates 140 ft of external conductor in three layers. The reel is supported on ball bearings at each end beyond the conductor storage area.

The reduction gear housing closes the drive end of the reel while the supporting plate for the flat tape conductor shaft closes the other end. The reel support bearings are mounted within the reel closure members, which in turn are attached to the cast aluminum mounting frame.

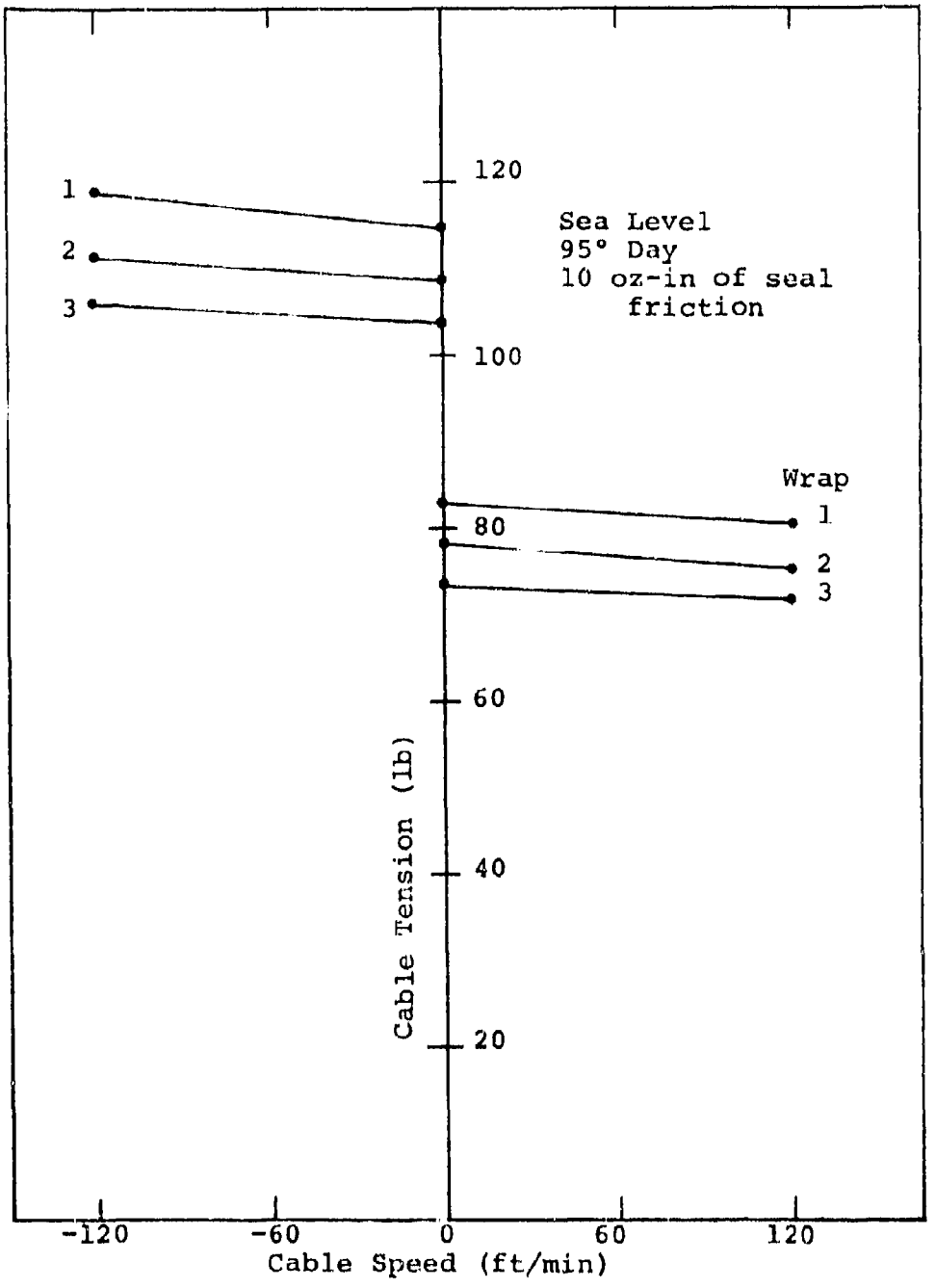


Figure 139. Reeling Mechanism Performance (Sea Level).

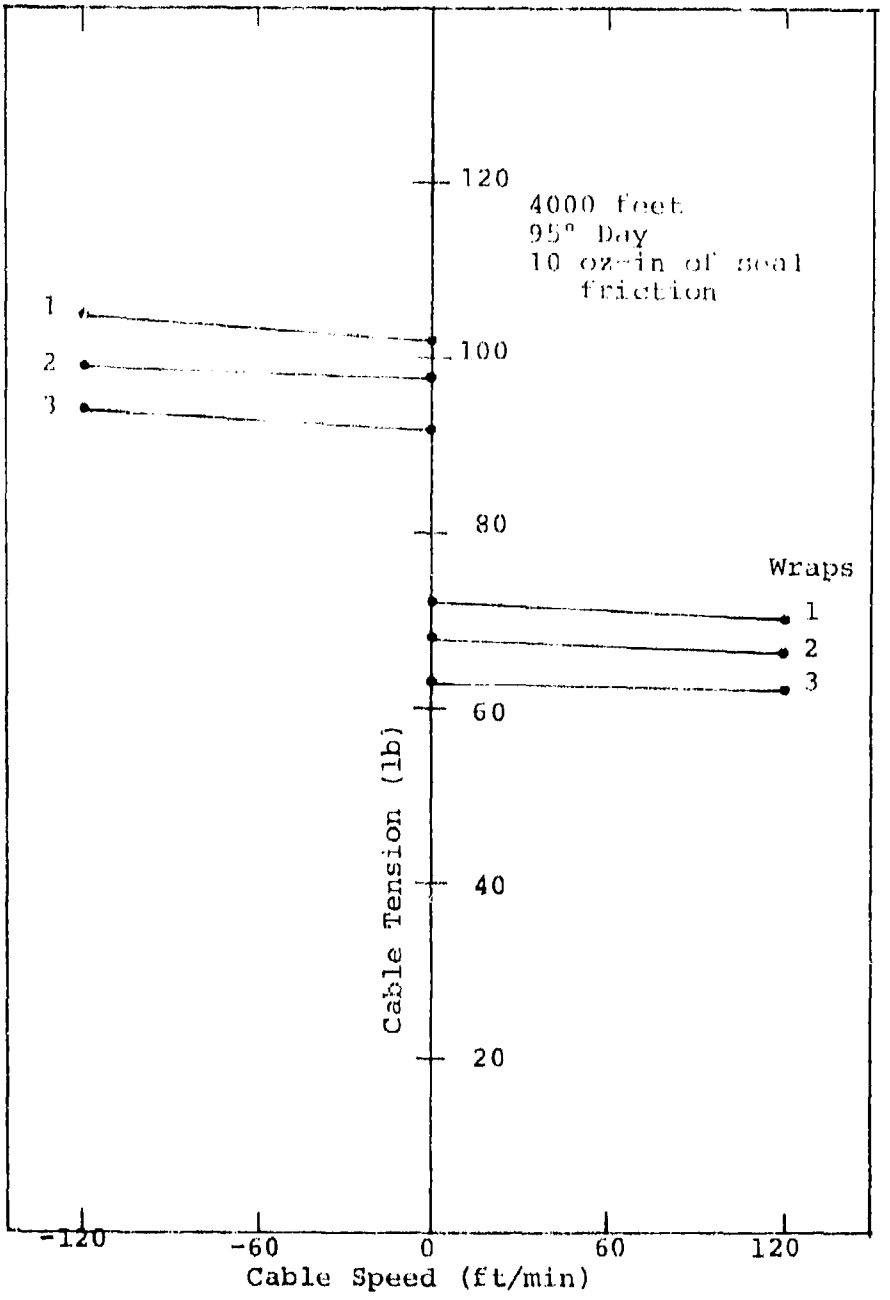


Figure 140. Reeling Mechanism Performance (4,000 Feet Altitude).

TABLE 18. DETAIL DESIGN SUMMARY OF GEARS.

	High-Speed Mesh		Middle Mesh		Low-Speed Mesh	
	Pinion	Gear	Pinion	Gear	Pinion	Gear
Pitch	20	20	20	20	12	12
Face Width	0.125	0.125	0.375	0.375	0.625	0.625
Number of Teeth	14	92	13	45	10	28
Speed (rpm) @ 120 ft/min	4310	657	657	190	190	67.9
Pitch Diameter (in)	0.700	4.60	0.650	2.25	0.833	2.33
Operating Torque in lb	4.75	31.21	31.21	108	108	302.5
Hook Release Torque	21.4	140	140	486	486	1360
Shear Torque	31.1	210	210	730	730	2050
*Bending Stress (ksi)	2.1	2.1	10.4	11.4	13.9	12.2
**Bending Stress (ksi)	16.3	16.4	83.6	91.3	111.2	98.1
*Contact Stress (ksi)	45.4	45.4	108.1	108.1	124.9	124.9

*Normal Operation
**During shearing of the shear section

The external conductor level wind mechanism is supported on sealed ball bearings mounted on arms extending from each end of the reel. These arms are supported on Teflon bearings concentric with the centerline of the reel such that the level wind shaft can rotate approximately 150° about the drum, permitting the level wind to align with the conductor exit angle. The level wind shaft has L.H. and R.H. helically machined grooves on its outside diameter such that pins within the follower nut engage these grooves and rotation of the shaft results in linear motion of the nut. The shaft is driven by a chain and sprocket mechanism from the reel. The follower nut has two nylon rollers to guide the conductor cable. Rotation of the nut about the shaft is prevented by a guide bar mounted parallel to the shaft.

Figure 141 shows the assembly drawing of the complete reeling mechanism.

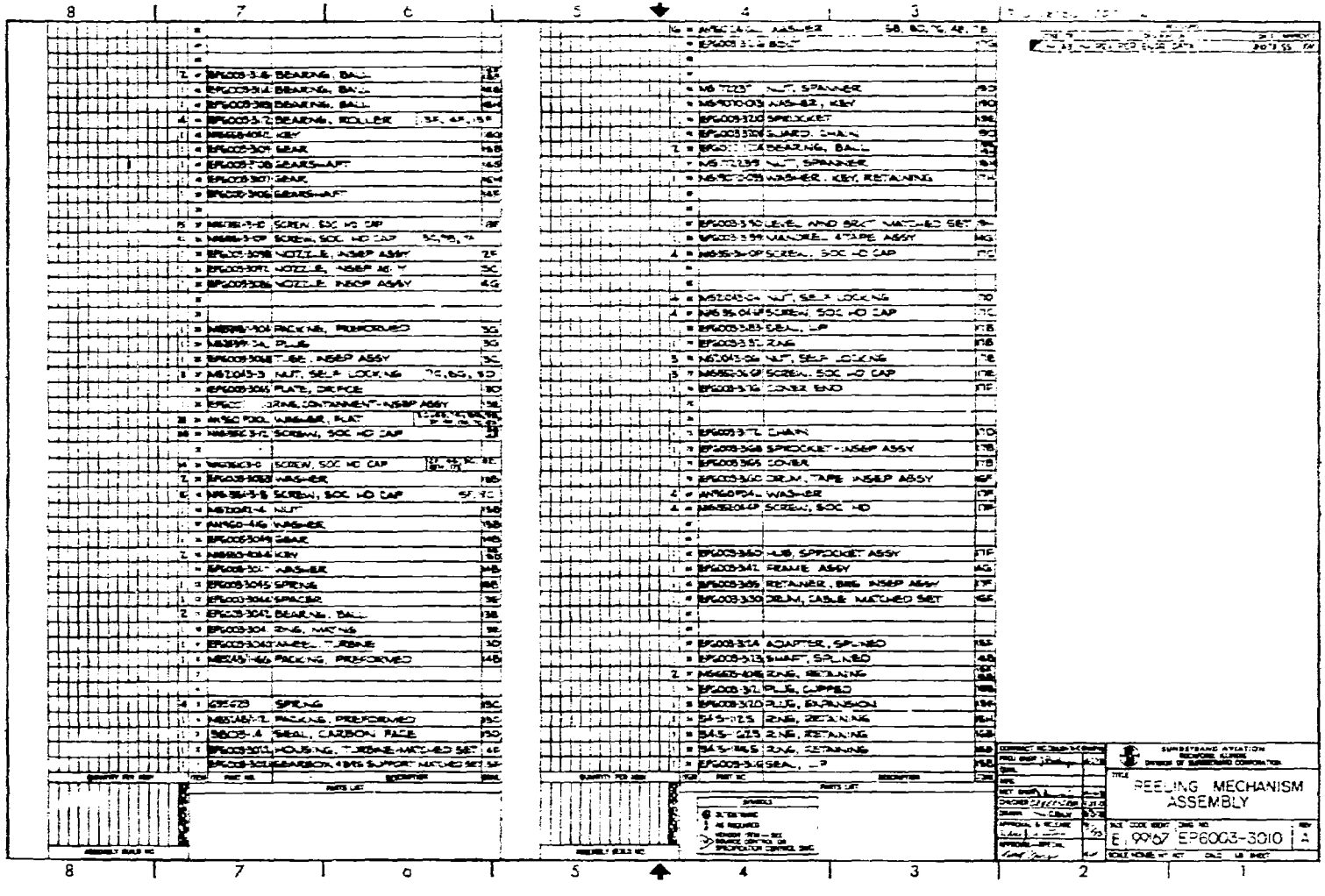


Figure 141. Design Layout of Signal Conductor Reel Assembly (Sheet 1 of 4).

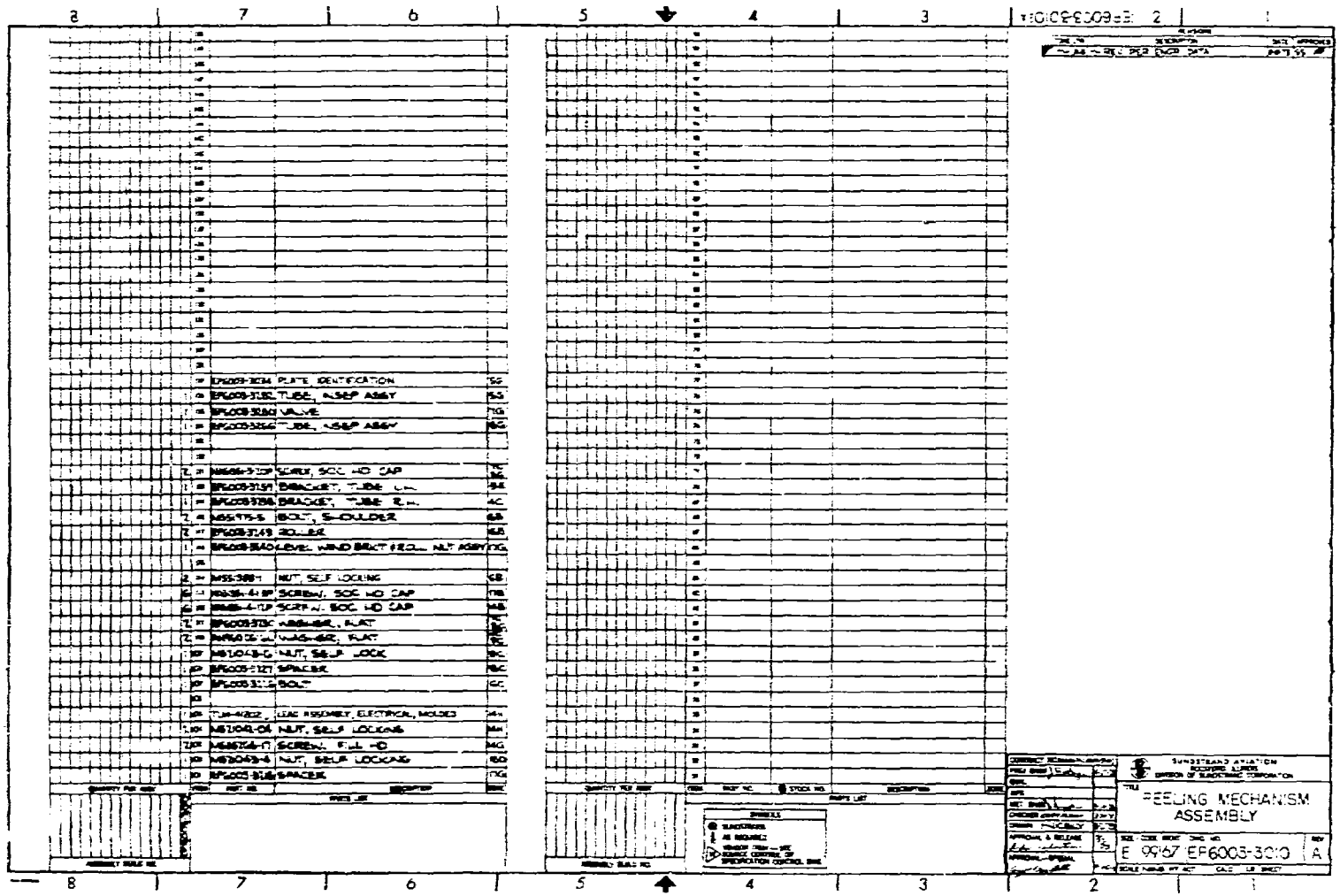


Figure 141. Continued (Sheet 2 of 4).

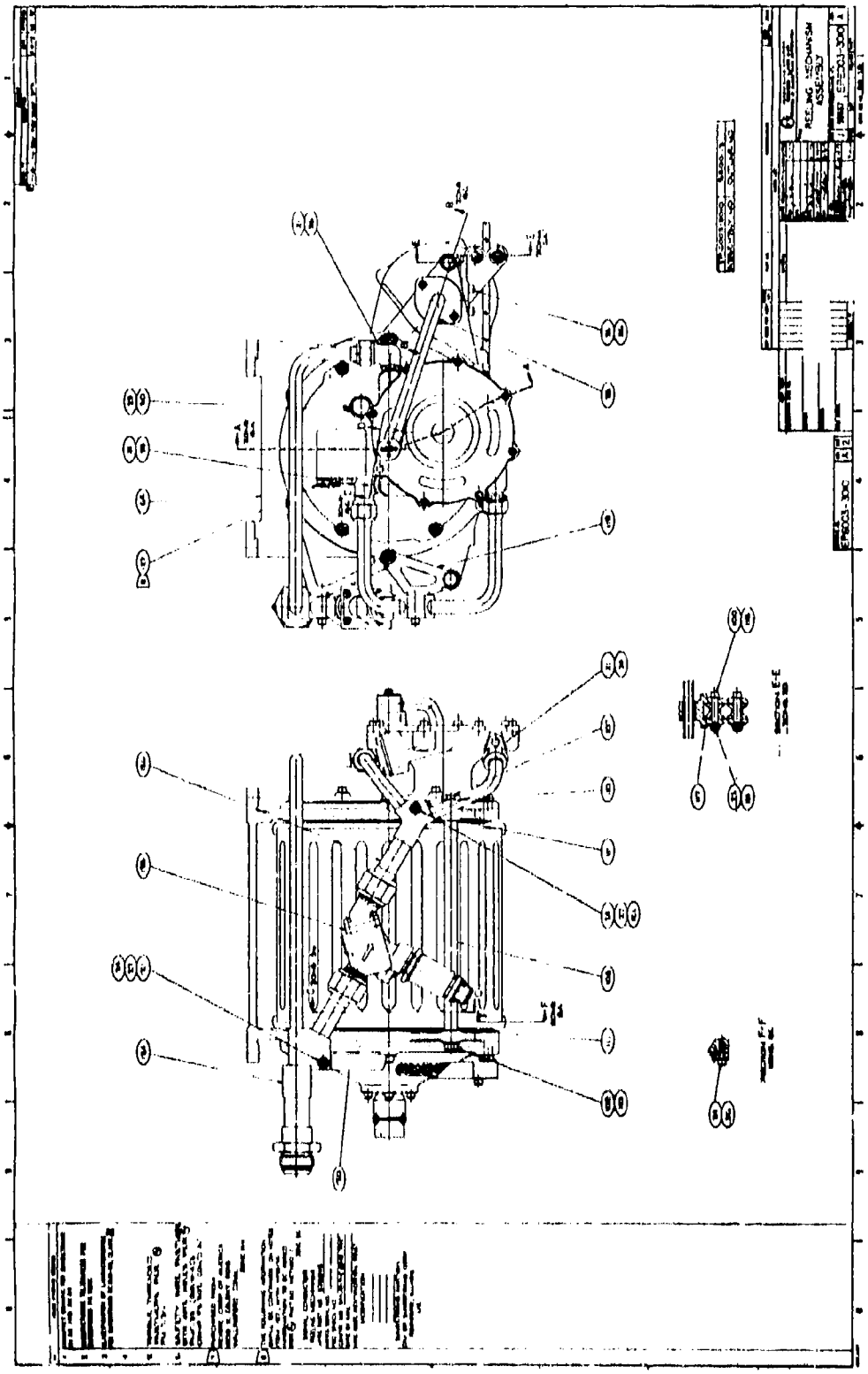


Figure 141. Continued (Sheet 3 of 4).

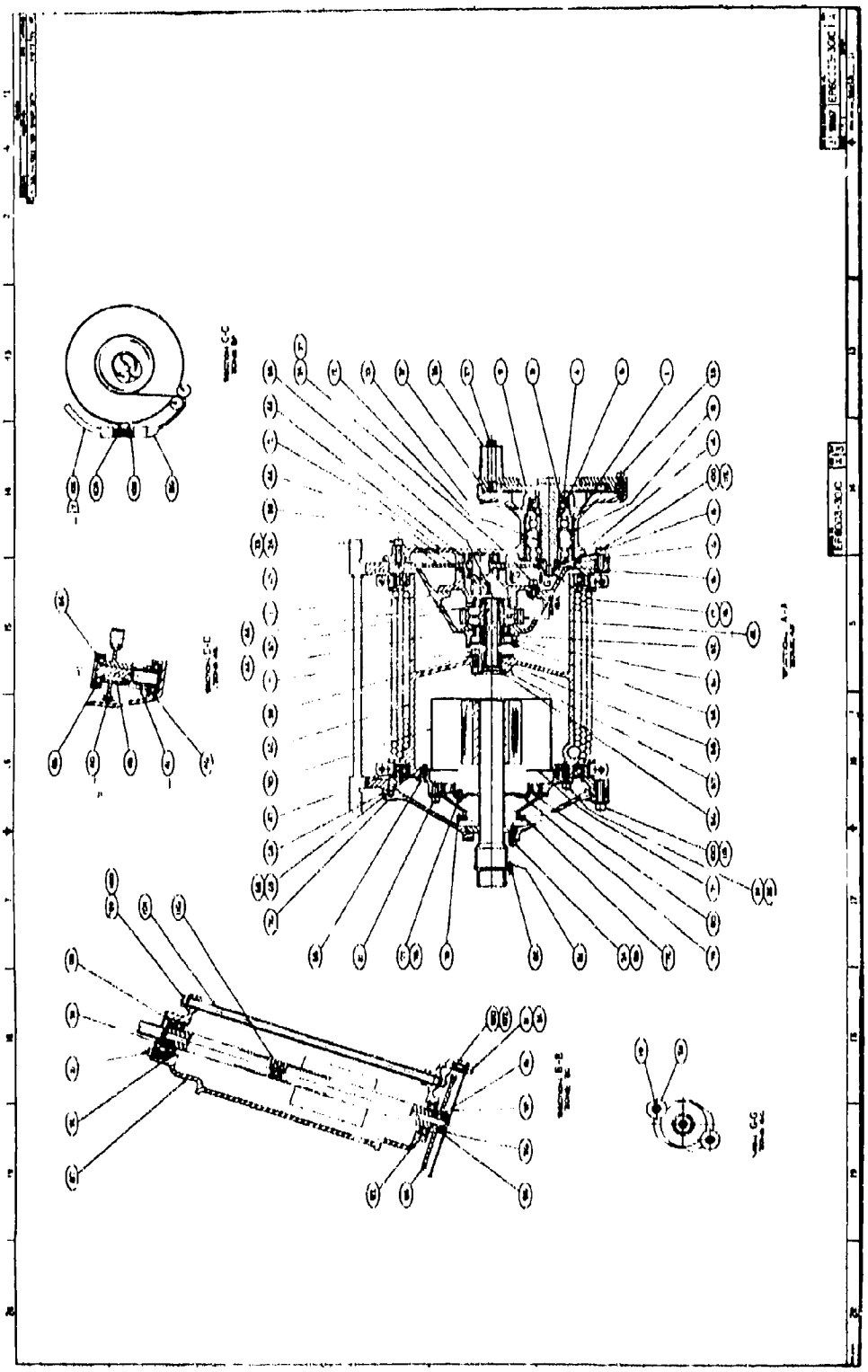


Figure 141. Concluded (Sheet 4 of 4).

CONTROLS AND DISPLAYS

Design Requirements

The general concept for cargo handling system controls and displays for the HLH was envisioned initially to be driven by four primary influencing factors:

1. The environmental conditions under which cargo handling operations are to be conducted.

2. The operational characteristics of the cargo handling system itself.

3. The accuracy with which cargo must be extracted or placed.

4. The precision with which aircraft/cargo system could be positioned in inertial space.

Those experienced in external cargo handling operations have for a long time realized the limitations associated with precise aircraft/load positioning under conditions of darkness, blowing dust or blowing snow. To aid in expanding operations into this heretofore restricted regime, a means for enhancing and augmenting a load controlling crewman's (LCCs) normal vision was considered mandatory. This facet of cargo system display is so important that it is discussed in a separate section. Even with a capability for visual augmentation, it was assumed initially that there is certain minimal information required which is not part of natural visual cueing, even under ideal meterological conditions. These cues rationally would include information pertinent to tension member loads, angles and extended lengths, as well as status of the couplings. Use of vertical scale and/or multi-mode displays was envisioned to provide these cues. In addition, it was assumed initially, based on experience in power-limited aircraft, that the operator would need some form of power display to assure that he would not call for more power than the aircraft could develop.

Initial concepts for external cargo system controls were predicated upon a hoist control system which provided both independent and synchronous, fully-variable speed control of the two hoists, with hoist speed directly proportional to the extent of control application, in displacement, force, or both. Based on consideration of existing helicopter flight control configurations, it was assumed the external cargo system controls would be manipulated with the operator's left hand in consort or time-shared with vertical control of the aircraft. In addition to hoist control, controls requirements also were envisioned for manual application of the hoist brake

and operation of emergency cable-cutting functions.

Studies, Analyses, and Procedures

The HLH Aircraft System Requirements Document (ASRD) contributed to more detailed definition of external cargo system controls/displays. It defined requirements for anthropometric and arctic clothing accommodations; system operation without release of flight controls; normal and emergency control, as well as release test circuitry; and invocation of MIL-H-46855 as a human engineering guideline to selection and arrangement of controls and displays. In order to limit technical consideration to those control/display concepts which would be feasible within the HLH ATC program time frame, one of the first steps in the preliminary design procedure was to produce an annotated bibliography and state-of-the-art projection of control/display technology for the 1970-1980 period. Since neither program schedule nor budget would permit advancement of the state of the art in control/display technology, a cutoff date of 1971 was established as a limiting date for technology which could be applied realistically to the External Cargo System ATC. Established state of the art is summarized as follows:

Controls: Mechanical, electromechanical, electromagnetic, electronic, push-button switches, modest computer assistance.

Displays: Conventional electromechanical, cathode ray tube (multi-gun, multi-colored, ported), vertical scale (electromechanical, electroluminescent, LED, fiber optic), alphanumeric (drum counter, vacuum tube, projected, solid state).

Establishment of Relationship Between External Cargo and Flight Control Systems

In order to rationalize the accuracy with which cargo must be extracted and placed, it was first necessary to define a composite operational scenario and mission profile representative of the broadest spectrum of worst case conditions under which the HLH might be required to operate. This scenario postulates a general ship-to-shore operation over a 5-mile course length and an approximate 12-minute sortie cycle time. An additional section of the scenario details the load controlling mission segment. In order to relate the cargo handling system to the flight control system in the context of this profile, several other relationships had to be considered.

1. The effect of precision hover system and load stabilization system on cargo handling operations.

2. The relationship of automatic flight path control to cargo handling.

3. The relationship of cargo load motion to aircraft flying qualities.

4. The relationship of ship motion to containership loading operations.

To gain insight into the relations of 1, 2, and 3 above, comments from operational pilots were reviewed pertinent to external cargo handling operations in the CH-46, CH-47, CH-53 and CH-54. Specific parameters considered were:

1. General external load handling capability.

2. Aircraft stability and handling qualities.

3. Capability for all weather cargo operations.

4. Load and load area visibility.

5. Current techniques for external cargo operations.

Particular attention was devoted to the details of CH-54 operation because of the aircraft considered, CH-54 operations most closely resembled those projected for the HLH. Selected project operational and technical personnel were permitted to experience cargo handling operations in the CH-54 to assure better understanding of the operational control and display problems involved.

Functional Analyses

Using the cited operational scenario/mission profile and knowledge of capabilities and limitations gained from analysis of and experience with existing cargo systems, functional flow diagrams for cargo system operation were generated down to the third level of analysis.

Determination of Action/Information Requirements

A survey questionnaire was prepared and circulated to thirteen subjects representing engineering and operational disciplines. Subjects were given a baseline list of action/information requirements, which they were asked to expand upon or reduce as they saw fit. Justification was required for retention, addition or deletion of each item. The survey resulted in the

identification of 66 action/information requirements. Items desired by a majority (7 or more evaluators) were considered mandatory for preliminary design. This process reduced the total number of action/information items from 66 to 20. These items were categorized into cargo and non-cargo system functions, as follows:

Cargo System Items

Actual Load Weight
*Hoist Mode (Configuration)
*Hoist Speed
Cable Extended Length
Cable Tension
Hook Position Relative to Load
Load Position Relative to Load Zone
Load Attitude (Pitch)
*Hook Open/Closed Condition
Hook Lock/Unlocked Condition
*Hook Armed/Safe Condition
*Hook Test Verification
*Night Vision Augmentation
*Dust/Snow Vision Augmentation
*Emergency Release

Non-Cargo System Items

*Absolute Altitude (Wheel Height)
*Aircraft Pitch Attitude
*Aircraft Roll Attitude
*Aircraft Heading

Those items marked (*) were assumed to require action controls, as well as information displays. From this listing, it was rationalized that all non-cargo system controls would probably be accommodated through the flight controller/s and that all non-cargo system display information could be either presented on conventional flight instruments or integrated into the VAS at some future date. The VAS control and display also would accommodate the night/dust/snow vision augmentation requirements, as well as those for hook/load and load/zone relative position information. It was further rationalized that the remaining cargo control system functions could be categorized into two groups:

Operational Controls	Mode Selection/Logic Controls
Hoist Speed	Hoist Mode (Configuration)
Coupling Release	Hook Armed/Safe
Emergency Release	Hook Test Verification

Similarly, cargo system display information was categorized into two groups:

Operational Displays	Mode/Logic Displays
Actual Load Weight	Hoist Mode (Configuration)
Hoist Speed	Hook Open/Closed Condition
Extended Cable Length	Hook Locked/Unlocked Condition
Cable Tension	Hook Armed/Safe Condition
Load Attitude	Hook Test Verification

In addition, it was realized that all crew stations probably would require a caution/advisory panel to provide discrete information relative to subsystems which interface with the cargo handling system. It is interesting to note that initial requirements for display of cable angle and manual application of hoist brake were not justified for inclusion. The supporting rationale for exclusion of cable angle is that the only real means of controlling cable angle is through either the alteration of flight control parameters (attitude, speed, etc.) or through alteration of load pitch attitude. Both of these information items have been provided for. Manual application of hoist brake was not required since the hoist brake system has been designed to function completely automatically.

Alternate Concept Definitions

Since the spectrum of available control/display technology was so broad, initial control display concepts were limited to two extreme configurations -- one representing an austere, segregated, electromechanical approach; the other representing a sophisticated, integrated, state-of-the-art approach. These two concepts were subjected to in-house review by 22 personnel representing various engineering and operational disciplines. The main conclusions and recommendations are summarized as follows:

1. Locate the cable cutter switch to itself or on an emergency panel, rather than on the normal control panel.

2. Orient cargo system control/display devices "fore and aft" wherever possible to correlate with actual hoist system.

3. Use words rather than abbreviations on legended lights wherever possible.

4. Vertical scale presentation of cable length and tension is more easily interpreted than round-dial presentation.

5. Scale cable tensions in 200 lb increments, with each 1000 lb increment numbered.

6. Load weight should be the sum of the weights on each of the two cables.

7. Illuminate the LCC's caution/advisory panel only when his performance is affected.

8. An overall approach somewhere between the most austere and the most sophisticated would be desirable.

The most controversial item of the in-house review was the configuration of the hoist speed controller. The simple two-lever approach presented represented an austere approach, but fell short of good functional/task relation and anthropmetric accommodation. Even though the U.S. Air Force Study on Design and Evaluation of Primary Hand Controllers (AFFDL-TR-71-16, dated December, 1970) had shown preference for lever type control for multi-mode operations, there was sufficient comment from the in-house review to merit reconsideration of the finger-tip type control.

Description of Control/Display Components

Based on conclusions and recommendations from the in-house design review, the following cargo system control/display components and functions were rationalized:

Hoist Controller

Hoist speed command
Hoist synchronization command
Hoist synchronization indication
Coupling release (This function alternately could be located as a right-hand function.)

Cargo System Control Panel

Hoist power on/off and indication
Hoist span position selection and indication
Coupling armed/safe selection and indication
Coupling locked/unlocked indication
Manual backup hook release
System test actuation and indication

Cable Tension Indicator

Actual load weight
Individual cable tension

Cable Length Indicator

Extended cable length
Hoist speed (Estimated from rate of change of cable length.)
Load attitude (Estimated from difference in cable length for given hoist span.)
Hoist span position (Tell-tale indicators)

Consideration of Safety Aspects of External Cargo/Flight Control Operations

The basic components, defined above, were reviewed with particular attention devoted to the safety implications of the basic concepts. Design reviews, both in-house and with the customer, resulted in several significant changes in concept which increased safety and improved operational effectiveness. These are summarized below:

1. Provide guillotine function to all crew stations with simple wiring (no interlocks to prevent guillotining of a stowed hook).

2. Hoist span function at LCC station only.

3. Use pictorial indicators for coupling open/closed/lock status.

4. Locate hook condition indicator on cable tension indicator rather than on cargo system control panel.

5. Eliminate hook release test function since it is superfluous.

Formal Design Review and Design Decisions

The external cargo system and LCC control/display concepts were subjected to formal design review by 13 Boeing Vertol and 9 Army operational and technical personnel. This review was conducted in conjunction with the Model 347 LCC Station Mockup Review so that the reviewers could visualize more easily the application of proposed controls/displays to the actual cargo handling task.

Vendor Proposal Solicitation

A vendor briefing and proposal solicitation for design, mockup and fabrication of the four cargo system control/display components was conducted for 22 vendors. As a result of this solicitation and briefing, the following proposals were received:

1. Contoured grip hoist controller

   Electro-Development Corporation
   Measurement Systems, Inc.
   Mason Electric Company

2. Cargo system control panel

   Barber-Coleman Company
   Canadian Marconi Company
   Electro-Development Corporation
   Hartman Systems, Inc.
   Simmonds Precision, Inc.

3. Cable tension and cable length indicator systems

   Canadian Marconi Company
   Electro-Development Corporation
   Hartman Systems, Inc.
   Simmonds Precision, Inc.
   Weston Instruments (Cable Length only)

Subsequent to evaluation of the proposals received, the following sources were selected:

1. Hoist controller - Measurement Systems, Inc.
2. Control panel - Barber-Coleman Company
3. Indicators - Electro-Development Corporation

Detail Design

As a result of negotiations and technical discussions with the subcontracted sources for the cargo system control/display hardware above, preliminary designs for each of the items of hardware were finalized. Each item is discussed below.

Contoured Grip Hoist Controller

The current configuration of the contoured grip hoist controller, based on the Preliminary Requirements Document, Hoist Control Grip, is shown in Figure 142. The grip is a palm-rest type providing "natural use of the thumb" to control hoist rate, in that up-down motion of the thumb produces up-down motion of the hoists. The two thumb switches also are oriented fore and aft to represent fore and aft location of the hoists. Experimentation with breadboard developmental models has shown that the thumb is sufficiently strong to operate these controls effectively without the use of a soft rubber covering over the thumb grip to reduce fatigue. Grip contours have been kept smooth to permit widest possible accommodation of different hand sizes and thumb lengths.

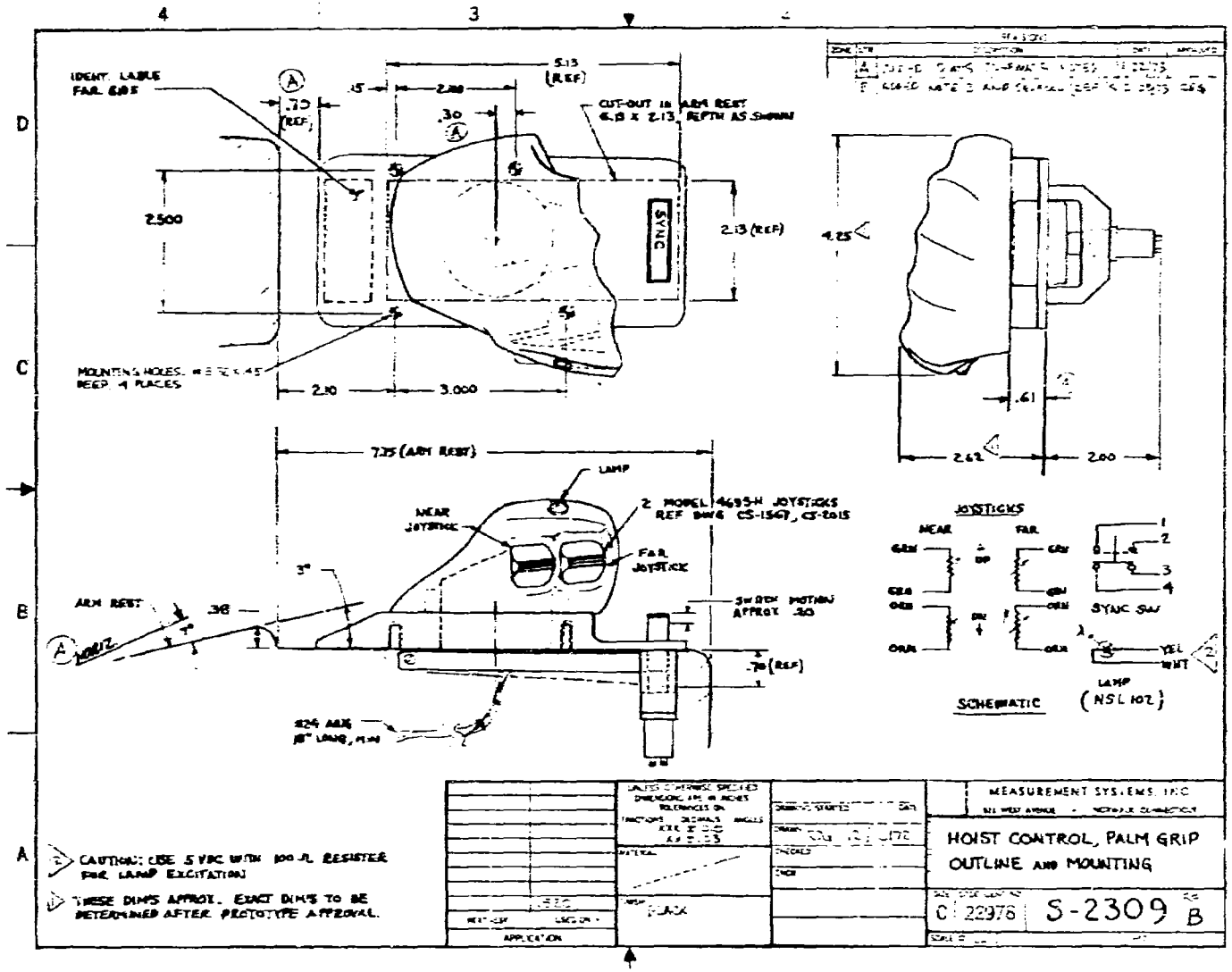


Figure 142. Contoured Grip Hoist Controller.

The switches themselves are MS Model 469 solid state, force switches containing no moving parts, but providing sufficient displacement to create adequate positional cueing and feel, even with an arctic gloved hand.

The output signal is directly and linearly proportional to the input force. Reliability of the Model 469 switches is 100,000 hours MTBF, double that of the connectors and wiring used. The lowest reliability item in the grip is the synchronization command (SYNC) switch, located in the base of the grip. Its 20,000-hour MTBF reduces the overall grip reliability to an estimated MTBF of 9,000 hours. (MSI points out that of more than 3,000 such grips in operation in the field, not one has been returned for repair in over three years.) In addition to the SYNC switch, a SYNC light is provided in the top of the grip to indicate to the operator when the synchronized mode of hoist operation has been selected. The grip and its switches are easily replaceable. In addition, the switch mechanisms are repairable. Since the grip is made around a metal grip shell, RFI/EMI requirements can be met easily. In addition, this construction is less subject to inadvertent damage and is safe during crashes. All components are available off-the-shelf and already are qualified to military helicopter environments.

Cargo System Control Panel

The procurement configuration of the cargo system control panel (see Figures 143 and 144) is closely similar to the suggested panel configuration in the Preliminary Requirements Document, Cargo System Control Panel. Two fully operational panels were procured. The rectangular switches themselves are lighted-legended push-button switches, whose characteristics are representative of MIL-STD switches. The control will permit complete operation of the cargo system from either of the two locations (cockpit or LCC station) selected by the control transfer switch. The legends on both panels will indicate the status of the controlled functions regardless of which station has assumed control. The mechanical hook release control is a ring-guarded, momentary contact switch which actuates the mechanical hook release sequence.

In operation, the control transfer switch selects the panel location to perform the control functions by "enabling" the other switches on the selected panel. The OPERATE/STOW switches are connected to the hoist electrical systems by switching logic such that the STOW function can occur only if the hook is unloaded and in a SAFE condition. When the STOW mode is selected, the hoist will raise the hook to its highest position and then disable the power to the hoist assembly. The OPERATE function makes power available to the

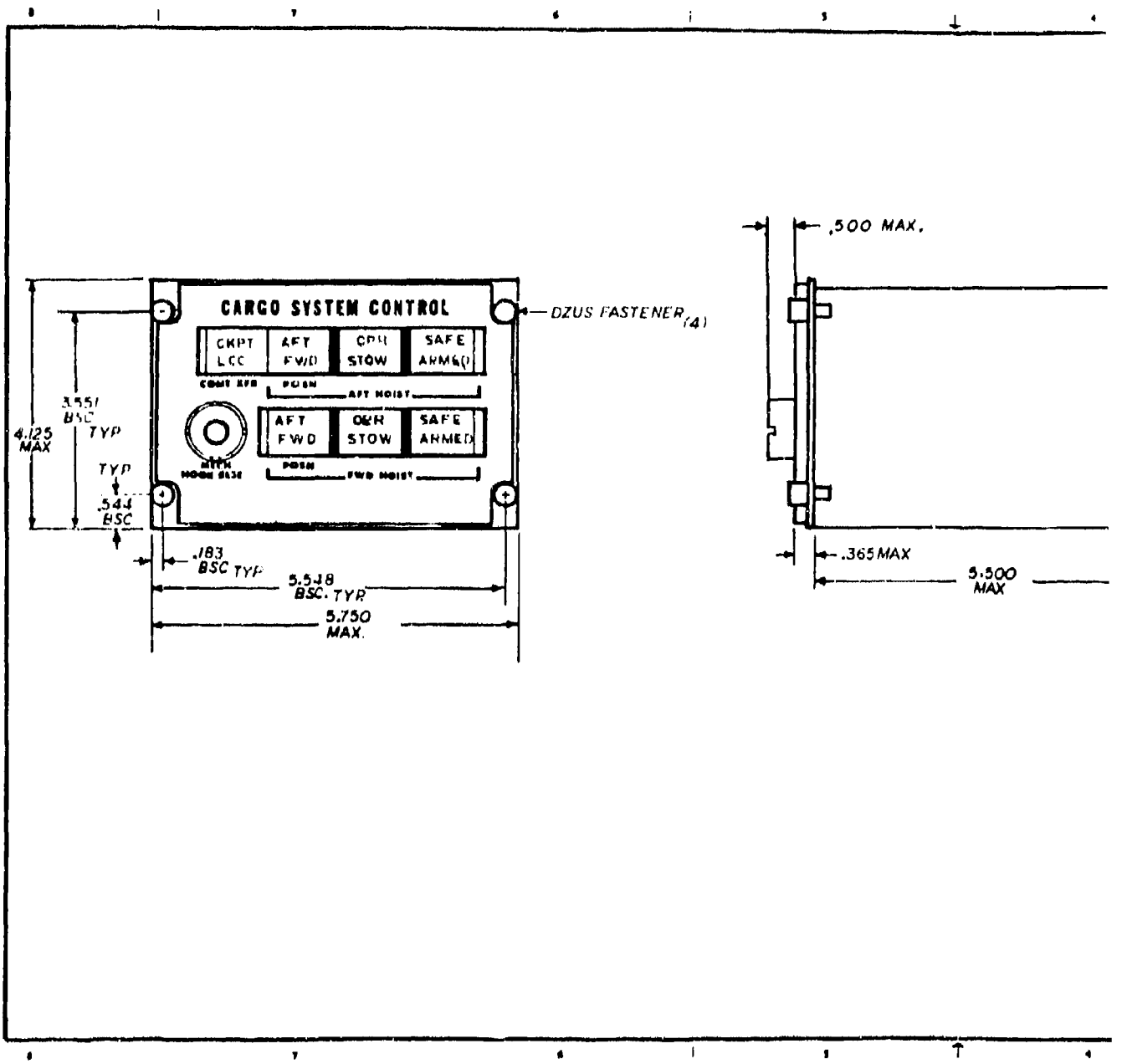
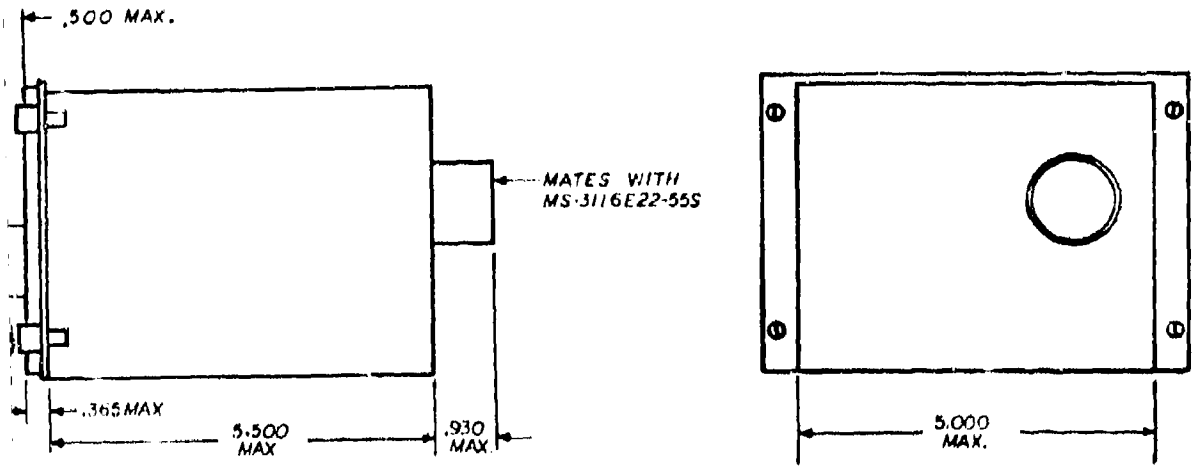


Figure 143. Cargo System Control Panel.

REVISIONS			
LTR	DESCRIPTION	DATE	APPROVED
A1	WAS MS3116E20-41S		
A2	CHANGED PANEL VIEW	2-28-73	LR



INSTALLATION DRAWING
SHEET 1 OF 1

REFERENCES: VERTOL 107-II Yl. 1601 TRUE POSITION TOLERANCING	DRAWN BY W. H. McHUGH DATE 2-14-73 CHECKED DATE 16 FEB 73 APPROVED DATE 16 FEB 73	UNLESS OTHERWISE SPECIFIED DIMENSIONS ARE IN INCHES TOLERANCES ON DECIMALS ANGLES	HARBER-COLMAN COMPANY ROCKFORD ILLINOIS U.S.A. NAME CONTROL BOX CARGO HOOIST SIZE D CODE IDENT NO 05624 PART NO FYLZ 50257 FINISH NONE

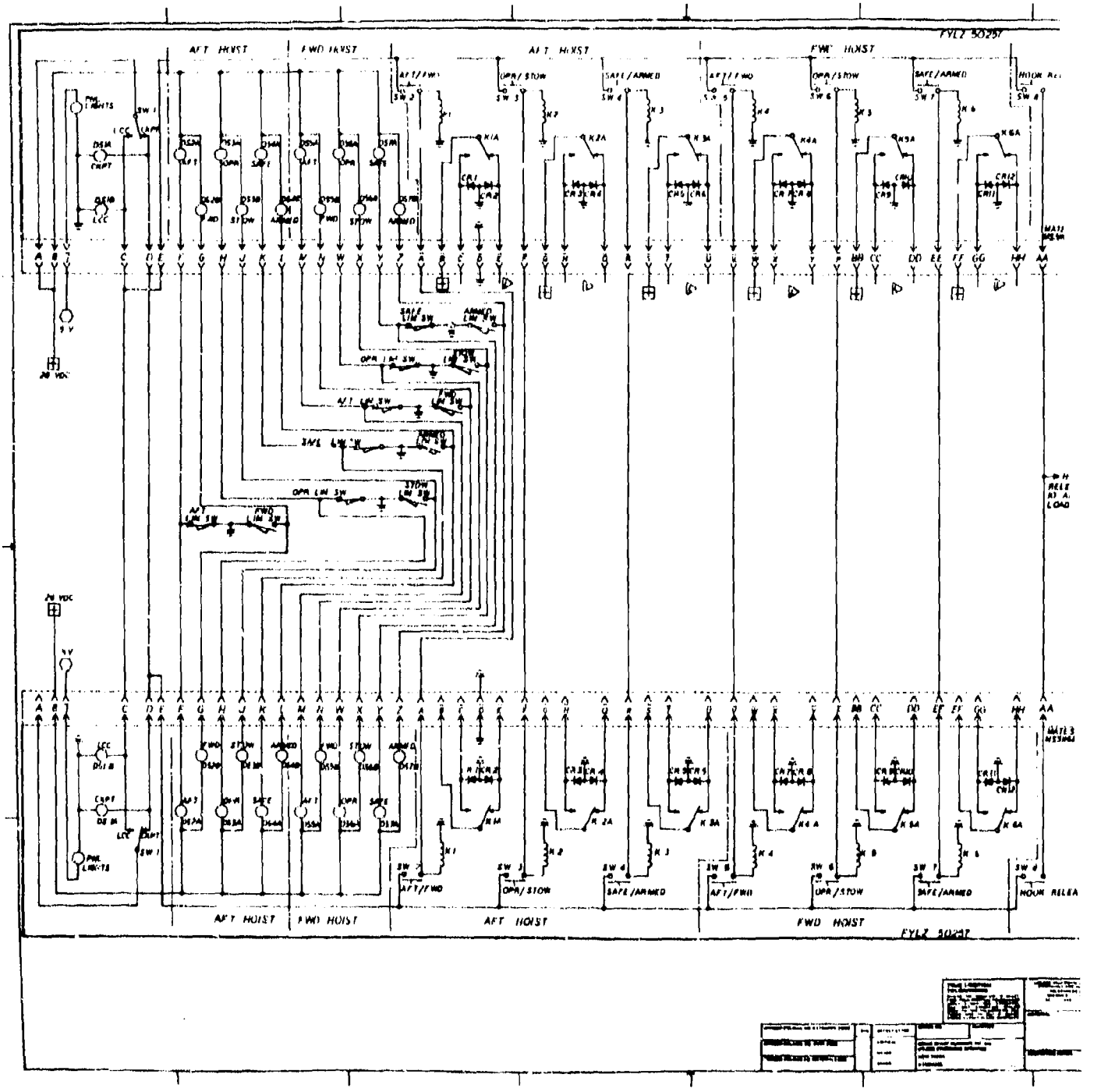
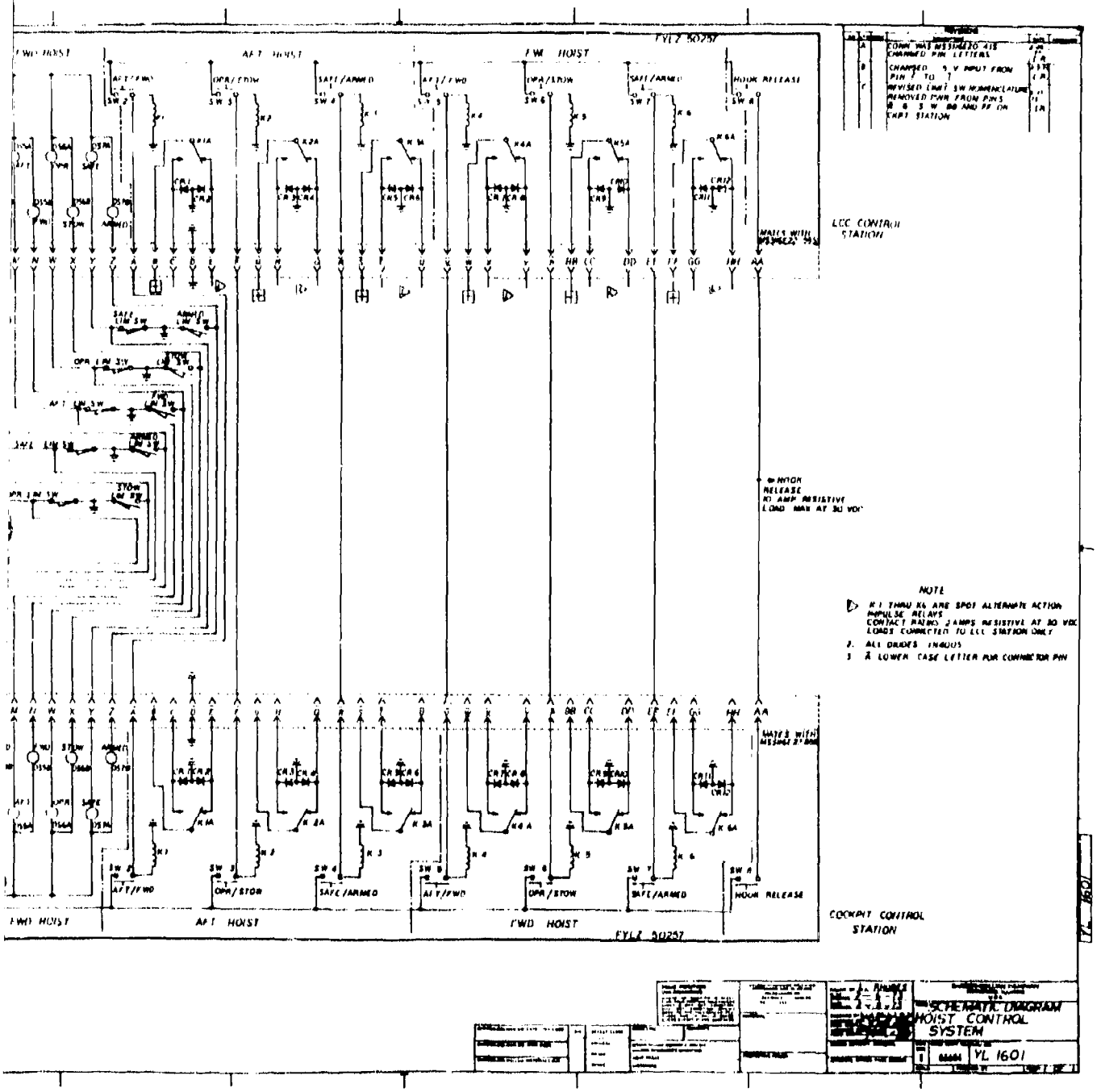


Figure 144. Schematic of Cargo Control System.



Schematic of Cargo Control System.

hoist system. The SAFE/ARMED switches enable the electrical hook release circuits in the ARMED condition and disables them in the SAFE position. The POS'N switches select the desired span position of the respective hoist assemblies. They are enabled only when the hooks are unloaded (less than 1,000 lb). The legend is illuminated when the selected position has been achieved. The controls are designed such that the last selected mode remains in effect upon control transfer or after a power interruption.

Display System

The cable tension and cable length indicating system consists of an interface electronics unit, a cable tension indicator, and a cable length indicator.

The cable tension indicator and cable length indicator are shown in Figures 145 and 146. The cable length indicator displays to the load controlling crewman (LCC) the length of cable payed out from each of the forward and aft hoists and in addition indicates the span position of both hoists.

The cable tension indicator displays to the LCC the tension in each of the forward and aft cables and the total load weight suspended on the cables. A caution flag is presented if the load weight exceeds 70,000 lb. In addition, it displays the status of the forward and aft cargo hooks, locked, unlocked, or open.

The interface electronics unit provides the interface between the cargo handling system sensors and the cable length and cable tension indicators. It computes the cable length, cable tension and total load weight from inputs of length, load isolator force, cable angle and the attitude of the helicopter. In addition to the signals to the indicators, the unit also provides warning outputs to indicate load unbalance, excessive cable tension or load overweight. A pictorial presentation is shown in Figure 147.

Interface Electronics Unit

Theory of Operation. The interface electronics unit provides the interface between the cargo handling system transducers and sensors and the cargo handling system cable length and cable tension indicators.

The interface electronics unit accepts inputs from the cable length, load isolator force, cable pitch angle and roll angle transducers, and provides the necessary signal conditioning and computation circuitry to provide analog outputs of cable length, cable tension and load weight for the indicators.

REPRODUCED FROM BEST AVAILABLE COPY

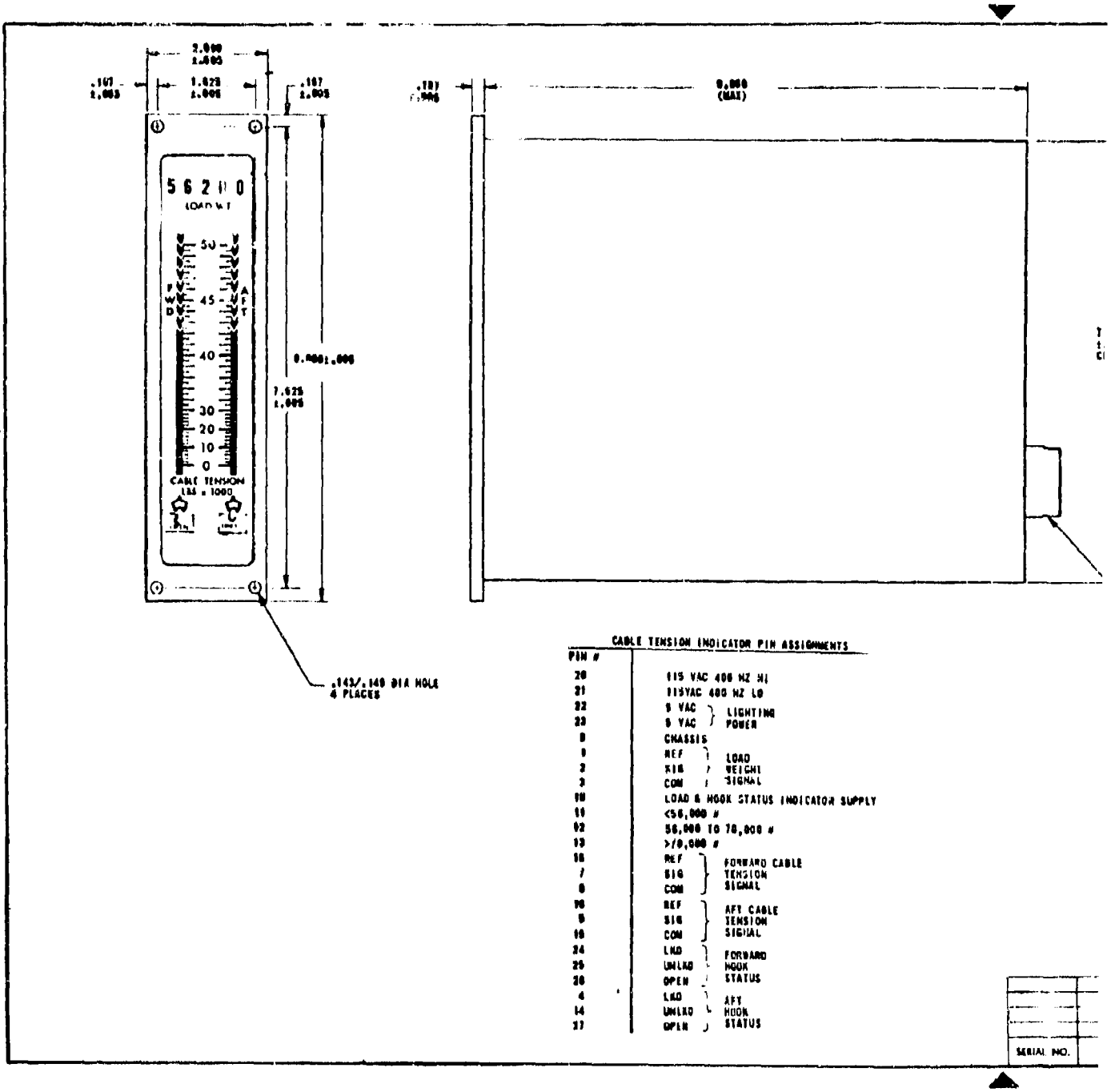
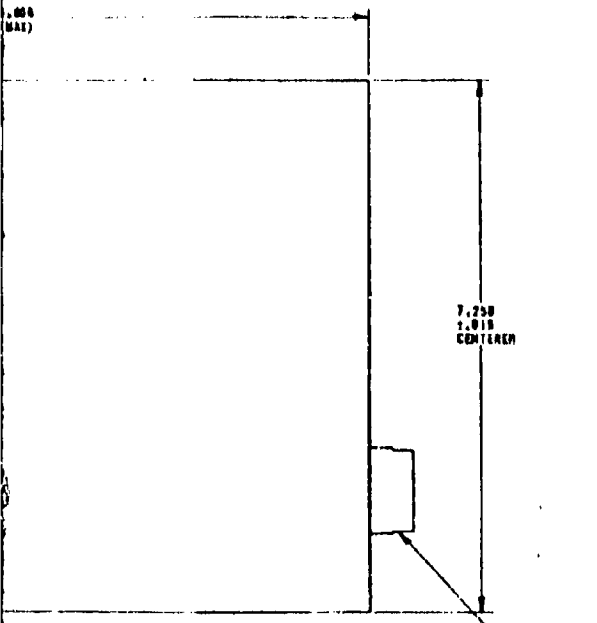
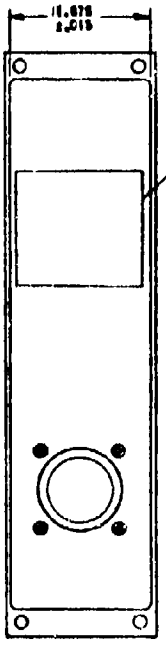


Figure 145. Cable Tension Indicator.

REVISIONS			
LTR	DESCRIPTION	DATE	APPROVED





PART IDENTIFICATION

NOTES:

1. THE B-170-01 IS AN UNLIT MOCKUP.
2. THE B-170-02 IS A WORKING MODEL, ACCEPTANCE TEST PER EDC DOCUMENT 130508 (TEST PLAN FOR HLH CABLE TENSION AND CABLE LENGTH INDICATING SYSTEM.)
3. B-170-02 IS PED 111 PER MIL-L-25467.
4. INDICIA AND NUMERALS ARE WHITE, COLOR #37875 PER FED-STD-595.
5. BACKGROUND IS BLACK COLOR #37038 PER FED-STD-595.
6. THIS EQUIPMENT IS PROCURED UNDER GOVERNMENT CONTRACT NO. DAAJ01-71-C-0040 (P40).
7. OUTSIDE FINISH IS BLACK, COLOR #37038 PER FED-STD-595.

CATOR PIN ASSIGNMENTS

00 HZ HI
0 HZ LO

LIGHTING
POWER

LOAD
WEIGHT
SIGNAL

ON STATUS INDICATOR SUPPLY

70,000 #

FORWARD CABLE
TENSION
SIGNAL

AFT CABLE
TENSION
SIGNAL

FORWARD
HOOK
STATUS

AFT
HOOK
STATUS

CONNECTOR "SEALTRON" 8803-18-8-31PN-AP MATES WITH MS24266R18B31SN AMP "340" SERIES

SERIAL NO.	PART NO.	QTY REQD	APPLICATION

UNLESS OTHERWISE SPECIFIED
DIMENSIONS ARE IN INCHES
TOLERANCES ARE
LINEAR .XX ±
.XXX ± NOTED
ANGULAR ±
BREAK ALL SHARP EDGES
ALL ANGLES & BENDS 90°
ALL DIMENSIONS PER STATE FIT & FINISH
PART MARK PER MIL STD-130
√ ALL MACHINE SURFACES

CONTRACT NUMBER
DRAWN
CHECKED
STRESS
WEIGHT
APPROVED

LYNNWOOD, WASHINGTON EDC

INTERFACE DRAWING
CABLE TENSION
INDICATOR

SIZE D | CODE IDENT NO 08748 | ID 9-170

SCALE 1/1 | SHEET 1 OF 1

2

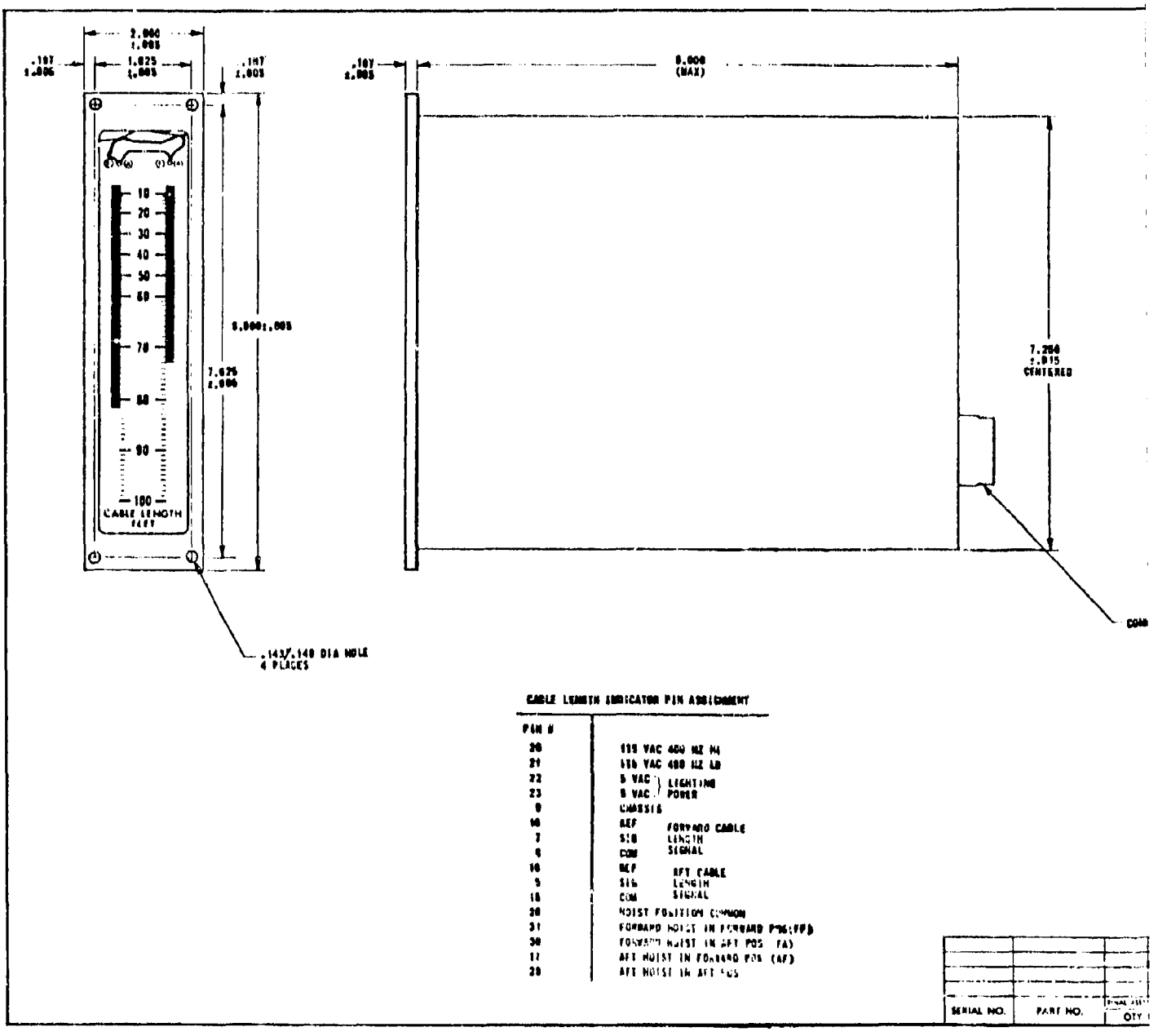
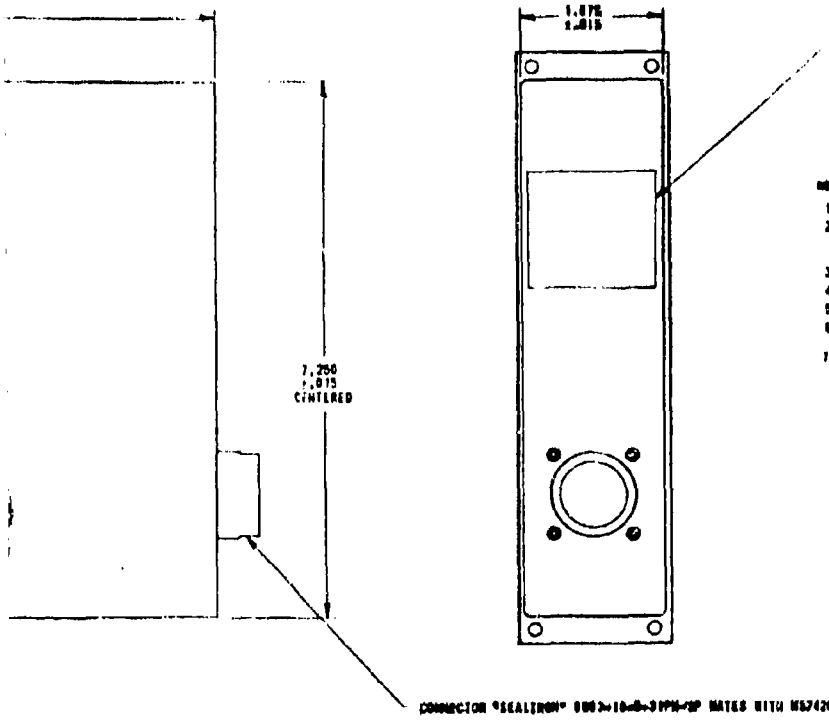


Figure 146. Cable Length Indicator.



NOTES:

1. THE B-171-01 IS AN UNLIT MOCKUP
2. THE B-171-32 IS A MARKING MODEL. ACCEPTANCE TEST PER EDC DOCUMENT 730508 (TEST PLAN FOR NLM CABLE TENSION AND CABLE LENGTH INDICATING SYSTEM.)
3. B-171-02 IS RED LIT PER MIL-L-25467.
4. INDICIA AND NUMERALS ARE WHITE, COLOR #37875 PER FED-STD-595.
5. BACKGROUND IS BLACK, COLOR = 37038 PER FED STD-595
6. THIS EQUIPMENT IS PROCURED UNDER GOVERNMENT CONTRACT NO. DAAJ01-71-C-0840 (P40).
7. OUTSIDE FINISH IS BLACK COLOR #37038 PER FED-STD-595.

CONNECTOR "SEALECTRO" 08[illegible] MATES WITH MS3426A10B31SW AMP "345" SERIES.

CONTRACT DAAJ01-71-C-0840(P40)

SERIAL NO	PART NO	QTY REQD	NEXT ASSY APPLICATION

UNLESS OTHERWISE SPECIFIED
DIMENSIONS ARE IN INCHES
TOLERANCES ARE
LINEAR .XX ± .XXX ±
ANGULAR ±
NOTED
BREAK ALL SHARP EDGES
ALL ANGLES 6 DEGS ±
ALL DIMENSIONS PER ASA B46.1
PART MARK PER MIL STD 130
ALL MACHINED SURFACES

CONTRACT NUMBER	
DRAWN	DATE
CHECKED	
ENGR	
QUALITY	
APPROVED	
ATTORNEY	

LYNNWOOD, WASHINGTON EDC

INTERFACE DRAWING
CABLE LENGTH
INDICATOR

SIZE	CODE IDENT NO.	ID's-171
D	08748	

SCALE 1:1 SHEET 1 OF 1

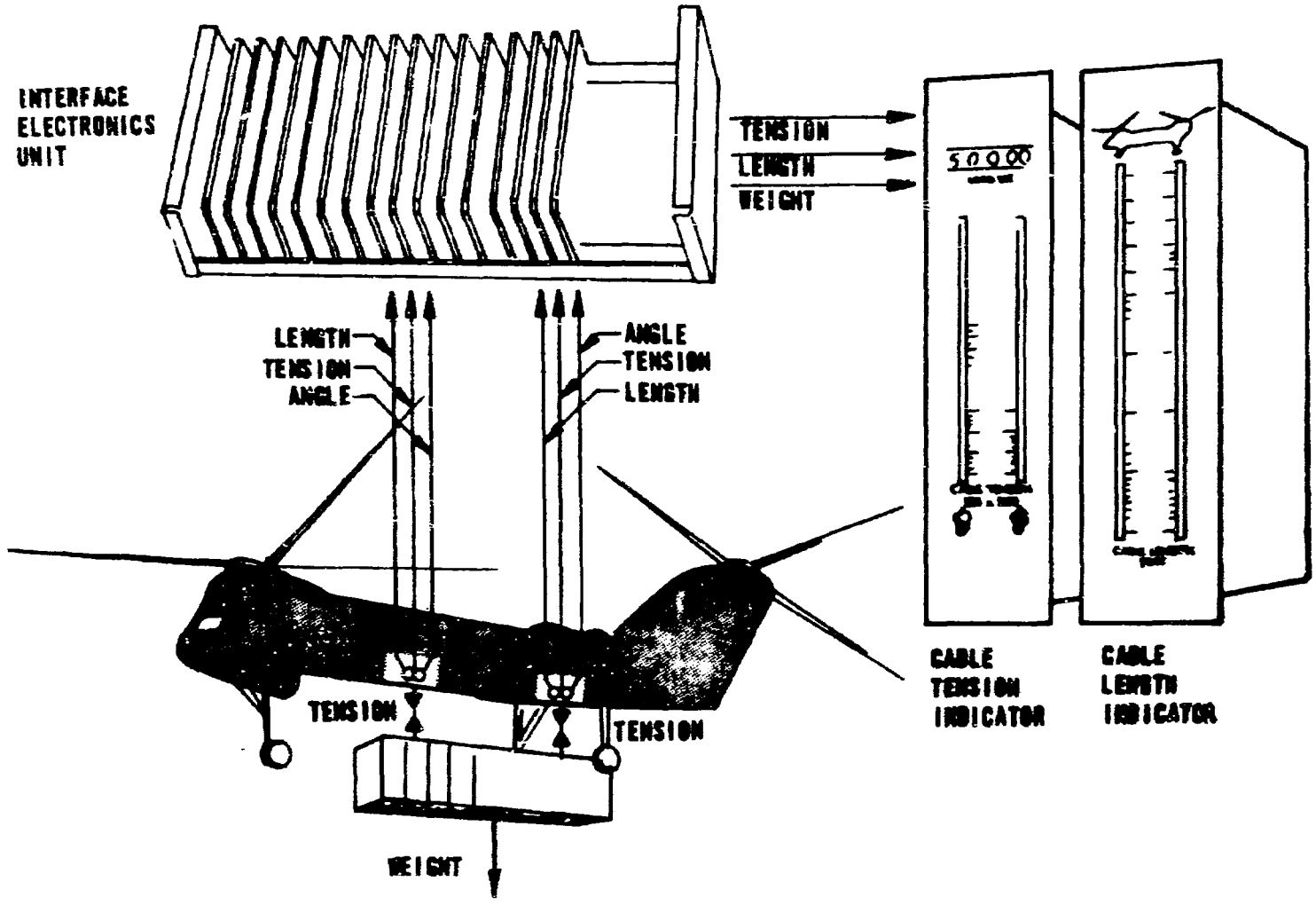


Figure 147. HLH Cable Tension and Cable Length Indicator System.

Cable Length. The cable length signal to the cable length indicator is computed as follows:

Two identical channels are used, one for the forward and one for the aft cable. Each cable length transducer is a linear transformer which provides a 400-Hz AC output signal proportional to the length of cable payed out. This is achieved by gearing the linear transformer off of the cable drum. The transducer is zeroed at 50 feet cable length and provides an output which increases in amplitude in phase with the transducer excitation for cable lengths above 50 feet and increases in amplitude out of phase for cable length below 50 feet.

The linear transformer output is phase sensitive demodulated to produce a DC voltage proportional to cable length. In addition, the linear transformer excitation voltage is also demodulated to provide a DC reference voltage: nominally 5 VDC. The length signal is then represented as the ratio between the DC signal to the DC reference voltage. The system thus operates ratiometrically, thus making the system accuracy independent of the amplitude of the transducer excitation voltage. This ratiometric technique is also used for the cable tension and load weight computations.

The output from the signal demodulator is fed to a two-segment function generator which shapes the cable length signal to provide a two-slope curve with a break at 60 feet. This matches the scale characteristic of the cable length and allows the indicator to use a linear feedback potentiometer. (This has the advantage that an identical linear feedback potentiometer can be used in the cable tension indicator, as its scale breaks are also produced by a function generator in the interface electronics unit.)

The cable length signal output from the interface electronics unit to the indicator is thus a three wire DC signal - reference, signal and common - which expresses cable length as the ratio between the characterized signal and the reference voltages. The reference voltage excites the servo follow-up potentiometer, thus completing the ratiometric measurements; i.e., the tape is positioned proportional to the voltage ratio between the input signal and the reference voltage.

Cable Tension. Two identical channels of signal conditioning compute the forward and aft cable tension signals which feed the cable tension indicator. As with the cable length signal conditioning, the system works

ratiometrically and in ides the function generator to characterize the cable nsion indicator scale break points.

Each hoist consists of two geared cable drums and two cables. A load isolator on each drum measures the reaction force on the drum which is a function of the cable tension.

For each hoist, the cable tension is computed by measuring the force in both the forward and aft load isolators and then shaping these signals to a function which represents the cable tension to load isolator force relationship as determined by the mechanics of the hoist. The resulting signals are summed to produce a signal proportional to the total tension on the two cables of the hoist. A warning output is provided if the tensions in each cable differ by more than a preset level. For the development unit this was set to 5,000 lb. A warning output is also given if the total tension in the cables on each hoist exceeds 50,000 lb.

The transducers used to measure the load isolator forces are strain gauge bridges. The bridges are excited with 10 V RMS and 400 Hz AC, and the bridge output is a 0 to 18 mV 400 Hz signal whose amplitude is directly proportional to the load isolator force. This millivolt signal is amplified by a high gain AC amplifier and then phase sensitively demodulated to reject noise and produce a DC signal proportional to the load isolator force. This signal is then fed to a function generator which approximates the load isolator force to cable tension transfer function, thus producing at its output a DC signal which is proportional to the cable tension on that drum. By summing this with the cable tension signal from the second drum, the total cable tension on that hoist is computed. This is then the forward or aft hoist cable tension which is to be displayed on the indicator. However, before sending these signals to the cable tension indicator, they are shaped by a three-segment function generator to provide break points at 30,000 and 40,000 lb tension to match the indicator scale characteristics. As mentioned above, this allows a linear feedback potentiometer to be used in the indicator servo, which results in the identical servo amplifiers and servo mechanisms in both indicators. As with cable length, the cable tension signal to the indicator is a three-wire signal which represents cable tension as the ratio between the characterized signal and the reference voltage. The reference voltage excites the servo follow-up potentiometer in order that the indicator will position the tape as a function of the input voltage ratio.

Load Weight. The total load weight is computed by summing the load weights on the forward and aft hoists. These are computed by multiplying the cable tension on the appropriate hoist by the cosines of the angles of the cable to the vertical in both the roll and pitch axes.

The angle of the cable to the vertical in pitch is derived by adding or subtracting the helicopter pitch angle (θ) from the longitudinal angle of the cable to the body axis of the helicopter (OC). Similarly, in the roll axis, the cable angle to the vertical is determined by adding or subtracting the helicopter roll angle (ϕ) from the lateral cable angle to the body axis of the helicopter (B).

The pitch and roll signals are 400 Hz AC signals from synchros in the vertical gyro,and the cable angle signals are 400 Hz AC signals from linear transformers. By using two of the three synchro wires,these signals are AC summed in the appropriate phase to give AC signals proportional to the cable angles to the vertical in both roll and pitch. (Note that as the gyro pitch and roll signals come from synchros and only two wires are used, their amplitudes are not linearly proportional to pitch and roll angle but are a sinusoidal function.) For small angles (less than 20 degrees), negligible error (0.28° at 20°) is introduced in the AC summation with the cable angle linear transformer outputs, but this increases to 1.2° at 30° and 3.2° at 40°.

The AC signals, proportional to the cable angle to the vertical,are phase sensitively demodulated to produce corresponding DC signals. These are fed to cosine function generators whose outputs are then proportional to the cosines of these angles and by multiplying these by the cable tension signals result in DC voltages directly proportional to the forward and aft load weights. These are summed to produce a total load weight signal which is sent to the indicator in the standard three-wire format. In the indicator an analog-to-digital convertor working on voltage ratio is used to drive the load weight digital display. The analog load weight signal in the interface electronics also feeds comparators set to trip at 56,000 lb and 70,000 lb. These provide the logic signals to drive the load weight caution and warning flags on the load weight display.

Hook Status Logic. The interface electronics also contains two identical logic circuits which provide signals to the cable tension indicator to drive the hook status legend to either the locked, unlocked or open position. A single input line from the hook controls the locked/unlocked legend and a second line, the open condition. However, the "open" signal is momentary and, therefore, is used to trigger a one-shot circuit which causes the "open" legend to be displayed for a fixed period of time in order that the LCC should not miss this information. The one-shot time period was set to 1-1/2 seconds in the development system.

Construction Details. An outline drawing of the interface electronics unit is shown in Figure 148, while a photograph showing internal construction details is shown in Figure 149.

The electronics is housed in an existing standard 1/2 ATR long case with all the circuitry on plug-in circuit cards. No attempt was made to improve the volumetric efficiency of the packaging design. However, the system was designed to be flexible with trimpots provided for all gains, zero offset adjustments, function generators characteristics and comparator trip points. The trimpots were accessible without removing the cover to facilitate calibration to the system transducers when installed in the test rig.

Printed circuit boards were used wherever more than one of a given board configuration was required, e.g., for the multipliers, function generators, and phase sensitive demodulators.

Cable Tension Indicator

Theory of Operation. The block diagram of the cable tension indicator is shown in the upper right-hand portion of Figure 150. The forward and aft cable tensions are displayed by two "thermometer" vertical tape displays, while the load weight is presented as a digital readout. The two tapes are driven by a direct drive DC torque motor (no gears are used) which provides torque in the upscale direction. A spring return mechanism provides downscale torque, which also drives the tape fully downscale and displays the word OFF when power is turned off. A follow-up potentiometer is attached coaxially with the torque motor and tape drive drum to provide tape position information for closed loop servo operation. A servo amplifier compares the voltage from the feedback pot with the input signal and

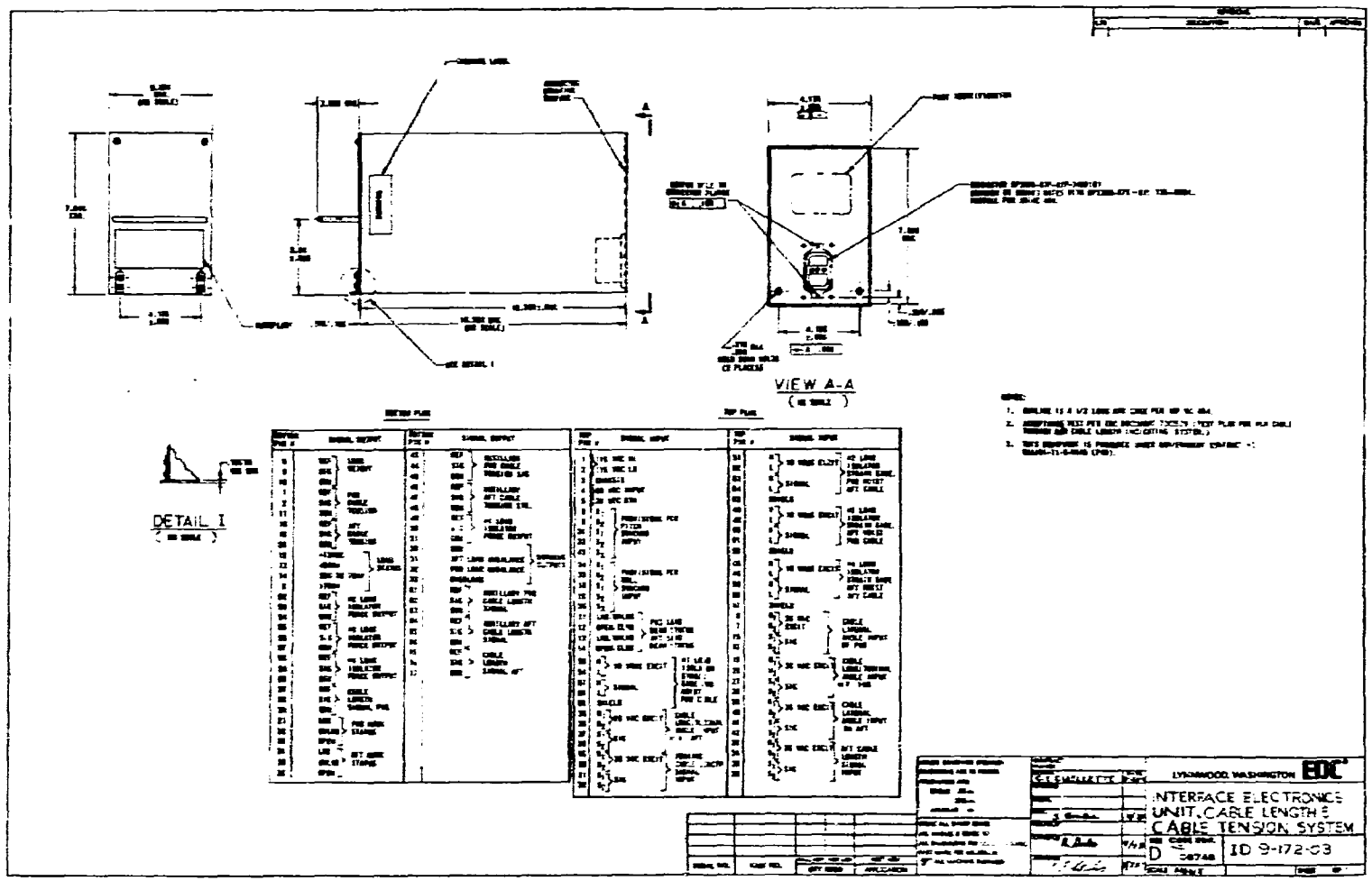


Figure 148. Interface Electronics Unit.

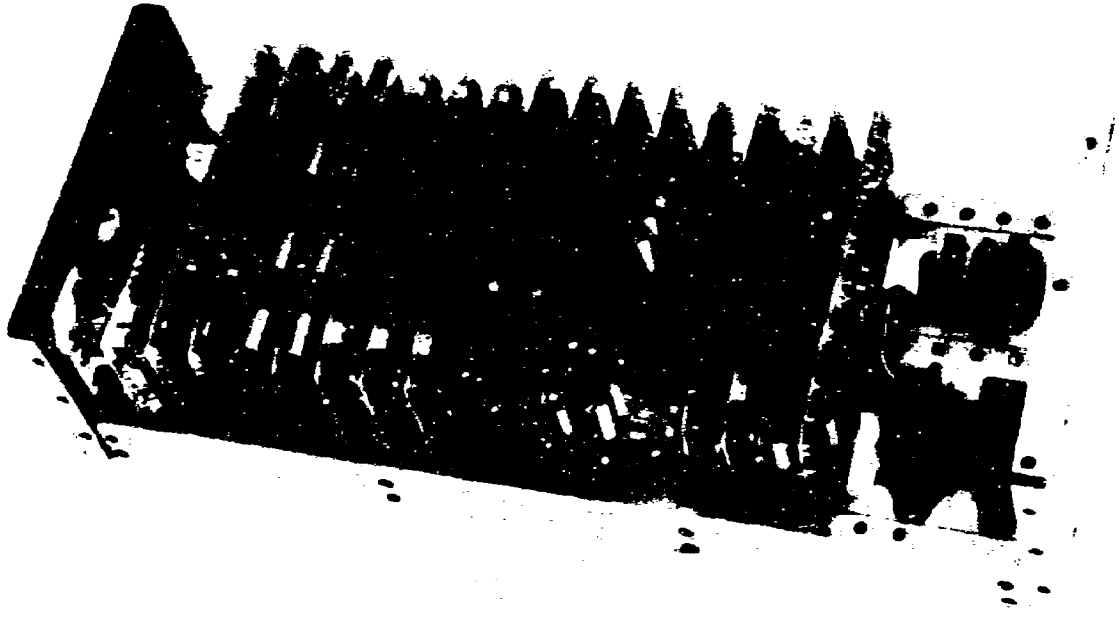


Figure 149. HLH Cable Tension and Cable Length Prototype Interface Electronics Unit (Internal Construction).

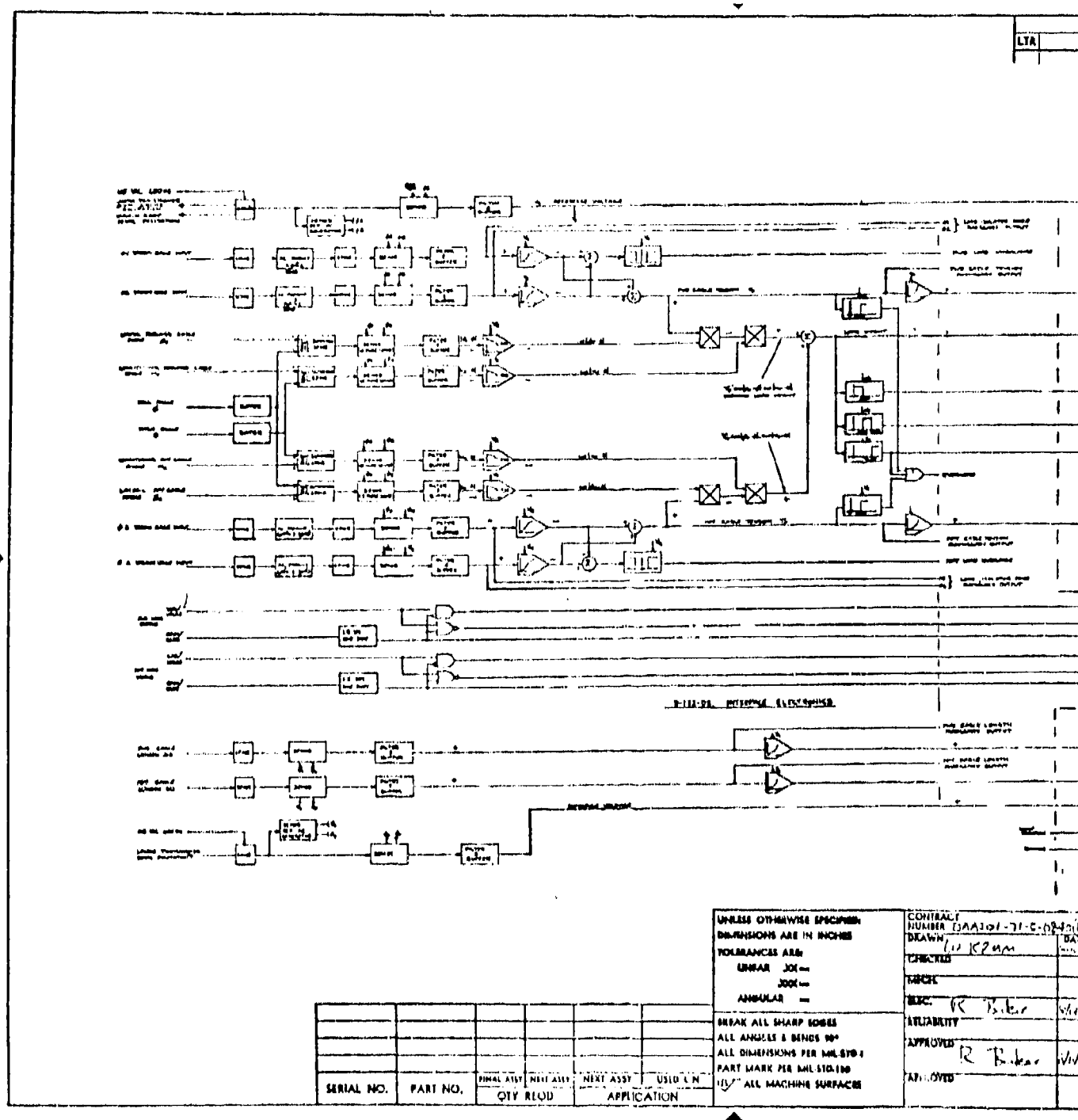
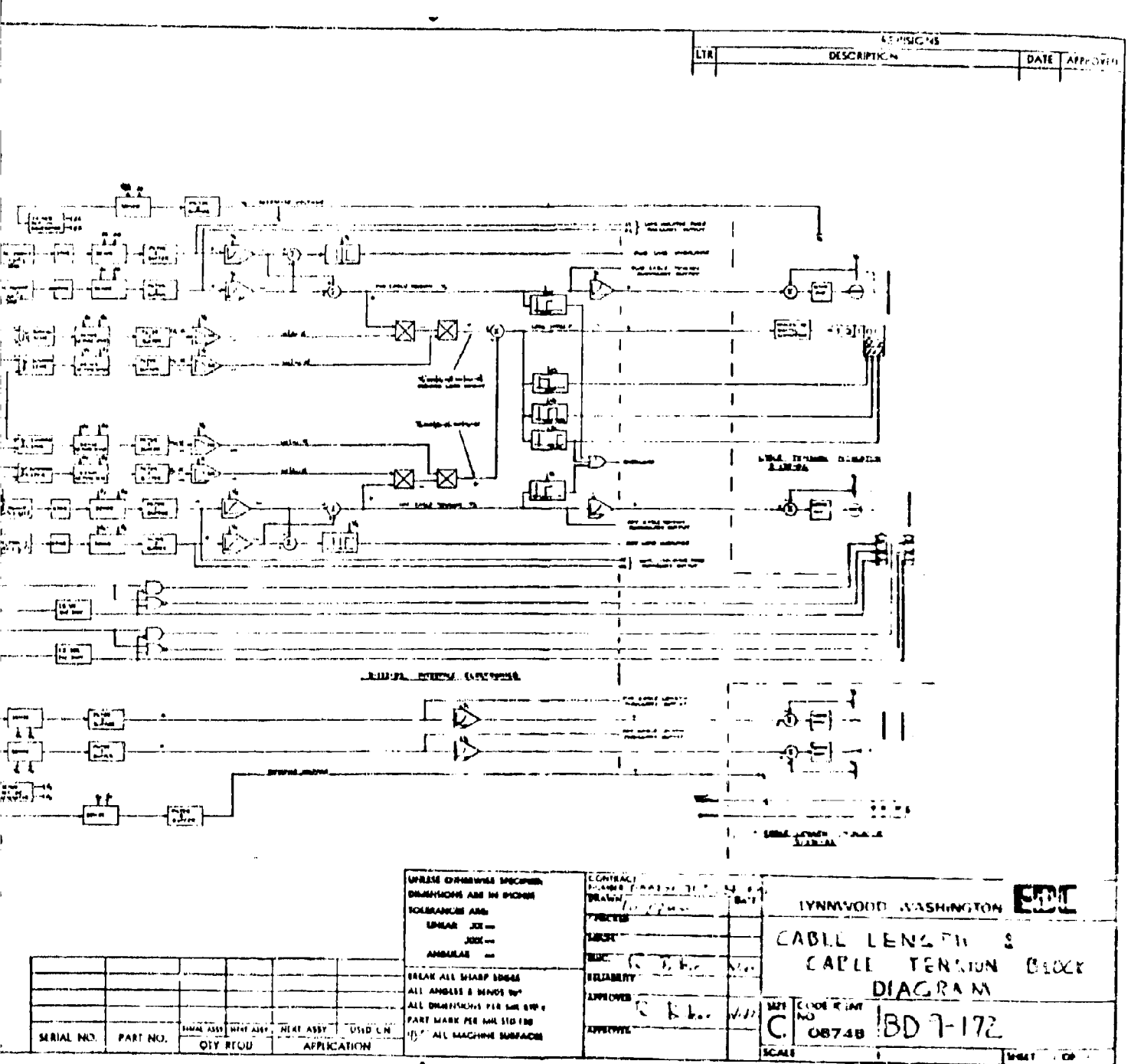


Figure 150. Cable Length and Tension Diagram.



Cable Length and Tension Diagram.

increases or decreases the signal to the torque motor so that the motor turns and the pot wiper voltage becomes equal to the input voltage. As the pot is excited with the reference voltage and the input signal information is represented as the ratio between the signal and reference voltage, the tape is also positioned proportional to this ratio. The servo follow-up pot is linear, thus the tape position is linearly proportional to the input signal voltage ratio. The scale breaks are achieved by shaping the signal in the interface electronics unit and this has the advantage of allowing identical servomechanisms to be used in both of the indicators.

As the torque motor is constantly exerting a torque to overcome the spring return torque, a switching mode servo amplifier was used in order to minimize the servo amplifier power dissipation. This is considerably more efficient than a linear amplifier (90%). The total power dissipation for each servo amplifier and DC torquer at null is approximately one and a half watts.

In order to achieve cautionary condition on the cable tension display, clear tapes were used. As the input signal increases, the clear tapes are driven upscale, uncovering more of the white background. This gives the "thermometer" type display required. Above 42,000 lb the background changes to a black and amber chevron to indicate that the cable tension is in the caution range. This is shown in Figure 151.

"Magwheels" (digital electromagnetic indicators) were used for the load weight readout. These were driven by an analog to digital converter which produced an output directly proportional to the signal to reference voltage ratio at i s input. A magwheel with a dual drum was also used for the least two significant digits of the load weight display which are used to display the load weight caution and warning flags.

For load weights up to 56,000 lb, two white zeros on a black background are displayed; between 56,000 and 70,000 lb, a caution flag consisting of two white zeroes on a black and amber diagonal stripped background is displayed; and above 70,000 lb a diagonal red and white stripped warning flag is displayed. The various flag conditions are also shown in Figure 151.

The remaining feature in the cable tension indicator is the forward and aft hook status legends. Once again, magwheels were used for this function. The hook body

PRECEDING PAGE BLANK-NOT FILMED

Figure 111. Types of Cable Tension Gauges

mimic was screened onto the dial face and the three different hook symbols were screened onto the magwheel. By energizing the appropriate magwheel positions, the "open", "unlocked" and closed hook symbols are presented. See Figure 151.

Display Figure 151 shows the dial presentation for the cable tension indicator.

From left to right these pictures show the following operating modes:

1. Power OFF condition - the OFF flags are visible on each tape. The hook status legend is shown in the "open" position.

2. Power ON condition, zero load weight - both tapes indicate zero cable tension, and the hook status legend is shown in the "unlocked" position.

3. Normal operation - less than 56,000 lb load weight and less than 42,000 lb on each cable; the load weight is shown at 50,000 lb load, and each cable tension at 25,000 lb. The hook status indicates a "locked" hook condition.

4. Caution range - the load weight is between 56,000 and 70,000 lb; a black and amber flag appears behind the two least significant digits of the load weight display.

5. Overweight condition - the load weight is greater than 70,000 lb; a red and white striped flag is displayed in the load weight readout to indicate this condition, also the cable tensions are over 42,000 lb, exposing a black and amber chevron which indicates excessive cable tension.

(It is possible to have excessive cable tension [42,000 lb] without being overweight or even in the cautionary load weight range. This can happen for large cable angles, which result in the sum of the cable tensions being much greater than the load weight.)

The change in vertical "tape" color as the cable tension increases is achieved by using a clear tape with the upper portion black. The boundary between the clear and

black portions becomes the tape reading line. By screening the white normal region and black and amber caution regions directly on the dial face and by uncovering them with the clear tape as the cable tension increases produces the effect of change in the "tape" color.

The design of the cable tension display was based on the following criteria:

1. Make the tape displays (scale factor) as large as possible. (Scale factor in terms of inches or tape travel per unit of displayed parameter.)

2. Use digital indicators (magwheels) for the "total load weight" and "coupling device status" indicators.

3. Have the largest possible reading angle with the smallest possible reading ambiguity. This turned out to be a 30° cone of visibility.

4. Use the same bezel cover, or assembly, for both indicators.

5. Red lighting was required.

The cable tension indicator (Figure 52) is housed in a 7.25-inch-high by 1.875-inch-wide, and approximately 9.00-inch-long metal case with a faceplate 2.00 inches wide, 8 inches high and 0.187 inch thick. The total glass area visible to the operator when viewed from the front is approximately 10 square inches. Both the total load weight indicators and the coupling device status indicators are made from 1-inch-diameter magwheels that were placed as close to the top and bottom of the instrument as possible.

Each movable tape consists of a strip of specially treated mylar that is wide enough to cover the painted tape strip on the scale face, thus when the tape moves, the clear section will uncover the painted tape strip below and appear as a two-color (white and amber/black) line. Various tape widths were evaluated before selecting one that was .125 inch wide. This width gives the operator good readability while being aesthetically appealing.

The original requirement for the caution region was that it be amber; however, under red light conditions the white tape region and amber tape region would both

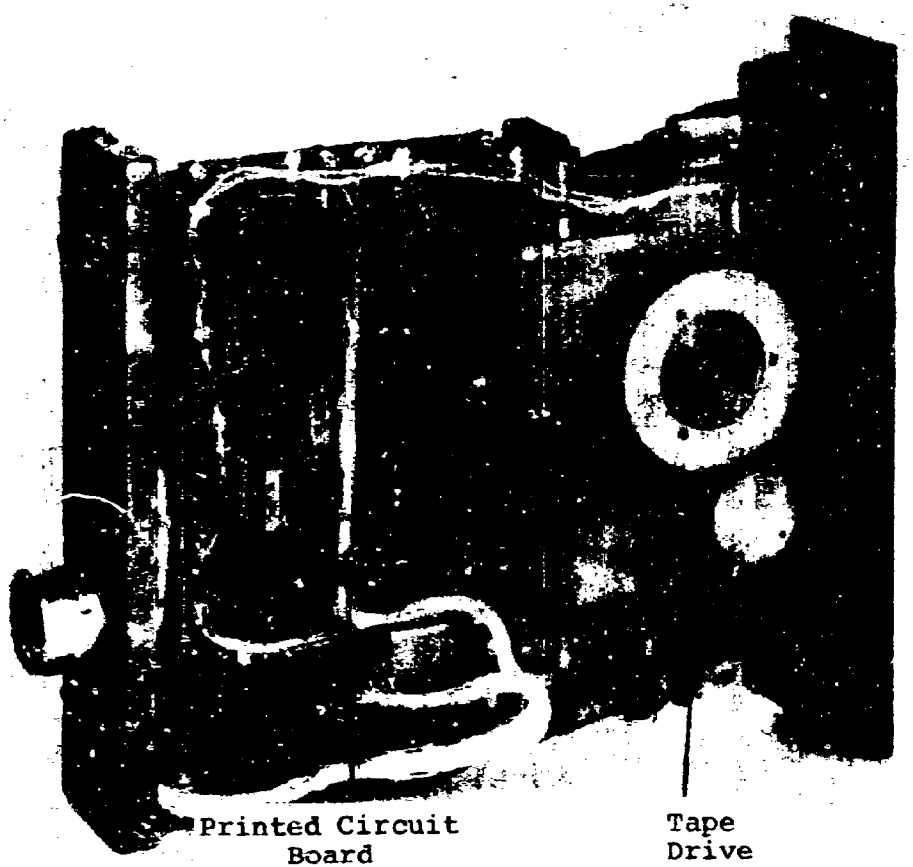


Figure 152. Internal Construction - Prototype HLH Cable Tension Indicator.

appear red and, thus, the caution band would not be identifiable to the operator.

Therefore, various other approaches were considered for identifying the caution region, with the requirement that it could be differentiated from the white region under red light. This was achieved by using a black and amber chevron pattern. When red lit, this appeared as a black and red chevron pattern and presented the caution information to the operator by pattern recognition rather than by color recognition.

The total visible tape length of each tape is 4.11 inches. The scales are 3.85 inches long from the center of the major graduation opposite the zero to the center of the major graduation opposite the fifty. The two tapes are .9 [illegible]h apart and are centered in the instrument, each tape width being .125 inch. The major graduations are .2 inch long and .030 inch wide and are spaced opposite each scale number. The sub-major graduations are .1 inch long and .015 inch wide and are spaced to indicate 2,000 pounds each in the range of 0 to 30,000 pounds, 1,000 pounds each in the range of 30,000 to 40,000 pounds, and 500 pounds each in the range of 40,000 to 50,000 pounds.

The dial face was selected after evaluating many different styles of graduations and numbers. Readability is the prime concern when selecting the dial face layout. It was felt that a simple, very clean, but adequate (for the resolution required), dial face should be proposed. This type of dial display was centered in the allowable space ensuring that it was readable within the 30° cone of visibility.

The total load weight presentation is a normal, five-magwheel display with the exception of the last two zeros. These zeros are silk-screened on a single, double width magwheel that also serves in two of its other positions as the caution flag and warning flag.

The magwheels are set back from the cover glass approximately .050 inch and framed in an aperture opening of .30 inch by 1.5 inches. In the selection of the magwheel position and distance from the cover glass, the viewing angle was always kept in mind. The dimension selected ensures the maximum possible viewing angle while not permitting the adjacent digits to be visible.

The caution flag associated with the load weight display was originally required to change the last two digits (fixed zeros) from white numerals on a black background

to amber numerals on a black background for load weights between 56,000 and 70,000 lb.

Under external ambient light and unfiltered white light, the amber numbers would have been sufficient to alert the operator to a caution condition. When the decision was made to adapt the instrument to red lighting, it was determined that the small amount of amber in the two zeros would not be readily discernable to the operator. To ensure that the operator would be unambiguously aware that a caution condition exists, many different flag configurations were evaluated. As with the chevrons on the cable tension tape display, it was determined that some black region was required on the flag. This resulted in the design with white zeroes on a black and amber stripped background. This design is readily visible under ambient white light, and under red light the black cross lines behind the zeros serves to alert the operator to a caution condition.

The overload condition flag (load greater than 70,000 lb) is a red and white diagonal stripe. Under red light both the white and red lines appear red, as contrasted to the background, and alert the operator to an overload condition. Under ambient white light the lines appear white and red and offer more contrast to the background than either a total white or a total red flag. The important consideration in the human engineering of this flag is the width of the white cross line. If the white line becomes too thin, then from a reasonable viewing distance the flag appears all red. An all red flag when framed with black is not as discernable as a red and white flag. If the white lines get too thick, then the warning red becomes lost to the operator. A good compromise appears to be a white line that is approximately one-half the width of the red line.

The hook status indication is presented as a mimic at the bottom of each movable tape. The hook and legends are silk-screened on a double-width magwheel, while the upper portion of the coupling device is silk-screened on a thin plastic pulley cover. Thus, when the magwheel is rotated, the hook and legends are changed. It should be noted that a mechanically moving device such as a magwheel (or flag) is the only technique that will not suffer from fading under ambient white light.

Construction. The outline drawing for the cable tension indicator is shown in Figure 145, and Figure 152 shows the internal construction of the indicator. The forward portion of the indicator contains the tape drive mechanism

which consists of the direct drive DC torque motor and the spring return mechanism.

The DC torque motor, follow-up potentiometer and tape drive drum are coaxially mounted as a single assembly which can be removed as a module.

The motors and spring returns are mounted on a T-shaped center plate which is attached directly to the bezel and also carries the scale face. The load weight mag-wheels and hook status indicators are mounted on brackets which also attach to the center plate.

The rear of the indicator houses the electronics, which in this prototype consisted of an analog to digital converter and two servo amplifiers (one for each servo mechanism).

Cable Length Indicator

Theory of Operation. The block diagram of the cable length indicator is shown in the lower right-hand portion of Figure 150. The forward and aft cable lengths are displayed by two "thermometer" vertical tape displays.

The mechanism for the tape drive and servo amplifiers are identical to those used in the cable tension indicator, with the exception that the tape is driven downward for increasing cable length rather than upward as in the cable tension indicator.

Display Design. The cable length indicator, see Figure 146, uses the same bezel assembly as the cable tension indicator. This maintains similarity and display balance between the two instruments. The tape width of the cable length indicator is the same as that of the cable tension indicator; however, the scale length is increased as much as practical. Increasing the length, the tapes appear to the operator more like a cable and at the same time increase the reading resolution. The major and minor scale graduations are the same length and width as those used on the cable tension indicator. The scale is laid out in two steps; the first starts at 10 feet and is divided in linear steps to 60 feet, with each minor graduation equal to 2 feet; the second is from 60 feet to 100 feet, with each minor graduation equal to 1 foot. The two downward moving tapes are situated below a helicopter legend and as close to it as practical to give the impression of hanging below the helicopter. However, they are not shown attached to the bottom of the helicopter since the

addition of the requirement to light the helicopter legend made it impractical to extend the tapes to the very bottom of the legend.

The two sets of lights located on either side of the top of the tapes are to indicate the fore and aft span position of the hoists. When operating, the appropriate hoist position lights illuminated red with the "F" or "A" for fore and aft position appearing as a black silhouette.

The tapes on the cable length indicator are driven in the opposite direction to those in the cable tension indicator, so that the scale indication increases in a downward direction. Because the tape is driven downward by the servo and returned upward by the spring return, the "off" flag appears at the bottom of the scale as opposed to the top of the scale as in the tension indicator.

Construction The outline drawing for the cable length indicator is shown in Figure 146.

With the exception of the dial face tapes and nameplate, the same parts used in the cable tension indicator were used in the cable length indicator. It should be noted that the same center T-shaped plate is used in each indicator for mounting the servo mechanical components even though the tapes on the cable length indicator are driven in the opposite direction from those on the cable tension indicator. This is achieved by inverting the center plate in the cable length indicator such that the motors are below the spring return mechanisms.

The plug-in circuit card, visible at the rear of the indicator, contains the two switching mode servo amplifiers which also are identical to those used in the cable tension indicator.

Integrated Test Rig

The controls and displays procured for the ATC program (and installed in the Integrated Test Rig) consist of:

1. LCC Hoist Controller (See Figures 153 and 154)

   Measurements Systems Incorporated Dwg. S2309 (Figure 142) describes delivered hardware.



Figure 153. LCC Hoist Controller.

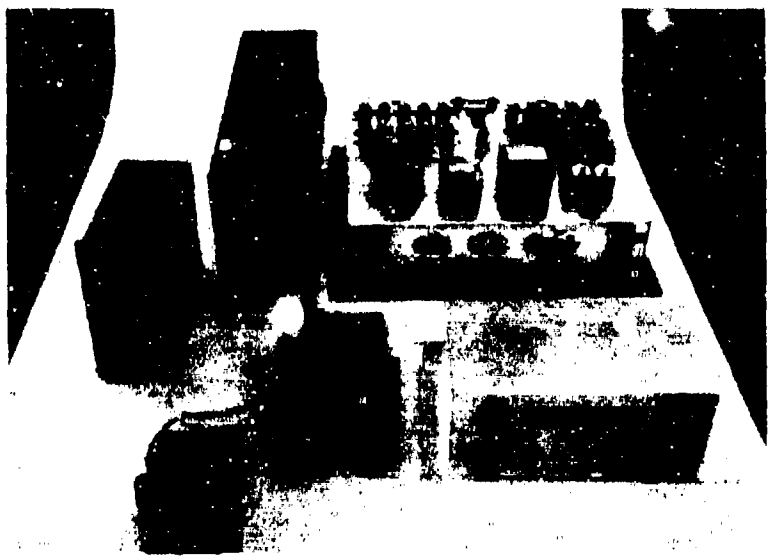


Figure 154. Controls and Displays Components.

2. Cargo System Control Panel (See Figures 143, 144, 155)

Barber-Colman Company Dwgs. FYLZ and YL1601 (Figures 143 and 144) describe the delivered hardware and circuitry of each of the two procured panels.

3. Cable Length and Cable Tension Indicators (See Figures 151, 152 and 154)

Electro Development Corporation Dwgs. ID9-170, ID9-171, ID9-172-03 and BD9-172 (Figures 145, 146, 148, 149 and 151) describe the delivered hardware and the inter-connections. The items received were:

a. Cable tension indicator (ID-170)
b. Cable length indicator (ID-171)
c. Interface electronics unit (ID-172)
d. Nonoperating models of ID-170 and ID-171 for use in cockpit mockup.

Because of the requirements established for operational instrumentation and auxillary instrumentation outputs and to facilitate the development circuitry fabrication, it was considered more economical of both time and money to provide a

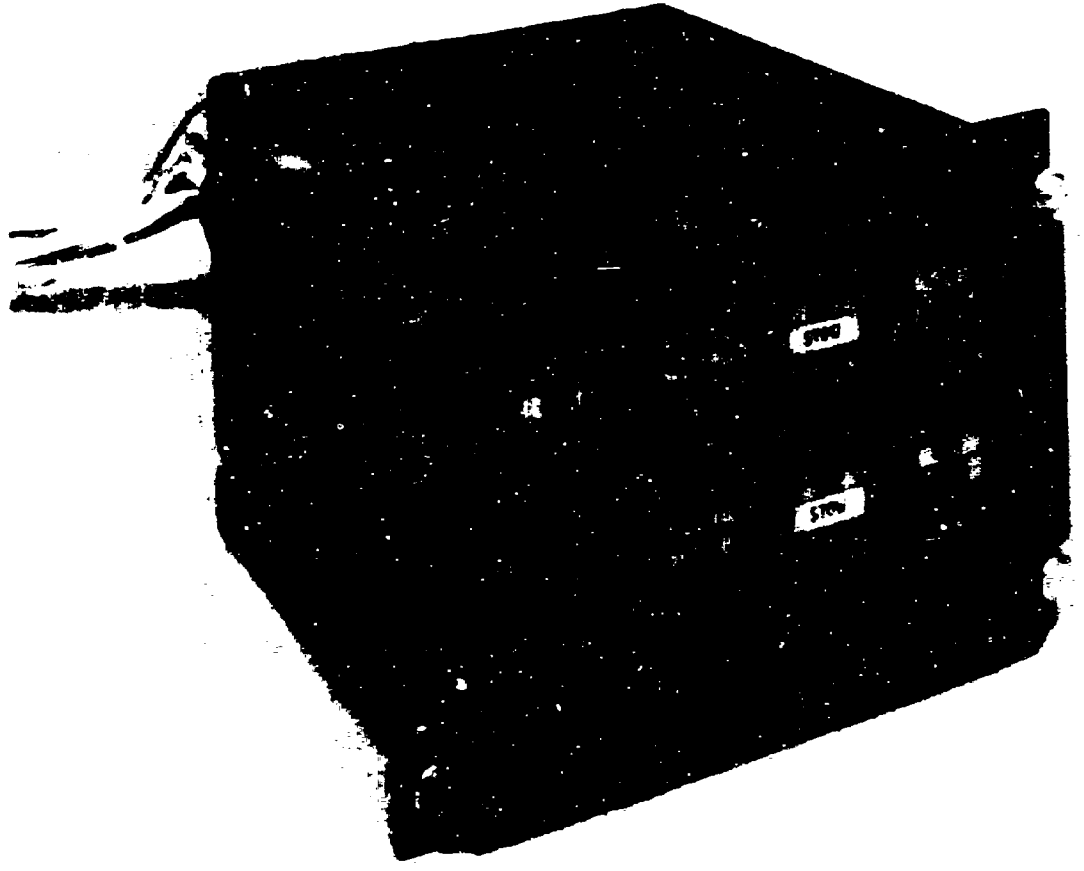


Figure 155. Cargo System Control Box.

third enclosure for the developmental processing and computational function necessary to actuate the tape servos in the respective displays, therefore the interface electronics unit was utilized for this function. (See Figures 148 and 154). The package size of the indicators themselves is sufficient to include the necessary electronics functions, when the ATC experience has refined the exact requirements and when it is appropriate to expend the nonrecurring funds for such packaging.

4. Signal Conditioning and Control Logic Unit

As the integrated test rig program developed and as the procurement of the components had not permitted a thorough system integration earlier, it was necessary to design and fabricate hardware to marry the components from the various vendors into an operating system in the ITR.

The ITR installs a full complement of the Cargo Handling ATC (except VAS) and in addition required auxiliary equipment for instrumentation signal conditioning, and control logic.

The Signal Conditioning Unit (Figures 154 and 156) provides the functions of:

1) Amplitude scaling and cubic parabola shaping of the SPEED COMMAND signals from the hoist control grip into the Sundstrand ATM controller.

2) Amplitude scaling of the cable length sensor signals between the EDC interface electronics unit and the ATM controller.

3) Amplitude scaling of the cable tension signals from the EDC interface electronics unit and the ATM controller.

4) Amplitude scaling of the pitch angle signals from the sensors and the ATM controller.

5) Amplitude scaling of the SPEED COMMAND, pitch angle, and roll angle signals for instrumentation.

6) Timing circuit for the EMERG hook release circuit.

7) Power supplies for above functions plus the LED "SYNCH" indicator in the control grip.

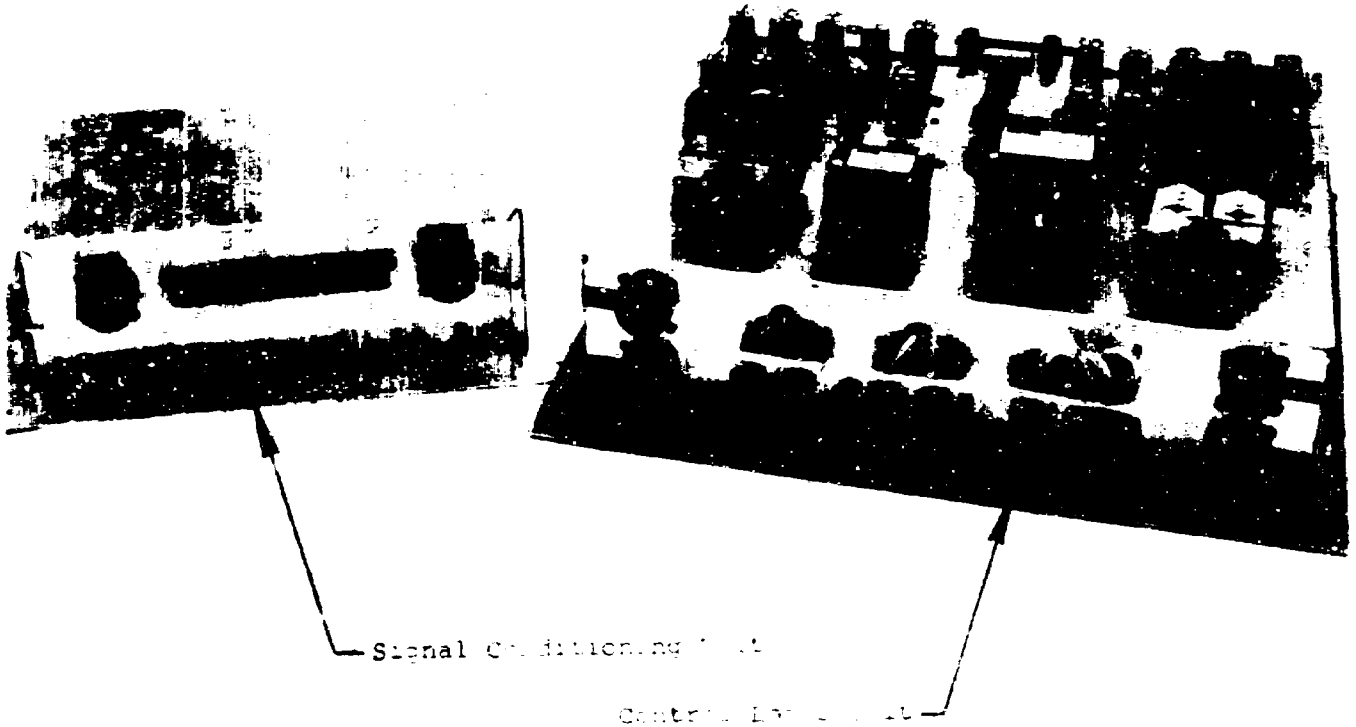


Figure 156. Signal Conditioning and Control Logic Units.

The control logic unit (Figures 154,156) consists of a relay test circuit and a duplicated set of relay logic to permit the automatic operation of the hoist traverse system and to integrate the cable length limits and span position interlocks into a system which allows winch operation only between upper and lower cable length limits when the control panel is in the OPER condition (hoist module in FWD or AFT position with pin locks engaged) or from upper length limit to stow limit after initiation of the STOW command.

This unit also serves as the power distribution unit of the ITR control system.

The control logic unit also contains the relay logic for the NORMAL and EMERGENCY hook release functions.

The auxiliary control panel provides a means of actuating the cable cutter and normal hook release circuits (not necessarily representative of an aircraft installation).

VISUAL AUGMENTATION SYSTEM (VAS)

Design Requirements

Limitations and restrictions in current external cargo operation imposed by conditions of darkness, fog, smoke, or blowing dust and snow established a mandatory goal for the HLH of providing a means for accurately positioning and orienting the aircraft and/or load when operating in a degraded visual environment. Toward this goal, Boeing Vertol proposed development and evaluation of a visual augmentation system to complement the precision hover capability concurrently developed under the flight control system ATC. Microwave, infrared and low light level television (LLLTV) were identified as possible sensor technologies which could be used. Since it was estimated that a single sensor might enhance visual acuity and range by a factor of three or four, it was not inconceivable that a combination of sensors might be required to accommodate the entire range and spectrum of obscurations which the HLH might encounter. However, the existence of developmental broad band sensors, coupled with state-of-the-art advances in wide angle optics, cathode ray tube (CRT) displays and symbology generation, indicated that a system to achieve the goal of the VAS was technically feasible and, if successful, economically beneficial. The major benefits to be derived were:

1. Increased productivity through conduct of operations over a broader range of meteorological conditions.

2. Increased efficiency through providing the pilot/copilot with a means of monitoring cargo operation from a remote location.

3. Possible elimination of a load controlling crewman (LCC's) glass cage by allowing cargo operations to be conducted entirely by remote viewing from the cockpit or an LCC station inside the fuselage.

Initially, it was rationalized that the VAS must have a field of view (FOV) equal to or better than the human operator. To provide such a FOV, use of an extremely wide angle lens (commonly referred to as a "fisheye" lens by the optics industry) was proposed.

Studies, Analyses and Procedures

Survey of Operational Experience and Technical Documentation

A survey was conducted of existing technical literature

and on-going projects devoted to the following subjects:

1. Hover position sensors and systems
2. Hover position indicator and displays
3. Vision enhancement systems
4. Low light level television systems
5. Infrared vision enhancement systems

The search identified two Army programs which might have technology bordering that associated with the VAS. These were:

1. Night vision surveillance system (NVASS)
2. Iriquois night fighter and night tracker (INFANT).

A second search identified ten projects, primarily related to helicopter flying characteristics and stability in hover. The following projects were identified to be of potential interest:

1. Helicopter-borne camera system for battlefield surveillance (ECOM)

2. Precision hovering with heavy sling loads (Princeton University for ECOM)

3. Overhead wide-field head-up display (ECOM)

4. Solid-state image motion sensor (Optonetics for USAFFDL)

5. Optical landing systems for helicopters (Naval Air Engineering Center).

From these searches, ECOM and its associated Night Vision Laboratory (NVL) were recognized for its technical expertise and active engagement in vision enhancement systems. Technical contacts were made with ECOM and NVL, as well as with interested parties in U.S. Air Force AFFDL and Naval Air Systems Command.

Definition of Visual Environment

To assist in arriving at the operational requirements for the VAS, a study was made of the worst case weather conditions, airborne particle concentrations and ambient light conditions potentially existent during the HLH cargo system operations. The Systems Evaluation Group used computer analysis to predict the effect on the LCC's visual capabilities over a range of conditions of drizzle or snowfall. It was recognized that the

theoretical worst case conditions are unlikely to occur during any HLH operation; however, the study results were useful in bracketing the sensor requirements for use in vendor proposal preparation and evaluation of submitted proposals.

Initial Concept Definition

At the initiation of the HLH ATC Program, it was noted that several HLH characteristics and subsystem requirements which could impact the design of the VAS had not been scheduled for definition. These included such items as C.G. computation, power/lift margin, navigation, collision avoidance, weather avoidance, station keeping, radar mapping, etc. In order to generate system control documentation for the VAS in a timely manner, certain ground rules were established pertinent to the design criteria and objectives for the VAS to be demonstrated during the ATC Program. These are summarized as follows:

1. Recognizing the potential of the CRT display for multi-mode operation, design effort will not be expended configuring the VAS display for multi-mode operation.

2. The VAS will not be designed for use as a navigation aid, and will be designed to provide enhanced vision only within a slant range of 350 feet.

3. The VAS will be optimized for use by the ICC. This configuration may not represent the optimum configuration for use by the pilot/copilot.

4. Presentation of master caution annunciation can be incorporated into the design of the VAS in accordance with the guidelines of MIL-STD-884.

5. Inputs of absolute altitude, pitch, roll and heading are assumed available from other HLH subsystems.

6. Display and panel lighting must possess red light capability to preserve night vision adaptation at the operators location.

Design guidelines were established for the VAS by maintainability, reliability, safety and human factors engineering personnel.

Initial System Definition

The VAS comprises five subsystem elements (see Figure 157):

1. Visual augmentation display (VAD)
2. Electro-optical sensor (ECS) group
3. VAS illuminator group
4. Electronics interface unit (EIU)
5. VAS control.

Visual Augmentation Display

The VAD comprises a cathode ray tube (CRT) presentation of the real-world load area with superimposed symbology, positioned in a suitable location in the load controlling crewman's (LCC) compartment.

Electro-Optical Sensor Group

The EOS group comprises a downward-looking, fixed mounted imaging device with very wide FOV and a gimbal mounted imaging device, stabilized and servo driven, with a narrow FOV and a range gating capability.

VAS Illumination Group

The VAS illumination group provides for both wide-angle (flood) and narrow-angle (spot) illumination of specified areas located in the hemisphere below the helicopter. Flood and spot illumination are operable independently of each other and may be used simultaneously. The VAS must not be dependent upon aircraft floodlights for night operations, but is expected to be compatible with their use in benign environments.

Electronics Interface Unit

The EIU contains the electronics interface between the EOS group, the VAD, the illumination group, and other helicopter systems, and includes low voltage power supply, signal data conversion, display programming and computation functions.

VAS Control

All controls for the VAS, including controls for the VAD, the EOS group, the illuminator group and the EIU are included in a separate control panel designed for installation in a standard 5.75-inch panel track.

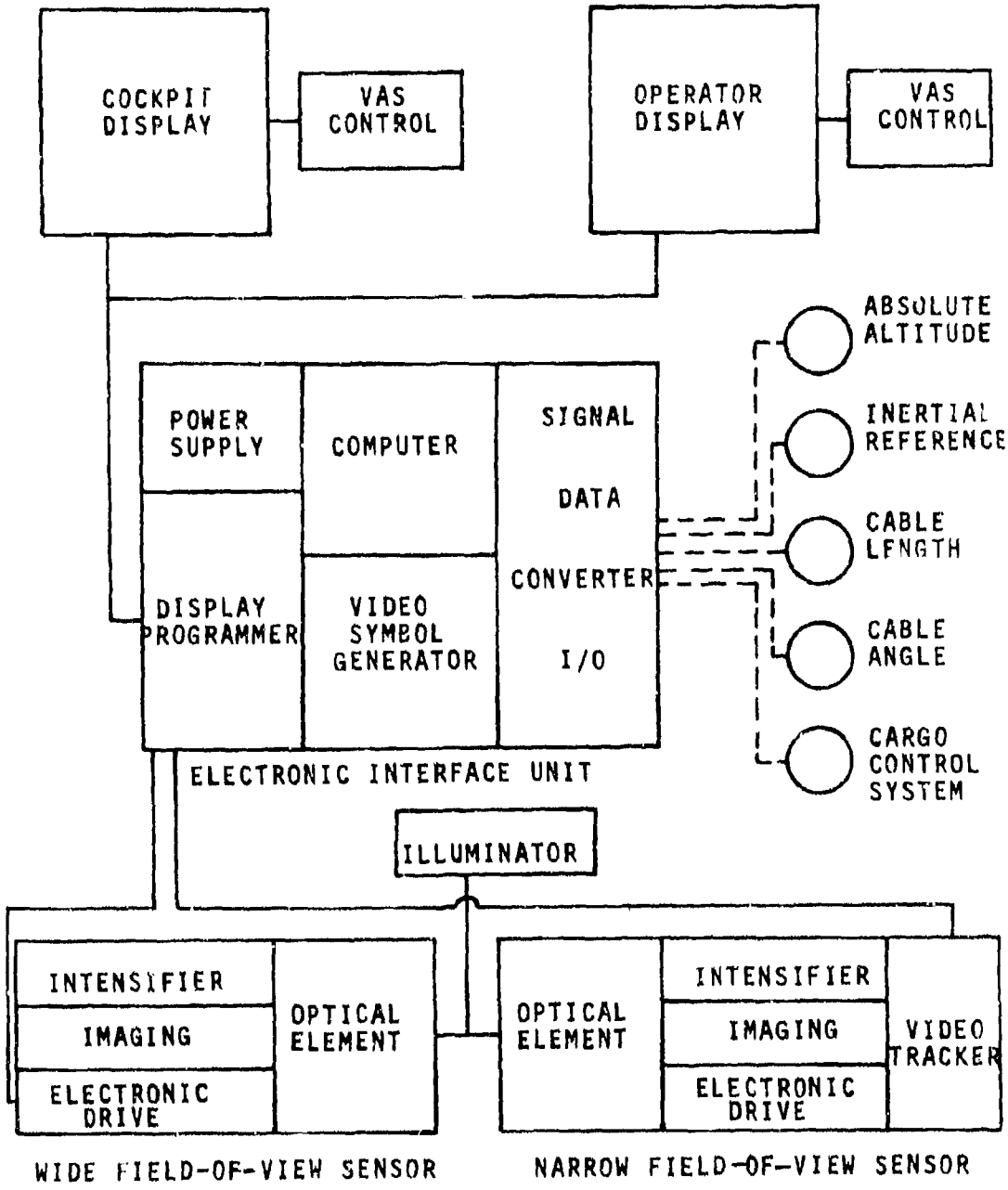


Figure 157. Visual Augmentation System Concept Block Diagram.

During the process of initial concept definition, it was rationalized that two fields of view and perhaps two sensor locations would be required to provide the high resolution and see-around-the-load capabilities required. Viewing and illumination schemes are depicted in Figure 158.

The initial system performance characteristics are summarized below:

System Resolution	- 3.75 TV lines/minute of viewing angle (NFOV) 55 TV lines/degree of viewing angle at center (WFOV) 5 TV lines/degree of viewing angle at edges (NFOV)
Display Brightness and Contrast	- Adequate to permit operation between bright sunlight and overcast starlight against a target having 1% contrast
Environment	- Sufficient atmospheric attenuation to reduce transmittance to 1%
Range	- 350-ft slant, 250-ft absolute altitude
Display Size and Format	- 10.5-in. round CRT with 9.5 in. screen
Fields of View	- 220° WFOV 4° NFOV
Heading	- Displayed around periphery of CRT
CRT Phosphor	- P4 with detachable green and red filters on display face
Raster	- Adequate to provide resolution and prevent flicker below 30 Hz
WFOV Lens Response	- Orthographic (Sinusoidal)
NFOV Lens Response	- Normal (tangetial)
Floodlight Spectra	- Overt - .556 principal wavelength Covert - .750 , gated as required to penetrate obscuration

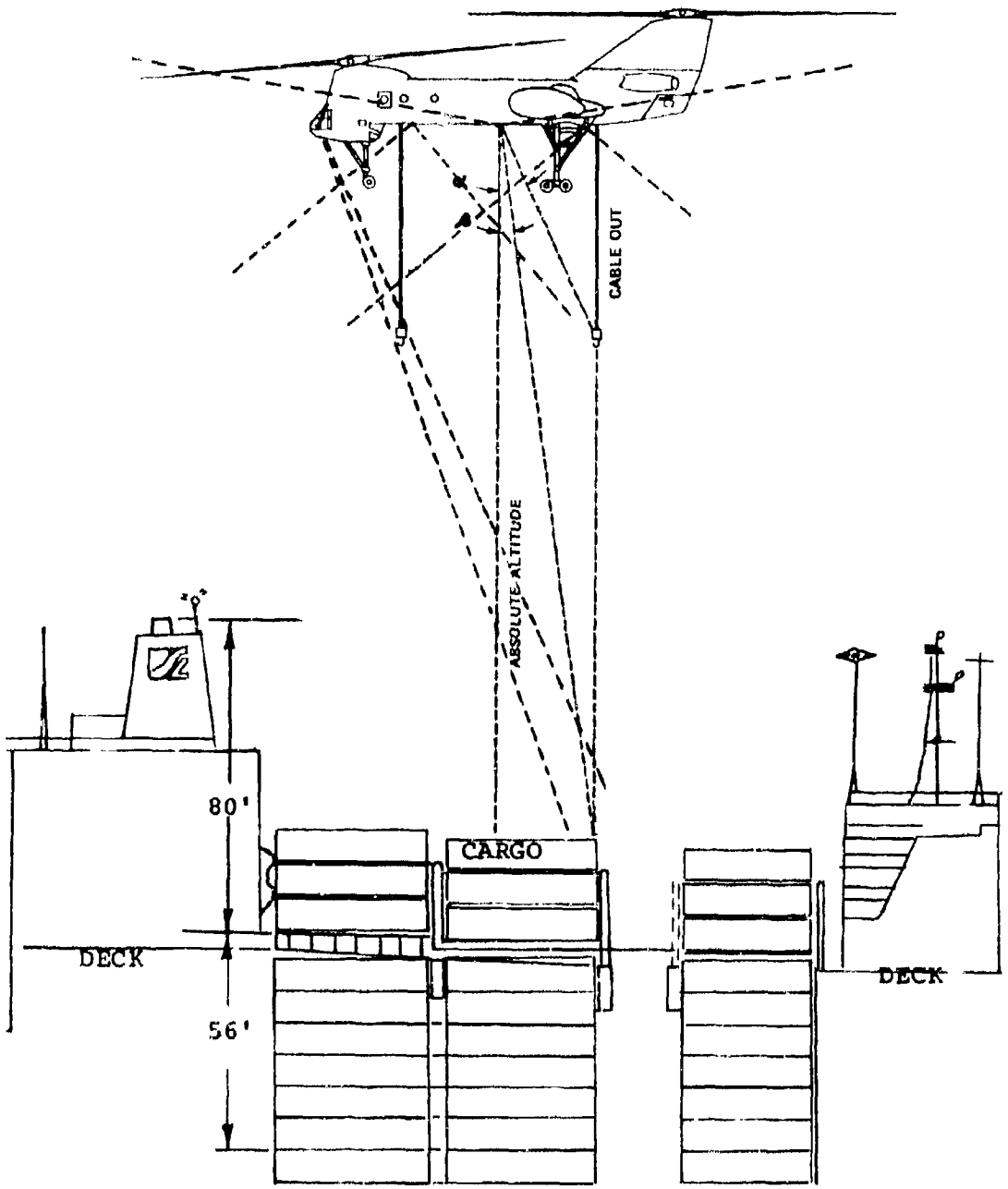


Figure 158. Viewing and Illumination Patterns For SL-7 Class Ship.

Technical Briefing and Vendor Symposium

A list of 530 companies claiming some degree of technical expertise in electro-optical systems and components was developed. From this list, 33 companies were identified as having total system capability and recognized qualifications. All of these were invited to attend a technical briefing on VAS. The 22 which attended the symposium were further invited to submit technical and planning proposals for implementation of the VAS concept, including identification of concept improvements or alternatives.

As a result of the vendor symposium, six proposals were received, four for total systems and two for displays and interface electronics only, as follows:

Concrac Corporation - Displays and electronics only
Martin-Marietta Corp. - LLLTV system
Kaiser Aerospace Co. - Display and electronics only
Dalmo Victor Co. - Stereo LLLTV
RCA/Honeywell - LLLTV system
Texas Instruments - FLIR.

The proposals were reviewed in-house, by the Army, and through cooperative arrangement with the Army Program Manager, by the Electro-Optical Department of NASA, Langley. A range-gated video LLLTV system, as proposed by both Martin Marietta and RCA/Honeywell appeared to show the greatest capability for meeting the VAS requirements and the highest potential for future technical growth. Both the Martin and RCA proposals were weak in the optics and display areas. Since both systems employed an RCA vidicon sensor, RCA's proposal was technically very strong in the sensor area. Additionally, RCA provided a selective list showing combinations of components which enabled consideration of a broad spectrum of cost, complexity and capability. As a result of these and other technical and logistical considerations, the RCA/Honeywell approach to VAS implementation was adjudged superior.

UH-1 Flight Tests to Support Concept Development

The VAS concept was proposed on the basis of flight test investigations conducted by Boeing Vertol under independent research and development funds. Viewing of the test films which resulted from this investigation resulted in a number of comments and questions concerning characteristics peculiar to fisheye viewing systems. In addition, all of the assessments had been based on the observation of color motion picture film. The next most logical step in evaluating the VAS concept was the assessment of an electro-optical system with real-time monochromatic CRT display. Toward that end a

cooperative flight test program was developed with USANVL to enable exposure of operational personnel to a fisheye viewing system and to accumulate subjective commentary which could be used in defining those characteristics (perspective, depth perception, color, resolution, range, field of view, symbology, target designation, heading orientation, screen size, magnification, distortion, disorientation, etc.) which could impact the effectivity of VAS design and feasibility demonstration.

The tests demonstrated sufficient potential of the VAS concept to merit continued investigation and development. Several other conclusions affecting the design of the VAS are:

1. Resolution greater than that of conventional 525 line systems is required.

2. Automatic brightness control is required.

3. High brightness phosphors and glare protection are required.

4. Apparent magnification must be increased.

5. Horizon information is of no value as a flight control cue, but has value as an orientation or comfort cue.

6. Care must be exercised in location of the sensor to keep landing gear and other airframe features from being a distraction in the presentation.

7. A compass heading indicator is of no apparent value and should be eliminated from the design.

8. Spectral filtering would enhance tonal contrast.

Unfortunately, the tests did not provide conclusive results pertinent to the optimum FOV. It was therefore mutually agreed upon by the Army and Boeing Vertol that the ATC demonstration program should examine both fisheye and conventional wide-angle optics applied in conjunction with a higher resolution sensor and a more stable vehicle platform.

General Component Definition

The VAS concept proposed by RCA was studied to determine where modifications could be made to simplify the concept, to conserve available resources, and to bring the concept for the VAS demonstrator system more into alignment with the ATC demonstration program in the Model 347. It was determined

that the demonstrator VAS should be an 875 TV-line system which would provide the next step of improvement over the existing 525 line system, and yet be less costly than the proposed 1500 line system. Analysis of the system alternatives provided by RCA indicated the cost breakdown per system element as shown in Table 19.

Electronics Interface Unit Selector

From the variances of the "% of system cost" data, it can be seen that the electronics interface unit, which includes the symbol generation, computation, display programming, and input/output interface functions, is the most expensive element. In addition, it can vary in cost by a factor of three, depending on the sophistication required. Since most of the sophistication required was associated with symbol generation and display programming when both a wide and a narrow field of view were displayed simultaneously, it appeared that the first area of economization was in the region of electronics interface. Simplification was accomplished in several ways:

1. Narrow field-of-view LLLTV systems have been under development for a number of years and have been evaluated under several programs. Experience with wide fields of view has been very limited and that with fisheye field of view is almost nonexistent. Therefore, a decision was made to display only wide fields of view during the demonstration. This automatically reduced the number of TV cameras and illuminators from two to one. The symbol generation was simplified, and electronic interface became easier because there was no longer a requirement to interface two different fields of view. In addition, the amount of optics and automatic light control was halved.

At this point RCA elected to divorce itself from Honeywell in this area, and proposed an EIU concept, built by RCA at an estimated cost less than $50K. Selection of RCA to produce the EIU has since proven to be technically and logistically sound in light of their responsibility for system development.

Tracker Elimination

The second most expensive element, particularly for an austere system, is the tracker. Trackers already have been developed and demonstrated on a number of missile and space programs. Since only one sensor was being considered, and since that sensor required a field of view sufficiently wide to detect a

TABLE 19. RCA ANALYSIS OF VAS ALTERNATIVES - COST BREAKDOWN PER SYSTEM ELEMENT.

System Element	Min Cost (%)	Max Cost (%)	Average (%)
Electronics	19.1	58.0	38.6
Image Tracking	11.6	14.0	12.8
TV Cameras	3.4	19.1	11.3
Displays	6.8	14.0	10.4
Cables & Hardware	5.3	10.1	7.7
Illuminators	4.8	10.1	7.5
Optics	4.3	4.7	4.5
Stabilization	3.9	5.1	4.5
Gimballing	1.9	3.8	2.9

target from an altitude of 250 feet and slant range of 350 feet, it was rationalized that the sensor must have a field-of-view capability of at least 113°. With such a field of view, automatic optical tracking should not be required, and the capability to steer the optical axis by manual methods should be adequate. Thus the tracker requirement was eliminated.

TV Cameras/Sensors Selection

The most variable element, as a function of sophistication, is the TV camera. In order to conserve program resources, two approaches were considered:

1. Modification of existing commercial grade equipment to meet operational and flight safety requirements of the demonstration program.

2. Bailment and modification of surplus Iroquois Night Fighter and Night Tracker (INFANT) System or the Cobra Night Fire Control System (CNFCS) to make maximum use of hardware already developed by the U.S. Army.

   The CNFCS, though a 525 line system, contained the same silicon intensified target (SIT) camera tube proposed for use by RCA in the VAS. In addition, since its R&D phase had been terminated, several systems were scheduled for moth-balling. The INFANT system, on the other hand, was equipped with a secondary emission conduction (SEC) camera tube, and would require both a tube and sweep frequency modification. Either system could be made to operate with minimum modification of the existing controls. Based on the technical factors above, and the fact that RCA had developed the CNFCS initially (thereby giving them access to technical and test data on the system), CNFCS became the prime candidate as a means for implementing the VAS. The AVSCOM HLH Program Manager effected loan of one CNFCS from Frankford Arsenal. In addition, use and/or modification of existing CNFCS cables, hardware, illuminator, and gimbals would result in cost-effectiveness and good utilization of technology and hardware already under development by the Army.

Display Section

Conrac suggested the use of a production model of their 10-inch CRT monitor developed for the Boeing B-52 Electro-Optical Viewing System (EVS). This offered the advantage of an off-the-shelf, military-qualified 875 line TV display which need only be modified to meet the specific requirements of helicopter environments and the HLH application. In addition, this display was already designed with the P-31 phosphor, which provided the higher brightness called for, and did not require a detachable green filter.

Prime Optics Selection

RCA's original proposal was based on specifically designed and fabricated optics to meet the VAS requirements. The one remaining problem yet unresolved was the analysis and trade of extremely wide angle optics with the horizon visible but with attendant problems in magnification and linear distortion, against conventional wide angle optics with suitable magnification and distortion characteristics but lacking horizon information and requiring at minimum the ability to gimbal the sensor longitudinally in order to track the load through its extreme travels in cable length. To provide insight into this problem as well as to establish and/or verify symbolic cueing requirements, additional flight investigation of the operational characteristics of a very wide angle electro-optical viewing system was undertaken by Boeing Vertol/U.S. Army Night Vision Laboratory. Unfortunately, because of significant differences in test site, target, test subjects, test aircraft and symbology, as well as limited time for testing, no conclusive results were achieved. However, use of the CNFCS provided a solution to the FOV problem. Since the CNFCS has an electronic zoom capability, use of this feature in conjunction with two different lenses, would permit examination of four fields of view during the demonstration program, with attendant loss of resolution in the zoomed condition due to the over-scanning techniques employed. In order to select the best available off the-shelf optics, representatives of RCA and Boeing Vertol visited Ehrenreich Photo-Optical Industries and Karl Heitz, Inc., both of New York, and U.S. Distributors of Nikkor and Kinoptik lenses, respectively. At Ehrenreich the Fisheye-Nikkor Auto 6MM f/2.8 (?20°) and OP (Orthographic Projection) Fisheye-Nikkor 10MM f/5.6 lenses were examined and discussed. At Heitz, the Kinoptik Super-Tegea 1.9MM f/1.9 (1970), the Kinoptik Tegea 9.8MM f/1.8 (130°), and Volpi Peri-Apollar were examined. Linear distortion curves for these lenses are compared with ideal fisheye and desired VAS curves in Figure 159. The response considered ideal for VAS application is expressed by:

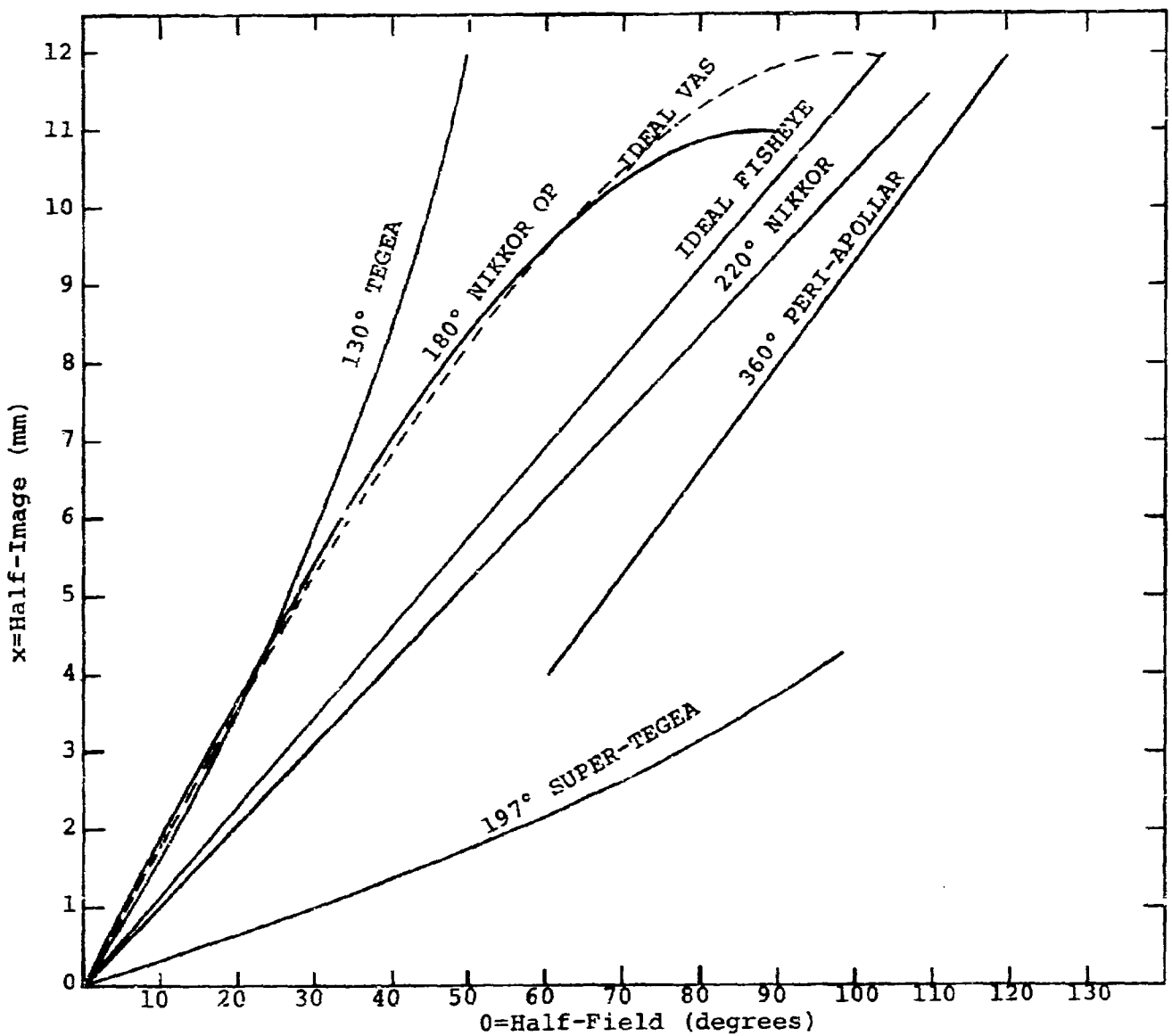


Figure 159. Comparison of Lens Responses Considered for VAS.

$$x = k_1 \sin\left(\frac{180}{k_2}\theta\right), \quad k_2 \geq 180$$

Where:

x is the half-image diameter
k_1 is the image format radius
k_2 is the desired FOV, and
θ is the half-field in degrees

For a 220° FOV projected onto a 24MM diameter format, the equation is:

$$x = 12 \sin(.865\,\theta)$$

It may be seen on Figure 159 that the ideal curve closely approximates the tangential (Tegea) and orthographic (Nikkor OP) curves in the region $0° \leq \theta \leq 20°$. In the region $20° \leq \theta \leq 60°$, the ideal curve closely follows the orthographic curve. For $\theta \geq 60°$ the ideal curve has the sinusoidal response of the OP expanded to broaden the field of view from 180° to 208° and the image size from 22MM to 24MM. No one lens examined had all of the characteristics desirable in the ideal lens. Therefore, RCA has elected to use three prime lenses in the VAS demonstration program, the 130° Tegea for conventional tangential response, the 180° Nikkor OP because it most nearly approximates the ideal response, and the 220° Nikkor Fisheye because it most closely approximates the desired FOV and has a light-gathering capability superior to the OP lens (f/2.8 vs. f/5.6). All three lenses have been procured by RCA from thier respective sources.

Minimum desired transmittance for an ideal lens would be as follows:

On Axis:	Blue (.420μ)	78.0%
	Green (.560μ)	93.3%
	Red (.640μ)	89.8%
	Average	87.0%
30° Off-Axis:	Blue	78.0%
	Green	92.1%
	Red	88.2%
	Average	86.1%
90° Off-Axis:	Blue	75.9%
	Green	88.8%
	Red	83.7%
	Average	82.8%

Since this level of transmissivity already has been achieved in 6MM Nikkor Fisheye f/2.8, it should pose no technical problems in an orthographic lens. Minimum transmittance curves for the ideal VAS lens are shown in Figure 160. It is expected that for 100 lines/MM, an optical transfer function of 30% on-axis and 20% 90° off-axis could be achieved. The high resolution of this lens, combined with its orthographic response, is expected to minimize the distortion and disorientation effects usually associated with conventional fisheye optics.

Detail Design

As a result of negotiations and technical discussions between the vendor, Boeing Vertol, Army Program Management, and Army R&D agencies, contracts were let with Conrac Corporation for a modified off-the-shelf 10-inch CRT television monitor, and to RCA Advanced Technology Laboratories for the following:

1. Development of the VAS Electro-Optical Sensor.
2. Development of the VAS Electronics Interface Unit.
3. Development of the VAS Control Panel.
4. Development of the VAS Illuminator.
5. Modification of the CNFCS to meet the developmental requirements of 1, 2, 3, and 4 above.
6. Integration of the modified CNFCS with new developmental hardware, including the VAS display, to produce a demonstratable VAS.

Simplified block diagrams of the CNFCS, with intended modifications are given in Figures 161 and 162. Preliminary design details for each of the VAS components will be discussed in the following paragraphs.

Visual Augmentation Display (VAD)

The VAS display is a 10-inch, 875-line, television monitor. Design details are covered in the Critical Item Development Specification (CIDS) for the HLH Visual Augmentation System 10-inch, Solid-State Militarized Airborne Television Monitor. The monitor shown in full-scale outline in Figure 163, and Conrac Drawing E-72737-61001B, Outline and Mounting, 10-inch Monitor, is identical to the B-52 EVS Monitor, with the exception that :

1. The display has undergone expanded vibration testing in the range of 0-150 Hz to assure compatibility with helicopter operational environments.

2. The CRT tube has been hand-picked to assure that maximum allowable beam spot size is not exceeded.

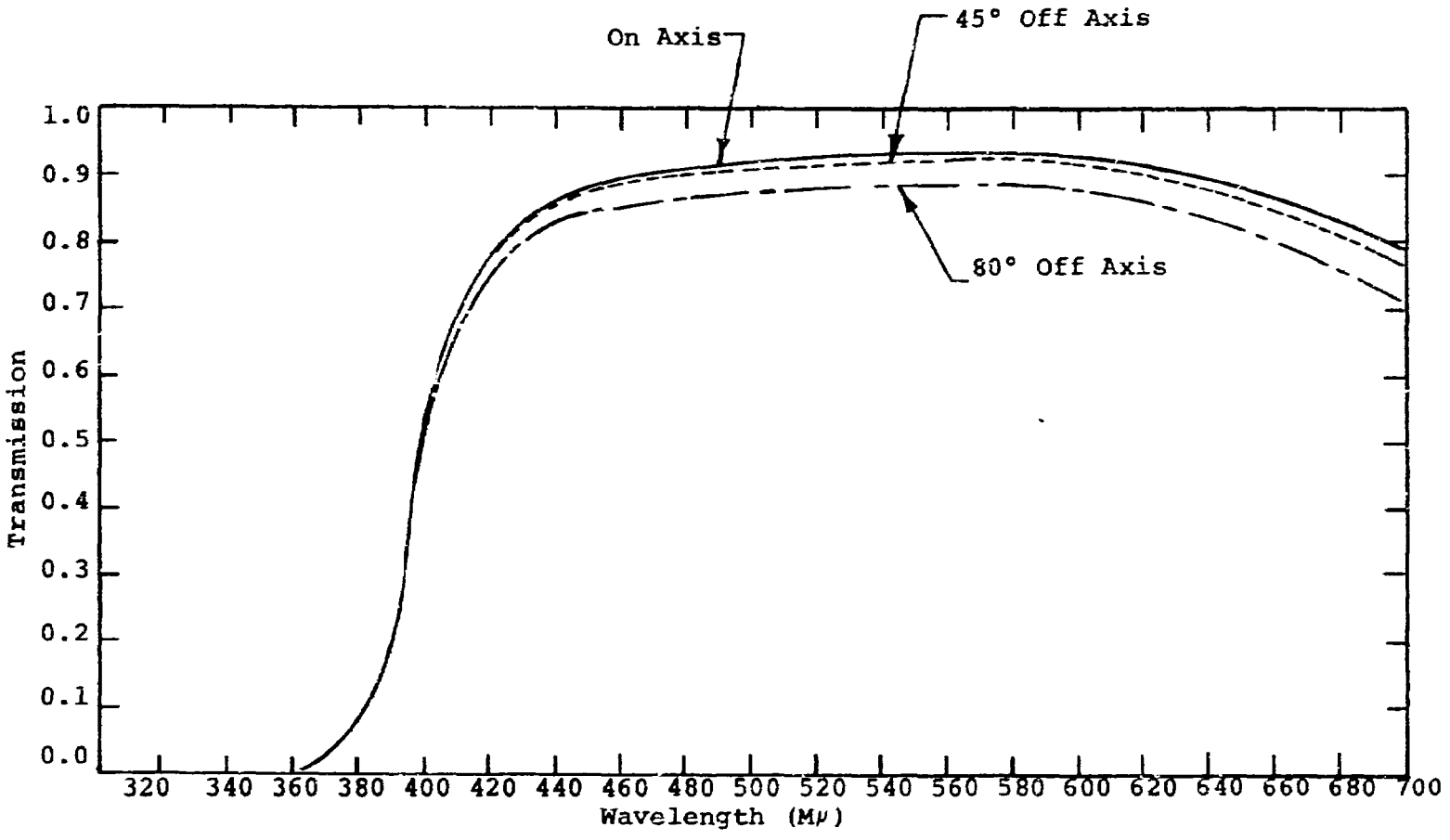


Figure 160. Minimum Spectral Transmittance Characteristics for Ideal VAS Prime Lens.

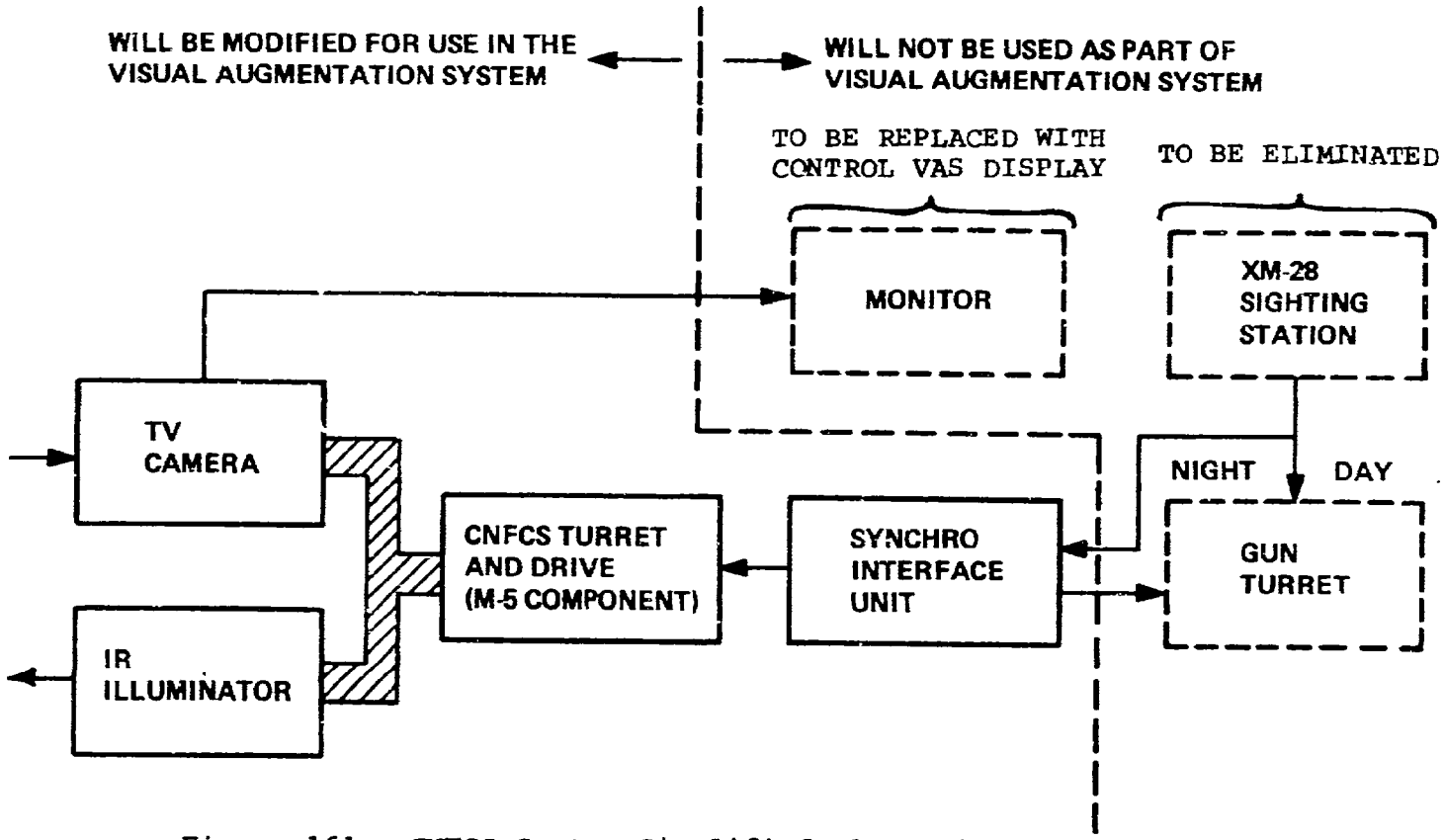


Figure 161. CNFCS System Simplified Block Diagram.

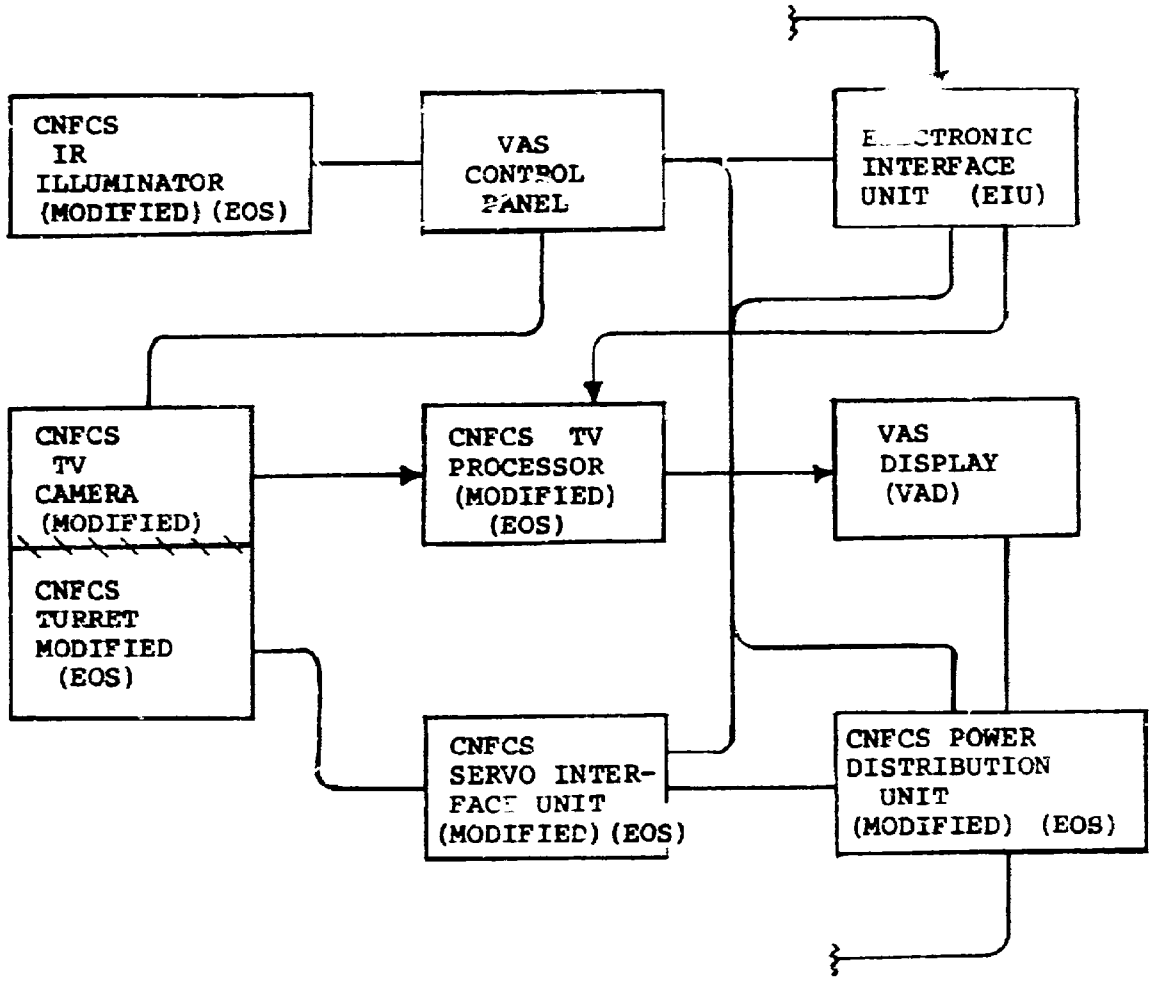


Figure 162. CNFCS Modifications for VAS.

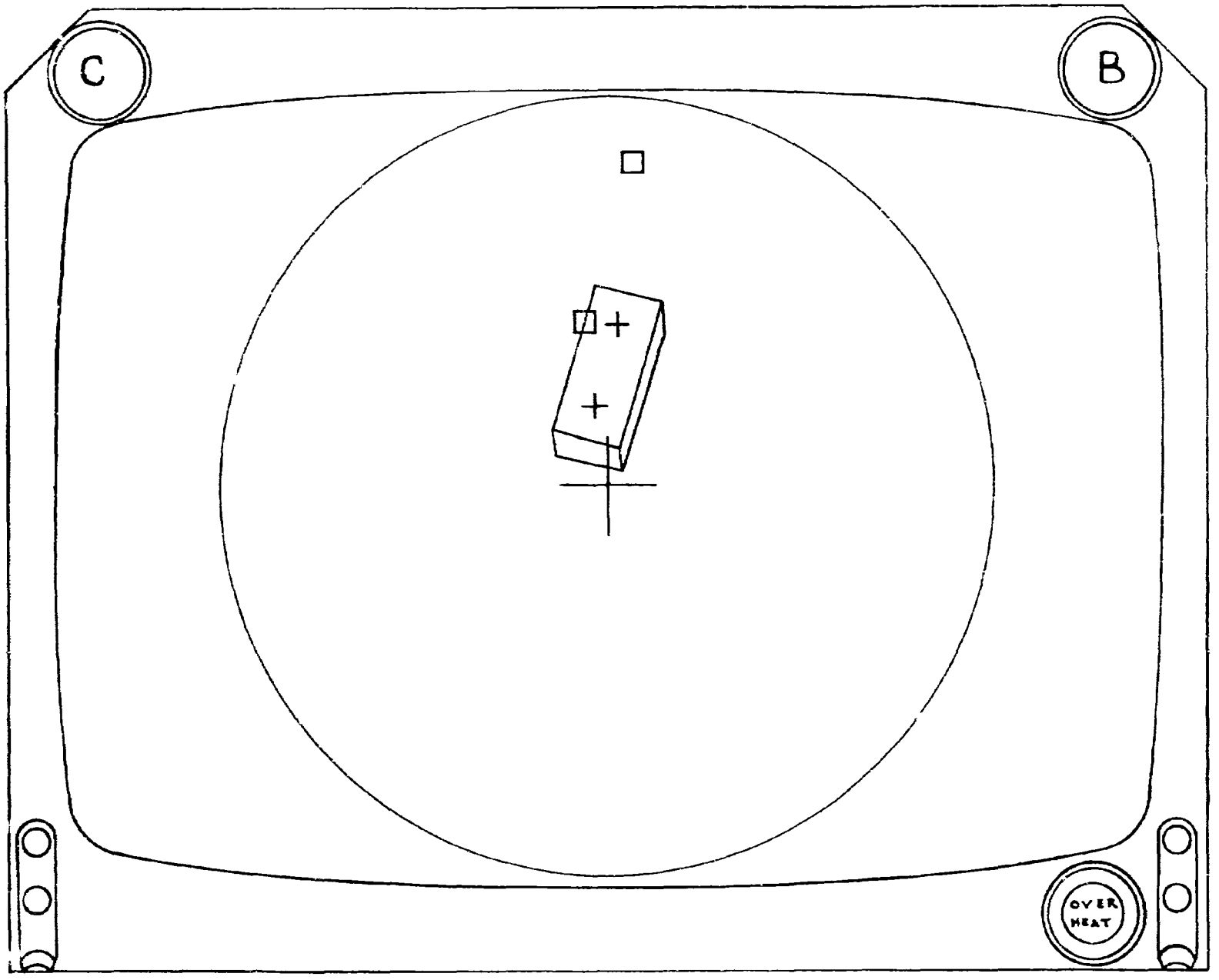


Figure 163. Full-Scale Outline of Visual Augmentation System Display.

3. The CRT tube face-plate has been gold-flashed to reduce EMI/RFI from the front of the tube which conceivably could interfere with low-frequency radio aids to navigation.

The display is designed to meet ambient lighting conditions of 5.83×10^3 foot-lamberts, compared with the 10^4 foot-lamberts currently specified for most Army aircraft. It is rationalized that in a production configuration, the display could be equipped with an ultra-high contrast filter to complement the P-31 phosphor and meet the 10^4 foot-lambert criterion.

Electro-Optical Sensor (EOS)

The Electro-Optical Sensor for VAS is a major modification of the CNFCS sensor. RCA coupled each of the prime lenses to its own field lens, which converges the image into the entrance pupil of the zoom optics. Each prime optics assembly is manually interchangeable at the front of the optical relay assembly. In a production configuration, should more than one prime lens be required by a single sensor, it is reasonable to assume that multiple lenses could be provided on a motor-driven turret.

The optical relay design is shown graphically in Figure 164 and pictorially in Figure 165. The 2:1 momentary zoom feature of the CNFCS employed an overscanning technique which resulted in loss of resolution in the zoomed condition. To eliminate this problem, RCA elected to use infinitely variable, motor-driven optical zoom. The Rank-Taylor-Hobson Zoom Telecommande was selected as the best off-the-shelf device for this application. The Telecommande normally has a 20-100MM (5:1) zoom capability. In order to make the one zoom compatible with all three prime lens elements, RCA modified the Telecommande to 25-125MM, which results in an apparent reduction of zoom capability of 3.5:1 in the worst case (130° lens). With the three prime lenses and the zoom optics, a capability exists to permit assessment during the demonstration program of all FOV's between 37° and 220° without loss of optical resolution. The zoom optics is followed by a wide band, hot mirror. The spectral response of this mirror combined with those of the prime lens and the intensifier photocathode will assure that VAS is not affected by radiation from the Precision Hover Sensor (PHS) illuminator operating in the .85 region. After passing through the hot mirror, the image is deflected by the folding optic mirror onto the original CNFCS prime lens (Aerojet Delft 150MM Deltamar) which is used as a final imaging lens for the CNFCS intensifier and TV camera. The CNFCS TV camera was modified by RCA's Burlington Division to operate at 875 lines rather than 525 lines.

RECEIVED [illegible] NOT FILMED

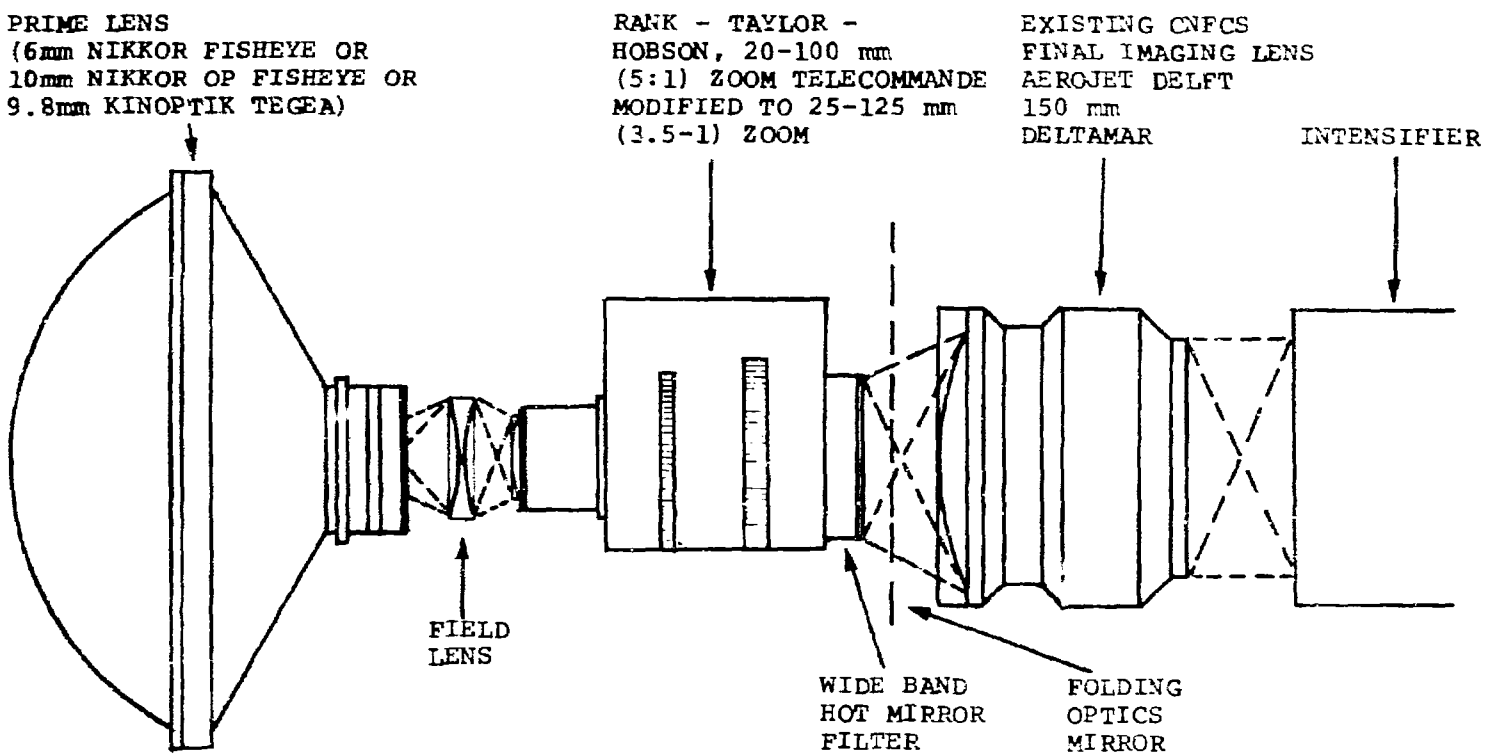


Figure 164. VAS Optical Relay Scheme.

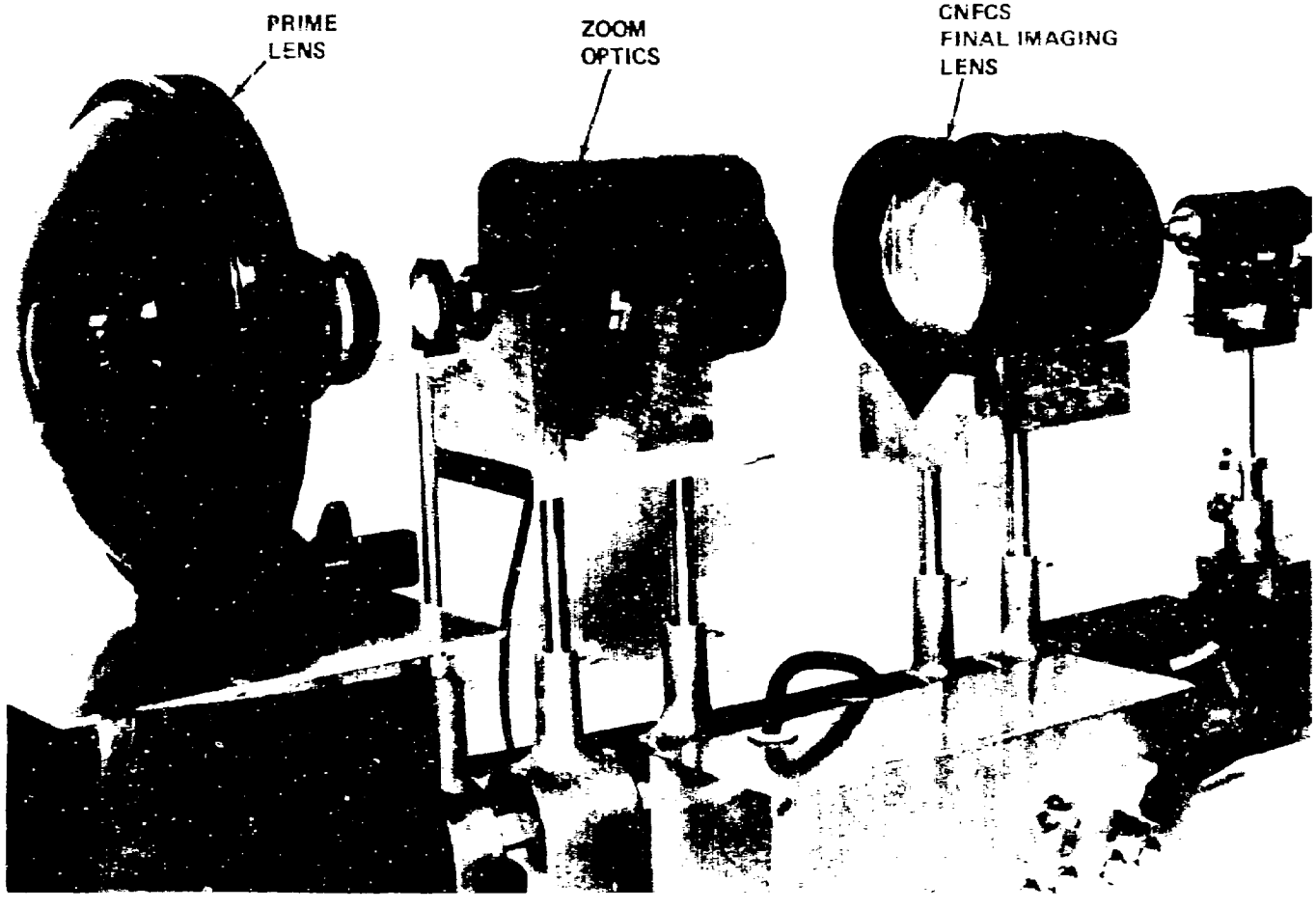


Figure 165. VAS Optical Relay System Mockup.

Electronic Interface Unit (EIU)

The EIU is the intelligence center for the VAS. Relationship of the EIU to other elements of the VAS/modified CNFCS is shown in Figure 166. The primary functions of the EIU are as follows:

1. Generates master clock signals for the sensor and display units.

2. Generates cargo handling symbology.

3. Computes desired symbol positions with respect to real-world video as a function of aircraft attitude, altitude and cable extended length.

4. Superimposes symbology on TV video.

Because the 347 will not have operable hoists, RCA has elected to input extended cable length as a manually inserted constant. In a production configuration, this parameter would be an infinitely variable input from the cable length sensors. Once cable length, altitude, and attitude information have been input to the EIU, desired symbol position is computed by the circuitry shown in the block diagram of Figure 167. Generated symbology is as shown (not to scale) in Figure 168. It will be noted that two symbol sizes are being offered for evaluation in the ATC demonstration program. It is anticipated that a single symbol size would be adequate for a production configuration.

Also, as a result of the Critical Design Review, it was proposed that the calibrated symbology be presented for both the wide field of view and the narrow field of view of 180° OP lens instead of only the wide field of view for the 220° fisheye lens. Subsequent negotiations between Boeing and the Army resulted in approval of this proposal, and RCA was authorized to provide two manually interchangeable sets of symbology memory with the delivered hardware, programmed for the wide and narrow fields of view for the 180° lens.

Illuminator

The illuminator for VAS is the CNFCS illuminator, with its optical modules modified to produce an overall illuminated field of 50 degrees. In a production system the field could be extended to 60 or more degrees, and the illuminator could be range gated to reduce the effect of backscattering and aid in the penetration of visual obscuration. The CNFCS illuminator is shown in Figure 169.

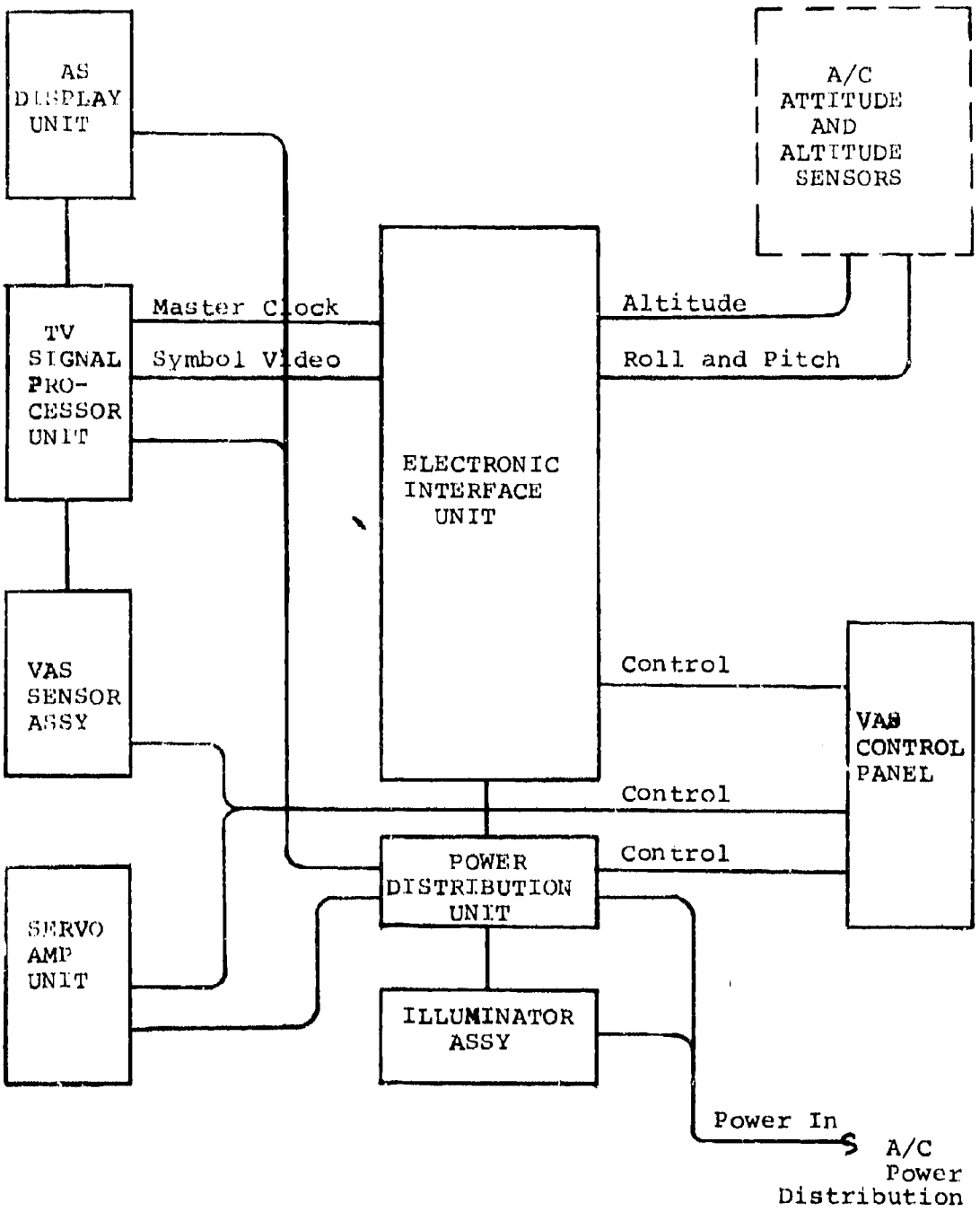


Figure 166. EIU Interface Diagram.

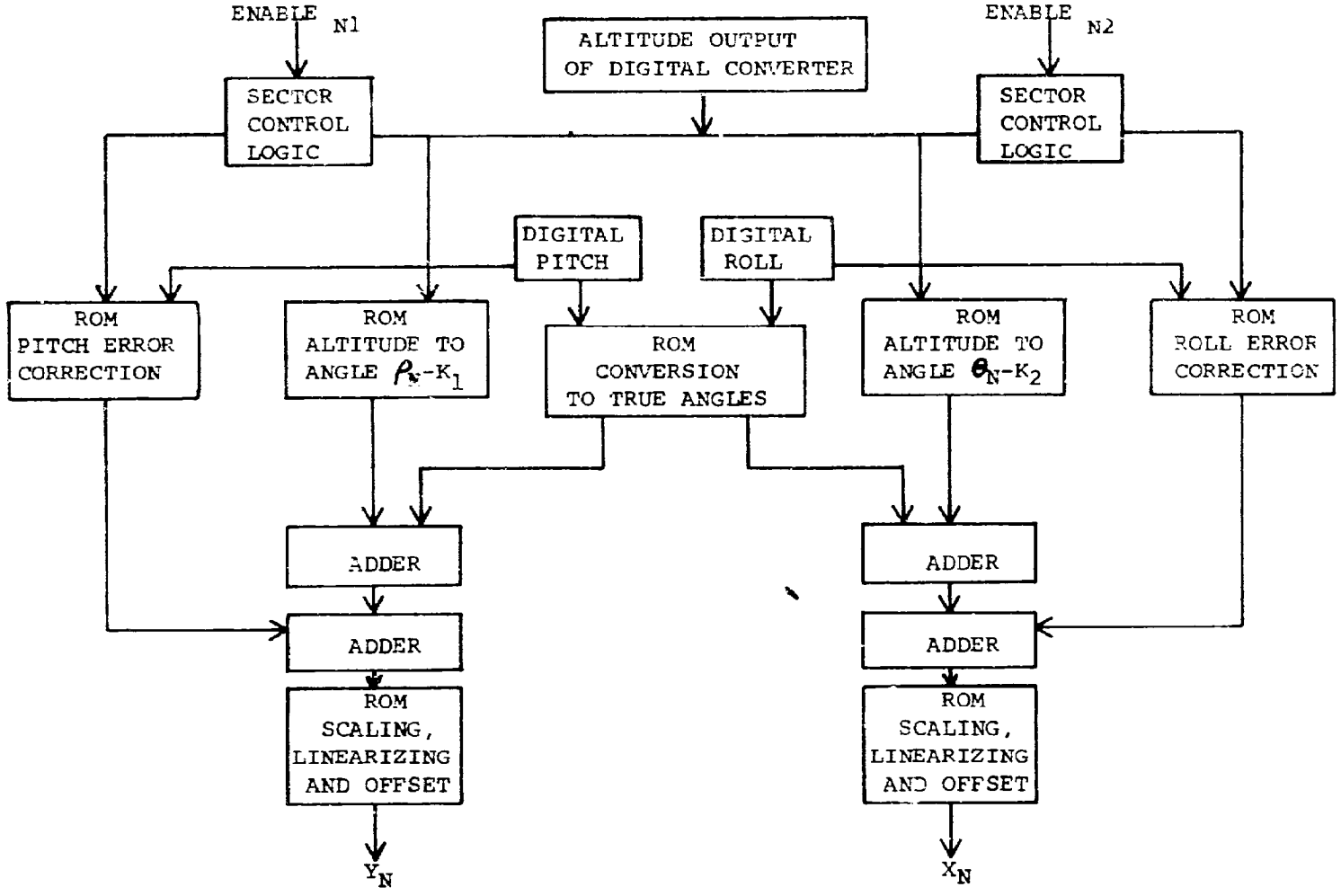
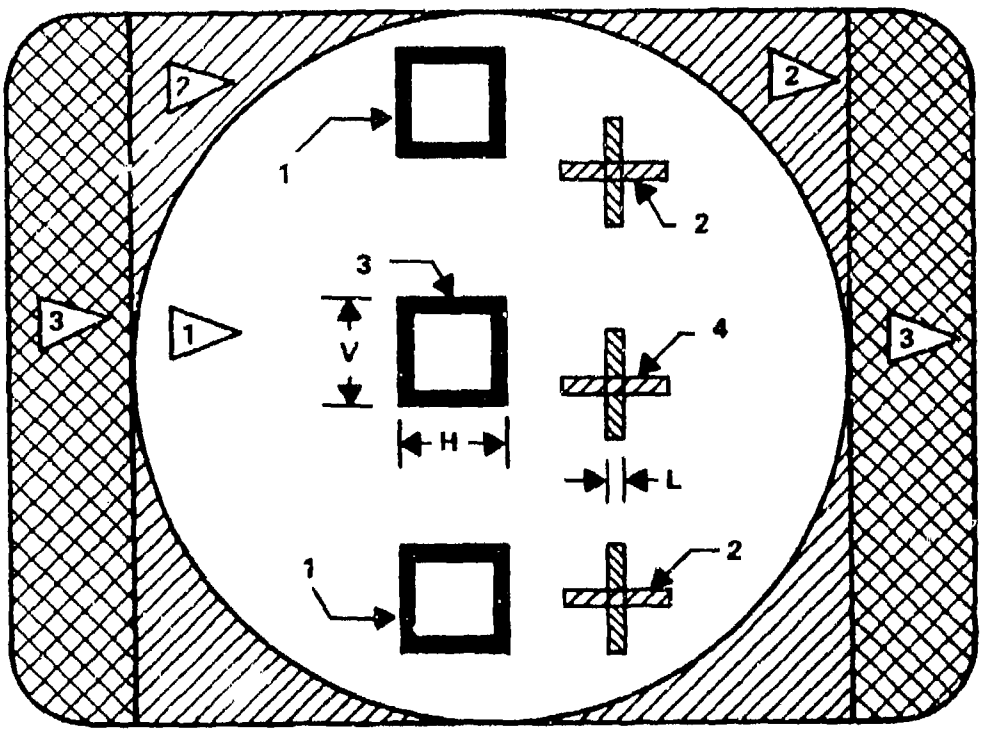


Figure 167. Symbol Positioning Logic.



NOTES:

1 Tension Member Hook Position: Aft (Top), Forward (Bottom)

2 Tension Member Projection: Aft (Upper), Forward (Lower)

3 Single Tension Member Hook Position

4 Centerpoint Projection (Dual Members)
Tension Member Projection (Single Member)

V Vertical Dimension of Symbols (in terms of resolution elements) will be preflight selectable to either 14 or 28

H Horizontal Dimension of Symbols (in terms of resolution elements) will be preflight coselectable with V to either 14 or 28

L Line width of symbols will be 2 resolution elements

1 Information area of display face (800 elements diameter)

2 Raster scanned area of display face (800 elements square)

3 Unscanned area of display face

Figure 168. VAS Symbology Characteristics.

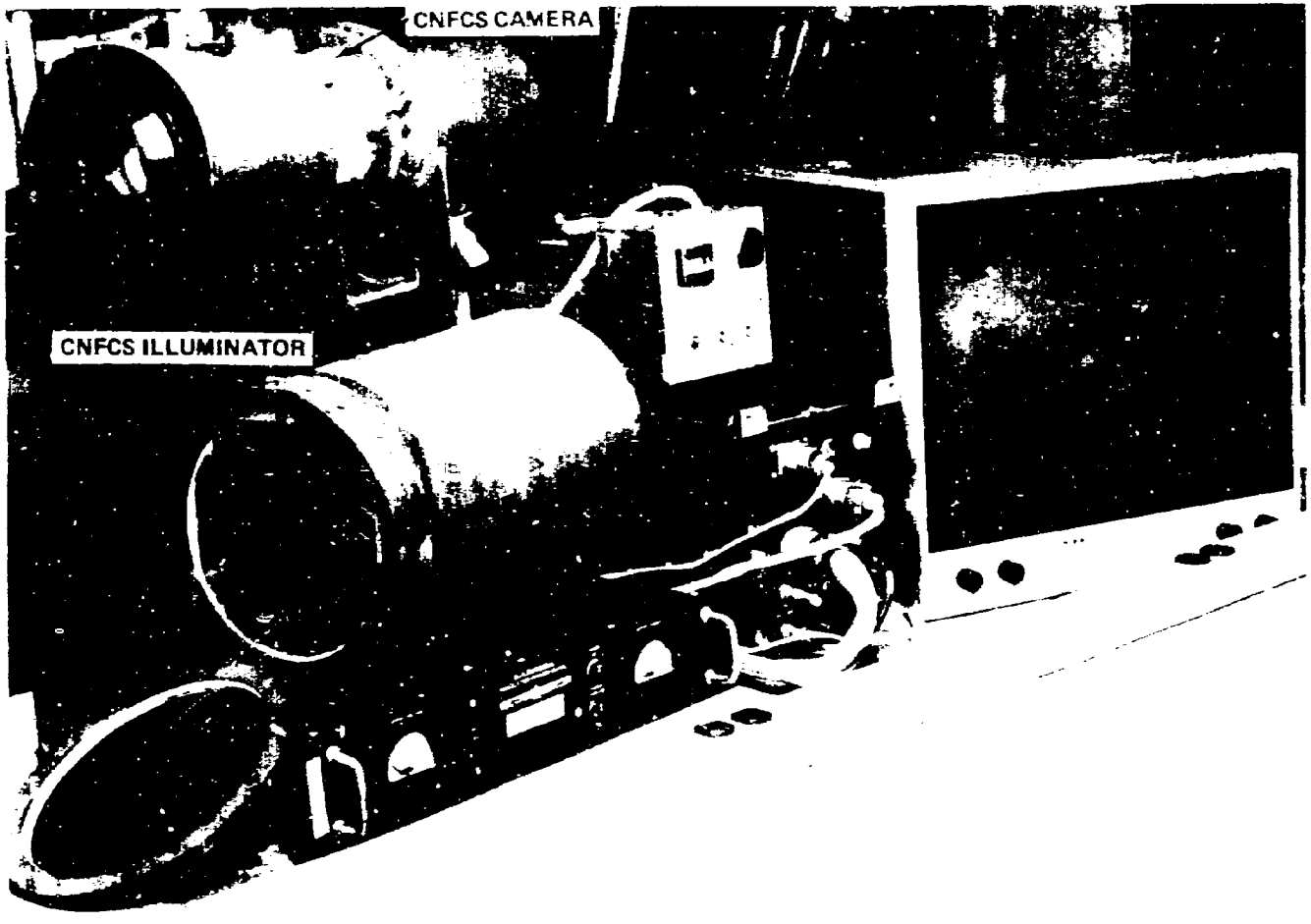


Figure 169. CNFCS Components.

VAS Control Panel

The VAS control panel is shown in Figure 170. This panel contains power and illuminator on/off switches as well as brightness and blanking controls for the symbology. Any or all hook symbology can be blanked to de-clutter the presentation. Camera elevation control is possible along with an indicator to show when the camera is in transit to or from its stowed position. Controls are provided for manual operation of the focus and zoom features of the camera, and for selection of manual or automatic mode of sensor brightness control. In the manual mode, the operator controls sensor brightness by varying the intensifier gain, opening or closing the iris, and if necessary, extending or retracting the glare shield to prevent the illuminator or sun from appearing in the field of view. When the self test function is actuated, selected inputs are fed to the EIU which drive the symbols to predetermined positions, thus indicating proper operation of the system.

CNFCS Modification

Fabrication of a demonstratable VAS required a series of modifications to the CNFCS system. The XM-28 Sighting Station, Servo Amp, Sight Distribution Cables, Range Pot, Turret Azimuth Control and TV Control Panel have been eliminated, as shown in Figure 171. The existing gimbal system has been modified to remove the trunnion (azimuth) axis, thus reducing complexity and system weight by about 40 pounds. In addition, CNFCS cables were acquired from an AH-1G undergoing refurbishing at ARADMAC. Modification and use of these cables have facilitated CNFCS component checkout and reduced cable costs in the demonstration system.

To better assure proper interface with the Model 347 helicopter, RCA constructed the sensor mounting jig shown in Figure 172. Examination of the sensor/gimbal assembly in this jig led to the selection of mounting locations for 374 demonstration shown in Figure 173. The line of sight of the camera is such that it bisects the angle formed between the lens and the two hooks over the full range of camera elevations.

Visual Augmentation System Hardware

The VAS is basically a closed circuit TV system with a very wide field-of-view and dynamic range of scene illumination characteristics. It consists of a modified Cobra Night Fire Control System TV Sensor and a Conrac 875 line Display for good resolution and a symbol generator to synthesize and position symbols representing cable couplings and ground intercept points of their vertical projections. A new control

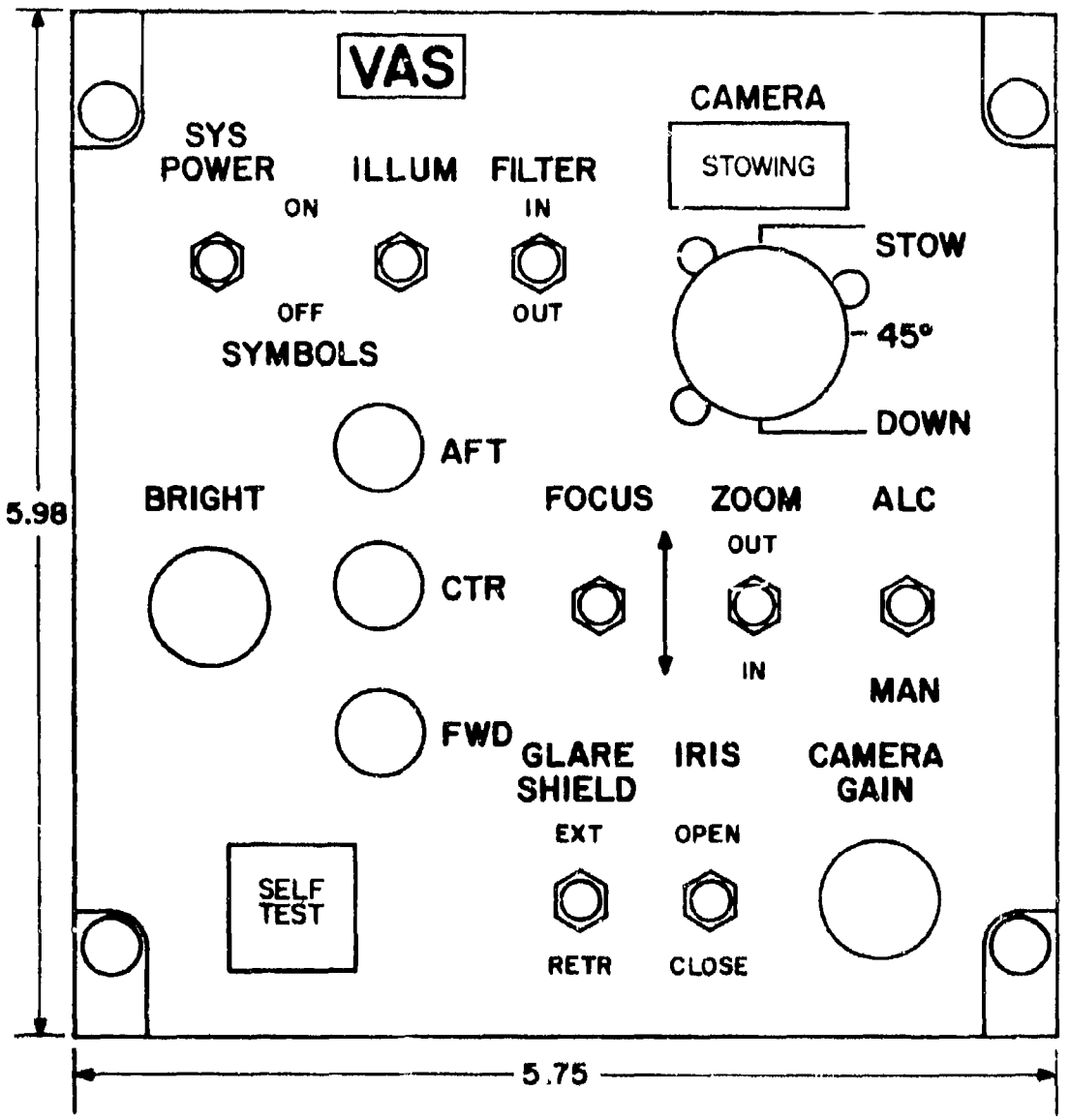


Figure 170. VAS Control Panel.

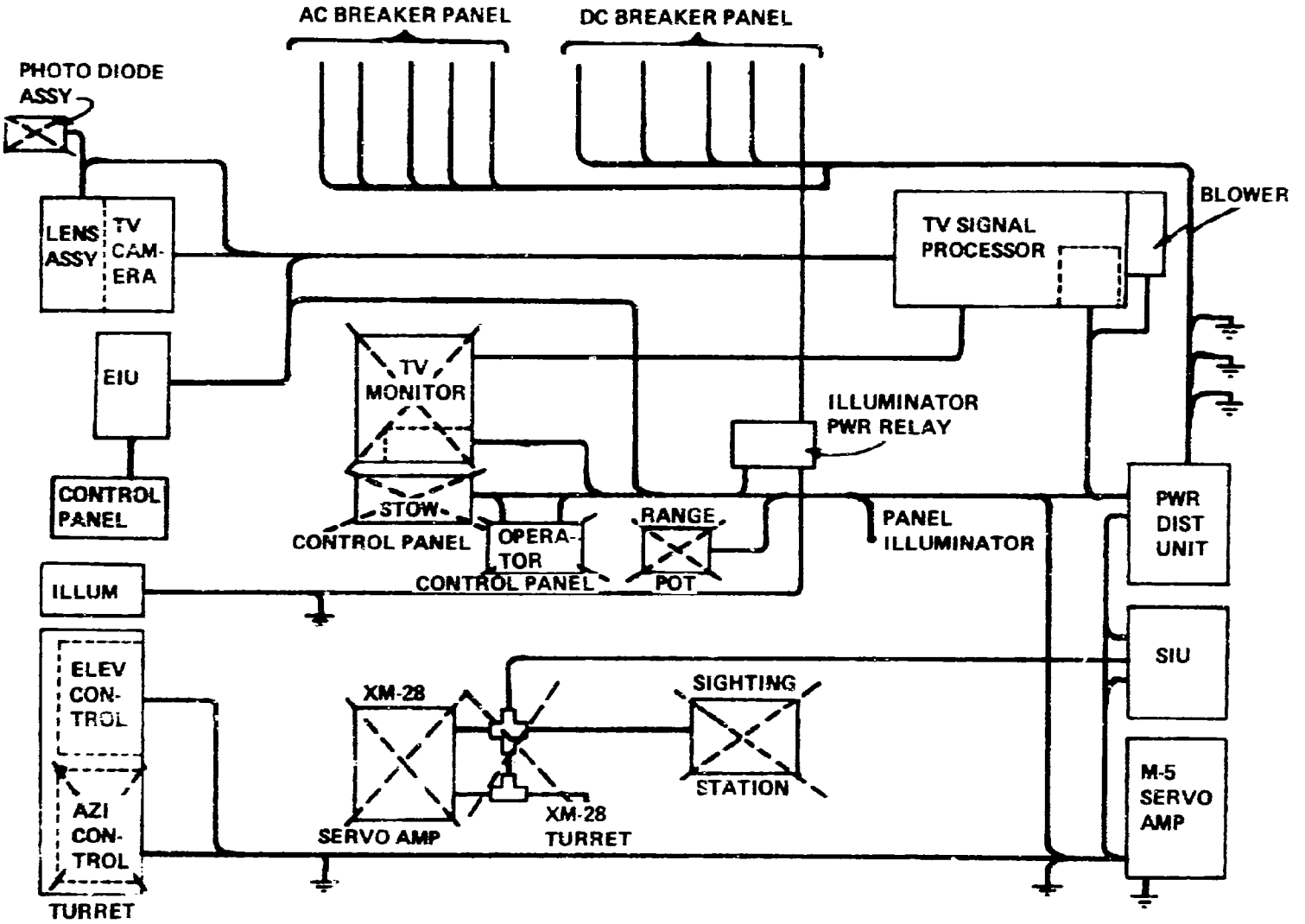


Figure 171. CNFCS System Modification Block Diagram.

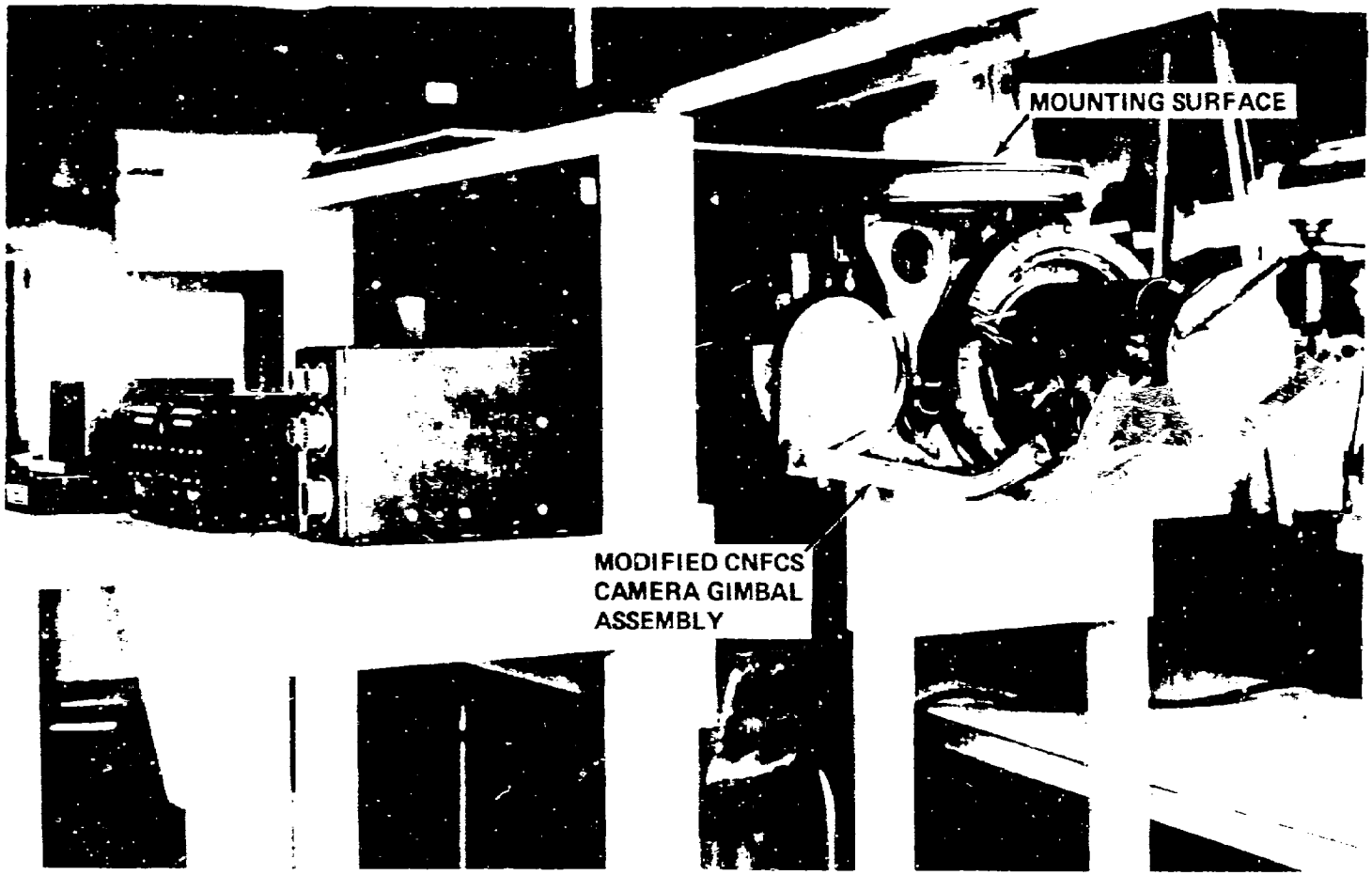
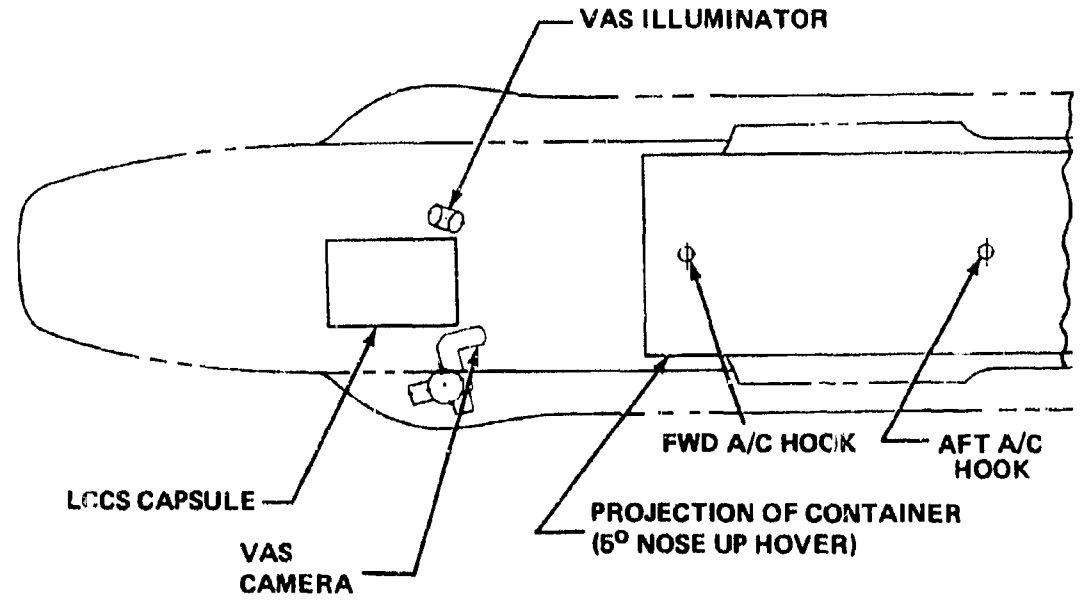
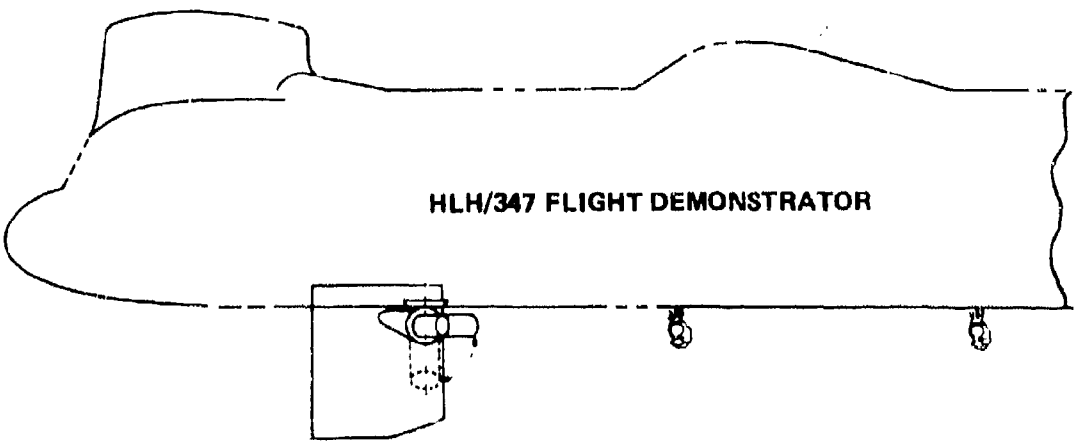


Figure 172. CNFCS Camera Mounting.



(Plan View)



(Side View)

Figure 173. VAS Equipment Location on Model 347 Helicopter.

panel and an auxiliary semi-covert illuminator for extremely low light level use are also provided.

Interconnection between the hardware is shown in Figure 174, and outline drawings for the components are shown in Figures 175 through 180.

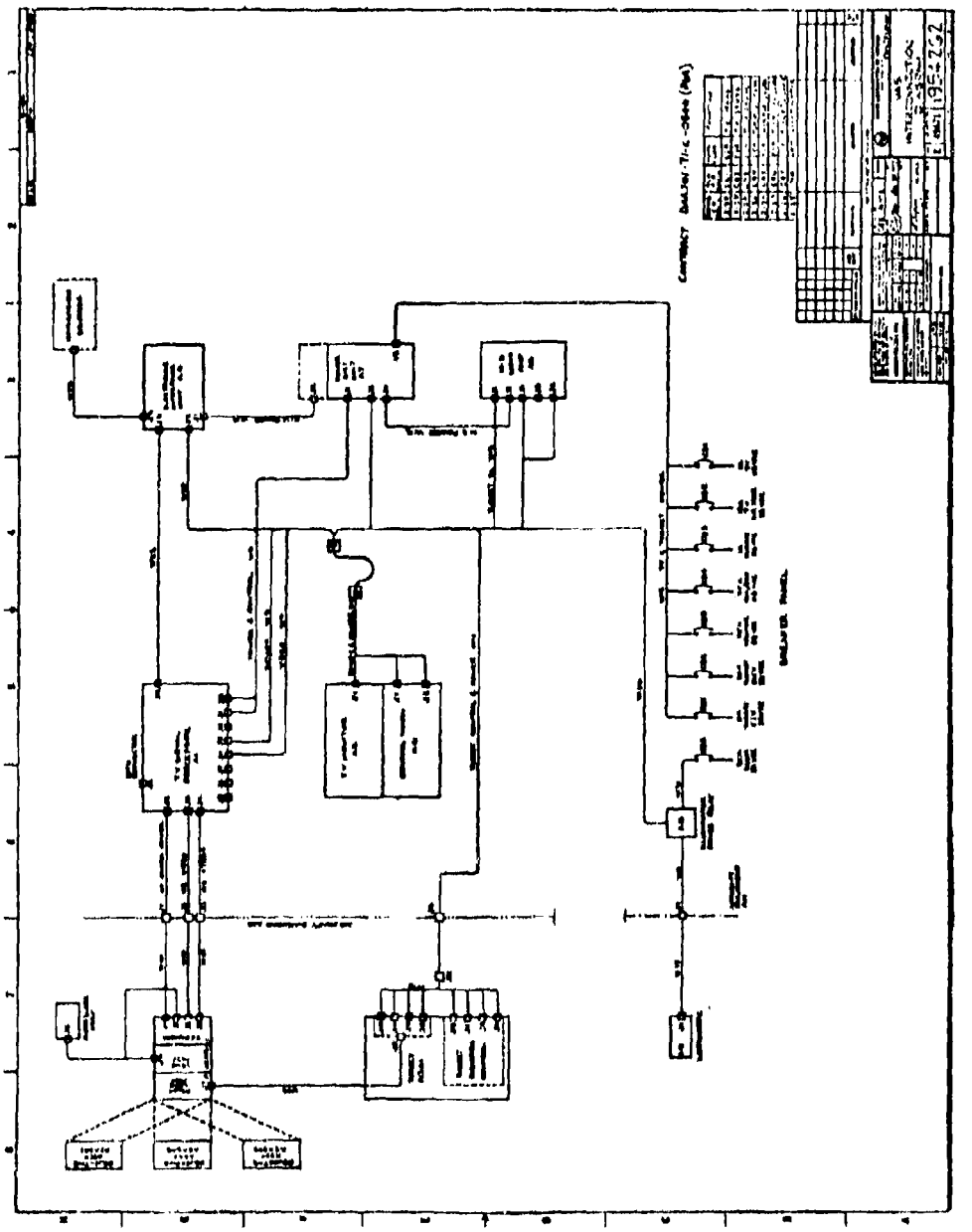


Figure 174. VAS Interconnection Diagram.

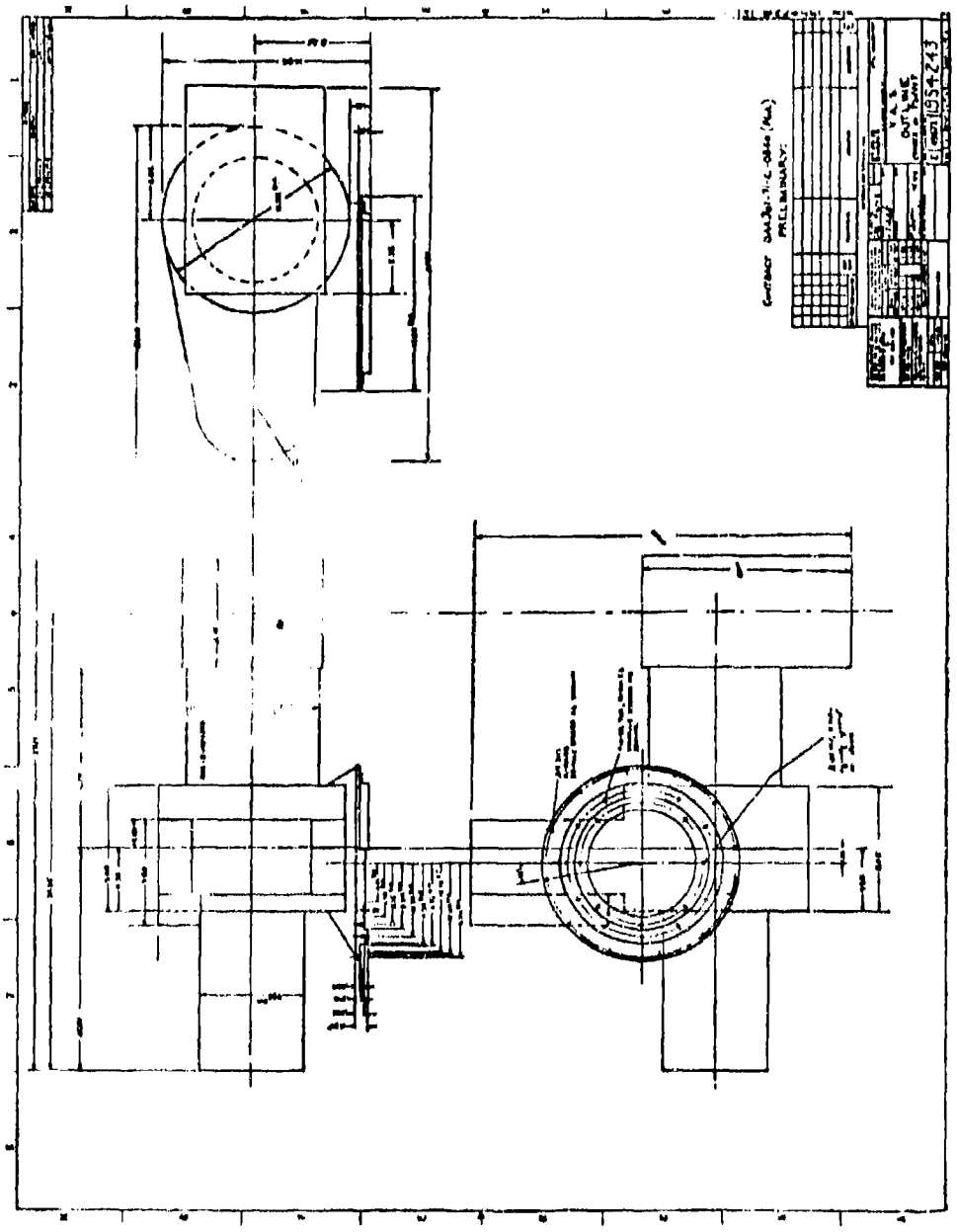


Figure 175. Camera and Turret Outline.

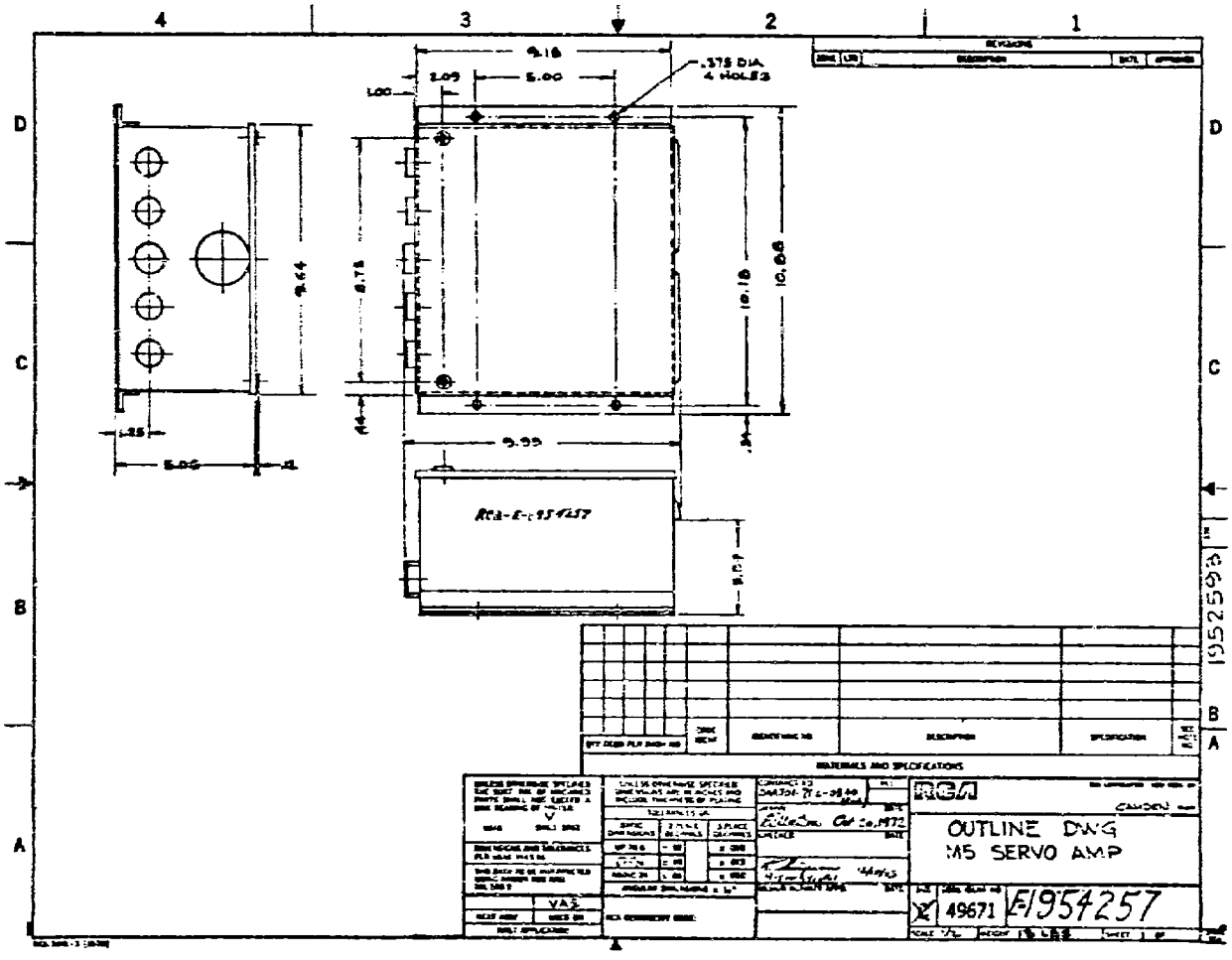


Figure 176. M5 Servo Amplifier Outline.

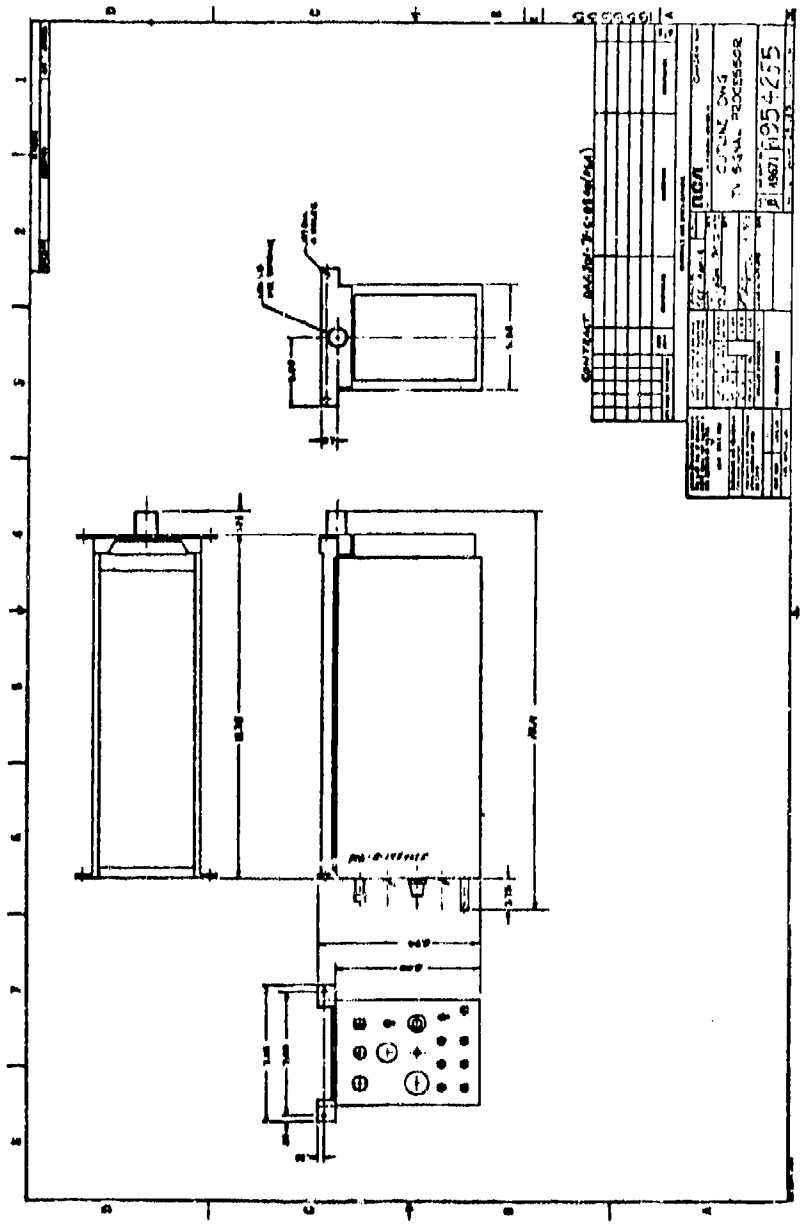


Figure 177. Signal Processor Outline.

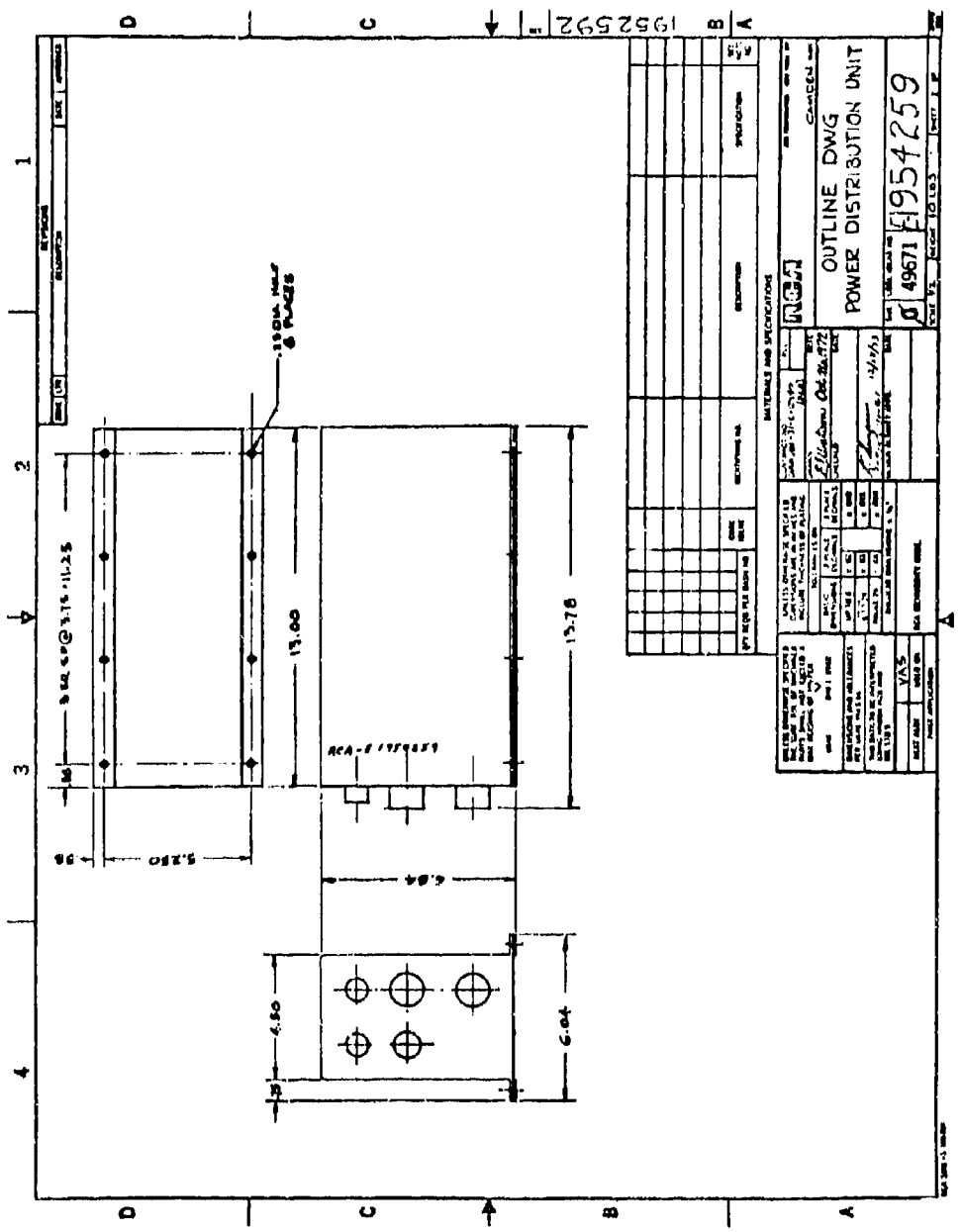


Figure 178. Power Distribution Unit Outline.

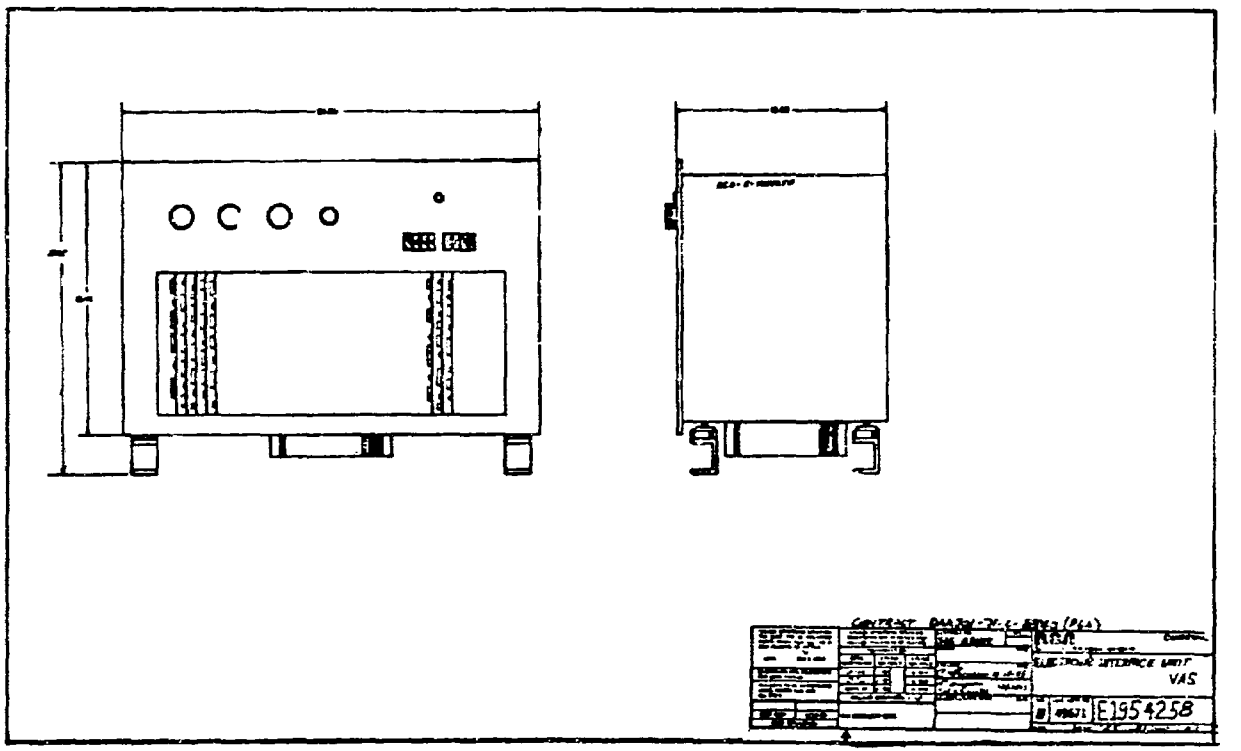


Figure 179. Electronic Interface Unit Outline.

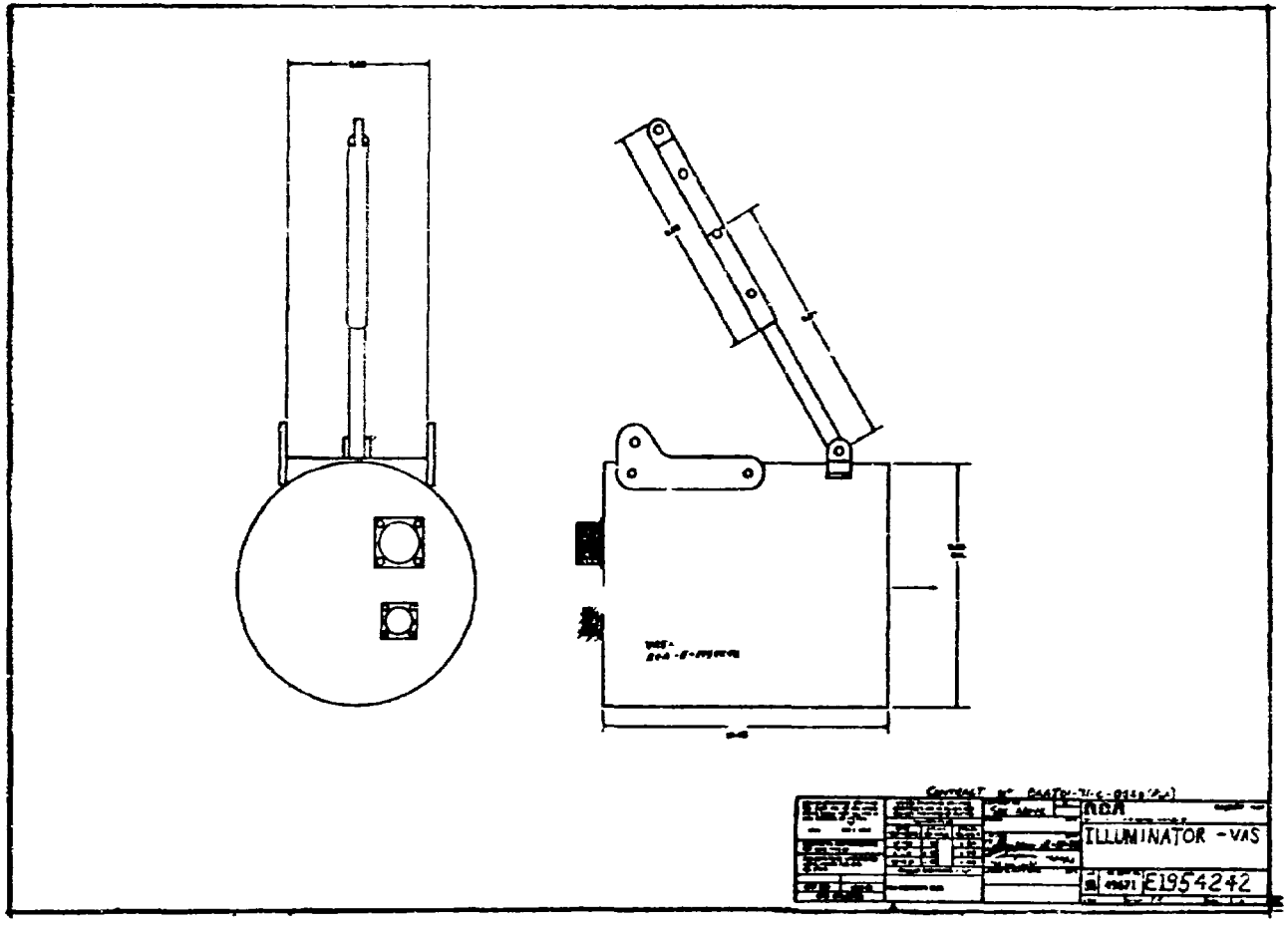


Figure 180. Illuminator Outline.

STATIC ELECTRICITY DISCHARGE SYSTEM

Objective

During forward flight and hover a helicopter can acquire an electrostatic potential, through several different mechanisms, which is different from that which exists on the ground. This potential can range as high as 200,000 volts on an HLH sized vehicle. When the helicopter lands, the electrostatic potential between itself and the ground is equalized either by a spark discharge or by direct ground contact through a conductive path.

When a helicopter acquires external cargo while in hover, without landing first, no conductive discharge path exists for the electrostatic potential equalization until the hookup man or a conductive sling or both touch the helicopter. Such electrical discharges through the human body are felt as shocks ranging from mild discomfort through levels which under certain circumstances could be dangerous or even lethal.

The purpose of the static electricity discharge system is to provide a safe means to equalize the electrostatic potential between a hovering helicopter and the ground, to protect ground handlers from severe shock and to minimize sparking which can alarm unsophisticated personnel and possibly ignite flammables and explosives.

Background

Two basic concepts exist for solution of the large hovering helicopter static electricity discharge problem:

1. Active Dissipation
2. Passive Dissipation

Active dissipation involves remote sensing of the potential difference between the helicopter and the ground in terms of magnitude and polarity of charge. This information is then used to control a high voltage bi-polar power supply which equalizes the potential by forcibly discharging proper polarity ions into the air surrounding the helicopter via electrified corona dischargers. When external cargo hookup operations are being conducted in natural charging conditions, such as blowing dust or snow, the active system must also be capable of rapidly following changes in the polarity and level of charging, which can vary from zero to maximum value in a matter of seconds.

Passive dissipation involves rotor blade mounted fully-passive corona dischargers to limit the maximum potential which the helicopter can attain before going into free body corona. In addition, a resistive grounding link is suspended from one cargo coupling to provide a low-spark conductive path to the ground before the ground handler can reach and touch the coupling or any other part of the helicopter.

The HLH contract initially called for the development of an active discharger system. Based on this stipulation, the three-part program[6] outlined below was performed.

1. Laboratory dissipator tests using a low-speed wind tunnel and a full-scale mockup of an engine exhaust and aft helicopter fuselage.

2. Helicopter ground tests of selected active dissipator configurations to evaluate the thermal, acoustic, soot and flow field effects of an actual engine exhaust plume.

3. Full-scale flight tests on a CH-47 helicopter at the U.S. Army Yuma Proving Ground to evaluate active dissipators and remote sensors under conditions of actual helicopter trioelectric charging while hovering in a dust cloud.

A summary of the program is provided in succeeding paragraphs.

Active System Elements

The design elements of the active system can be divided into:

1. Powered high voltage dissipating system capable of up to ±600 microamperes net current. (Net current equals discharge element current minus recirculation current.)

2. Remote sensing system capable of establishing the magnitude and polarity of charge on the helicopter with an accuracy such that an indicated potential equalization would allow no more than 14,000 volts residual helicopter voltage (200mJoule discharge energy).

3. Electronic feedback control loop system connecting the sensing and dissipating elements into an automatic discharge system. Design of a stable control loop depends on the accuracy of sensing and response speed of the system.

6. Solak, B.J. and Wilson, G.J.; TECHNOLOGY DEVELOPMENT REPORT - RESULTS OF STATIC ELECTRICITY DISCHARGE SYSTEM TESTS (ACTIVE AND PASSIVE) HEAVY LIFT HELICOPTER; Boeing Vertol Company; USAAMRDL Technical Report 74-22, U.S. Army Air Mobility Research & Development Laboratory, Ft. Eustis, Va.; 1974.

Dissipating Systems

The following dissiptaing methods were tested and found feasible:

1. Dissipation into the turbine exhaust; three corona rings located 5 turbine exhaust orifice diameters aft, fed by 200 to 250 KVolts.

2. Dissipation into the helicopter downwash, eight corona points located approximately 6 feet away from the fuselage, fed by 200 to 250 KVolts.

In order to reduce the recirculation to the fuselage, two additional dissipation methods were investigated, namely;

1. Aerosol Discharge System developed by the U.S. Army Electronics Command, Fort Monmouth. This method uses a relatively low voltage (6 to 8 KV) but requires a supply of compressed air and of conductive liquid (water with NaCl added).

2. Repetitive pulse technique (100 KVolt pulse voltage) investigated for Boeing Vertol by ION Physics Corporation.

Both methods show relatively minor improvements in the dissipation efficiency at a considerable expense in design penalties. They were not pursued further, especially in view of a fundamental difficulty in sensing which is described next.

Sensing System

The only known method to remotely sense the voltage between two objects is to infer it from the measurement of the electric stress (field) between them. As long as the intervening space is free of electric charges, voltage can be uniquely related to the electric field. This is, however, not the case with electrostatic charging. Flight test experience indicated the presence of charges between the helicopter and the ground which falsify the voltage sensing. Since the intervening charges produce an error signal in the voltage sensing scheme, it was decided that a measurement of this error would be decisive in determining the lowest possible residual helicopter voltage achievable with a "perfect" servo loop controlling the discharge apparatus.

Prior to the active discharge program the generally accepted schematic of charging of the helicopter was as shown in Figure 181and was based on the experience and measurements conducted on fixed-wing aircraft. It was reasoned that lowering the sensor some distance away from the negative ion cloud generated by collisions of dust with the blades, would

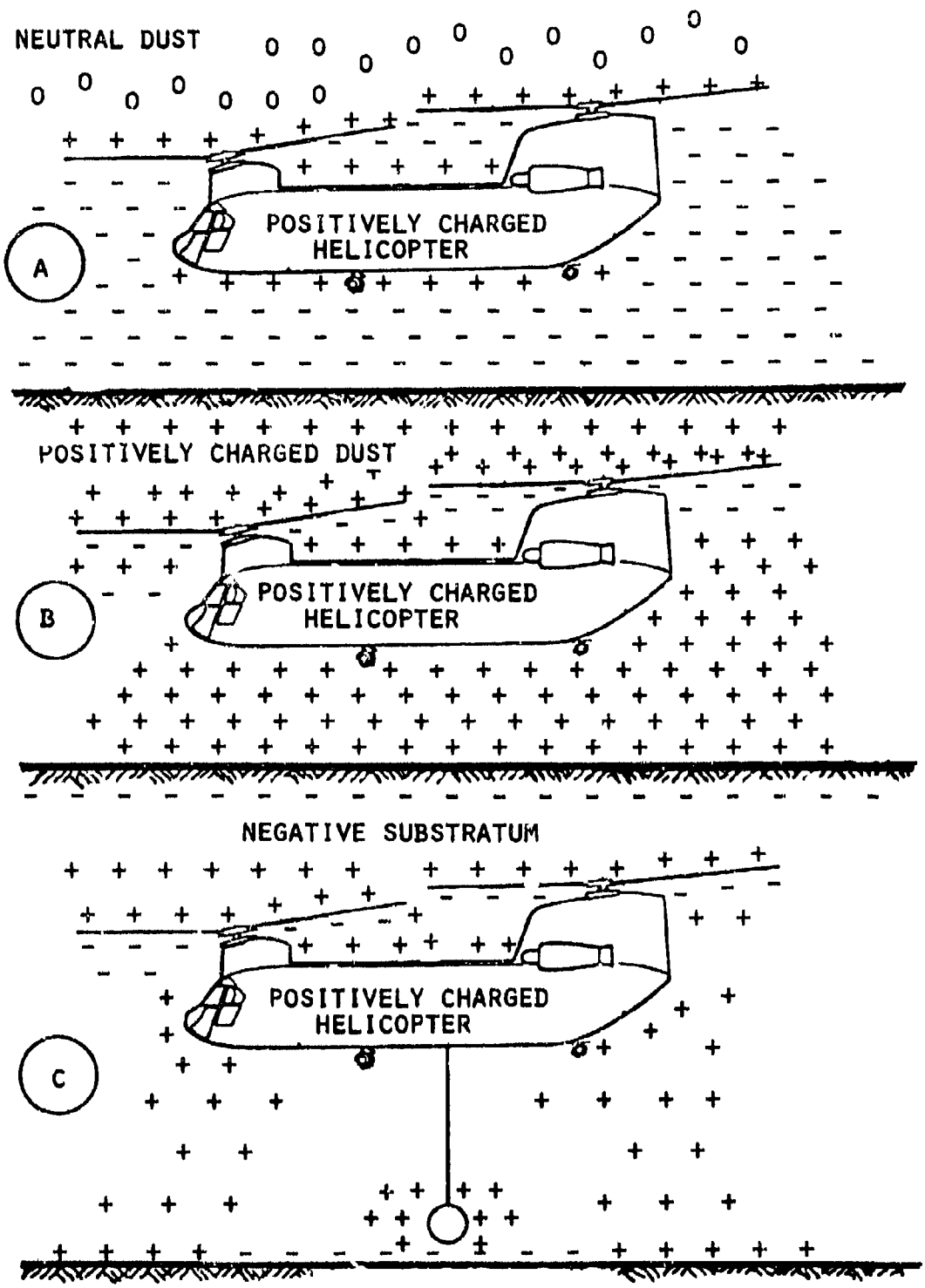


Figure 181.Charging Schematics.

eliminate or significantly reduce the sensing error and would allow a stable closing of the control loop for the dissipating system. The conditions measured during the active discharge showed a radically different structure of the dust cloud as shown in Figure 181. The dust cloud surrounding the helicopter is of the same sign (positive) as the charge deposited on the helicopter. In the positively charged dust cloud the negatively charged particles bouncing away from the blades are barely detectable. The question arose, where were the negative charges which neutralize the positive helicopter charge when contacting the hovering helicopter? The only plausible explanation is that the negative charges are in the conductive substratum of the desert and come to the surface as the altitude of the helicopter or cargo hook over the desert is decreased as depicted in Figure 181.

To measure the voltage sensing error, the hovering helicopter was grounded directly to a stake. Under such conditions any electric field measured by helicopter-borne field mills is an error due to the surrounding ion cloud. When the field mill indications are driven to zero by an active discharge apparatus, the required power supply voltage is a measure of the potential error (since the helicopter is grounded). Conversely, a measure of the error can also be obtained by inferring the helicopter potential from the measured electric field with the helicopter grounded and the power supply set to zero. The HLH discharge energy, which would be encountered with this "residual" potential (under actual operational circumstances), can then be calculated from the residual potential and the estimated HLH capacity of 2000 pF.

Since the residual potential error was random in nature, varying widely in polarity and magnitude, statistical analysis was the only suitable method of interpreting the experimental results.

In Figure 182 a statistical summary of the probability of a shock when touching a helicopter using field mills and hovering in a dust cloud is presented in terms of precentage of time that the discharge energy will exceed the energy on the ordinate axis. The acceptable shock level, based on experiments conducted during the passive static electricity flight tests, was shown to be 200 millijoules. As can be seen, the 200-millijoule level will not be exceeded 3% of the time for Field Mill #3, 14% for Field Mill #2, 25% of time for Field Mill #1 when suspended half way between the helicopter and the ground and 50% of time when it is suspended 5 feet over the desert. Following the probability curve of Field Mill #1 suspended 5 feet over the desert, we find that a 500-millijoule level will be exceeded 26% of time and a 1-joule level may be exceeded a small percent of time in hover in the dust. It can be estimated that to increase the sensing accuracy to ensure that 200 millijoule will not be exceeded while hovering in dust, the sensor would have to be placed 2 to 3

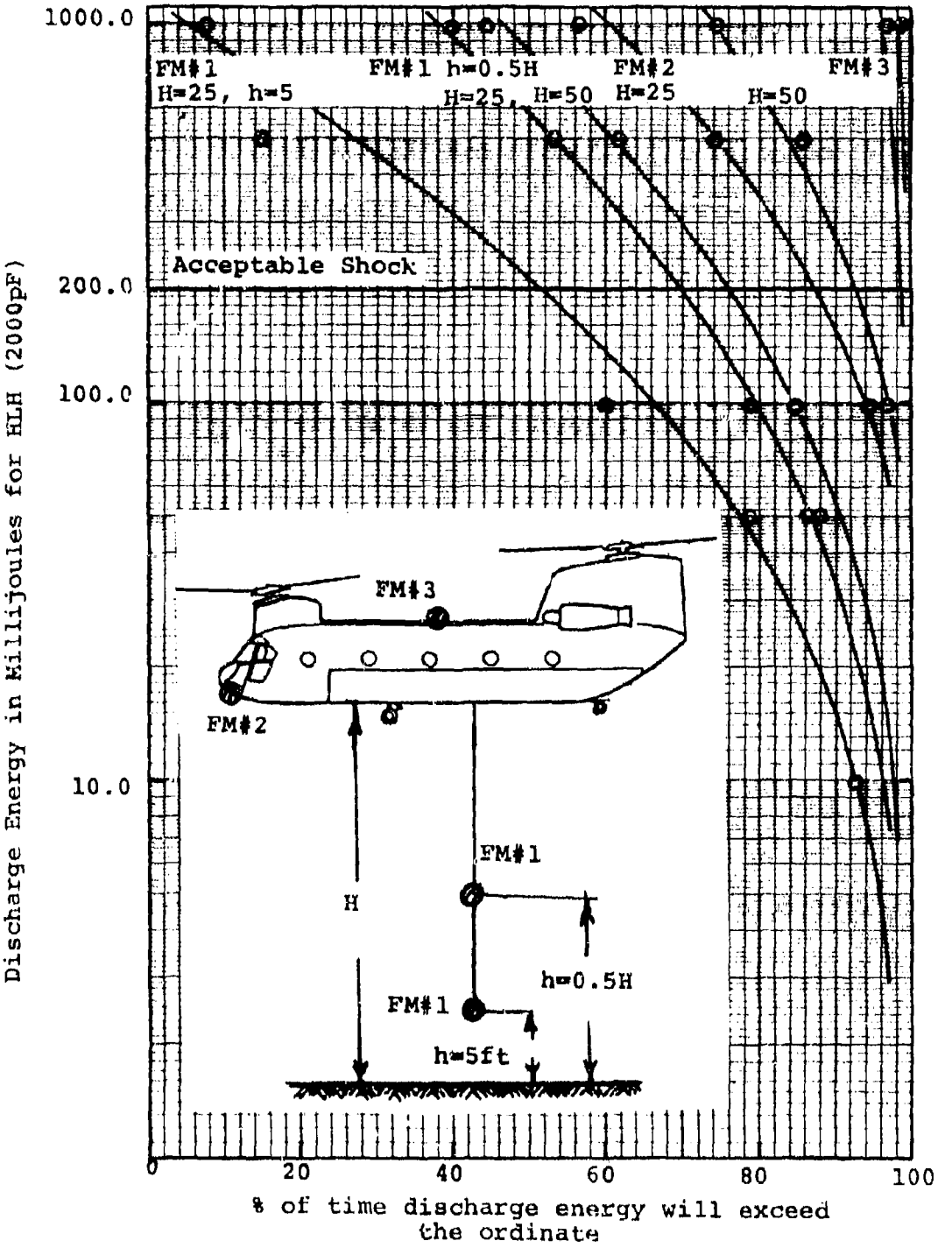


Figure 182. Accuracy of Voltage Sensing and Residual Shock Energy for HLH Hovering in Dust (Yuma Desert).

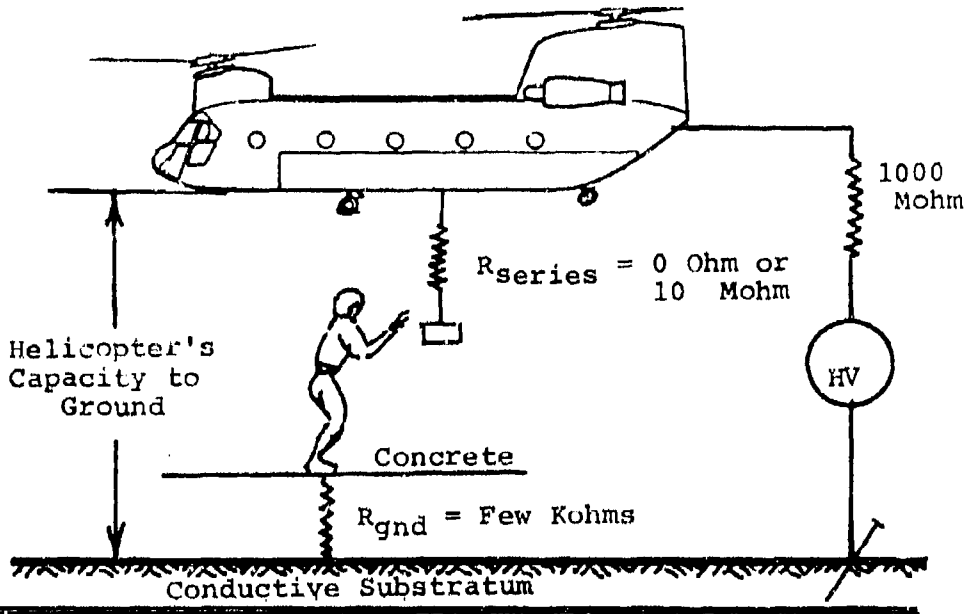
feet above the ground surface or from the extended hand of the cargo handler. Such placement accuracy of a freely suspended sensor under a hovering helicopter was considered to be unacceptable, and the static electricity program was redirected toward the dissipation of static charge by dropping a grounding electrode 2 to 3 additional feet, i.e., resting it on the ground surface.

Physiological Response to Static Electricity Discharge

Defining the levels of impulse shock (up to the lethal level) is difficult due to the complex way in which electrical shock affects the body. A case is described in the literature (Dalziel) in which a young man was killed by an impulse estimated to be 24 joules. The same source quotes cases in which people received comparable or higher shocks and survived with burns, unconciousness or severe headache. In the U.S.A., the reported injuries due to static electricity discharge from a hovering helicopter are limited to minor injuries such as small burns, split fingernails or backing off into some dangerous object. Experiments conducted by Dalziel indicate that a 0.1-second current pulse of 0.2 ampere will start fibrillation of the heart, and that the fibrillating current value is inversely proportional to time constant. The time constant of the HLH through the same 5000 ohms is 10^{-5} secs, giving 20 amperes as the fibrillating current. This corresponds to 100 KV potential difference between the HLH and the cargo handler on a good ground. Assuming that the maximum HLH voltage will not exceed 200 KV, calculations indicate that the minimum series resistance required to prevent fibrillation is of the order of 3 megohms.

Figure 183 shows the shock tests conducted with humans during the passive flight tests. The tabulation shows test results for 0 series resistance. An acceptable shock level was found to be 200 millijoules, which compares well with the 250-millijoule level established by Dalziel on animals.

When a 10-Mohm series resistance was inserted, the maximum acceptable discomfort level of 200 millijoules was established at 100 KVolt helicopter voltage. It was concluded that a 10-Mohm series resistance is a suitable design compromise between the lowest shock from the residual helicopter voltage after grounding and the highest helicopter voltage against which the cargo handler inadvertently touching the grounding electrode prior to grounding will be protected.



Aircraft Voltage (kV)	CH-47 Discharge Energy (mJ)	Equivalent HLH Voltage (kV)	Comments
2.5	3	1.8	
5.0	12.5	3.5	
6.0	20	4.5	(Dalziel threshold)
7.5	28	5.2	"Slight shock"
10.0	50	7.0	"Shock in fingers"
12.5	78	8.8	
15.0	112	10.2	"Sensible shock"
17.5	152	12.5	"Shock felt in wrist"
20.0	200	14.0	"Distinct shock felt in wrist and ankles"
23.7	250	16.0	"(Dalziel: Strong shock, not dangerous)"

Note: Assumed capacities CH47 1000 pF; HLH 2000 pF. R_{series} = 0 Ohms

Figure 183. Physiological Response of Subject Evaluating Anticipated Electric Shock.

Limiting the Maximum Voltage Level

The maximum voltage which a helicopter acquires when hovering under triboelectric charging conditions is reached when the charging current equals the corona current leaving the helicopter from points of high electric stress. Maximum voltages recorded were 200 KVolt for small helicopters hovering in snow or tropical rain and 120 KVolt for CH-47 helicopters hovering in severe dust (300 microamperes charging current).

By providing points of high electric stress in the form of passive dischargers, installed on the blade tips, the maximum voltage for a proven charging current can be lowered substantially as the experiments by ECOM and Princeton University have shown. However, the residual voltage is much too high to prevent severe shock to the man touching the helicopter.

It was reasoned that placing a corona discharger on the line suspended from a hovering helicopter may lower the residual voltage to an acceptable level.

To assess the contribution of a corona point suspended under the helicopter, controlled experiments were run at the General Electric Company, High Voltage Laboratory in Pittsfield, Massachusetts. Several corona point configurations were tested with voltages up to 500 KV. Typical results for a single corona brush are shown in Figure 184. It can be observed that in order to be effective and dissipate a substantial part of 600 microamperes charging current, the brush must be lowered very close to the ground. For example, at 100 KVolt, the corona point lowered within 3 feet off the ground will dissipate only 50 microamperes. Considering that the CH-47 was charged to 120 KVolt by 300 microamperes, it is obvious that a corona point suspended under the helicopter can alleviate the problem somewhat, but cannot discharge the helicopter to the desired level of 10 to 20 KVolt.

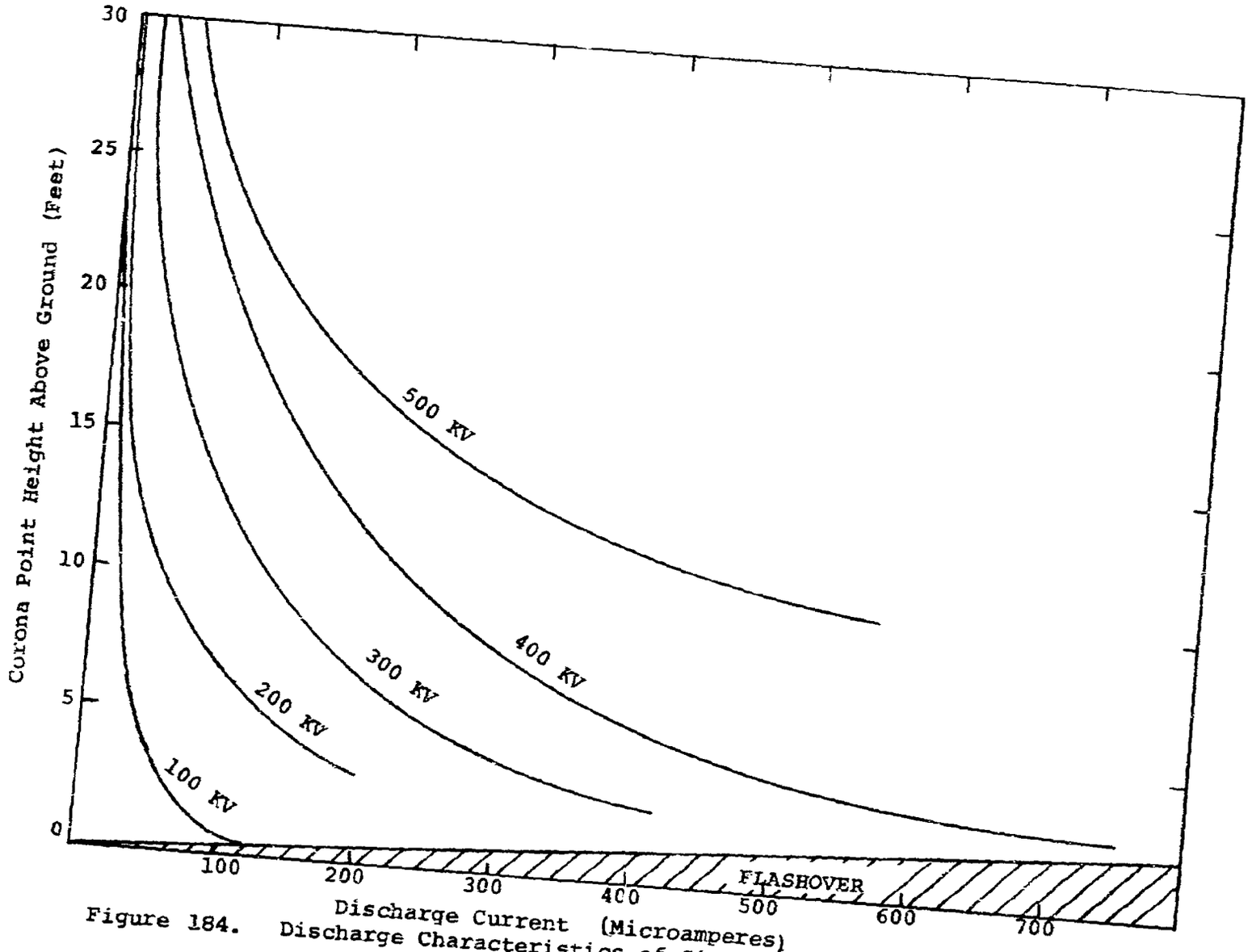


Figure 184. Discharge Characteristics of Single Corona Brush.

Passive Static Electricity Program

Background

Based on the findings of the active dissipation program, the static dissipation program was redirected to a passive system. The passive system was developed and subsequently demonstrated at the U.S. Army Yuma Proving Ground. USAAMRDL TR74-22, Test Development Report - Static Electricity, contains a full description of the tests and demonstration. Subsequent paragraphs summarize the passive static electricity system development program.

Objective

The primary objective of the passive system is the protection of the cargo handler during cargo hookup operations. This objective presents a design compromise:

1. A highly conductive grounding link (such as a low-resistance wire) between the helicopter and the ground surface will leave the minimum residual voltage on the helicopter. However, in case of inadvertent contact with the cargo handler (prior to contact with the ground surface), it will expose the cargo handler to the full discharge energy stored by the helicopter.

2. If a resistor of several megohms is inserted in the grounding line, it will protect the cargo handler against very high voltages on the helicopter (e.g., 10 megohms will allow a contact up to 120,000 volts, 20 megohms over 200,000 volts, etc.), but will leave a residual voltage under heavy charging conditions due to the ohmic voltage drop. At the HLH design maximum charging current of 600 microamperes, a total resistance between the helicopter and ground of 10 megohms will leave a residual voltage of 6,000 volts on the helicopter, and 20 megohms will leave a residual voltage of 12,000 volts.

Design Approach

Two pieces of grounding hardware were considered for the HLH. The first is a resistive grounding link, commonly called a grounding line, which is attached to one cargo coupling and dangles approximately 7 feet below it. As the HLH winches are used to lower the cargo coupling for load hookup, the grounding line contacts the cargo or the ground and thereby discharges the helicopter prior to any handling of the cargo coupling by ground hookup personnel. The second hardware item is a resistive grounding pole intended to be used under

the special circumstances of a depot location and a requirement to handle or guide cargo before it touches the ground. In this situation, the grounding pole, which is a loose piece of ground handling equipment, is used to contact the cargo and to thereby discharge the cargo and the helicopter, making it safe for ground handler manipulation.

Passive Method

The success of passive dissipation depends on the resistance between the grounding electrode and the conducting layer of the ground. Previous measurements have quoted resistances as high as 10^{10} ohms. Even a resistance of 2×10^8 ohms would keep the helicopter at 120 KV level when the charging current reaches the 600 microampere level, precluding passive dissipation. However, the resistance measurements conducted during the passive flight test program have shown that the contact resistance decreases dramatically with increasing voltage and never exceeds 10^7 ohms. In Figure 185 the resistance between the grounding electrode (2 feet of commercial chain) and the desert is plotted as a function of applied voltage, for various contact surfaces. The line drawn for 600 microamperes charging conditions cuts the resistance curves well below the 14 KVolt limit, except for the conditions shown for the chain resting on dry rocks when the voltage is of the order of 16 KVolt. If both the cargo handler and the chain rest on the same rocks, the cargo handler is tapping the charges through 30 megohm resistor in series. As discussed in the preceding praragraph, shock experiments on humans have shown that when 10 megohm resistor is placed in series with the cargo handler, he is able to touch the helicopter with up to 120 KVolt potentials. It is concluded that in the worst case of dry rocks he will feel no sensations if standing on the same rocks and only slightly higher than acceptable shock (260 millijoules) if he is grounded to the conductive substratum while the chain rests on the dry rocks. Such a circumstance may be considered an improper grounding procedure, similar to dropping the grounding chain on a fiberglass container, then touching the helicopter while standing on a good ground.

Protection Against Inadvertent Contact with the Grounding Line Prior to Its Contact with the Ground

There is a possibility that the cargo handler may accidentally touch the grounding line prior to the grounding electrode (chain) touching the ground. He would then receive the full discharge energy from the helicopter, if some additional protection is not provided. To guard against this possibility, a 10 megohm resistor is incorporated between the grounding electrode and the helicopter. The cargo handler will be protected, but the residual voltage on the grounded

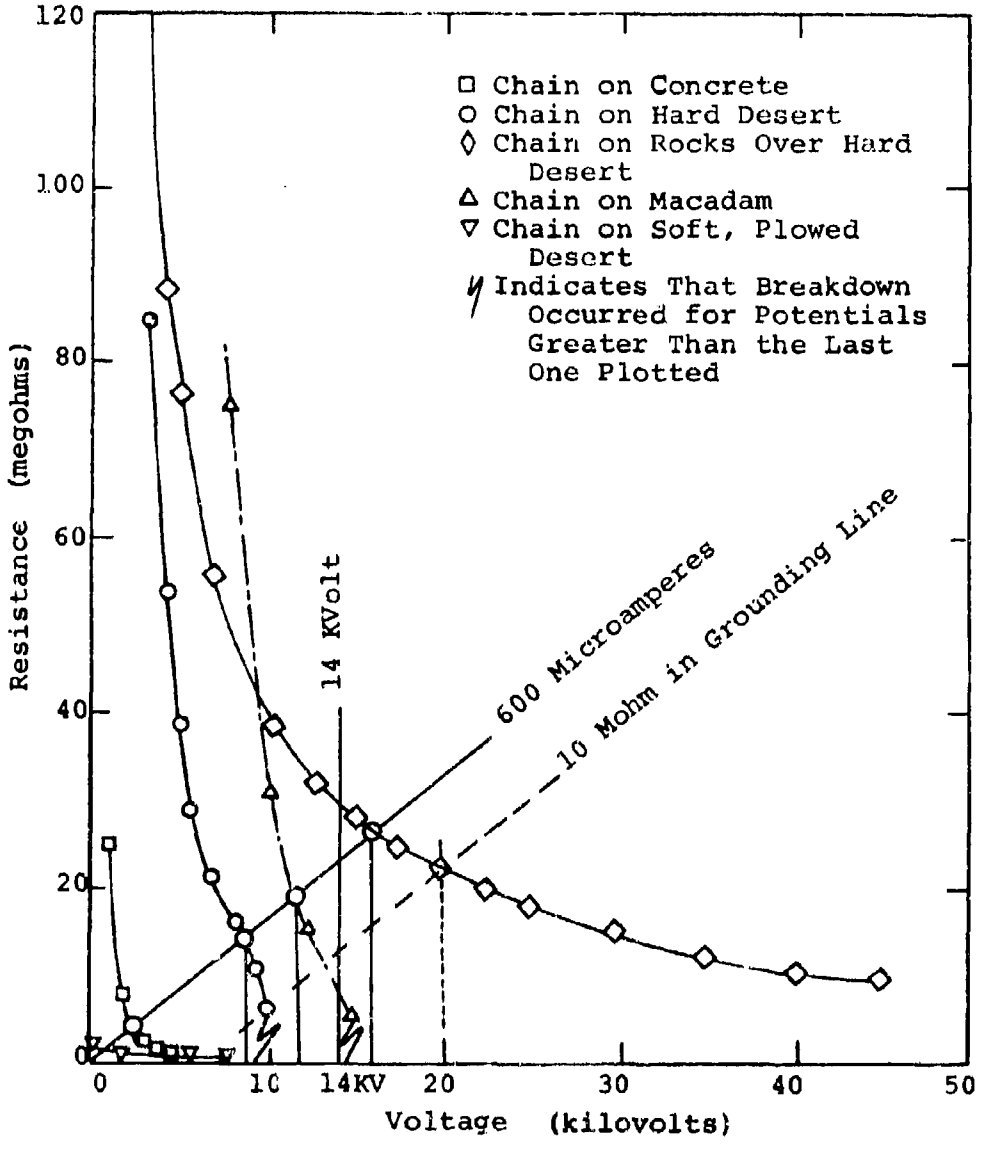


Figure 185. Resistance as a Function of Voltage For Various Surface Materials.

helicopter is increased by 6 KVolt maximum under maximal charging conditions (see Figure 4), even then the voltage remains below 14 KVolt for concrete macadam or desert, and rises to 20 KVolt when the grounding electrode is resting on rocks. The handler standing on good ground would receive a 400-millijoule shock, admittedly severe, but considered to be much less severe than 14 joules discharge when accidentally touching a good conducting grounding line.

Passive Dissipation Hardware

Two types of dissipation hardware were tested:

1. Grounding Pole
2. Grounding Line

Grounding Pole - The grounding pole consists of the following elements:

1. Conductive Contact Element
2. One Megohm Resistive Element (Optional)
3. Lead Wire
4. Ground Contact Element
5. Insulating Rod

Conductive Contact Element - This item consists of a 1/4-inch-diameter anodized aluminum rod threaded at one end and bent into the shape of a shepherd's crook. Its purpose is to contact the cargo and to accept direct spark discharges which are then carried to the ground. It also provides a means for gripping or hooking onto most types of external cargo.

One Megohm Resistive Element - This item consists of a 12-inch-long rigid tubular fiberglass center body overcoated with polurethane doped with a carbon dust content sufficient to provide the required resistance. Attachments are provided at each end to maintain electrical conductivity with the conductive contact element and the lead wire. This element may be omitted. It was originally intended for allocation of shock or sparking under compounded circumstances, e.g.,contact resting on spilled fuel, intermittent contact with cargo hook, severe charging.

Lead Wire - This item consists of a 120-inch piece of No. 6 AWG copper braid inside an equal length of heat shrinkable Teflon tubing. Disconnect couplings of the MS electrical type are provided at each end to permit field replacement if the lead wire becomes damaged. The purpose of this element is to carry the static discharge from the conductive contact element to the ground and also to serve as a drain for a lightning strike to the helicopter after the grounding pole has been attached to the cargo.

Ground Contact Element - This item consists of a 2-foot length of cadmium plated steel chain. Welded tabs are provided on each end link for compatibility with forked bolts,which in turn are attached to disconnect couplings. A feed-through wire is provided to ensure end-to-end electrical conductivity. The purpose of this element is to provide a reasonable contact electrical path to ground under widely varying terrain conditions in the presence of hovering helicopter rotor downwash.

Insulating Rod - This item consists of a hollow insulating fiberglass pole 6 feet in length covered with heat shrinkable Teflon tubing for water repellency. Its resistance exceeds 100 megohms. A series of polypropylene water droplet collars is provided to prevent rain from forming a continuous conductive path down the length of the pole. A rubber hand-grip is provided at the lower end to facilitate one-hand usage. The purpose of the insulating rod is to protect the ground handler from the shock energy levels of helicopter discharging.

Grounding poles are in a wide use by the British Navy and by the U.S. Coast Guards. The operational problem they present is as follows: If the contact is accidentally broken, the helicopter regains full voltage in a matter of seconds. For this reason, one ground handler must be exclusively allotted the task of maintaining the contact.

Since it was found that the grounding line has worked satisfactorily, the grounding pole is not recommended for use with the HLH, but is useful optional equipment for such applications as discharging hovering helicopters in fixed bases and onboard ships.

Grounding Line - In order to meet the normal service abuse (stepping, flexing), the original design called for a flexible resistive element of 10 Mohms. It was found that the flexible resistive element, supplied for the flight tests, changed resistance by a factor of 3 to 4 under normal mechanical strain, such as whipping in the helicopter downwash, deployment, etc. A subsequent search for a flexible 10 Mohm resistor, which would not change more than $\pm$ 10% under full voltage and temperature range, established that none was available commercially. It was decided to take the following approach on the design of the grounding line:

1. Long Term Solution - Flexible resistor, fully tested for environmental conditions, will be adopted when it is offered by the resistor industry.

2. Short Term Solution - Fixed resistive elements of suitable stability properly protected from service abuse, will be used to form a flexible grounding line.

Proposed Design for HLH Resistive Grounding Line

Basic Design - The resistive line will consist of three elements: 3.3 Mohm, 70 KVolt resistor, and 7 inches long, as shown in Figure 186. Each resistor will be encased in a strong protective tubing for mechanical protection, and potted on ends to exclude water ingress and corrosion.

Resistance Stability Requirements - The resistor must hold its resistance within +10% from -65°F to 160°F under maximum voltage of 200 KVolt (120 KVolt for dry desert climate, 200 KVolt anticipated for the Arctic).

Industry Standards - The resistor industry uses definitions given below:

1. Temperature Stability - Percentage per °C.

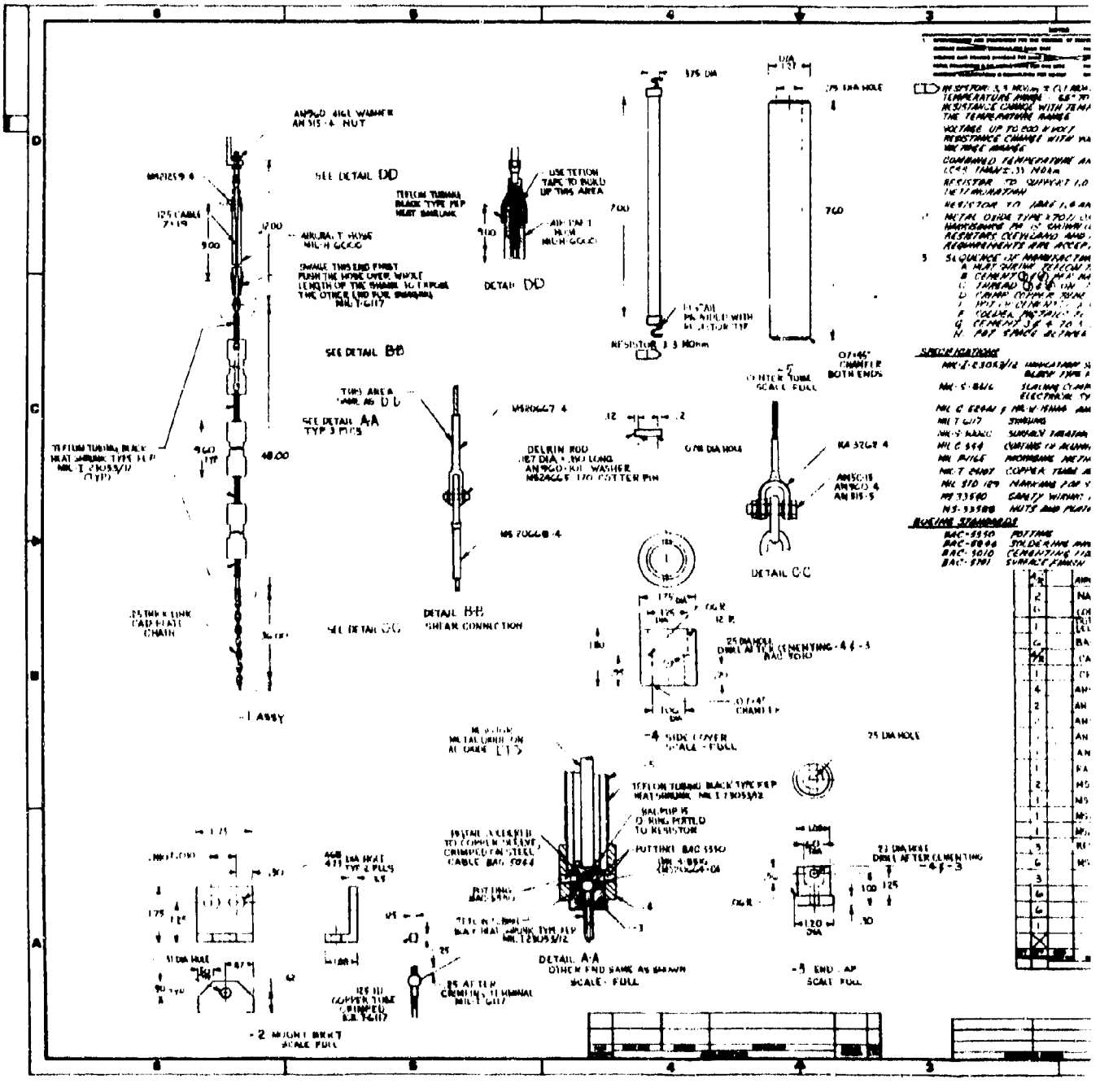
2. Voltage Stability - Resistance is measured at 1/10 voltage, then at full voltage. The resistance change per volt is defined as:

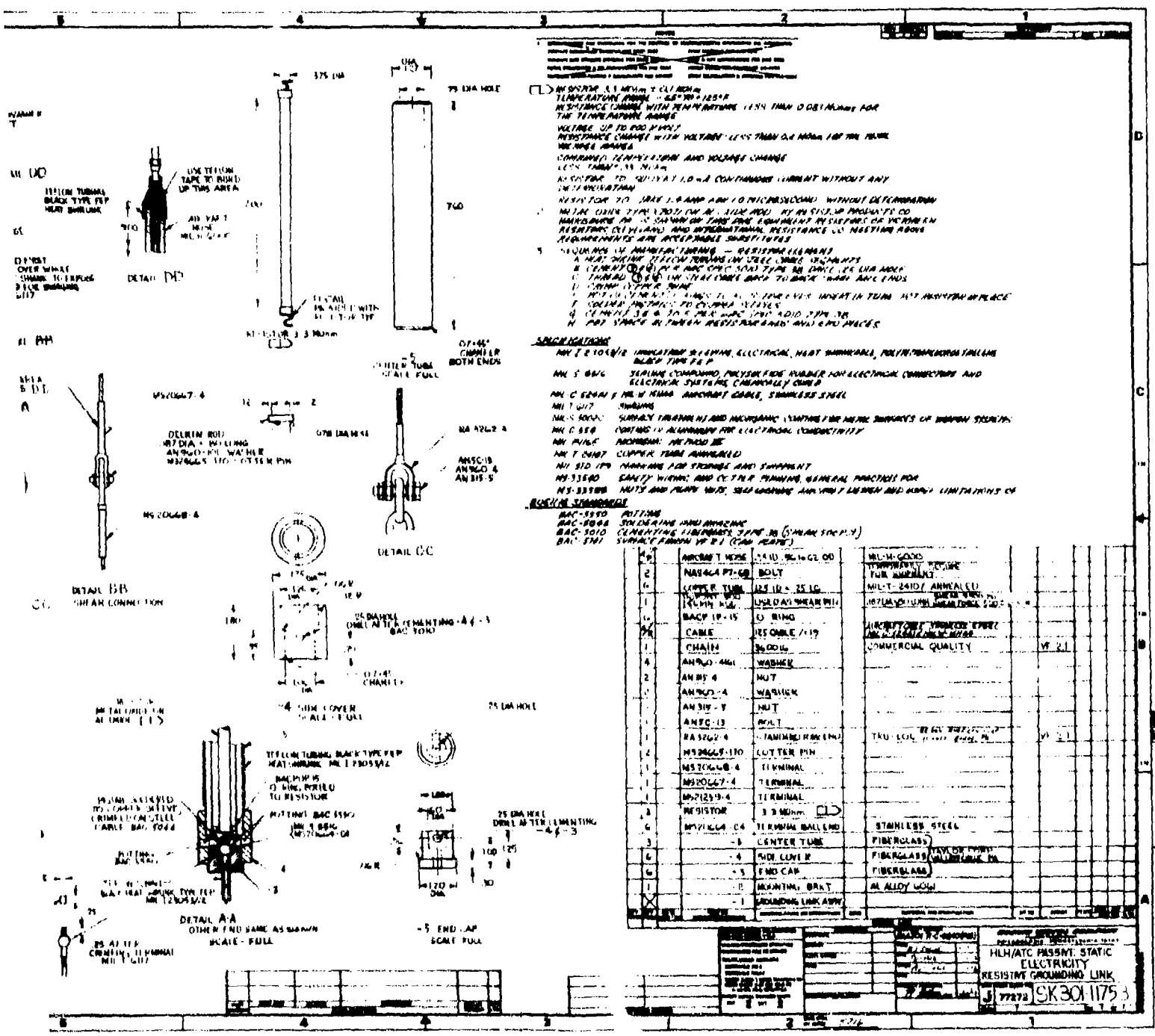
$$\frac{R \text{ at } 0.1 \text{ volt} - R \text{ full volts}}{\text{Volts} - 1/10 \text{ Volts}}$$

Types of Resistors Available - Two resistor types are available from the resistor industry, namely:

1. Carbon film deposited on fiberglass. This type of resistor has the advantage of some flexibility from the fiberglass rod, but the carbon coating exhibits large temperature and voltage coefficients.

2. Metal oxide film deposited on ceramic. This resistor type has the disadvantage of a rather brittle rod (aluminum oxide), but the oxide deposit has superior temperature and voltage characteristics.


SEE DETAIL DD
SEE DETAIL BB
SEE DETAIL A-A
TYP 3 PLCS
SEE DETAIL CC
DETAIL DD
DETAIL BB
SHEAR CONNECTION
DETAIL CC
DETAIL A-A
OTHER END SAME AS SHOWN
SCALE - FULL
-1 ASSY
-2 MOUNT BRKT
SCALE FULL
-4 SIDE COVER
SCALE - FULL
-5 END CAP
SCALE FULL
DELRIN ROD
.187 DIA x .190 LONG
AN960-10L WASHER
MS24665-120 COTTER PIN
TEFLON TUBING BLACK TYPE FEP
HEAT SHRINK TYP
MIL-T-23053/10
(TYP)
AIRCRAFT HOUSE
MIL-H-6000
SHRINK THIS END FIRST
PUSH THE HOSE OVER WHOLE
LENGTH OF THE SHRINK TO ENSURE
THE OTHER END FOR SHRINK
MIL-T-6117
USE TEFLON
TAPE TO BUILD
UP THIS AREA
AIR DRY 1
HOUR
MIN
MIL-H-6000
.375 DIA
.75 DIA HOLE
.07 x 45°
CHAMFER
BOTH ENDS
CENTER TUBE
SCALE FULL
.078 DIA HOLE
.25 DIA HOLE
DRILL AFTER CEMENTING - 4 & - 5
BAC 5010
.07 x 45°
CHAMFER
.25 DIA HOLE
DRILL AFTER CEMENTING
- 4 & - 5
.25 DIA HOLE
DRILL AFTER CEMENTING
- 4 & - 5
.25 AFTER
CRIMPING TERMINAL
MIL-T-6117
.125 ID
COPPER TUBE
CRIMPED
BAC 9403
.468 DIA HEAT
FIT TYP 2 PLCS
TEFLON TUBING BLACK TYPE FEP
HEAT SHRINK MIL-T-23053/2
BALLPIP IS
O RING MTLD
TO RESISTOR
POTTING BAC 5550
MIL-A-8625
TYPE I
CLASS 1
GRADE A
TOTAL CRIMPED
TO COPPER SLEEVE
CRIMPED TO STEEL
CABLE BAC 5004
POTTING
BAC 5550
TEFLON TUBING BLACK TYPE FEP
HEAT SHRINK TYP
MIL-T-23053/10
.125 CABLE
7 x 19
AN960 416L WASHER
AN315-4 NUT
MS21259-4
MS20667-4
MS20668-4
MS24665-120
RA 3267-4
AN515-10
AN960-4
AN815-5
.25 THICK LINK
LOAD RATE
CHAIN
.187 DIA HOLE
.25 DIA HOLE
.125 DIA HOLE
.25 DIA HOLE
.25 DIA HOLE
.25



Resistive Grounding Line.

2

The metal oxide type resistor was selected based on the following calculations:

1. Carbon Deposited on Fiberglass - 3.3 Mohm, 70 KVolt, 126°C Temperature Range.

2. Resistance change with temperature

   10^{-3} per °C

   10^{-3} X 126 = 12.6% = 1.26 Mohm for 10 Mohm

3. Resistance change with voltage

   3×10^{-6} per Volt

   Change: $3 \times 10^{-6} \times 21 \times 10^{4}$ Volt X 3.3 Mohms = 2.1 Mohms

   Total Change = Change with temperature + change with voltage = 3.36 Mohm

4. Metal Oxide (Resistor Products Co. Type X7071) on Ceramic (aluminum oxide).

   Resistance change with temperature

   200×10^{-6} per °C = 2×10^{-4} per °C
   for 126°C and 10 Mohms = 0.25 Mohms

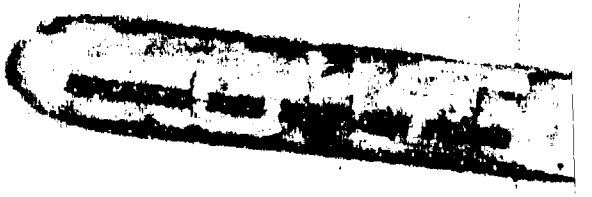
   Resistance change due to voltage

   10^{-6} per Volt
   10 Mohms X 10^{-6} X 189×10^{3} = 1.8 Mohms

   Total Change = Change with temperature + change with voltage = 2.05 Mohms

Resistor Data - The 7.0 inches length was selected based on a voltage drop of 10 Volt/mil, which is customary in resistor design.

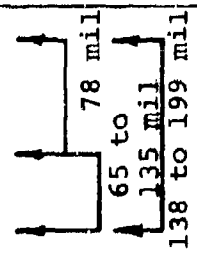
Continuous current carrying capability - 1 mA, maximum 1.6mA surge capability - 1.4 A for 1 microsecond.



Thermal Expansion and Potting Considerations - The aluminum oxide is not flexible, hence it must be protected from mechanical abuse. Enclosing the resistor inside a Teflon cylinder provides good water repellency and a strong case. Potting is used as the solution against water ingress and dielectric strength. The difference in thermal expansion of the materials used excludes potting of the whole resistor length as shown in Table 20.

TABLE 20. THERMAL EXPANSIONS OF GROUNDING LINE MATERIALS.

Material	Linear Thermal Expansion Coeff.	Total Expansion on 7" Length for 126°C	Expansion for 126°C
Alum.Oxide	7×10^{-6} per °C	6.3 mil	
Fiberglass	8×10^{-6} per °C	8.0 mil	
Teflon	95×10^{-6} per °C	84 mil	
Potting Compound BAC 5550	160 to 230 X 10^{-6} per °C	142 to 205 mil	



It is obvious that potting the whole length of 7 inches would present very difficult packaging. The 40 mil expansion difference between the Teflon and aluminum oxide presents a problem, which would require some flexible bellows on both sides of the resistor. A suitable compromise was a fiberglass case, covered with heat shrinkable Teflon tubing.

PART 2. STRUCTURAL DESIGN AND WEIGHTS ANALYSIS

GENERAL

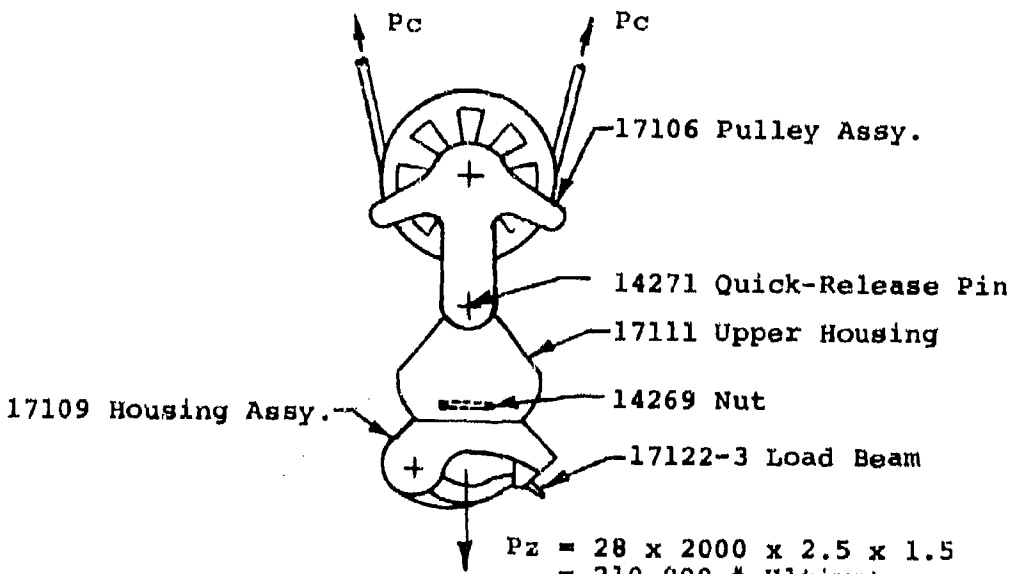
The following is a summary of the structural capabilities of the major components of the cargo handling system, including:

1. Coupling device
2. Tension member
3. Hoist (with load isolator)
4. Hoist drive.

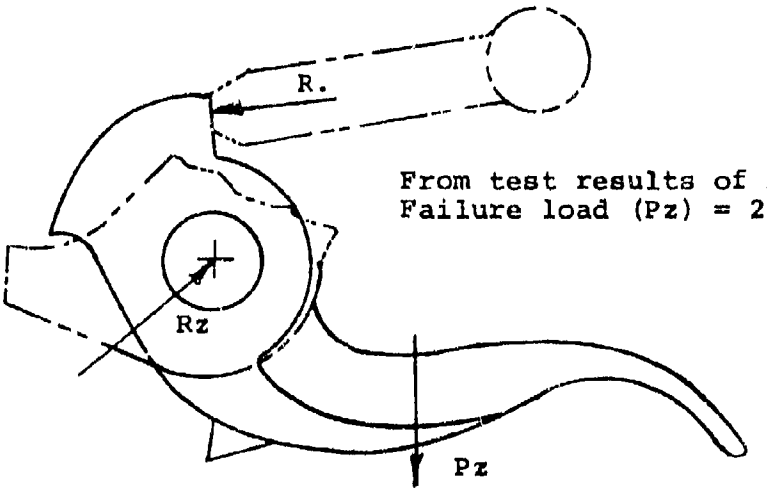
Each of the components listed above is presented with a sketch of the basic critical static loads, followed by a listing of the margins of safety. These static loads are derived from the requirements presented in Part 3 of this report.

Coupling Device

Design Condition - Single-point pickup
28 ton load
nz = 2.5 limit



17122-3 Load Beam



From test results of Ref. B:
Failure load (Pz) = 243,500 lb

$$m.s. = \frac{243,500}{210,000} - 1 = .16$$

TABLE 21. CARGO SYSTEM COUPLING DEVICE - SUMMARY OF MARGINS OF SAFETY.

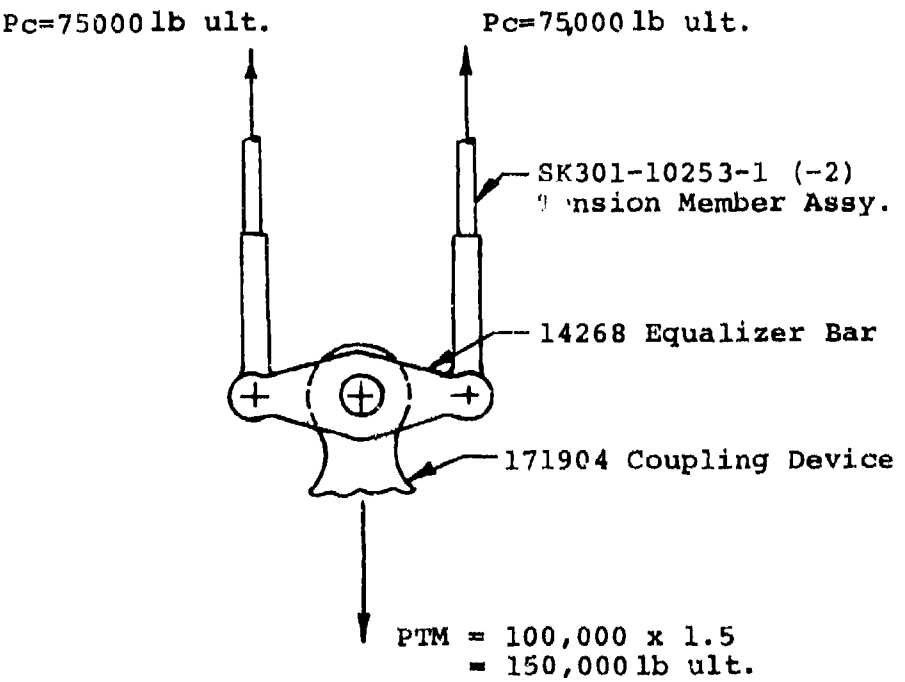
Part No.	Description	M.S.	Load Condition	Type of Failure
17102	Housing Assembly		(1)	Shear Bearing of Lug
14269	Nut	>1.0	(1)	Thread Disengagement
17111	Upper Housing		(1)	Lug Tension
14271	Quick-Release Pin	.06	(1)	Pin Bending
17106	Pulley Assembly	.33	(1)	Bending of Rim
14268	Equalizer Bar		(2)	Bending

(1) Single-point pickup load on coupling = 210,000 lb Ultimate.

(2) Dual-point pickup load on coupling = 150,000 lb Ultimate.

Tension Member

Ult. Design Condition - Dual-point pickup
28 ton load
nz = 2.5 limit



Design Development Test Results on SK301-10253-1(-2) Tension Member Assy. (With 0.70 Inch 36x7 Cable):

1. Min. Ult. Strength Before 10,800 Load Cycle Fatigue = 75,100 lb ult.
   $$M.S. = \frac{75,100}{75,000} - 1 = 0.0$$

2. Min. Ult. Strength After 10,800 Load Cycle Fatigue = 69,900 lb ult.
   $$M.S. = \frac{69,900}{75,000} - 1 = -0.07$$

3. Min. Ult. Strength After 10,800 Load Cycle Fatigue Plus Corrosive Atmosphere = 62,100 Ult.

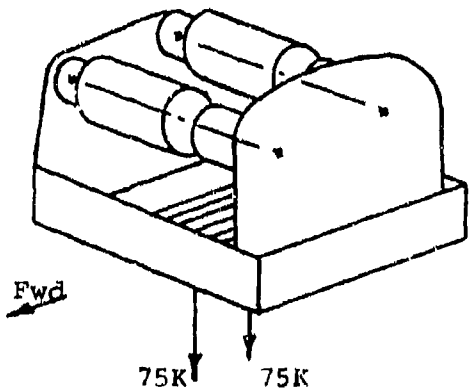
$$M.S. = \frac{62,100}{75,000} - 1 = -0.17$$

This analysis, which is based on the results of development testing of the 0.70-inch-diameter cable, indicated negative margins of safety. A 0.72-inch-diameter 36x7 cable has, therefore, been selected for the HLH/ATC tension member design.

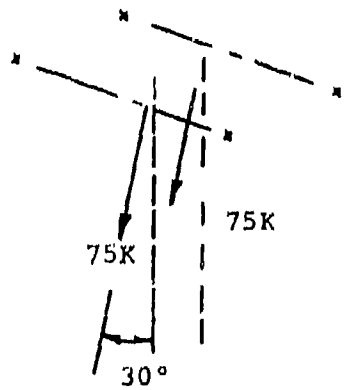
Hoist Assembly

Ult. Design Load Conditions - Dual-point pickup
28 ton load
nz = 2.5 limit

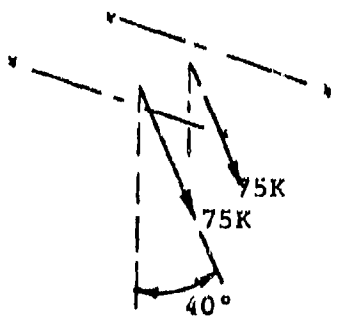
Cond. 1
Load Vertical



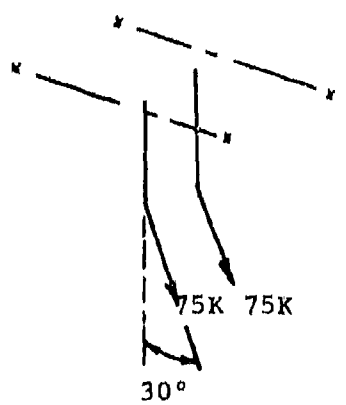
Cond. 2
Load 30° Fwd.



Cond. 3
Load 40° Aft



Cond. 4
Load 30° Lateral



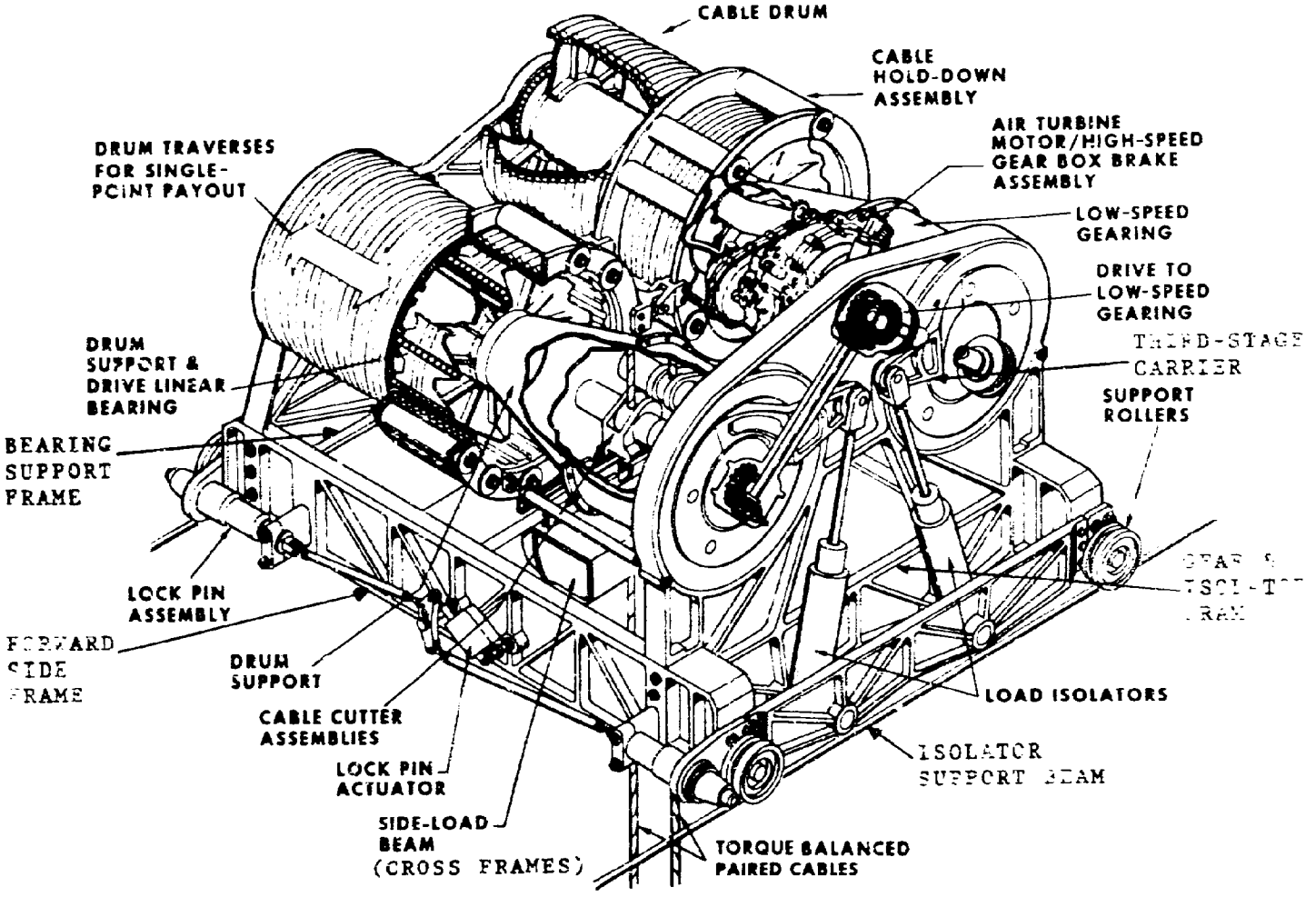


Figure 187. Dual Drum Hoist Assembly.

TABLE 22. CARGO SYSTEM HOIST ASSEMBLY - SUMMARY OF MARGINS OF SAFETY.

Part No.	Description	Load Cond.	Type of Failure	M.S.	Life (Hrs)
42198R180	Bearing Support Frame	3	Bending	.167	--
42198R179	Gear & Isolator Frame	3	Bending	.283	--
42198R183	Isolator Frame	3	Bending	.027	--
42198R181	Fwd Side Frame	3	Bending	.027	--
42198R182	Aft Side Frame	3	Bending	.262	--
42198R184 & 42198F185	Cross Frames	4	Bending	.081	--
42198R101 & 42198R132	3rd Stage Carrier	1	Shear	.012	--
200646002	Load Isolator	1	Column	>0.0	--
42198R178	Drum Support	*	Fatigue	--	5,400

*Fatigue loading of 10,800 cycles (3,600 hours) as defined in Part 3 of this report.

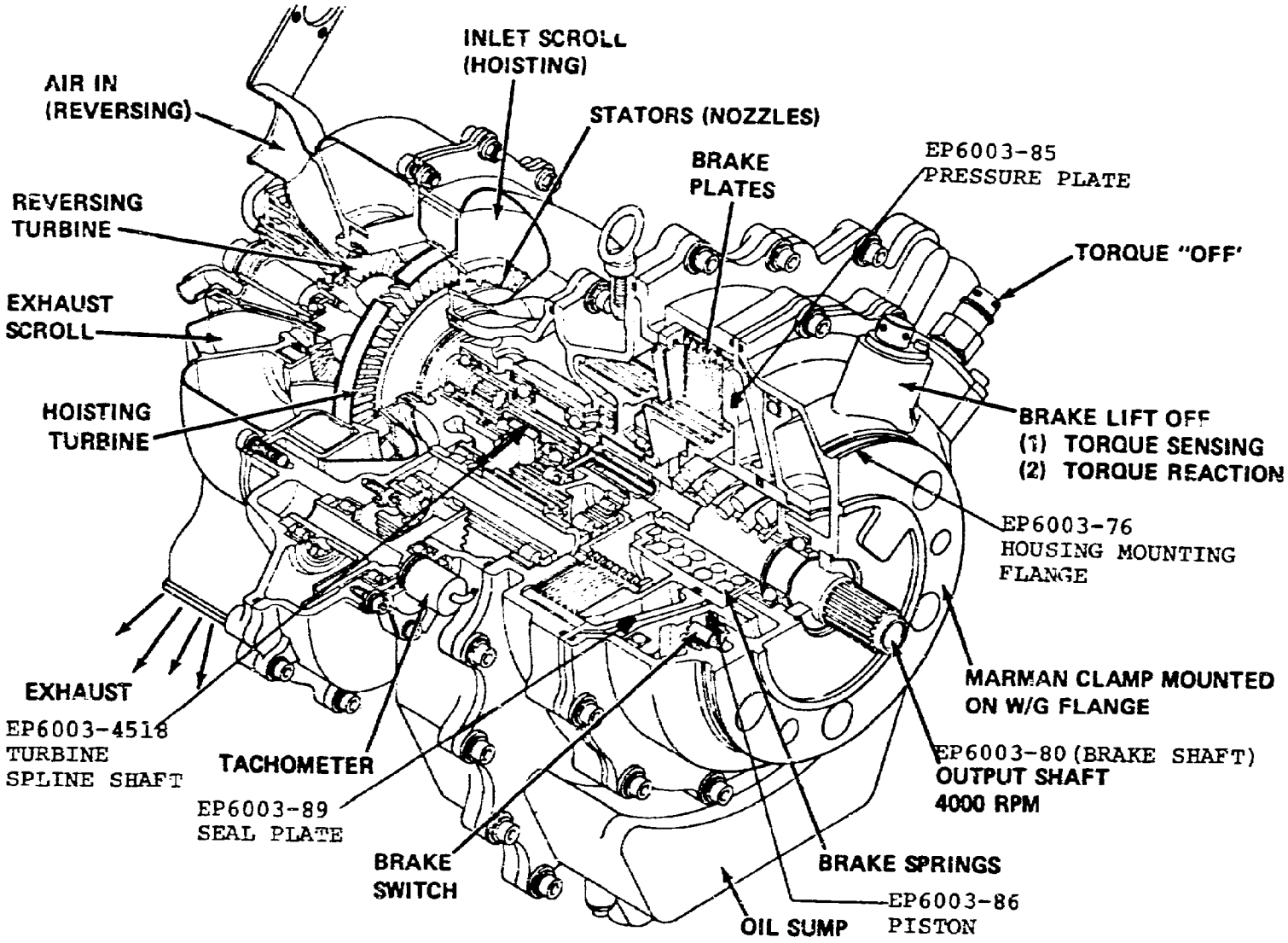


Figure 188. Hoist Drive.

TABLE 23. CARGO SYSTEM AIR TURBINE MOTOR - SUMMARY OF MARGINS OF SAFETY.		
Part No.	Description	M.S.
EP6003-76	Housing Mounting Flange	.24
EP6003-4518	Turbine Spline Shaft	.11
EP6003-80	Brake Shaft	1.0
EP6003-86	Brake Plate Ram	1.0
EP6003-89	Seal Plate	.44
EP6003-86	Piston	.68
	Turbine Blade	.17

Weight Analysis

A weight comparison of the cargo handling system is presented in Table 24. Listed are the major component target weights, the comparable ATC actual weights, and the potential weight reductions that can be visualized in future redesign efforts.

The potential weight reductions are shown below as negative numbers in parentheses followed by a detailed breakdown of the affected hardware and the proposed method of attaining each weight saving.

Hoist Assembly (-150 lb)

-34 lb drum - reduce length due to dead wrap reduction from 4.5 to 3.

-12 lb drum end plate - change from steel to titanium.

-40 lb frame - improve design and reduce moment due to shorter drum.

-24 lb side load beams - revise criteria to delete 2.5g @ 30°.

-20 lb drum support structure - refine design.

-10 lb roller assemblies - refine design.

-10 lb miscellaneous details - refine design.

Hoist Drive System (-14 lb)

-3.0 lb ATM/brake - material removal.

-11.0 lb ATM/brake - material change, aluminum to magnesium.

Cable Cutters (-4 lb)

Change end caps from steel to aluminum.

Tension Member Assembly (-28 lb)

Reduce 15 feet per hoist.

TABLE 24. CARGO HANDLING SYSTEM WEIGHT SUMMARY.

	Spec. Target Weights	ATC Actual Weights	Potential Wt.Reduction To ATC
Hoist Assembly (2)	1,996	2,456	-150
Hoist Drive System (2)	116	143	- 14
Load Isolators (4)	180	194	
Cable Cutters (4)	27	18	- 4
Tension Member Assy.(4)	454	483	- 28
Coupling Assy.& Equalizer Beams (2)	178	289	- 38
Reel and Conductor Instl.(2)	65	106	- 21
Hoist Positioning System (2)	48	65	
Hoist Position Locking Sys.		44	
Roller & Fitting Instl.	125	65	
Supports - Structural		*	
Tracks	43	*	
Misc. Hardware	30	0	
Controls	40	38	
Single-Point Adapter Assy.	87	100	- 3
Controllers	40	76	- 4
	3,429	4,077	-262

*Not aircraft component - used only with integrated test rig.

Coupling Assembly (-38 lb)

-28 lb change housing material from 7075 aluminum to 6.4 titanium (high tool cost) and refine design.

-10 lb remove remote mechanical release.

Reel and Conductors (-21 lb)

-.8 lb material removal.

-1.2 lb material change from steel to aluminum.

-4.5 lb material change from aluminum to magnesium.

-10.0 lb eliminate override control valves.

Controllers (-4 lb)

Refine design.

Single-Point Adapter (-3 lb)

Reduce sheave assembly weight due to cable diameter reduction.

Extension Pendant Design

The estimated weight of the 150-foot extension pendant design shown in Figure 114 is 502 pounds excluding the coupling. Use of a coupling similar to the ATC design will result in a total pendant and coupling weight of 623 pounds.

PART 3. STATIC AND DYNAMIC LOAD ANALYSIS

The ATC Contract ASRD dictated a system capacity of 28 tons with a 2.5 inertia factor to limit load and a 1.5 factor to ultimate. The ASRD also specified the requirement to accommodate a ± 10% longitudinal shift in the c.g. location of a loaded MILVAN. The system life was defined as 3,600 flying hours with three hoist cycles per flight hour. Time between overhaul was specified as 3600 hoist cycles. A fatigue spectrum was defined as follows:

10% of fatigue life cycles at 125% design load
75% of fatigue life cycles at 100% design load
10% of fatigue life cycles at 50% design load
5% of fatigue life cycles at 25% design load

From the above requirements, together with the specified speeds and lengths, the following analysis was made to determine the system and component design criteria.

Hoist Design Capacity

In order to determine the design load, limit load, and ultimate load requirements for each hoist in the dual hoist system, the following parameters were reviewed:

1. Effect of asymmetric loads
2. Effect of cable departure angle
3. Effect of aerodynamic forces on the payload
4. Effect of coupling and tension member weight.

In addition, the specification requirement for a 2.5 inertia factor was reviewed using available analytical and flight test data. This review is summarized on the two curves in Figure 189. Note that the "hook acceleration" on the lower curve refers to an aircraft mounted hook. The upper curve illustrates that, as the load mass approaches that of the aircraft, the maximum acceleration at the load decreases. From this plot, the contract requirement for a 2.5g inertia factor would appear to be conservative.

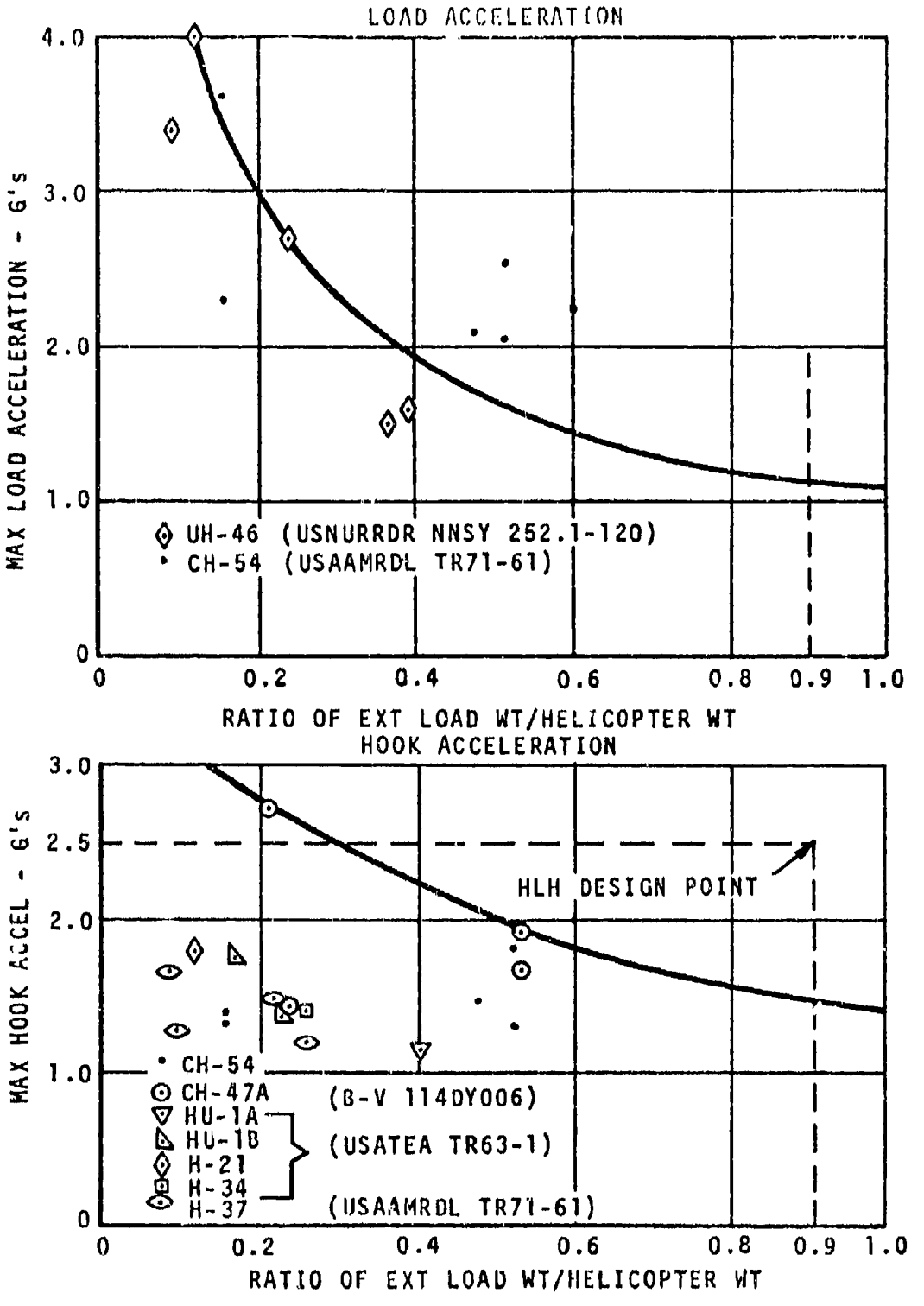


Figure 189. Maximum G Levels Experienced With External Loads.

Effect of Asymmetric Loads

The ASRD requires the system design be capable of accepting a ± 10% shift in the longitudinal c.g. of a loaded MILVAN. From the specification, MIL-C-52661, the maximum gross weight for a MILVAN is 20 long tons (44,800 lb). The container length is 20 feet, therefore the most off-center cg will be 8 feet from one end. In the dual-point mode with a hoist separation of 18 feet, hoist reaction will be: $\frac{44,800}{18} \times 11 = 27,380$ lb for the hoist closest to the cg, and 17,420 pounds for the other hoist. In order to accommodate cg variations in longer commercial containers loaded to 28 tons, and cg variations in non-containerized loads, the individual hoist capacity was selected as 60% of the system capacity, i.e., 56,000 x .6 = 33,600 lb. Using this value for each hoist design load, Table 25 provides a summary of the cg variations that can be accommodated.

TABLE 25. LOAD ASYMMETRY ACCOMMODATION (18-FOOT HOIST SEPARATION)

Load Length (ft)	Load Weight (lb)	Permissible CG Shift (ft)	CG Shift % of Length
20	44,800 *	4.5	22.5
20	56,000	1.8	9.0
30	45,000 *	4.44	14.8
30	56,000	1.8	6.0
40	45,000 *	4.44	11.1
40	56,000	1.8	4.5

*Rotary-Wing Mode Operating Gross Weights for Containers per MHS.1-1970 (Container Standard)

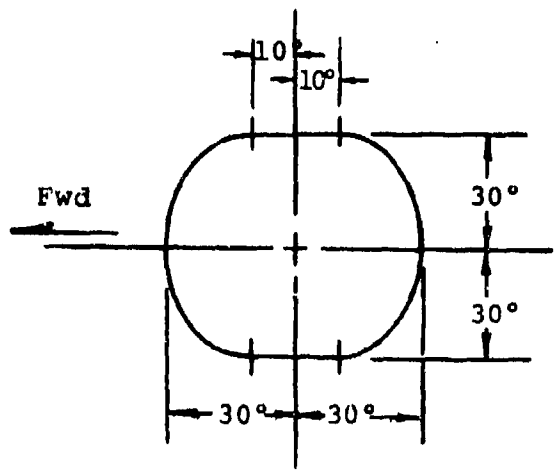
The design of the single-point adapter ensures a 50/50 load split in the single-point mode.

Effect of Cable Departure Angle

The contract ASRD required that the hoist tension member exit be designed to permit the tension member to swing through a 30° cone. A review of the possible cable angles resulting from static suspension geometry, aerodynamic drag, aircraft attitude, and longitudinal pendulum motion indicated that the design should consider the following:

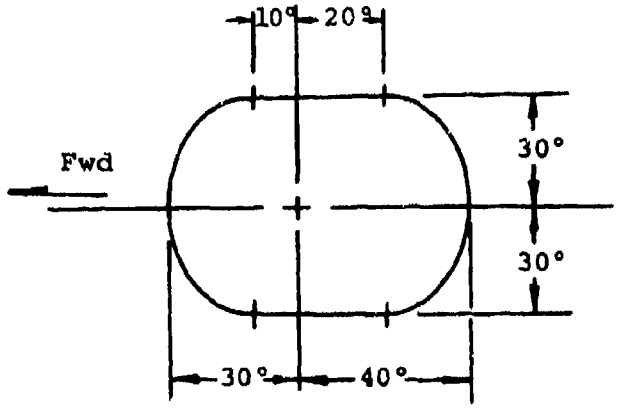
The maximum tension member inclination angles, measured from true vertical at which the maximum load can be applied is as defined below.

1. For the design of the hoist drive torque, the cargo hook (coupling) assemblies and the tension members, the maximum inclination is described by an irregular cone. A section through this cone, perpendicular to true vertical, is shown below.



Design inclination angles for the couplings and tension members consider static displacements caused by a dual to single-point suspension and drag forces, and dynamic displacements caused by external load oscillations and helicopter maneuvering.

2. For the hoist assemblies and the hoist supporting structure, the maximum inclination is described by an irregular cone. A section through this cone, perpendicular to true vertical, is shown below.



Design inclination angles for the hoists and supporting structure consider static displacements caused by a dual- to single-point suspension and drag forces, dynamic displacements caused by external load oscillations in helicopter pitch attitude prior to external load response.

As a result of this review, a factor of 1.15 is used in the design of the hoist, tension member and coupling to account for the 30° angle. The hoist frame and supporting structure also consider the increased angle 40 degrees in the aft direction.

Effect of Aerodynamic Forces on the Payload

Aerodynamic forces acting on a container in forward flight can contribute to the load in the tension member. From wind tunnel tests conducted at the University of Maryland in 1969, a plot of lift/pitch angle for various yaw angles was established. Assuming a maximum nose-down pitch angle on a 20-foot container of 15° and a maximum yaw angle of 6°, then the negative force on the container would be 2780 lb. This force would be additive to the limit load and is spread between the two hoist tension members. Assuming a 60/40 split, the additive load is 2780 x .6 = 1668 lb.

Effect of Coupling and Tension Member Weight

The total load on the hoist will include the weight of the coupling, equalizing bar and deployed tension member. The maximum load will be representative of 100 feet of deployed cable and equal to 140 lb + 194 lb = 334 lb.

From the preceding considerations, the hoist design load may be determined:

Hoist design load = (max. asymmetric load + coupling & T.M. weight) x cable angle factor
= (33,600 + 334) x 1.15
= 33,934 x 1.15
= 39,024

Using the 2.5 inertia factor and aerodynamic down load, hoist limit load will be:

Hoist limit load = Hoist design load x 2.5 + 1670
= 39,024 x 2.5 + 1670
= 97,560 + 1670 = 99,230 lb

This value was rounded out to 100,000 pounds.

The hoist ultimate load will be:

Ultimate load = hoist limit load x 1.5
= 100,000 x 1.5
= 150,000 lb

This value was also used for the design of the dual cable tension member resulting in each cable requiring a minimum breaking strength of 75,000 lb with a minimum yield strength of 50,000 lb.

Single-Point Mode

The geometry of the single-point adapter ensures equal loading on each hoist. The coupling would not be influenced by cable geometry angles, and as single-point loads are generally irregular high density pieces of equipment, there is no significant aerodynamic down load.

The coupling design, limit and ultimate load values will be:

Coupling design load = 56,000 lb
Coupling limit load = 56,000 x 2.5 = 140,000 lb
Coupling ultimate load = 140,000 x 1.5 = 210,000 lb

The tension members of the single-point adapter consist of dual cables attached to each hoist tension member termination with the single-point coupling attached to a sheave supported by the adapter cables. Individual ultimate cable loads will be:

Coupling ultimate load/4 x cable angle factor
= 210,000/4 x 1.15
= 60,400 lb

As the cable for the single-point adapter is identical to the hoist tension member cable, the latter requirements will design the cable.

System Design Life

The system life is predicated on an aircraft life of 3600 hours. Using the estimate of three complete hoist cycles in each flying hour, the required system life is 10,800 hoist cycles.

A hoist cycle is defined as:

Deploy unloaded coupling 100 feet
Hoist load 100 feet
Lower load 100 feet
Hoist unloaded coupling 100 feet.

The design time between overhauls is 3600 hoist cycles.

The fatigue load spectrum is defined as follows:

10% of hoist cycles will be at 125% of design load
75% of hoist cycles will be at 100% of design load
10% of hoist cycles will be at 50% of design load
5% of hoist cycles will be at 25% of design load

CONCLUSIONS AND RECOMMENDATIONS

The HLH helicopter cargo handling system developed under this program is viable for future HLH system RDTE and production programs.

As a result of the testing, the following recommendations are made to improve the effectiveness of the various elements of the system.

- Hoist Drive - An additional iteration of the design of the hoist drive nozzle and turbine wheel should be performed to optimize the efficiency of this power unit. The hoist drive gear ratio should be modified to provide increased hoisting and lowering speeds at design load, above those specified for the ATC design, to further reduce operational cycle time.

- Hoist - A detail design iteration of the major structural elements of the hoist should be performed for weight reduction and to reduce production fabrication costs.

- Cargo Coupling - The release criteria for the cargo coupling should be reevaluated to justify the necessity for the mechanical release mode. A modification should be incorporated to provide additional protection against entry of water.

- Signal Conductor Reeling Mechanism - The level wind deployment mechanism of the conductor cable should be modified to provide a more wear-resistant deployment exit. A design iteration should be performed to provide a more reliable system for electrical signal transfer.

- Tension Member - The configuration of the tension member should be a .72-inch-diameter 36x7 construction mill run wire cable, in order to eliminate the reduction in ultimate tensile strength after exposure to a fatigue life cycle.

- Load Isolator - The envelope constraints relative to the configuration of the load isolator should be reviewed so that a larger dynamic seal can be incorporated to increase the seal life.

LITERATURE CITED

1. Stein, D. et al; ADVANCED TECHNOLOGY HIGH CAPACITY HOIST DRIVE SYSTEM: Boeing Vertol Company; USAAMRDL Technical Report 72-21, U.S. Army Air Mobility Research and Development Laboratory, Fort Eustis, Virginia; April 1972, AD746629.
2. Gibson, P. T. et al; TORSIONAL PROPERTIES OF WIRE ROPE; ASME Report 69-DE-34; 1969.
3. Black, R.; MARK 7 ARRESTING GEAR PURCHASE CABLE AND DECK PENDANT DEVELOPMENT PROGRAM; NAEC Report ENG-7625, Naval Air Engineering Center, Philadelphia, Pennsylvania; May 1970.
4. Jacobsen, Ayre; ENGINEERING VIBRATIONS; McGraw-Hill Book Company, New York, New York; 1958; Page 474.
5. Nutley, W.; TECHNOLOGY DEVELOPMENT REPORT - MODEL 301 HLH/ATC CARGO HANDLING SYSTEM COUPLING; Boeing Vertol Company; USAAMRDL Technical Report 73-88, U.S. Army Air Mobility Research and Development Laboratory, Fort Eustis, Virginia; January 1974, AD778770.
6. Solak, B. J. and Wilson, G. J.; TECHNOLOGY DEVELOPMENT REPORT - RESULTS OF STATIC ELECTRICITY DISCHARGE SYSTEM TESTS (ACTIVE AND PASSIVE) HEAVY LIFT HELICOPTER; Boeing Vertol Company; USAAMRDL Technical Report 74-22, U.S. Army Air Mobility Research and Development Laboratory, Fort Eustis, Virginia; May 1974, AD784130.

LIST OF SYMBOLS

ABS	Aggregate Breaking Strength
AC	Alternating Current
A_e	Effective Nozzle Area
APU	Auxiliary Power Unit
ARADMAC	Army Aeronautical Depot Maintenance Center
ASRD	Aircraft Systems Requirements Document
ATC	Advanced Technology Component
ATM	Air Turbine Motor
BOD	Bending Over Drum
BTU	British Thermal Unit
°C	Degrees Centigrade
C_c	Flow Coefficient
CG	Center of Gravity
CNFCS	Cobra Night Fire Control System
COZID	Cable Operated Zero Impedance Device
CRT	Cahtode Ray Tube
cu-in	Cubic Inch
C_v	Velocity Coefficient
D, d, dia	Diameter
D/d	Ratio Drum Diameter to Cable Diameter
DBS	Design Breaking Strength
DC	Direct Current
ECOM	United States Army Electronics Command
EGCS	Electrogalvanized Carbon Steel
EIU	Electronic Interface Unit

EMI	Electro Magnetic Interference
EOS	Electro Optical Sensor
EVS	Electro Optical Viewing System
°F	Degrees Fahrenheit
FLIR	Forward Looking Infr Red
Ft, ft	Feet
ft-lb	Foot-pound
FOV	Field of View
ft/min.	Feet per Minute
g	Acceleration of Gravity
gal	Gallon
GPM	Gallons per Minute
HLH	Heavy Lift Helicopter
HP, hp	Horsepower
HV	High Voltage
HVE	Hoist Valve Enable
HZ, Hz	Hertz, cycles per second
in	inch
INFANT	Iriquois Night Fighter and Night Tracker
IR	Infra Red
IWRC	Independent Wire Rope Core
ksi	kips per square inch
KVolt	Kilovolt
LB, lb	pound
lb/min	pounds per minute

lb/sec	pounds per second
LCC	Load Controlling Crewman
LED	Light Emitting Diode
L/d	Ratio Lay Length to Diameter
LH	Left Hand
LL	Lang Lay
LLLTV	Low Light Level Television
LW	Level Wind
M	Maintainability
mA	Milliampere
MBS	Minimum Breaking Strength
MDE	Malfunction Detection System
Mil	One thousandth of an inch
Min	Minute
mJ	Millijoule
MM	Millimeter
Mohm, MΩ	Megohm
MP	Multipoint
MPU	Magnetic Pick-up
MTBF	Mean Time Between Failures
mV	Millivolts
MVD	Modulating Valve Disable
NFOV	Narrow Field of View
NVASS	Night Vision Surveillance System
NVL	Night Vision Laboratory
OD	Outside Diameter

OP	Orthographic Projection
pF	Pico farad
PHS	Precision Hover Sensor
P/M	Powdered Metal
P/N	Part Number
psi	Pounds per square inch
psia	Pounds per square inch absolute
psig	Pounds per square inch gage
$\underline{R}$	Reliability
°R	Degrees Rankin
R_B	Rockwell Hardness, B scale
R_C	Rockwell Hardness, C Scale
R, r, rad	Radius
Rev	Revolution
RFI	Radio Frequency Interference
RH	Right Hand
RL	Regular Lay
RMS	Root Mean Square
rpm	Revolutions per Minute
Sec	Second
SIT	Silicon Intensified Larget
SL	Sea Level
SPP	Single Point Payout
Sq-in	Square Inch
T	Torque
TOD	Tension Over Drum

U/Co	Velocity Ratio
USAFFDL	United States Air Force Flight Dynamics Laboratory
UTS	Ultimate Tensile Strength
VAD	Visual Augmentation Display
VAS	Visual Augmentation System
VDC	Volts Direct Current
W	Weight
WFOU	Wide Field of View
ΔT	Delta Temperature
ηA	Microampere
#	Pounds
μ	Coefficient of Friction